THE *VICINAL* DIFLURO MOTIF IN ORGANIC CHEMISTRY: THE SYNTHESIS AND BEHAVIOUR OF COMPOUNDS DERIVED FROM 2,3-DIFLUROSUCCINIC ACIDS

Martin Schueler

A Thesis Submitted for the Degree of PhD
at the
University of St. Andrews

2006

The *vicinal* difluoro motif in organic chemistry: The synthesis and behaviour of compounds derived from 2,3-difluorosuccinic acids.

Martin Schueler

Ph.D. Thesis

The Edinburgh and StAndrews
Research School of Chemistry

Declarations

I, Martin Schueler, hereby certify that this thesis , which is approximately 35,000 words in length, has been written by me, that it is the record of work carried out by me and that it has not been submitted in any previous application for a higher degree.

Date: 3/4/2006 Signature: [redacted]

I was admitted as a research student in October 2002 and as a candidate for the degree of Ph.D. in Organic Chemistry. The study for which this thesis is a record was carried out at the Department of Chemistry and Centre of Biomolecular Sciences at the St Andrews University.

Date: 3/4/2006 Signature: [redacted]

I hereby certify that the candidate has fulfilled the conditions of the Resolution and Regulations appropriate for the degree of Ph.D. in the University of St Andrews and that the candidate is qualified to submit this thesis in application for that degree.

Date: 12/4/06. Signatu[redacted]

Copyright

Acknowledgements

I wish to express my sincere appreciation to Professor David O'Hagan for giving me guidance and the scientific freedom throughout my time in his laboratory. I am also thankful for helpful suggestions and discussions.

I am indebted to Professor Alex M. Z. Slawin for her expertise and significant contribution to this work, also for her kind and motivating manner, and her endless attempts to extract crystallographic data even in the most hopeless cases.

I am grateful to the technical and support staff at the department, in particular Melania Smith, Tomaš Lebl, Silvia Williamson, Caroline Horsburgh, and Catherine Botting. I am also thankful to Professor R. J. Abrahams & Professor H. Rzepa for NMR analysis and theoretical calculations.

Many sincere thanks to everybody in the DOH group for an exiting time in St Andrews, useful discussions in the laboratory, competition on the golf courses and the evenings in the Central.

Finally, I would like to express my gratitude to EPSRC for funding and I am grateful for the excellent working conditions throughout my PhD time in St Andrews.

“Je zielstrebiger wir vorgehen, desto wirkungsvoller trifft uns der Zufall.”

Friedrich Dürenmatt

Table of Contents

Abbrevations

BAST	Bis-(methoxyethyl)aminosulfur trifluoride
bp	boiling point
CI	Chemical ionisation
CDS	Cambridge Structural Database
d	doublet
DAST	Diethylaminosulfur trifluoride
de	diastereomeric excess
DCC	Dicyclohexylcarbodiimide
DCM	Dichloromethane
DEAD	Diethyl azodicarboxylate
DMF	*N*-dimethylformamide
DMSO	Dimethylsulfoxide
DSC	Differential scanning calorimetry
de	Diastereomeric excess
ee	enantiomeric excess
EDC	Ethyl
EI	Electron ionisation
EPSRC	Engineering and Physical Sciences Research Council
GC-MS	Gaschromatography-Mass spectrometry
HOBt	Hydroxybenzotriazole
HOMO	Highest occupied molecular orbital
HRMS	High resolution mass spectroscopy
IR	Infrared spectroscopy
EDG	Electron donating group

EWG	Electron withdrawing group
LDA	Lithium diisopropylamide
LUMO	Lowest unoccupied molecular orbital
m	multiplet
MOST	*N*-morpholinosulfur trifluoride
mp	melting point
m/z	molecular mass to charge ratio
NMM	N-methylmorpholine
NMR	Nuclear magnetic resonance
PPHF	Pyridinum polyhydrogenfluoride
ppm	parts per million
py	pyridine
q	quartet
s	singlet
t	triplet
TBAB	*N*-tetrabutylammonium bromide
TBAC	*N*-tetrabutylammonium chloride
TBAF	*N*-tetrabutylammonium fluoride
TBAI	*N*-tetrabutylammonium iodide
THF	Tetrahydrofuran
TLC	Thin layer chromatography
PTC	Phasetransfer catalyst
RT	Room temperature
VT	Variable temperature

Abstract

The following work describes the synthesis of compounds carrying a *vicinal* difluoro motif and the evaluation of this structural element to influence the conformation of organic molecules. The synthesis of *erythro* and *threo* 1,2-difluoro-1,2-diphenylethane was achieved by bromofluorination and subsequent halogen exchange from stilbene. Oxidative degradation of the phenyl rings allowed to access *erythro* and *threo* 2,3-difluorosuccinic acids and a variety of derivatives thereof. The conformations of these compounds were investigated by means of X-ray analysis and NMR spectroscopy. Conformational analysis of derivatives of 2,3-difluorosuccinic acid was carried out using J_{HF} and J_{HH} NMR coupling constants. A clear preference for the conformations in which the two *vicinal* C-F bonds are *gauche* emerged from these calculations, which was confirmed by temperature and solvent dependent NMR analyses.

The *vicinal* difluoro motif was incorporated into small peptide structures. In the solid state, a strong preference to align the *vicinal* C-F bonds *gauche* to each other was observed and when adjacent to an amide moiety, the C-F bond was found to prefer an *anti* periplanar orientation with respect to the carbonyl bond. These effects appeared to override steric and electrostatic interactions. The conformation of these fluorine-containing peptides showed a clear dependence on the stereochemical orientation of the C-F bonds, and this appears to be an effective tool for influencing the secondary and consequently tertiary structure in a predictable manner. In order to access single enantiomers of peptides having the *vicinal* difluoro motif, a stereoselective route to *R,R* and *S,S* 2,3-difluorosuccinic was developed. This involved nucleophilic fluorination of the cyclic sulfates generated from (*R,R*)- and (*S,S*)- diethyl tartrates and subsequent deoxofluorination of the intermediate fluorohydrins.

1 Introduction

Fluorinated compounds have found wide application in our all daily lives. A large number of agrochemicals and drugs, but also polymers, lubricants, coatings, liquid crystals, owe their unique properties to the introduction of fluorine. Fluoroorganic compounds can have extreme properties. Molecular fluorine for instance is extraordinarily reactive, a powerful fluorinating reagent and the most powerful oxidant known. If applied in undiluted form, fluorine spontaneously combusts or explodes on contact with organic compounds. In contrast, the inertness of perfluorocarbons and halofluorocarbons can make them persistent on a geological time scale, an effect, which can causes ecological problems in certain cases.

The introduction of fluorine has a strong influence on the physical properties of organic compounds. Dipole moment, lipophilicity, acidity/basicity, thermal and oxidative stability of a given molecule can be significantly influenced by the presence of a fluorine atom. Neighbouring functional groups are directly affected by fluorine substitution, thereby strongly influencing chemical reactivity and biological activity of organic compounds. The magnitude of such changes is influenced by the proximity of the fluorine atom, but can be significant even when the fluorine is remotely attached to the functional group.

Naturally occuring organofluorine compounds are rare and thus fluoroorganic compounds have to be obtained by organic synthesis. With respect to the so-called inductive and resonance effects caused by fluorine, conventional synthetic methods are however not always applicable, and surprises that emerge in predicting the behaviour and reactivity of fluoroorganic compounds have led to such terms as

"flustrates" being coined.[1] A specialised understanding of reaction mechanisms, reagents, and synthetic strategies based on the unique chemical and physical properties of fluorine is essential for the synthesis of structurally complex organofluorine compounds. Despite the development of novel fluorinating reagents that have emerged as an answer to the increasing demand for fluorine containing substances, selective fluorination remains one of the most challenging aspects in modern organic chemistry. The application of modern fluorinating reagents and the development of new synthetic strategies for the regio- and stereoselective introduction of fluorine is described which adds a contribution to the important field of fluoroorganic chemistry.

1.1 Electronic and steric properties of fluorine

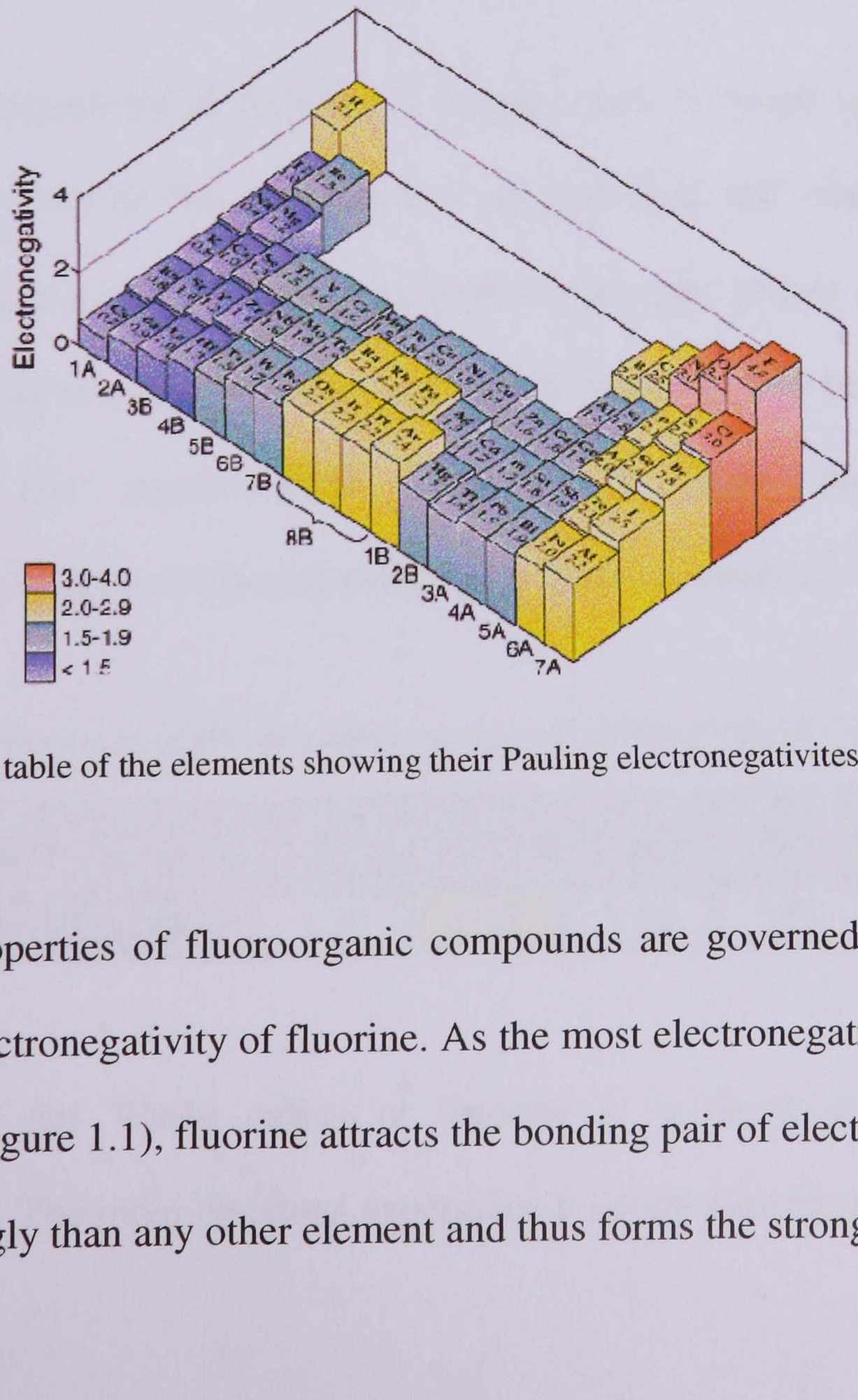

Figure 1.1. Periodic table of the elements showing their Pauling electronegativites.

The physical properties of fluoroorganic compounds are governed by the moderate size and high electronegativity of fluorine. As the most electronegative element in the periodic table (Figure 1.1), fluorine attracts the bonding pair of electrons in a covalent bond more strongly than any other element and thus forms the strongest bond to many

elements including carbon. The high electronegativity of fluorine arises from the high positive charge of the fluorine nucleus, which causes a strong attraction for its electrons. The valence shell electrons are relatively close to the fluorine nucleus due to the absence of d or f orbitals, and consequently experience a strong attraction (Figure 1.2).

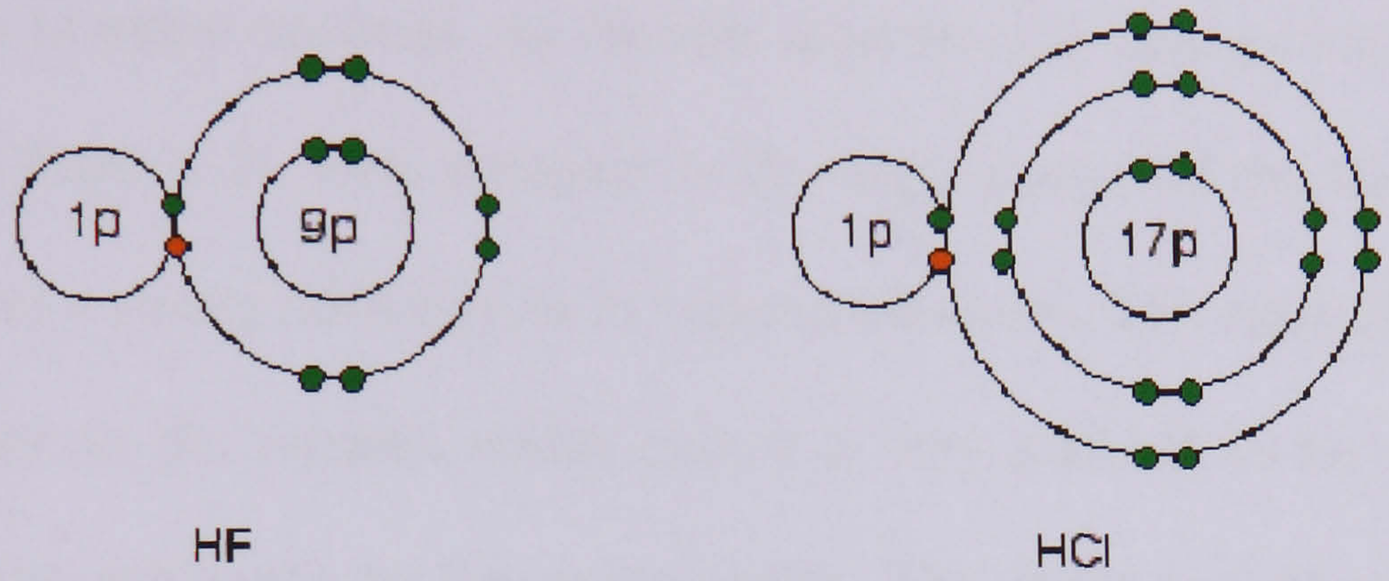

Figure 1.2. Valence shell electrons for the molecules hydrogen fluoride and hydrogen chloride. Despite the same nuclear charge, the chlorine nucleus attracts the valence electrons somewhat less strongly than the fluorine nucleus due to the shielding effect of the 8 inner p electrons.[2]

The high electronegativity of fluorine is coupled with its small size. The Van der Waals radius of fluorine lies between that of hydrogen and oxygen (Table 1.1). Therefore substitution of fluorine for hydrogen or oxygen causes only minor steric perturbations in organic molecules, a strategy which has widely been applied in the pharmaceutical and agrochemical industries to alter physiological and pharmacokinetic properties of biologically active lead compounds.[3]

Table 1.1. Van der Waals radii of elements often encountered in biologically active lead structures.

Element	H	F	O	Cl	Br	I
van der Waals radius [Å]	1.20	1.35	1.40	1.80	1.95	2.15

The small Van der Waals radius of fluorine is a direct effect of its high electronegativity. The outer electrons experience a strong attraction from the nucleus

which is not offset by extra shielding orbitals from inner electrons, and consequently the valence shell of fluorine comes closer to its nucleus than that of any other element with the exception of hydrogen and helium.

The small size of fluorine comes along with a low polarisability. Although fluorine has nine times as many electrons, the fluorine atom has the same atomic polarisability as hydrogen (Table 1.2). One rationale is the high charge of the fluorine nucleus which exercises a strong attraction to its valence electrons. The outer electrons are in close proximity to the nucleus which makes it very difficult to be influenced by external charges, and hence the low polarisability. The ability to form covalent bonds, and the nature of such bonds, is directly affected by the polarisability of the bonded atoms. In general, the bonds formed by fluorine are more ionic in character and therefore extraordinarily strong. For example, aluminium fluoride is considered to be ionic because the small fluoride ion cannot be polarised sufficiently to form a covalent bond, even though the "charge density" of the aluminium ion is very high. In contrast, aluminium iodide is entirely covalent due to the higher polarisability of iodine (Table 1.2).

Table 1.2. Atomic polarisability A^3 for hydrogen and the halogen atoms given in 10^{-24} cm^3.[4]

	H	**F**	**Cl**	**Br**	**I**
A^3 [10^{-24} cm^3]	0.5	0.5	2.2	3.1	4.7

Fluorine has a strong tendency to accommodate a single electron in its valence shell and form fluoride ion. With an electronic configuration of $1s^2 2s^2 2p_x^2 2p_y^2 2p_z^1$ it needs only one more electron to fill its valence shell and arrive at the electronic

configuration of the noble gas neon. The electron affinity refers to the tendency of an element to take up an electron and is thus a measure of attraction between an additional electron and the nucleus. Fluorine has a higher electron affinity than bromine or iodine (Figure 1.3).

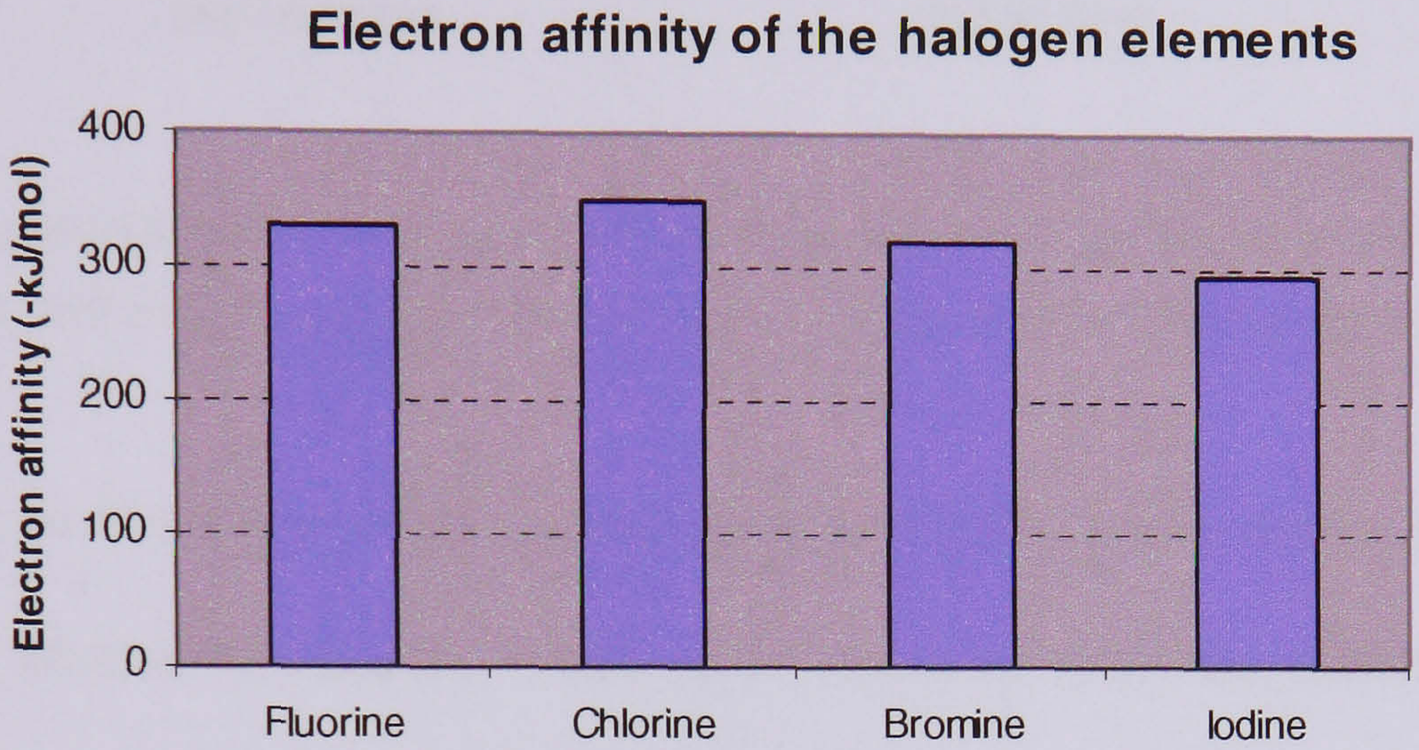

Figure 1.3. Electron affinities of the group 7 elements in comparison.

Surprisingly, the first electron affinity of fluorine is smaller than that of chlorine, which is assumed to be a result of electrostatic repulsion between the incoming electron and the valence electrons. The relatively high electron affinity of fluorine is as a result of the proximity of the incoming electron to the nucleus (Figure 1.4). On the other hand, the ionisation energy of fluorine is very high compared to any other halogen atom. The first ionisation potential shows periodicity and varies from Li to Ne, and from Na to Ar in a sequential manner (Figure 1.5). These variations in the first ionisation potential can be explained in terms of the electronic structures. In going across the period, the increasing number of protons in the nucleus will pull the electrons in more tightly, and therefore, the ionisation energies become higher towards the end of each period.

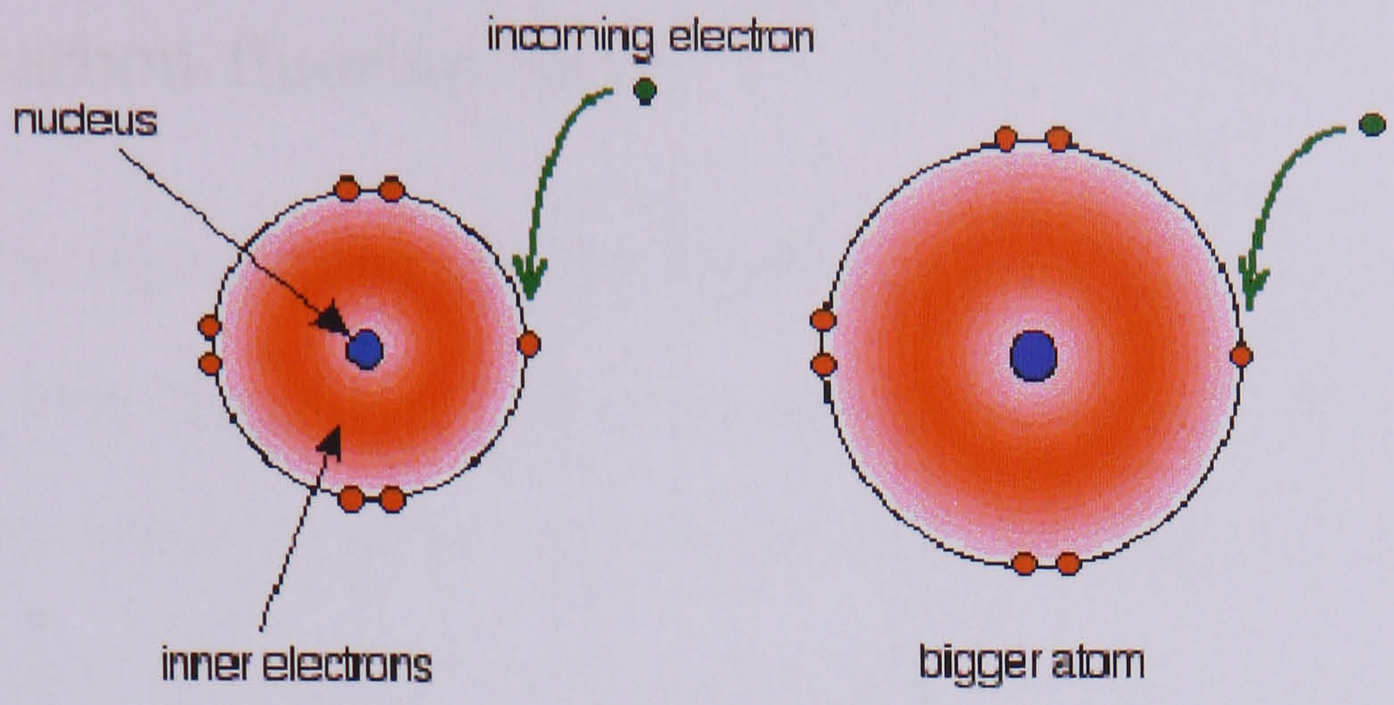

Figure 1.4. The attraction that an incoming electron experiences is dependent on the distance of the valence electron shell from the nucleus. This will directly affect the first electron affinity of the atoms.

The decrease in ionisation energy when going down the group can be understood in terms of the increasing distance of the outer electrons from the nucleus. The large ionisation energy for fluorine (Figure 1.5) shows a high degree of attraction between the outer electrons and the nucleus and is a measure of the energy to generate a positively charged fluoronium ion (F^+).

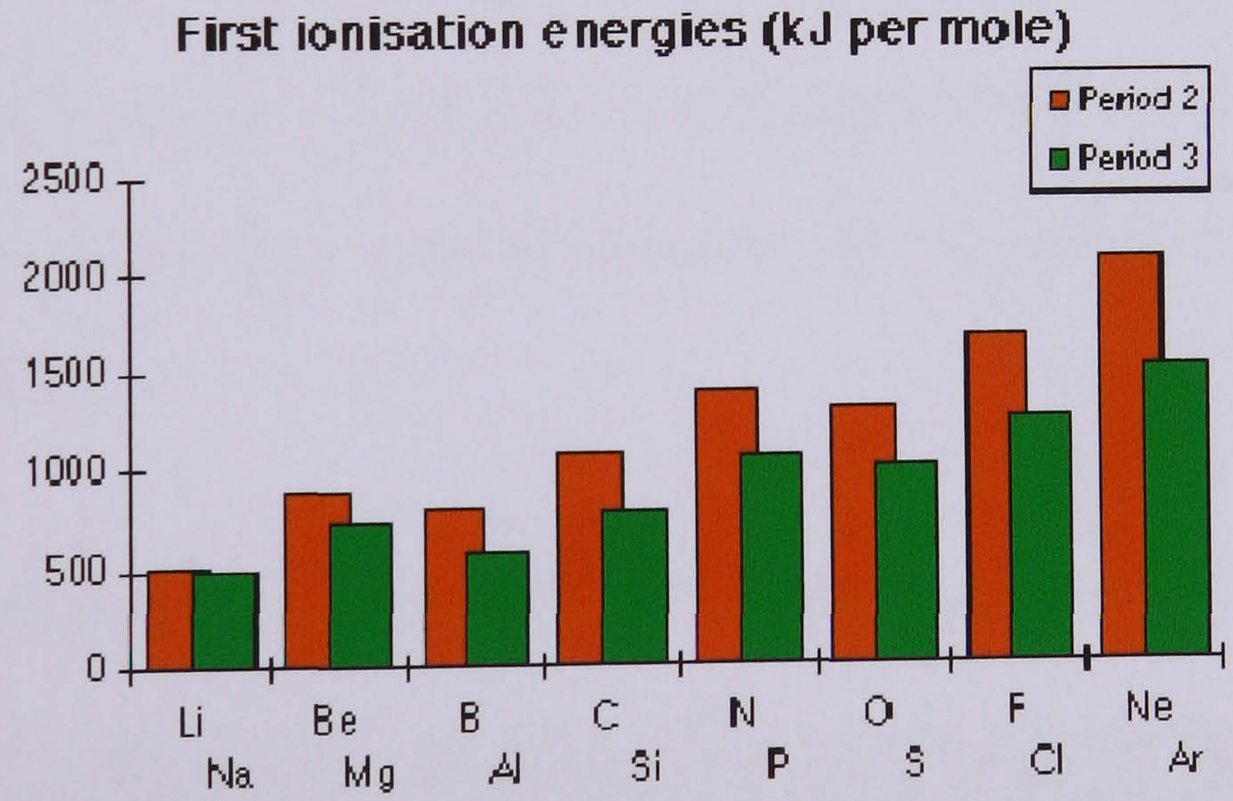

Figure 1.5. The first ionisation energies for the period 2 and period 3 elements.

1.2 The carbon-fluorine bond

As a result of its high electronegativity, fluorine forms the strongest covalent bonds known (Table 1.3). That applies in particular to hydrogen, carbon, silicon, and boron, where the bonds to fluorine are stronger than with any other element.[5] The strength of the carbon-fluorine bond has also been rationalised in terms of an excellent match of the 2s or 2p orbitals of fluorine with the corresponding orbitals of carbon.

Table 1.3. Bond dissociation energies for some atoms and functional groups bonded with fluorine.[6]

D^o [kJ/mol]	H	F	Cl	Br	I	CH_3	CF_3
H	436	570	432	366	298	439	450
CH_3	439	472	350	293	239	377	423
CF_3	450	547	362	294	227	423	413

For carbon, the bond energy increases with increasing degree of fluorination. For instance, the C-F bond dissociation energy in CF_4 is significantly highenr than in CH_3F. The high bond energy is reflected in the high thermal and chemical stability of fluorinated organic compounds and the resistance of sp^3 centred carbon to undergo nucleophilic attack.

Table 1.4. Bond length of the C-F bond compared to some other elements.[7]

Bond	C-H	C-C	C-O	C-F	C-Cl	C-Br	C-I
Length [Å]	1.09	1.53	1.42	1.39	1.79	1.94	2.13
Energy [kJ/mol]	416	347	326	485	326	64.3	50.7

The C-F bond length is most similar to that of the C-H bond (Table 4). Therefore substitution of fluorine for hydrogen generates molecules that closely resemble the

corresponding non-fluorinated compound in size. The CH_2F and CF_2H groups have been proposed to be isosteric (and also isopolar) replacements for the hydroxyl group because of their comparable size and electronic distribution. The CF_2H group is especially attractive in this regard due to its potential to act as a hydrogen donor, allowing interactions with solvent and other molecules.

1.3 Electronic effects induced by fluorine

The stability of the carbon-fluorine bond increases with the number of fluorine substituents bound to the carbon atom. The increase in stability is reflected by the C-F bond length: CH_3F (140 pm) > CH_2F_2 (137 pm) > CHF_3 (135 pm) > CF_4 (133 pm). This stabilisation has been rationalised in terms of the dipolar resonance structures **1** and **2**, which cause a self-stabilisation of multiple fluorine substituents by back-bonding of the fluorine lone pairs onto the same carbon atom (Scheme 1.1).[8]

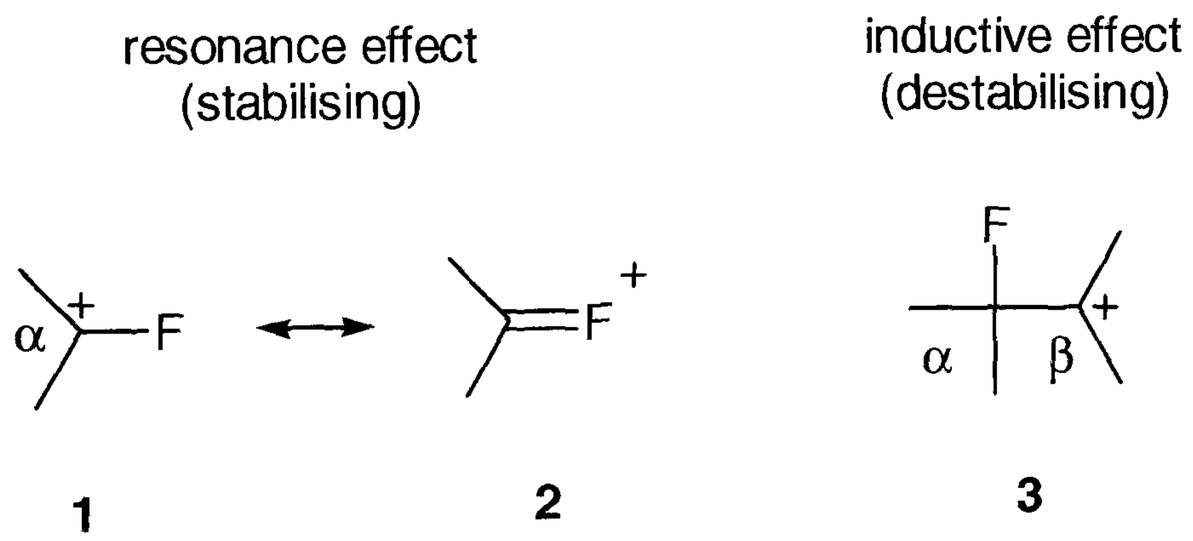

Scheme 1.1. Electrostatic and resonance effects in fluoroalkanes. The resonance effect of fluorine leads to stabilisation of α-fluoro cations, whereas β-fluoro cations are destabilised by the inductive effect caused by the fluorine atom.

In addition, perfluorocarbons gain kinetic stability by shielding of the central carbon atom. This shielding or "coating" originates from the tightly bound lone pairs of the fluorine atoms, that are effective in delivering enough electrostatic repulsion to

prevent nucleophilic attack at the carbon atom. This "coating effect" for instance renders perfluorinated compounds extremely inert to basic hydrolysis.[9]

The presence of fluorine strongly influences the stability of adjacent carbanions and carbocations, a tendency which has been referred to as "α-fluorine effects". Carbocations that are adjacent to a fluorine substituent are stabilised by donation of the nonbonding electron pairs. Experimental proof has been found by gas-phase hydride affinity measurements which suggest a stability order for fluoromethyl cations as: $CH_3^+ < CF_3^+ < CH_2F^+ < CHF_2^+$.[10] The trifluorinated species is less stable than its mono and difluorinated analogues, presumably due to destabilising electrostatic repulsion between the fluorine lone pairs.

Table 1.5. Reactivities of alkyl bromides towards nucleophilic attack of NaOPh in MeOH at 20 °C. [11]

Substrate	k ($l*mol^{-1}s^{-1} \times 10^4$)
CH_3CH_2Br	39.1
$CH_3CH_2CH_2Br$	25.6
FCH_2CH_2Br	4.95
$ClCH_2CH_2Br$	5.61
$BrCH_2CH_2Br$	4.99

In contrast, β-fluorocarbocations **3** are destabilised due to the inductive effect of the fluorine (Scheme 1.1). This can have a substantial effect upon reactivity of contiguous nucleophilic centres. Thus, introducing fluorine α–, β–, or γ– to the reaction centre usually reduces reactivity towards nucleophilic substitution,[12] while fluorine attached directly to the reaction centre has an activating effect.[13] The deactivating effect of β-fluorine substitution on carbocation formation is illustrated by comparison of different substituted alkylbromides towards nucleophilic substitution (Table 1.5). From the

data, it becomes clear that the effects are not very different for the individual halogens, and so halogen substitution in general reduces S_N2 reactivity by comparison with non-halogenated substrates.

Table 1.6. Base-catalysed deuterium exchange in various haloforms at 0 °C in D_2O.[14]

Haloform	Rate of exchange 10^5 *k* ($l*mol^{-1}s^{-1}$)
CHF_3	Too slow to measure
$CHCl_2F$	16
$CHCl_3$	820
$CHBr_2F$	3600
$CHBr_3$	101000

Intuitively one would expect, that the high electronegativity of fluorine will stabilise an adjacent carbanion. This is not the case as electrostatic n-π repulsion between the anionic centre and the fluorine lone pairs actually lead to destabilisation of an α-fluorocarbanion **4** (Scheme 1.2).[15] This effect has been confirmed by measuring the exchange rates and acid strength for a variety of halogenated compounds (Table 1.6 and 1.7).

Table 1.7. Apparent ionisation constants of substituted nitromethanes in water at 25 °C . The fluoro nitromethane has a much lower acidity than its chlorinated analogue.[16]

$XCH(NO_2)_2$	pK_a
X = H	3.57
X = Cl	3.80
X = F	7.70

β-Fluoroanions **5** on the other hand, are stabilised by β-fluorine. This effect has been confirmed by measuring the relative acidities of hydrogen in polyfluoro compounds.[17] A large contribution in stabilising β-carbanions results from negative hyper-conjugation (Scheme 1.2).

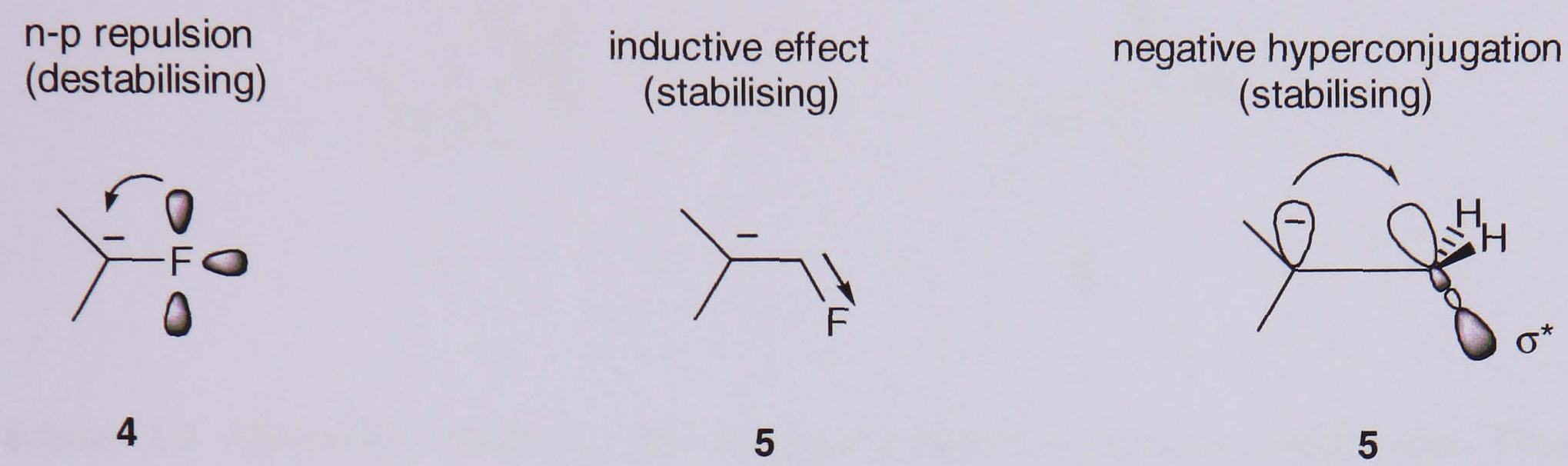

Scheme 1.2. Influence of fluorine on the stability of α-fluorocarbanions **4** and β–fluorocarbanions **5**.

A large contribution for this stabilisation has also been concluded from the rates of sodium methoxide catalysed deuterium exchange of monofluorohydrocarbons (Table 1.8). The significant differences in exchange rates reflect fluorocarbanion stabilities, in the sequence of $3^{o} > 2^{o} > 1^{o}$. The results indicate that nine β-fluorine atoms are much more stabilising for the carbanion than three α-fluorine atoms. In general, the larger the number of β-fluorines the more equivalent resonance structures can be drawn, and consequently, the more stabilised is the carbanion.

Table 1.8. Relative rate of sodium methoxide catalysed deuterium exchange between methanol-d^6 and monohydrofluorocarbons at -29 °C. [18]

Compound	Relative rate	pK_a estimated
CF_3-H	1.0	28
$CF_3(CF_2)_5CF_2$-H	6.0	27
$(CF_3)_2CF$-H	$2x10^5$	18
$(CF_3)C$-H	$1x10^9$	11

In vinyl fluorides n-π repulsion between the fluorine lone pairs and the π electrons leads to destabilisation of the double bond. This is accompanied by a resonance effect in which the lone pairs of the fluorine substituent conjugate with the π-system (Scheme 1.3).

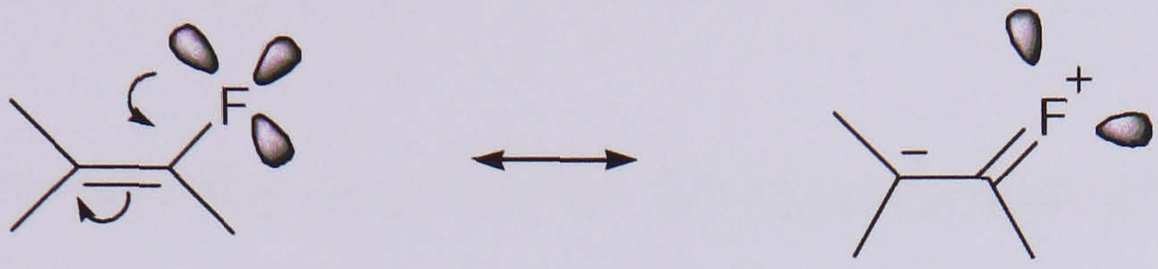

7 **8**

Scheme 1.3. Electrostatic repulsion **7** and resonance effects **8** operating in vinylfluorides. These compounds generally are destabilised relative to nonfluorinated alkenes due to n-π orbital repulsion.

The combined effects cause a strong preference for sp^2 fluorine-substituted centres to rehybridise to sp^3, which is consistent with the increased reactivity of fluoroalkenes and fluorinated enol ethers in pericyclic reactions. For example, it has been observed that vinyl fluorides are much better substrates in Claisen rearrangements than their nonfluorinated analogues, a reaction which involves rehybridisation of sp^2 to sp^3 centres.[19]

Nucleophilic substitution on sp^2 centres is usually accelerated by fluorine substitution. This effect is not attributed to the lower stability of vinylic fluoride, but is rather the result of a two-step addition-elimination process.[20] The nucleophilic attack towards vinyl fluoride **9** is accelerated by inductive effect of fluorine. The process affords a β-fluorocarbanion **10** which undergoes fluoride elimination to yield the substituted alkene **11** (Scheme 1.4).

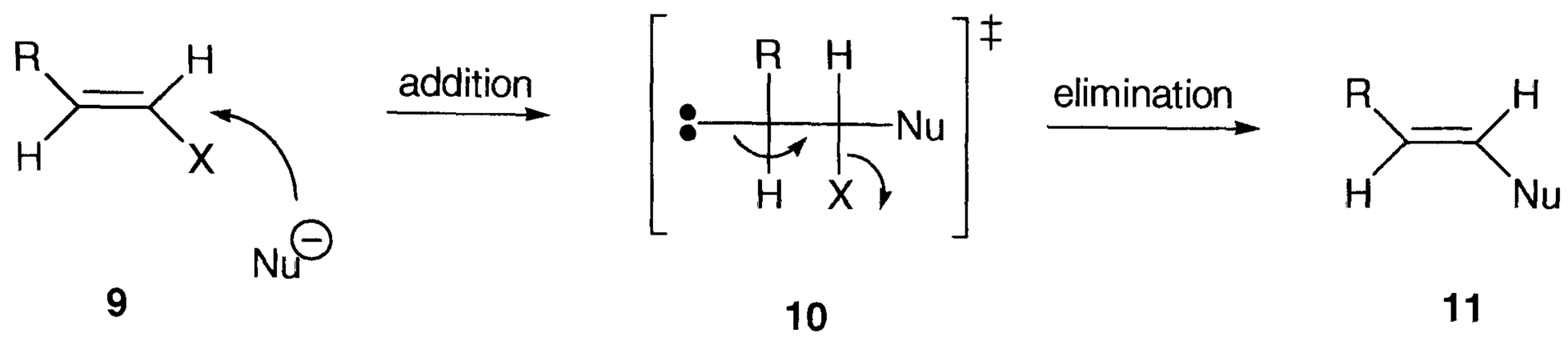

9 10 11

Scheme 1.4. The two-step addition-elimination mechanism for nucleophilic substitution at sp^2 centres.

Mechanistically, the transition state involves a β-fluorocarbanion, which is stabilised by negative hyperconjugation into the σ* C-F orbital. The appearance of geometric mixtures for the vinyl fluoride **12** may be the direct result of a more stable and longer-lived β-fluorocarbanion that allows time for rotation and thus gives rise to the isomeric products **13** and **14** (Scheme 1.5).

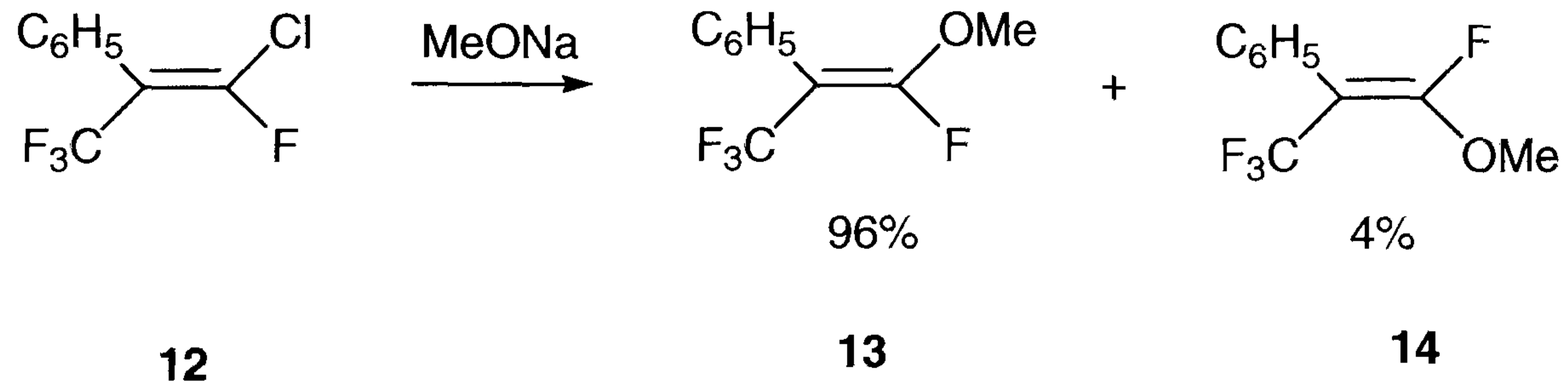

12 13 14

Scheme 1.5. Vinyl fluorides undergo nucleophilic substitution readily to eliminate fluoride ion.[21]

The rate determining step of the reaction is the addition of the nucleophile, which is strongly influenced by the inductive effect of fluoride. Comparison of the reaction rates of several haloalkenes illustrate this effect.[22] Interestingly, when both F and Cl are attached to the same vinylic carbon, chlorine is selectively displaced over fluorine (Scheme 1.5). This seems to be in contrast to the superior reactivity of vinylfluorides, but can be rationalised in terms of the better leaving group ability of chlorine over fluorine. [23]

1.4 Effect of fluorine substitution on physical properties

The introduction of fluorine will have a significant impact upon the physical properties of organic compounds. In particular, the parameter most obviously influenced are boiling point, refractive indexes, surface tensions, lipophilicity, acidity and basicity of the molecules. For instance, perfluorocarbons have extremely low surface tensions which makes them nearly ideal liquids with high vapour pressures and high compressibility. This can be attributed to the small inter- and intra-molecular forces operating in perfluorocarbons, an effect which mainly result from electrostatic repulsion of the electronegative fluorine atoms.

Table 1.9. $p\mathrm{K_a}$ and $p\mathrm{K_b}$ values of organic acids and bases in comparison with their fluorinated analogues.[24]

Carboxylic acid	$p\mathrm{K_a}$
CH_3COOH	4.76
CH_2FCOOH	2.59
CHF_2COOH	1.34
CF_3COOH	0.52
CCl_3COOH	0.56

Most obviously, fluorine substitution influences the $p\mathrm{K_a}$ and $p\mathrm{K_b}$ of organic acids and bases. This is due to the high electronegativity of fluorine and its correlated negative inductive effect. The acidifying effect of fluorine increases with the number of fluorine substituents, and is highest for the trifluoromethyl substituted compounds (Table 1.9).

The influence of the fluorine on acidity significantly falls off with distance. For example, trifluoroacetic acid is four orders of magnitude more acidic than acetic acid. However, trifluoropropionic acid is considerably less acidic and the acidity is further decreased in trifluorobutyric acid (Table 1.10).

Table 1.10. Acid constants of a series of aliphatic acids $X_3C\text{-}(CH_2)_n\text{-}COOH$ and their trifluoro derivatives relative to acetic acid ($pK_a = 4.8$).[25]

X	n	ΔpK_a
H	0	0.0
F	0	-4.6
H	1	+0.1
F	1	-1.9
H	2	0.0
F	2	-0.6
H	3	0.0
F	3	-0.3

In general, the introduction of fluorine reduces the basicity of functional groups. The decreasing effect of fluorine substitution on basicity can be understood in terms of the high electronegativity of fluorine, which decreases electron density at the electron donor group. The effect of fluorination on basicity is directly related to a higher acidity of their conjugated Brønstedt acids. The effect is illustrated for fluorinated aliphatic ammonium salts (Table 1.11). Again, the effect is dependent on the distance between the fluorine atoms and the basic functional group. Accordingly, the pK_a values of trifluoroalkylammonium salts steadily decrease from fluoroethyl to fluorobutylammonium salts. It is important to mention that the nucleophilicity of amines is much less affected by fluorine substitution than its basicity.

Table 1.11. Dissociation constants of fluoroalkylammonium salts $X\text{-}(CH_2)_n\text{-}CH_2\text{-}NH_4$ relative to the halogen-free ethyl, propyl, and butyl ammonium salts ($pK_a = 10.7$).[26]

X	n	ΔpK_a
H	1	0.0
F	1	-4.8
H	2	0.0
F	2	-1.8
H	3	0.0
F	3	-1.1

Changes in acidity or basicity of a given molecule due to fluorine substitution will strongly influence the ability of a molecule to interact with the solvent (e.g., to form hydrogen bonds) and thus will strongly affect their lipophilicity. The influence of fluorine substitution on lipophilicity can be complex, in particular for multiple fluorinated compounds, or molecules that contain various functional groups or heteroatoms. Lipophilicity is usually decreased in cases, where the introduction of fluorine strongly affects the overall dipole moment of the molecule. This is the case for fluorinated carbonyl compounds, monofluorinated saturated alkanes, and trifluoromethylated saturated alkanes.

The relative lipophilicity of α-fluorinated carbonyl compounds is usually decreased compared to their non-fluorinated analogues. This effect can mostly be attributed to hydration of the carbonyl group, which drives partitioning relative to the non-fluorinated analogues towards the aqueous phase. On the other hand, lipophilicity is increased for fluorinated aromatic compounds, fluorine adjacent to heteroatoms, or fluorination adjacent to atoms with π-bonds such as fluoroolefins. Perfluorinated aliphatic or aromatic hydrocarbons generally have the highest degree of lipophilicity.

1.5 Stereoelectronic Effects

The introduction of fluorine into an organic compound can strongly alter the conformation of the molecule due to stereoelectronic effects that arise from the high electronegativity of fluorine. Stereoelectronic effects in general include electrostatic dipole-dipole interactions, and effectsthat arise from bonding, non-bonding or *anti*-bonding orbital interaction. Such effects can have a profound influence on molecular conformation, and thus, are fundamental to understanding the chemical and physiological properties of organofluorine molecules.

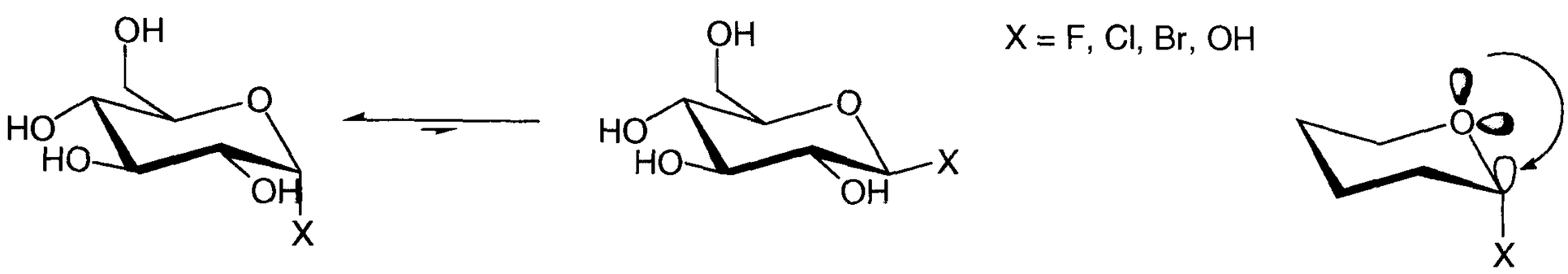

15 **16** **17**

Scheme 1.6. The α-anomer **15** with the glycosylic substituents axial is stabilised over the β-anomer **16** by hyperconjugation of the antiperiplaner nonbonding orbital of oxygen into the C-X bond of **17**.

The "anomeric effect" originally described the thermodynamic preference for polar groups bonded to the anomeric carbon of a glycopyranosyl sugars to take up an axial position (Scheme 1.6).[27] The stabilisation of the axial conformation of the glycosylic substituent can be explained in terms of n-σ* hyperconjugation between the ring oxygen lone pair and the carbon-halogen bond. The orbital overlap is more effective when the orbitals are antiperiplanar to each other, and consequently, the axial conformer **17** is electronically stabilised (Scheme 1.7).

The stereoelectronic preference for the axial conformation of α-D-glucose can also be argued in terms of dipole interactions of the endocyclic oxygen and the anomeric hydroxyl group. For the β-anomer **20** the dipoles are pointing in the same direction

and are thus electrostatically unfavoured, whereas in the α-anomer **19** the axial hydroxyl can partially compensate the dipole of the endocyclic oxygen (Scheme 1.7).

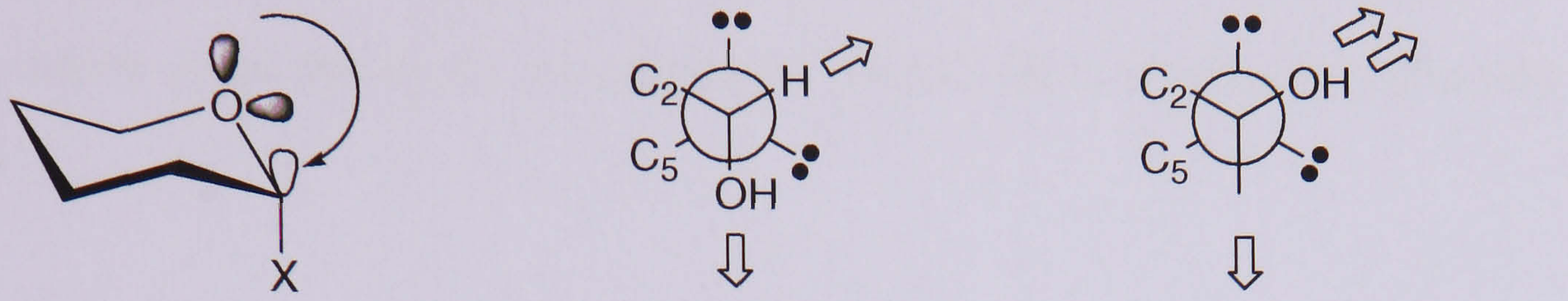

18 **19** **20**

Scheme 1.7. Dipole moments for the α–anomer **19** and the β-anomer **20** of a glucoside are illustrated by a Newman projection. The dipole moments of the ring oxygen and the anomeric substituent can be better compensated for in the α-anomer making the conformation thermodynamically more stable.

In aqueous solution however, the β-conformation is favoured over the α-conformer in glucopyranosyl sugars. This is due to hydration of the molecules by the solvent which renders steric effects more influential, and in addition, the effective dipole moments of the structures are decreased by hydration.[28] The anomeric effects is not only of theoretical importance, but can have a strong influence on the chemical stability and reactivity of organic molecules. This is demonstrated impressively by the difference in stabilisation energy in the desymmetrisation of glycerol (Scheme 1.8).

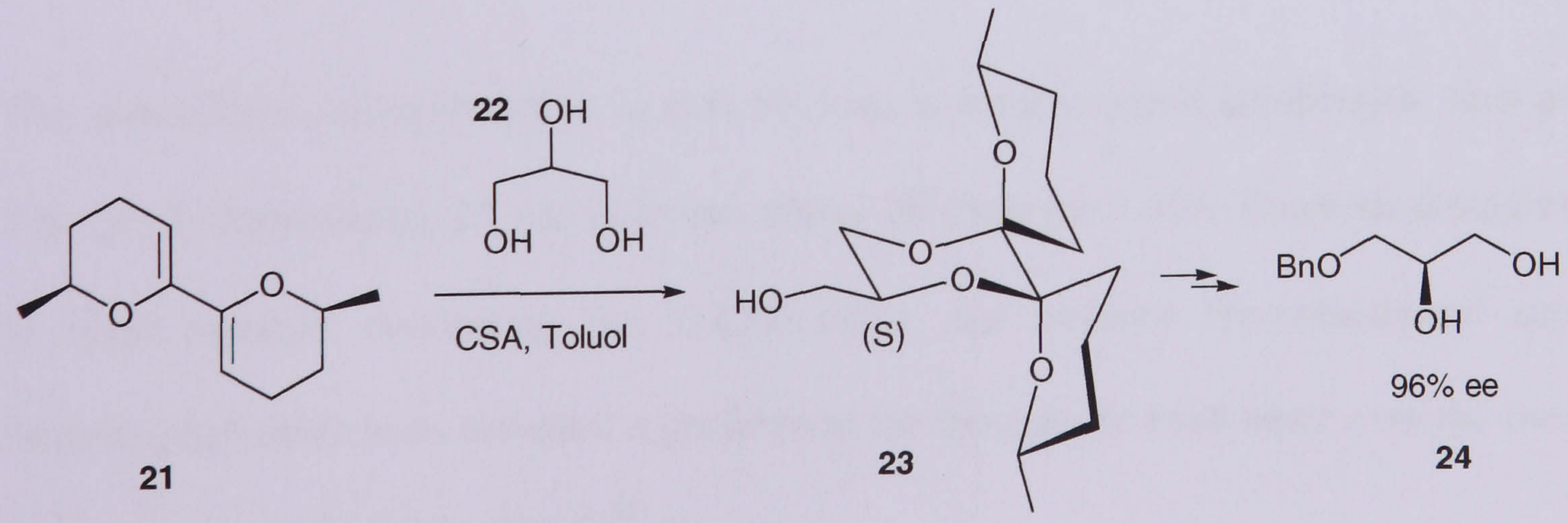

21 **23** **24**

Scheme 1.8. Protection of glycerol **22** with the chiral di-dehydropyran **21** results in formation of spiroketal **23**. The free hydroxyl group is then derivatised and gives the monoprotected glycerol **24** after acidic hydrolysis.

In the synthesis of optically active glycerol **24**, a chiral auxiliary reacts with glycerol to form a spiroketal, which is stabilised by a double anomeric effect over all other possible products. The parent spiroketal **23** can thus be obtained in high enantiomeric excess, which gives rise to the monoprotected alcohol **24** in enantiomerically pure form.[29]

The conformational preference for the axial conformation in glucosides is a special case of the "generalised anomeric effect". According to the theory, a preference for the *gauche* over the *anti* conformation of the C-Y bond exists in systems of the general structure C-Y-C-X.[30] The effect is illustrated for chloromethoxy methane, where the *gauche* conformation **25** is of higher stability than the *anti* conformation (Scheme 1.9).

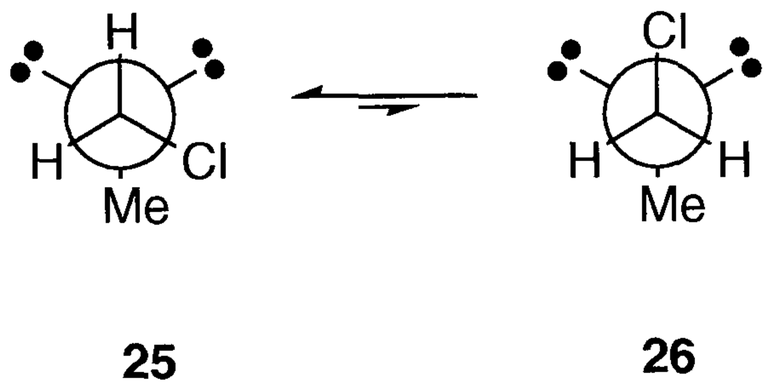

25 **26**

Scheme 1.9. The *gauche* conformation **25** is electronically preferred over the anti structure **26**. The stabilisation most likely arises from n-σ* hyperconjugation and dipole-dipole compensation.[31]

The generalised anomeric effect is also obvious in fluoroorganic compounds such as 2-deoxy-2-fluorosugars **27** and α-fluoro ethers **28** (Scheme 1.10). Theoretical studies in small systems containing the O-C-F motif, for instance fluoromethanol and fluoromethyl ether have revealed a preference for the *gauche* conformer over the *anti* conformer by up to 6.0 kcal/mol.[32]

27 28

Scheme 1.10. 2-Fluoro-2-deoxysugars and α-fluoroethers prefer a conformation in which the nonbonding orbital of oxygen aligns antiperiplanar to the electron-deficient C-F bond.

Probably the most widely discussed stereoelectronic effect associated with the C-F bond is the "*gauche* effect", which commonly refers to the preference for two *vicinal* C-F bonds to align *gauche* rather than *anti* to each other (Scheme 1.11).

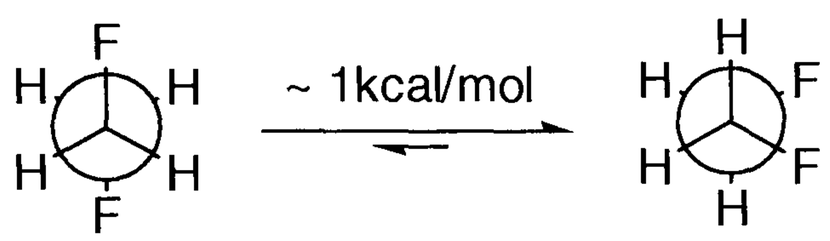

29 30

Scheme 1.11. *Gauche* and *anti* conformation of difluoroethane. In the gas phase, the *gauche* conformer **30** is stabilised over the *anti* structure **29** in the gas phase by about 1 kcal/mol.[33]

The conformation of 1,2-difluoroethane has been investigated extensively, and the preference for the *gauche* conformation has been confirmed by NMR,[34] electron diffraction,[35] FTIR and Raman spectroscopy.[36] The changes in rotation energy about the carbon-carbon bond were investigated by *ab initio* calculations and found to be similar to those for *n*-butane.[37] The preference for the *gauche* conformation in 1,2-difluoroethane is particularly surprising as this structure does not accommodate dipole compensation and appears to override electrostatic repulsion of the fluorine atoms. Apparently, an electronic effect operates within the *vicinal* difluoro alkane by which these effects are compensated for.

Table 1.12. The energies and percentage of population for the rotational isomers of 1,2-disubstituted ethanes at 20 °C. Estimated errors are given in parentheses.[38]

	FCH_2CH_2F	$ClCH_2CH_2Cl$	$BrCH_2CH_2Br$
% gauche	> 67	27(7)	11(5)
% trans	< 33	73(7)	89(5)
more stable isomer	*gauche*	*trans*	*trans*
ΔG° (kcal/mol)	0.59-1.42	0.89	1.63

In contrast, 1,2-bromo and 1,2-dichloroethane prefer the conformation in which the carbon-halogen bonds align *anti* to each other (Table 1.12). The higher relative stability of the *trans* over the *gauche* isomers in these molecules can be understood in terms of electrostatic effects and steric repulsion of the bigger halogen atoms.[39]

The "*gauche* effect" has initially been described as the tendency for a molecule to adopt a conformation with the maximum numbers of *gauche* interactions between the most polar bonds or non-bonded electron pairs.[40] The most obvious explanation for the stabilisation of the *gauche* conformer **31** arises from hyperconjugation (Scheme 1.12).

31

Scheme 1.12. Hyperconjugation in 1,2-difluoro ethane **31**. The interaction of the bonding σ C-H orbital with the nonbonding σ* C-F orbital is assumed to stabilise the *gauche* conformation.

The stabilisation is optimal when the best σ-donor bond is *anti*-periplanar to the best acceptor bond, consequently the electron-rich C-H bond and the electron-deficient C-

F bond will have a tendency to be opposite to each other. In *vicinal* difluoroalkanes the occupied σ-orbitals of the C-H bond and the *anti*-bonding σ* orbitals of the C-F bond may favourably interact as their energy difference is largest. Evidence for hyperconjugation has emerged from both theoretical calculations and experimental data to support hyperconjugative electron donation in neutral fluorocarbons.[41]

The "*gauche* effect" has also been rationalised by the so-called "*bent bond hypothesis*". According to the theory, a covalent bond can be described as the path of maximum charge density between a pair of bonded atoms.[42] In case of the *trans* isomer of 1,2-difluoroethene, the path of the C-C bond seems distorted towards opposite directions, which leads to reduced overlap and weakening of the σ C-C bond. In the *cis* isomer on the other hand the electron density is bent in the same direction, thus leading to better orbital overlap in a "bent bond" and thereby stabilisation of that conformer (Figure 1.6).

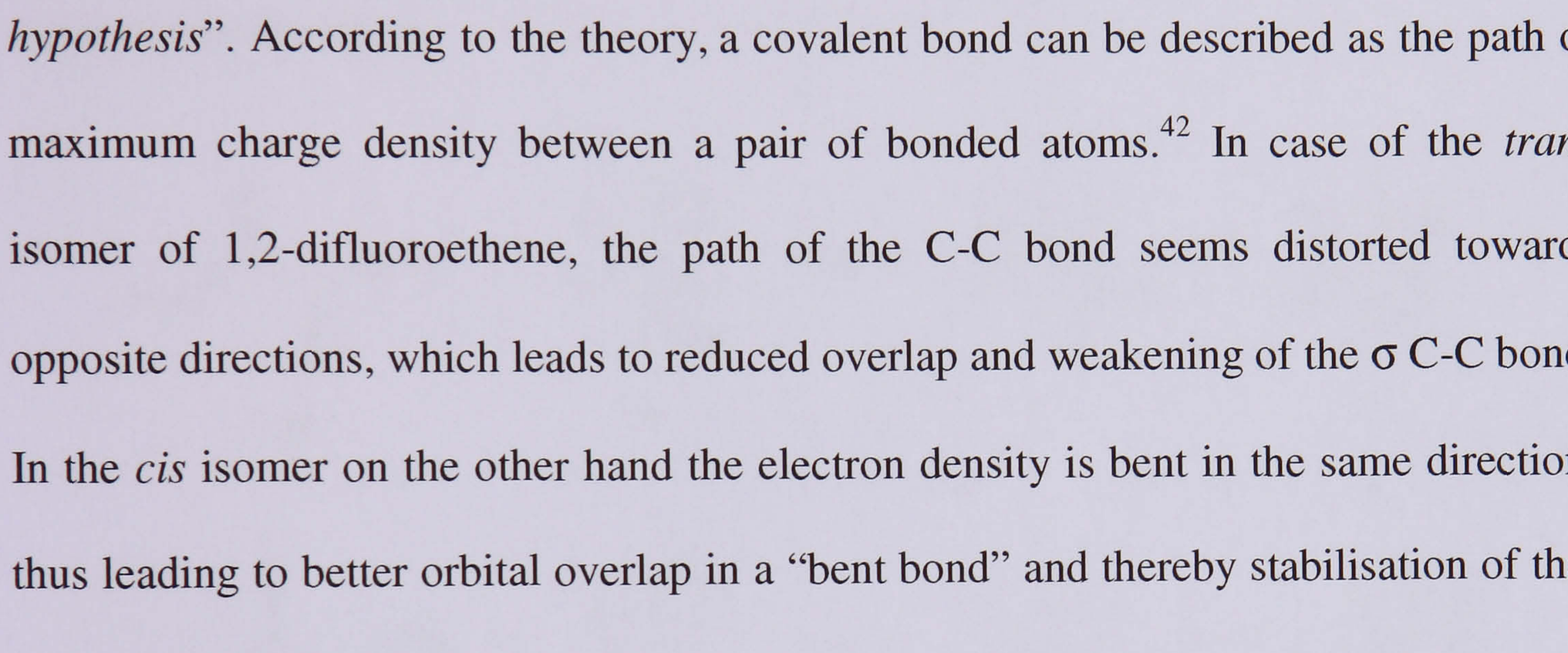

Figure 1.6. Difference between the electron density map for *trans*-1,2-difluoethene (left) and *cis*-1,2-difluoethene (right) using 6-31+G* basis sets.[43] The solid contours indicate regions of high electron density, and clearly define the form of the C-C and C-F bonds.

The preference for the *gauche* conformation extends to *erythro* and *threo* 2,3-difluorobutane.[44] The rotamer in which the two methyl groups are *anti* and the fluorines are *gauche* is lower in energy by about 0.8 kcal/mol. This effect can be illustrated by the Newman projections of 2,3-difluorobutane (Scheme 1.13). In the case of the *erythro* isomer the two enantiotopic rotamers **e** and **f** with the carbon-fluorine bonds *gauche* to each other are preferentially populated. This indicates that the energy in bringing the larger methyl groups together is compensated for by the stereoelectronic effect.

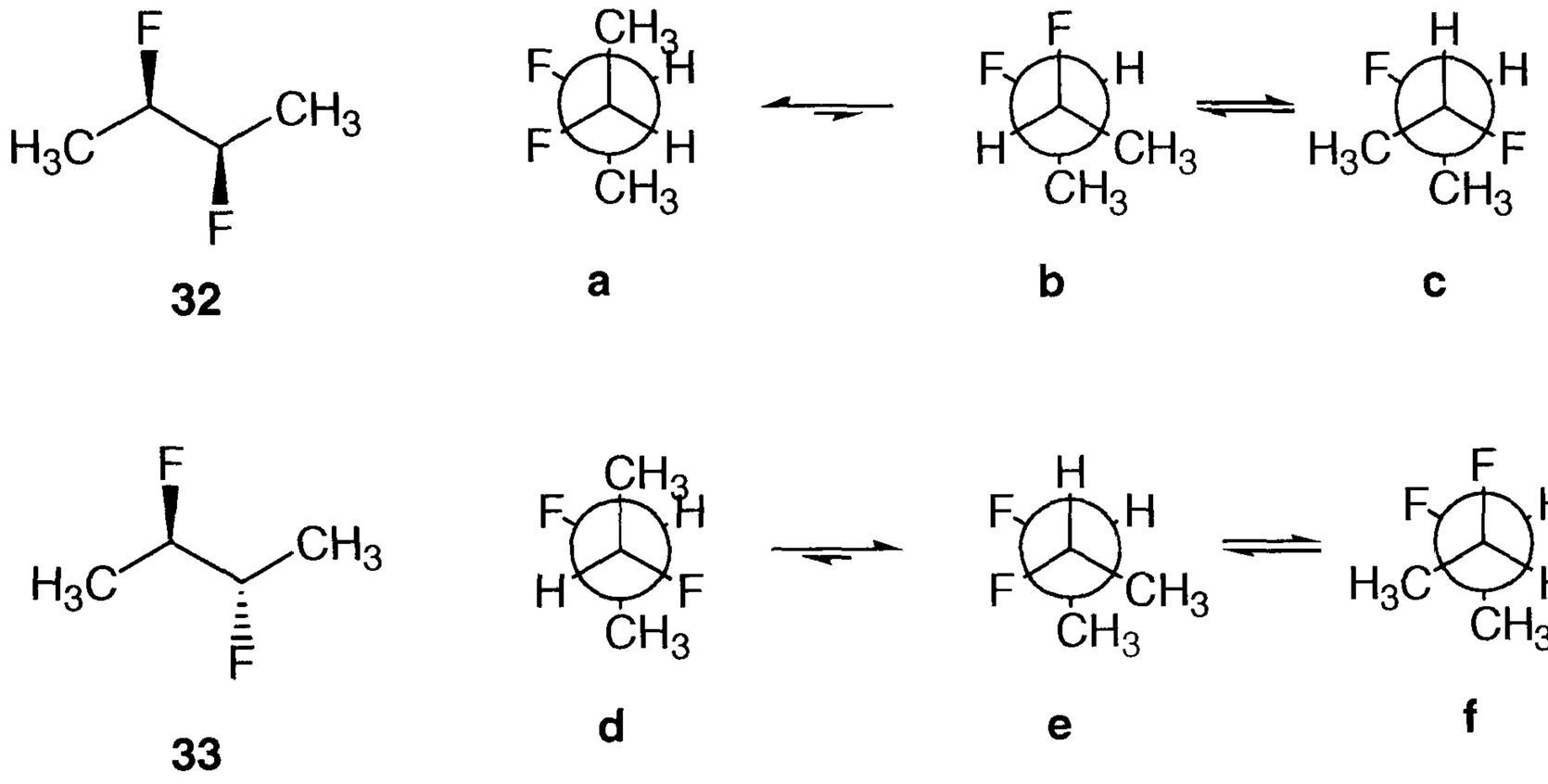

Scheme 1.13. Staggered conformations of *erythro* and *threo* 2,3-difluorobutanes **32** and **33** respectively. *Ab initio* calculations suggest a preference for the rotamers with their C-F bonds *gauche* to each other.

The preference for a *gauche* arrangement is not restricted to carbon-halogen bonds. *Gauche* effects are also apparent in organofluorine systems where the second C-F bond is replaced with another polarised bond. Since the electronegativity of oxygen is second only to fluorine, the theory applies to fluoroalcohols equally well. The influence of a *gauche* effect in 2-fluoroethanol **34** has been investigated, and a pronounced preference for the *gauche* conformation **34a** over the *anti* structure **34d** has emerged from these calculations. This preference however was attributed almost

entirely to intramolecular O-H···F hydrogen bonding, as the *gauche* structures **34b** and **34c** had a similar energy compared to their respective *anti* structures **34e** and **34f** (Scheme 1.14). In this system, the stabilisation for the *gauche* structure resulting from the *gauche* effect was estimated with 0.1 – 0.2 kcal/mol only.[45]

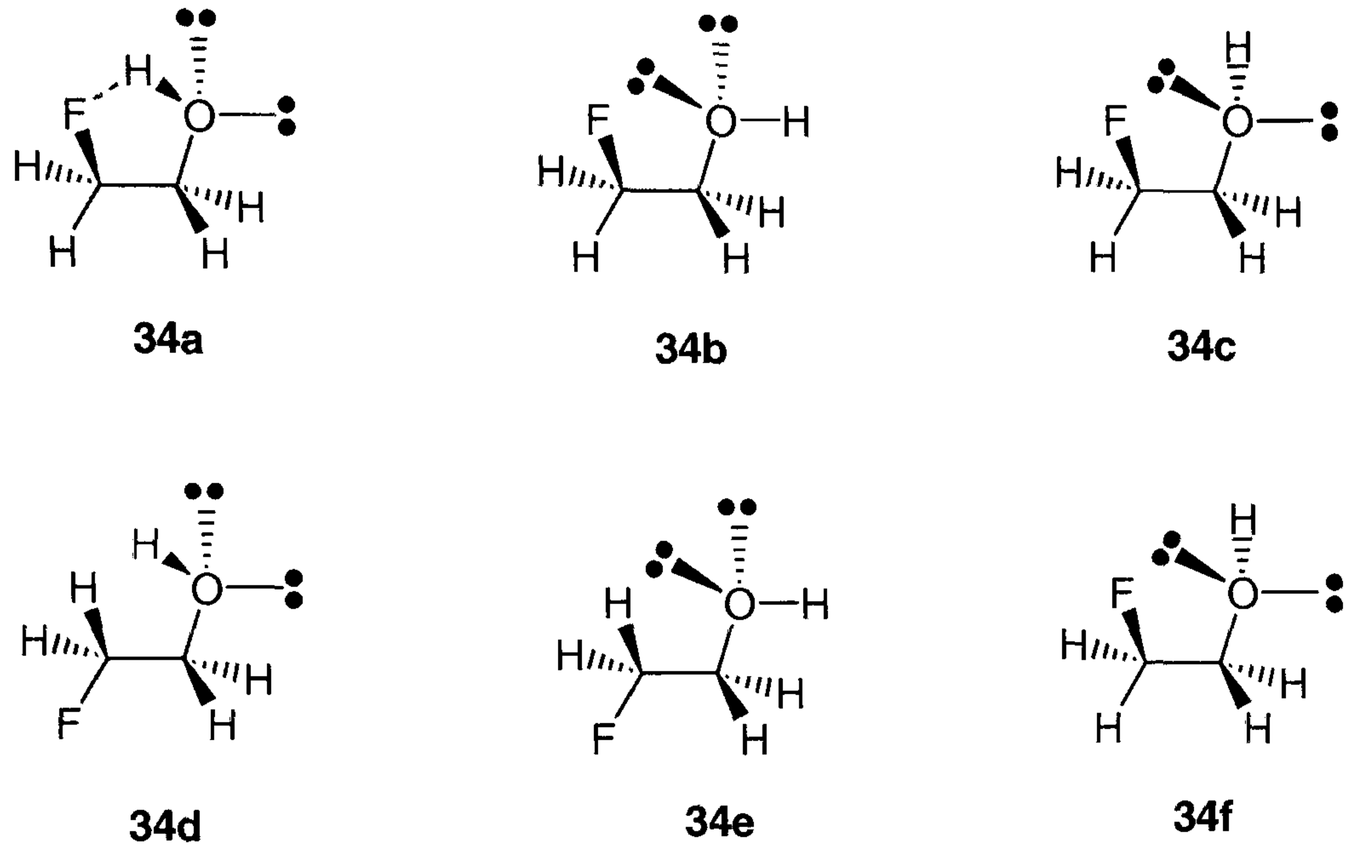

Scheme 1.14. Possible molecular conformations of monofluoroethanol **34**. *Ab initio* calculations suggest a preference for the structure **34a** by about 2.0 kcal/mol over the energetically next higher conformation **34d**.

When the hydroxyl group in 2-fluoroethanol becomes protonated (Scheme 1.15), the calculated energy differences between the individual conformers is much more pronounced. In all cases, the *gauche* structures were found to be significantly more stable than their *anti* counterparts. The energy difference between *gauche* and *anti* structures **35b** and **35e** on one hand, and **35c** and **35f** on the other hand, was largest at 7.0 and 7.2 kcal/mol respectively. The *gauche* conformation **35a** was lower in energy over the *anti* structure **35d** by 4.4 kcal/mol. The *gauche* preference observed in the latter case appears to arise from a true stereoelectronic effect.

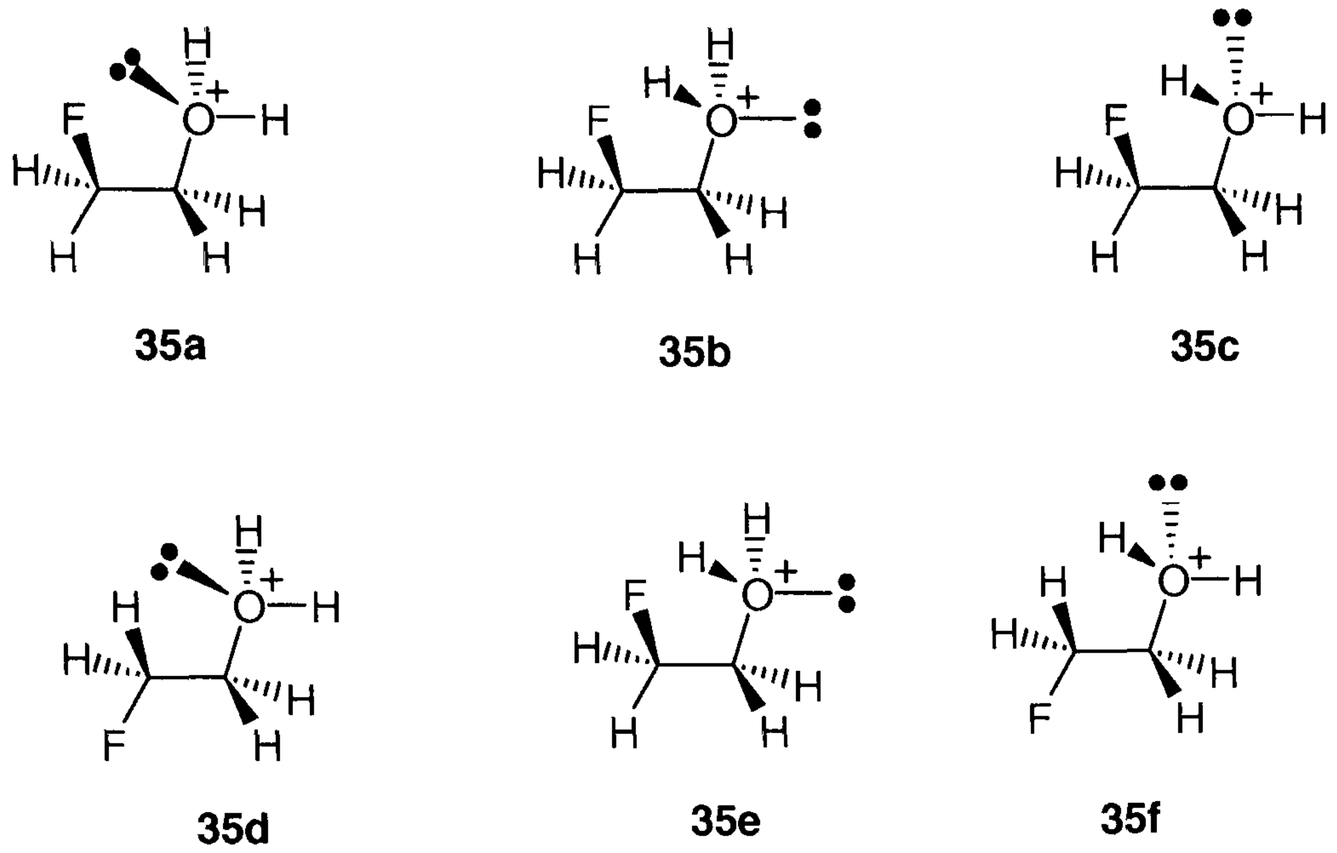

35a **35b** **35c**

35d **35e** **35f**

Scheme 1.15. Molecular conformations of protonated monofluoroethanol. *Ab initio* calculations suggest a preference for the *gauche* structure **35a** over the *anti* conformations **35d** by about 4.4 kcal/mol

The studies were extended to the 2-fluoroethylamine and 2-fluoroethylammonium systems. In the latter case a strong preference for the *gauche* conformation **36a** over the *anti* structure **36b** emerged from the calculations, supported by the X-ray structure of the fluoroethylammonium salt (Scheme 1.16).

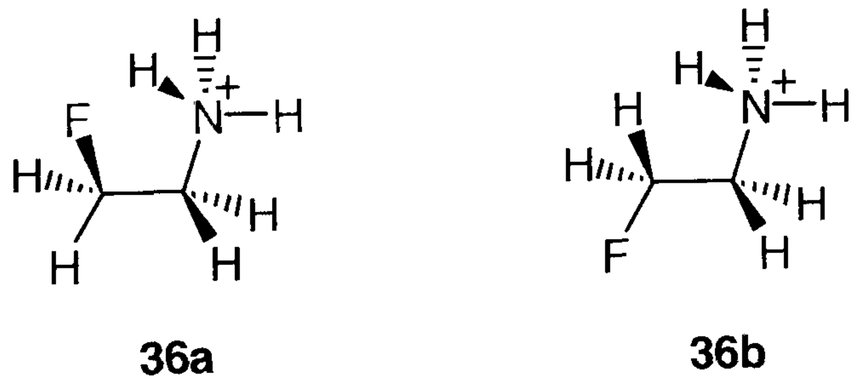

36a **36b**

Scheme 1.16. The *gauche* and *anti* conformation of fluoroethylamonnium salt **36**.[46]

X-ray analysis of dibenzylammonium chloride **37**, 4-(Fluoroethyl) morpholinium chloride **38**, and the diphenylpyrrolidine derivative **39** revealed a strong preference of the F-C-C-F motif to adopt a *gauche* conformation. Double *gauche* relationships were observed in the crystal structure of di(2-fluoroethyl)amine **40** (Scheme 1.17).

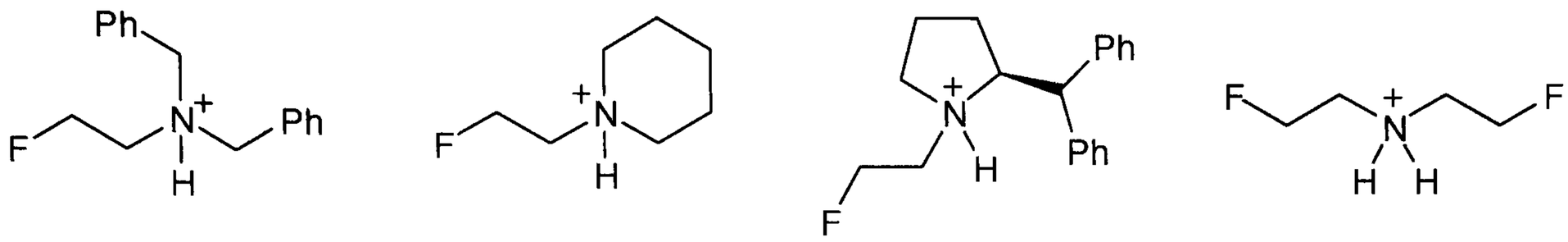

37 **38** **39** **40**

Scheme 1.17. The structures of dibenzylammonium chloride **37**, 4-(fluoroethyl) morpholinium chloride **38**, diphenylpyrrolidine **39**, and bis-(2-fluoroethyl)amine **40**.[47]

1.6 Stereoelectronic effects in α-fluorocarbonyl compounds

Stereoelectronic effects also exist when the C-F bond is adjacent to a carbonyl group such as in α-fluoroesters,[48] α-fluoroketones,[49] and α-fluoroaldehydes.[50] Stabilisation energies are relatively small and have been found in the range of 0.8 to 2.0 kcal/mol. The effect is strongest in α-fluoroamides, which align their C-F bonds *anti* periplanar to the carbonyl group and *syn* planar to the N-H bond (Scheme 1.18).

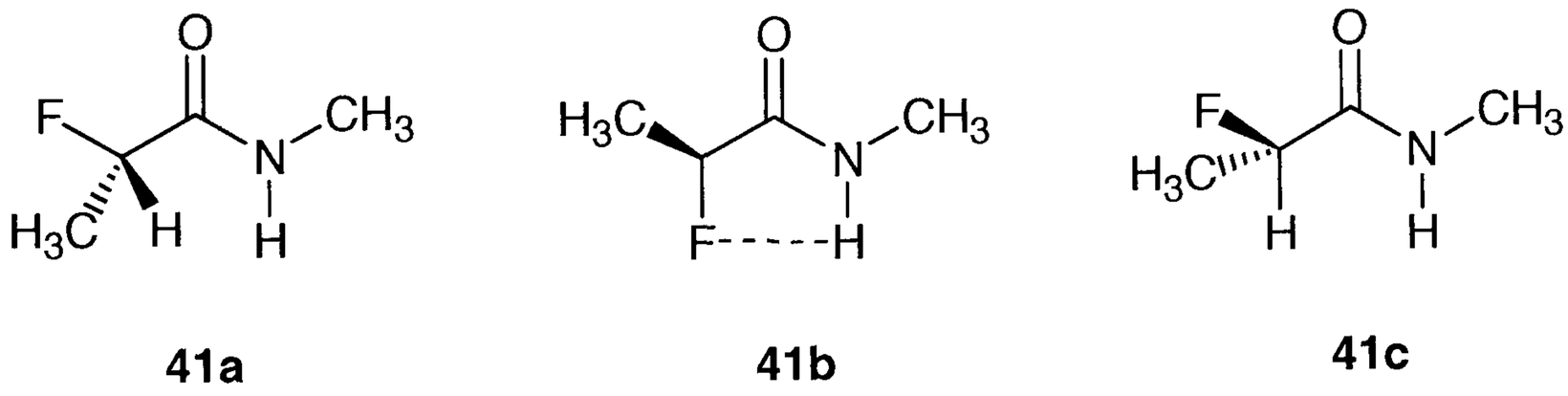

41a **41b** **41c**

Scheme 1.18. Possible conformations of *N*-methyl 2-fluoropropionamide **41**. The stereoelectronically preferred structure is the *trans* isomer **41b** which has the C-F bond *anti* periplanar to the carbonyl bond and *syn* planar to the N-H bond.

A*b initio* calculations for α-fluoropropionamide **41** indicate a deep energy well of up to 8.0 kcal/mol for the *trans* isomer **41b** with an energy difference of about 7.0 kcal/mol to the *cis* structure **41a**. (Figure 1.7).

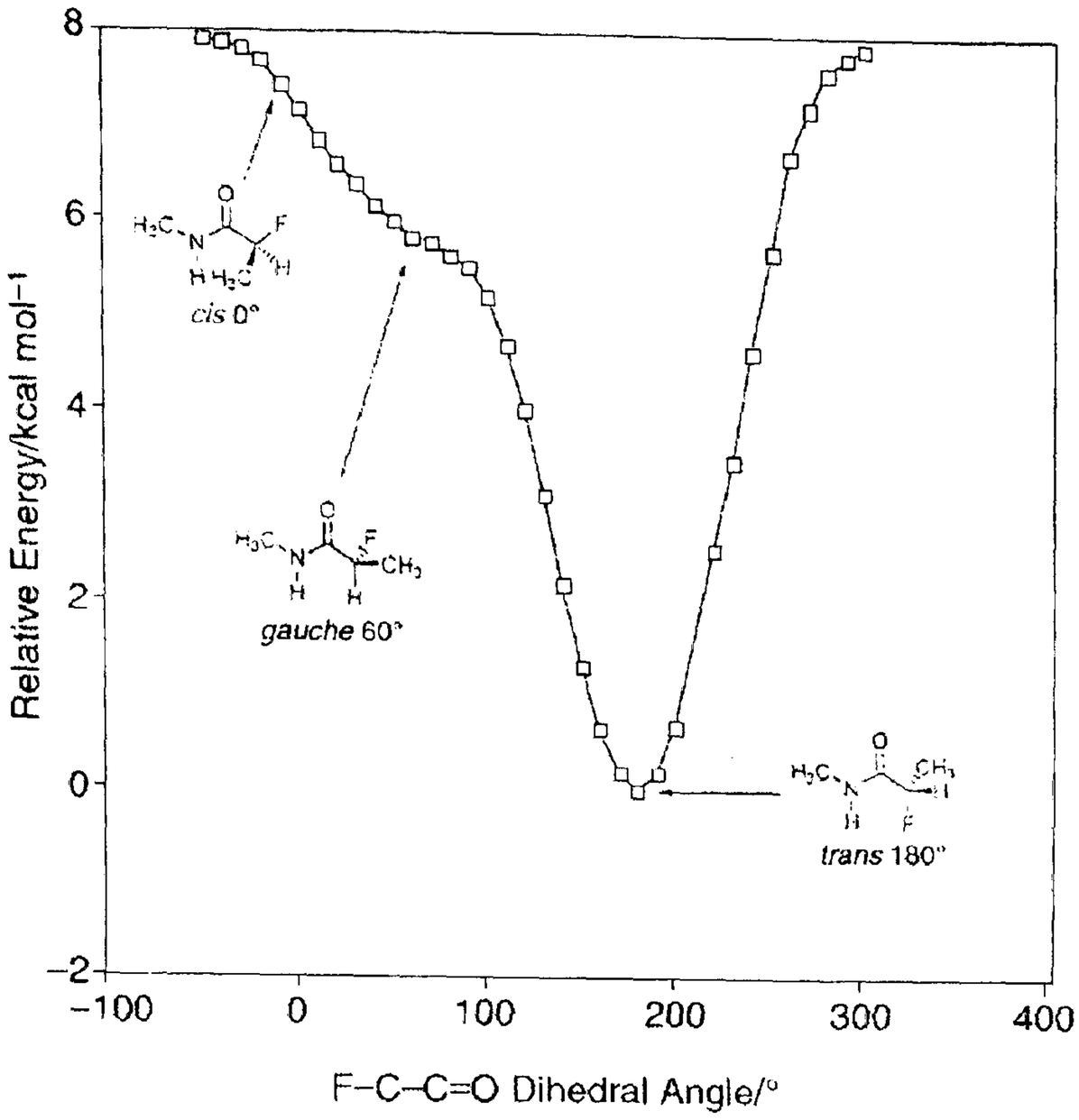

Figure 1.7. Rotational profile around the C(O)-C(F) bond for *N*-methyl 2-fluoropropionamide **41**.[51]

The major contribution to the stabilisation of the *trans* isomer (~3.1 kcal/mol) arises from the interaction of the fluorine lone pairs and the σ* orbital of the N-H bond.[52] Other stabilising effects involve hyperconjugation between the σ C-F orbital into the σ* orbital of the *anti* periplanar carbonyl group, and dipole-dipole relaxation of carbonyl and the C-F bond in their *trans* conformation (Scheme 1.19). Formation of N-H···F hydrogen bonding may also play a role in stabilising the *anti* periplanar structure.

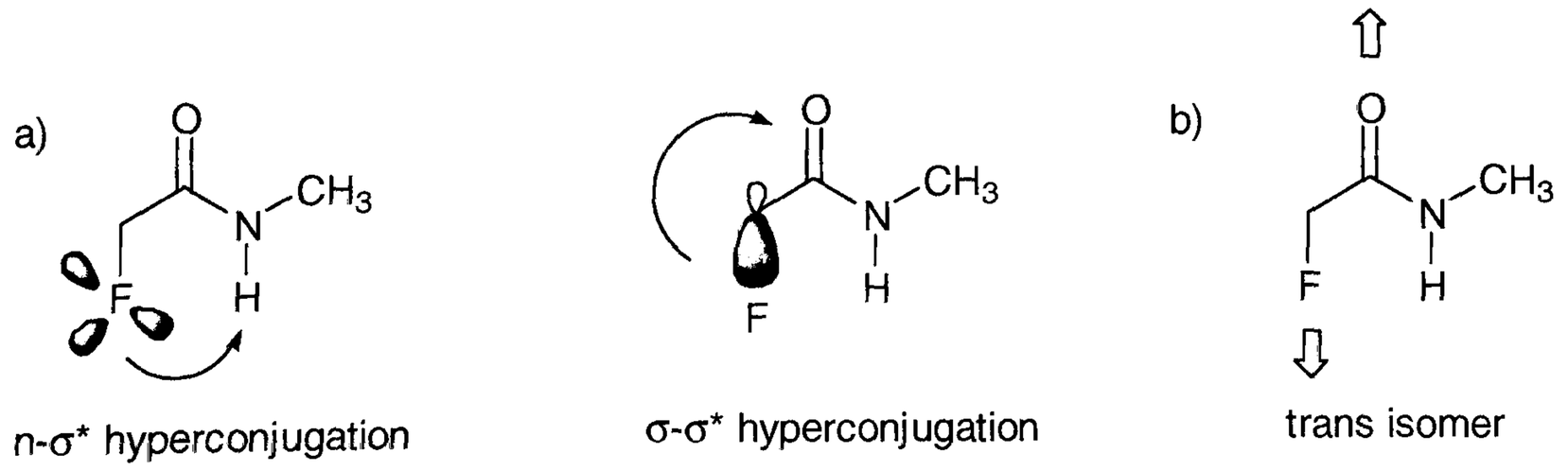

Scheme 1.19. Hyperconjugation (a) and dipole-dipole relaxation (b) are assumed to be stabilising effects for the *trans* structure of N-methyl 2-fluoropropionamide **41**.

Theoretical calculations are supported by X-ray analysis of α-fluoroacetamides such as **42**,[53] and related structure.[54] In the solid state, the α-fluoroamide moieties adopts *trans* planar conformations in 2-fluoropropionamides **42** and **43** consistent with the predicted stereoelectronic effect for these compounds (Scheme 1.20).

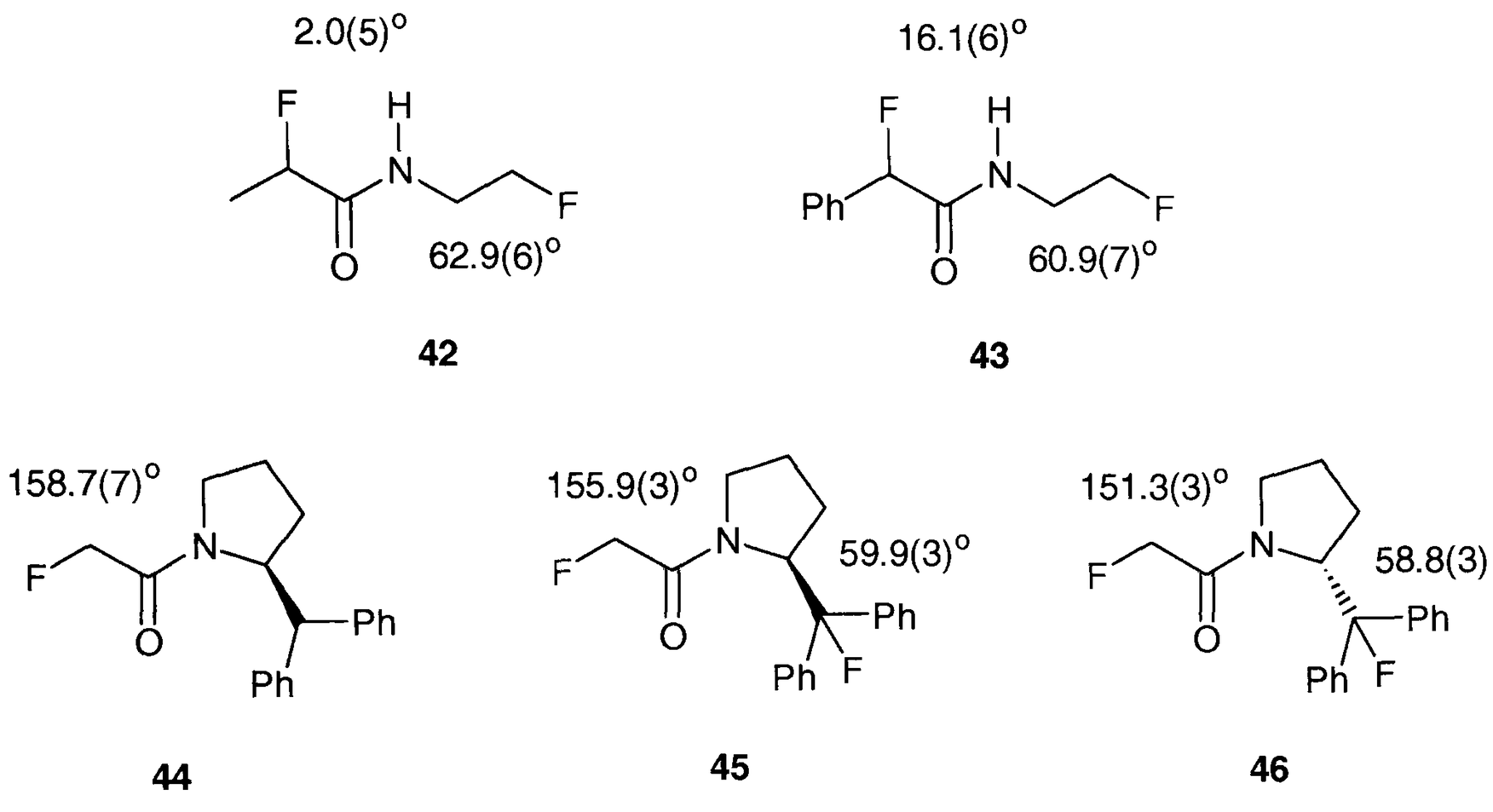

42 **43**

44 **45** **46**

Scheme 1.20. The X-ray structures of primary α-fluoroamides indicate a preference to align the C-F bond *syn* planar to the N-H bond. The F-C-C-N torsion angles are given in parentheses.

Surprisingly, with secondary amines the effect seems to reverse. Crystal structures of secondary α-fluoro amides **44-46** show that the C-F bond is now *syn* planar to the carbonyl, an observation consistent with theoretical calculations for *N,N*-dimethylfluoroacetamide.[55] The presence of an additional substituent on the amide nitrogen induces a destabilising steric interaction which is not observed in primary amides. The *N*-β-fluoroamide moiety in compounds such as **45** and **46** adopts a conformation, in which the C-F bond is *gauche* to the *vicinal* C-N bond (Scheme 1.20). This conformational preference has analogy with the "*gauche* effect" in *vicinal* difluoroalkanes. The *gauche* conformation in *N*-β-fluoroamides may be stabilised due

to polarisation of the C-N bond adjacent to fluorine by the amide group. The α-fluoroamide moiety is of considerable electron-withdrawing character and, according to the more general definition of the "generalised *gauche* effect", the most electronegative substituent relative to fluorine. This is supported by theoretical calculations and experimental data for *N*-acetyl-β-fluoroethylamine, which suggest a preference for the *gauche* over the *anti* conformation.[56] The energy difference was calculated to be approximately 1.8 kcal/mol, indicating a two to three-fold increase in stabilisation relative to 1,2-difluoroethane.

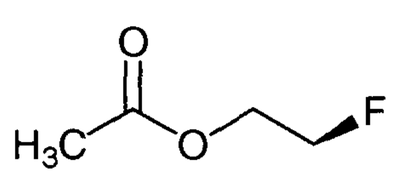

47

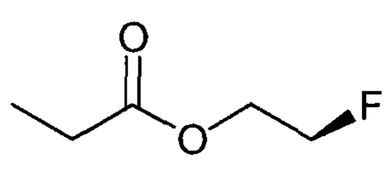

48

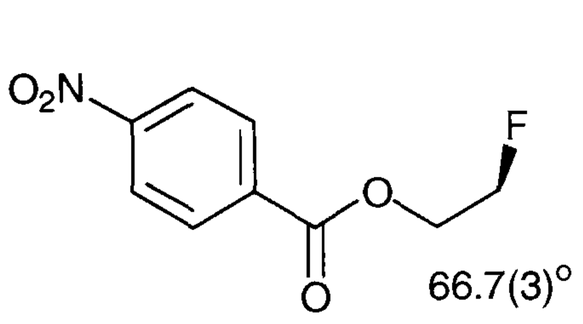

49

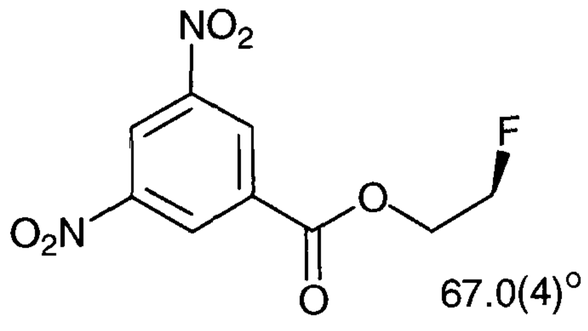

50

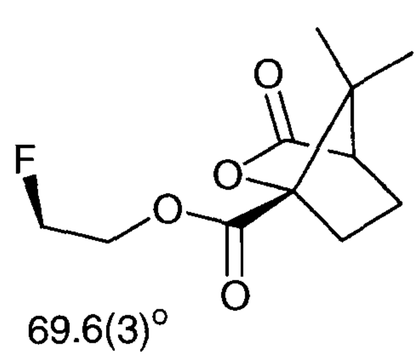

51

Scheme 1.21. Several β-fluoroesters and their O-C-C-F torsion angles found in the X-ray structures.

The *gauche* preference also exists in *O*-2-fluoroesters (Scheme 1.21). The X-ray structures of a variety of compounds **47-51** reveals that the C-F bond is in all cases perfectly *gauche* relative to the C-O bond. The *gauche* effect for *O*-2-fluoroesters has been supported by theoretical calculations,[57] but was estimated to be less significant in energy terms than in *N*-2-fluoroamides or *vicinal* difluoroalkanes.[58]

1.7 Hydrogen bonding, C-F···H-X

Hydrogen bonding is one of the most fundamental interactions in chemistry and biology,[59] and as such important in understanding the properties and reactivity of compounds.[60] Hydrogen bonding is particularly strong to oxygen and this interaction can contribute up to 10 kcal mol^{-1} in stabilisation energy.[61] The binding energies are usually in the range of 1-10 kcal mol^{-1} depending on the polarity and polarisability of the donors and acceptors involved. A structural criterion for hydrogen bonding is the distance between the proton and the acceptor atom, which is most commonly obtained from X-ray analysis of the compounds or their derivatives. The existence of hydrogen bonding can also be established by means of NMR,[62] and IR spectroscopy.[63]

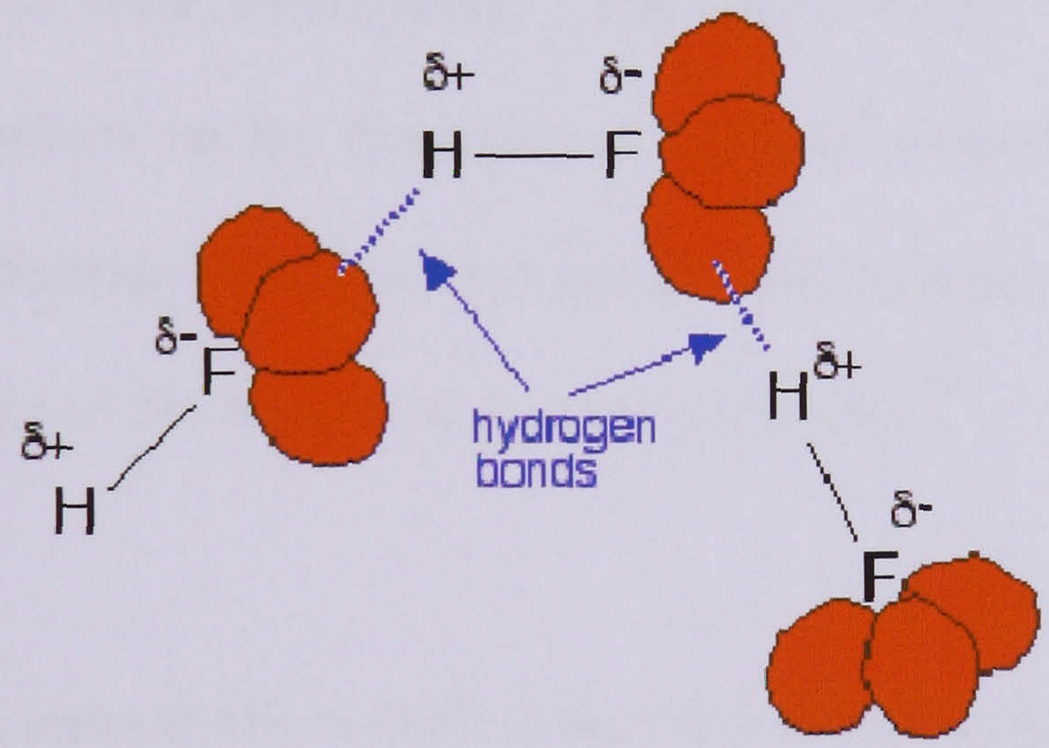

Figure 1.8. Schematic structure of polyhydrogen fluoride. The dashed lines indicate F-H···F hydrogen bonding between the protons and the free electron pairs of fluorine.

Inorganic fluoride ion can act as a very strong proton acceptor which is reflected in the extraordinary strong hydrogen bonds of hydrofluoric acid $(HF)_n$ (Figure 1.8). Another striking example is the bifluoride ion (HF_2^-) with a bond energy of 40 kcal/mol, making it by far the strongest known hydrogen bond.[64]

The bond energy for covalently bound, so-called organic fluorine is very weak compared to those of the fluoride ion. Interactions of the type C-F···H-X usually approach values that are typical for van der Waals interactions. Contacts in the range of less than 2.5-2.6 Å are considered as hydrogen bonding as the distance is close to the sum of the van der Waals radii of hydrogen and fluorine. Theoretical calculations estimate the strength of a typical C-F···H bond to be in the range of 2 - 3.2 kcal mol,[65] which is approximately half than that of X-H···O bonding. It is however commonly accepted that fluorine is a stronger acceptor than the other halogens.[66, 67]

The weak hydrogen bonding capability of fluorine may appear paradoxical in view of the large electronegativity difference of fluorine compared to carbon and historically, has been the subject of some controversy.[68] The effect of C-F···H hydrogen bonding can have profound effects on the reactivity of organic compounds. Replacement of allylic and benzylic fluoride by a hydroxyl group is accelerated under strongly acidic conditions with respect to the respective chloro compounds.[69]

Table 1.14. Statistic data obtained from a search of the CSD for short F···H contacts < 2.35 Å for sp^3 bound carbon.[70]

C(sp^3)-F	Compounds	C-F Bonds	Intramolecular contacts	Intermolecular contacts
O-H	71	89	5	1
N-H	69	85	8	3
C-H	177	237	16	18
Total	*177*	*237*	*29*	*22*

The relevance of electronegativity generally is obvious for a proton donor group. The greater the electronegativity of the proton donor, the greater is the effective positive charge on the hydrogen atom, and hence the more easily the latter participates in hydrogen bonding.

Table 1.15. Statistic data obtained from a search of the CSD for short F···H contacts < 2.35 Å for sp^2 bound carbon.[71]

C(sp^2)-F	Compounds	C-F Bonds	Intramolecular contacts	Intermolecular contacts
O-H	89	177	3	3
N-H	113	214	9	8
C-H	360	929	53	39
Total	*371*	*926*	*65*	*50*

The influence on hydrogen bonding acceptor ability however is less clear. Fluorine can be considered to be an extremely weak base and therefore a poor hydrogen bond acceptor. The poor polarisability of the fluorine atom means that it forms hydrogen bonds which are unfavourable soft donor-hard acceptor interactions. Fluorine's ability to act as an hydrogen bond acceptor has been explored by analysis of the Cambridge Structural Database, looking for C-F···H contacts shorter than 2.3 Å. The data illustrate that C-F···H bonding is relatively rare which is an indication for the weak acceptor ability of organic bound fluorine (Tables 1.14 and 1.15).

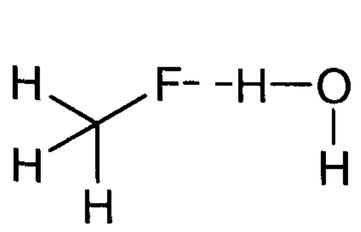

52

2.38 kcal/mol

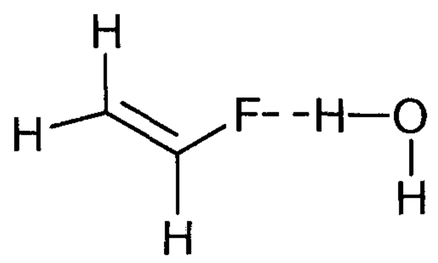

53

1.48 kcal/mol

Scheme 1.22. C-F···H interaction energies for fluoromethane **52** and fluoroethene **53** in H_2O.

The statistical data were supported by theoretical calculations on fluoromethane **52** and fluoroethene **53**. The data also indicated a stronger interaction of aliphatic over vinylic fluorine (Scheme 1.22). The energy difference of this interaction was rationalised by hyperconjugation of the fluorine lone pairs with the π-orbitals in the vinylic system, which makes the fluorine less able to participate in hydrogen bonding. The calculations indicate that C-F···H-C interactions are less stable than C-F···H-O interactions. With an energy minimum of 0.2 kcal/mol the interaction of fluorine to carbon bound hydrogen lies in the region of van der Waals complexes.

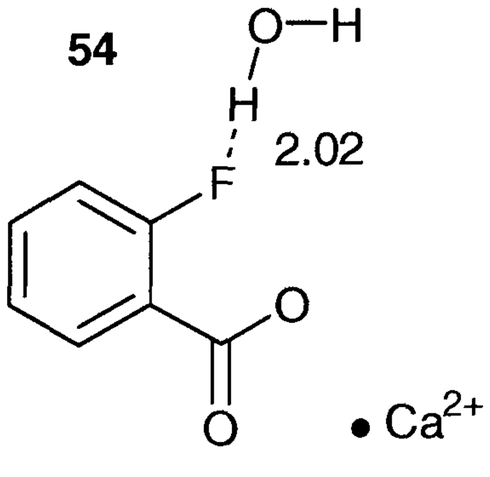

54

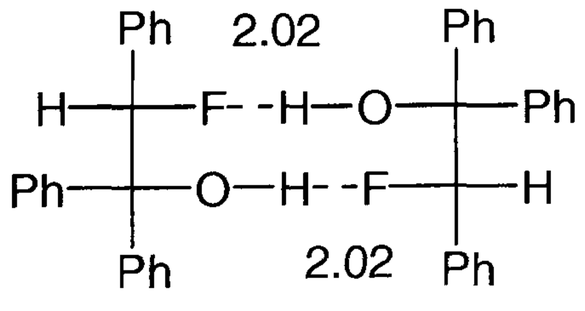

55

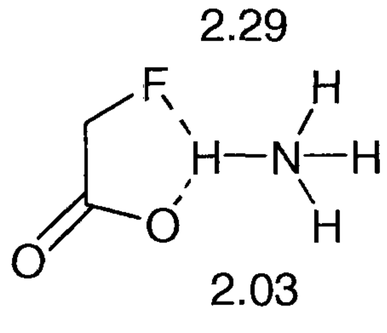

56

Scheme 1.23. C-F···H-O interactions in calcium bis(2-fluorobenzoate) dihydrate **54**, 2-fluoro-1,1,2-triphenylethanol **55**, and ammonium monofluoroacetate **56**.

A later study on fluorine hydrogen bonding also based on the Cambridge Structural Database confirmed these results.[72] C-F···H-X interactions with distances less than 2.3 Å were found only in 37 out of 5947 C-F bonds. Only a few structures, e.g. **44** and

45, were classified as molecules exhibiting true hydrogen bonds to fluorine (Scheme 1.23). These experimental results led to the conclusion that "covalently bonded F hardly ever acts as a H-bond acceptor and then only in exceptional molecular and crystal environments". This includes the requirement that fluorine forms hydrogen bonds only in the absence of a better acceptor group. For instance, in monofluoroacetate **46** the hydrogen bonded proton was dragged towards the carboxylic acid group rather than to the fluorine. Even though the molecule contains four hydrogen donors per anion, there was no clear proof of a C-F···H bonding.

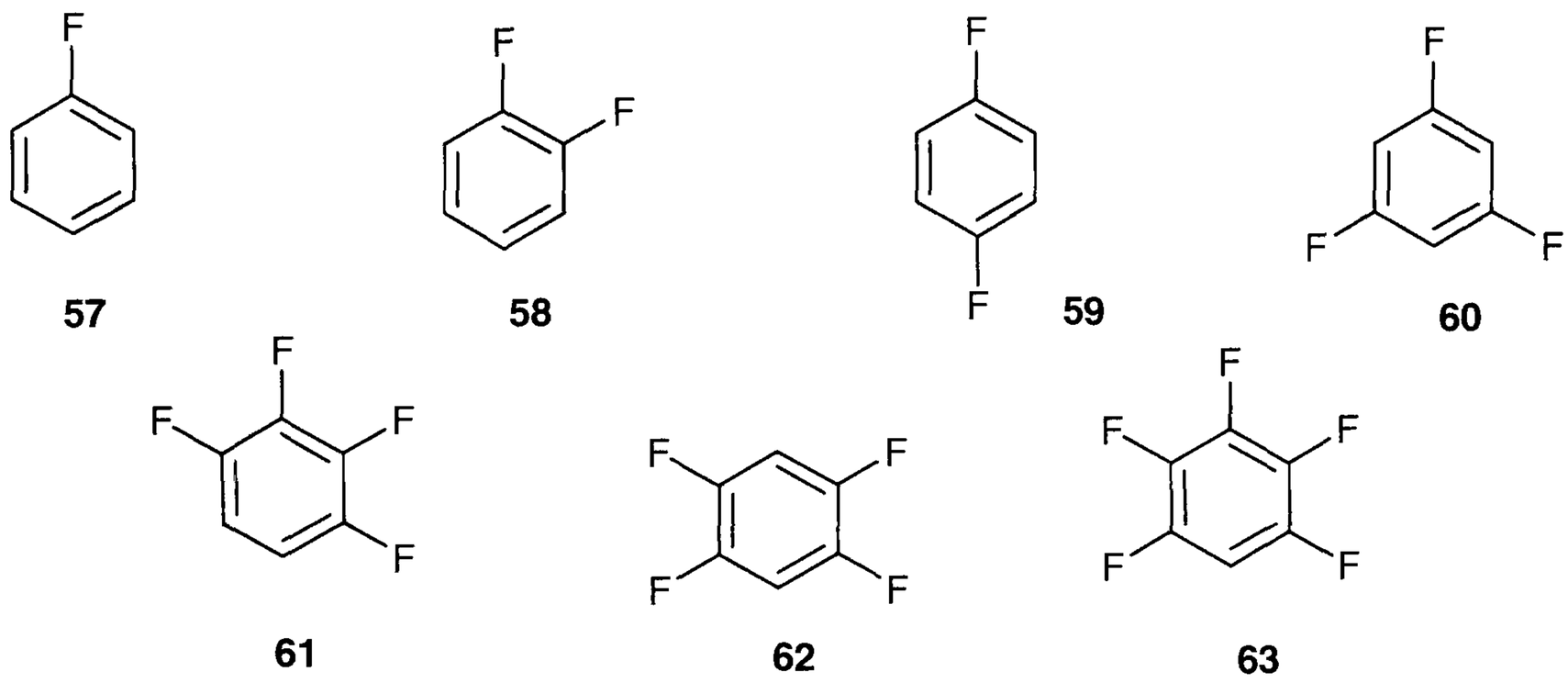

57 **58** **59** **60**

61 **62** **63**

Scheme 1.24. Short C-F···H contacts have been observed in the crystal structures of various fluorobenzenes **57-63** deposited in the Cambridge Structural Database (CSD).

Another CSD study reported on C-F···H interactions in a series of fluorobenzenes (Scheme 1.24). Shorter H···F distances were observed with increasing fluorine content, as may be expected from a greater degree of C-H bond activation.[73] In the study, the H···F distances were plotted against the C-H···F angles for all interactions between $C(sp^2)$-H and $C(sp^2)$-F (Figure 1.9).

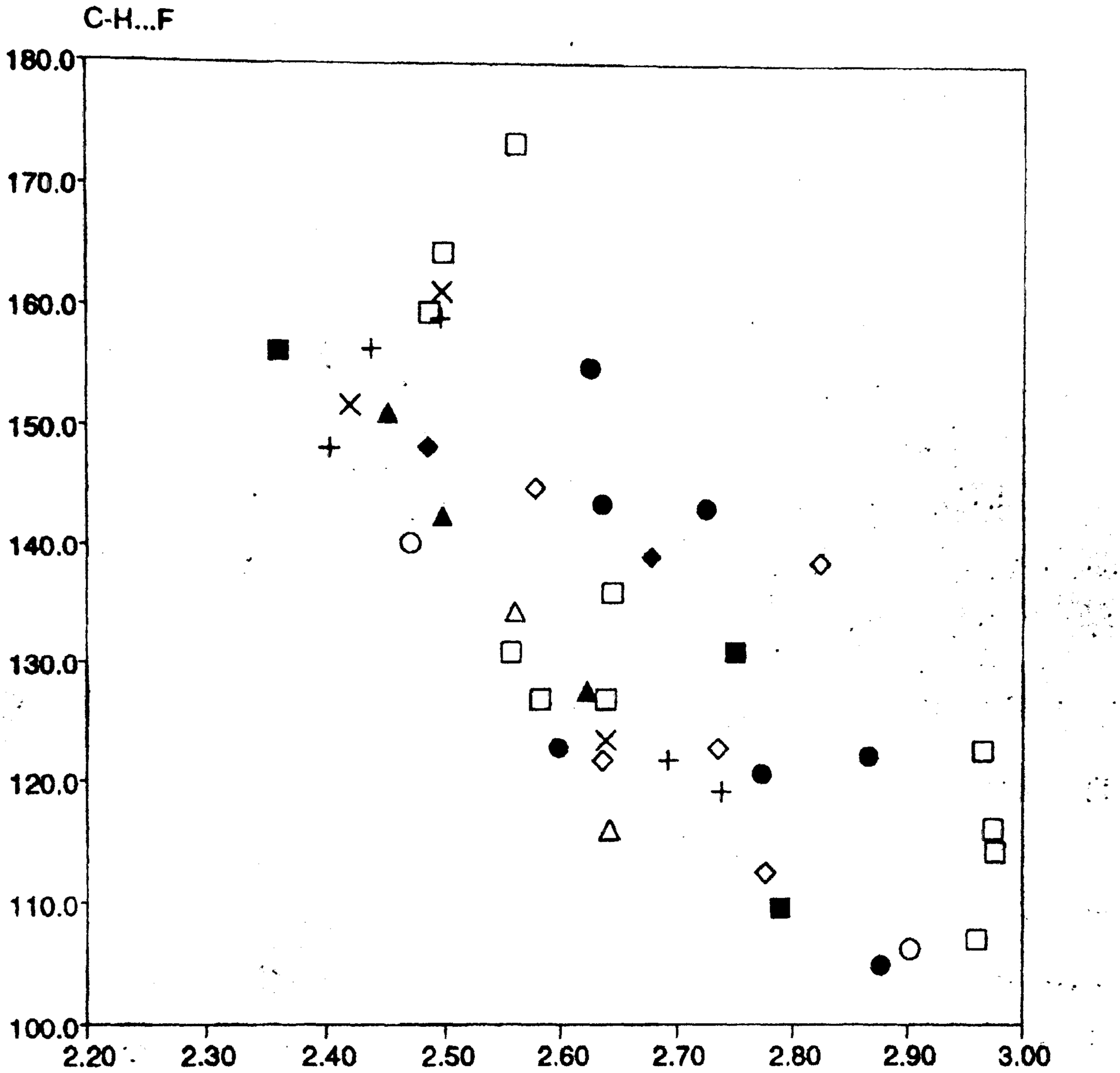

Figure 1.9. Distance of C-F···H interactions plotted against angle of the hydrogen bonds for the fluorobenzenes **57** (○), **58** (◊), **59** (♦), **60** (▲), **61** (□), **62** (■), **63** (●).

In case of the fluorobenzenes studied a negative correlation between distance and angle of the hydrogen bridges was observed, characteristic of hydrogen bonding. The data suggested that the fluorine hydrogen contacts in these fluorobenzenes were for a chemical reason rather than merely a result of the overall (isotropic) crystal packing. From these experimental results it can be concluded that organic fluorine can act as a hydrogen bond acceptor in certain cases especially when the fluorine is attached to an sp^2 carbon centre.

References

[1] D. Seebach, *Angew. Chem. Int. Ed.*, 1990, **29**, 1320.

[2] Images obtained from web pages in, www. chemguide.co.uk

[3] A. M. Thayer, *Chemical & Engineering News*, 2006, **5**, 15; A. M. Thayer, *Chemical & Engineering News*, 2006, **5**, 27.

[4] B. E. Smart, *J. Fluorine Chem.*, 2001, **109**, 3.

[5] J. D. Dunitz, *ChemBioChem*, 2004, **5**, 614.

[6] P. Beier, In *Partially fluorous molecules and lipase mediated enantiomeric resolutions in fluorous solvents*, PhD thesis, St Andrews University, 2004.

[7] P. Beier, A. M. Z. Slawin, D. O'Hagan, *Tetrahedron: Asymmetry*, 2004, **15**, 2447.

[8] P. Kirsch, In *Modern Fluoroorganic Chemistry*, Wiley-VCH, 2004, 15.

[9] P. Kirsch, In *Modern Fluoroorganic Chemistry*, Wiley-VCH, 2004, 91.

[10] A. D. Allan, T. T. Tidwell, *Adv. Fluorine Chem.*, 1973, **7**, 69.

[11] R. D. Chambers, *Fluorine in Organic Chemistry*, Blackwell Publishing Ltd, Oxford, 2004, 122 and references cited herein.

[12] S. Alunni, V. Laureti, L. Ottavi, R. Ruzziconi, *J. Org. Chem.*, 2003, **68**, 718.

[13] G. Kohnstamm, D. Routledge, D. L. H. Williams, *J. Chem. Soc., Chem. Comm.*, 1966, 113.

[14] J. Hine, N. W.Burske, M. Hine, P. B. Langford, *J. Am. Chem. Soc.*, 1957, **79**, 1406.

[15] M. Schlosser, *Angew. Chem. Int. Ed.*, 1998, **37**, 1496.

[16] G. Adolph, M. J. Kamlet, *J. Am. Chem. Soc.*, 1966, **88**, 4761.

[17] M. Hudlicky, *Coll. Czech. Chem. Comm.*, 1991, **56**, 1680.

[18] S. Andreades, *J. Am. Chem. Soc.*, 1964, **86**, 2003.

[19] G. DiMartino, M. B. Hursthouse, M. E. Light, J. M. Percy, N. S. Spencer, M. Tolley, *Org. Biomol. Chem.*, 2003, **1**, 4423.

[20] D. Chambers, *Fluorine in Organic Chemistry*, Blackwell Publishing, CRC Press, Oxford, 2004, 132.

[21] B. Bacerzac, M. Fedorynski, *J. Chem. Soc., Chem. Comm.*, 1991, 826.

[22] D. Chambers, *Fluorine in Organic Chemistry*, Blackwell Publishing, CRC Press, Oxford, 2004 and ref cited therein.

[23] D. Chambers, *Fluorine in Organic Chemistry*, Blackwell Publishing, CRC Press, Oxford, 2004, and references cited herein.

[24] B. E. Smart, *J. Fluorine Chem.*, 2001, **109**, 3.

[25] M. Schlosser, *Angew. Chem. Int. Ed.*, 1998, **110**, 1496.

[26] V. J. Jasys, R. A. Volkmann, *J. Am. Chem. Soc.*, 2000, **122**, 466.

[27] A. J. Kirby, In *The Anomeric Effect and related Stereoelectronic Effects at Oxygen. Reactivity and Structure*, Concepts in Organic Chemistry 15, Springer Verlag, Berlin, 1983.

[28] W. Walter, H. Beyer, In *Lehrbuch der Organischen Chemie*, Hirzel Verlag, Stuttgart, 1991, 440.

[29] G. J. Boons, D. A. Entwistle, S. V. Ley, M. Woods, *Tetrahedron Lett.*, 1993, **34**, 5649.

[30] P. Deslongchamps, In *Stereoelectronic Effects in Organic Chemistry*, Pergamon Press, Oxford, 1983.

[31] S. Wolfe, A. Rauk, L. M. Tel, I. G. Csizmadia, *J. Chem. Soc. (B)*, 1971, 136.

[32] H. Senderowitz, P. Aped, B. Fuchs, *Tetrahedron*, 1993, **49**, 3879; M. Hayashi, H. Kato, *Bull. Chem. Soc. Jpn.*, 1980, **53**, 2701.

[33] K. B. Wiberg, *Acc. Chem. Res.*, 1996, **29**, 229.

[34] G. Angelini, E. Gavuzzo, A. L. Segre, M. Speranza, *J. Phys. Chem.*, 1990, **94**, 8762.

[35] R. J. Abrahams, E. Bretschneider, In *Internal Rotations in Molecules*, Wiley & Sons, London, 1974, 498.

[36] J. R. Durig, J. Liu, T. S. Little, V. F. Kalasinski, *J. Phys. Chem.*, 1992, **96**, 8224.

[37] N. C. Craig, A. Chen, K. H. Shu, S. Klee, G. C. Mellau, B. P. Winnewieser, M. Winnewieser, *J. Am. Chem Soc.*, 1997, **119**, 4789; P. Huber-Waelchli, H. H. Guenthard, *Spectrochim. Acta*, 1981, **37A**, 285.

[38] R. J. Abrahams, E. Bretschneider, In *Internal Rotations in Molecules*, Wiley & Sons, London, 1974, 498.

[39] K. Tanabe, *Spectrochim. Acta.*, 1972, **A28**, 407, and references cited therein.

[40] S. Wolfe, *Acc. Chem. Res*, 1972, **5**,102.

[41] W. T. Borden, *J. Chem. Soc., Chem. Comm.*, 1998, 1919.

[42] R. F. W. Bader, *Atoms in molecules: A quantum theory*, Clarendon Press, Oxford, 1990.

[43] K. B. Wiberg, *Acc. Chem. Res.*, 1996, **29**, 229.

[44] G. Angelini, E. Gavuzzo, A. L. Segre, M. Speranz, *J. Phys. Chem.*, 1990, **94**, 8762.

[45] C. R. S. Briggs, M. J. Allan, D. O'Hagan, D. J. Tozer, A. M. Z. Slawin, A. E. Goeta, J. A. K. Howard, *Org. Biomol. Chem.*, 2004, **2**, 732.

[46] C. R. Briggs, *The gauche effect*, PhD Thesis, St Andrews University, 2002.

[47] C. R. Briggs, *The gauche effect*, PhD Thesis, St Andrews University, 2002.

[48] B. J. Van der Veken, S. Truyen, W. A. Herrebout, G. Watkins, *J. Mol. Struct.*, 1993, **193**, 55.

[49] R. J. Abrahams, A. D. Jones, M. A. Warne, R. Rittner, C. T. Tormena, *J. Chem. Soc., Perkin Trans. 2*, 1966, 533.

[50] H. V. Phan, J. R. Durig, *J. Mol. Struct.*, 1990, **209**, 333.

[51] J. W. Banks, A. S. Batsanov, J. A. K. Howard, D. O'Hagan, H. S. Rzepa, S. Martin-Santamaria, *J. Chem. Soc., Perkin Trans. 2,* 1999, 2409.

[52] A. E. Reed, L. A. Curtis, F. Weinhold, *Chem. Rev.*, 1988, **88**, 899.

[53] C. R. S. Briggs, D. O'Hagan, J. A. K. Howard, D. S. Yufit, *J. Fluorine Chem.*, 2003, **119**, 9.

[54] C. R. Briggs, *The gauche effect*, PhD Thesis, St Andrews University, 2002.

[55] C.F. Tormena, R. Rittner, R. J. Abrahams, *J. Chem. Soc., Perkin Trans. 2*, 2000, 773.

[56] D. O'Hagan, C. Bilton, J. A. K. Howard, L. Knight, D. J. Tozer, *J. Chem. Soc., Perkin Trans.*, 2000, **2**, 605-607.

[57] R. J. Abraham, J. R. Monasterios, *Org. Mag. Reson.*, 1973, **5**, 305.

[58] C. R. S. Briggs, D. O'Hagan, H. S. R. Rzepa, A. M. Z. Slawin, *J. Fluorine Chem.*, 2004, **125**, 19.

[59] A. Warshel, A. Papazyan, P. A. Kollman, *Science*, 1995, **269**, 102.

[60] G. C. Pimentel, A. L. McClellan, In *The Hydrogen Bond*, Freeman, San Francisco, CA, 1960.

[61] P. Gilli, V. Bertolsasi, V. Feretti, G. Gilli, *J. Am. Chem. Soc.*, 2000, **122**, 10405.

[62] J. E. Del Bene, S. A. Perera, R. J. Barlett, *J. Phys. Chem. A.*, 1999, **103**, 8121; A. Bagno, G. Saielli, G. Scorrano, *Chem. Eur. J.*, 2002, **8**, 2047.

[63] G. R. Desiraju, *Acc. Chem. Res.*, 2002, **35**, 565.

[64] A. L. Mcclellan, *Ann. Rev. Phys. Chem.*, 1971, **22**, 2532.

[65] D. A. Dixon, B. E. Smart, *J. Phys. Chem.*, 1991, **95**, 1602.

[66] R. West, D. L. Powell, L. S. Whatley, M. K. T. Lee, P. R. Schleyer, *J. Am. Chem. Soc.*, 1962, **84**, 3221.

[67] C. Laurence, M. Berthelot, *Persp. Drug Discovery Des.*, 2000, **1**, 39.

[68] L. Pauling, In *The nature of the chemical bond*, 2nd ed., Cornell University Press, Ithaca, New York, 1940, 286.

[69] C. G. Swain, R. E. T. Spalding, *J. Am. Chem. Soc.*, 1960, **82**, 6104; G. M. LeFave, *J. Am. Chem. Soc.*, 1949, **71**, 4148.

[70] J. A. K. Howard, V. J. Hoy, D. O'Hagan, G. T. Smith, *Tetrahedron*, 1996, **52**, 12613.

[71] J. A. K. Howard, V. J. Hoy, D. O'Hagan, G. T. Smith, *Tetrahedron*, 1996, **52**, 12613.

[72] J. D. Dunitz, R. Taylor, *Chem. Eur. J.*, 1997, **3**, 89.

[73] G. R. Desirau, *Acc. Chem. Res.*, 2002, **35**, 565.

2 Results and Discussion

The aim of the PhD project was to obtain *vicinal* difluoro compounds by chemical synthesis and investigate the influence of stereoelectronic effects on their molecular conformation. In particular, the synthesis of 2,3-difluorosuccinic acids **64** and **65** was envisaged. The molecule containes the *vicinal* difluoro motif and offers access to several derivatives such as esters and amides.

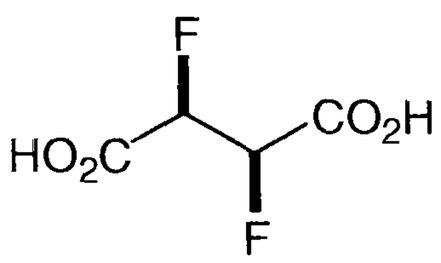

64

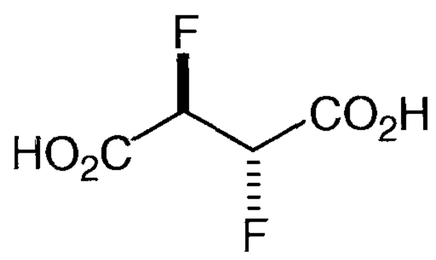

65

The amides derived from 2,3-difluorsuccinic acids incorporate two adjacent α-fluoroamide moieties which were expected to exhibit pronounced stereoelectronic effects. Due to the preference of the C-F bond to align *anti* periplanar to the carbonyl group and the *gauche* effect, the main chain conformations of the *erythro* and the *threo* stereoisomers **66** and **67** were anticipated to be very different and predictable in each case.

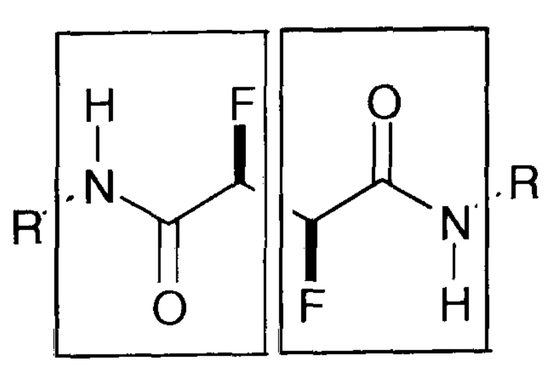

66

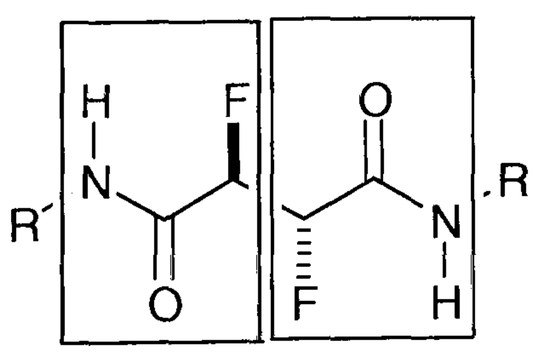

67

New synthetic routes towards *vicinal* difluoro compounds had to be explored in order to access the stereoisomers **66** and **67** in a diastereoselective manner. X-ray analysis and NMR techniques were then used in order to establish conformational preferences as a result of stereoelectronic effects induced by the C-F bonds.

2.1 Synthesis of stereoisomers of 2,3-difluorosuccinic acid

The introduction of fluorine into organic molecules is an important and challenging subject, which has led to fluorine chemistry as an independent area of research. Synthetic methods towards fluorine-containing compounds may be broadly classified into selective fluorination or the so-called building block approach. The building block approach involves the incorporation of a structural element already containing fluorine. The strategy usually allows for standard experimental procedures which commonly applied in synthetic chemistry.[1] The synthesis of fluorinated analogues of the antimalaria drug artemisenine represents an example for the building block approach (Scheme 2.1).

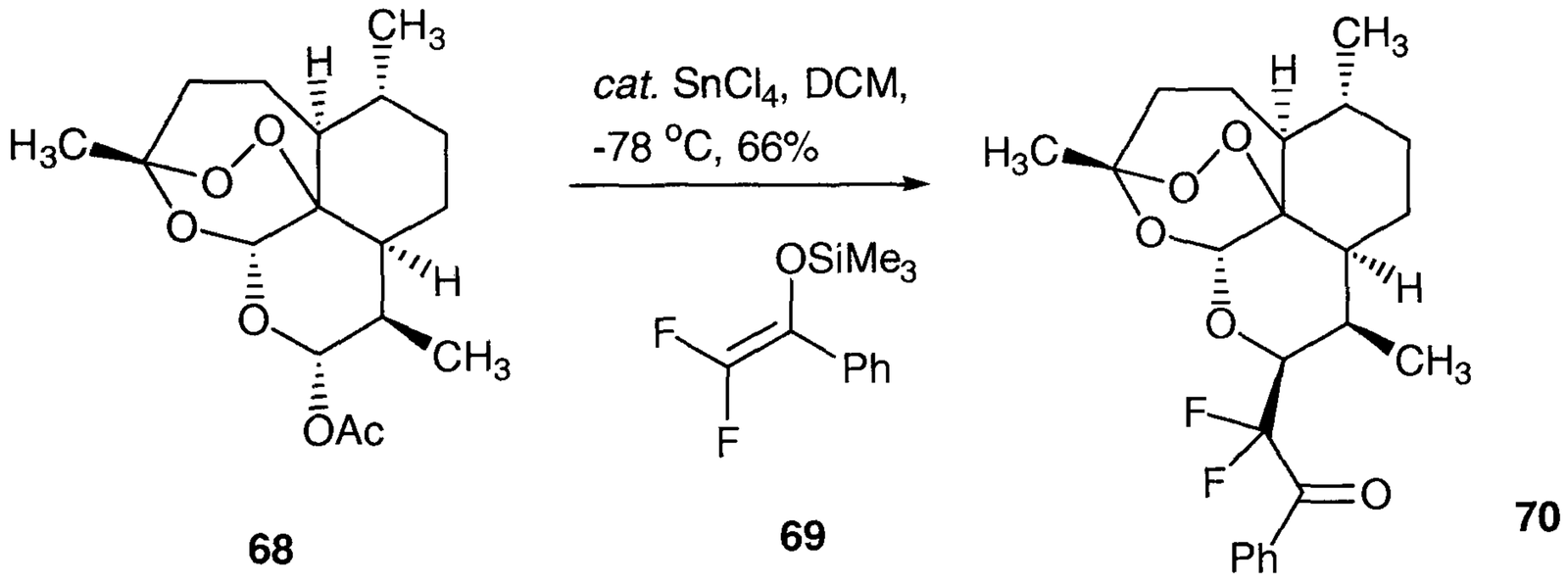

68 **69** **70**

Scheme 2.1. Synthesis of a fluorinated analog of artemisinine. The silyl enol ether **69** is introduced as a fluorinated building block into the natural product **68** to form the fluorinated antimalaria drug **70**.

Selective fluorination aims at functional group interconversion with the aim to introduce a C-F bond. This typically involves treatment of the starting material with a suitable fluorinating reagent. The method has historically involved elemental fluorine, hydrogen fluoride, or derivatives thereof.[2] These reagents are of extraordinary reactivity and toxicity and typically require special equipment when used in the

laboratory. A variety of alternative reagents have been developed in recent years that have moderate reactivity and can be employed more safely and under milder conditions on a laboratory scale, making fluorination a more straightforward and less hazardous process.[3] The use of such fluorinating reagents is described in this thesis, and the variety of fluorination strategies developed for the synthesis of *vicinal* difluoro compounds has clearly broadened their scope of application and may be of interest for the synthetic organic chemist in general.

2.1.1 Current synthetic routes to *vicinal* difluoro compounds

Of the 298,876 registered fluorinated compounds in the Beilstein Chemical Database, 51,447 structures have two adjacent carbon-fluorine bonds. However, there are only 279 compounds that contain a genuine *vicinal* difluoro motif -CHF-CHF- with the majority of them being perfluorinated substances. The rare presence of this class of compounds may certainly be attributed to the difficulty of their selective synthesis. Synthetic methods for the preparation of *vicinal* difluoro compounds most frequently start from an alkene and elemental fluorine,[4] XeF_2,[5] or electrochemical methods (Scheme 2.2).[6]

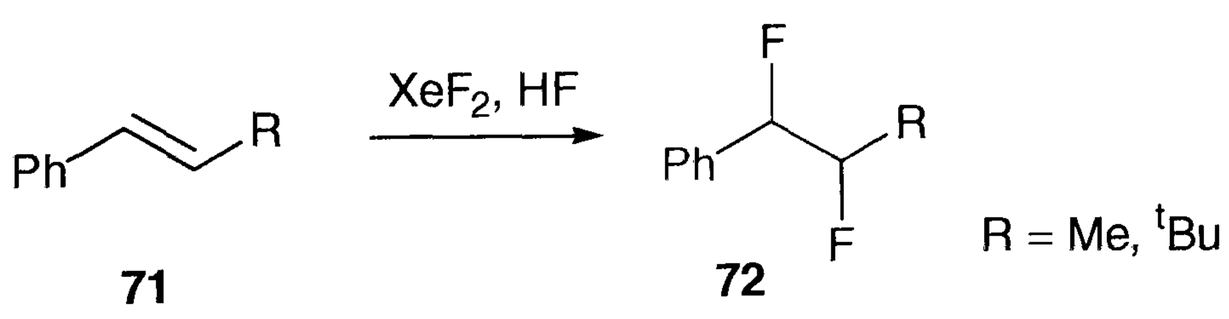

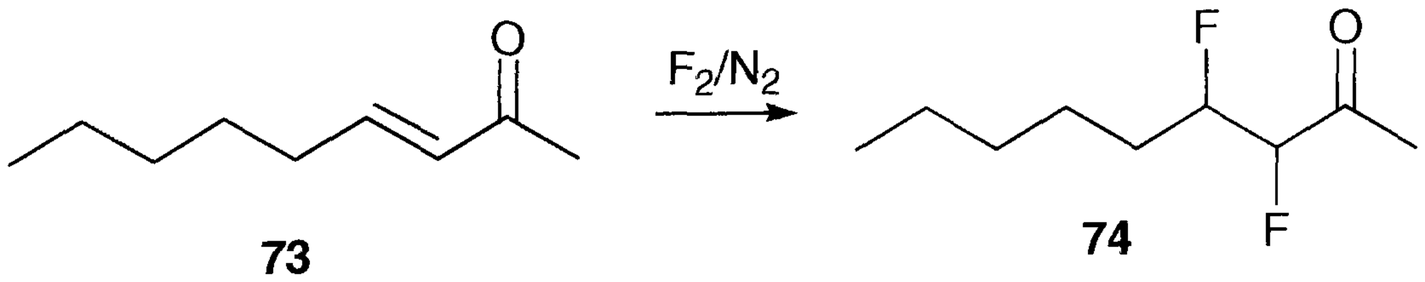

Scheme 2.2. Synthetic methods that have been used previously for the synthesis of *vicinal* difluoro compounds.

Such reactions however are either difficult to carry out with standard laboratory equipment and are hazardous, or lack general applicability. Alternative methods that involve the ring opening with "tamed" hydrogen fluoride have been developed recently that are less hazardous and result in a high degree of diastereoselectivity. For example, the stereoselective ring opening of epoxides with pyridinium polyhydrogen fluoride (PPHF) facilitated the synthesis of *threo* and *erythro* 9,10-difluorostearic acids **78** and **82**. Each diasteroisomer was prepared as the diastereomerically pure material starting from their respective *E* or *Z* methyl oleates **75** and **79** (Scheme 2.3).

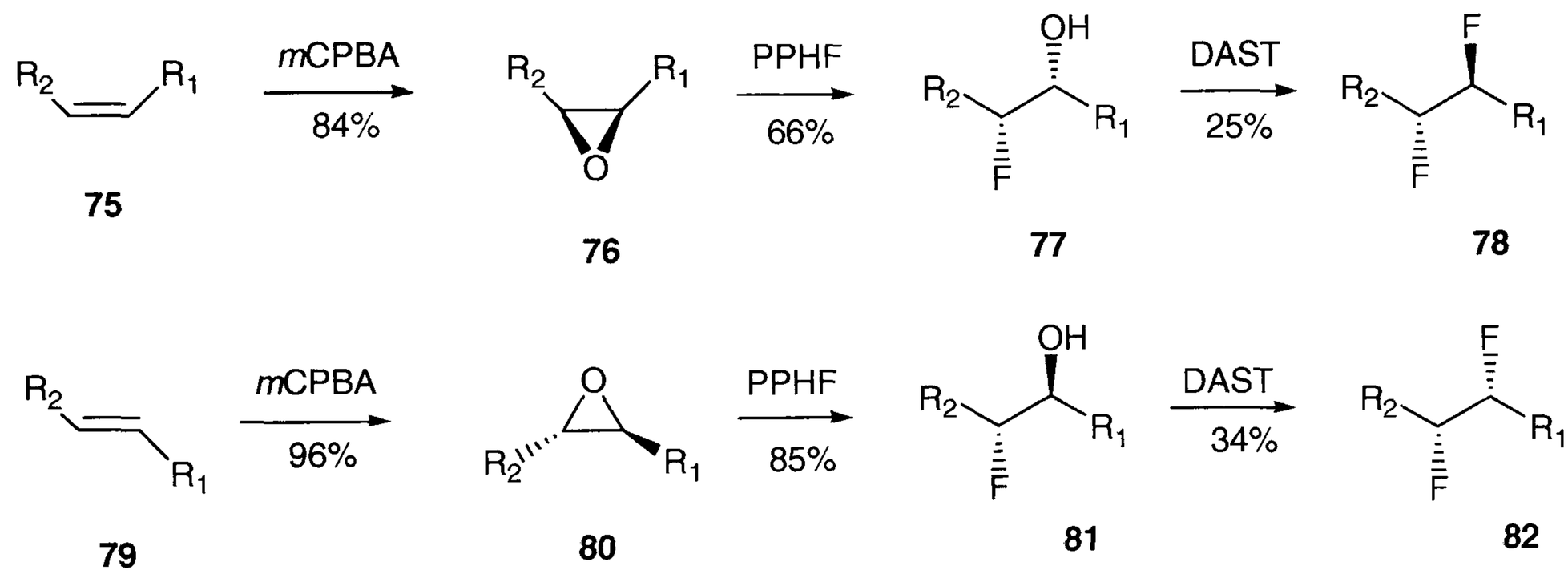

$R_1 = (CH_2)_7CO_2Me$, $R_2 = (CH_2)_7CH_3$

Scheme 2.3. Diastereoselective synthesis of *erythro* and *threo* 9,10-difluorostearic acids. Ring opening of the epoxides **76** and **80** with PPHF generated the respective fluorohydrins **71** and **75** as a 1:1 mixture of regioisomers (only one regioisomer shown). The products **72** and **76** are obtained as their racemic mixtures after treatment with DAST.

Due to the problems in handling pure hydrogen fluoride, the reactions were carried out with pyridinium polyhydrogen fluoride complex (PPHF). The reagent is considerably less hazardous than free hydrogen fluoride due to complexation with the pyridinium base and can be safely employed in the laboratory.[7] Ring opening of the epoxides **76** and **80** with PPHF generated the respective fluorohydrins as a 1:1

mixture of regioisomers. The mixture was directly converted with DAST into the *threo* and *erythro* difluoro compounds **72** and **76** respectively. The deoxyfluorination gave considerable amounts of byproducts that arise from elimination, which however could be removed conveniently by ozonolysis and work-up.[8]

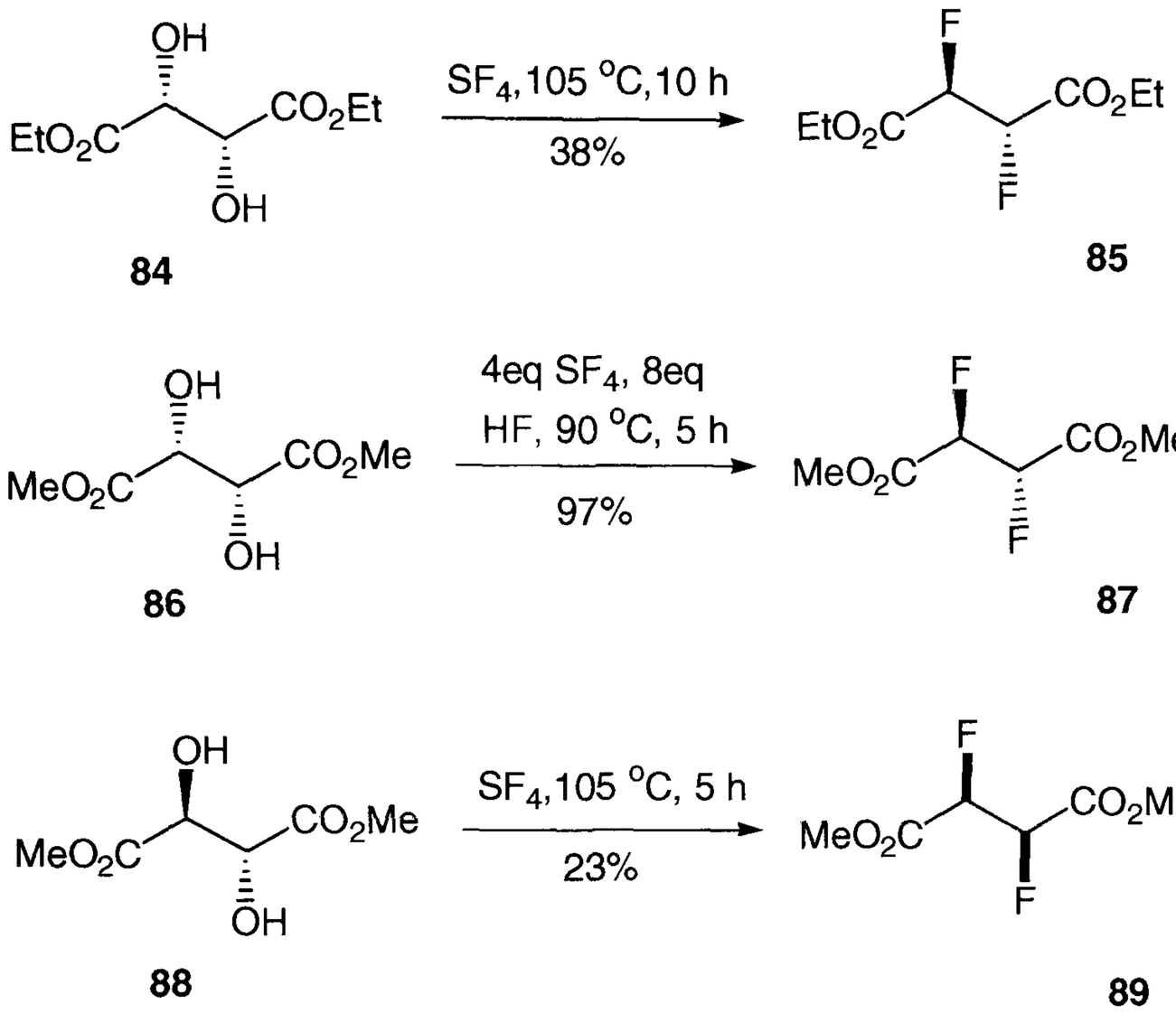

84 **85**

86 **87**

88 **89**

Scheme 2.4. Synthesis of *vicinal* difluorosuccinates, which requires the application of hazardous reagents SF_4 and HF.

Interestingly, stereoisomers of 2,3-difluorosuccinic acid were found amongst the *vicinal* difluoro compounds listed in the Beilstein Database. Both stereoisomers were obtained either from L-(+)-tartrate **84** and **86** or *meso*-tartrate **88** (Scheme 2.4). The synthesis of these compounds however involves the action of sulfur tetrafluoride,[9] the application of which is restricted for laboratory use due to its low boiling point, high corrosiveness and toxicity. The lethal concentration of SF_4 is very low and in the range of that for phosgene, and neat HF had to be added to the mixture which renders the process even more hazardous.[10]

Alternative preparative methods have involved catalytic hydrogenation of 2,3-difluoromaleic acid **90**. The reaction yields *meso* 2,3-difluorosuccinic **65** acid but only in poor yield.[11] Significant by-product formation results from the hydrogenolysis of the olefinic carbon-fluorine bond, a reaction that predominates when difluorofumaric acid **91** is applied to the same reaction conditions (Scheme 2.5).

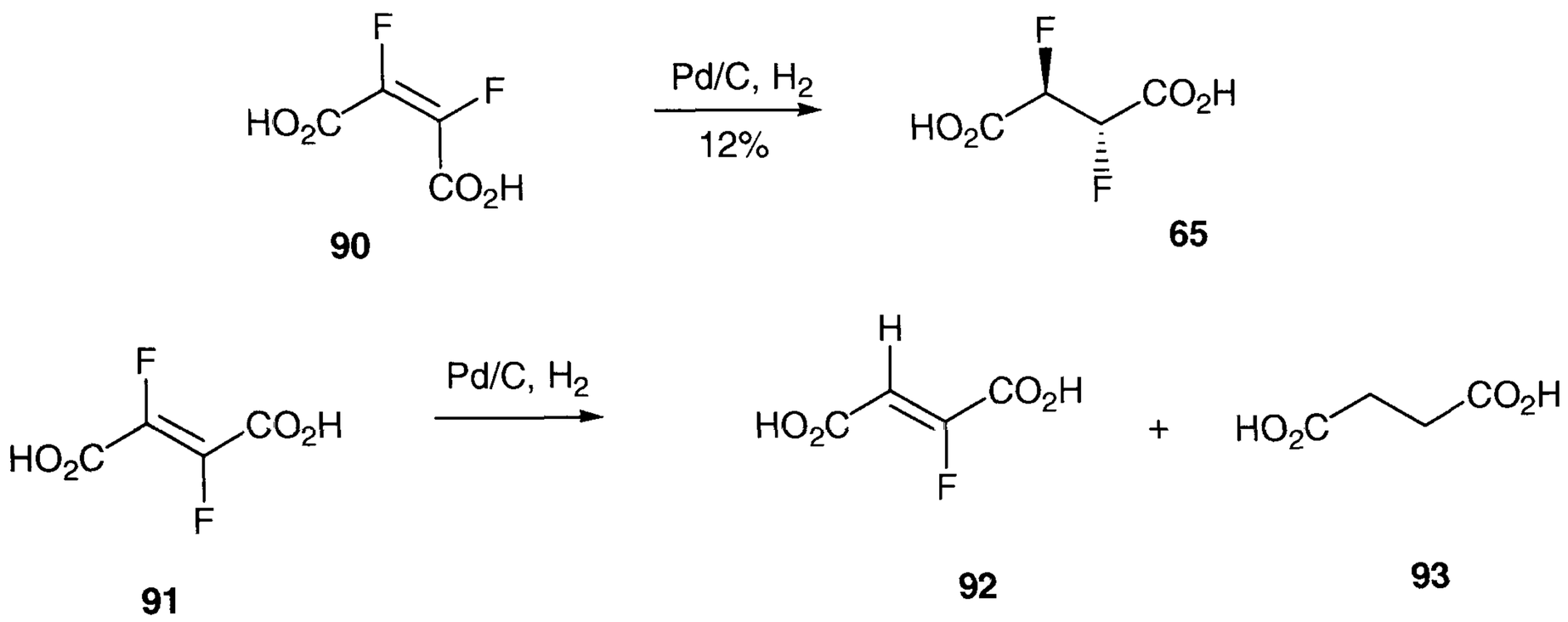

Scheme 2.5. Alternative synthetic route to *vicinal* difluoro compounds *via* catalytic hydrogenation.

Different reaction conditions were applied resulting either in low yields or product mixtures that arose from elimination or perfluorination processess.[12] The low yielding reactions in the latter cases and the highly hazardous reagents used for the previous methods made an alternative synthetic approach necessary to access the 2,3-difluorosuccinic acids.

2.1.2 Synthesis of 1,2-difluoro-1,2-diphenylethanes

Vicinal difluoro compounds have also been prepared by halofluorination of alkenes followed by addition of silver fluoride (Scheme 2.6). Initially, α-halo-β-fluoro compounds are generated which undergo halogen exchange reaction in the presence of the silver salt. The reaction is applicable to a variety of alkenes that have unactivated, isolated double bonds.[13]

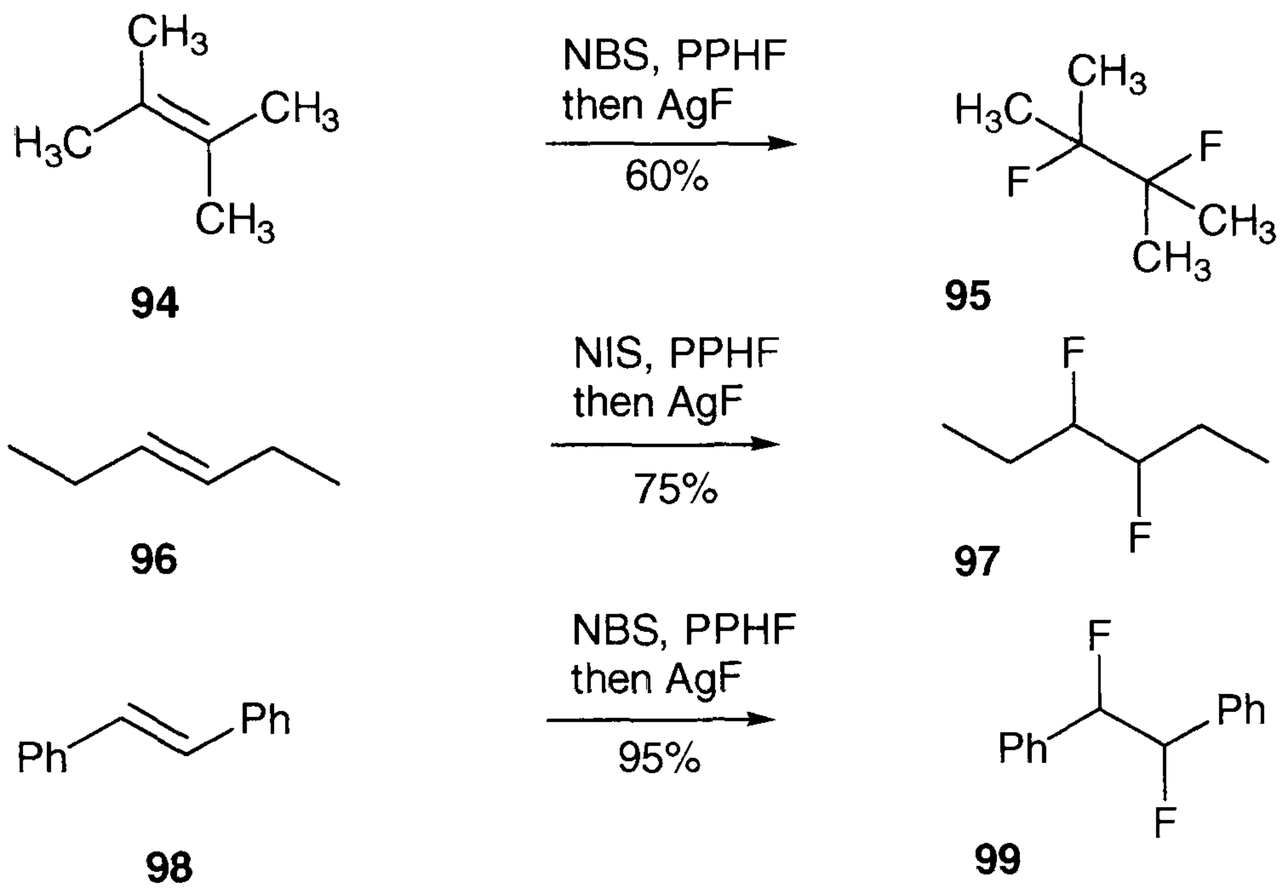

Scheme 2.6. Halofluorination of electronrich alkenes followed by halogen exchange reaction results in formation of *vicinal* difluoro compounds.

For instance, 1,2-difluoro-1,2-biphenylethane **99** can be obtained in excellent yield from *trans* stilbene **98** according to this method. As this compound contains two terminal phenyl groups that may be transformed to carboxylic groups by oxidative cleavage, the compound emerged as a useful precursor for the synthesis of 2,3-difluorosuccinic acid.

According to the literature procedure,[14] stilbene **98** was readily converted into its bromofluoro adduct **100** by treatment with NBS and PPHF. The reaction was carried out with an excess of hydrogen fluoride as a 1:1 mixture in diethyl ether at room temperature.

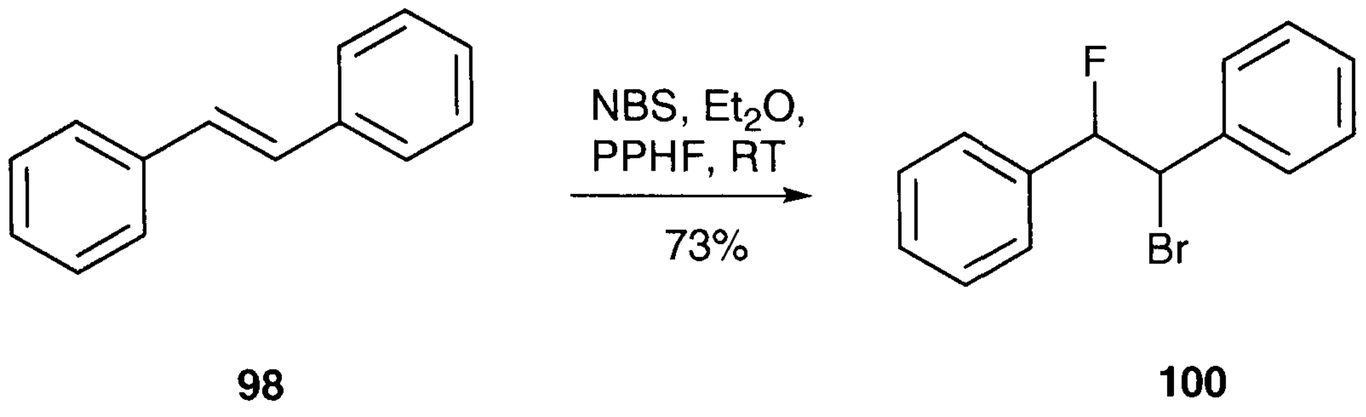

98 **100**

Scheme 2.7. Bromofluorination of stilbene according to Olah's procedure using NBS and PPHF.

GC-MS analysis indicated that the reaction had gone to completion within 2 - 3 hours. The reaction was clean indicated by a single peak with the correct mass for the expected bromofluoro compound **100**. ^{19}F-NMR confirmed that the reaction proceeded in a highly diastereoselective manner, consistent with previous observations (Figure 2.1).[15]

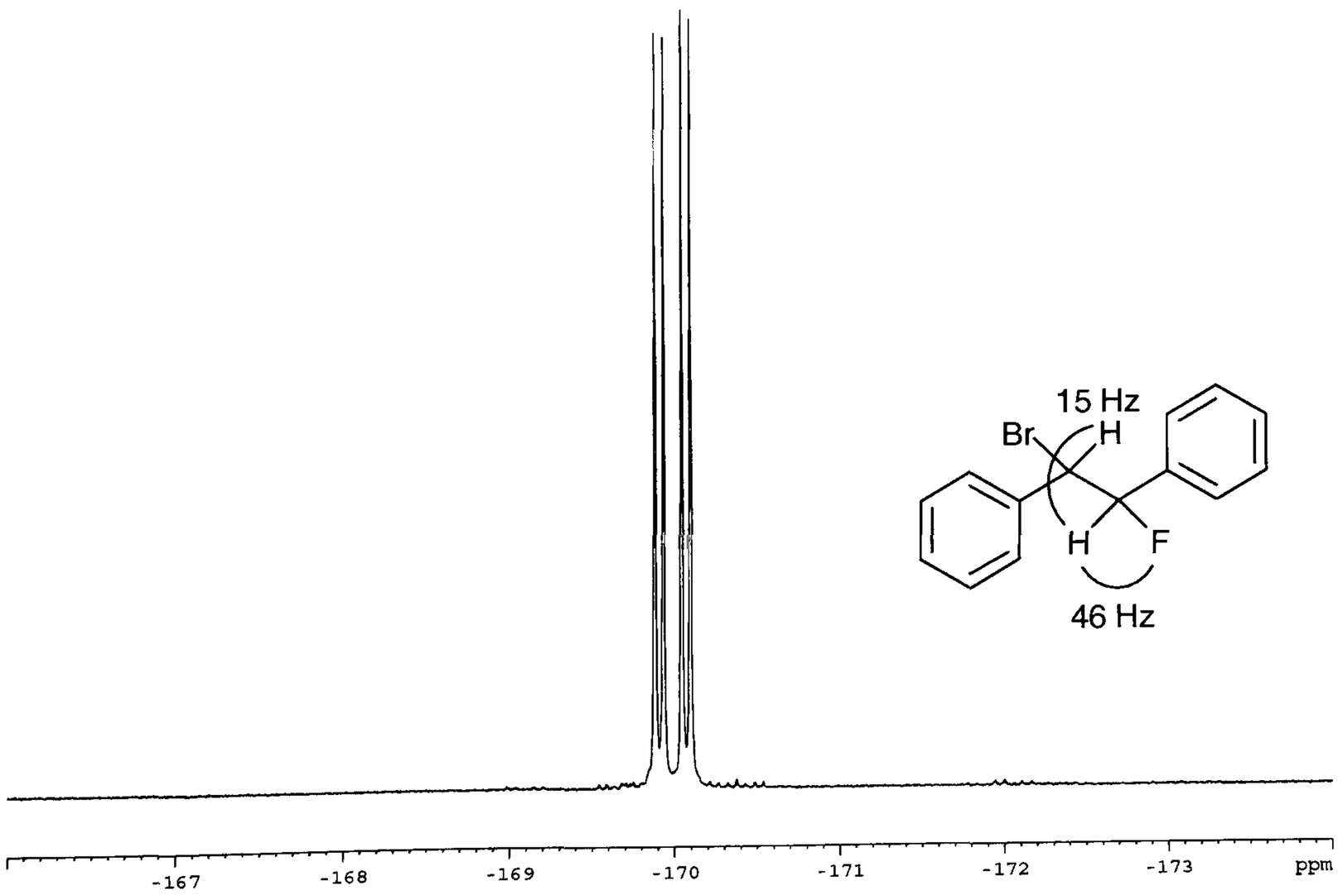

Figure 2.1. ^{19}F NMR spectrum of 1-bromo-2-fluoro-1,2-diphenylethane **100**. ^{19}F-NMR analysis of the product shows a doublet of doublets corresponding to a *geminal* and a *vicinal* HF coupling.

The relative stereochemistry of the fluorobromo compound **100** had not been elucidated previously, and NMR spectroscopic data of the pure *erythro* and *threo* diastereoisomers were not available. However, it had been reported previously that the halofluorination generally proceeds stereospecifically according to an *anti* addition mechanism.[16] In order to prove the stereochemistry of the product, compound **100** was crystallised in an effort to obtain X-ray crystallographic data. Although clear, colourless crystals of the compound were obtained (Figure 2.2), the X-ray structure could not be resolved and the relative stereochemistry had to be elucidated otherwise.

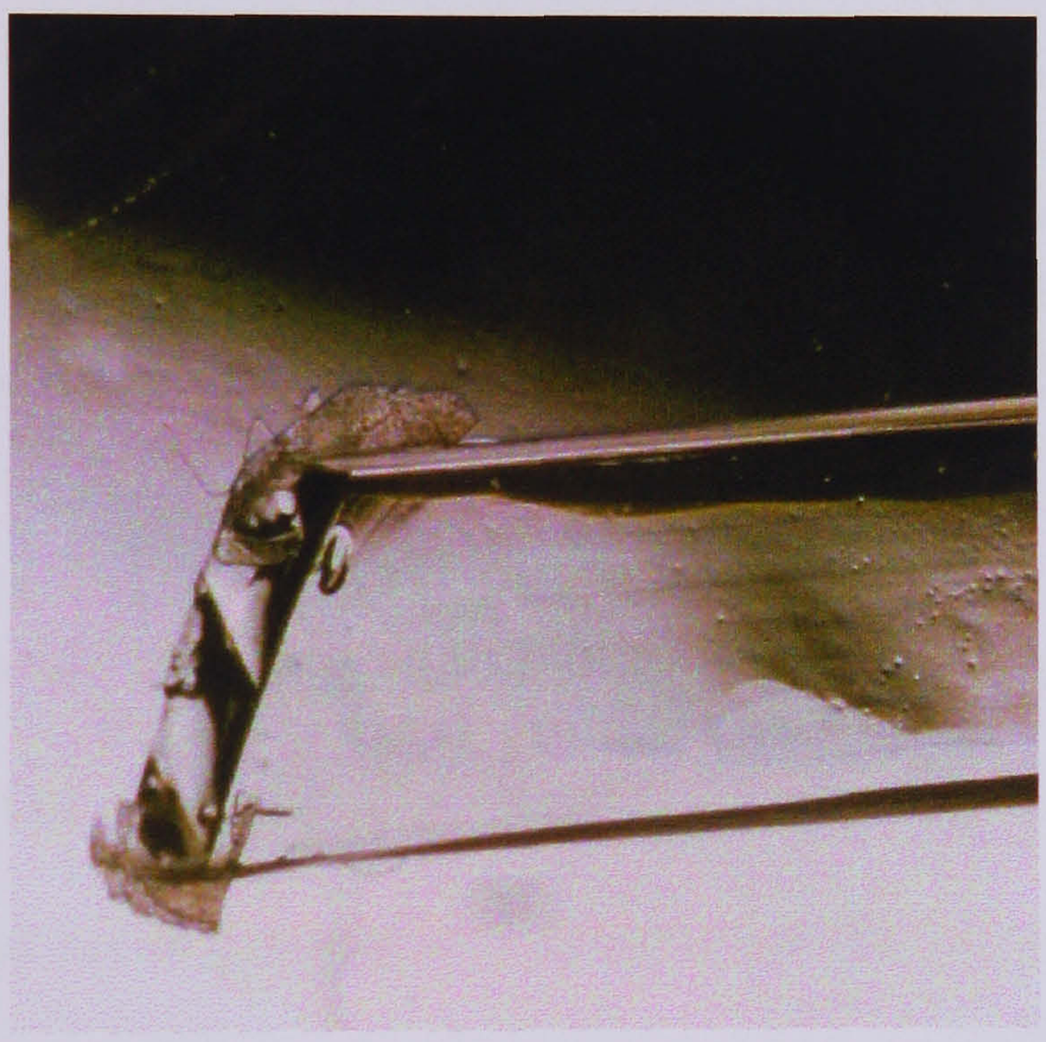

Figure 2.2. 1-Bromo-2-fluoro-1,2-diphenylethane **100** as obtained after recrystallisation from hexane.

1,2-Diphenylethane is often used as a tool to evaluate the stereochemical outcome of fluorination reactions.[17] The *anti* stereochemistry of **100** was established from the coupling constants of the products obtained after dehydrobromination. A preparative method for the elimination of hydrogen bromide from such β-fluorohalides had been developed previously, as the resulting vinyl fluorides are useful synthetic building blocks in organic chemistry.[18]

According to a literature procedure,[19] treatment with potassium *tert*-butoxide in a refluxing solution of hexane or pentane leads to stereospecific *anti*-elimination of hydrogen bromide (Scheme 2.8).[20]

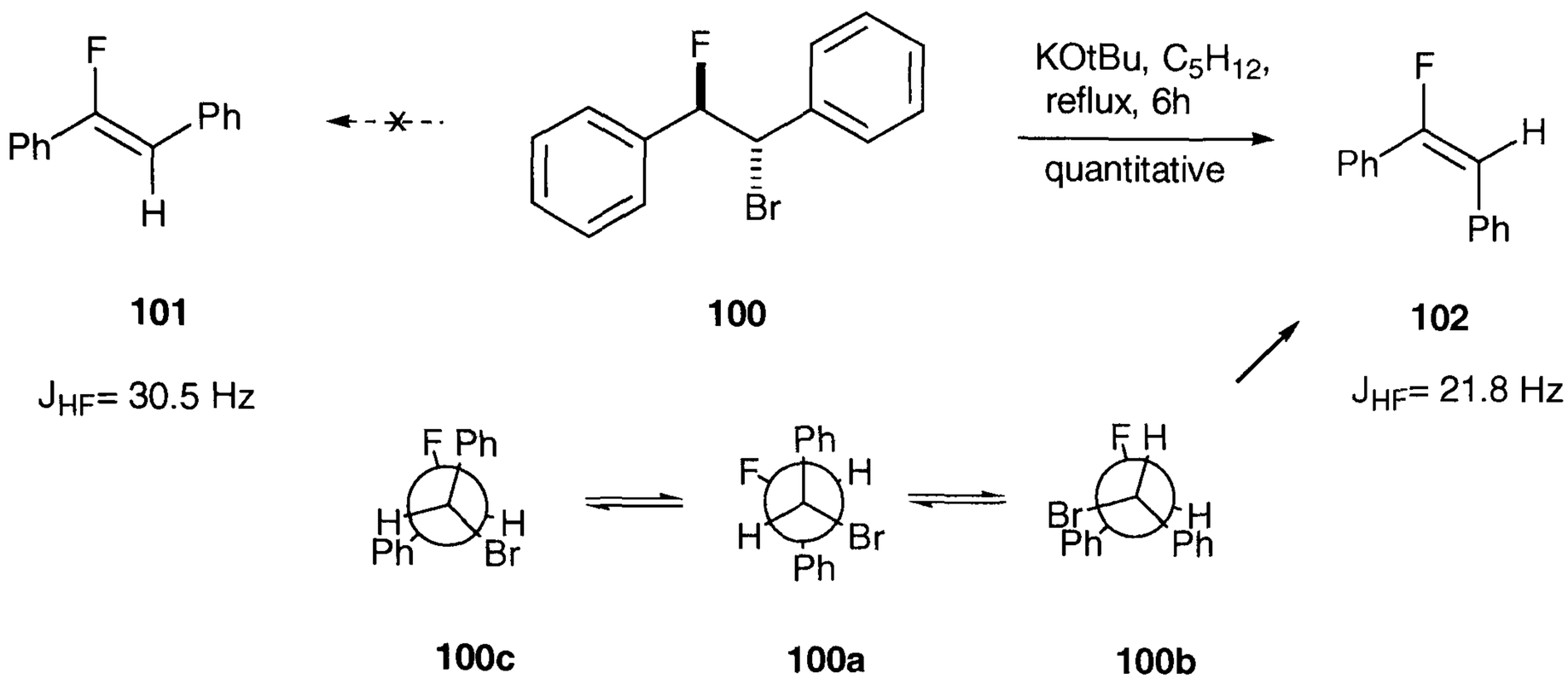

Scheme 2.8. Treatment of the bromo compound **100** with base leads to HBr elimination, a reaction which proceeds stereospecifically to afford the *E*-fluorostilbene **102** according to an *anti* elimination mechanism.

The two vinyl fluorides **101** and **102** can be readily distinguished by their $^3J_{HF}$ coupling constants. The $^3J_{HF}$ coupling constant of 21.1 Hz obtained from the ^{19}F-NMR spectrum of the crude product is indicative for the formation of the *E*-alkene **102** (Figure 2.3). From the resultant geometry of the fluorostilbene **102** it is immediately obvious that the precursor **100** must have the *erythro* configuration with the bromine and the fluorine *anti* to each other in the extended chain conformation. Vinyl fluorides are interesting molecules in their own right and may be useful fluorinated building blocks in organic synthesis. For instance, vinyl fluorides have found application in cycloaddition reactions,[21] and Claisen-rearrangements.[22]

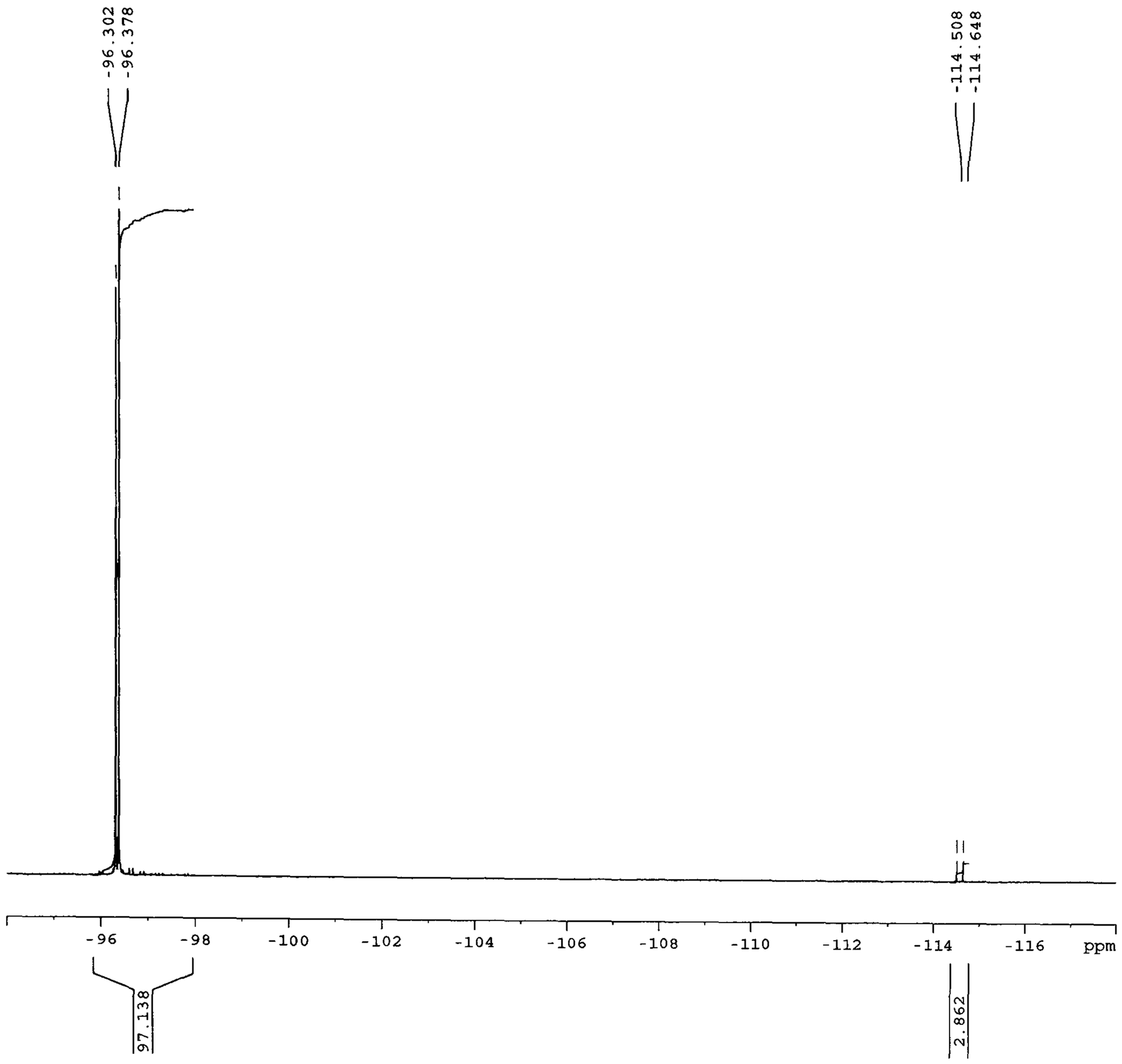

Figure 2.3. ^{19}F NMR spectrum of the crude product obtained after HBr elimination from **100**. The diastereomeric ratio of the *E*-alkene **102** at -96 ppm and *Z*-alkene **101** at -115 ppm indicates a stereoselective reaction.

Substitution of bromine with fluorine was then accomplished by use of silver(I)-fluoride. The silver metal drives the substitution of the bromide ion forward by formation of a stable silver bromide complex. The reagent clearly requires a polar aprotic solvent in order to ensure solubility of the silver salt, and most commonly, acetonitrile is applied as the solvent. The reaction has to be carried out in the dark, as the silver salt is light sensitive. Under these conditions, the fluorination proceeds smoothly and yields the difluorinated product **99** (Scheme 2.9). The product is formed as a 5:1 mixture of stereoisomers indicating some degree of stereochemical crossover

in the reaction. The reaction is sluggishly under these conditions and requires several days to go to completion. The use of a sonicator considerably accelerated the reaction affording complete conversion in 6-8 hours.

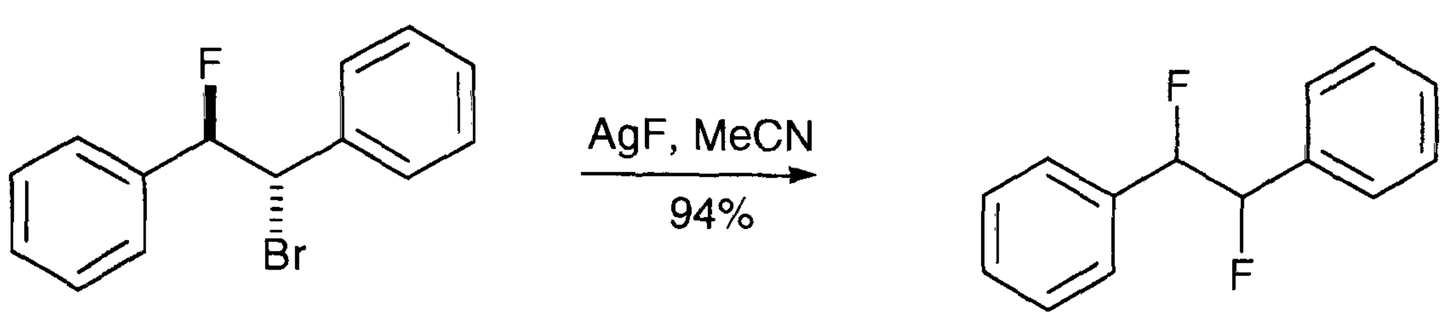

100 99

Scheme 2.9. Halogen exchange reaction with silver(I)-fluoride leading to formation of 1,2-difluoro-1,2-diphenylethane **99**.

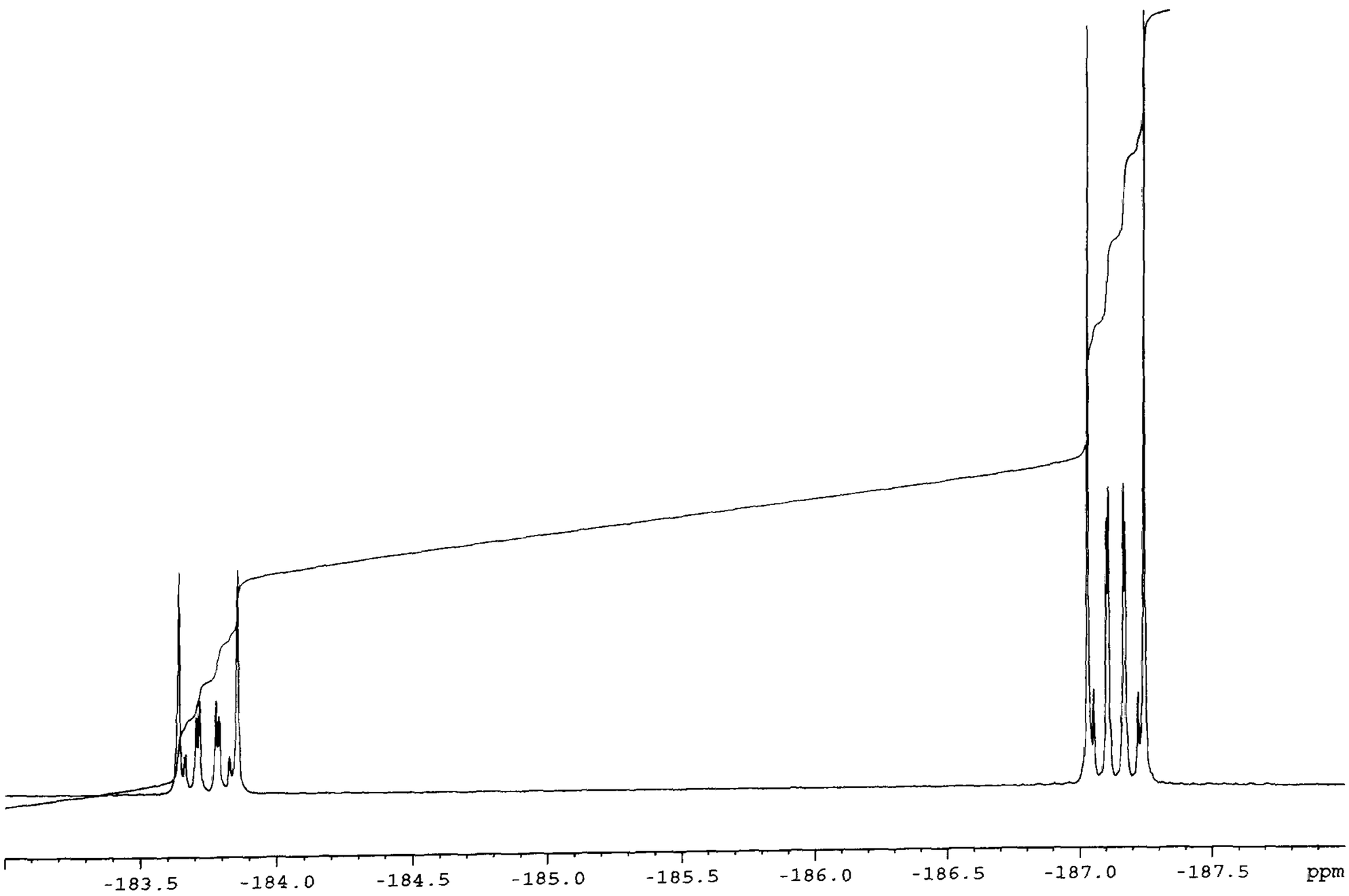

Figure 2.4. ^{19}F NMR spectrum of crude 1,2-difluoro-1,2-diphenylethane **99** obtained after the one-pot procedure. The major isomer has the *erythro* configuration, which appears upfield (-187.1 ppm) relative to the *threo* isomer (-183.5 ppm). [23]

The reaction is considerably faster when silver fluoride is added directly after the previous reaction step without isolating **100**. The one-pot reaction however lead to significant loss of stereoselectivity as indicated by GC-MS and ^{19}F NMR spectroscopy, where both stereoisomers were obtained in a 3:1 ratio (Figure 2.4). It was assumed that the highly polar HF/pyridine complex stabilises a possible carbocation-like intermediate during nucleophilic substitution, such that the reaction proceeds with considerable S_N1 character.

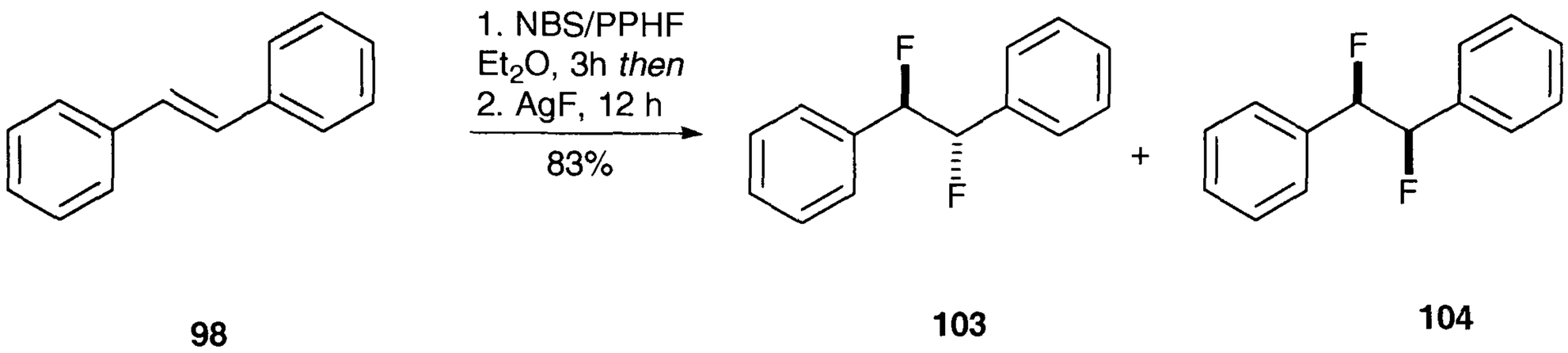

98 **103** **104**

Scheme 2.10. Olah's one pot double fluorination procedure generates 1,2-difluoro-1,2-diphenylethanes as a mixture of *erythro* and *threo* diastereoisomers **103** and **104**. The *erythro* compound **103** is obtained as the major isomer in the reaction.

The one pot procedure yields *erythro* 1,2-difluoro-1,2-diphenylethane **103** as the major isomer (Scheme 2.10). The compound was isolated by crystallisation, which afforded the pure stereoisomer after several crystallisation steps. In contrast, isolation of the *threo* stereoisomer **104** proved to be a tedious process. Although enough material was obtained for crystallographic studies (Figure 2.8, page 61), the amount of pure *threo* 1,2-difluoro-1,2-biphenylethane **104** was insufficient for preparative purposes. Therefore, alternative methods were investigated to obtain 1,2-difluoro-1,2-biphenylethane **104**. It was assumed that the stereogenic centre of the bromofluoro intermediate **103** can be inverted by means of a Finkelstein reaction, which involves the exchange of bromide or chloride with iodide in acetone as the solvent.[24]

Compound **103** was initially unreactive towards iodide even at elevated temperatures.[25] This observation is somewhat unexpected as benzyl halogenides, as well as allyl halogenides and α-halocarboxylic acids are known to be readily amenable to this conversion.[26] Clearly, the C-F bond adjacent to the reactive centre has a deactivating effect and renders the starting material unreactive.

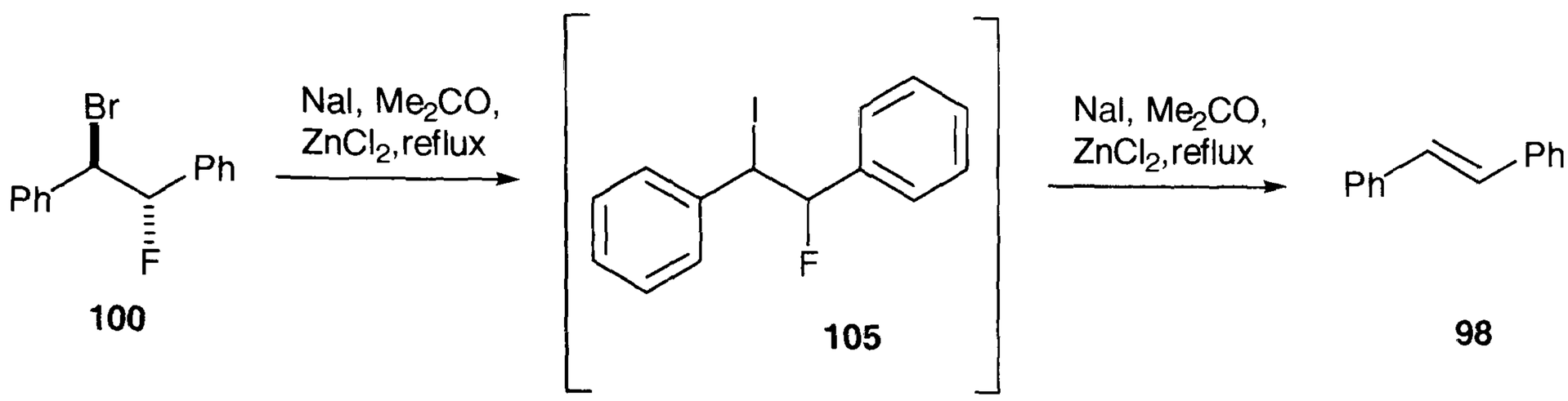

Scheme 2.11. Attempted Finkelstein conversion of 1-bromo-2-fluoro-1,2-diphenylethane **100**.

The reaction was repeated in the presence of zinc chloride (Scheme 2.11). The presence of the Lewis acid has been reported to accelerate the Finkelstein exchange by complexation of the carbon bound halogen.[27] According to the literature procedure, a complex product mixture was obtained in which the iodofluoro compound **105** was identified as a minor product by GC-MS analysis. Surprisingly, *trans*-stilbene **98** was identified as the major component in this reaction.

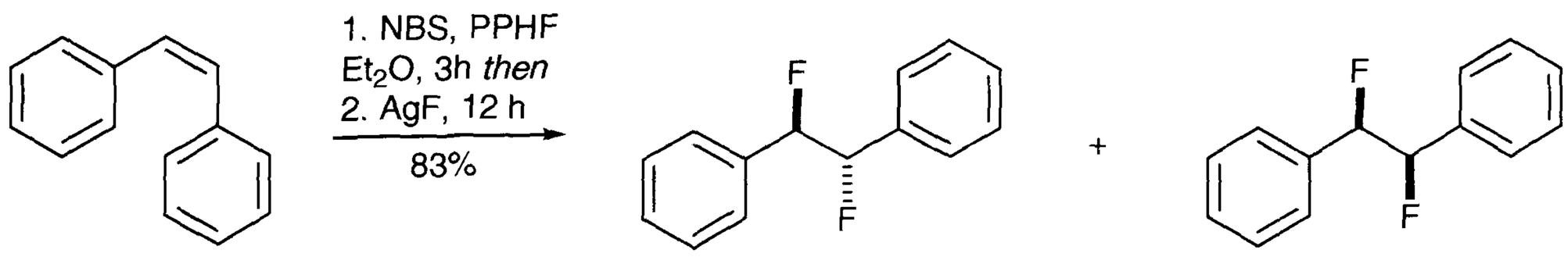

105 **103** **104**

Scheme 2.12. Conversion of *cis*-stilbene **106** again leads to formation of the *erythro* 1,2-difluoro-1,2-diphenylethane **103** as the major isomer.

The possibility of obtaining *threo* 1,2-difluoro-1,2-biphenylethane **104** by using *cis*-stilbene **102** as the starting material was also investigated. The reaction proceeds smoothly under the standard conditions and gave the difluoro compounds after addition of silver fluoride. Surprisingly, the *erythro* compound **103** again emerges as the major stereoisomer in the reaction. The reaction is less stereoselective in comparison with the conversion of *trans* stilbene **98** (Table 2.1).

Table 2.1. Diastereoisomeric ratios of **103** and **104** formed from *cis* and *trans* stilbene.

Starting material	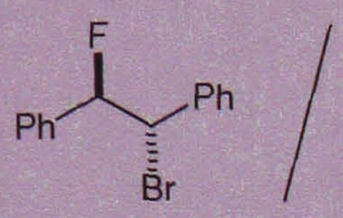	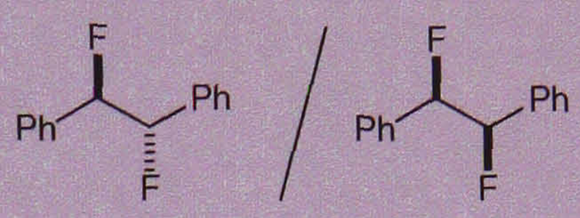
***trans*-stilbene**	94% de	56% de
***cis*-stilbene**	76% de	47% de

The formation of the *erythro* isomer **100** as the major product is clearly a result of internal rotation about the central carbon-carbon bond after initial formation of a bromonium ion **106**. The driving force for this process is most likely a steric clash between the large phenyl substituents. The carbocationic centre of the intermediate **107** may then be shielded from one side by the large bromine atom forcing fluoride ion attack from the opposite side to give the *anti*-addition product **100** (Scheme 2.13).

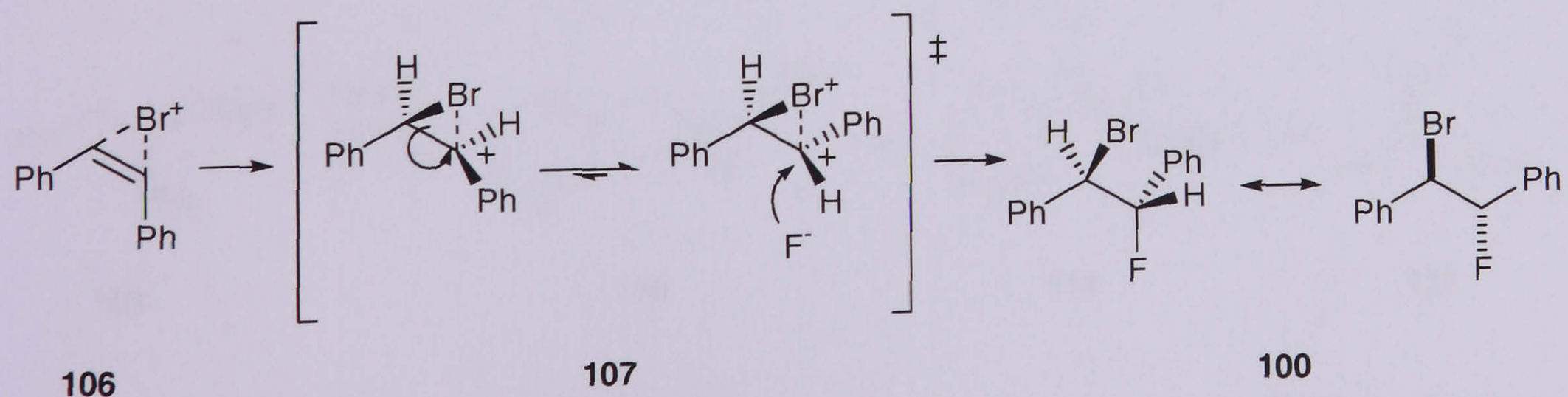

106 **107** **100**

Scheme 2.13. Proposed mechanism of the bromofluorination reaction according to an *anti* addition mechanism.

The substitution process may also involve neighbouring group participation by the phenyl ring. The stereochemical outcome of the reaction suggests a double inversion mechanism, in which bromine is activated as a silver complex, and the carbocation **108** thus formed is stabilised by the adjacent phenyl ring (Scheme 2.14).

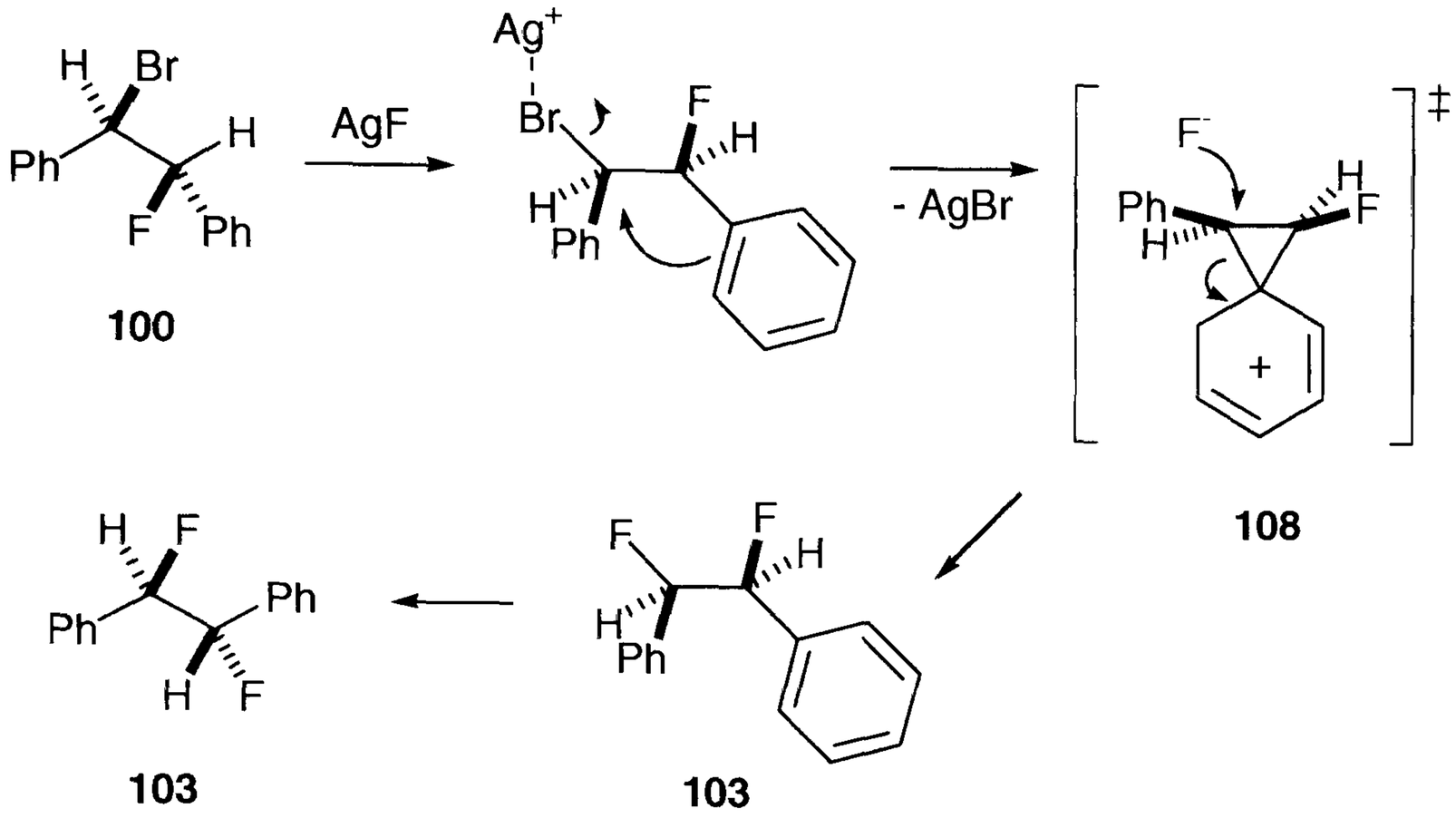

Scheme 2.14. Proposed mechanism for the formation of *erythro* 1,2-difluoro-1,2-diphenylethane **103** from 1-bromo-2-fluoro-1,2-diphenylethane.

Various examples for neighbouring group participation or anchimeric assistance by phenyl groups have been reported in the literature.[28] For example, the existence of a phenonium ion was suggested in benzilic rearrangements,[29] and also to explain the rearranged products resulting from diazotisation of phenylalanine (Scheme 2.15).

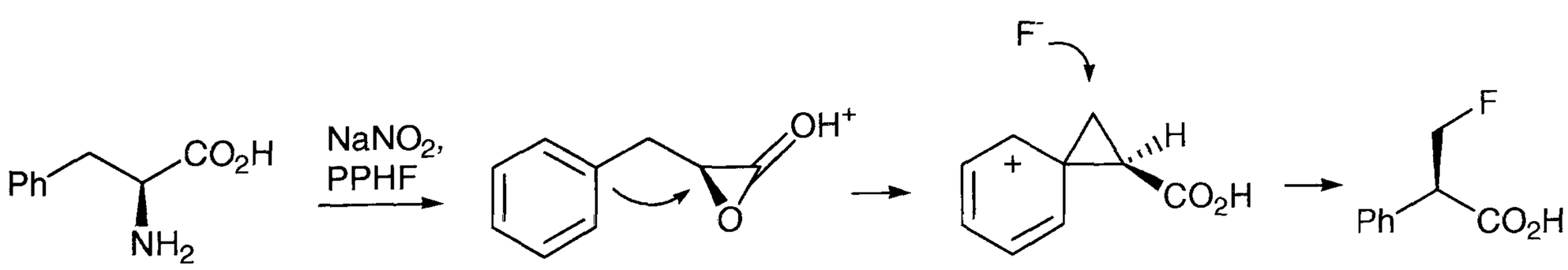

109 **110** **111** **112**

Scheme 2.15. The rearrangement of L-phenylalanine **109** presumably proceeds *via* the phenonium ion **111**, which results in the formation of β-fluoro acid **112**.[30]

An elegant experiment to prove the existence of the phenonium ion has been developed from tosylate esters of 3-phenylbutan-2-ol. Treatment of optically active *threo*-tosylate **113** with acetic acid led to complete loss of stereochemical integrity by formation of racemic *threo* acetates **115** and **116** (Scheme 2.15).

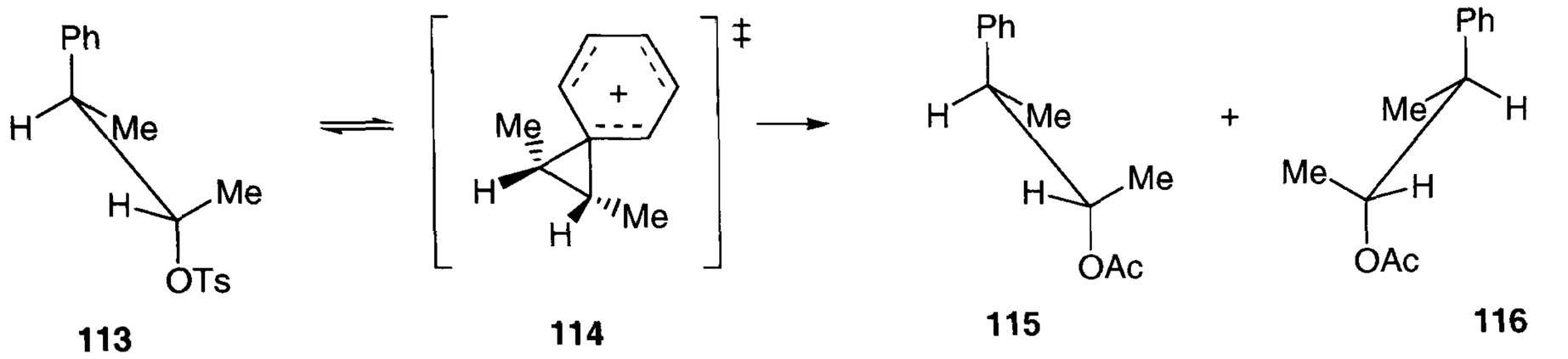

113 **114** **115** **116**

117 **118** **119**

Scheme 2.15. Solvolysis of the optically active *threo*-tosylate ester **113** leads to the formation of enantiomers **115** and **116**. In contrast, the *erythro* tosylate **117** gives only a single enantiomer **119**.[31]

In contrast, the optically active *erythro* tosylate **117** afforded the optically active *erythro*-acetate **119** in a similar reaction. The stereoselectivities can be understood by formation of intermediate phenonium ion **114** and **118**, which are subsequently attacked by the solvent from either side of the structure.

Investigation of the physical properties of 1,2-difluoro-1,2-diphenylethanes required separation of the diasteroisomers. The *erythro* compound **103** was readily purified from the mixture of diastereoisomers after several crystallisation steps. The crystals appeared as white needles after crystallisation in cold methanol or hexane (Figure 2.5).

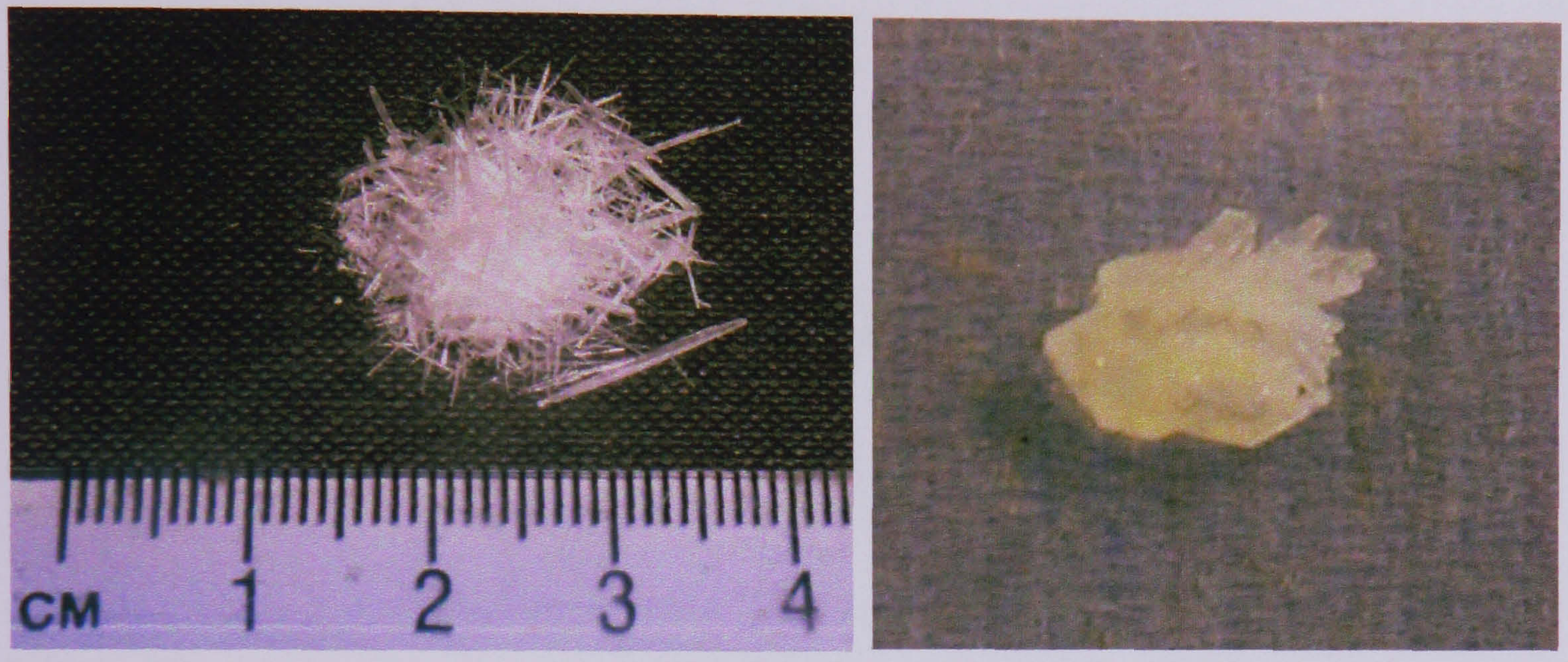

Figure 2.5. Crystals of *erythro* 1,2-difluoro-1,2-diphenylethane **103** (left) and its *threo* isomer **104** (right) obtained after recrystallisation from hexane.

Isolation of the *threo* isomer **104** however proved to be more challenging. Separation of a 1:1 mixture of diasteroisomers obtained on silica led to quick elution of the compounds. Interestingly, under GC-MS conditions using a polar column the diastereoisomers separated readily with the *threo* isomer **104** eluting before the *erythro* isomer **103**. This may indicate a lower boiling point of the *threo* isomer **104** compared to **103**, rather than a difference in polarity of the two compounds.

In the crystal structure, *erythro* 1,2-difluoro-1,2-diphenylethane **103** adopts a conformation in which the large phenyl substituents are *anti* to each other, with a C(2)-C(1)-C(1A)-C(2A) torsion angle of 180 °. The C-F bonds align *anti* with respect to each other, with a F(1)-C(1)-C(1A)-F(1A) torsion angle close to 180 ° (Figure 2.6).

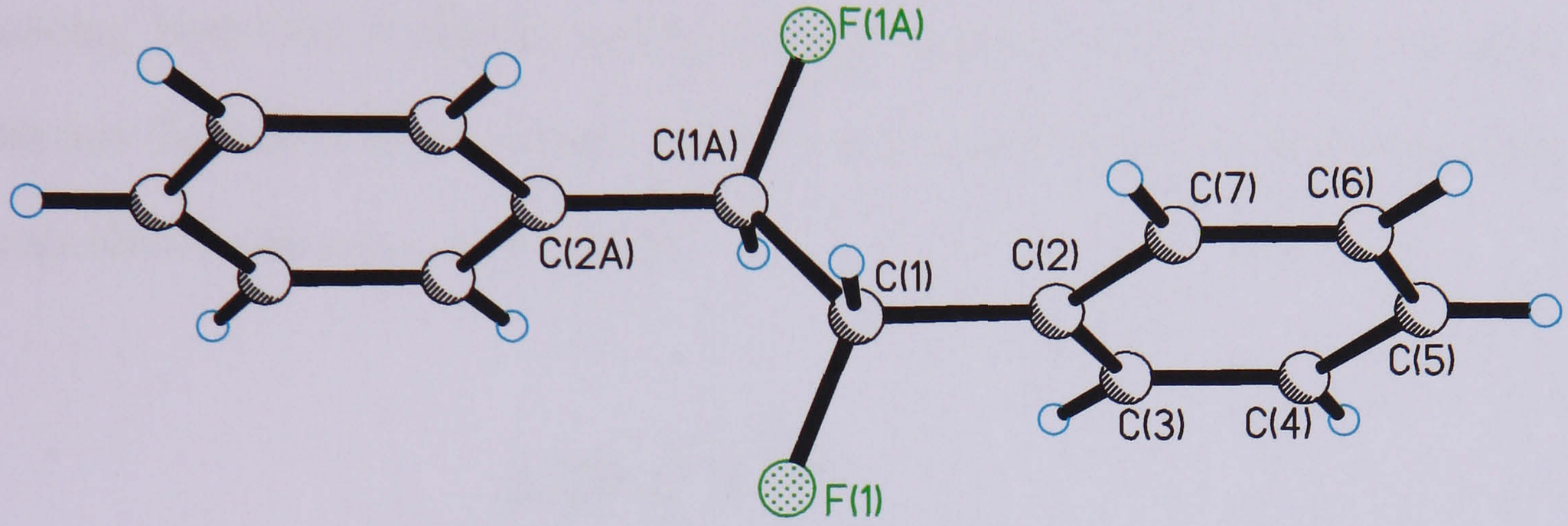

Figure 2.6. Crystal structure of *erythro* 1,2-difluoro-1,2-diphenylethane **103**. Selected bond lengths (Å), bond angles (°), and torsion angles (°): C2A-C1A 1.538(11), C1A-F1A 1.343(7), C1A-C1 1.314(15), C1-F1 1.343(7), C1-C2 1.538(11); C2A-C1A-F1A 112.4(6), F1A-C1A-C1 118.4(10), F1A-C1A-H1AA 100.7, C2A-C1A-C1 119.2(9), C1A-C1-C2 119.2(9), F1-C1-C2 112.4(6); C2A-C1A-C1-C2, F1A-C1A-C1-C2, F1A-C1A-C1-F1, F1-C1-C1A-C2A.

The *gauche* effect predicts a conformation in which two *vicinal* C-F bonds align *gauche* rather than *anti* to each other. This is clearly not the case for this molecule. Although a stereoelectronic preference to align the C-F bond *gauche* may exist, this conformation has to compete with the sterically less strained structure in which the large phenyl substituents oppose each other. The current conformation is not only the most favourable in terms of steric effects, but also avoids electrostatic repulsion of the electronegative fluorine nuclei. Also dipole-diplole compensation may play an important contribution in stabilising the current structure.

Intermolecular forces may be crucial in influencing the molecular conformation. This includes in the first instance hydrogen bonding which is however considered to be weak in case of C-H···F interactions. In general, stabilisation by hydrogen bonding is essentially limited to distances of approximately 2.7 Å (Chapter 1.7), and thus, the C-H···F contacts obtained are too long to indicate significant stabilisation from hydrogen bonding. Both C-H···F distance and bond angles suggest that this interaction is weak and that the short C-H···F contacts merely appear as a result of the geometry of the molecular conformation in the unit cell.

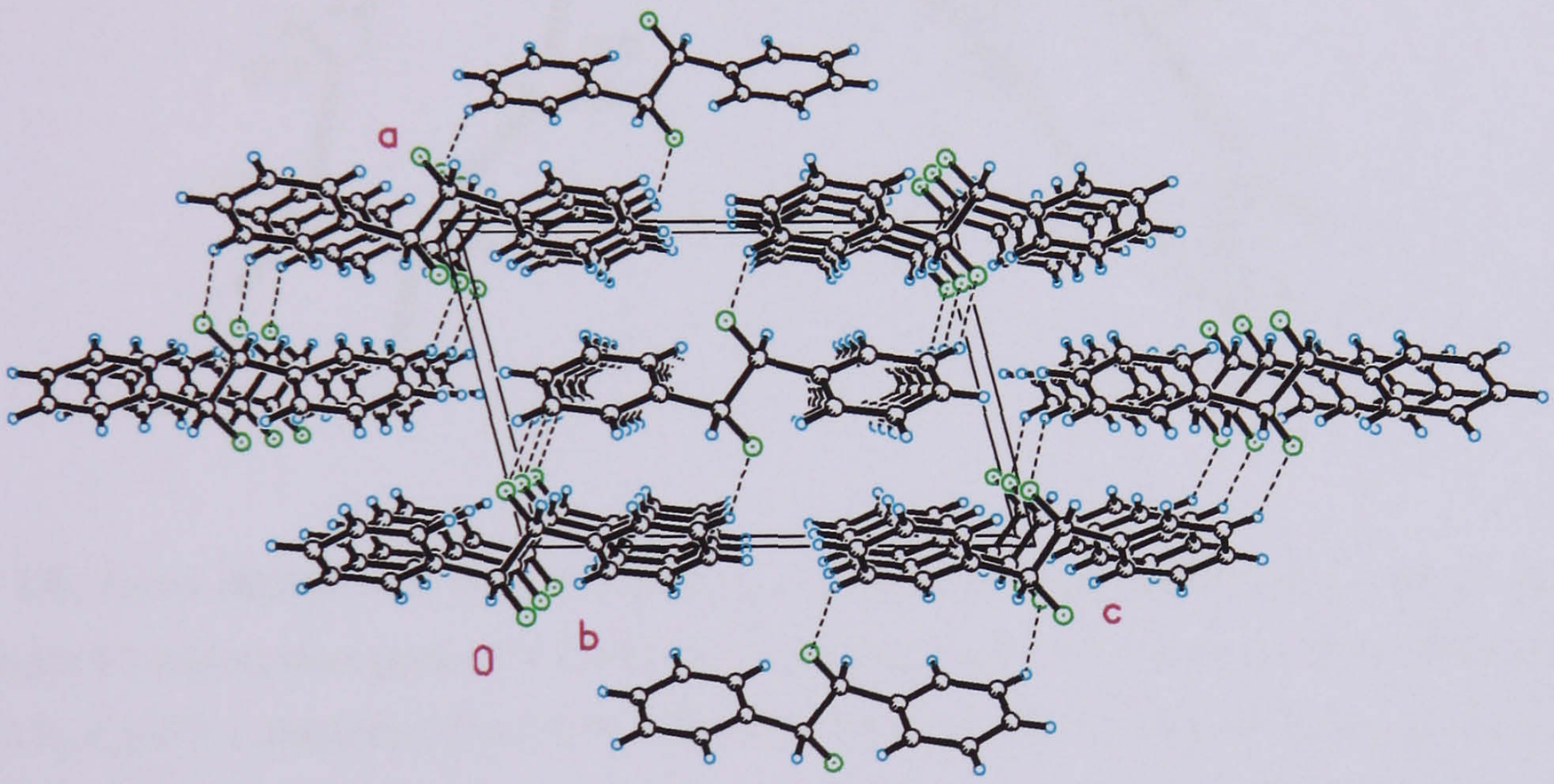

Figure 2.7. Crystal packing and unit cell of *erythro* 1,2-difluoro-1,2-diphenylethane **103** as viewed along the c-axis. The dashed lines indicate short C-H···F contacts.

More important for the current structure may be intermolecular forces that arise from interaction of the phenyl rings, so-called π–stacking interactions. The molecules align along the c axis in such a way that the phenyl groups are parallel and in close proximity to each other, which may indicate face to face π-stacking (Figure 2.7). Such effects have been reported previously to stabilise such structures in the solid state.[32]

Samples of pure *threo* isomer **104** were obtained from diastereomerically-enriched mixture of **103** and **104** obtained from thin-layer chromatography (TLC). The samples could be crystallised to purity, which afforded crystals suitable for X-ray analysis (Figure 2.8).

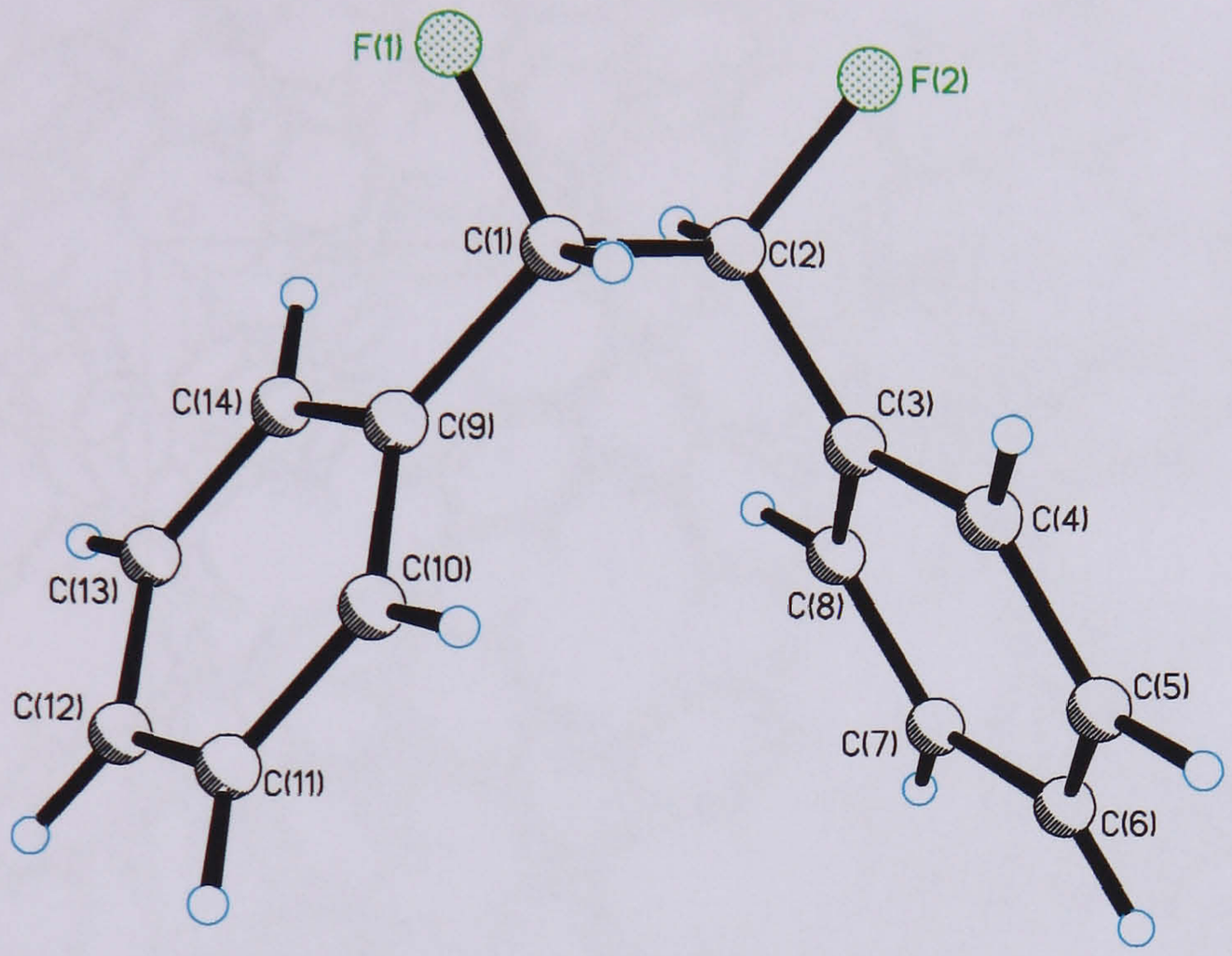

Figure 2.8. X-ray structure of *threo* 1,2-difluoro-1,2-biphenylethane **104**. Selected bond length (Å), bond angles (°) and torsion angles (°): C9-C1 1.5066(16), C1-F1 1.4124(12), C1-C2 1.5190(16), C2-F2 1.4143(13), C2-C3 1.5064(16); C9-C1-F1 109.29(9), F1-C1-C2 106.33(9), F1-C1-H1A 109.4, C1-C2-F2 106.40(9), F2-C2-C3 109.64(9), C1-C2-C3 113.29(9); C9-C1-C2-C3 -59.31(13), F1-C1-C2-C3 -179.24(9), F1-C1-C2-F2 60.23(11), F2-C2-C1-C9 -179.84(9).

The most obvious feature in the X-ray derived structure of the *threo* isomer **104** is the *gauche* relationship of the C-F bonds. This conformation is rather unexpected, as the large phenyl groups come close in proximity to each other, as do the fluorine atoms. This conformation certainly results in some degree of steric and electrostatic repulsion, which has to be compensated for by electronic effects. The argument of a σ - σ^* hyperconjugation of C-H and C-F bond is certainly not valid for the stabilization of this particular *gauche* structure, as the C-F bonds are rather perpendicular to the C-H bonds. A possible rationale may derive from the bend bond theory,[33] which predicts

better σ C-C orbital overlap in the *gauche* conformation compared to the *anti* in *vicinal* difluoro compounds. The crystal packing was analysed in order to assess the influence of intermolecular forces on molecular conformation (Figure 2.9).

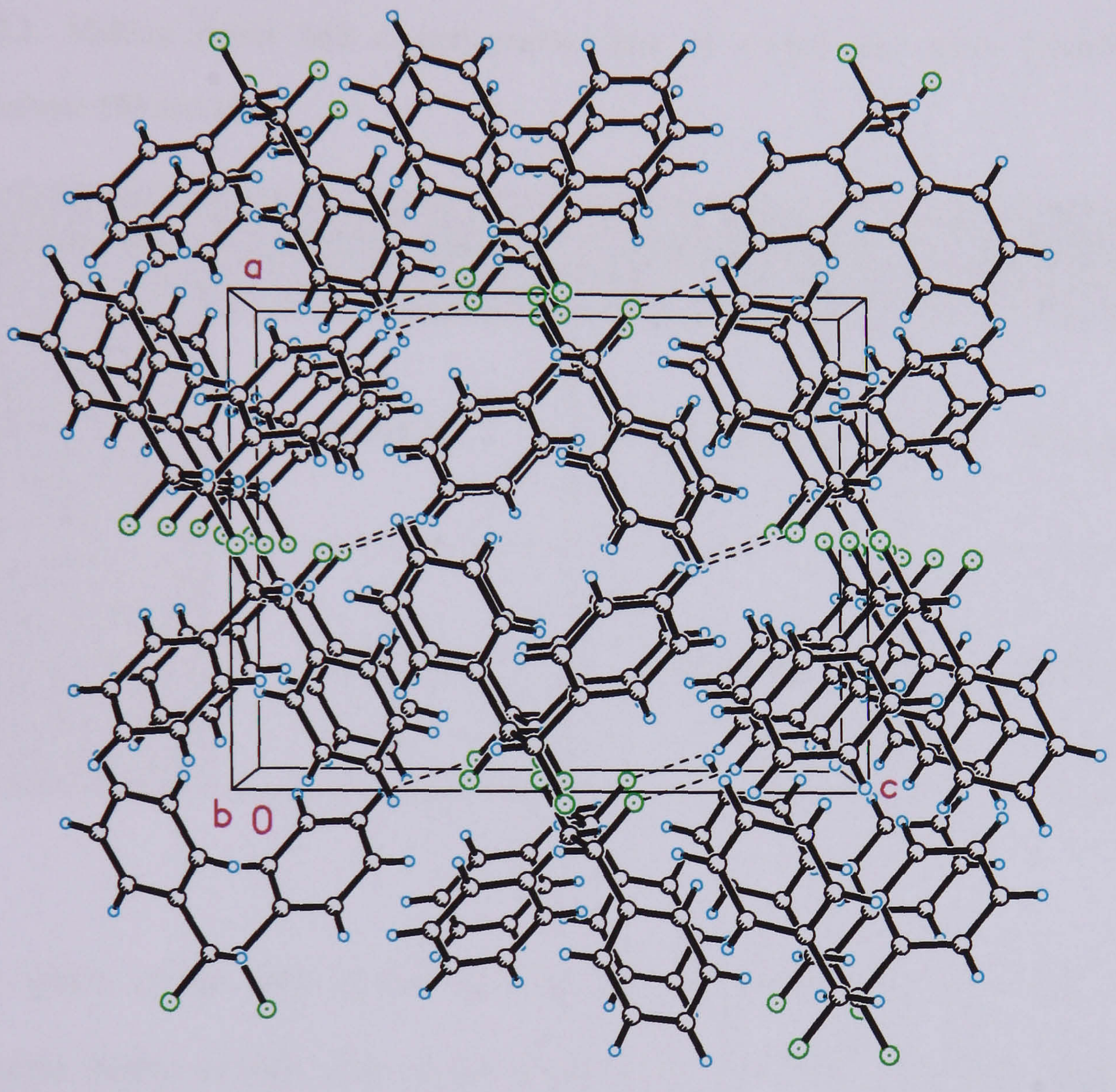

Figure 2.9. Crystal packing of *threo* 1,2-difluoro-1,2-diphenylethane **104** as viewed along the c-axis. The dashed lines denote short C-H···F contacts.

The crystal packing is dominated by face to face π-stacking of the phenyl rings. Again the distance of the C-H···F contact does not suggest a significant contribution to stabilising this conformation. Stabilisation of the conformations by hyperconjugation would be most effective when the C-F bonds are *anti* to the C-H bonds, which is not observed in both structures. Thus, the conformations of both diastereoisomers do not appear to be influenced significantly by stereoelectronic effects.

Melting points of analytically pure samples of the diasteroisomers were compared in order to establish differences between the two diastereoisomers in terms of their physical properties (Table 2.2).

Table 2.2. Melting points and crystallographic data of *erythro* and *threo* 1,2-difluoro-1,2-diphenylethane **103** and **104**.

Compound	Melting point	Crystal system	Space group
 **104**	94-95 °C	monoclinic	P2(1)/n
 **103**	102-103 °C	monoclinic	P2(1)/n

Similar space group and crystal systems for the diastereoisomers may indicate comparable lattice energy. The observed melting point difference may in principle arise from conformational mobility of the individual molecules in the crystal packing, which in turn may be related to steric, electrostatic or stereoelectronic effects. A more likely explanation however arises in this case from the fact that the racemic mixture of the *threo* isomer **104** is compared to the *meso* compound **103**, which represents a single stereoisomer. The melting point difference of the diastereoisomers may therefore be entirely a result of their stereochemical integrity.

2.1.3 Synthesis of 2,3-difluorosuccinic acids

The synthesis of 2,3-difluorosuccinic acids **120** was achieved from 1,2-difluorobiphenylethanes (Scheme 2.16). This transformation involves oxidation of the aryl rings into carboxylic acids, which requires strong oxidising conditions often resulting in low yields and by-product formation. Some literature is available on this process, however it had to be established if the carbon-fluorine bonds would be amenable to such conditions.

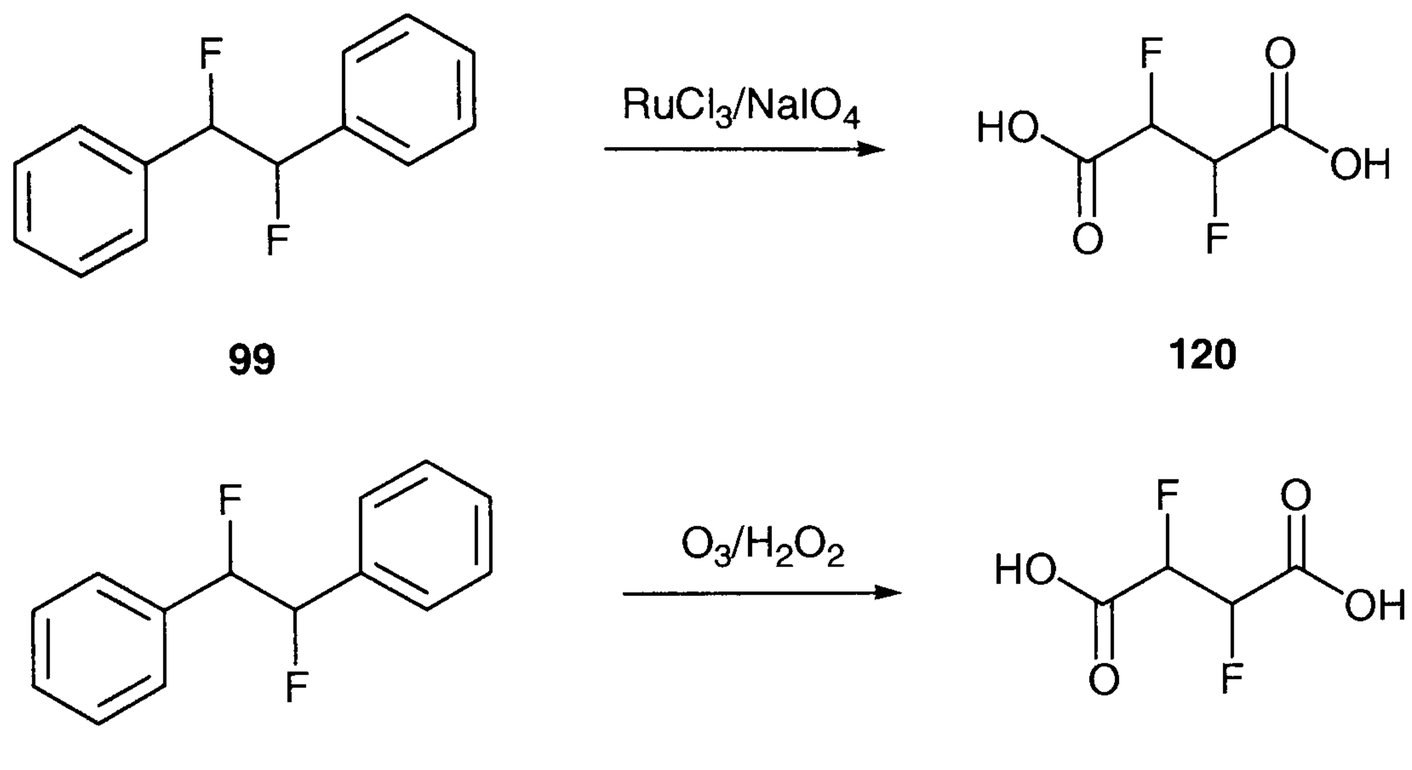

99 **120**

99 **120**

Scheme 2.16. Oxidation of 1,2-difluoro-1,2-diphenylethanes **99** to generate the stereoisomers of 2,3-difluorosuccinic acid **120**.

Oxidative degradation of aromatic rings can be achieved with ruthenium tetraoxide, generated *in situ* from $RuCl_3$ and $NaIO_4$ (Scheme 2.16).[34] The reagent is most commonly used for the oxidation of terminal hydroxyl groups to carboxylic acids, a process that tolerates the presence of a carbon-fluorine bond.[35] A clean and rather gentle method involves ozonolysis followed by oxidative work up with hydrogen peroxide (Scheme 2.16).

The most obvious synthetic approach in generating the target compounds **120** involved halofluorination of the double bond in fumarate and maleate **121**. The reaction has been reported using a combination of *N*-bromoacetamide and anhydrous hydrogen fluoride.[36] Conversion of diethyl maleate and fumarate **121** has been reported to result in the formation of the bromofluoro adducts **122**, which may undergo a halogen exchange reaction to afford the *vicinal* difluorosuccinates **120**. The conversion of α-bromoesters has been achieved with silver fluoride in refluxing acetonitrile (Scheme 2.17).[37]

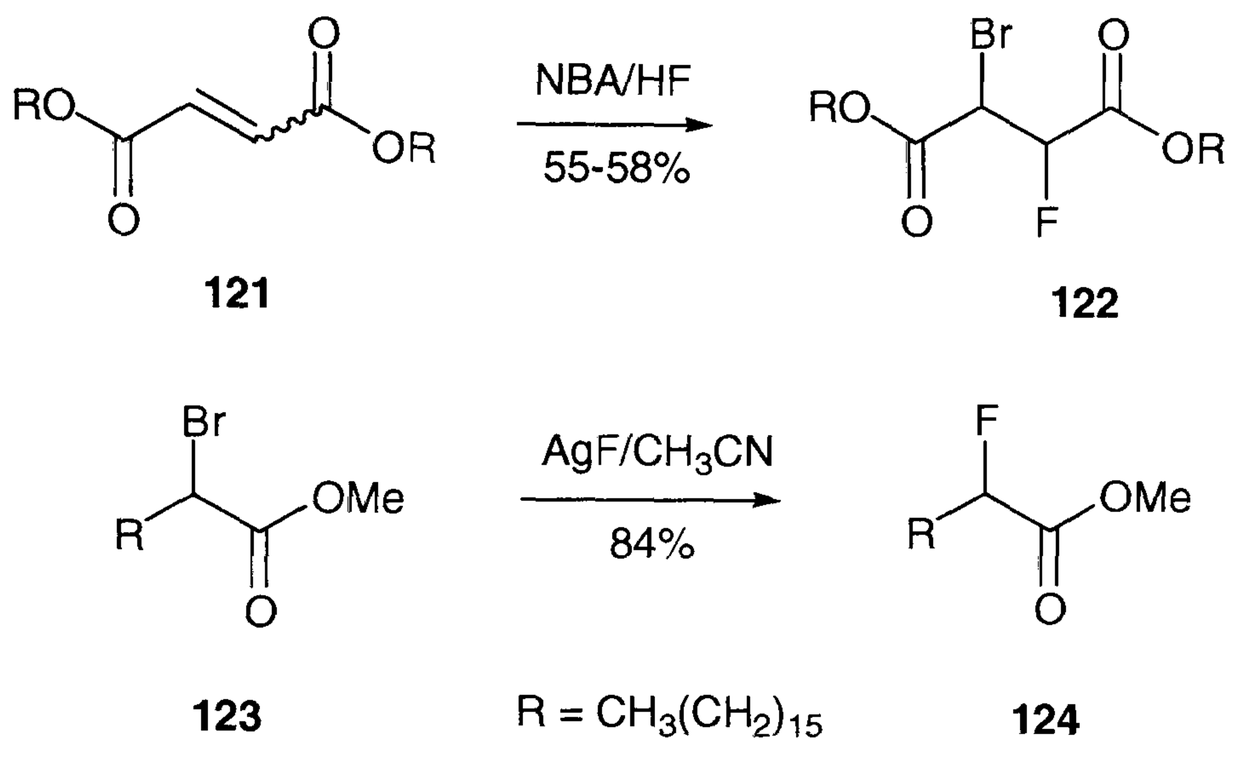

Scheme 2.17. Alternative routes to 2,3-difluorosuccinic acid **120** involving a bromofluorination step with *N*-bromoacetamide (NBA) and hydrogen fluoride and subsequent halogen exchange.

The reaction did not proceed when hydrogen fluoride was substituted for the safer alternative PPHF. Employing NBS and PPHF at room temperature for the conversion of diethyl maleate or diethyl fumarate, the desired products were not formed. Also, the conversion of the free carboxylic acids was not achieved under these conditions and application of *N*-iodosuccinimide or *N*-bromoacetamide did also not facilitate the reaction. Apparently, the process crucially depends on the presence of free hydrogen fluoride and consequently, alternative methods had to be considered.

The phenyl group may be considered to be a latent carboxylic acid functionality, which can be demasked by oxidation of the aromatic ring. The conversion of 1,2-difluoro-1,2-biphenylethanes **99** would thus furnish the desired 2,3-difluorosuccinates **120** (Scheme 2.18).

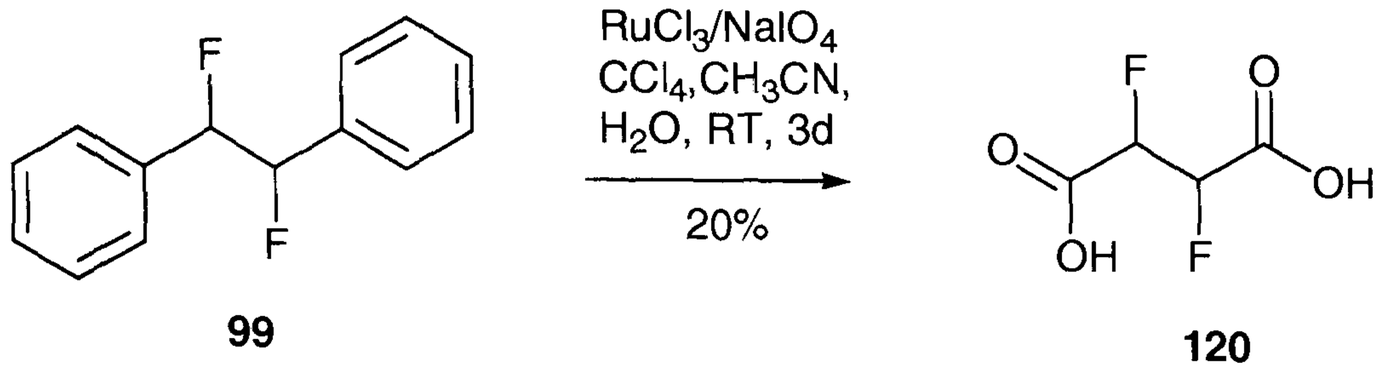

Scheme 2.18. Synthesis of 2,3-difluorosuccinic acid **120** by oxidative degradation of the aromatic rings of 1,2-difluoro-1,2-diphenylethane **99**.

The reaction requires strong oxidants as aromatic rings are chemically stable. The reaction can however be achieved using ruthenium tetroxide, which is commonly generated *in situ* from ruthenium-(III)-chloride and sodium periodate as the co-oxidant. This allows for catalytic amounts of the highly toxic ruthenium species to be used, although large amounts of inorganic waste are formed in this process.[38] The reaction afforded the desired product **120**, but only partial conversion of the starting material was observed. The crude reaction was investigated by ^{19}F NMR spectroscopy and showed various fluorine signals in the spectrum, which indicated by-product formation. Besides the lack of chemoselectivity, the reaction yields significant amounts of waste solid resulting from the 30 to 40 equivalents of sodium periodate that are necessary for the reaction. Filtration of the solid and recrystallisation in acetone indicated that the products are difficult to separate from the waste and thus the reaction did not seem to be especially useful for this particular reaction.

An alternative method for the conversion of aromatic rings into carboxylate groups involves the use of ozone (Scheme 2.16). Aromatic compounds are much less reactive towards ozone than alkenes or alkynes. The reactivity is furthermore dependent on the substituents attached to the aromatic ring. In general, electron deficient substituents decrease the rate of ozonolysis whilst the reaction becomes more feasible with electron donating substituents attached to the aromatic system. The order of increasing ease of ozonolysis in the benzene series follows the qualitative relationship: benzotrichloride < benzyl chloride < ethyl benzoate < benzene << xylenes < mesitylene < hexamethylbenzene.[39] As ozone is an aggressive, toxic, and explosive gas it is usually generated and applied as a dilute solution (approximately 3 vol%) in oxygen. Exposure to ozone can however be prevented, when the exhaust is vented through a solution of potassium iodide, thereby reducing ozone to oxygen before being released into the fume hood.

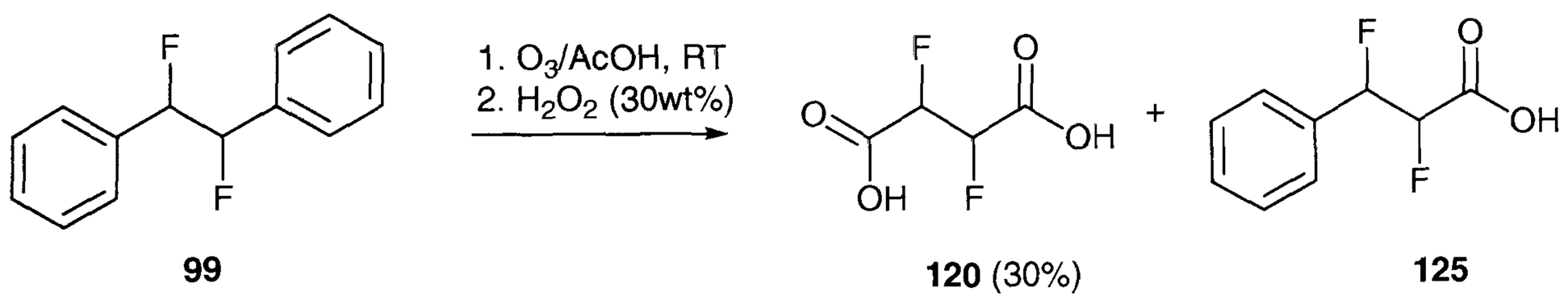

Scheme 2.18. Synthesis of *erythro* 2,3-difluorosuccinic acid **120** by oxidative degradation of the aromatic rings of 1,2-difluoro-1,2-diphenylethane **99**.

Ozonolysis of aromatic compounds had been used previously to achieve the conversion of biphenyl alkanes into dicarboxylic acids.[40] The literature procedure was carried out at room temperature using acetic acid as the solvent.[41] According to the literature procedure 1,2-difluoro-1,2-diphenylethane **99** was treated with ozone on a small scale (Scheme 2.18).

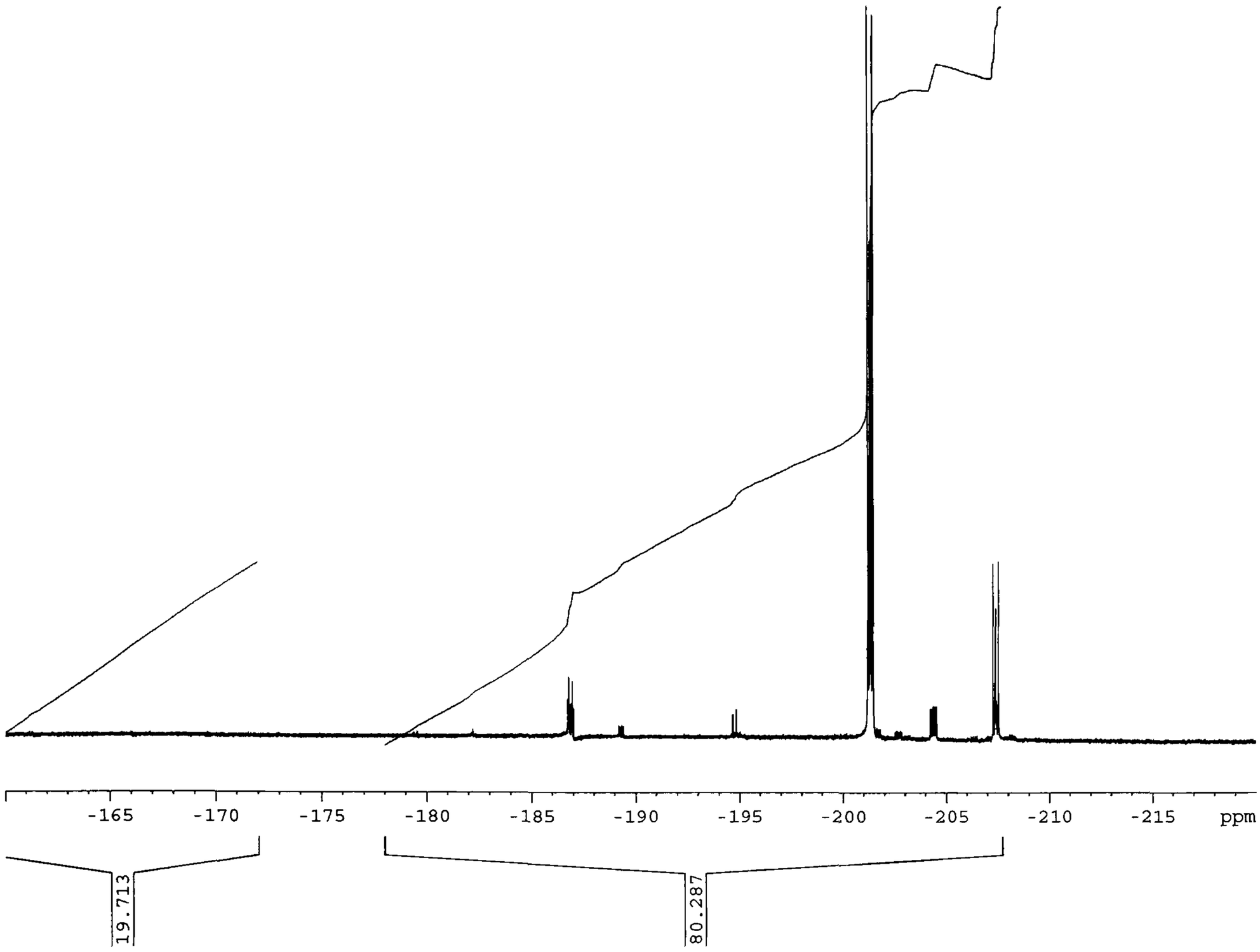

Figure 2.10. ^{19}F NMR spectrum of the crude reaction product after ozonolysis. The spectrum shows the AA'XX' pattern of the *erythro* and *threo* isomers of **120** at –202 ppm and –207 ppm respectively.

The product obtained from the reaction was investigated by means of ^{19}F NMR spectroscopy. The appearance of a new AA'XX' multiplet at –202 ppm indicated the formation of the desired product (Figure 2.10). Several other peaks were observed, including the monocarboxylic acid **125** resulting from partial oxidative degradation. Despite the occurrence of this by-product the reaction was relatively clean. Reaction of a 4:1 mixture of *erythro* and *threo* 1,2-difluoro-1,2-difluorobiphenylethane **103** and **104** led to formation of *erythro* and *threo* 2,3-difluorosuccinic acids. These compounds showed different chemical shifts at –202 ppm and –207 ppm respectively, which enables straightforward identification of the products.

Esterification of these products with methanol gave their respective dimethyl esters **126-128**. GC-MS analysis on a chiral column gave a splitting of the minor product indicating a racemic mixture. This was a clear indication that the minor stereoisomer possesses the *threo* configuration as only this compound comprises of two enantiomeric structures (Scheme 2.19).

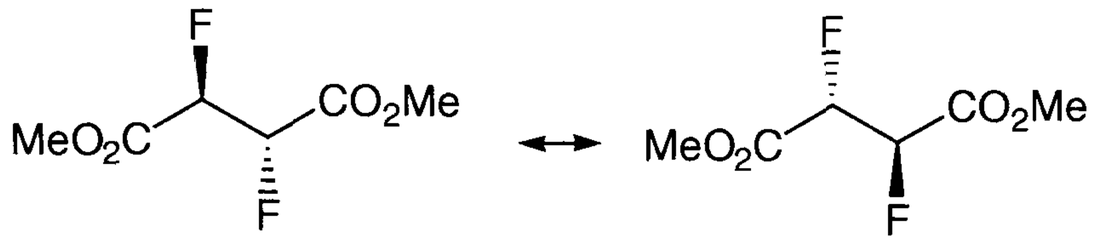

87

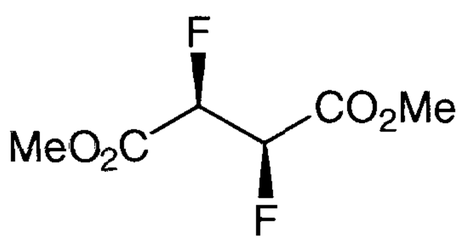

127

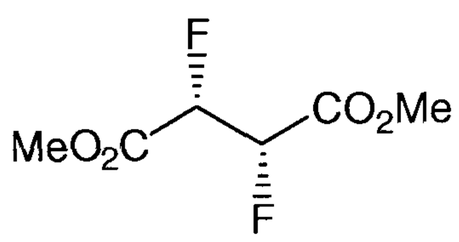

128

Scheme 2.19. The *threo* compound is a racemic mixture of **127** and **128**, whereas the *erythro* isomer **87** contains a mirror plane and therefore has a *meso* configuration.

The results were later confirmed by X-ray spectroscopy of the respective dicarboxylic acid **130** (Figure 2.11). *Erythro* 2,3-difluorosuccinic acid **130** was obtained in pure form starting from a purified sample of *erythro* 1,2-difluorobiphenylethane **103** (Scheme 2.20).

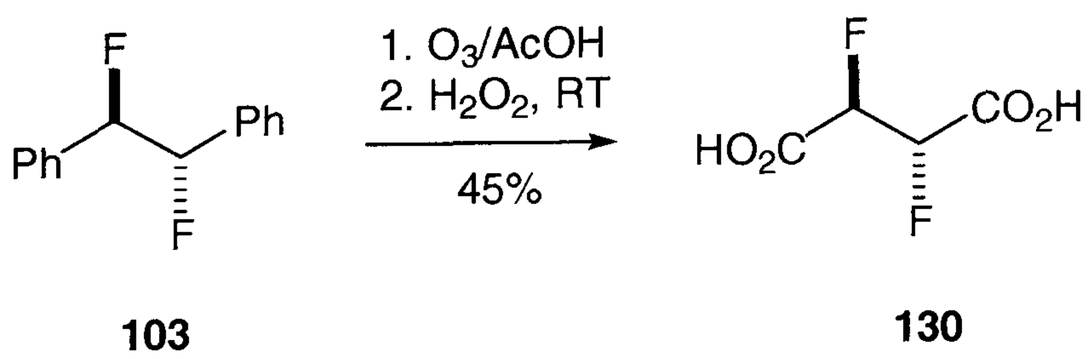

103 **130**

Scheme 2.20. Synthesis of *erythro* 2,3-difluorsuccinic acid **130** *via* ozonolysis of compound **103**.

Crystallisation of *erythro* 2,3-difluorosuccinic acid **130** proved to be difficult due to the formation of amorphous material in several common solvents. Crystals suitable for X-ray analysis were finally obtained by sublimation of the compound in *vacuo* (Figure 2.11).

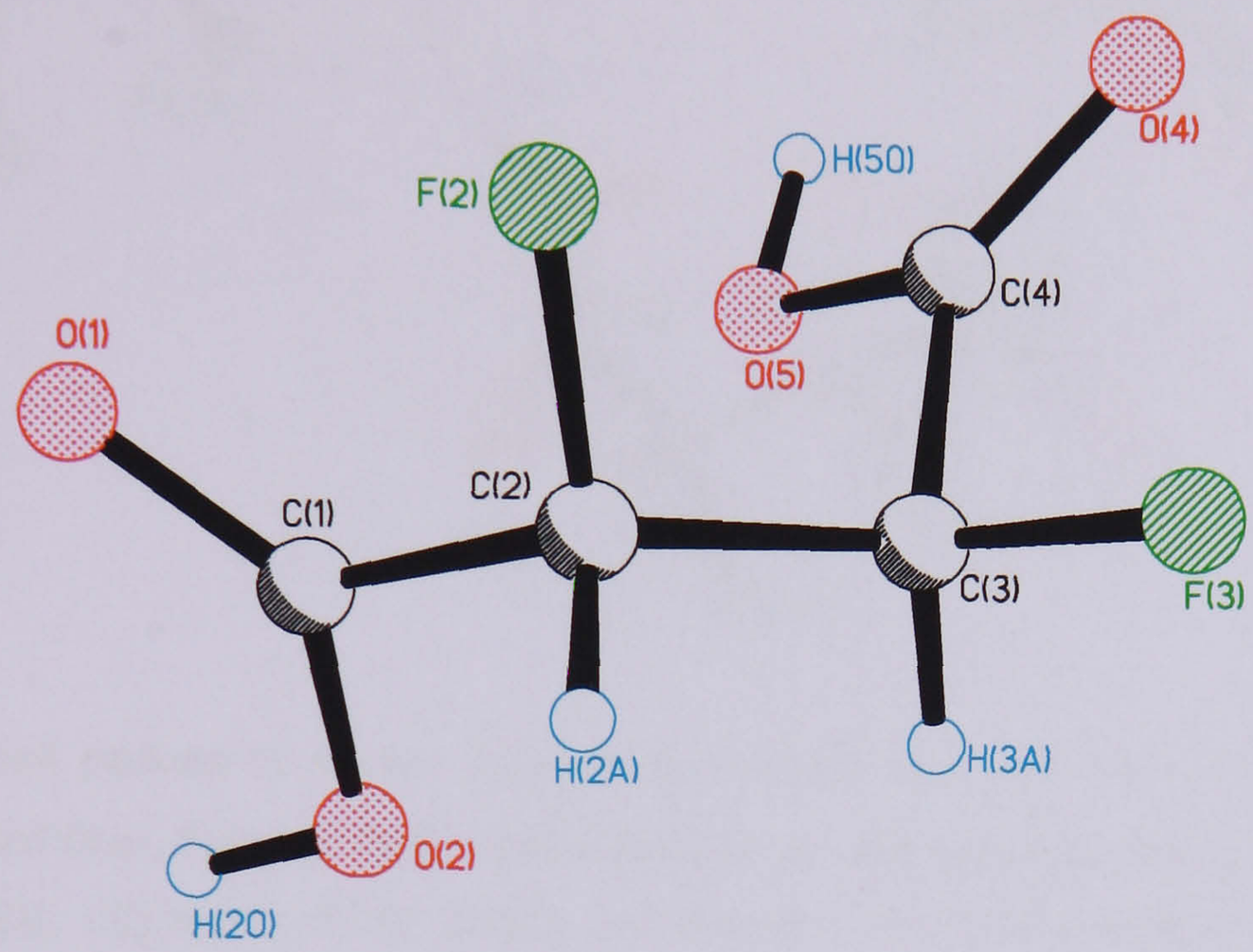

Figure 2.11. X-ray structure of *erythro*-2,3-difluorosuccinic acid **130**. Selected bond length (Å) and related angles [°]: O2-C1 1.302(2), O1-C1 1.210(2), C1-C2 1.517(3), C2-F2 1.384, C2-C3 1.525(3), C3-F3 1.380(2), C3-C4 1.524(3), C4-O4 1.203(2), and C4-O5 1.308(2) Å; O1-C1-C2-F2 10.2(2), O2-C1-C2-F2 171.70(14), F2-C2-C3-F3 65.18(17), C1-C2-C3-C4 67.7(2), F3-C3-C4-O4 –6.5(2), and F3-C3-C4-O5 173.11(14)°.

The crystal structure clearly indicates a *gauche* relationship between the *vicinal* fluorine atoms. This is consistent with the *gauche* effect, which predicts such a conformation. Interestingly both carboxyl groups prefer a specific planar conformation, which shows the carbonyl bond *syn* periplanar with respect to the C-F bonds. In the crystal packing, the carboxyl groups of two neighbouring molecules are hydrogen bonded which clearly determines the three dimensional structure of *erythro*-2,3-difluorsuccinic acid **130** (Scheme 2.12). Short O-H···F contacts are observed that are within the sum of the Van der Waals radii. These interactions are generally weak in energy terms, but they contribute to the overall stability of the crystal lattice.

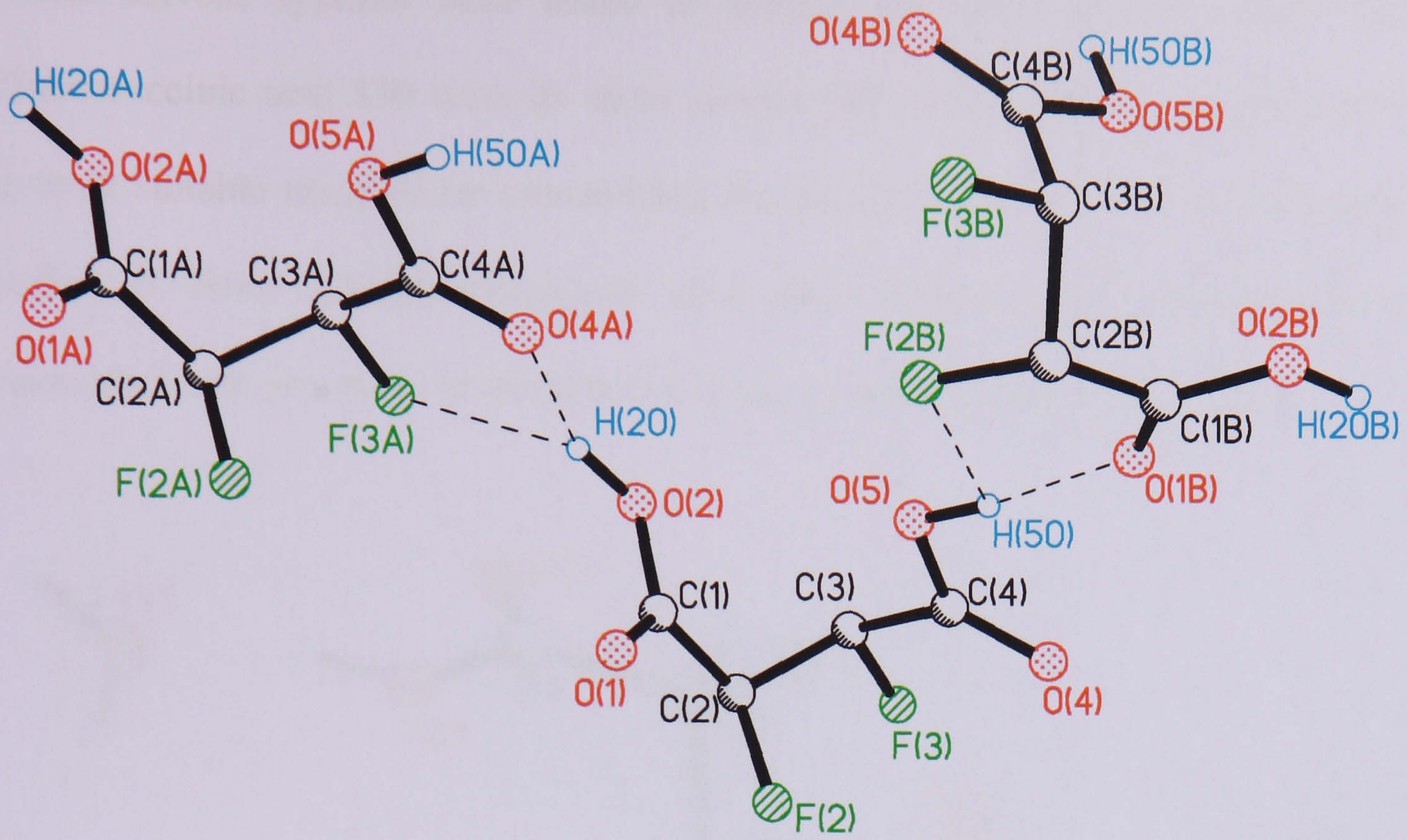

Figure 2.12. Crystal packing of *erythro* 2,3-difluoro succinic acid **130**. Short O-H···O contacts are illustrated by dashed lines. Selected interatomar distances (Å) and related angles [°]: O2-H(2O)···O4#1 1.709(10) [<159(2)], O2-H(2O)···F3#1 2.28(2) [<118.6(18)], O5-H(5O)···O1#2 1.697(6) [<167(3)], O5-H(5O)···F2#2 2.52(3) [<112.0(19)].

Crystallisation of a mixture of 2,3-difluorsuccinic acids **130** and **132** did not facilitate the isolation of the *threo* isomer **132**. Therefore the mixture was converted to the corresponding methyl esters and purified by silica gel chromatography. Acidic hydrolysis allowed the 2,3-difluorosuccinic acids **120** to be isolated as a mixture of diastereoisomers (Scheme 2.21).

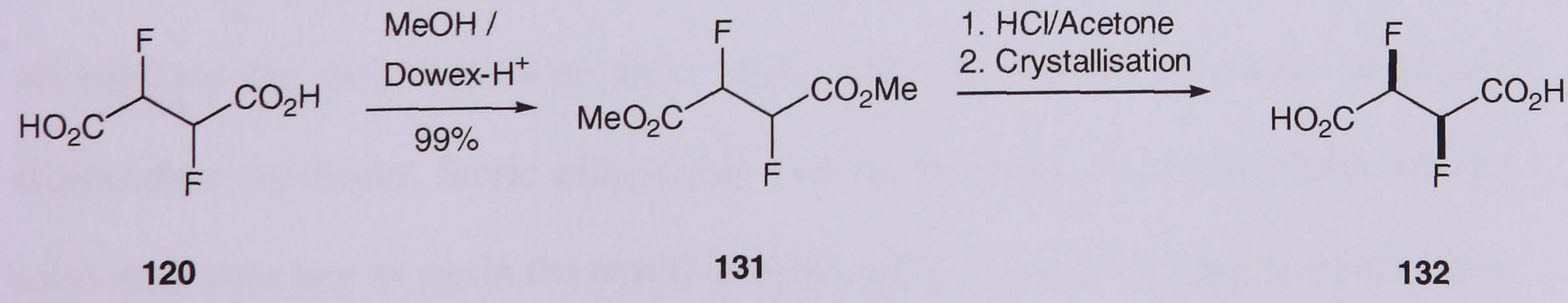

120 **131** **132**

Scheme 2.21. Purification of 2,3-difluorosuccinic acid. The crude dicarboxylic acid **120** is converted into its dimethyl ester **131** and then hydrolysed with hydrochloric acid. Selective crystallisation of the *threo* isomer **132** is achieved in a benzene/acetone mixture.

Several solvent systems were tested to achieve the separation of *erythro* 2,3-difluorosuccinic acid **130** from its *threo* isomer **132**. Acetone/benzene proved to be the most suitable medium for crystallising the racemic *threo* isomer. The colourless needles of *threo* 2,3-difluorosuccinic acid **132** obtained from crystallisation in acetone/benzene proved to be suitable for X-ray crystallography (Figure 2.13).

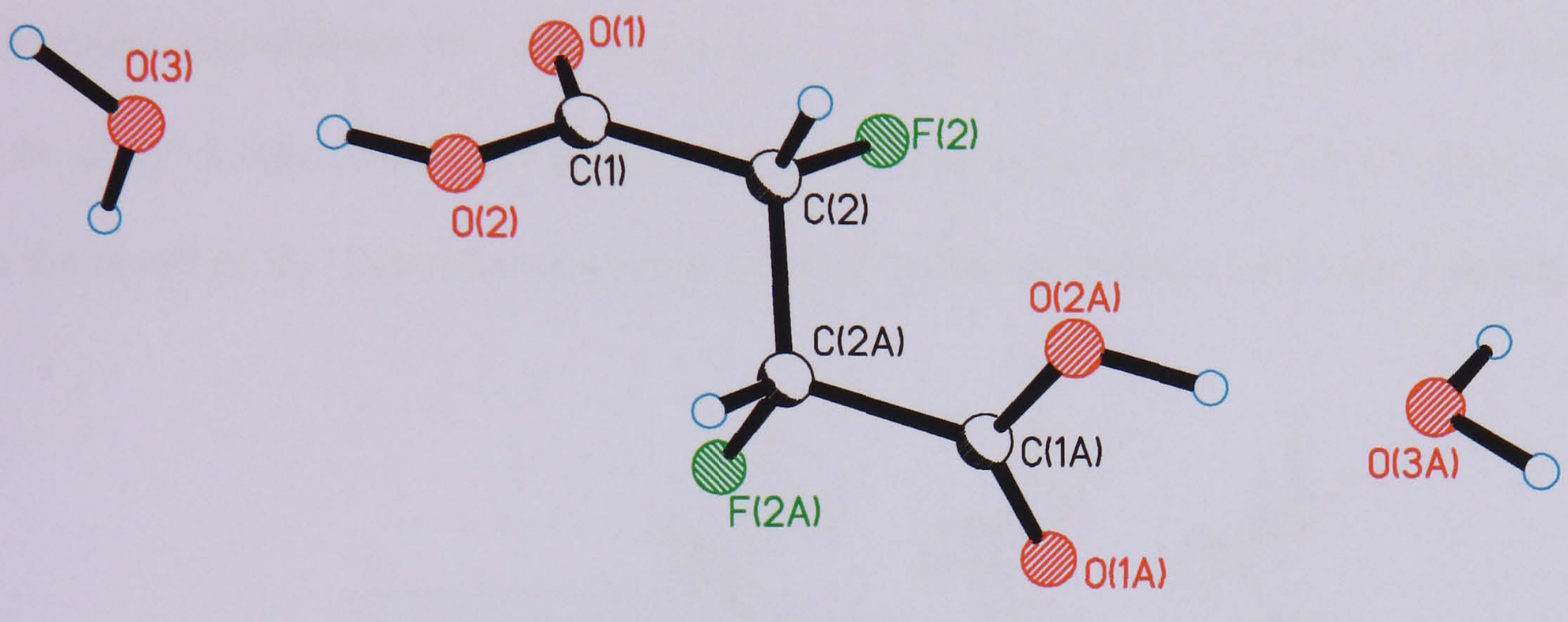

Figure 2.13. X-ray structure of *threo* 2,3-difluorosuccinic acid **132**. Selected bond lengths (Å) and torsion angles [°]: O1-C1 1.3059(17), O2-C1 1.3059(17), C1-C2 1.5297(17), C2-F2 1.3799(16), C2-C2A 1.518(2) Å; O1-C1-C2-F2 –5.57(17), O2-C1-C2-F2 175.62(9)°, F2-C2-C2A-F2A 65.3(20)°. The C2A-F2A bond length and O2A-C1A-C2A-F2A torsion angle are identical to the aforementioned values due to the symmetry of the molecule. The molecule has a symmetry plane and therefore the O-H···F distance outlined for the F(2) atom is the same for the F(3) atom.

The crystal structure shows the molecule in an extended chain conformation with both C-F bonds *gauche* to each other. Not surprisingly, the carboxyl groups as the largest substituents are pointing away from each other as a result of steric strain and electrostatic repulsion. Steric effects may not be the only controlling factor for this solid state structure as again the two C-F bonds are *gauche* with respect to each other. In addition, intermolecular hydrogen bonding has to be considered as another influencing factor. One molecule of H_2O is bound for every succinic acid molecule, clearly participating in hydrogen bonding with the carboxyl groups.

Generally, O-H···O interactions are strong in energy terms and thus can override conformational preferences of the isolated molecule. In addition, there are relatively short O-H···F contacts between the bound H_2O and the fluorine atoms, as illustrated by dashed lines in the crystal structure in Figure 2.14. Although within the sum of their van der Waals radii, interatomic O-H···F distances of 2.45 Å are comparatively long and they will contribute very little stabilisation energy to the crystal. From theoretical calculations the stabilisation energy of two *vicinal* C-F bonds is estimated to be of 0.5-1.0 kcal/mol (Introduction). For this reason, the O-H···F contacts may just be the result of the molecular geometry rather than due to genuine hydrogen bonding.

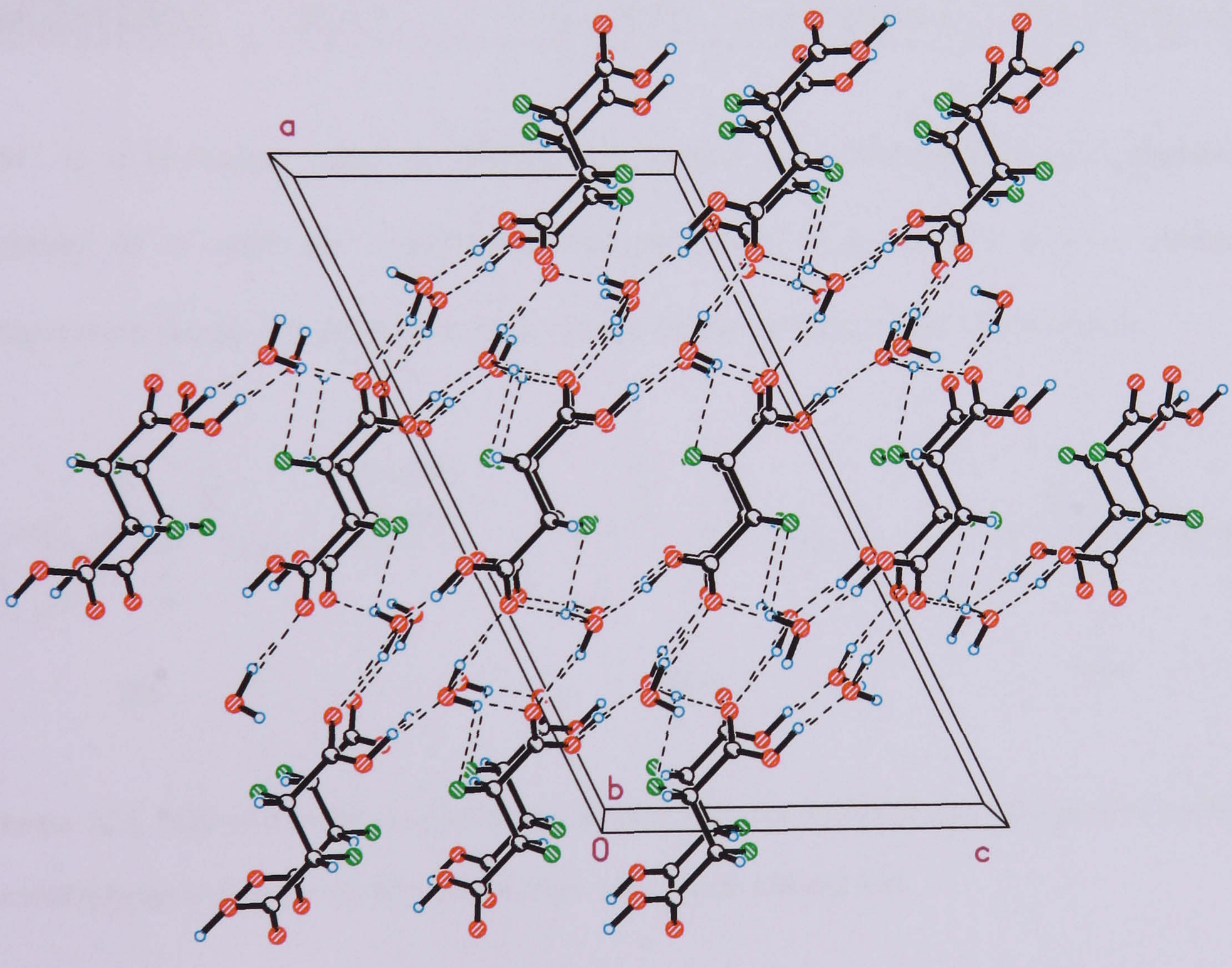

Figure 2.14. Crystal packing of *threo* 2,3-difluorosuccinic acid **132**. Short O-H···O contacts are illustrated by dashed lines. Selected interatomar distances (Å) and angles [°]: O2-H(2O)···O3 1.568(4) [<168.5(19)], O3-H(3A)···O1#2 1.901(11) [<156(2)], O3-H(3A)···O3#2 2.67(2) [<112.6(17)], O3-H(3B)···O1#3 1.814(3) [<172.5(19)], and O3-H(3B)···F2#3 2.447(19) [<112.5(14)].

The melting points of the two diasteromers **130** and **132** were determined using both a melting point apparatus and by Differential Scanning Calorimetry (DSC). The melting points obtained are significantly different. Interestingly, the *threo* isomer **132** has a much higher melting point than the *erythro* isomer **130** by about 30 °C, which may be due to stabilisation of the crystal-bound H_2O molecule (Figure 2.13).

Table 2.3. Melting points of the difluorosuccinic acids **130** and **132**. Crystallographic data indicate different crystal systems and space groups for the two diastereoisomers.

Stereoisomer	Melting point (DSC)	Melting point (manually)	Crystal system	Space group
threo **132**	200.8 °C	203-204 °C	monoclinic	C2/c
erythro **130**	180.3 °C	174-175 °C	orthorhombic	P2(1)-2(1)-2(1)

DSC is a technique used to obtain information on polymorphism and chemical stability of a particular compound and measures heat transfer over a defined temperature range. It also gives exact values for the melting point of materials.

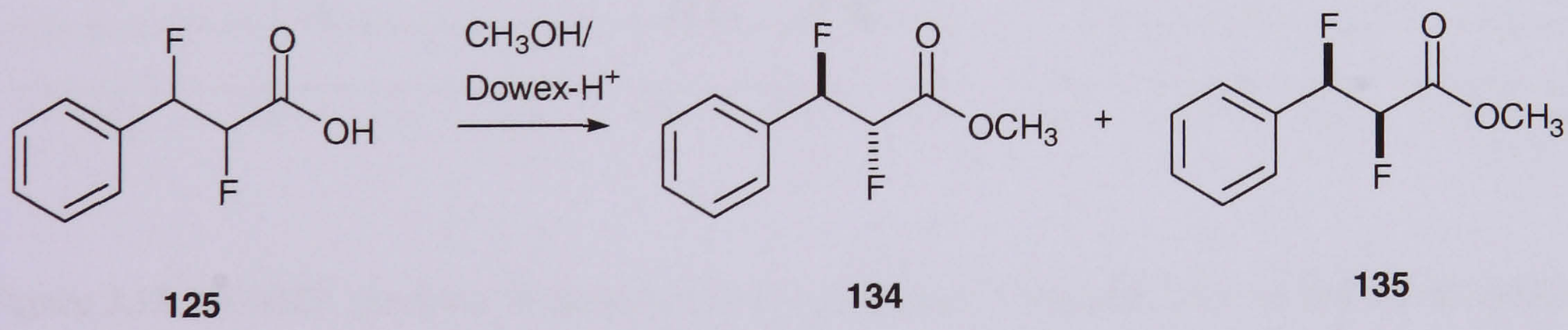

125 **134** **135**

Scheme 2.22. Methyl 2,3-difluoro-3-phenylpropionate **133** was esterified and then purified by flash chromatography to give the *erythro* and the *threo* compounds **134** and **135**.

The major by-product from the ozonolysis of difluorodiphenylethane **99** was the difluoromonocarboxylate **125**. The compound was purified by esterification with methanol and subsequent purification by silica gel chromatography (Scheme 2.22). Hydrolysis of the monoesters **134** and **135** as a mixture of diastereoisomers was

achieved under acidic conditions. Freeze-drying and recrystallisation afforded **125** in pure form. The methyl esters **134** and **135**, as well as the free carboxylic acids **125**, exhibited interesting NMR couplings (Figure 2.15).

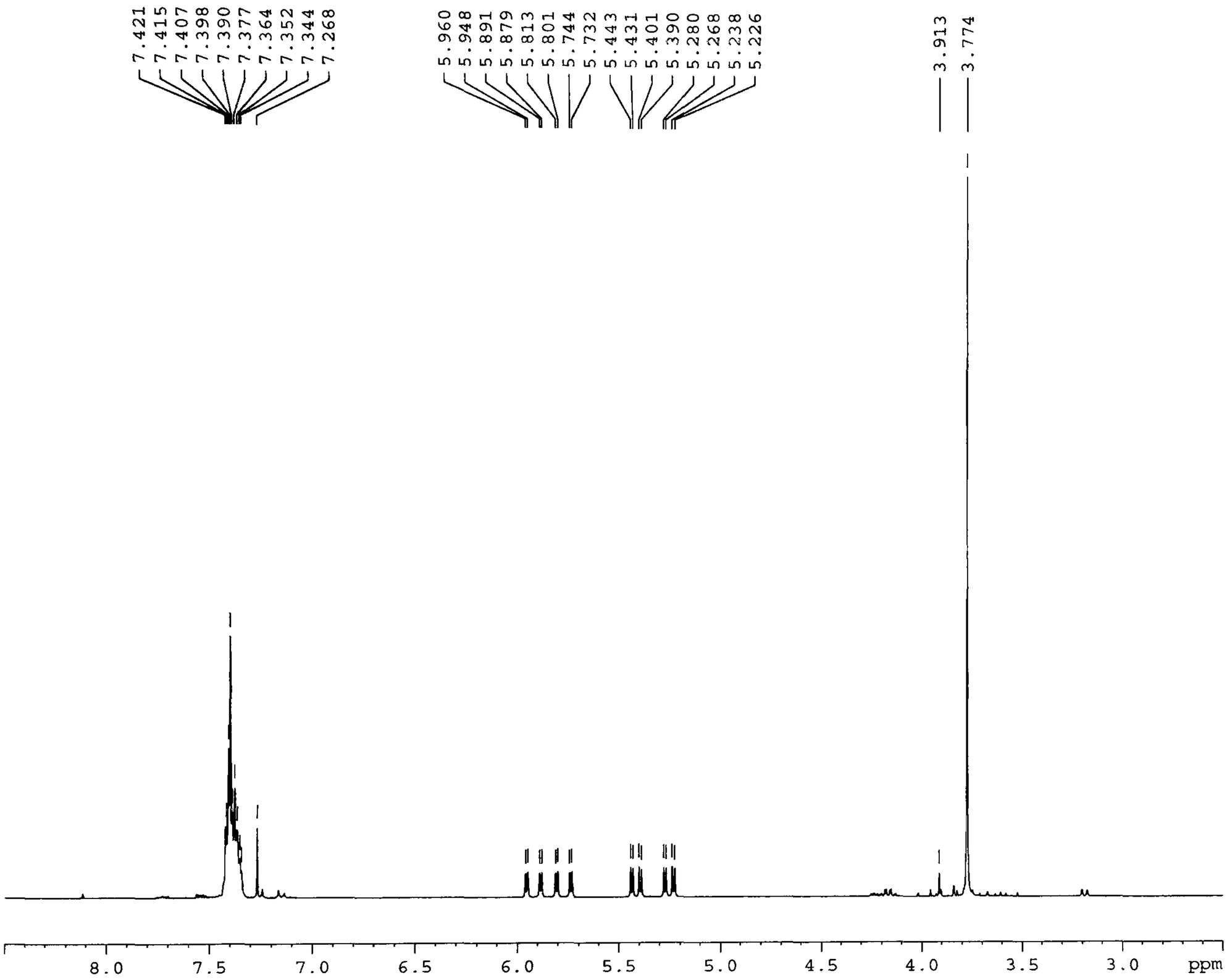

Figure 2.15. ^{1}H NMR spectrum of methyl *erythro* 2,3-difluoro-3-phenylpropionate **134**. C2-H and C3-H are dddd at 5.8 ppm and 5.3 ppm respectively. The compound was obtained by ozonolysis of a diastereoisomerically pure sample of *erythro* 2,3-difluorosuccinic acid and subsequent crystallisation.

The fluorines and their *geminal* protons in **134** and **135** are no longer chemically equivalent, and therefore a first order spectrum is obtained with a ddd pattern for each nucleus (Figure 2.15). Thus coupling constants can be read directly from the spectrum, however the conformational analysis is more complex. This is because the coupling constants are no longer affected only by the dihedral angle but also by the

adjacent functional groups. As a result two *vicinal* H-F and two *geminal* H-F couplings are obtained for each fluorine or proton nucleus. The signals for both fluorine nuclei are shifted upfield for the *threo* isomer **135** with respect to the *erythro* isomer **134**. This large chemical shift difference is useful for the immediate identification of the compounds obtained from oxidative degradation of the aromatic precursors.

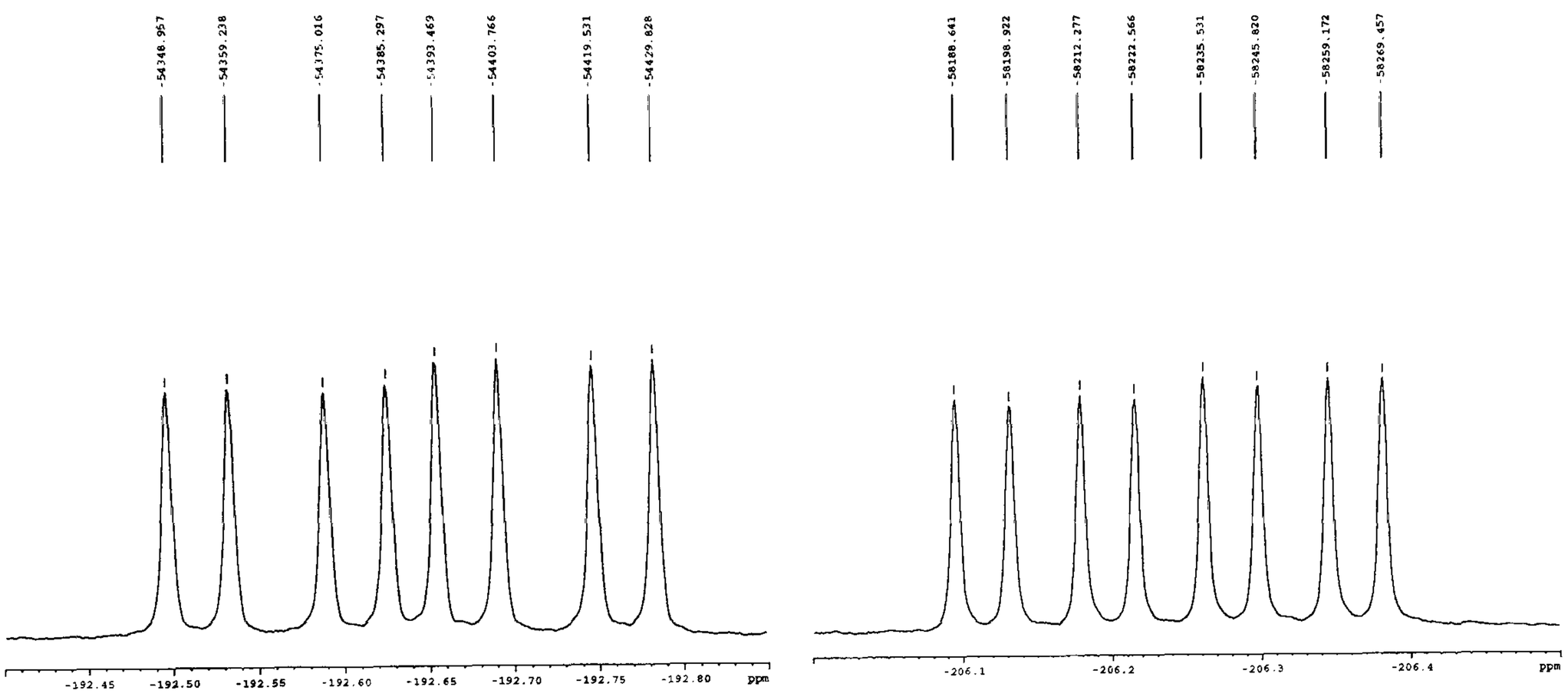

Figure 2.16. ^{19}F NMR spectrum of methyl *threo* 2,3-difluoro-3-phenylpropionate **135**. Both ^{19}F resonances for C3-F and C2-F at -193 ppm and –206 ppm show a ddd pattern according to a first order spectrum.

In the *erythro* isomer **134**, the chemical shifts of the ^{19}F nuclei resemble those of the *erythro* difluorosuccinates and biphenylethanes (Table 2.4). This is not the case for the *threo* compound **135** where the fluorine signal adjacent to the ester group is shifted downfield with respect to the *threo* difluorosuccinate. The C3-F adjacent to the phenyl group is shifted upfield in comparison to *threo* biphenylethane **104**.

Table 2.4. ^{19}F chemical shifts for 2,3-difluoro-3-phenylpropionates **134** and **135** compared with 1,2-difluoro-1,2-diphenylethanes **103** (**104**) and methyl 2,3-difluorosuccinates **87** (**127**).

Structure	*Threo*-isomer	*Erythro*-isomer
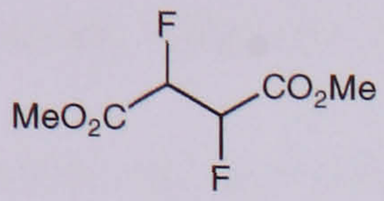	-207.1	-202.0
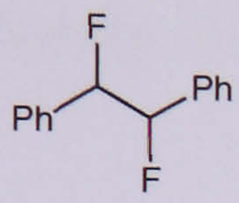	-183.8	-187.1
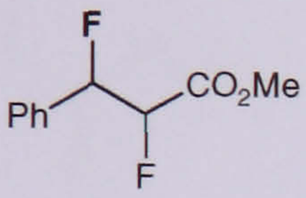	-193.2	-187.9
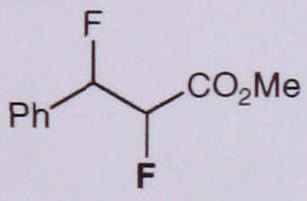	-205.6	-202.5

Coupling constants for both diastereoisomers were determined in order to carry out conformational analysis. There is generally one $^{3}J_{HF}$ coupling constant for each diasteroisomer as the two protons couple directly with each other. The coupling constants observed remain small and indicate a *gauche* relationship between these protons (Scheme 2.23).

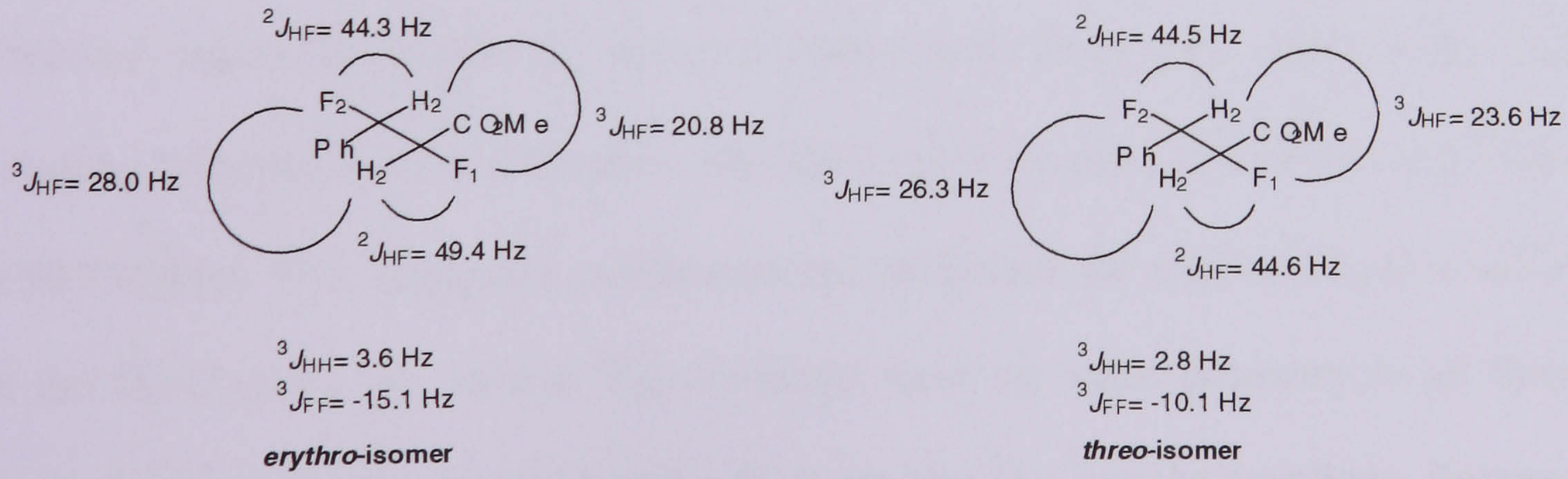

Scheme 2.23. NMR coupling constants of *erythro* and *threo* 2,3-difluoro-3-phenylpropionates **134** and **135**. The NMR spectra were recorded in $CDCl_3$ at room temperature.

Interestingly, in both compounds the C2-F nuclei adjacent to the carbonyl group show a smaller $^3J_{HF}$ than the C3-F adjacent to the phenyl group. The $^3J_{HF}$ coupling constants within the *erythro* isomer **134** shows a large difference (~7 Hz), while that in the *threo* isomer **135** is small (~3 Hz). The geometry of the rotational isomers in the *erythro* series allows for different $^3J_{HF}$ coupling constants depending on the conformation of the molecule. Rotamers **e** and **f** contain a *gauche* and a *trans* relationship for the *vicinal* ^{1}H and ^{19}F nuclei (Scheme 2.24).

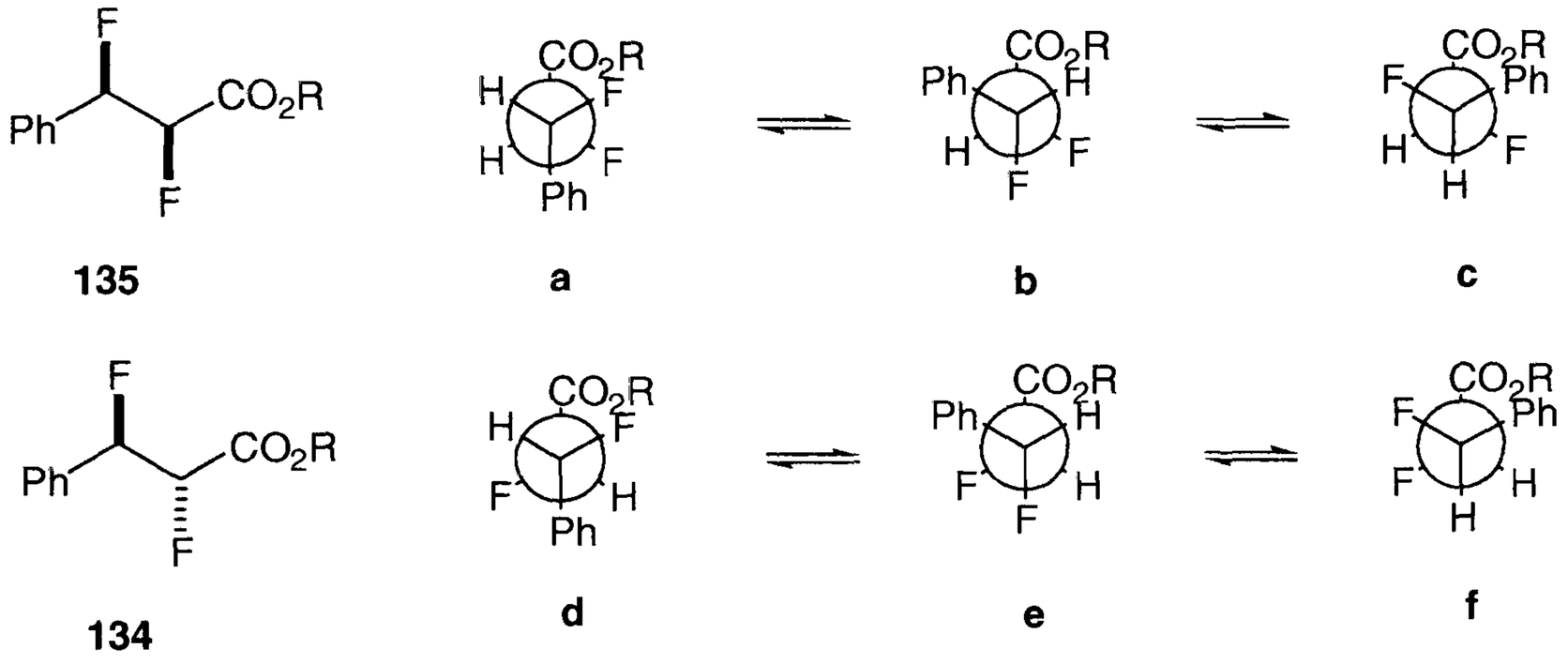

Scheme 2.24. Staggered conformations of *erythro* and *threo* 2,3-difluoro-3-phenylpropionates **134** and **135** shown by Newman will contribute differentially to the overall observed coupling constants.

Naturally, the average overall *erythro* $^3J_{HF}$ coupling constants will be different for the α- and the β-fluorine, provided that rotamers **e** and **f** are not equally populated. The observed values for *erythro* 2,3-difluoro-3-phenylpropionate **134** show a large $^3J_{HF}$ coupling constant for the β-fluorine (PhCHF), but a smaller one for the α-fluorine ($CHFCO_2Me$). This suggests a conformational preference for rotamer **f** over **d** and **e**. In the *threo* series, the *vicinal* $^3J_{HF}$ couplings have the same geometry in all three rotational isomers. For rotamer **b** and **c** there are two $^3J_{HF}$ *gauche* couplings. Rotamer **a** on the other hand has two *trans* $^3J_{HF}$ relationships. The overall $^3J_{HF}$ coupling constant should therefore be similar for the fluorine nuclei, but in fact, these coupling

constants are different (7 Hz versus 3 Hz). Substituent effects may give a likely explanation, as the phenyl and the ester group are very different in electronic nature.

Figure 2.17. X-ray structure of methyl *threo* 2,3-difluoro-3-phenylpropionate **135**. Selected bond length (Å), bond and torsion angles [°]: C7-C8 1.507(6), C7-F7 1.398(5), C7-C8 1.507(6), C8-F8 1.358(5) C17-F17 1.395(5), C17-C18 1.500(5), C18-F18 1.369(5) Å; C1-C7-F7 109.3(4), C7-C8-F8 110.2(4), F8-C8-C9 108.8(4), C11-C17-F17 109.6(3), F17-C17-C18 106.6(3), C17-C18-F18 109.8(3), F18-C18-C19 108.7(3)°; F7-C7-C8-F8 63.2(4), C1-C7-C8-C9 –179.1(4), F8-C8-C9-O9 –10.9(6), F8-C8-C9-O10 168.0(3), F17-C17-C18-F18 64.0(4), C11-C17-C18-C19 –178.5(4), F18-C18-C19-O19 –9.9(6), F18-C18-C19-O20 170.8(3)°.

In the solid state, the C-F bonds of *threo* 2,3-difluoro-3-phenylpropionate **135** adopts a *gauche* relationship (Figure 2.17). This is consistent with the preference for rotamer **a** found in solution. Unfortunately, a similar X-ray structure is not available for the *erythro* isomer **134**, as this compound is not a solid at room temperature. Attempts to crystallise its free carboxylic acid resulted only in the formation of amorphous material.

2.1.4 Mechanistic considerations on the ozonolysis reaction

The mechanism for the ozonolysis of alkenes has been investigated extensively by Criegee.[42] A mechanism was proposed which has recently been revised using ^{17}O NMR spectroscopy.[43] The first step is a 1,3-dipolar cycloaddition of ozone onto the double bond of the alkene **136**, which leads to the formation of a molozonide **137** (Scheme 2.25).

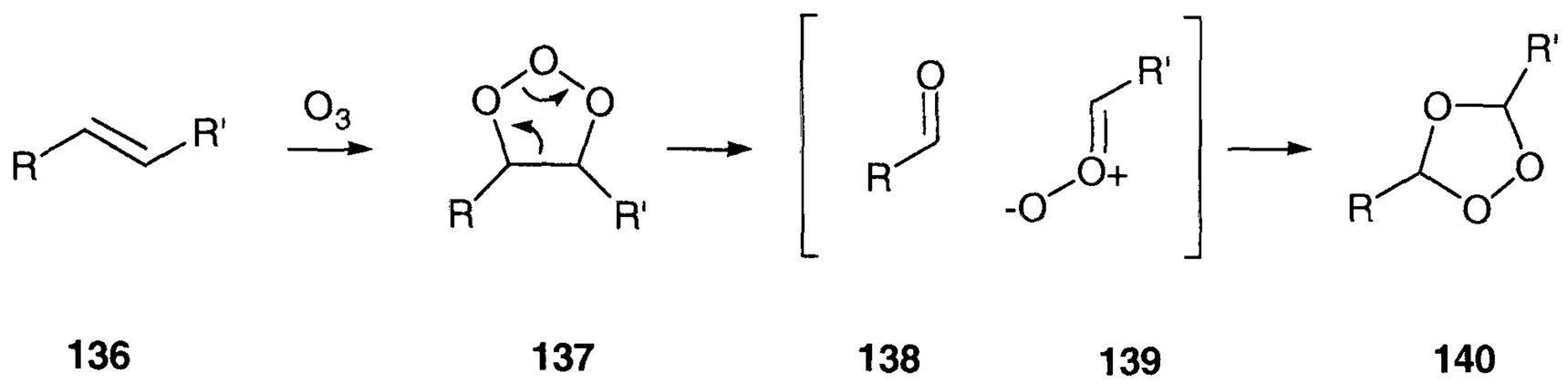

Scheme 2.25. Criegee mechanism for the formation of a molozonide **137** involves a [3+2] cycloaddition of ozone and an alkene **136**.[44]

The molozonide **137** is not stable and decomposes on formation to give a carbonyl compound **138** plus a carbonyl oxide **139**. The carbonyl oxide **139** is similar in reactivity to ozone and undergoes a 1,3-dipolar cycloaddition with the carbonyl compound **138**. This gives rise to a more stable secondary ozonide **140**. Although such compounds have been isolated previously, they are generally explosive species and represent a serious hazard to the research worker. Accordingly, it is necessary to perform the reaction and work up in a fumehood or behind a safety shield. The secondary ozonide can be reduced with sodium borohydride to give alcohols, oxidised with hydrogen peroxide to give carboxylic acids, or treated with dimethyl sulfide or triphenyl phosphine to obtain aldehydes (Scheme 2.26).

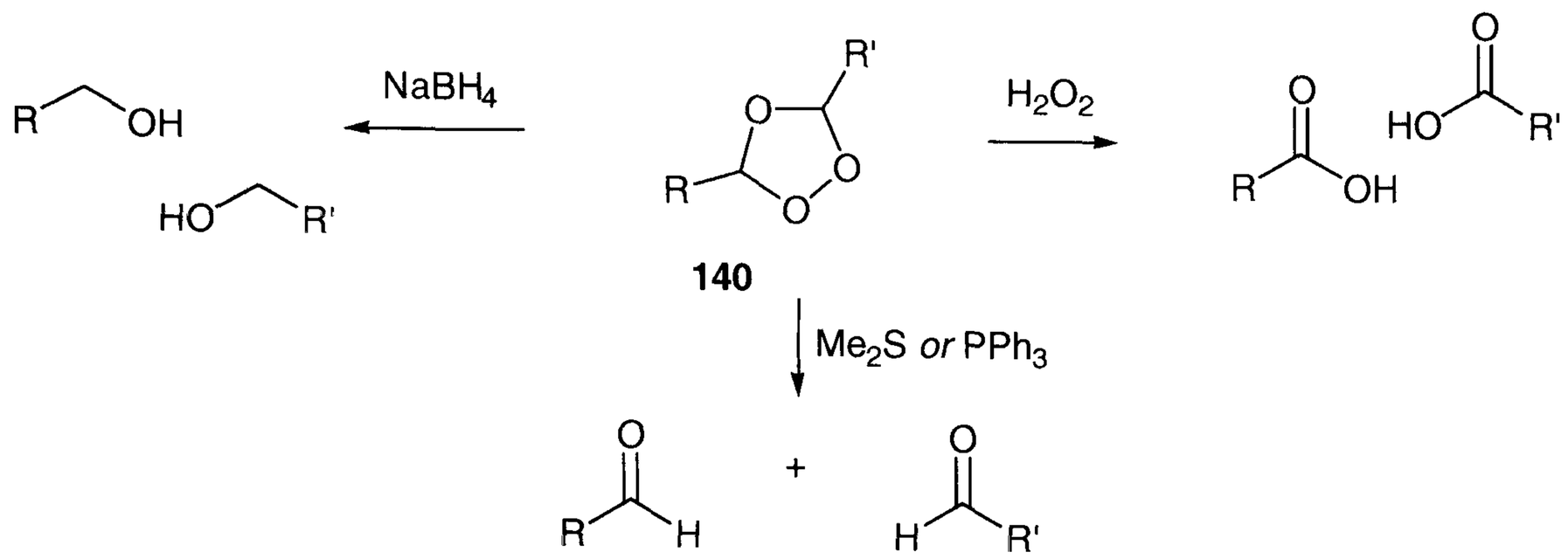

140

Scheme 2.26. The ozonide **140** can be interconverted to yield aldehydes or ketones, reduced to alcohols, or oxidised to carboxylic acids.

The Criegee mechanism is valid in apolar solvents such as hydrocarbons and dichloromethane. If the reaction is carried out in protic solvents such as alcohols, a hydroperoxyhemiacetal **141** is formed, which can rearrange to give an ester **142**.

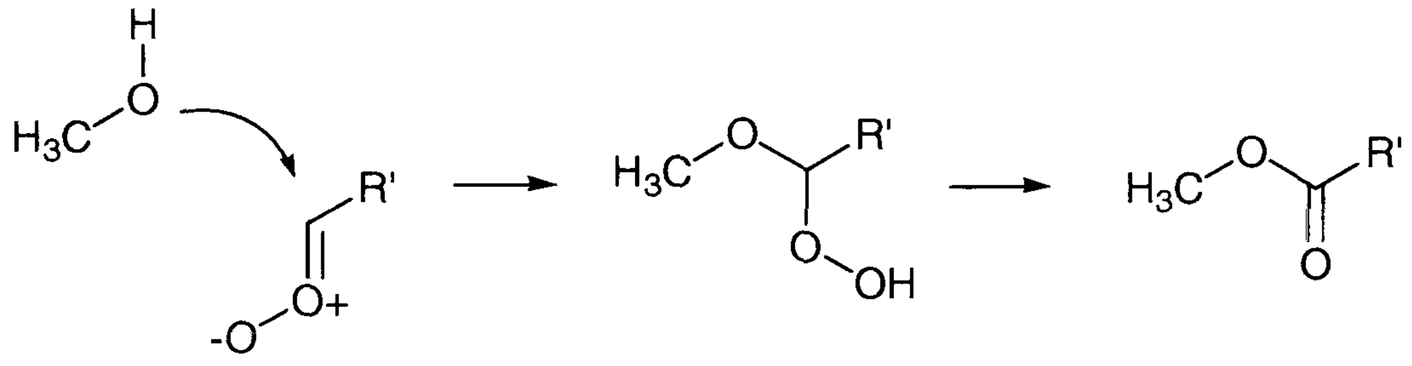

139 **141** **142**

Scheme 2.27. In protic solvents such as methanol the solvent presumably participates in the reaction to form a reactive hydroperoxyhemiacetal **141**, an intermediate which eventually affords an ester **142**.

Mechanistically, the oxidative depletion of aromatic compounds by ozone is a complex process, and opposing theories exist. The concept of localised π-complexes and the formation of an initial triozonide **144** from the interaction of benzene with three molecules of ozone has been postulated (Scheme 2.28). It has however been pointed out, that the resulting tetracyclic intermediate imposes considerable steric strain, and in particular formation of the respective secondary ozonide appears rather unlikely.

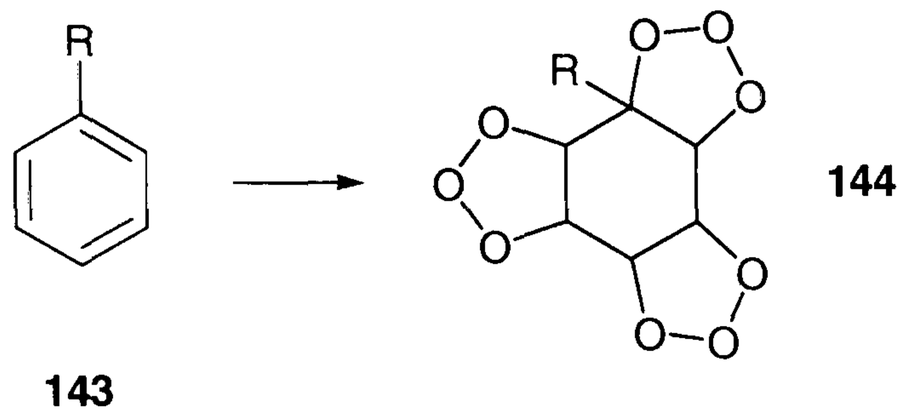

Scheme 2.28. Proposed formation of triozonide **144** in the ozonisation of an aromatic compound **143**.[45]

An alternative mechanism involves the electrophilic attack of one molecule of ozone on to a localised π-complex (Scheme 2.29). The molozonide **145** collapses into zwitterions such as compound **146**. In the presence of a protic solvent such as acetic acid the zwitterion will be quenched to form the acetohydroperoxide **147**. Formation of this intermediate has been concluded from the presence of degradation products such as formic acid, acetic acid, and glyoxal. Mechanistic considerations for the degradation of the acetohydroperoxide intermediate **147** are rather speculative, but may proceed by a second electrophilic addition of ozone onto the conjugated double bond of **147**. The possible intermediates will then breake down further in the presence of hydrogen peroxide to give the desired carboxylic acid **148**.

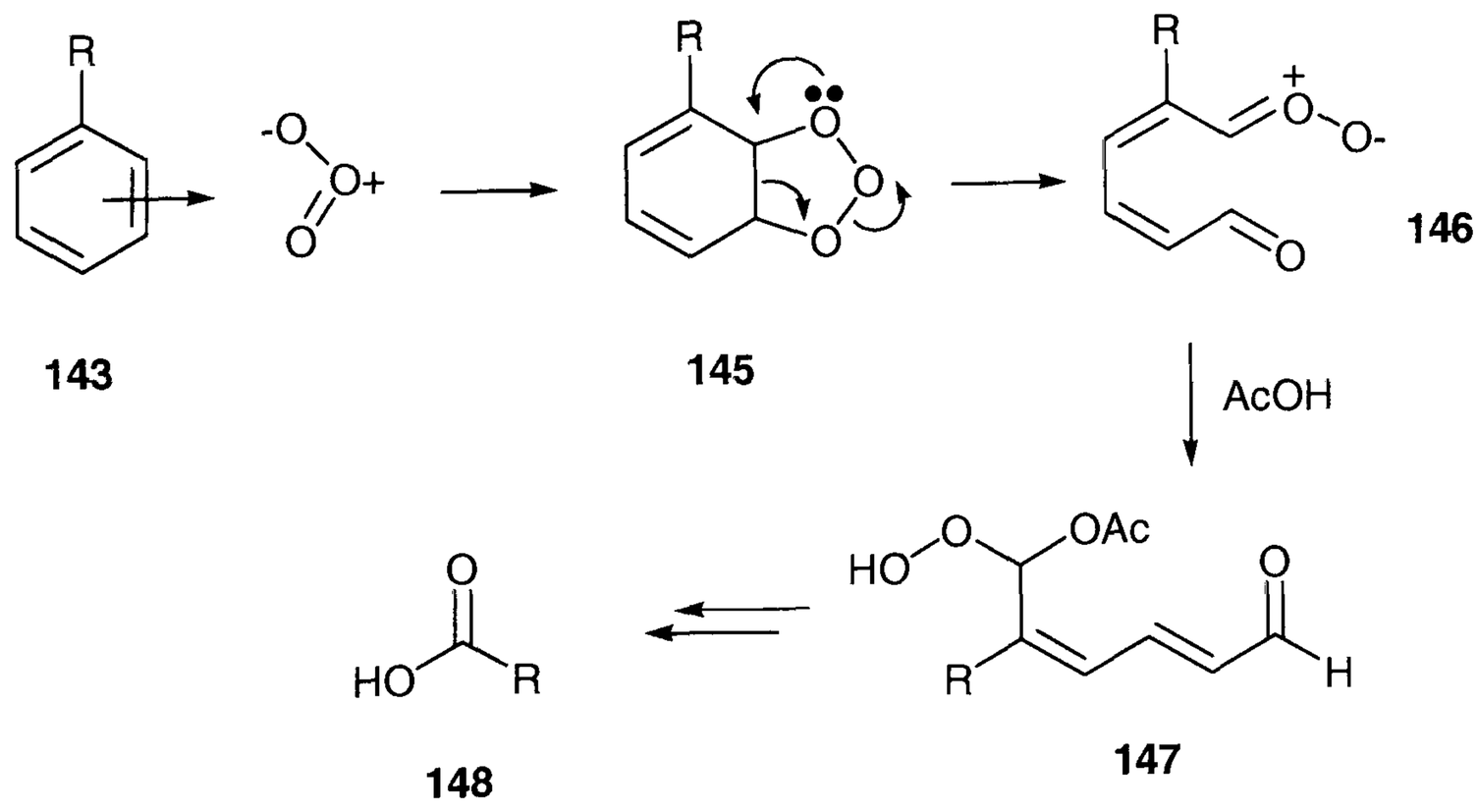

Scheme 2.29. Proposed mechanism for the oxidative degradation of aromatic rings by ozone.[46]

The hydroperoxide intermediate **147** has some stability and may thus remain in the reaction mixture even after treatment with aqueous hydrogen peroxide. For this reason, removal of the solvent and handling of the crude product has to be carried out with care. In addition, palladium-black can be added prior to solvent removal in order to decompose all remaining peroxides in solution. This treatment allows for safe handling of the materials involved even on a large scale. In principle, the rate of decomposition of all unsaturated intermediates should be high considering the reactivity of alkenes towards ozone under the reaction conditions. The first step in the reaction, namely the electrophilic addition of ozone onto the localised π-complex of the aromatic compound is the rate- determining step. Thus, improvement of reaction rate and yield will require changing the nature of the starting material.

2.1.5 Scale up of the difluorosuccinic acid synthesis

In the following, attempts to improve the yield of the ozonolysis and scale up of the synthetic route to 2,3-difluorosuccinic acids are described. Ozonisation requires solvents that are inert towards ozone attack, especially when the reaction is performed at room temperature. The most common solvents are dichloromethane, ethers, or hexanes, but also methanol has been used successfully at low temperature. Protic solvents such as alcohols are known to stabilise the polar breakdown intermediates of the ozonide, thereby considerably accelerating the reaction. However, these solvents are significantly reactive towards ozone and therefore must be used below –20 °C. Formic acid and acetic acid represent alternative solvents; they are stable to ozone and may accelerate the rate of reaction due to their inherent polarity. Acetic acid appeared to be the solvent of choice for this reaction as the 1,2-difluoro-1,2-biphenylethanes **99** have only a low solubility in formic acid.

Performing the reaction at 30 °C and 60 °C respectively did not alter the rate of the reaction significantly. Concentration of the starting material proved to be a crucial factor. In general, concentrations higher than 1.0 μM led to extremely low yields due to incomplete degradation of the phenyl groups. The low concentrations of starting material tolerated presented a serious problem for scale up. Because of this, attempts were made to improve the yield by using more reactive starting materials. In the ozonolysis of aromatic compounds, electron-donating groups activate aromatic systems toward electrophilic ozone attack. An example of this effect is provided in Woodward's strychnine synthesis, in which methoxy substitution allowed for selective oxidation of one aromatic ring of **149** over two others to afford an terminally functionalised (*Z*,*Z*)-diene **150** (Scheme 2.30).

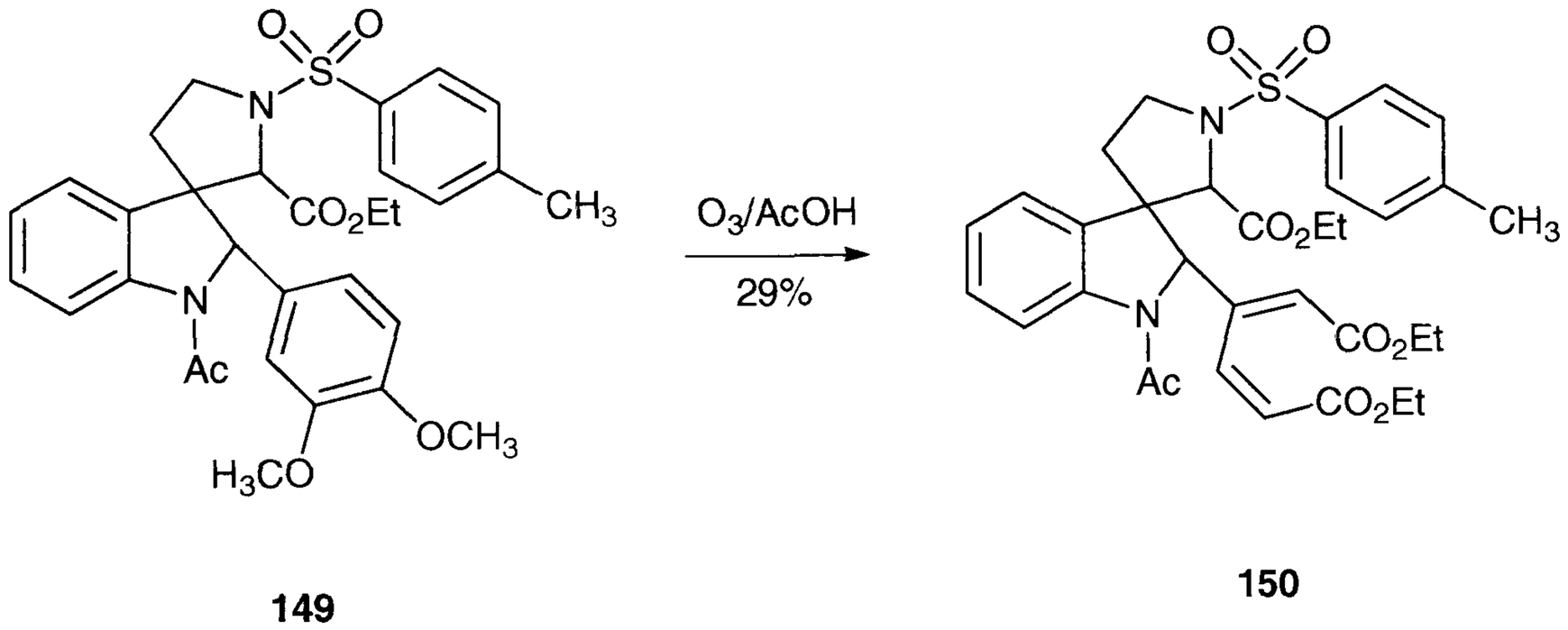

149 **150**

Scheme 2.30. Woodward's strychnine synthesis involves a selective ozonisation step in which a dimethoxy substituted aromatic ring reacts selectively over the two others.[47]

In order to improve the rate of oxidation of 1,2-difluoro-1,2-biphenylethane **99** by ozone, methoxyl substitution of the aromatic rings was envisaged. An obvious strategy to synthesise such compounds was to use 4,4'-dimethoxystilbene **151** as the starting material for Olah's difluorination procedure (Scheme 2.31).

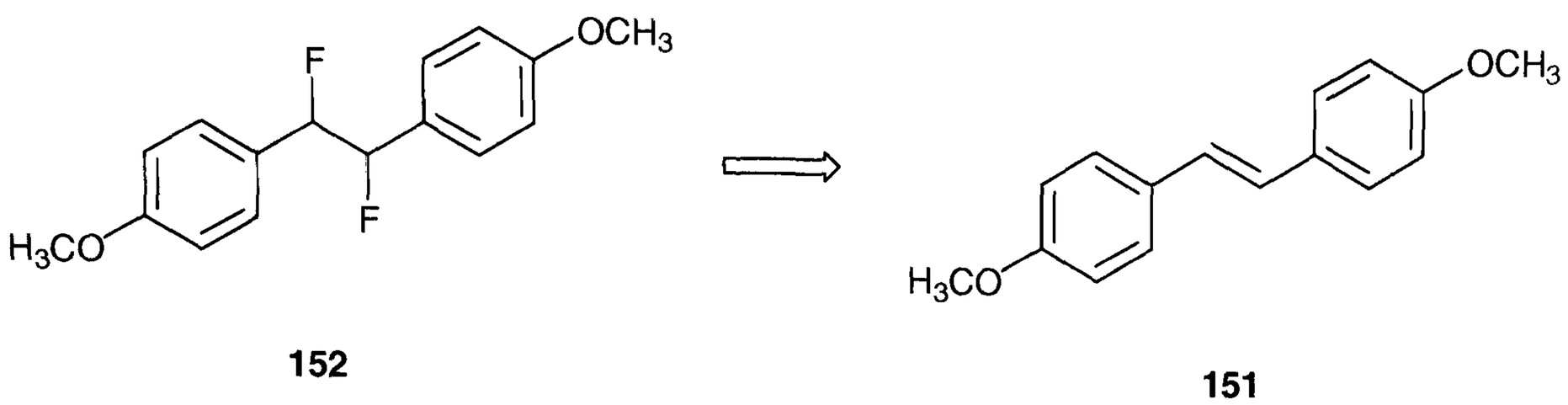

152 **151**

Scheme 2.31. Fluorobromination of 4,4'-dimethoxystilbene **151** with *N*-bromosuccinimide and PPHF.

4,4'-Dimethoxystilbene is commercially available as the *trans* isomer. Surprisingly, the compound proved to be virtually insoluble in all common solvents and even PPHF. The poor solubility of the starting material **151** completely impeded its application. The solubility problem was eventually solved by treatment of a THF suspension of 4,4'-dimethoxystilbene **151** with ultraviolet light (Scheme 2.32).

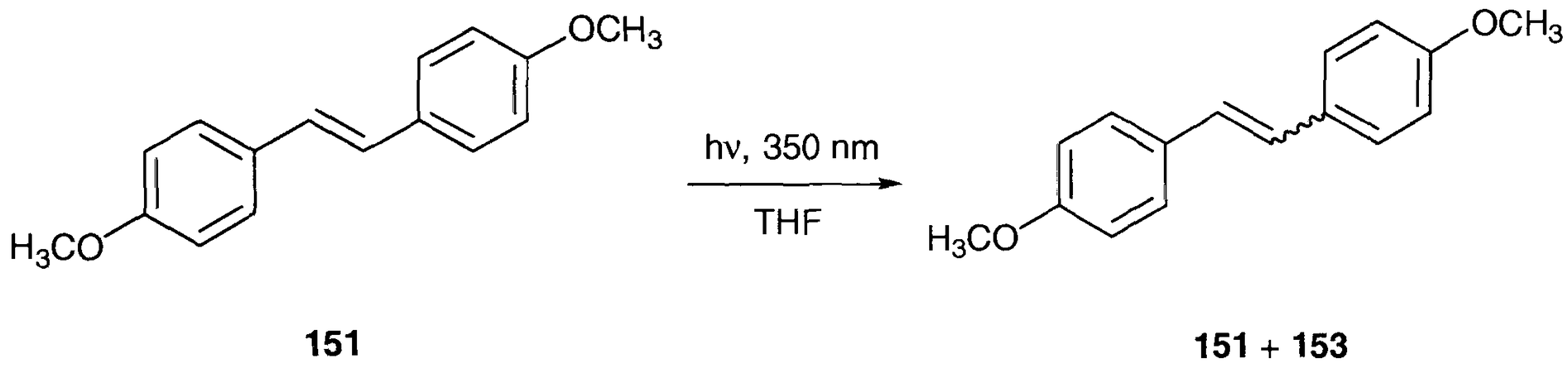

151 **151 + 153**

Scheme 2.32. Isomerisation of *trans* 4,4'-dimethoxystilbene **151** by means of UV irradiation.

The treatment of **151** with ultraviolett light generated a homogeneous solution, presumably due to the formation of an E and Z mixture of stereoisomers **151** and **153**. The transformation was carried out in Pyrex glassware, which is perfectly permeable to light above 300 nm, the wavelength necessary for excitation of the *trans* conjugated double bond. On the other hand it absorbs most of the electromagnetic radiation below 200 nm which is necessary for excitation of the Z-isomer **153** and therefore a one way conversion of the E to Z isomer is achieved. Disappointingly, conversion of the E/Z-mixture of 4,4'-dimethoxystilbene with NBS in PPHF under the standard

reaction conditions did not result in the expected fluorination of the double bond. Several attempts were made in a variety of solvents such as tetrahydrofuran, diethyl ether, dichloromethane, and neat PPHF, but in all cases only the unreacted starting material was recovered from the reaction. It was assumed that conjugation of the methoxyl groups with the aromatic ring and the central double bond may be responsible for this lack of reactivity.

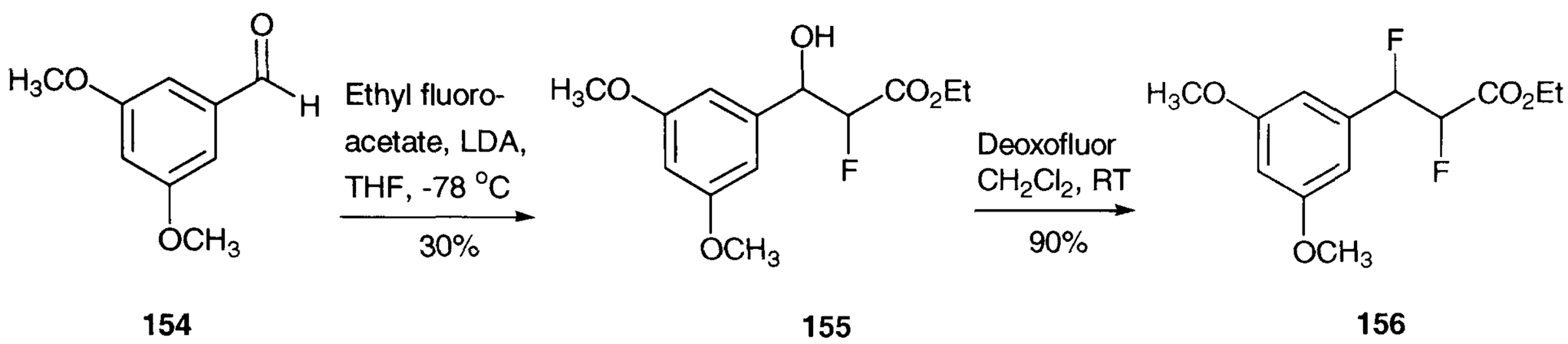

154 **155** **156**

Scheme 2.33. Synthesis of ethyl 2,3-difluoro-3-[3,5-dimethoxyphenyl]-propionate **156** *via* the aldol reaction of ethyl monofluoroacetate and 3,5-dimethoxybenzaldehyde **154**.

The synthesis of more reactive precursors for the ozonolysis reaction was finally achieved by a sequence of an aldol reaction followed by nucleophilic fluorination (Scheme 2.33). Aldol reaction of ethyl fluoroacetate with 3,5-dimethoxybenzaldehyde **154** using lithium diisopropylamide as the base led to formation of fluorohydrin **155**. The compound was obtained as a 1:1 mixture of diastereoisomers. After purification by flash chromatography the diasteroisomeric mixture of **155** was treated with Deoxofluor to afford **156**. As expected, the difluoro compound readily underwent ozonolysis to give the symmetrical ester **157**, which was hydrolysed without purification to give 2,3-difluorosuccinic acids **120** as a mixture of *threo* and *erythro* isomers.

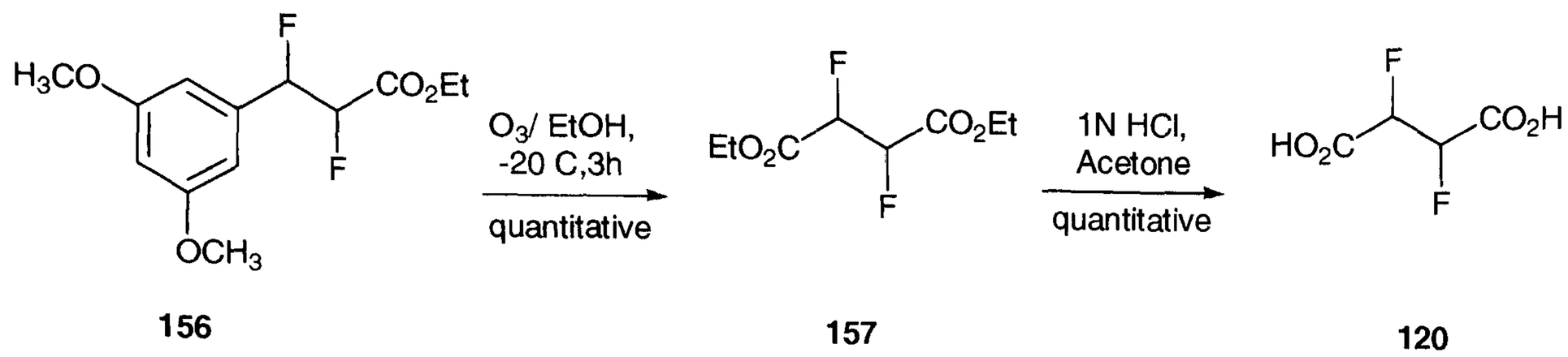

156 157 120

Scheme 2.34. Synthesis of 2,3-difluorosuccinic acid **120** by ozonolysis of ethyl 2,3-difluoro-3-[3,5-dimethoxyphenyl]-propionate **156**.

The aldol addition is the more problematical step in the synthesis of the difluorinated precursor **157**. ^{19}F NMR spectroscopy was used to analyse the conversion of ethyl fluoroacetate to the fluorohydrin **155**, the formation of which is indicated by a doublet of doublet. Surprisingly, a large excess of base was required to achieve a reasonable conversion of ethyl fluoroacetate. Attack of the lithium enolate **158** onto aldehyde **154** results in the formation of alkoxide **157**, which itself is a strong base (Scheme 2.35).

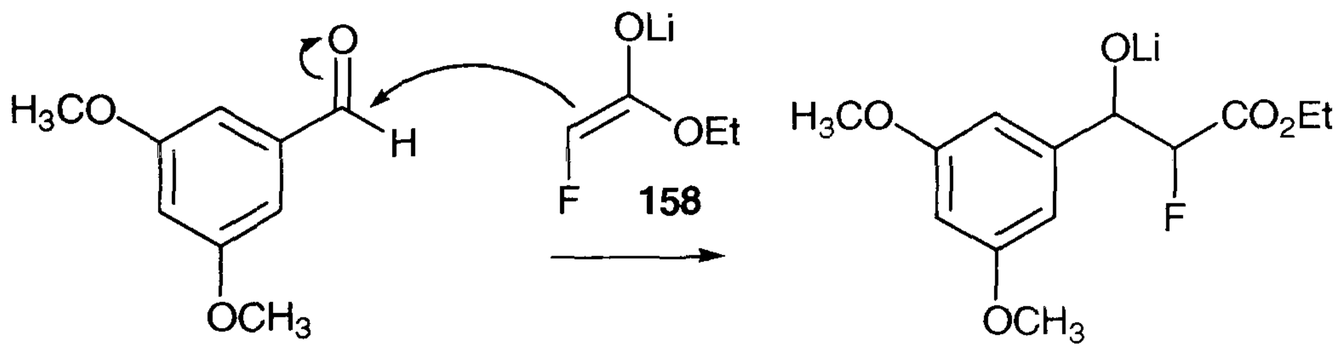

154 157

Scheme 2.35. The addition of the lithium enolate **158** on to aldehyde **154** yields lithium alkoxide **157**.

The reaction mixture was quenched at low temperature to prevent the persistence of strongly basic conditions. Formation of inorganic fluoride as a result of elimination was not observed by ^{19}F NMR spectroscopy. A drawback of this method is that the compounds were obtained as a mixture of all possible stereoisomers, and that the separation of diasteroisomeric ethyl 2,3-difluoro-2-[3,5-dimethoxyphenyl]propionates **156** as well as their precursors **155** was not possible.

2.1.6 Synthesis of amides and esters of 2,3-difluorosuccinic acid

Derivatisation of *erythro* and *threo* 2,3-difluorosuccinates was envisaged in order to compare their physical properties. Different sets of diastereoisomers were obtained, which exhibited quite different NMR coupling constants and solid state conformations. The diamides where anticipated to yield crystals that allow for X-ray analysis and the synthesis of the diethylesters facilitated the variable temperature NMR experiments which were used for conformational analysis of the *vicinal* difluoro compounds (Chapter 2.5).

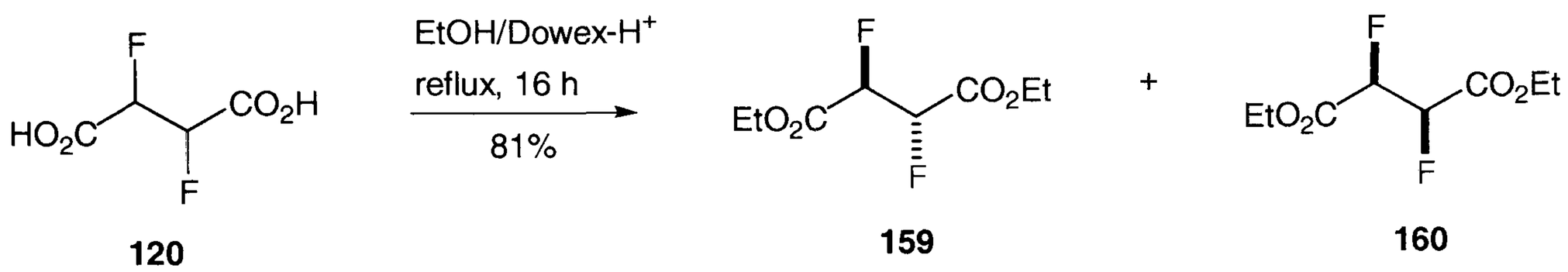

120 **159** **160**

Scheme 2.36. 2,3-Difluorosuccinic acid **120** was heated under reflux in ethanol using ion-exchange resin as the acid catalyst in the formation of diesters **159** and **160**.

The synthesis of *erythro* and *threo* ethyl 2,3-difluorosuccinates **159** and **160** was achieved by treatment of 2,3-difluorosuccinic acid **120** with ethanol in the presence of strongly acidic ion-exchange resin (Scheme 2.36). Several solvent combinations were tested in order to achieve isolation of the individual diastereoisomers by means of silica gel chromatography. Unfortunately, e*rythro* and *threo* 2,3-difluorosuccinates **159** and **160** could not be separated, and had to be synthesised individually from their diastereomerically pure *erythro* and *threo* 2,3-difluorosuccinic acids **130** and **132**.

The synthesis of 2,3-difluorosuccinamides **161** and **162** was of major interest, as these derivatives were anticipated to be solids at room temperature and as such amenable to X-ray analysis. These would than be used to assess the preferred solid state conformation for the diastereoisomers. The compounds were obtained from the racemic 2,3-difluorosuccinic acids **120** using standard peptide coupling procedures (Scheme 2.37).

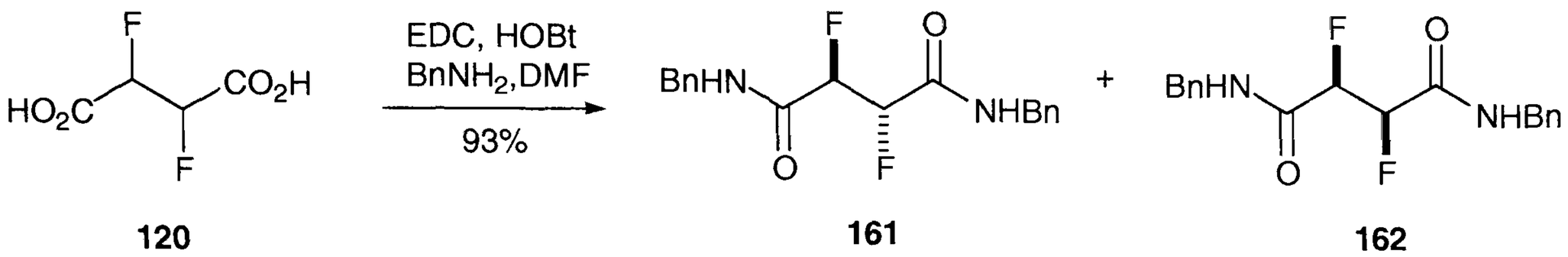

120 **161** **162**

Scheme 2.37. The synthesis of dibenzyl 2,3-difluorosuccinamides **161** and **162**. The *erythro* and *threo* diastereoisomers were separated by silica gel chromatography.

Initially, the reaction was carried out with dicyclohexylcarbodiimide (DCC), a reagent, which is effective for activation of carboxylic groups to undergo aminolysis. The reaction is typically carried out in the presence of HOBt, which prevents from side reactions and racemisation of adjacent stereogenic centres. The reaction was conveniently followed by 19F NMR analysis, which indicated clean conversion of the starting materials. When DCC was used as the coupling reagent, isolation of the pure compounds was hampered by the formation of dicyclohexylurea as the co-product, which is generated in 2 molar excess. In order to ease purification of the amides, DCC was substituted by EDC, which forms a urea that can be conveniently removed by aqueous wash. Using the improved procedure, the diasteroisomers **161** and **162** could be separated by silica gel chromatography simply after work up. Recrystallisation of the pure diasteroisomers allowed for X-ray analysis of both diastereoisomers.

The *erythro* isomer **161** crystallised in two independent structures, which very similar conformations. The more abundant (70%) conformer is shown in Figure 2.18.

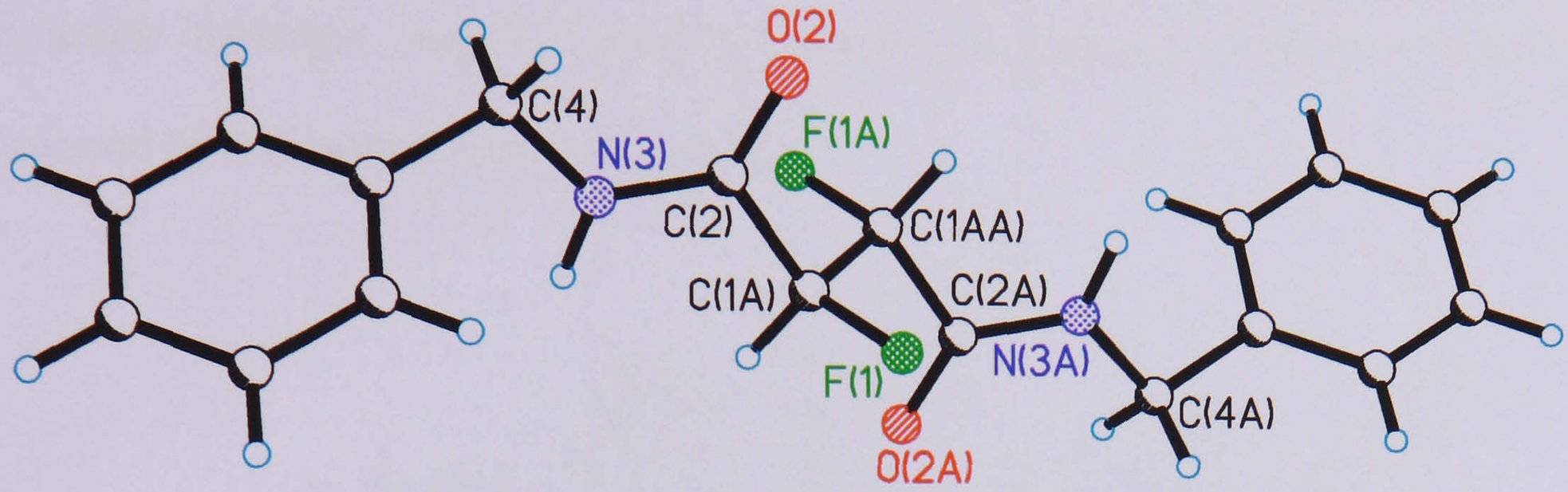

Figure 2.18. X-ray structure of *erythro* dibenzyl 2,3-difluorosuccinamide **161**. Selected bond lengths (Å), bond angles (°), and torsion angles: N3-N2 1.333(5), C2-O2 1.235(4), C1A-C2 1.553(8), F1-C1A 1.368(8), C1A-C1AA 1.533(13); F1-C1A-C2 115.0(4), F1-C1A-C1AA 107.2(7), F1-C1A-H1AA 109.6; C4-N3-C2-O2 0.2(7), C4-N3-C2-C1A 171.2(4), N3-C2-C1A-F1 -115.0(5), O2-C2-C1A-F1 56.5(7), O2-C2-C1A-C1AA -61.5(8), C2-C1A-C1AA-C2A, F1-C1A-C1AA-F1A.

The bond lengths, bond angles, and torsion angles on either side of the difluorosuccinamide moiety are identical as a result of the symmetry of the molecule. The main chain of **161** adopts an extended conformation in which the C-F bonds are *anti* with respect to each other. In that conformation the large benzyl substitiuents point in opposite directions minimising steric interactions within the molecule. Although the α-fluoroamide groups are planar, as it is typical for these groups, the C-F bonds are 23° off the ideal *syn* planar arrangement typical of the α-fluoroamide moiety. Also the C-F bonds adopt an *anti* conformation which is unusual for the *vicinal* difluoro moiety. Apparently, the conformation of **161** is mainly controlled by steric effects, although the main chain does somewhat deviate from the ideal zig-zag conformation.

An additional factor obviously influencing the solid state conformation is intermolecular hydrogen bonding. This becomes evident in considering the crystal packing of **161**. There is apparently strong intermolecular hydrogen bonding between the amide hydrogen and the carbonyl oxygen of adjacent molecules, which is illustrated by the dashed lines in Figure 2.19.

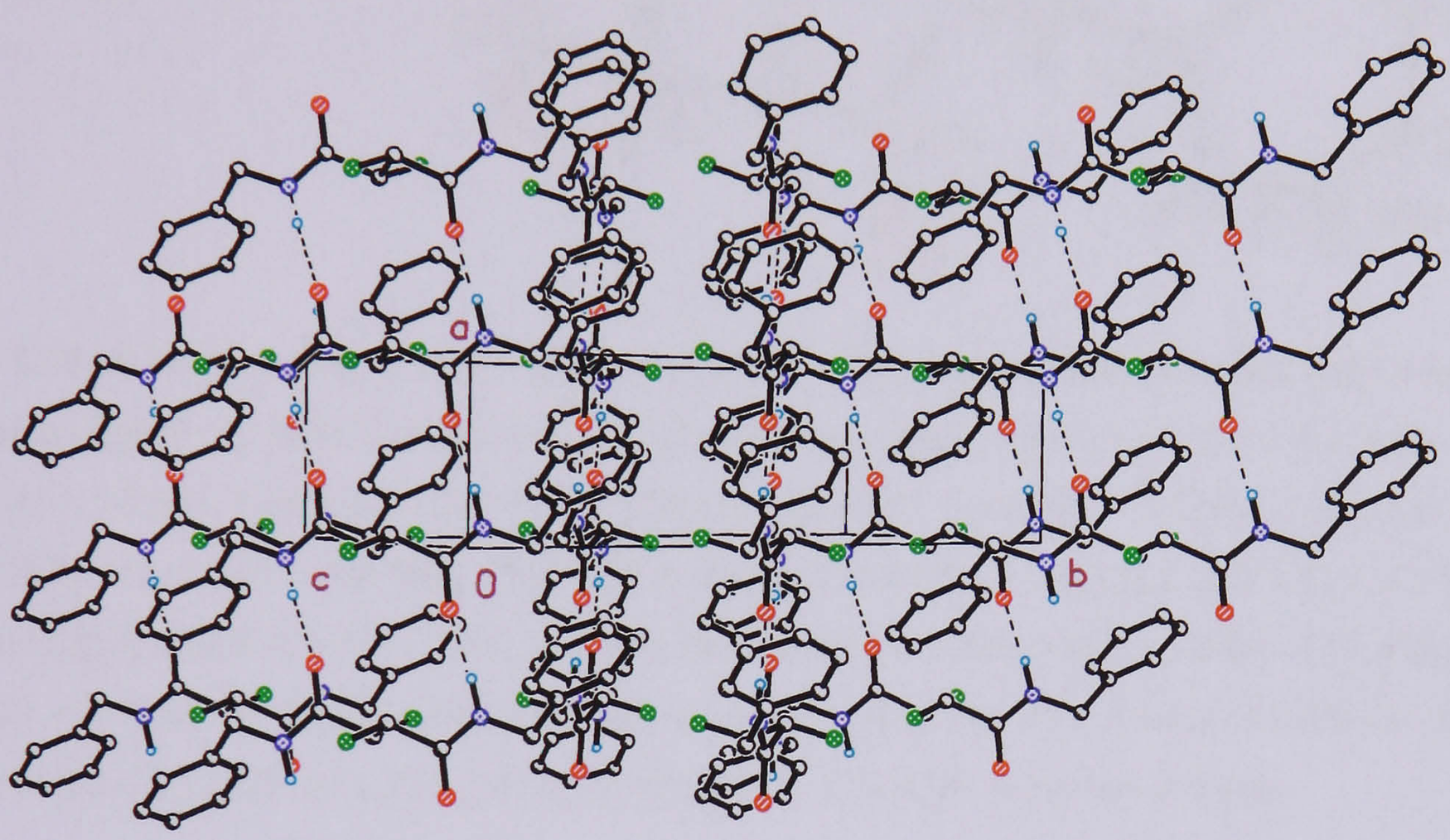

Figure 2.19. Crystal packing of **161**. The crystal system is monoclinic with space group P2(1)/c and R factor of 0.1372. There are short N3-H···O2#2 contacts of 1.8651(53) Å length, clearly indicating intermolecular hydrogen bonding.

These interactions are naturally strong and can override stereoelectronic effects in energy terms readily. Therefore, involvement of N-H···O hydrogen bonding is most likely the origin for the deviation of the α-fluoroamide groups from its ideal *anti* periplanar conformation and this may in turn affect the overall conformation of the main chain and the dihedral angle of the C-F bonds.

In contrast, the crystal structure of the *threo* isomer **162** shows both C-F bonds perfectly *syn* planar with respect to the N-H bond, consistent with the typical *anti* planar arrangement of the α-fluoroamide group (Figure 2.20).

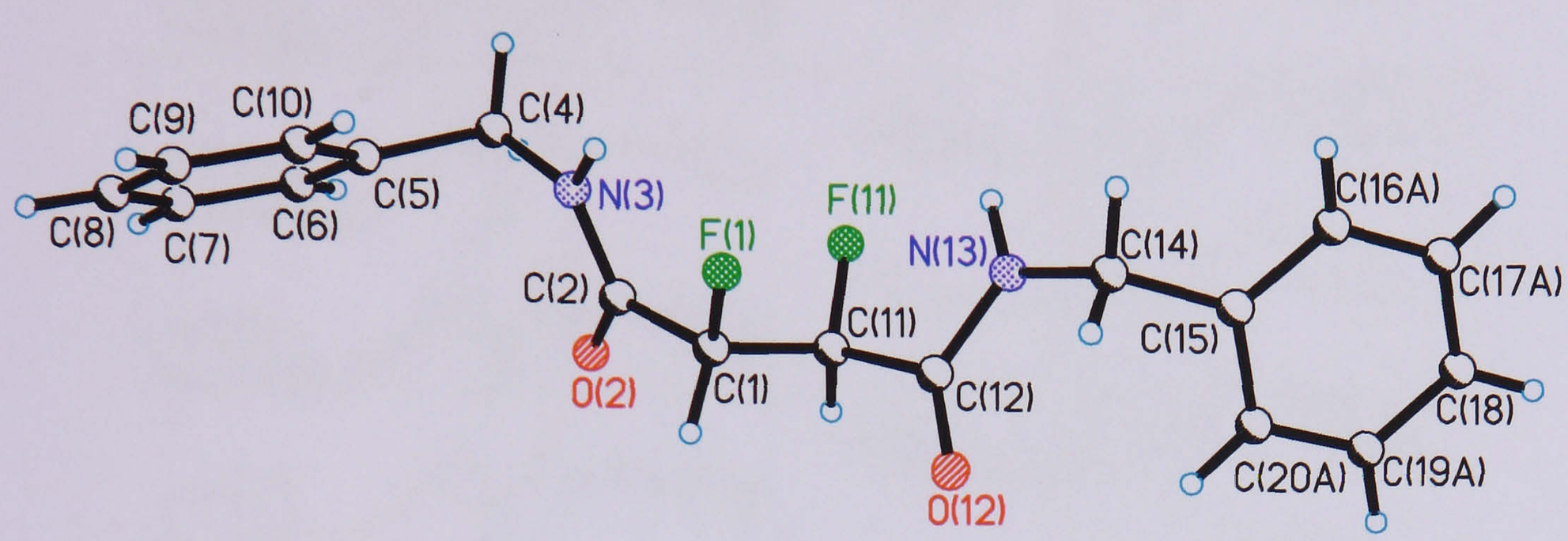

Figure 2.20. X-ray structure of *threo* dibenzyl 2,3-difluorsuccinamide **162**. Selected bond lengths (Å) and torsion angles (°): N3-C2 1.349(10), C2-O2 1.229(9), C2-C1 1.518(11), C1-F1 1.411(8), C1-C11 1.544(10), C11-F11 1.365(10), C11-C12 1.558(13), C12-O12 1.204(10), C12-N13 1.388(11); F1-C1-C2 109.2(6), F1-C1-C11 108.5(6), F1-C1-H1A 110.0, F11-C11-C1 109.3(6), F11-C11-C12 110.8(6), F11-C11-H11A 109.9; C4-N3-C2-O2 -4.4(10), N3-C2-C1-F1 7.7(8), O2-C2-C1-F1 -173.3(6), C2-C1-C11-C12 167.0(6), F1-C1-C11-F11 -72.0(8), F1-C1-C11-C12 48.1(7), C1-C11-C12-N13 -110.7(7), F11-C11-C12-O12 -172.4(7), F11-C11-C12-N13 8.4(8), C11-C12-N13-C14 176.4(6).

The compound crystallises in two independent molecules, which differ only in the orientation of one of the phenyl rings at the end of the chain. Bond length and torsion angles of the second independent molecule are identical to the aforementioned values. Remarkably, the *vicinal* C-F bonds align *gauche* with respect to each other, which is consistent in terms of the *gauche* preference for *vicinal* difluoro compounds. The planarity of the α-fluoroamide moiety and the *gauche* arrangement of the C-F bonds suggest that the conformation is determined to a high degree by stereoelectronic effects operating between the amide group and the C-F bond. Such effects would reasonably explain the slight deviation of the main chain from the ideal extended zig-zag conformation.

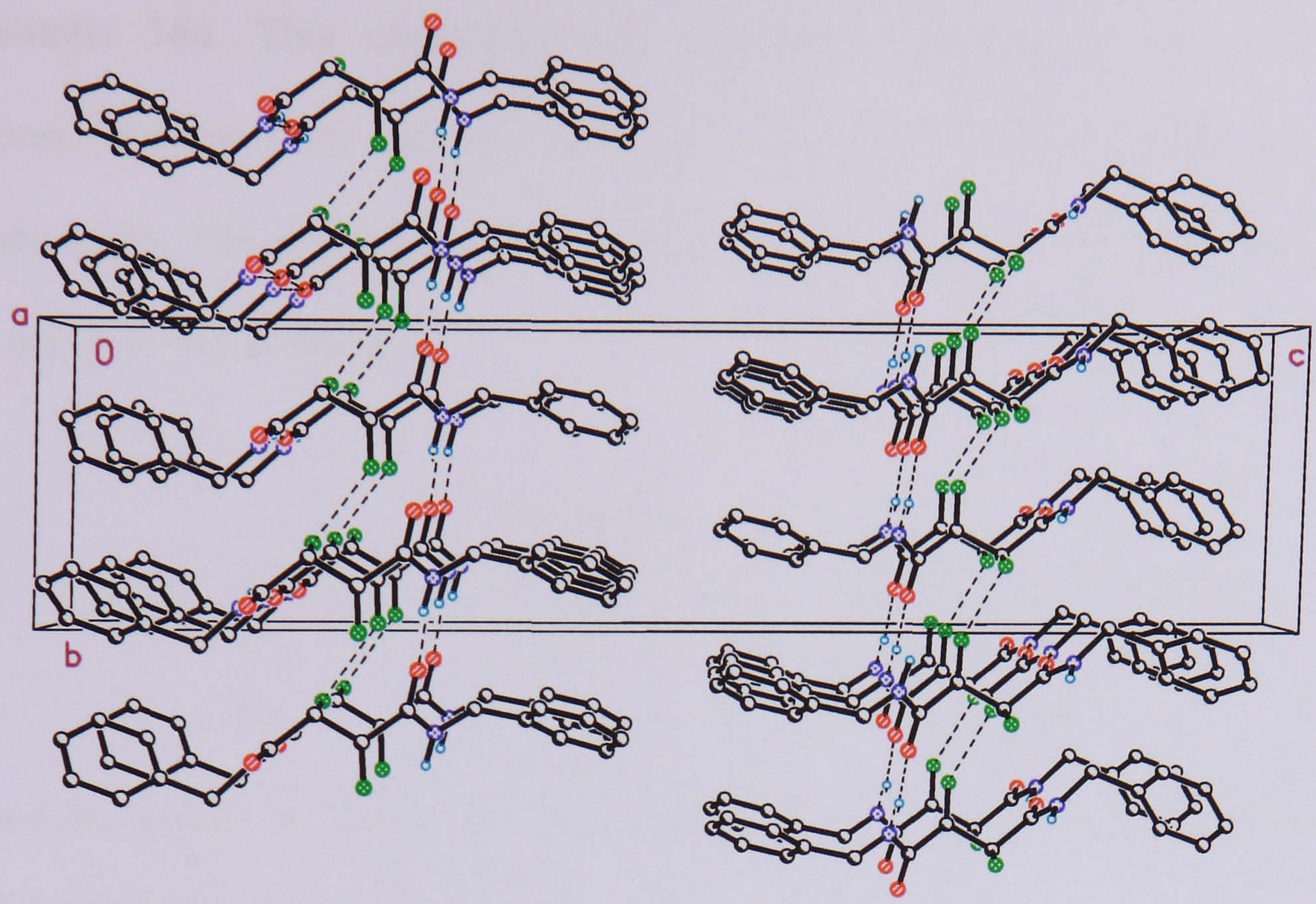

Figure 2.21. The crystal packing of **162** is viewed along the c-axis. Short N-H···O contacts are illustrated by dashed lines. Selected interatomic distances (Å) and angles [°] for msdh16: N(3)-H(3N)···O2#1 1.98 [<155.2], N13-H(13N)···O(32)#1 1.97 [<157.1], N23-H(23N)···O(22)#1 2.04 [<152.5], N33-H(33N)···O12#2 1.98 [<159.9].

The diastereoisomers show quite different melting points, which were determined by DSC analysis. Not surprisingly, the *threo* isomer **162**, which consists of a racemic mixture, has the lower melting point compared to the *erythro* isomer **161** (Table 2.5).

Table 2.5. Comparison of physical properties of *erythro* and *threo* dibenzyl 2,3-difluorosuccinamides **161** and **162**.

Stereoisomer	Melting point (DSC)	Melting point (manually)	Crystal system	Space group
threo	133.1 °C	133-147 °C	Monoclinic	P2(1)/c
erythro	165.1 °C	159-160 °C	Triclinic	P-1

A comparative structure without the fluorine substituents is provided by dibenzyl succinamide **164**. This compound was prepared in analogy to the fluorinated structures, starting from succinic acid using the EDC/HOBt coupling procedure (Scheme 2.38). The product could be recrystallised to purity and crystals suitable for X-ray analysis were obtained.

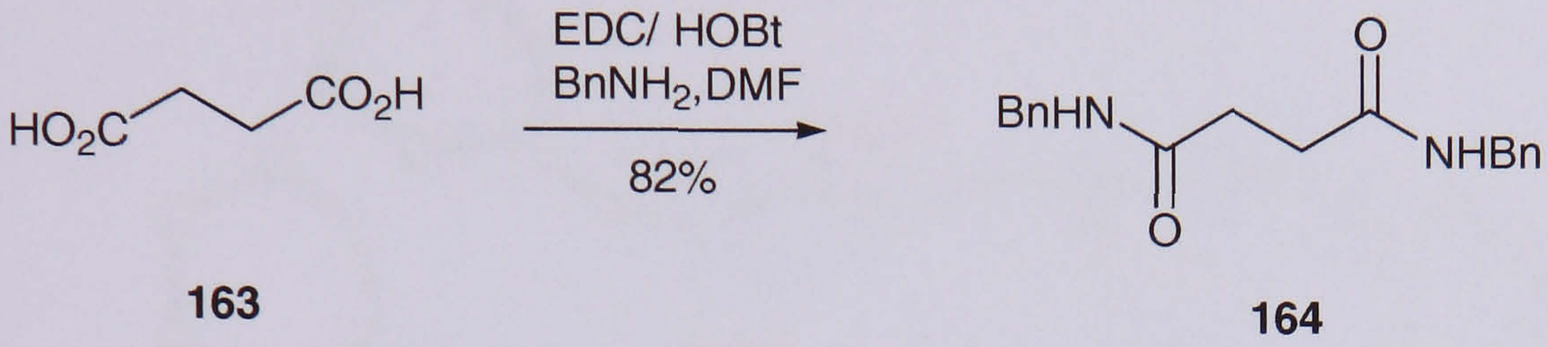

163 **164**

Scheme 2.38. Synthesis of dibenzyl succinamide **164**. The diamide was obtained by EDC coupling of succinic acid **163** with excess benzylamine.

The crystal structure of dibenzyl succinamide shows the main chain to be almost perfectly linear, consistent with minimal steric strain. The carbonyl groups point in opposite directions, which reduces electrostatic repulsion and also results in dipole-dipole compensation of the amide moieties (Figure 2.22).

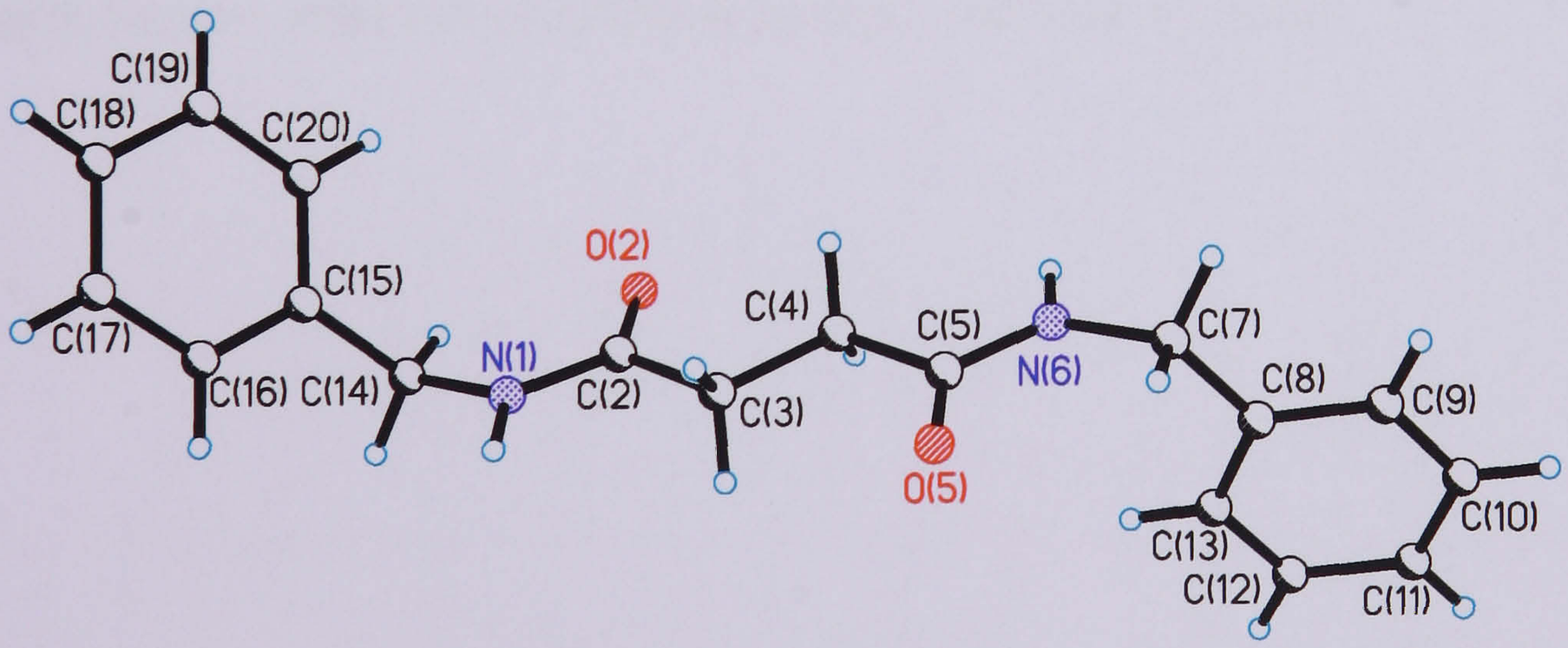

Figure 2.22. X-ray derived structure of dibenzyl succinamide **164**. Selected bond lengths (Å) and torsion angles (°): N1-C2 1.343(3), C2-O2 1.236(3), C2-C3 1.501(4), C3-C4 1.511(3), C4-C5 1.514(4), C5-O5 1.230(3), C5-N6 1.346(3); C14-N1-C2-O2 5.0(4), C14-N1-C2-C3 -174.8(3), O2-C2-C3-C4 4.6(4), N1-C2-C3-C4 -175.6(3), C2-C3-C4-C5 -179.7(3), C3-C4-C5-N6 178.9(2), C4-C5-N6-C7 176.6(3), O5-C5-N6-C7 -2.6(4).

There is clearly intermolecular hydrogen bonding between the carbonyl oxygen and the amide hydrogen as indicated by the dashed lines (Figure 2.23). The geometry of the molecule allows for an antiparallel orientation of the individual molecules in the crystal packing, which is analogous to that found in *anti* parallel β-sheet of peptides.

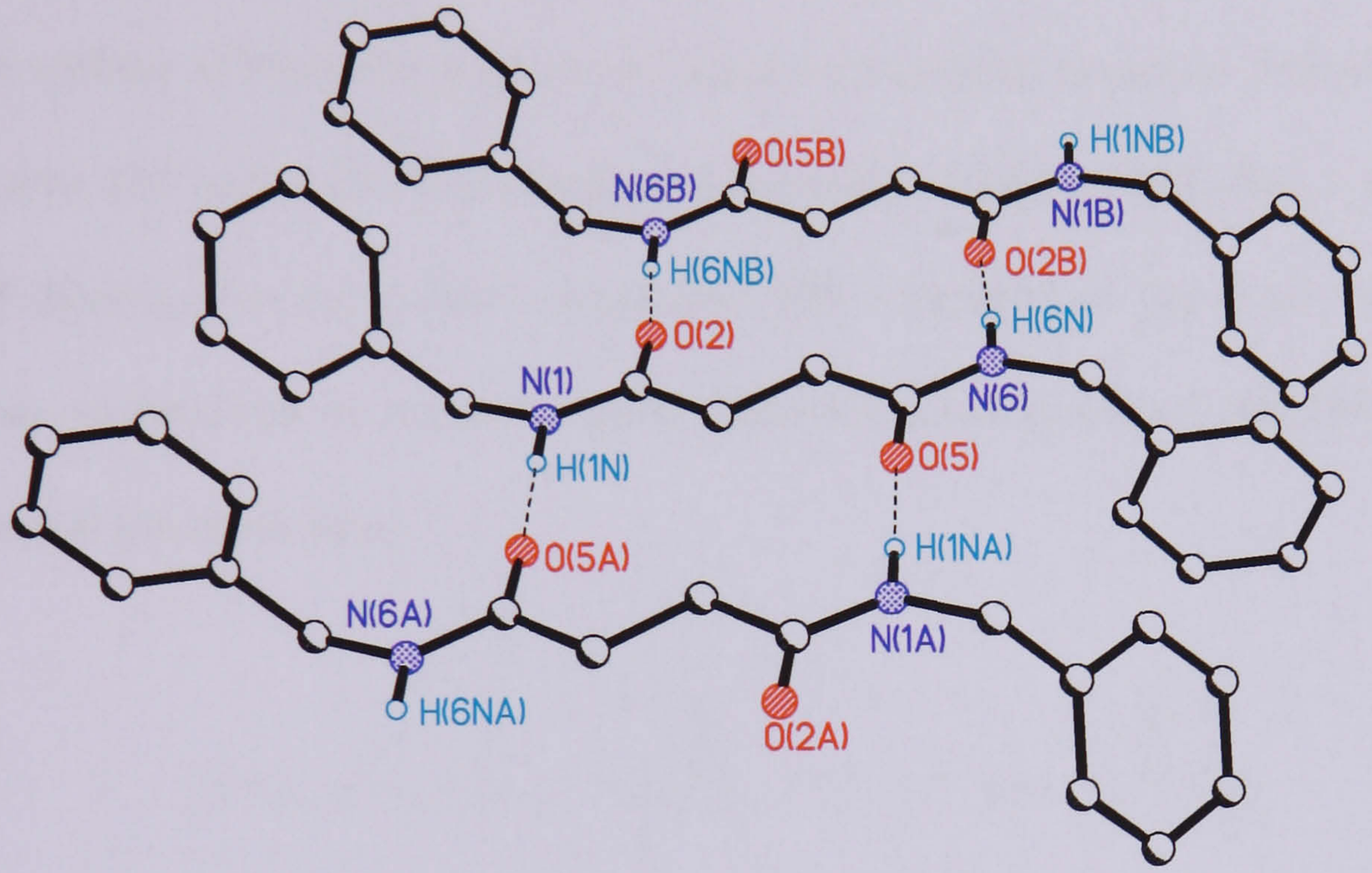

Figure 2.23. The crystal packing of dibenzyl succinamide **164**. Short N-H···O contacts are indicated by dashed lines, which suggest intermolecular hydrogen bonding. Selected distances (Å) and angles [°] for msdh18: N1-H1N···O5#1 1.877(3) [<179(2)], N6-H6N···O2#2 1.844(3) [176(2)].

2.1.7 Langmuir isotherm analysis

Langmuir isotherm analysis has been used as a tool in which to assess conformational stability of structurally related compounds.[48] For example, the technique has been used to investigate the conformational stability of 9,10-difluorostearic acids **165** and **166** (Scheme 2.40).[49] As part of the analysis, each of the stearic acids was deposited onto the surface of ultrapure water in a Langmuir trough to measure surface pressures *versus* area per molecule. The resultant Langmuir isotherms indicated a significant level of disorder for the *erythro* compound **165** compared to the *threo* isomer **166**. This was rationalised in terms of quite different conformational stabilities for the individual diastereoisomers.

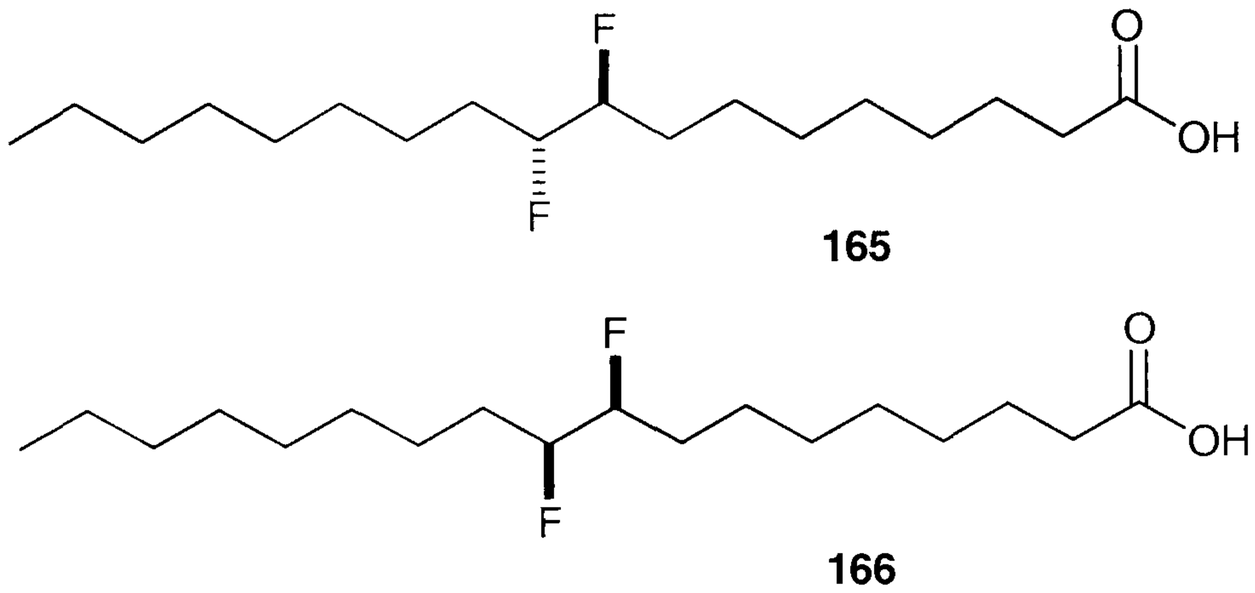

165

166

Scheme 2.40. Langmuir isotherm analysis of compounds **165** and **166**, and comparison of their Langmuir isotherms allows for investigation of conformational mobility of the compounds.

Attachment of long alkyl substituents onto the difluorosuccinic acids would allow for Langmuir isotherm analysis of these compounds. Ideally, the substituents require polar groups at the end of the chain in order to associate with the water surface. The planarity of the α-fluoroamide moieties will impart some degree of rigidity to the molecule that will amplify the effect around the F-C-C-F motif (Scheme 2.41).

It was anticipated that the *threo* isomer in Scheme 2.41 would be more extended than the *erythro* isomer due to the *vicinal* fluorine *gauche* effect. The *threo* compound has the C-F bonds *gauche* in the extended zig-zag conformation, which is stereoelectronically preferred. Applying pressure to the *threo* isomer **166** will require additional energy compared to the *erythro* isomer **165** in Scheme 2.41 that has the two C-F bonds *anti* with respect to each other. As a result, the diastereoisomers may exhibit quite different Langmuir isotherm behaviour, an effect that can be directly attributed to the conformational mobility of these compounds.

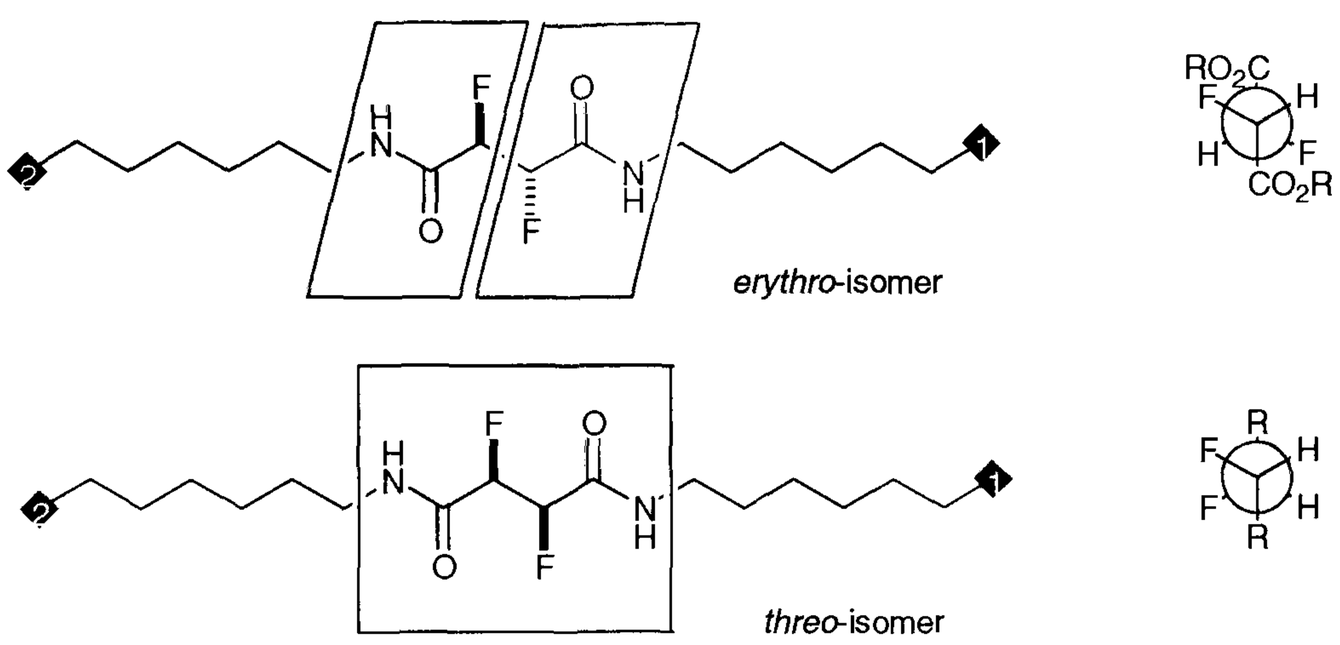

Scheme 2.41. The diasteroisomers of alkyl amides derived from 2,3-difluorosuccinic acid **130** and **132**. The rhombuses indicate polar groups necessary for effective adsorption onto the water surface. The squares drawn over the α-fluoroamide moieties indicate their conformational rigidity.

Suitable substituents to be attached to 2,3-difluorosuccinic acid **130** and **132** may be long chain carboxylic acids or their ammonium salts to ensure binding to the water surface. 11-Aminoundecanoic acid **167** emerged as the molecule of choice to be attached to the difluorosuccinic acid scaffold. This transformation required protection of the carboxyl group prior to amide formation. Several methods are available for this reaction, the most classical of which involves a protection/deprotection sequence of the amino group.[50]

According to the literature procedure, protection of the amino group was carried out with butoxycarbonyl anhydride. The N-protected amino acid was then esterified under basic conditions with methyl iodide, and the final building block 170 obtained by deprotection of the butoxycarbonyl group with acetyl chloride/methanol (Scheme 2.42).

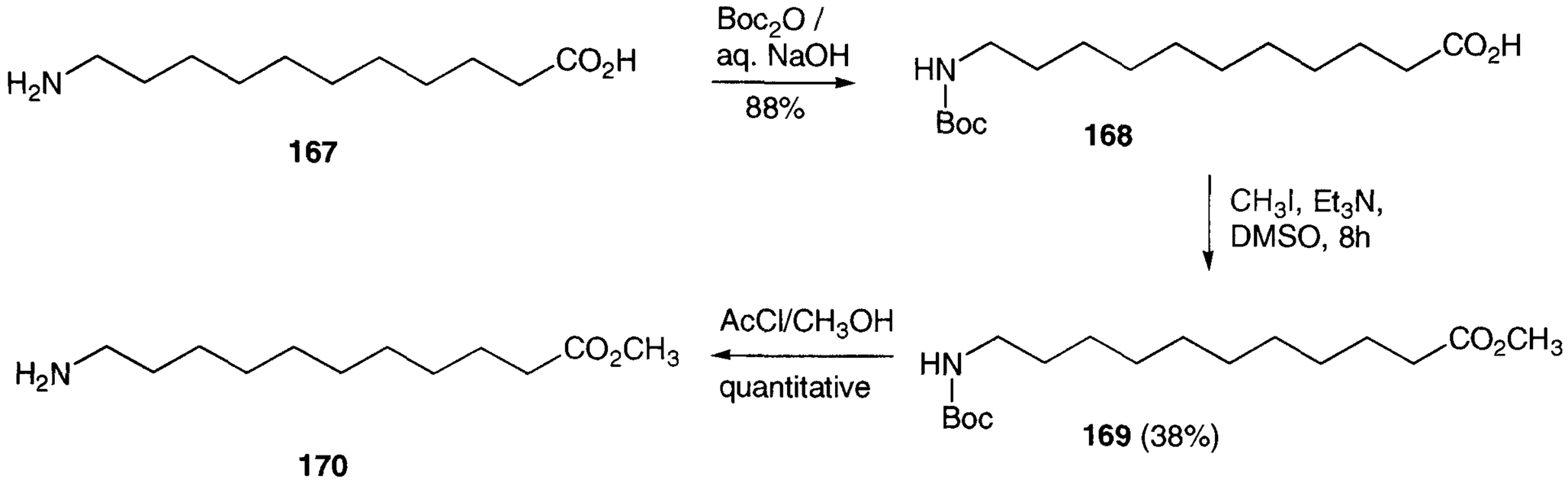

Scheme 2.42. Synthesis of methyl 1-aminoundecanoate **170** required for EDC coupling to 2,3-difluorosuccinic acids **130** and **132**.

The reaction of acetyl chloride in excess methanol generates dry hydrochloric acid which can facilitate esterification of the carboxyl group. The combination of acetyl chloride and an alcohol has been used as a synthetic protocol for simultaneous esterification and deprotection of amino acids.[51] In principle the coupling of esterification and deprotection should furnish the amino ester in a single step. Application of this methodology to the protected amino ester **169** indeed gave the amino ester **170** directly, however in a disappointingly low yield. An attempt aimed at direct esterification of 11-aminoundecanoic acid **167** with trimethylsilyl diazomethane proceeded equally sluggishly.[52] Material was therefore brought through using the established esterification/ deprotection protocol.

The amino ester **170** can be readily coupled with 2,3-difluorosuccinic acids **130** and **132** using the established EDC peptide coupling protocol. The resultant amides **171** and **172** were readily hydrolysed under acidic condition to give the free carboxylic acids **173** and **174** (Scheme 2.43).

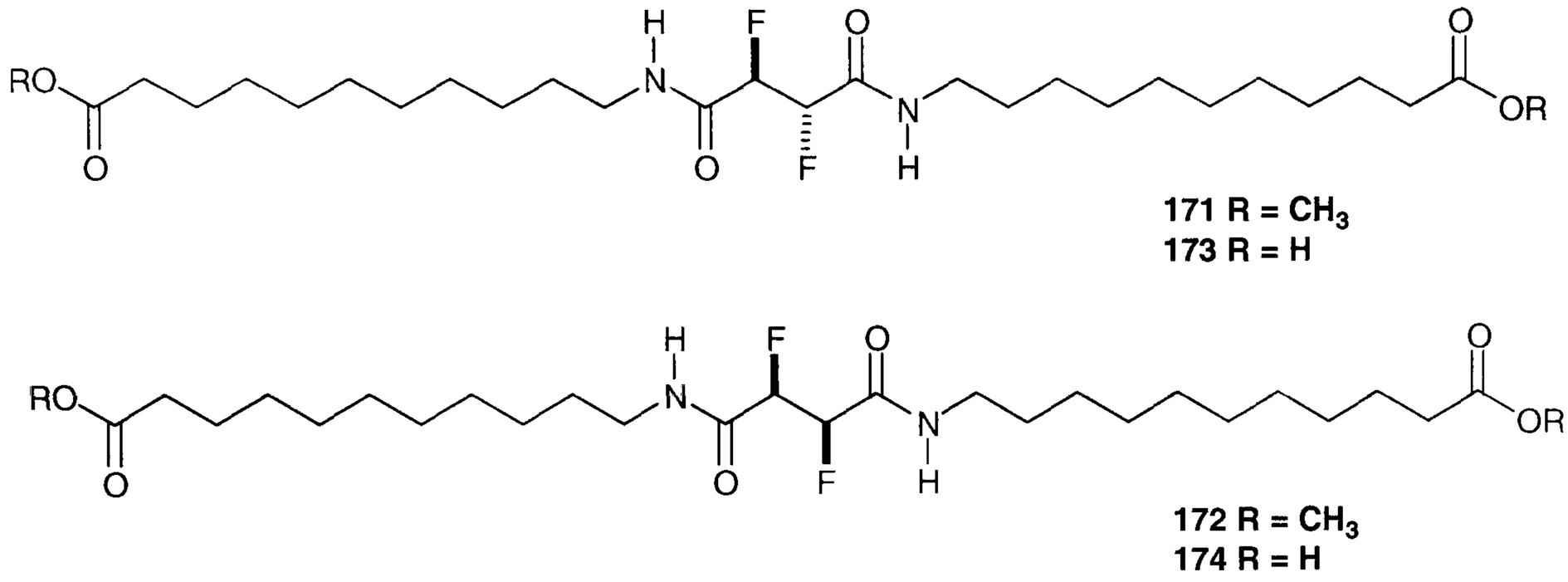

Scheme 2.43. The diasteroisomerically pure diamides **171** and **172** were obtained by EDC/HOBt coupling of methyl 1-aminoundecanoate **170** with 2,3-difluorsuccinic acids **130** and **132** in DMF at RT.

The Langmuir isotherm analysis was carried out with compound **174**, however, due to the solubility properties of compound **174** these results were not unambiguous. Addition of chloroform as a co-solvent to the water phase facilitated the measurement of a surface to pressure isotherm, which however has to be confirmed by additional experiments. The experiment indicated an extended surface area at low pressure, which underwent some sort of phase change with at higher pressures. In particular, the analysis of the *erythro* isomer **173** will be of major interest for comparison. Although compound **173** was conveniently obtained in the same manner as compound **174**, purification proved to be somewhat more difficult. Purification of **173** to pass elemental analysis and the synthesis of a non-fluorinated analogue will be in the focus of further work in this area.

Compounds **173** and **174** were solids at room temperature and were obtained as white crystals. The melting points of **173** and **174** were investigated in order to establish differences in terms of physical properties for the diastereoisomers. The melting points are very similar and the differences observed are likely to be within experimental error (Table 2.6).

Table 2.6. Melting points of compounds **173** and **174** obtained from DSC analysis and melting point apparatus.

Stereoisomer	Melting point (manually) R = OH	Melting point (DSC) R = OH
threo	145-146 °C	151.1 °C (1^{st}) 131.5 °C (2^{nd})
erythro	138-141 °C	146.7°C

The difference in purity of the two isomers may have significant influence on the melting point. In order to establish the melting points unambiguously, the melting points were measured by DSC analysis (Table 2.6). The experiment shows a slightly higher melting point for the *threo* isomer in the first heat cycle, but a lower melting point in the second cycle. The appearance of phase changes at different temperatures for the same compound indicates the appearance of different polymorphs. The effect of polymorphism was anticipated for the *erythro* compound, which may have a tendency to adopt either a F-C-C-F *gauche* conformation, or the extended zig-zag conformation of the main chain on the other hand. However the *erythro* isomer **173** did not indicate such an effect and thus concise conclusions are not forthcoming from these experiments.

2.1.8 Effect of the *vicinal* difluoro motif on chemical reactivity

In order to explore the effect of conformation on chemical reactivity, *bis*-allyl amides **175** and **176** of 2,3-difluorosuccinic acids were prepared. The *erythro* and *threo* diastereoisomers **175** and **176** were expected to show different reactivity towards ring closing methathesis, a reaction, which has recently attracted much attention in organic synthesis.[53] Cross metathesis (CM) and ring closing metathesis (RCM) have also found application in fluoroorganic chemistry. [54,55] The reaction has been shown to be especially useful in generating medium ring sizes, which are traditionally problematic in organic synthesis due to enhanced ring strain. The reaction therefore appeared to be ideal to benchmark the influence of two *vicinal* C-F bonds in **175** and **176** on chemical reactivity. As a consequence of the *gauche* effect, it was anticipated that the *erythro* isomer **175** would cyclise more readily than the *threo* isomer **176**.

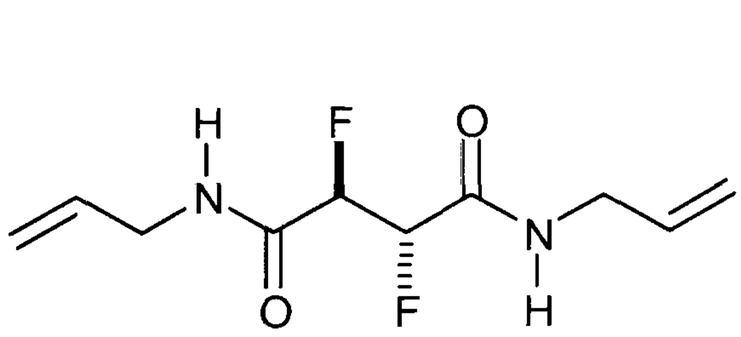

175

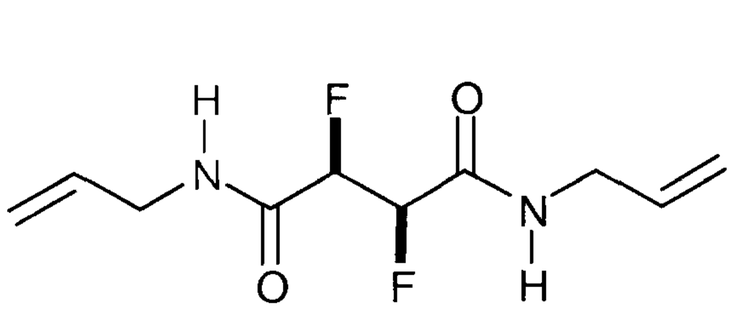

176

Scheme 2.44. The preparation of *bis*-(1-propenyl)-2,3-difluorosuccinamides **175** and **176** was achieved using the standard EDC/HOBt coupling protocol.

Synthesis of the RCM precursors was accomplished using the standard EDC peptide coupling protocol as outlined previously. The *threo* and *erythro* isomers **175** and **176** were obtained as a mixture of stereoisomers starting from a 1:1 mixture of *threo* and *erythro* 2,3-difluorosuccinic acids **120**. No attempt was made to separate the diastereoisomers and the stereoisomers **175** and **176** were used as a mixture in order to compare the rates of reaction under identical conditions. The progress of the

reaction was monitored using ^{19}F NMR spectroscopic analysis and ESI mass spectrometry. The reaction was performed according to a literature procedure using 2 mol% of Grubbs catalyst in dichloromethane (Scheme 2.45).[56]

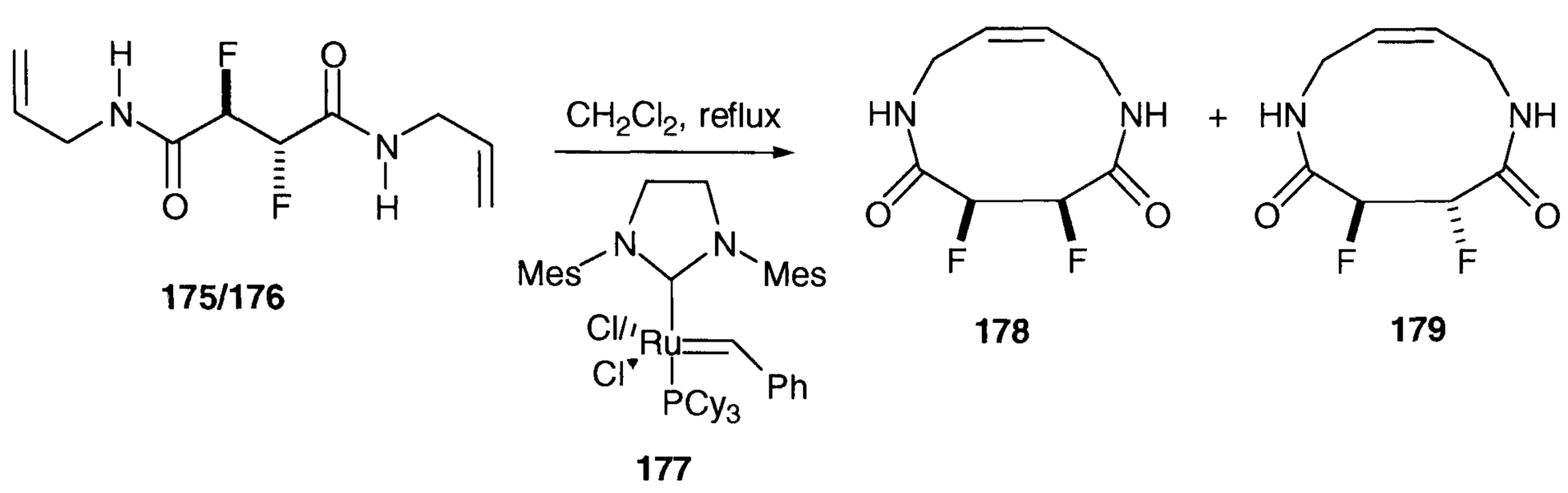

Scheme 2.45. Attempted ring closing metathesis of 2,3-difluorosuccinamides **175** and **176**.

In the methathesis reaction, there was no clear indication of product formation from either of the diastereoisomers. A variety of signals were observed in the ^{19}F NMR spectrum possibly indicating the formation of various oligomers. The formation of oligomers of **175** and **176** may be favoured kinetically due to the presence of the fluorine substituents. The strong preference of the α-fluoroamide moiety to adapt a *syn* planar conformation may render the intramolecular ring closure difficult as steric and stereoelectronic effects have to be overcome in bringing the molecular termini together. Considerable ring strain in the cyclic bisamides **178** and **179** will also render the process thermodynamically less favourable, as well as the presence of the endocylic double bound in the 10-membered ring. Consequently, the formation of a cyclic structure comprising the *vicinal* difluorosuccinamide moiety may be hard to achieve, even though there are a number of other synthetic methods for this transformation available.

References

[1] J. M. Percy, *Top. Curr. Chem.*, 1997, **193**, 131.

[2] J. Hutchinson, G. Sandford, *Top. Curr. Chem.*, 1997, **193**, 1.

[3] M. Shimizu, T. Hiyama, *Angew. Chem. Int. Ed.*, 2005, **44**, 214.

[4] S. Rozen, *J. Org. Chem.*, 1986, **51**, 3607.

[5] M. Zupan, A. Pollak, *J. Org. Chem.*, 1977, **42**, 1559.

[6] V. Dinoiu, T. Fukuhara, S. Hara, N. Youeda, *J. Fluorine Chem.*, 2000, **103**, 75.

[7] L. Paquette, In *Reagents in Organic Synthesis*, Volume 6, Elsevier, 1998.

[8] M. Tavasli, D. O'Hagan, C. Pearson, M. Petty, *J. Chem. Soc., Chem. Comm.*, 2002, 1226.

[9] A. I. Burmakov, L. A. Motnyak, B. V. Kunshenko, L. A. Alexeeva, L. M. Yagupolskii, *J. Fluorine Chem.*, 1981, **19**, 151.

[10] LC_{50} (rats) for SF_4 = 40 ppm, $COCl_2$ = 5 ppm, HF = 1278.

[11] M. Hudlicky, *J. Fluorine Chem.*, 1983, **23**, 241.

[12] R. G. Syvret, D. L. Vassilaros, D. M. Parees, G. P. Pez, *J. Fluorine Chem.*, 1994, **67**, 277.

[13] G. Olah, *J. Org. Chem.*, 1979, **44**, 3872.

[14] G. Olah, M Nojima, I. Keres, *Synthesis*, 1973, 780.

[15] G. Alvernhe, A. Laurent, G. Haufe, *Synthesis*, 1987, 562.

[16] R. D. Chambers, In *Fluorine in Organic Chemistry*, Wiley & Sons, New York, 2004.

[17] G. Stavber, M. Zupan, M. Jereb, S. Stavber, *Org. Lett.*, 2004, **6**, 4973.

[18] T. Ernet, G. Haufe, *Tetrahedron Letters*, 1996, **37**, 7251.

[19] T. Ernet, Haufe, *Synthesis*, 1997, 953.

[20] H. Saga, T. Hamatani, Y. Gugginberg, M. Schlosser, *Tetrahedron*, 1990, **46**, 4255.

[21] M. Essers, C. Mueck-Lichtenfeld, G. Haufe, *J. Org. Chem.*, 2002, **67**, 4715.

[22] G. DiMartino, J. M. Percy, *J. Chem. Soc., Chem. Comm.*, 2000, 2339.

[23] D. H. R. Barton, R. H. Hesse, G. P. Jackman, L. Ogunkoya, M. M. Pechet, *J. Chem. Soc., Perkin Trans. 1*, 1974, 739.

[24] M. Finkelstein, *Chem. Ber.*, 1910, **43**, 1531.

[25] J. A. Miller, M. J. Num, *J. Chem. Soc., Perkin Trans 1*, 1976, 416.

[26] A. Roedig, *Methoden Org. Chemie (Houben-Weyl)*, 1960, Vol. 5/4, 595.

[27] J. A. Miller, M. J. Num, *J. Chem. Soc., Perkin Trans. 1*, 1976, 416.

[28] F. Faustini, S. De Munari, V. Villa, C. A. Gandolfi, *Tetrahedron. Lett.*, 1981, 4533.

[29] D. J. Cram, *Electrophilic rearrangements, in Fundamentals of Carbanion Chemistry*, Academic Press, 1965, 223-243.

[30] R. Keck, J. Retey, *Helv. Chim. Acta*, 1980, **63**, 769.

[31] L. Harwood, *Polar rearrangements*, Oxford Chemistry Primers, Oxford University Press, 1995, 12.

[32] Z.-T. Zhang, X.-B. Wang, Q.-G. Liu, J.-B. Zheng, K.-B. Yu, *Acta Cryst.*, 2005, C61, 29.

[33] K. B. Wiberg, *Acc. Chem. Res.*, 1996, **29**, 229.

[34] K. Cho, M. Park, Y.-K. Shim, K. Lee, *Bull. Korean Chem. Soc.*, 2002, **23**, 1830.

[35] N. A. Fokina, A. M. Kornilov, I. B. Kulik, V. P. Kukhar, *Synthesis*, 2002, 2539.

[36] A. K. Bose, K. G. Das, P. T. Funke, *J. Org. Chem.*, 1963, **29**, 1202.

[37] S. A. Pogany, G. M. Zentner, C. D. Ringeisen, *Synthesis*, 1987, 718.

[38] S. Norsikian, *Chem, Eur. J.*, 1999, **5**, 2055.

[39] S. D. Razumovskii, G. E. Zaikov, In *Ozone and its reactions with organic compounds*, Elsevier, Amsterdam, 1984.

[40] T. Aoyama, *J. Chem. Soc. Perkin Trans. 1*, 1995, **15**, 1905; M. Imuta, *J. Org. Chem.*, 1978, 43, 3319.

[41] M. Nakajima, K. Tomioka, K. Koga, *Tetrahedron*, 1993, **49**, 9735.

[42] R. Criegee, *Rec. Chem. Prog.*, 1957, **18**, III/20.

[43] S. Berger, C. Geletniki, *Eur. J. Org. Chem.*, 1998, 1625.

[44] R. Criegee, *Angew. Chem. Int. Ed.*, 1975, **87**, 745.

[45] L. Long Jr., *Chem. Rev.*, 1940, **27**, 437.

[46] P. S. Bailey, *Chem. Rev.*, 1958, **58**, 925.

[47] R. B. Woodward, M. P. Cava, W. D. Ollis, A. Hunger, H. U. Daenicker, K. Schlenker, *Tetrahedron*, 1963, **19**, 247.

[48] D. O'Hagan, I. Kumadaki, M. Petty, H. Takaya, C. Pearson, *J. Fluorine Chem.*, 1998, **90**, 133.

[49] M. Tavasli, D. O'Hagan, C. Pearson, *J. Chem. Soc., Chem. Comm.*, 2002, 1226.

[50] K. W. Laue, G. Haufe, *Synthesis*, 1998, 1453.

[51] A. Nudelman, *Synth. Comm.*, 1998, **28**, 471.

[52] T. W. Greene, P. G. M. Wuts, In *Protective Groups in Organic Synthesis*, 3rd edition, 1999, Wiley & Sons, New York, 494.

[53] For general review on cross-metathesis: A. K. Chatterjee, T.-L. Choi, D. P. Sanders, R. H. Grubbs, *J. Am. Chem. Soc.*, 2003, **125**, 11360; S. J. Connon, S. Blechert, *Angew. Chem., Int. Ed.*, 2003, **42**, 1900.

[54] C. Audouard, J. Fawcett, G. A. Griffiths, J. M. Percy, S. Pintat, C. A. Smith, *Org. Biomol. Chem.*, 2004, **2**, 528.

[55] S. Thibaudeau, R. Fuller, V. Gouverneur, *Org. Biomol. Chem.*, 2004, 1110.

[56] K. S. Dunne, F. Bisaro, B. Odell, V. Gouverneur, *J. Org. Chem.*, 2005, **70**, 10803.

2.2 Pseudopeptides

The term pseudopeptide refers to a molecule that is structurally related to a peptide. Peptides are made up of specific sequences of amino acids, and they represent a universal building block in nature of which all living organisms are constructed. Small peptides are used as therapeutic agents due to their ability to influence neurological, immunological, and enzymatic processes with high specificity and prodigious potency.[1] Many artificial peptides have found application in various fields of medicine such as in the control of pain, cancer therapy, cardiovascular problems, connective tissue diseases, digestive disorders, mental illnesses, and in the regulation of fertility and growth.[2] There are currently more than 40 marketed peptide therapeutics worldwide, and today, the global peptide pharmaceutical market has reached an annual growth rate of over >15 %.[3] Peptide structures are also of growing interest in materials science where proteins form polymers of amazing stability, strength and elasticity. As an example, the silk of the garden spider *Araneus diadermatus*, which consists of protein domains of 200-300 kDa, has strength comparable to that of nylon and a superior elasticity to all known materials.

The concept of introducing fluorine into peptide structures is relatively new, probably due to synthetic limitations to regio- and stereoselective fluorination.[4] Nevertheless, fluorine containing aminoacids and peptides have found widespread bio-organic applications for instance as enzyme inhibitors, biological tracers, and in medical applications including the control of blood pressure, allergies, and tumor growth.[5] Due to the small size of fluorine its replacement for other substituents such as hydrogen or hydroxyl does not induce significant steric perturbations, and once introduced, the strong carbon-fluorine bond is particularly resistant to metabolic

transformations.[6] This effect is extremely important in maintaining activity and improving bioavailability of therapeutic agents, given the fact that these are usually administered far from the site of action. Moreover, the high electronegativity of fluorine can also have a significant effect on the basicity and acidity of neighbouring functional groups and on the electron distribution of the molecule. Hence, it may change the overall reactivity and stability of a given compound and often, profound and unexpected changes in their activity and pharmacokinetic profiles are observed. In addition, the sensitivity of the fluorine nucleus to the surrounding environment along with large ^{19}F-^{1}H coupling constants renders fluorine incorporation a particularly powerful tool for the investigation of biological processes. Proteins can be analysed conveniently by ^{19}F NMR spectroscopy in their natural environment without any background noise. The fluorine chemical shift is of such sensitivity that an increase or decrease by as much as 8 ppm can be observed when the protein is denatured.[7]

Proteins form well-defined three-dimensional structures, which are the basis of their biological function. The term peptidomimetics has been coined for compounds that mimic the action of certain peptide motifs and the efficiency of such compounds will crucially depend upon its ability to adopt specific secondary and tertiary structures. As the inherent conformational flexibility of a peptide can result in a large number of possible structures, it is of importance to predict and control the conformation of peptides or peptidomimetics in the development of new therapeutics. In this context, the introduction of fluorine may add a valuable tool in tuning the secondary and tertiary structure of peptides by stereoelectronic effects.

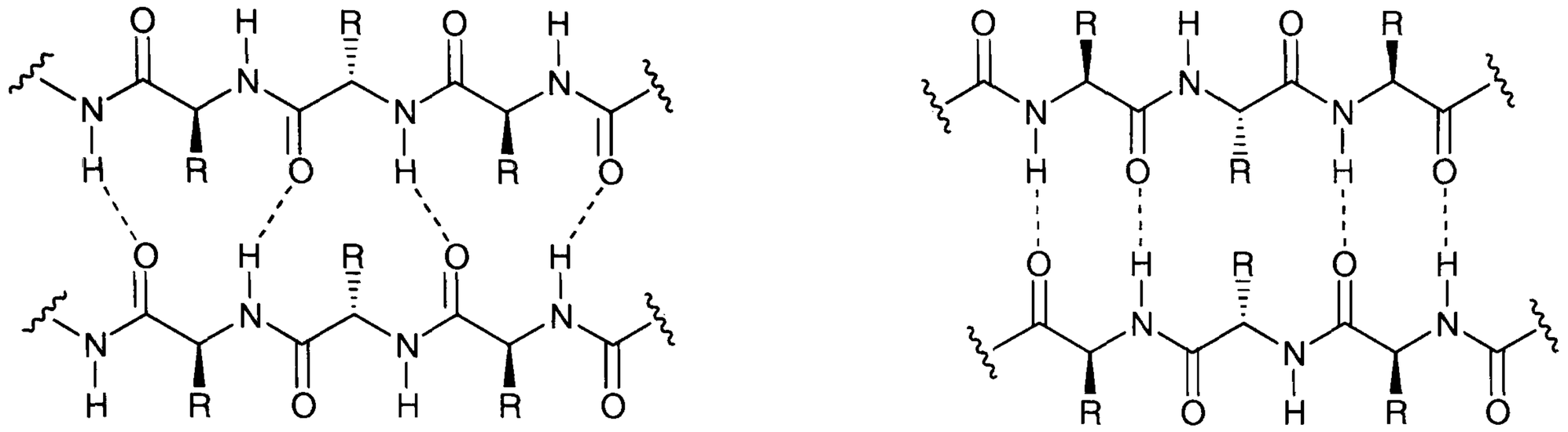

a b

Scheme 2.47. Parallel (**a**) and antiparallel (**b**) β-sheets are common features in peptide structures.

The most common secondary structures in peptides are α-helices, β-sheets, and β-turns. These structural elements are important in inducing the three-dimensional structure and biological activity of all proteins. β-Sheets consist of peptide strands that are knitted together by hydrogen bonding in a parallel or antiparallel manner (Scheme 2.47). Parallel or antiparallel β-sheets are fundamental structural elements that can be recognised in protein structures.[8] In the major histocompatibility complex (MHC) for instance, proteins selectively bind the extended β-strand conformation of peptides derived from viral, bacterial and endogenous proteins,[9] a process which is implicated in leukemia, inflammatory, and neurological diseases.[10] Therefore, small molecules that mimic β-strands can have important potential applications in medicine as enzyme inhibitors and antagonists. Fluorinated analogues of β-strands and α-helices have been prepared and found to form novel secondary structures along with having superior metabolic stability.[11]

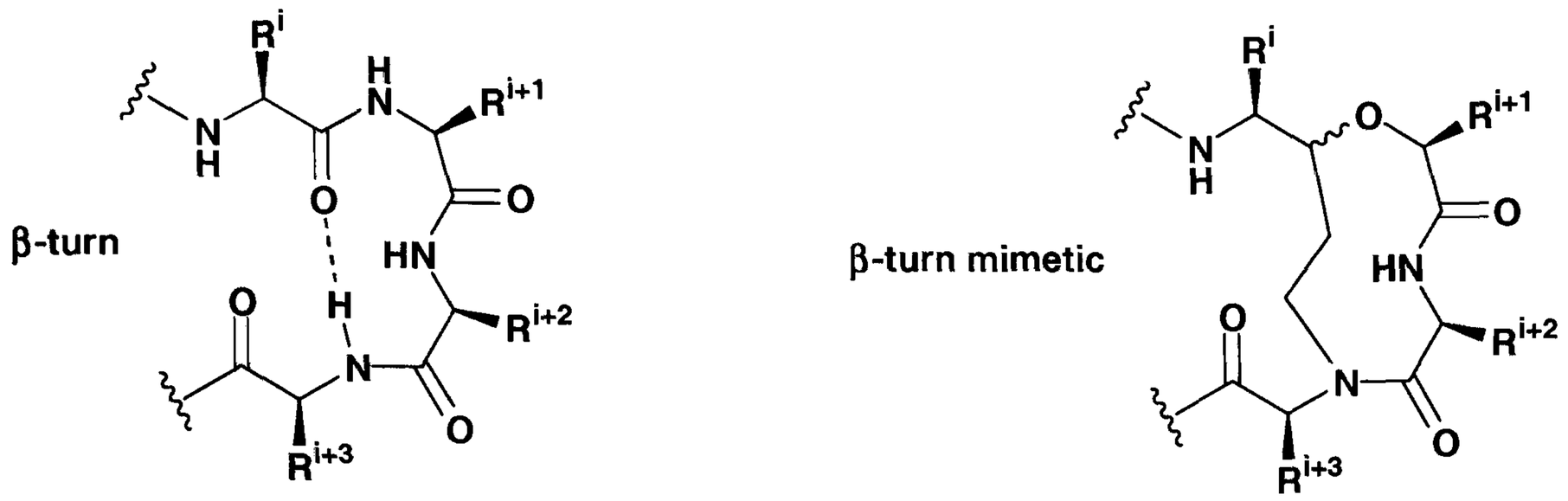

Scheme 2.48. Synthesis of a β-turn mimetic in which the intramolecular hydrogen bond is replaced by an ethylene bridge.[12]

β-Turns represent frequently encountered structural elements within proteins, where they can serve as recognition sites at protein surfaces. In addition, small biologically active peptide hormones such as LHRH and somatostatin have been found to adopt β-turn conformations.[13] Synthetic β-turn mimetics have been developed in order to nucleate β-sheet formation in small peptides and to improve the biomedicinal activity of peptides through conformational restriction (Scheme 2.48). Such conformationally restricted β-turn mimetics have been synthesised, but most of them have only been successful in nucleating β-sheet formation.

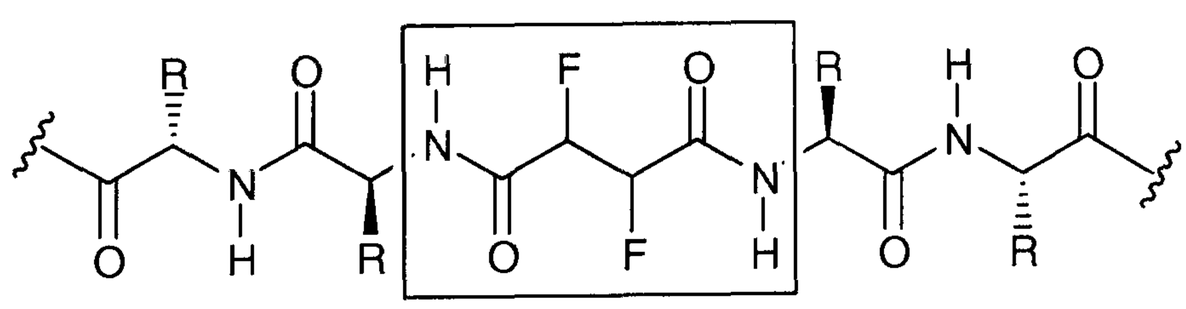

Scheme 2.49. Putative peptide structure derived from 2,3-difluorosuccinic acid. The *vicinal* difluoro motif can be introduced stereoselectively, presumably giving rise to different secondary structures.

The synthesis of pseudopeptides, which can reversibly adopt β-turn structures, would represent a step forward in this area of research. The incorporation of two *vicinal* fluorines into a given peptide molecule may induce conformational preferences by

stereoelectronic effects, which could ensure both conformational reversibility and tunability. The synthetic advantage of this approach is obvious. The *vicinal* difluoro motif can be introduced simply by attachment of amino acids on either side of the 2,3-difluorosuccinic acid moiety, rather than to elaborate complex synthetic routes to generate fluorinated amino acids stereoselectively (Scheme 2.49). The amino esters of the natural amino acids are all commercially available, and coupling of the various esters would allow for orthogonal deprotection under basic and acidic conditions, or by hydrogenation.[14] The peptide bond can be formed using the EDC/HOBt coupling protocol. Coupling of an enantiomerically pure amino acid **199** with 2,3-difluorosuccinic acid **120** will generate the symmetrical pseudopeptide of general structure **200** (Scheme 2.50).

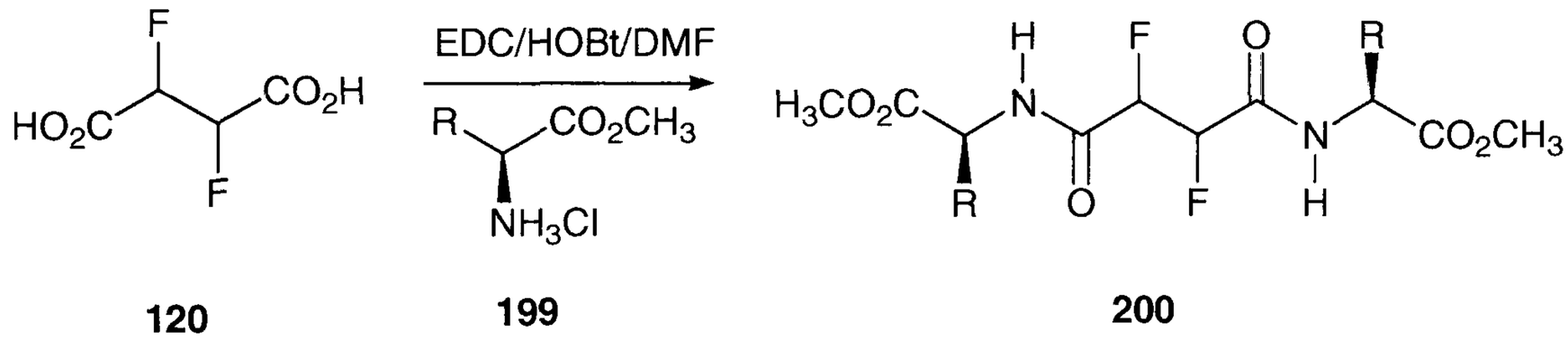

120 **199** **200**

Scheme 2.50. Formation of symmetrical fluorinated pseudopeptides of the general structure **200**.

The mechanism of the coupling reaction involves activation of the carboxyl groups **201** by the carbodiimide reagent **202** to give an *O*-acylisourea **203**. The formation of this intermediate is rapid and leads to peptide **204** either by immediate aminolysis or *via* a symmetrical anhydride **205** (Scheme 2.51). The intermediates **203** and **205** are very reactive and may undergo side reactions. Especially the formation of an *N*-acylurea **206** may compete significantly with intramolecular acyl transfer or aminolysis, leading to reduced yield and purification problems. This difficulty can be avoided in the presence of a suitable α-nucleophile such as hydroxybenzotriazole **207**, which rapidly reacts with the *O*-acylisourea **203** before side reactions can intervene.

The intermediate **208** is still reactive enough to undergo aminolysis, but is less reactive towards other nucleophiles avoiding racemisation and other side reactions.

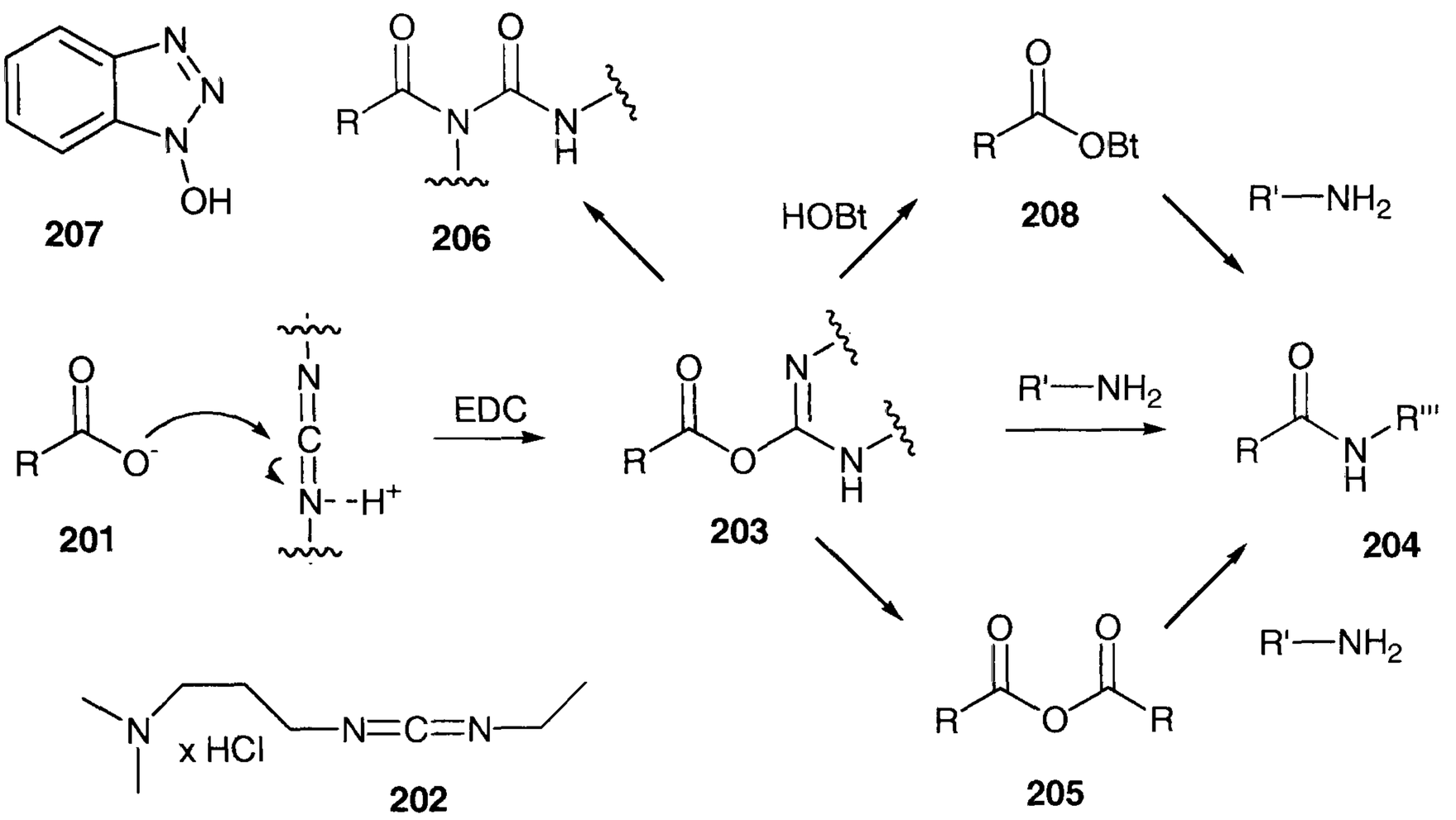

Scheme 2.51. Currently accepted mechanism for the EDC catalysed peptide bond forming reaction.[15]

Starting from pure *erythro* 2,3-difluorosuccinic acid **130**, a series of pseudopeptides **209-212** were derived from L-amino esters of phenylalanine, alanine, valine, and leucine (Scheme 2.52).

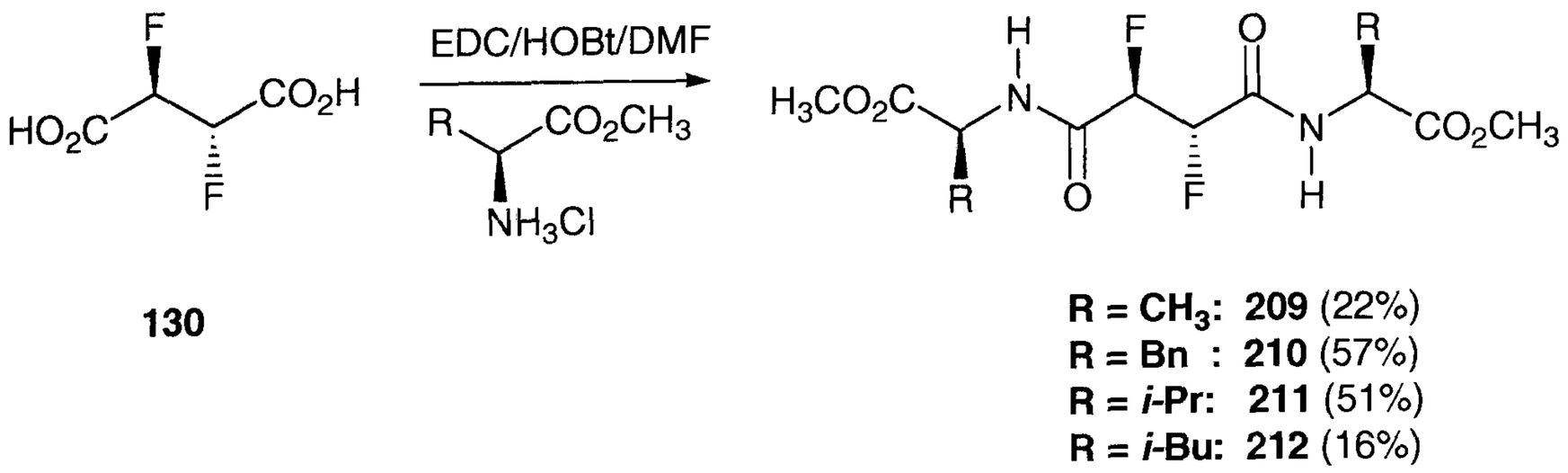

Scheme 2.52. Synthesis of pseudopeptides **209-212** derived from 2,3-difluorosuccinic acid **130**.

These pseudopeptides were investigated by ^{19}F and ^{1}H NMR spectroscopy and their analysis is described in Chapter 2.4. The respective *threo* isomers can be obtained by coupling of the same amino esters with enantiomerically pure *threo* 2,3-difluorosuccinic acid, the synthesis of which was developed from (*R,R*)- and (*S,S*)-tartaric acids (Chapter 2.3). Furthermore, the coupling of unnatural D-amino acids to enantiomerically pure 2,3-difluorosuccinic acids gives access to all possible stereoisomers of **200**. In choosing different natural amino acids, a large variety of *vicinal* difluorinated pseudopeptides is accessible. Coupling of L-phenylalanine with 2,3-difluorosuccinic acids **120** lead to the three diastereoisomeric structures **214**, **215**, and **216** (Scheme 2.53).

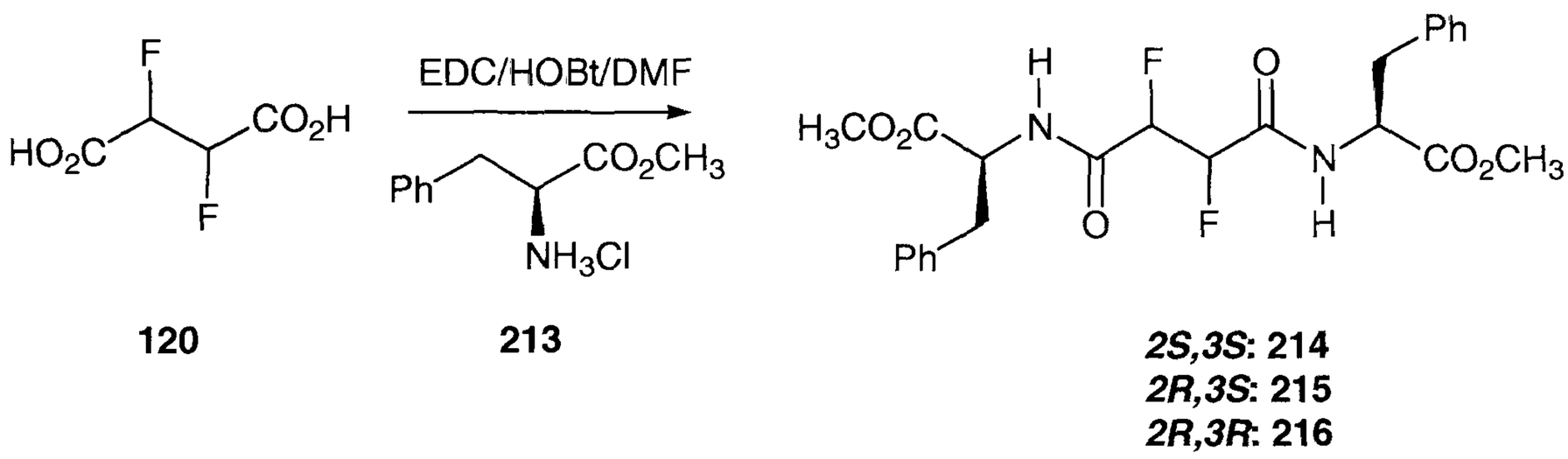

120 **213**

***2S,3S*: 214**
***2R,3S*: 215**
***2R,3R*: 216**

Scheme 2.53. EDC coupling of methyl L-phenylalanine **213** and a mixture of 2,3-difluorosuccinic acid **120** generates the respective pseudopeptide as a mixture of diastereoisomers **214-216**.

The synthesis and isolation of the different stereoisomers **214-216** derived from the mixture **120** was explored. Progress of the reaction was conveniently monitored by ^{19}F NMR spectroscopy. The reaction proceeded cleanly indicated by the appearance of the signals depicted in Table 2.7. Surprisingly, all three diastereoisomers could be readily separated by a combination of flash chromatography and preparative TLC.

This indicates a significant difference in terms of polarity for the stereoisomers **214-216,** which is particularly evident between the *erythro* and *threo* diastereoisomers.

Table 2.7. Expanded region of ^{19}F NMR spectra (282 MHz, $CDCl_3$) for the diastereoisomers **214**, **215**, and **216**. The compounds are listed according to their relative polarity from the top to the bottom.

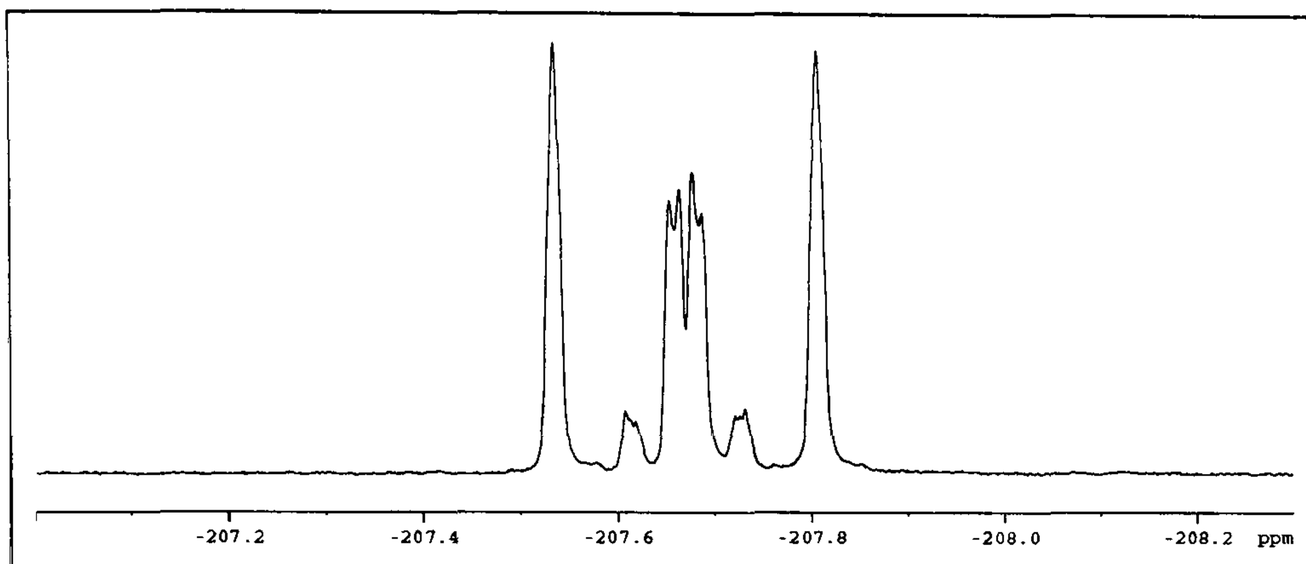

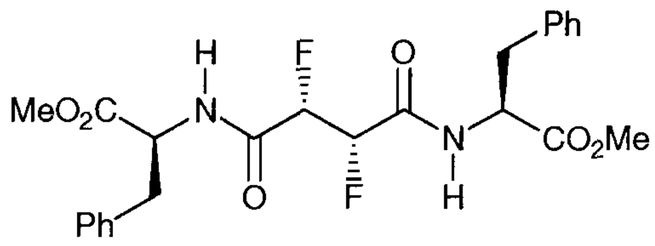

214

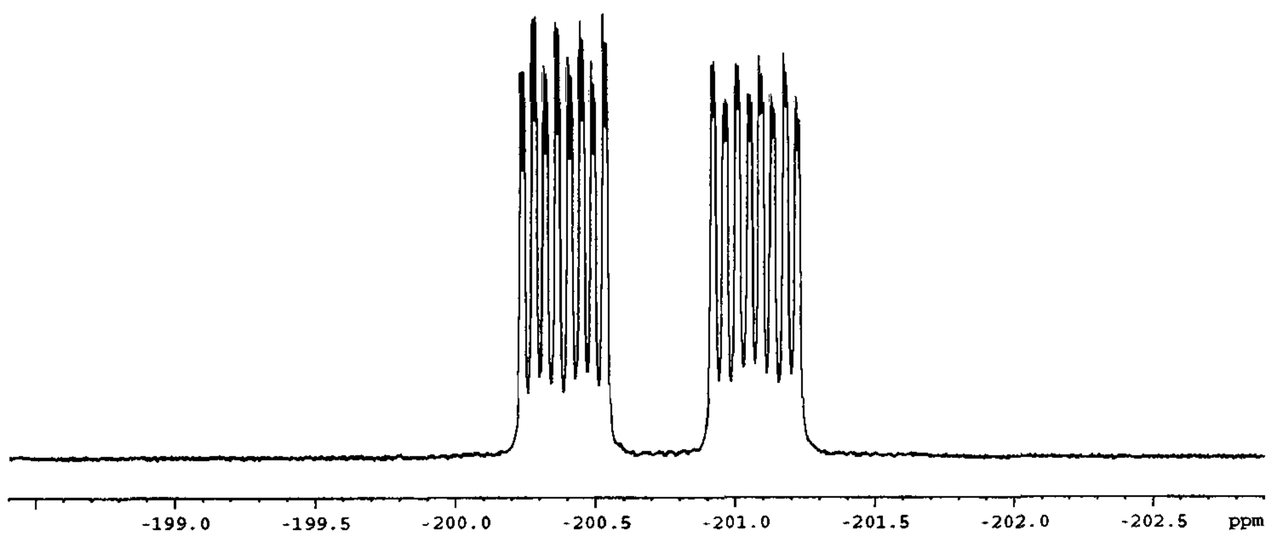

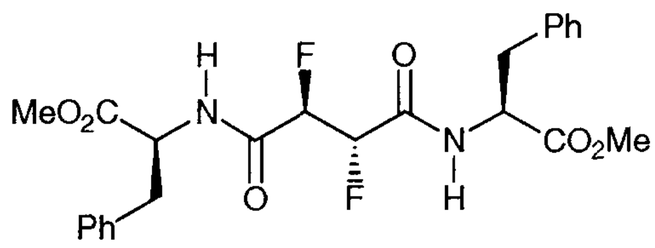

215

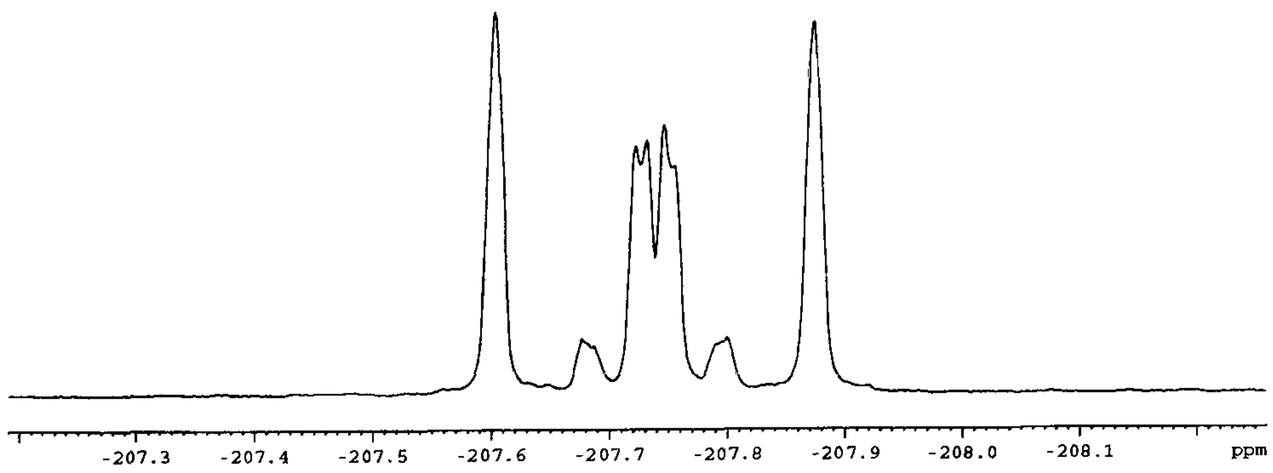

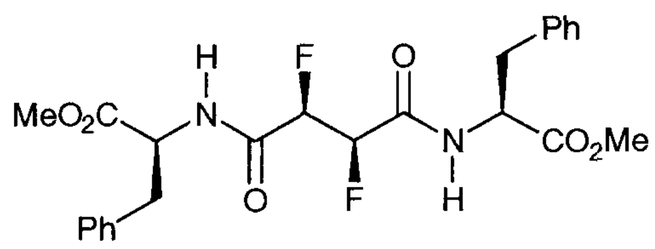

216

The *threo* compounds **214** and **216** have chemically equivalent fluorine nuclei, which are however magnetically nonequivalent. This results in a second order ^{19}F NMR spectrum with an AA'XX' spin pattern (Table 2.7). In contrast, the *erythro* compound **215** has chemically non-equivalent fluorine nuclei as a result of diastereoisomeric interactions with the L-phenylalanine residues. The chemical shifts for the two nonequivalent fluorine nuclei are sufficiently different and give rise to resolved

resonances. Hence, the coupling pattern is first order and two ordinary ddd pattern are observed for each nucleus. The coupling constants for the *erythro* stereoisomer can be extracted directly from the spectrum. Analysis of the spectra for the *threo* isomers is more complex and will be described in chapter 2.5.

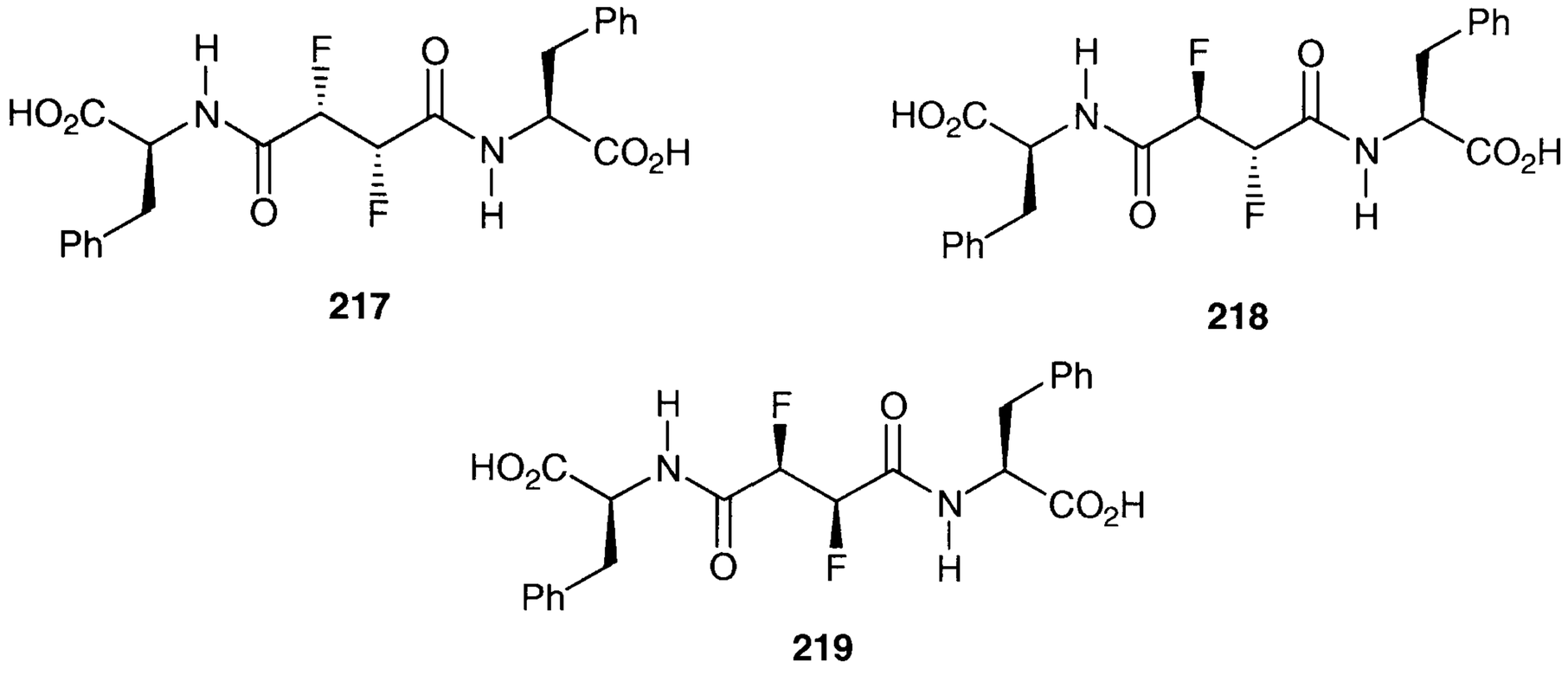

Scheme 2.54. Dicarboxylic acids **217-219** obtained by acid hydrolysis of the dimethyl esters **214-216**.

Both of the *threo* isomers **214** and **216** are solids at room temperature, but repeated crystallisation of these compounds in various solvent systems did not succeed to give crystals suitable for X-ray analysis. The single diastereoisomers of **214** – **216** were hydrolysed to give the free dicarboxylic acids **217-219** (Scheme 2.54). Hydrolysis was achieved in refluxing diluted hydrochloric acids with acetone as the co-solvent. The reactions were monitored by ^{19}F NMR spectroscopy, which indicated a clean reaction under these conditions. The *erythro* compound **218** crystallised in dichloromethane to give crystals suitable for X-ray analysis. The solid state structure of **218** shows the C-F bonds *gauche* to each other, consistent with predicted stereoelectronic effects. The large phenyl groups are bent towards each other, thereby causing a deviation of the main chain from the zig-zag conformation (Figure 2.24).

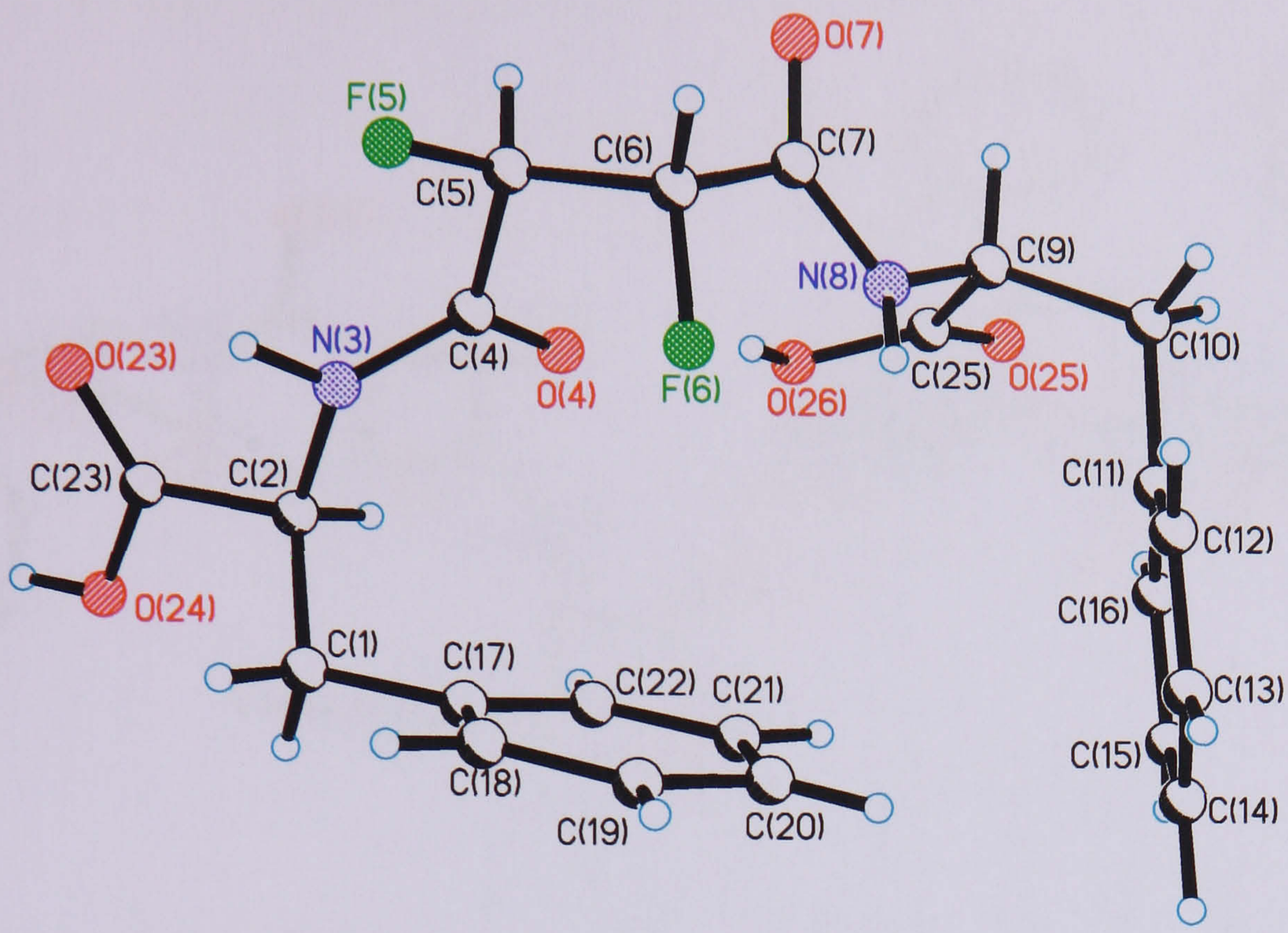

Figure 2.24. X-ray structure of **218**. Selected bond lengths (Å) and torsion angles (°): N3-C4 1.349(9), C4-O4 1.236(8), C4-C5 1.507(9), C5-F5 1.406(7), C5-C6 1.538(9), C6-F6 1.406(7), C6-C7 1.512(9), C7-O7 1.229(8), and C7-N8 1.345(8); N3-C4-C5-F5 4.8(8), O4-C4-C5-F5 -176.1(6), F5-C5-C6-F6 75.2(6), F6-C6-C7-O7 -178.0(5), and F6-C6-C7-N8 3.4(8). The donor-hydrogen-acceptor distances and angles (°): H(26O)···O4 1.89(4) [137(5)], H(26O)···N8 2.11(5) [122(4)], and H(8N)···F6 2.13(9) 112(7)].

An interesting feature in the crystal structure of **218** is the anticipated planarity of the α-fluoro amide groups. This conformation is apparently stabilised over the *anti* structure by stereoelectronic effects, dipole-dipole relaxation and N-H···F interaction (Introduction). There is intramolecular hydrogen bonding between the two opposing carboxyl groups that may contribute to stabilising this particular conformation. Intermolecular hydrogen bonding apparently occurs between the carboxyl oxygen and the carboxyl hydrogens of adjacent molecules. For instance, O23 is bonded to O54-H and also to N33-H of an adjacent molecule. Likewise O53 is bonded to N3-H and O24-H of the next molecule. Although the O-H···O contacts are short, their geometry is not particularly linear, perhaps due to additional hydrogen bonding with the amide hydrogens.

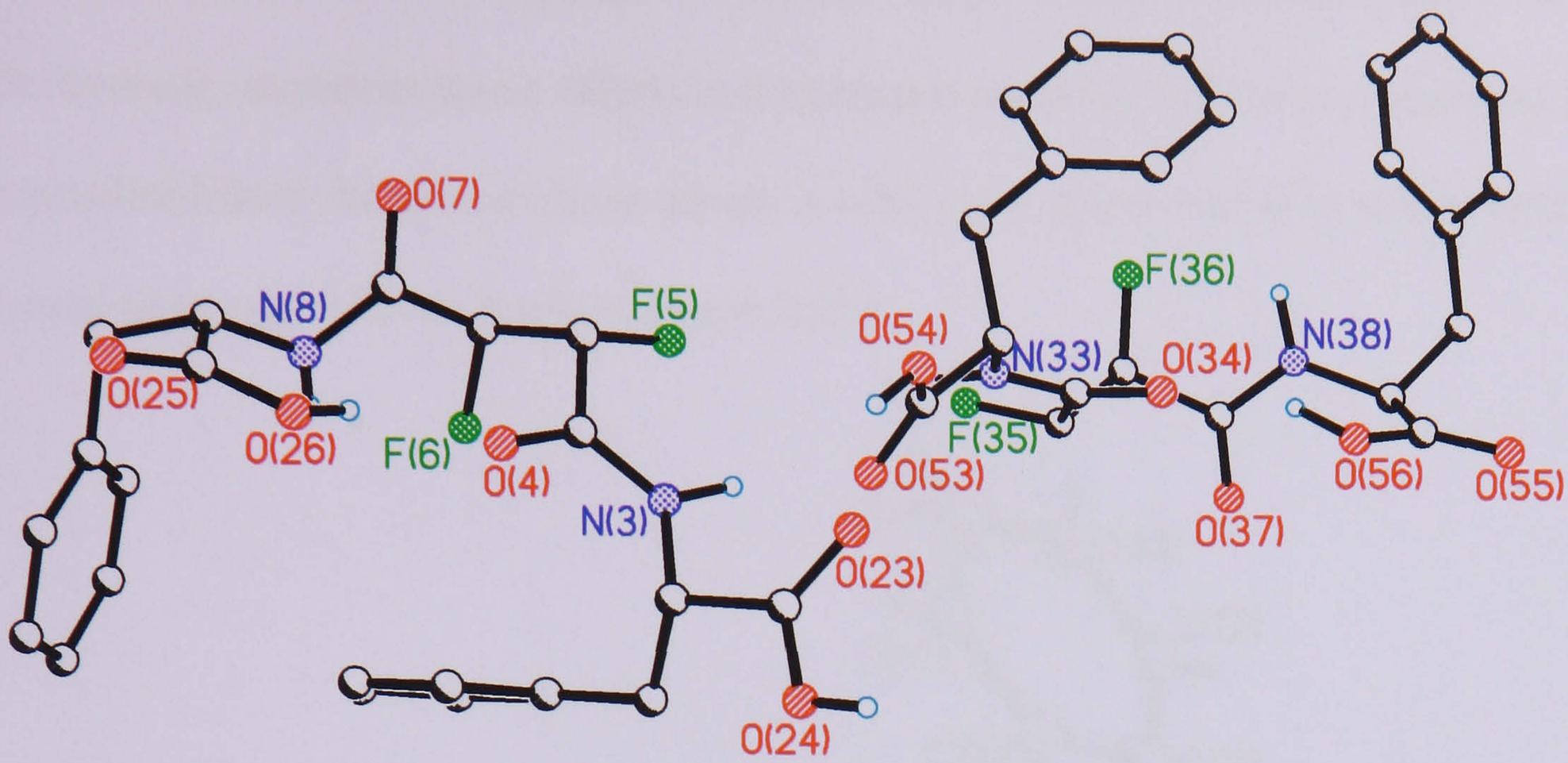

Figure 2.25. Crystal packing of **218**. Short interatomar distances (Å) are given as well as donor-hydrogen-acceptor angles [°]: H(54O)···O23 1.73(7) [<144(10], H(24O)···O(53)#1 1.69(5) [<157(12)], H(33N)···O(23)#2 2.12(3) [<157(7)], and H(3N)···O(53) 2.161(16) [<172(8)].

The conformation in which the two C-F bonds align *anti* is stereoelectronically less favoured due to the *gauche* effect. Also this conformation would cause considerable steric strain, considering the planarity of the α-fluoroamide groups, perhaps comparable with 1,3-diaxial repulsion in substituted cyclohexanes.[16] There could also be a considerable degree of electrostatic repulsion between carbonyl oxygens and fluorine atoms in that conformation (Scheme 2.55).

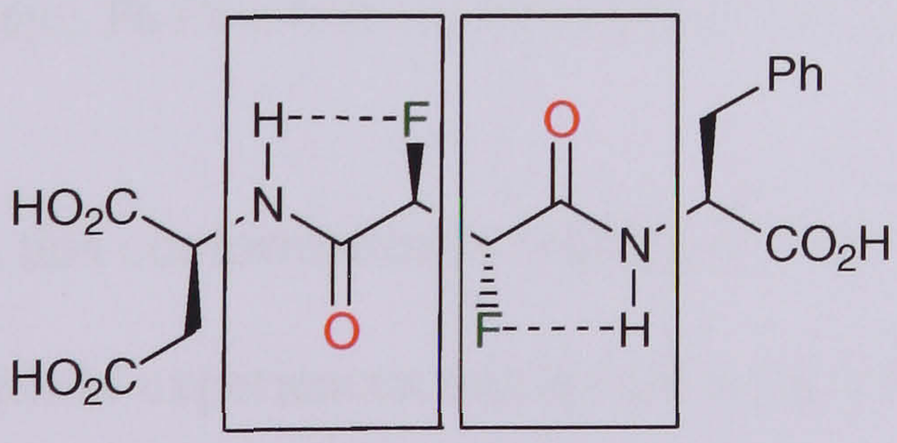

Scheme 2.55. The extended zig-zag conformation of *erythro* **218** would lead to a structure in which the planes of both α-fluoroamide groups are parallel, a situation that would result in steric and electrostatic repulsion between the fluorine and the carbonyl oxygen atoms in each motif (boxed).

The conformation of the molecule is determined by a complex combination of steric, electrostatic, stereoelectronic effects and hydrogen bonding. The *threo* compound **219** crystallised from dichloromethane adopts a solid state conformation in which the C-F bonds align *gauche* to each other (Figure 2.26).

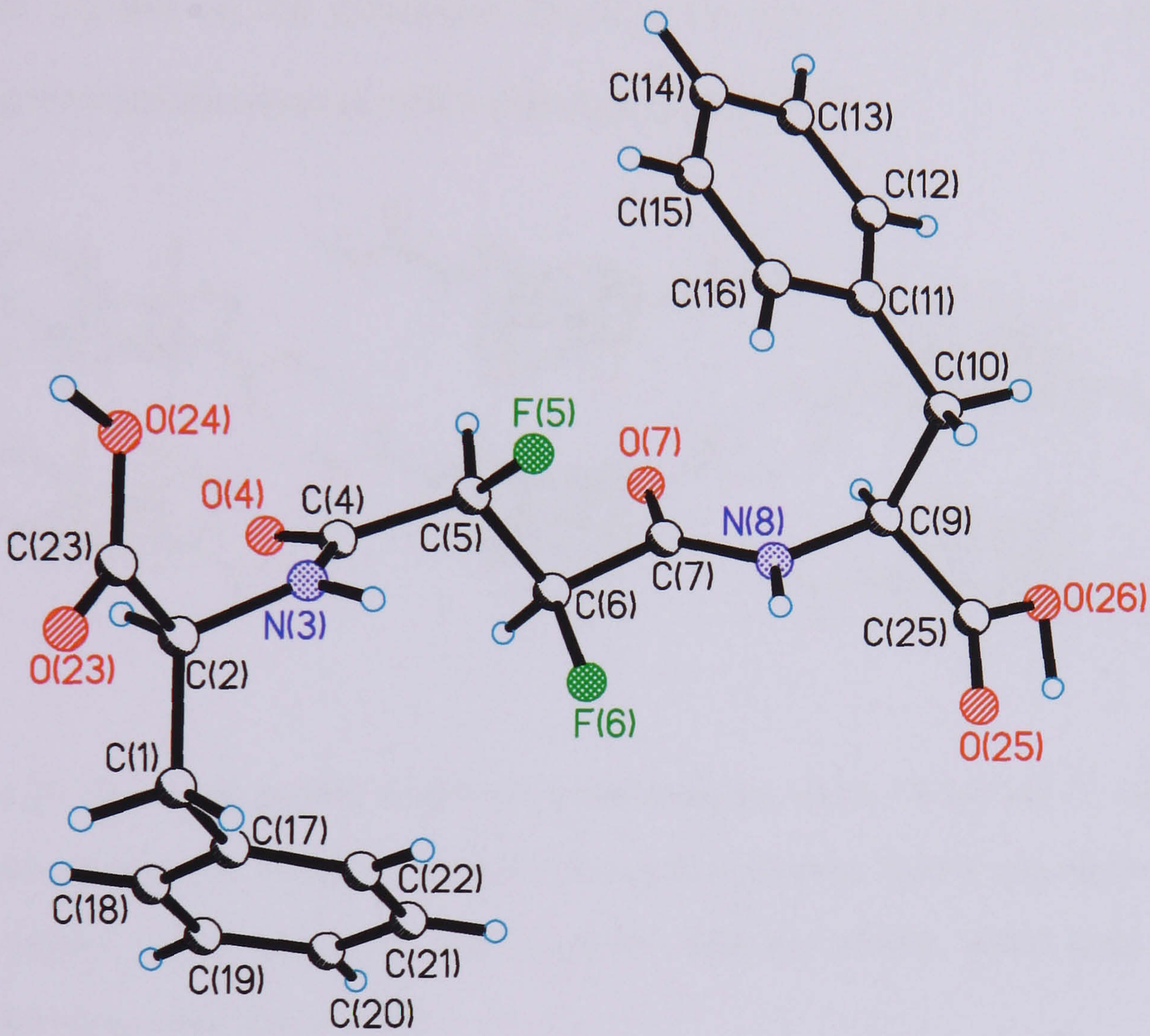

Figure 2.26. X-ray derived structure of **211**. Selected bond lengths (Å) and torsion angles (°): N3-C4 1.338(7), C4-O4 1.214(7), C4-C5 1.512(9), C5-F5 1.397(7), C5-C6 1.495(10), C7-O7 1.220(7), C7-N8 -12.2(8); N3-C4-C5-F5 -23.8(8), O4-C4-O5-F5 155.4(6), F5-C5-C6-F6 49.0(6), C4-C5-C6-C7 163.1(5), F6-C6-C7-O7 165.6(6), F6-C6-C7-N8 -12.2(8); H(8N)···F6 2.23(7) [<105(5)].

This is not surprising as this conformation is stabilised by the g*auche* effect, and also, the extended carbon scaffold experiences minimised steric clash within the molecule. The *gauche* conformation of the C-F bonds and the planarity of the α-fluoro amide moieties is obvious. The carbonyl groups both point away from the C-F bonds and align *anti* periplanar to each other. This conformation is favourable due to

stereoelectronic effects, dipole-dipole compensation, and hydrogen bonding. The N-H···F distance of 2.23 Å is well within the Van der Waals radius of the two atoms thereby supporting the existence of genuine fluorine-hydrogen bonding, an effect that is lively discussed in the literature (Introduction). Within the unit cell, the molecules are held together in the horizontal direction by strong intermolecular hydrogen bonding between the terminal carboxyl groups (Figure 2.27).

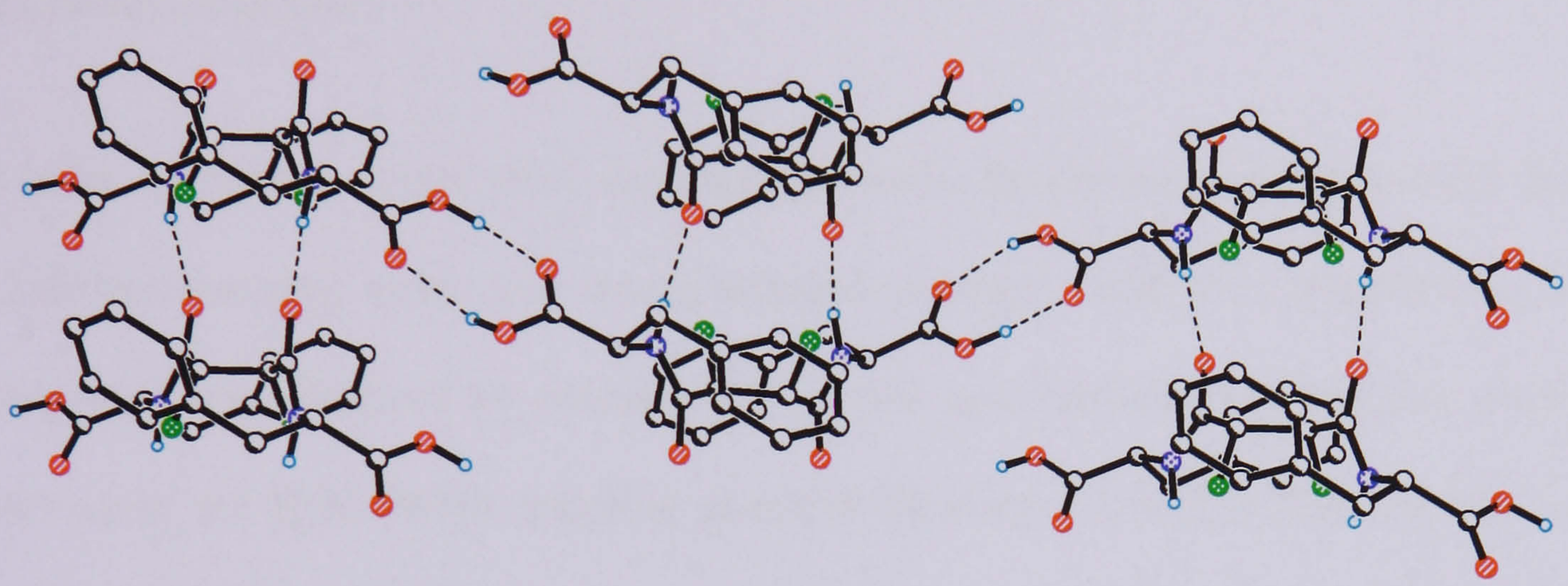

Figure 2.27. The crystal packing of **219** as viewed along the c-axis. Short O-H···O contacts are illustrated by dashed lines. Interatomic distances (Å) as well as the donor-hydrogen-acceptor angles [°]: H(24O)···O25#2 1.70(3), [<170(13)]; H(26O)···O23#3 1.98(10), [126(9); H(3N)···O4#1 1.84(2), [<158(5)]; H(8N)···O7#1 2.01, [<144(6).

The individual molecules alternate constantly throughout the crystal packing to form V shaped chains that are interconnected by hydrogen bonds in the vertical direction. The image in Figure 2.27 highlights the unusual conformation that the 2,3-difluorosuccinamide core adopts. Remarkably, both of the carbonyl oxygen's point to one side of the molecule whereas the fluorine atoms point to the other side. The main chain is extended with both terminal carboxyl groups outstretched in opposite directions.

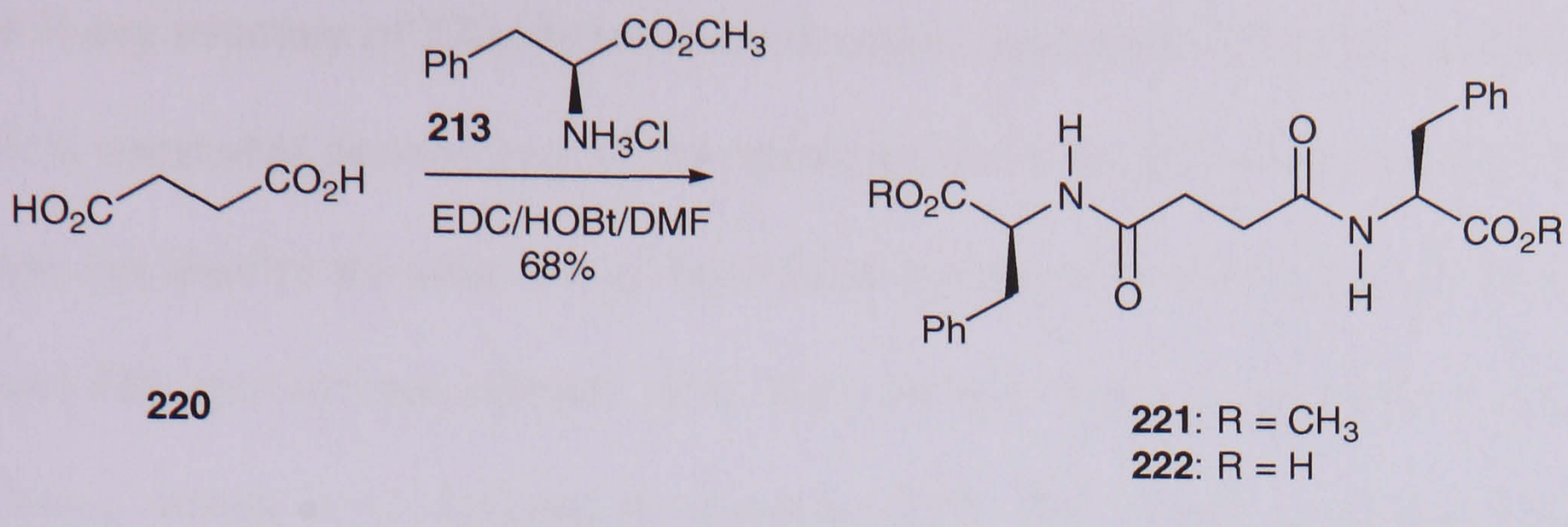

220

221: R = CH_3
222: R = H

Scheme 2.56. Synthesis of the pseudopeptide **221** derived from succinic acid **220** and L-phenylalanine **213**. The reaction affords a single stereoisomer, which was hydrolysed under acidic conditions to give the dicarboxylic acid **222**.

In order to compare solid state structures between the pseudopeptides derived from 2,3-difluorosuccinic acid, the non-fluorinated analogue **222** was synthesized. The compound was obtained by reaction of succinic acid with L-phenylalanine methyl ester using the EDC/HOBt coupling protocol (Scheme 2.56). The diamide **221** was purified by chromatography. Hydrolysis of 221 was accomplished under acidic conditions according to the procedure for the synthesis of **217**-**219**. Recrystallisation in chloroform afforded crystals suitable for X-ray analysis (Figure 2.28).

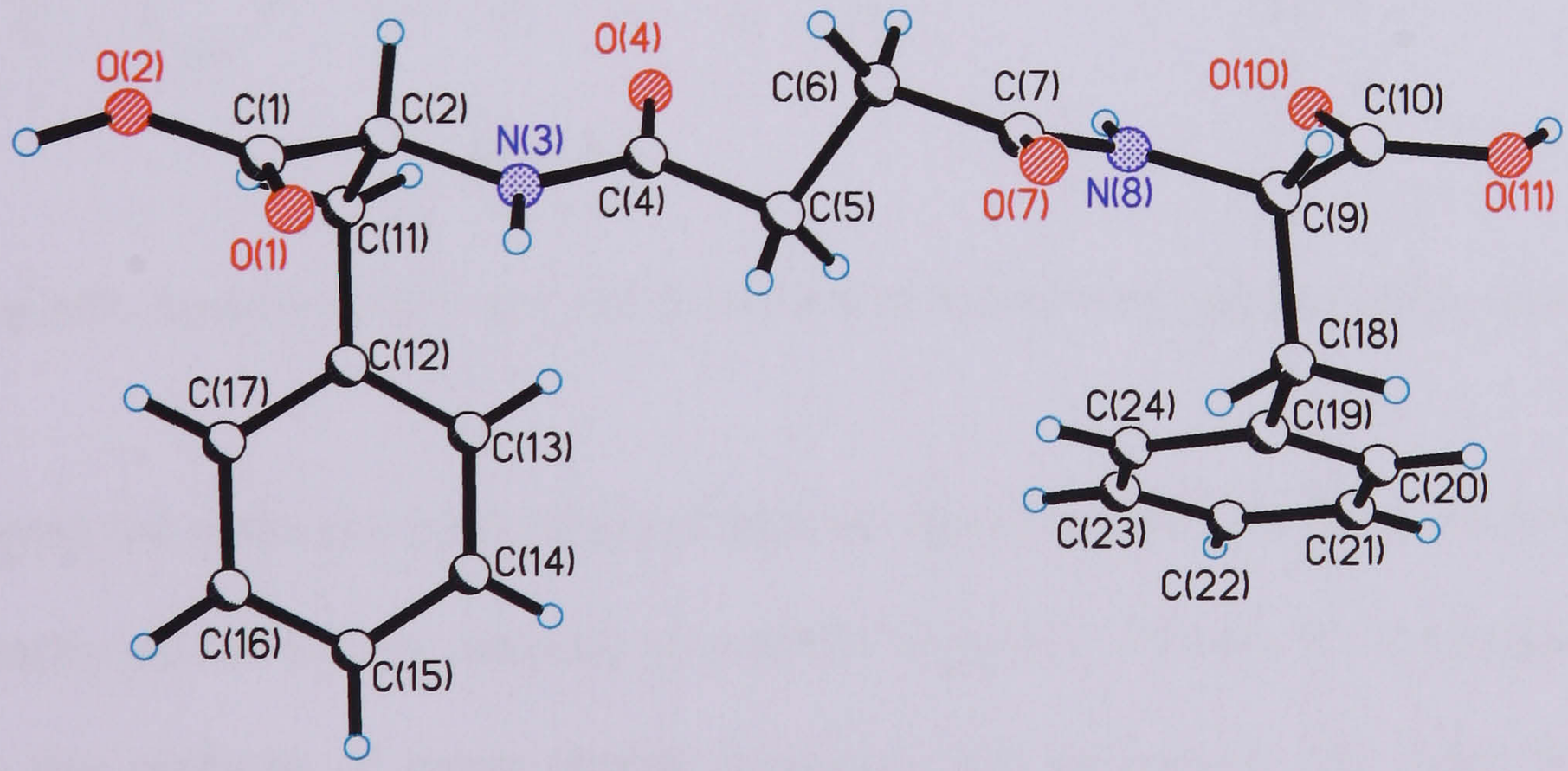

Figure 2.28. X-ray derived structure of **222**. Selected bond lengths (Å) and torsion angles (°): N3-C4 1.338(5), C4-C5 1.524(5), C5-C2 1.547(5), C6-C7 1.507(5), C7-O7 1.248(4), C7-N8 1.336(5); C2-N3-C4-C5 178.5(2), N3-C4-C5-C6 -111.4(3), C4-C5-C6-C7 179.3(3), C5-C6-C7-N8 89.9(4), C6-C7-N8-C9 177.9(3).

In the X-ray structure of **222**, the main chain adopts an extended zig-zag conformation which is somewhat twisted around the amide bonds. This allows the carbonyl bonds to align *synclinal* to the adjacent sp^3 hybridised centres, and unlike those of structures **218** and **219**, they are not eclipsed. Also, the carbonyl oxygen atoms point in opposite directions, which is in contrast to structure **219**. The crystal packing of **222** is dominated by hydrogen bonding of the amide hydrogens and carboxyl hydrogen with the carbonyl oxygen atoms in the structure. The obvious structural difference of **222** compared to its fluorinated counterparts suggests that the *vicinal* difluoro motif is influencing the pseudopeptide conformation by stereoelectronic effects.

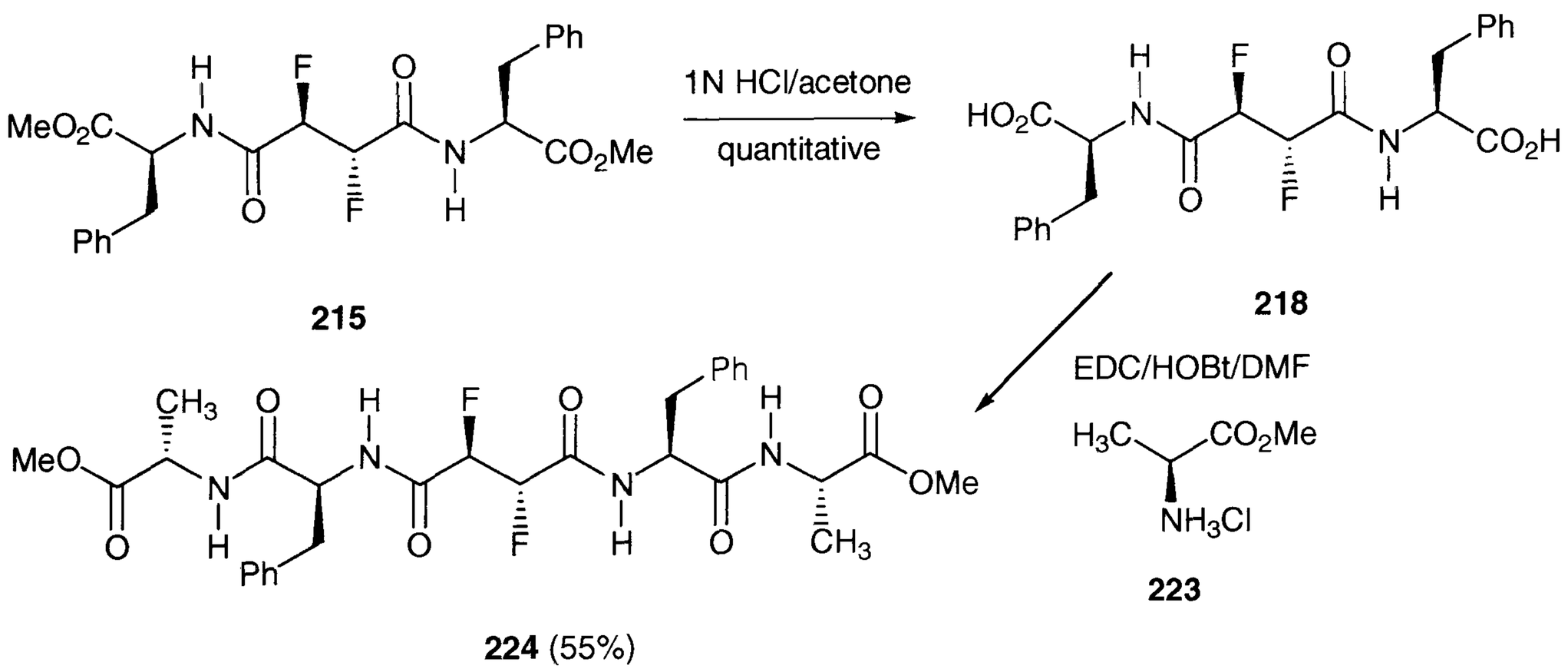

Scheme 2.57. Synthesis of the larger peptide structures *via* hydrolysis and peptide coupling sequences.

Changing the molecular conformation can have dramatic effects on the secondary and eventually on the tertiary structure of peptides in general. In order to investigate this effect the synthesis of larger peptide structures was envisaged. The most obvious approach to access extended peptide structures follows a hydrolysis and coupling sequence from the pseudopeptide esters **214-216** (Scheme 2.57). The reaction was carried out under the standard reaction conditions after hydrolysis of the *erythro*

compound **215** in a mixture of dilute hydrochloric acid and acetone. EDC coupling afforded the symmetrical tetrapeptide **224**. Separation of the stereoisomers **214-216** was clearly of major importance to isolate **224** as enantiomerically pure material.

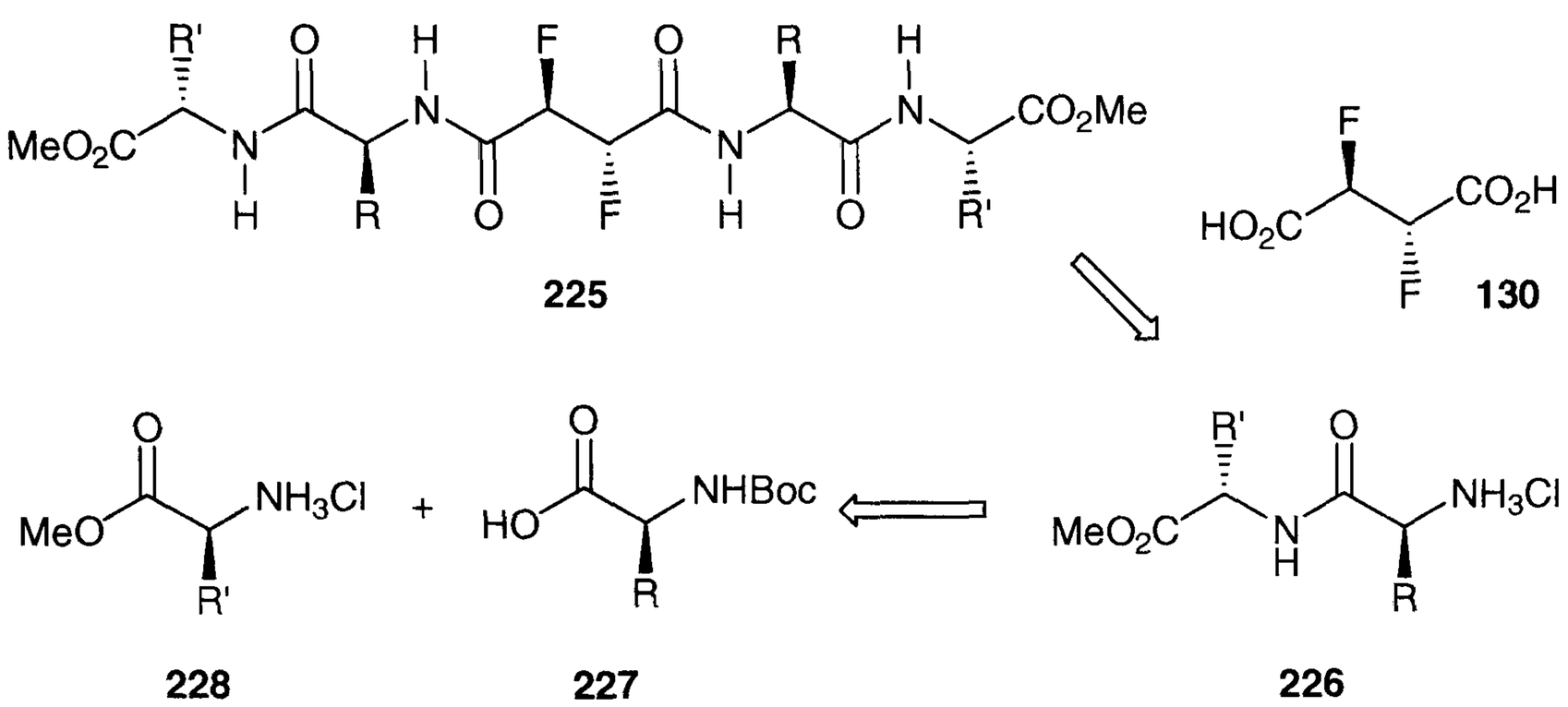

Scheme 2.58. Convergent approach for the synthesis of larger peptide structures **225**. The peptide substituents **226** are assembled by coupling of the protected peptides **227** and **228** prior to attachment to the *vicinal* difluoro succinic acid motif **130**.

Theoretically, a more efficient strategy for accessing larger peptide structures involves the use of peptides that are already assembled prior to coupling to the 2,3-difluorosuccinic acid core (Scheme 2.58). This convergent approach would permit the crucial coupling step to be carried out at the latest stage, without having to perform multiple purification steps. Also, the method would allow for application of solid phase peptide synthesis for the assembly of the terminal substituents.[17]

The synthesis of the individual peptide chains can also be achieved economically and efficiently using an ethyl chloroformate coupling.[18] The method is known to prevent from side reactions and racemisation. Using this methodology, the dipeptide **230** was formed in excellent yield and stereoselectivity (Scheme 2.59).

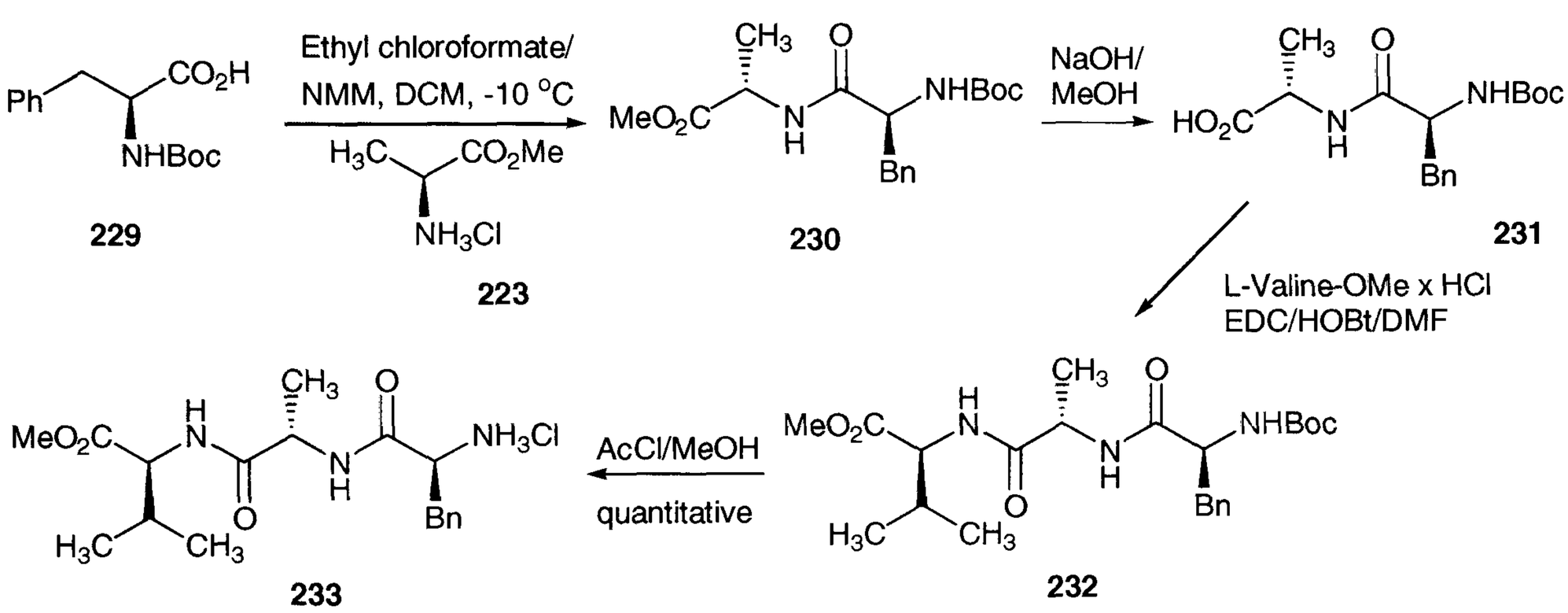

Scheme 2.59. Synthesis of the tripeptide Phe-Ala-Val **233** for use in the synthesis of larger pseudopeptide structures.

The ethyl chloroformate method is a somewhat conventional, but nevertheless effective and frequently applied strategy for the coupling of amino acids. The reaction proceeds *via* a carboxylic-carbonic anhydride **236**, which is formed after nucleophilic attack of the carboxylic acid **234** with ethyl chloroformate **235** (Scheme 2.60). The mixed anhydride **236** subsequently undergoes aminolysis to form the peptide **237**. Two oxygen atoms flank one of the carbonyl groups of the intermediate **236**, which reduces its activity relative to the other carbonyl group. Therefore nucleophilic attack of the amine is regiospecific and urethanes are not usually formed.

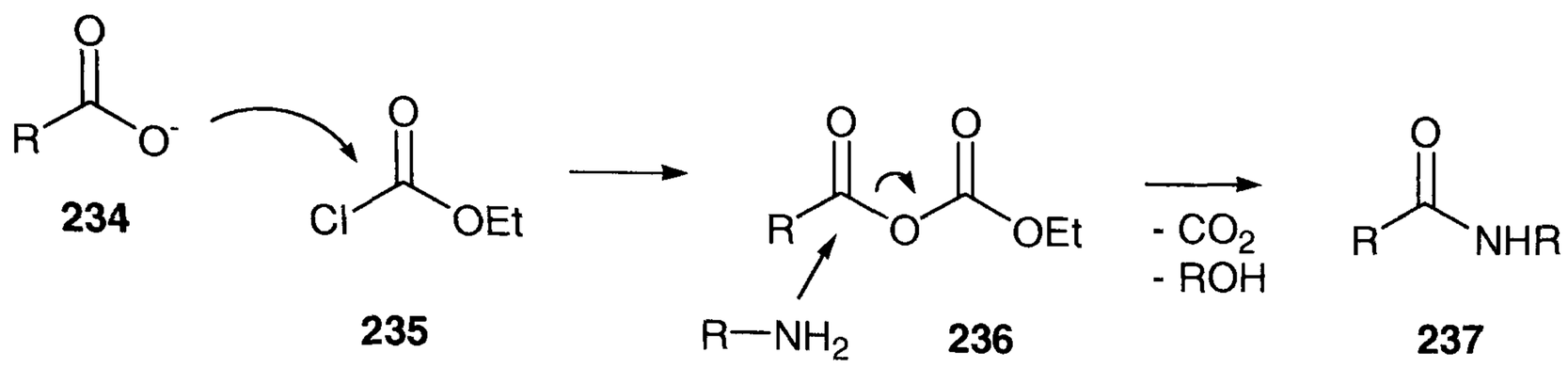

Scheme 2.60. Mechanism of ethyl chloroformate peptide coupling which proceeds *via* carboxylic anhydride intermediate **236**.

Deprotection of the amino group was initially carried with trifluoroacetic acid.[19] The deprotection was efficient but problems in the subsequent coupling step occurred. Therefore the application of acetyl chloride and methanol for this transformation was investigated. Reaction of acetyl chloride with methanol generates anhydrous hydrochloric acid, which removes the Boc-group effectively and gives rise to the ammonium chloride salt of these oligopeptides.

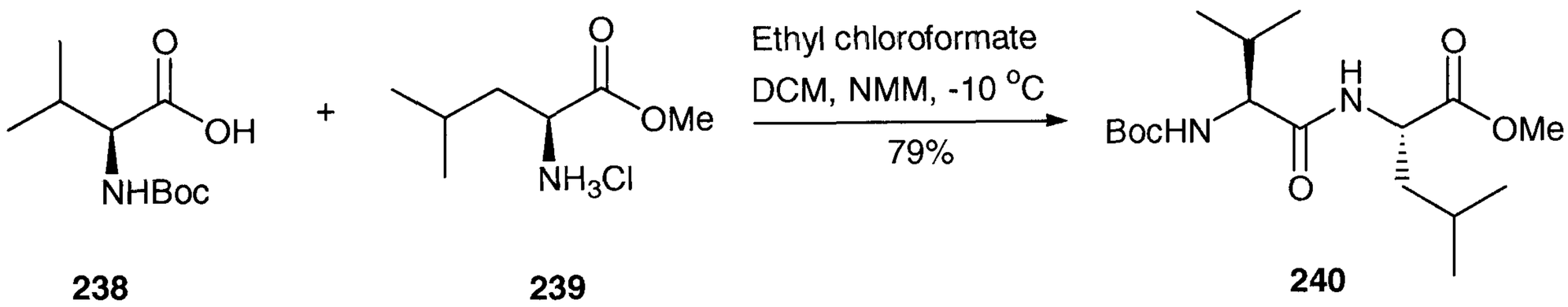

Scheme 2.61. Synthesis of the dipeptide Val-Leu using the ethyl chloroformate coupling procedure.

The peptide **240** was synthesised as a building block for the formation of larger peptide substituents such as **233** (Scheme 2.61). Initial attempts to attach such larger peptides by the standard EDC protocol however proved to be rather unsuccessful. For instance, reaction of the tripeptide **233** to *erythro* 2,3-difluorosuccinic acid **130** using the EDCI/HOBt mixture failed even after addition of excess *N*-methylmorpholine and EDC.

References

[1] C. M. Bladon, In *Pharmaceuticals Chemistry: Therapeutic Aspects of Biomacromolecules*, New York, Wiley & Sons, 2002.

[2] N. Seewald, H.-D. Jakubke, *Peptides: Chemistry and Biology*, Wiley-VCH, 2002.

[3] Frost & Sullivan, Pharmaceutical News, 2005.

[4] J. T. Welch, *Tetrahedron*, 1987, **43**, 3123.

[5] R. Filler, Y. Kobayashi, L. M. Yagupolskii, In *Biomedical Aspects of Fluorine Chemistry*, Elsevier, Amsterdam, 1993; C. T. Walsh, *Annu. Rev. Biochem.*, 1984, **53**, 493.

[6] D. F. Hook, F. Gessier, C. Noti, P. Knast, D. Seebach, *Org. Biomol. Chem.*, 2004, **2**, 691.

[7] N. C. Yoder, K. Kumar, *Chem. Soc. Rev.*, 2002, **31**, 335.

[8] W. A. Loughlin, D. A. Tyndall, *Chem. Rev.*, 2004, **104**, 6085 and references cited herein.

[9] D. R. Madden, J. C. Gorga, J. L. Strominger, *Cell*, 1992, **70**, 1035.

[10] D. Leung, G. Abbenante, D. P. Fairlie, *J. Med. Chem.*, 2000, **43**, 305.

[11] F. Gessier, C. Noti, M. Rueping, D. Seebach, *Helv. Chim. Acta*, 2003, **86**, 1862.

[12] S. Hanessian, G. McNaughton-Smith, H.-G. Lombard, W. D. Lubell, *Tetrahedron*, 1997, **53**, 12769.

[13] P. Kreye, J. Kihlberg, *Tetrahedron Lett.*, 1999, **40**, 6113.

[14] T. W. Greene, P. G. M. Wuts, In *Protective Groups in Organic Synthesis*, 3rd edition, 1999, Wiley & Sons, New York, 494.

[15] J. Jones, In *Amino acid and peptide synthesis*, Oxford University Press, 2002, 33.

[16] K. P. C. Vollhardt, N. E. Schore, In *Organische Chemie*, 2. Auflage, VCH, 1995, Weinheim, 117.

[17] E. Atherton, R. C. Sheppard, In *Solid Phase Peptide Synthesis*, Oxford University Press, 1989.

[18] D. Seebach, A. Thaler, D. Blaser, S. Y. Koo, *Helv. Chim. Acta*, 1991, **74**, 1102.

[19] P. Meffre, R. H. Dave, J. Leroy, B. Badet, *Tetrahedron Lett.*, 2001, **42**, 8625.

2.3 Stereoselective synthesis of 2,3-difluorosuccinates

The stereoselective synthesis of difluorosuccinates has been achieved by Burmakov *et al.*[1] Treatment of (*R,R*)-tartaric acid with sulfur tetrafluoride led to a complex product mixture containing *erythro* 2,3-difluorosuccinic acid. The reaction was most successful using the esters of 2,3-difluorosuccinic acid. Treatment of dimethyl (*2R,3S*) tartrate **241** with sulphur tetrafluoride led to the formation of dimethyl (*2R,3S*)-2,3-difluorosuccinate **249** in the presence of catalytic amounts of hydrogen fluoride. The stereochemical outcome of the reaction is rather unexpected, and a mechanism for the reaction has been proposed (Scheme 2.62).

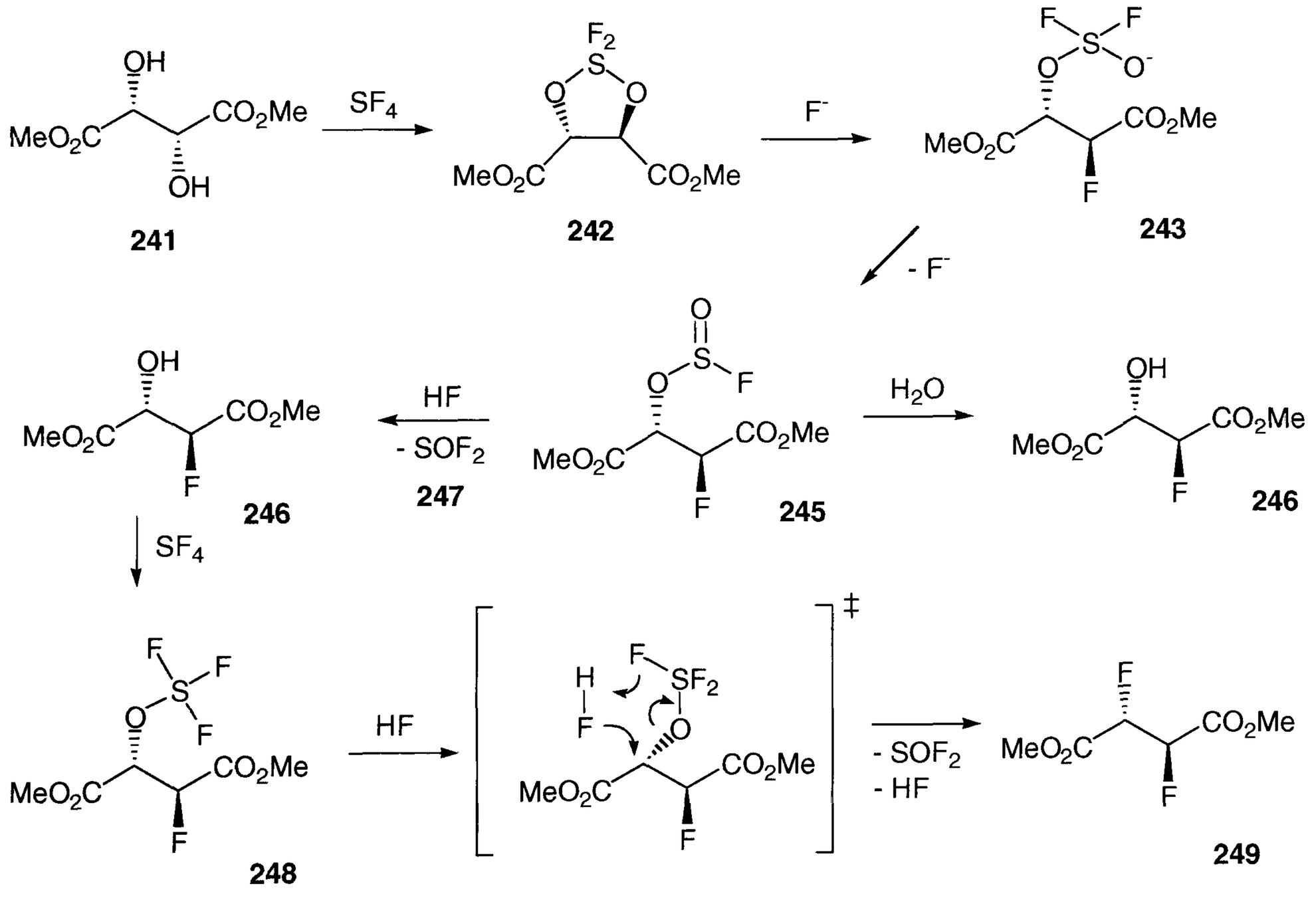

Scheme 2.62. Stereoselective synthesis of dimethyl 2,3-difluorosuccinate **249** using SF_4 and catalytic amounts of hydrogen fluoride.

The reaction presumably involves formation of a fluorohydrin **246** after initial generation of a fluorosulfite **245**. Only traces of the difluoro compound **249** were obtained after treatment

with SF_4 at ambient temperatures, and the fluorohydrin **246** is the main product. The presence of hydrogen fluoride however changes the course of the reaction significantly. Presumably the intermediate fluorosulfite **245** is cleaved in the presence of HF to generate the fluorohydrin **246**, which further reacts with excess SF_4 in a second fluorination step. The second fluorination apparently proceeds with retention of configuration at the C2 carbon atom, which may be rationalised by an intramolecular nucleophilic substitution. The fluorination of fluorohydrin **246** eventually results in formation of *erythro* (*2R,3S*)-2,3-difluorosuccinate which proceeds in a highly stereospecific manner. Although the method yields the *vicinal* difluoro compounds in good yields, the reaction involves highly noxious chemicals such as SF_4 and HF, which renders the process unsuitable for laboratory applications. For instance, sulfur tetrafluoride is a gas with toxicity comparable to that of phosgene, and its handling requires extensive safety precautions. This is even more so the case for hydrogen fluoride, a low boiling liquid (bp. 19 °C) of extraordinary toxicity and corrosiveness. HF is a highly hazardous substance to the living organism as it penetrates tissue rapidly to cause severe burns that are extraordinary painful and difficult to heal. Moreover, the handling of HF requires special laboratory equipment as it etches glassware and in contact with moisture even causes corrosion of steel. In the first instance, the application of alkylaminosulfur trifluorides **250-252** was envisaged as a safe alternative to SF_4 and HF (Scheme 2.63).

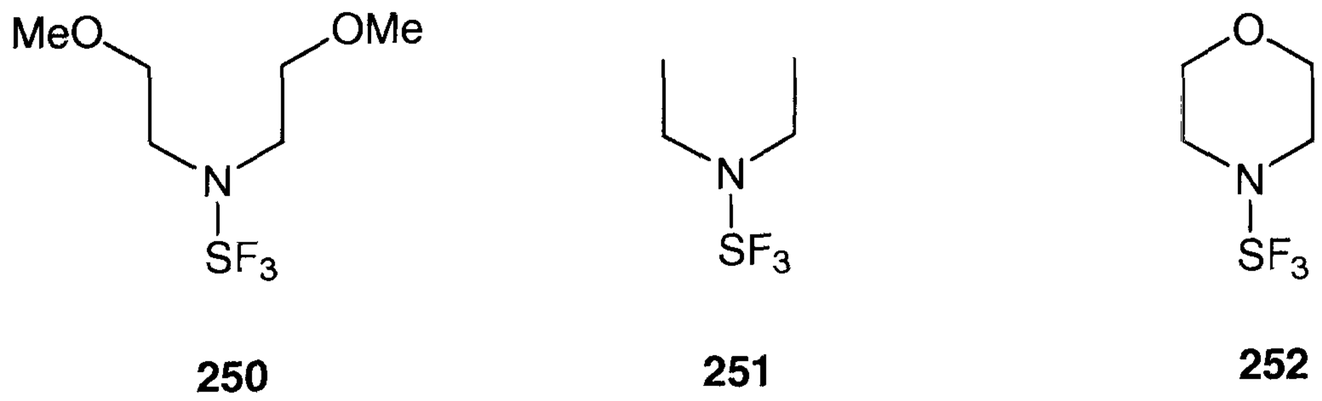

250 **251** **252**

Scheme 2.63. Bis-(methoxyethyl)-aminosulfur trifluoride (BAST) **250**, diethylaminosulfur trifluoride (DAST) **251**, and *N*-morpholinosulfur trifluoride (MOST) **252** are nucleophilic fluorinating reagents that can safely be used in the laboratory.

Alkylaminosulfur trifluorides are reagents that can be employed safely and conveniently on laboratory scale to achieve nucleophilic fluorination.[2] The most popular of this class of reagents is DAST, which can be used for the direct conversion of primary, secondary, and tertiary alcohols into their respective fluoroorganic compounds.[3] A wide variety of functional groups such as esters, amides, and certain silyl protecting groups are tolerated which makes the reagent a valuable tool for the selective synthesis of fluoroorganic compounds under mild reaction conditions. The reaction of DAST with an alcohol proceeds stereospecifically with inversion of configuration. However, retention of configuration can occur when nucleophilic functional groups are present as a result of double inversion. Also, in some cases rearranged products will be obtained, a tendency, which is of synthetic importance in certain cases such as for the synthesis of α-fluoro-β-amino acids (Scheme 2.64).

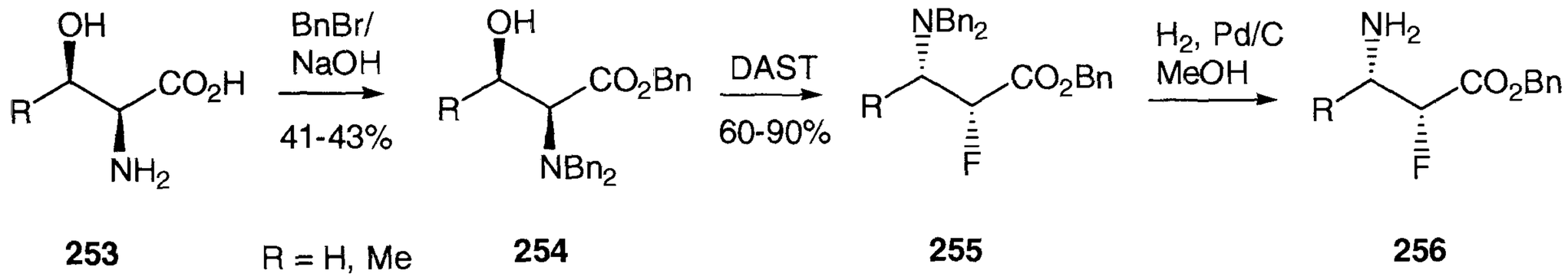

253 R = H, Me **254** **255** **256**

Scheme 2.64. Synthesis of α-fluoro-β-amino acids according to the method developed by Seebach *et al.*[4]

An alternative strategy for nucleophilic fluorination is the conversion of an alcohol into a leaving group followed by S_N2 reaction with fluoride ion. Fluorination can be achieved with inorganic fluoride salts such as potassium fluoride. The solubility of KF in organic solvents is low, even for the most polar solvents DMF or DMSO. Efficiency and rate of the reaction can be greatly improved by addition of phase transfer catalysts (PTC) such as quaternary ammonium and phosphonium salts, or crown ethers. A popular example is *N*-tetrabutylammonium fluoride (TBAF), which is a common reagent for nucleophilic fluorination in the laboratory. Due to its low cost, TBAF is usually employed in equimolar

amounts to achieve rapid fluorination of mesylates or triflates. The reaction can go to completion within minutes, which has been exploited for the synthesis of radioactive labelled rediopharmaceuticals.[5]

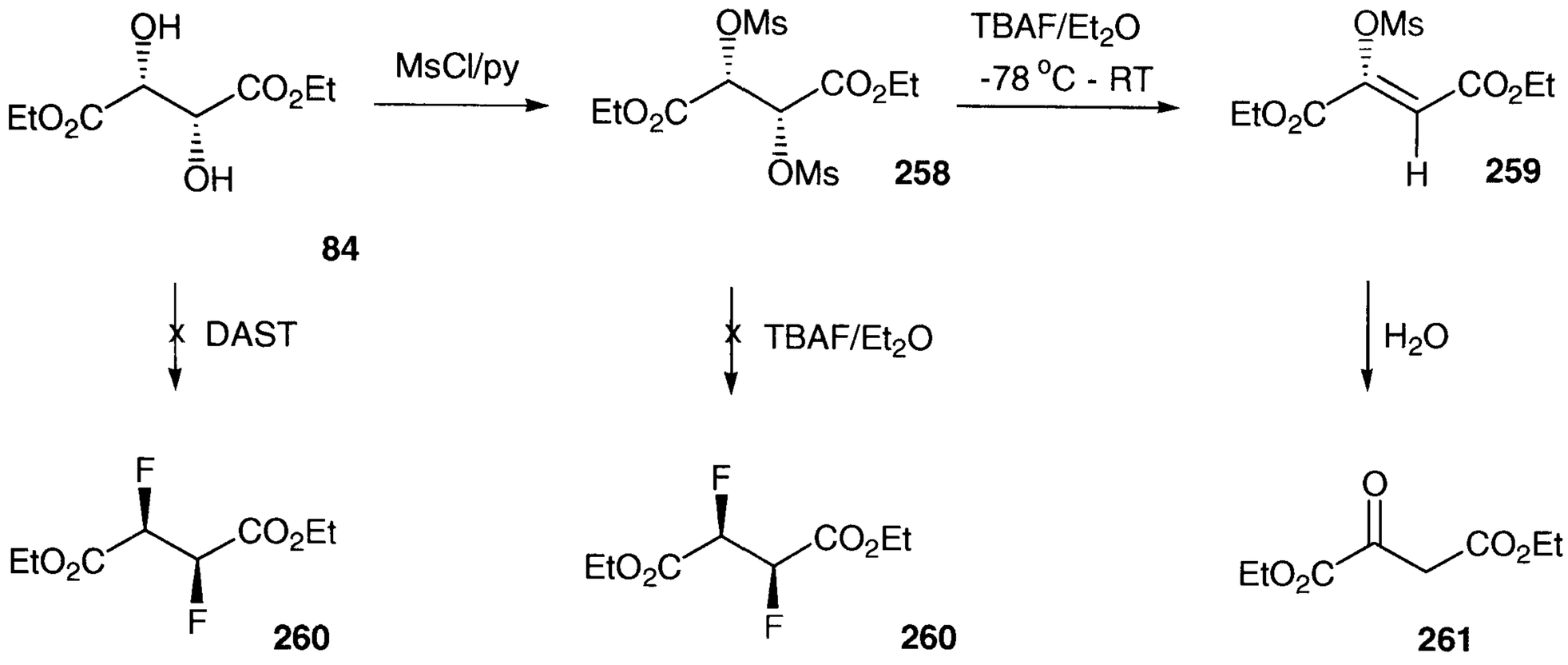

Scheme 2.65. Attempted direct nucleophilic fluorination of (*R,R*) tartrate *via* its mesylate **258** using DAST.

After initial attempts to achieve direct fluorination of the tartrate **84** with DAST failed, an attempt was made to access the 2,3-difluorosuccinates **260** from the corresponding dimesylate **258** by action of TBAF. Conversion of both hydroxyl groups of the tartrate **84** was achieved by treatment with mesyl chloride in pyridine (Scheme 2.65). Fluorination of the dimesylate **258** with TBAF however did not yield the desired difluorinated compound. The major product was diethyl oxalacetate **261** identified by means of ^{1}H-NMR spectroscopy and GC-MS analysis. This product may have formed during the aqueous work up from methanesulfonyl-enolester **259**, an intermediate that arises from deprotonation by strongly basic fluoride ion. The preference for the dimesylate to undergo elimination over substitution has also been reported by Seebach *et al.* for attempts to synthesise 2,3-diaminosuccinates.[6]

An alternative method for the synthesis of *vicinal* difluoro compounds involves the formation of epoxides as intermediates. The ring opening reaction of epoxides with fluoride generally proceeds in a highly stereospecific manner. The Sharpless asymmetric epoxidation,[7] and the Jacobsen/Katsuki epoxidation[8] on the other hand represent methods for the stereoselective epoxidation of allylic and also unfunctionalised alkenes, and therefore chiral fluoroorganic compounds are accessible. The introduction of fluorine and nucleophilic cleavage of epoxides can be achieved with alkylaminosulfur trifluorides **250**-**252**. However, the reaction often results in poor yields due to rearrangements frequently giving mixtures of *vicinal* and *geminal* difluoro compounds which are difficult to separate.[9]

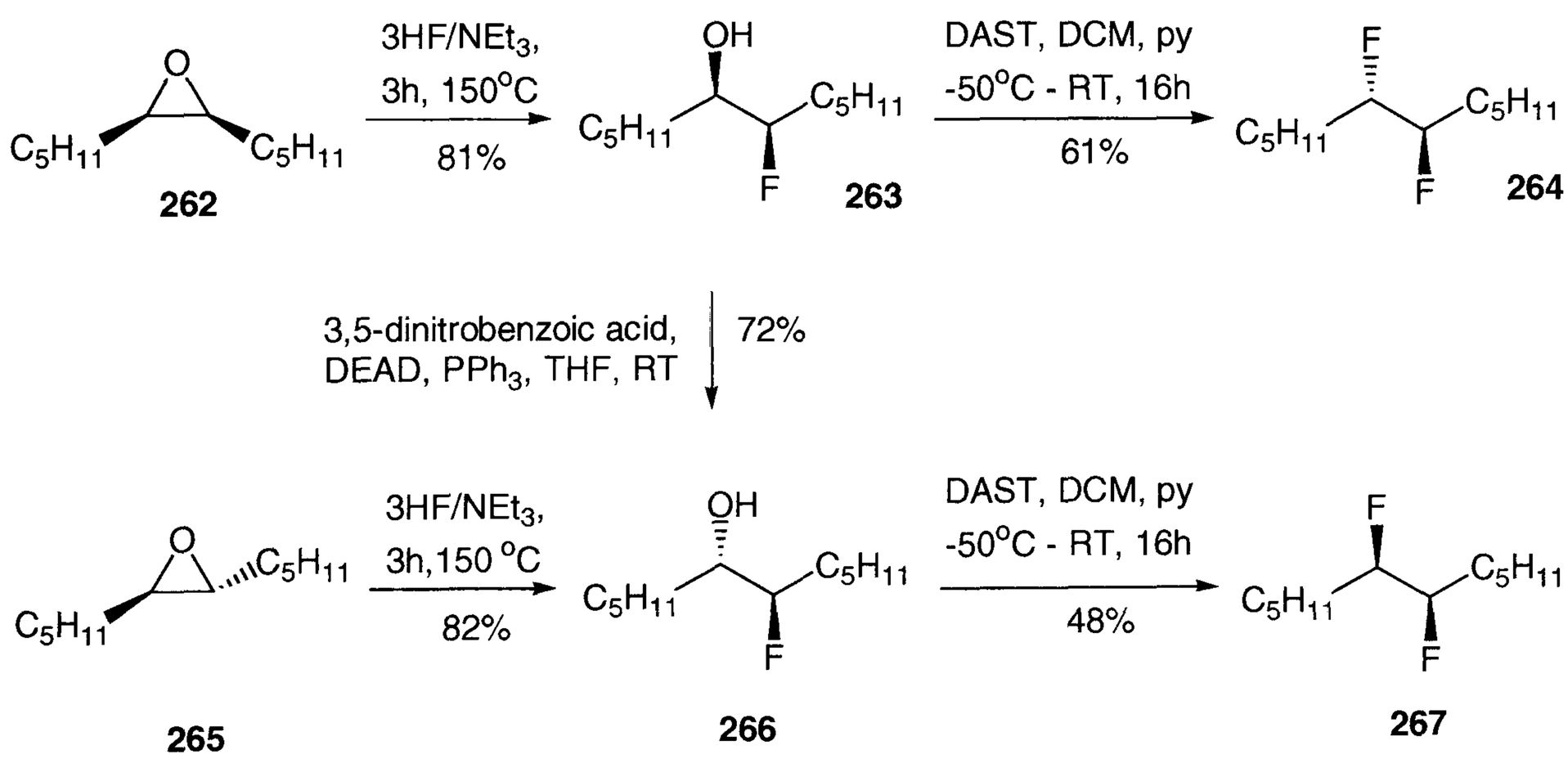

Scheme 2.66. Schlosser's synthesis of *vicinal* difluoroalkanes **264** and **267** involves diastereoselective ring-opening of epoxides with hydrogen fluoride triethylamine complex.[10]

Alternatively, *vicinal* difluoro compounds can be prepared by ring opening of epoxides with the much less expensive, readily available pyridinium polyhydrogen fluoride PPHF or related amine-hydrogen fluoride complexes.[11] This methodology has been used successfully for the stereocontrolled synthesis of *vicinal* difluoroalkanes by Schlosser *et al.* (Scheme 2.66). The

method represents a straightforward synthetic route to access diasteromerically pure *vicinal* difluoro compounds **264** and **267**. Fluorination of the epoxides with hydrogen fluoride triethylamine complex afforded the *threo* and *erythro* fluorohydrins **263** and **266** in a stereoselective manner. Conversion of the resulting hydroxyl group was accomplished using DAST. The epoxides **262** and **265** can be synthesised selectively from their respective *cis*- and *trans* alkenes, which in turn can be obtained by means of a Wittig reaction. The major advantage of using epoxides for the introduction of fluorine is that the reaction proceeds with inversion of configuration at the carbon-oxygen bond.

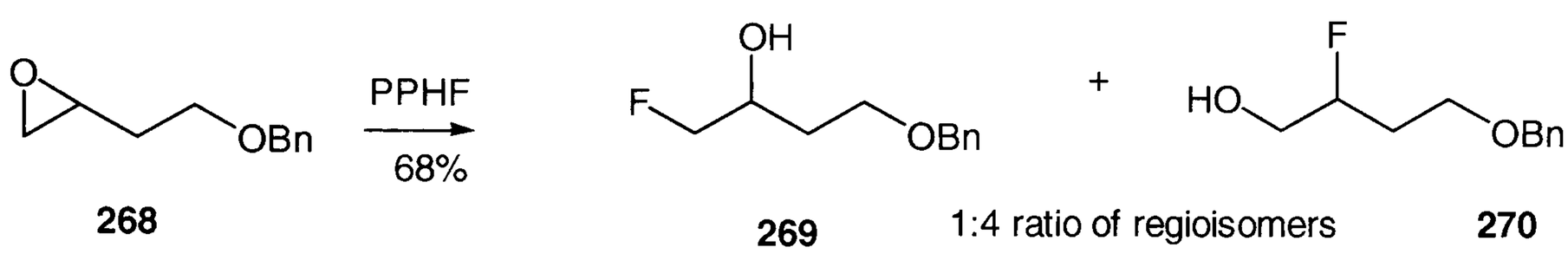

268 **269** 1:4 ratio of regioisomers **270**

Scheme 2.67. Influence of the base in the hydrogen fluoride complex on regioselectivity of epoxide opening.

Pyridinium polyhydrogen fluoride (PPHF), also called Olah's reagent, represents a "tamed" form of hydrogen fluoride in which hazardous hydrogen fluoride is complexed with pyridine. This generates a stable liquid that can be safely handled in the laboratory, although its application is restricted to plastic or stainless steel equipment. The reagent is especially effective for the fluorination of epoxides to generate fluorohydrins in a stereoselective manner. Regioselectivity can be tuned by choice of the amine that is used in combination with hydrogen fluoride.[12] Pyridine for instance is considerable less basic than triethylamine or diisopropylamine and will therefore increase the relative acidity of the reagent. Aprotic solvents such as dichloromethane and ethers that are inert towards the reagent are typically used in combination with the reagent.[13] Hence, the ring opening reaction preferentially yields the products arising from a more stable carbocation intermediate (Scheme 2.67).

The electronic nature of the oxirane substituents is less important for the more basic reagents, and a shift of regioselectivity to the sterically more accessible site of the oxirane ring is generally observed (Scheme 2.68).

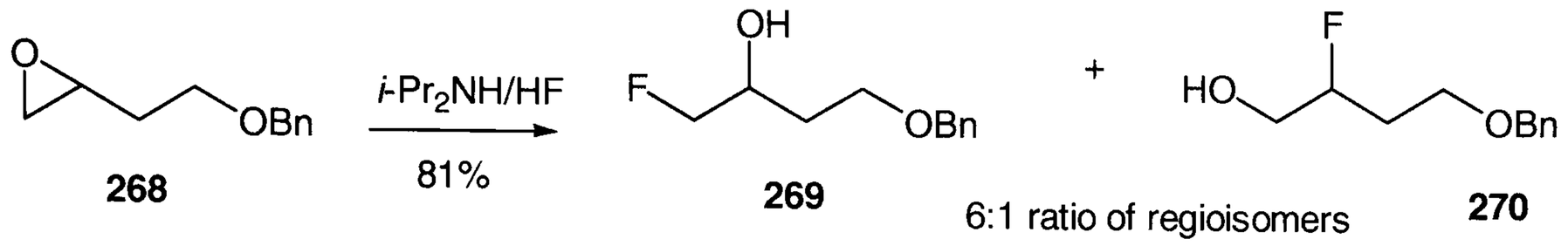

Scheme 2.68. Regioselectivity of epoxide ring opening with hydrogen fluoride/diisopropylamine complex.

Under acidic conditions caused by PPHF, the ring opening of epoxides proceeds *via* a borderline S_N1 mechanism, in which the transition state presumably possesses substantial S_N1 character.[14] The reaction occurs through the initial formation of an epoxonium ion **271**, which may be in equilibrium with two secondary α-hydroxycarbenium ions **272** and **273**. The stability of the α-hydroxycarbenium ions strongly influences the regioselectivity of the reaction. Carboxylate, amide, and cyano groups have been reported to prevent stretching of a contiguous C-O bond, thereby directing nucleophilic attack to the β-carbon.[15] Hence, fluorination will preferentially occur at the site where a positive partial charge can be more readily established (Scheme 2.69).

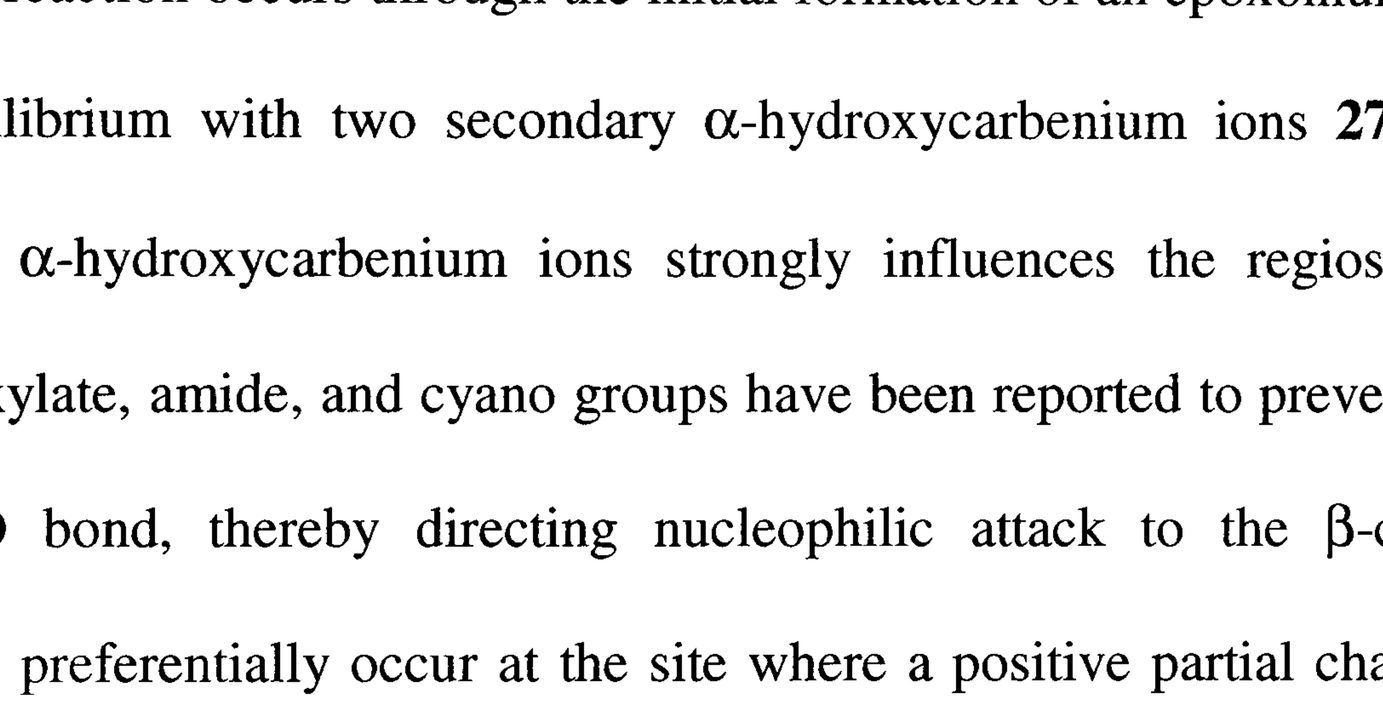

Scheme 2.69. Proposed mechanism for the fluorination of epoxides with PPHF. The electron-withdrawing group (EWG) will direct fluoride attack to the β-carbon.

The synthesis of diethyl 2,3-difluorosuccinate **260** was envisaged *via* ring opening of epoxide **276** with PPHF. The generation of the epoxide **276** is difficult to achieve directly from fumaric and maleic acids due to the electron-deficient character of these double bonds. The reaction has been achieved in moderate yield using lithium *t*-butyl hydroperoxide,[16] and also with a tungsten catalyst.[17] An alternative method for the generation of the epoxide intermediate involves the generation of a bromohydrin, which can be obtained from the respective tartrates. Accordingly, diethyl *(R,R)*-tartrate **77** was reacted with bromine in acetic acid which yielded diethyl 2-bromo-3-acetoxysuccinate **274** (Scheme 2.70).

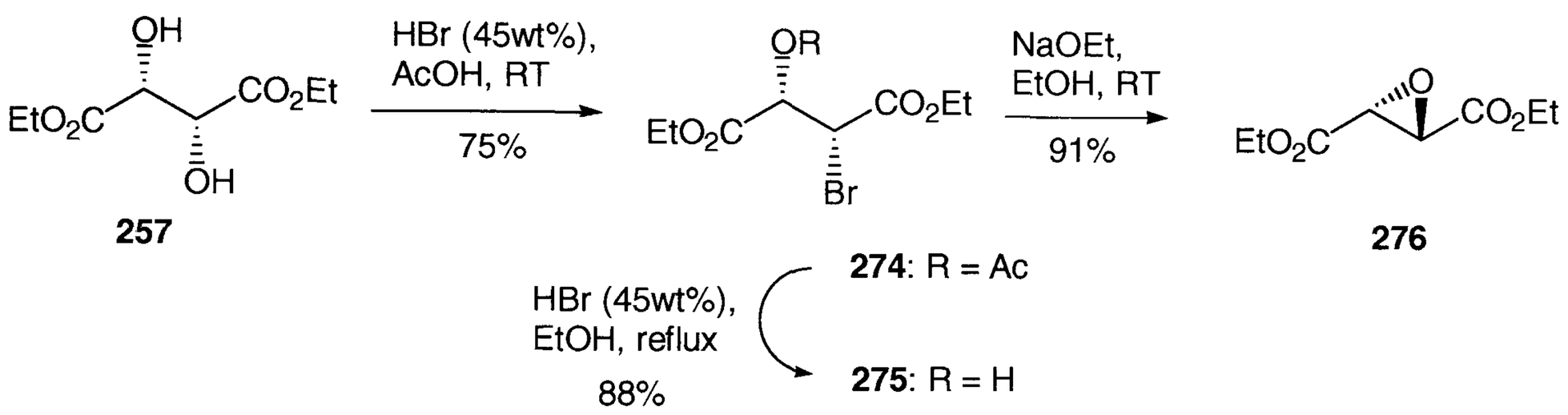

Scheme 2.70. Synthesis of diethyl *trans*-epoxysuccinate **276** as reported by Crout *et al.*[18]

Spectroscopic and physical data for the epoxide **276** thus obtained matched those previously published.[19] The geometry of the epoxide allows for nucleophilic attack of fluoride ion from either side of the molecule to generate a fluorohydrin in a stereoselective manner. Treatment of epoxide **276** with PPHF (Olah's reagent) generated the fluorohydrin **277** in moderate yield (Scheme 2.71).

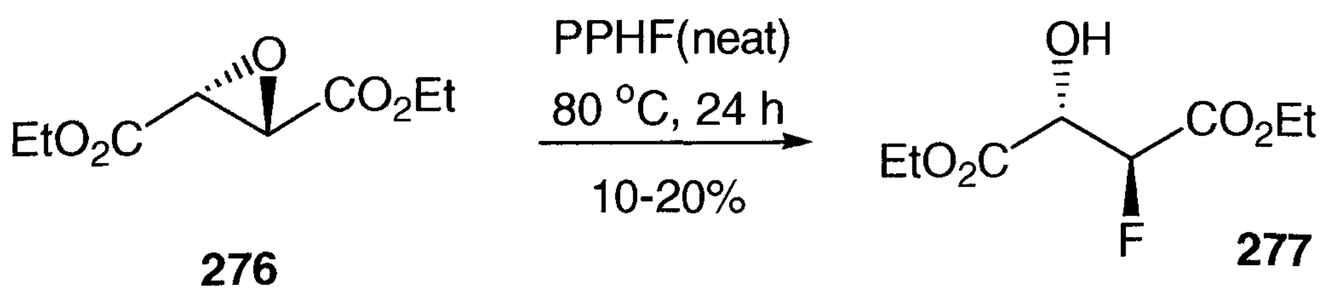

Scheme 2.71. Synthesis of diethyl *(2R,3S)*-2-fluoro-3-hydroxysuccinate **277** *via* epoxide cleavage with PPHF.

Long reaction time and elevated temperatures were required to initiate the ring opening reaction. The low yield of **277** indicated side reactions such as decarboxylation and fluoride elimination. Moreover due to the aggressive nature of the reagent special teflon equipment had to be used and the reaction was eventually abandoned. Considering the formation of a carbocation-like transition state **272** in the reaction of PPHF, the poor reactivity of the epoxysuccinate **276** may be rationalised in terms of the strong electron-withdrawing character of the α-ester groups. As the parent epoxide possesses ester groups on either site, the ring opening reaction with PPHF is only sluggish and generates the fluorohydrin only in moderate yield.

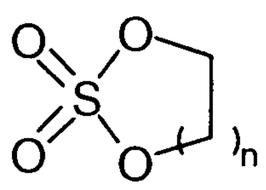

dioxathiolane: n = 1
dioxathiane: n = 2
dioxathiepane: n = 3

1,3,2-dioxathiolane-2,2-dioxide: "Cyclic Sulfate"

Scheme 2.72. Cyclic sulfates of various ring size derived from aliphatic diols and their IUPAC nomenclature.

Cyclic sulfates are useful intermediates in organic synthesis offering the same advantages such as reactivity to a wide range of nucleophiles and good accessibility as epoxides. They are particularly useful for the synthesis of aziridines, oxiranes, cyclopropanes, tetrathiofulvalenes, phospholanes, and for deoxygenation reactions.[20] The most common cyclic sulfates are the 5, 6 and 7 membered heterocyclic compounds of the general structure shown in Scheme 2.72. The conversion of a *vicinal* diol into a cyclic sulfate allows for the stereospecific introduction of a wide range of nucleophiles. Even weak nucleophiles such as carboxylates and fluoride ion are readily introduced into the molecule. The high reactivity of cyclic sulfates has been rationalised in terms of ring strain and partial double bond character between the ring oxygen atoms and the sulfur atom.[21]

The reaction of a nucleophile with the cyclic sulfate **278** leads to cleavage of a carbon oxygen bond to generate a monoalkylsulfate **279**. The nucleophilic attack proceeds with high S_N2 character to give **279** as a single stereoisomer (Scheme 2.73).

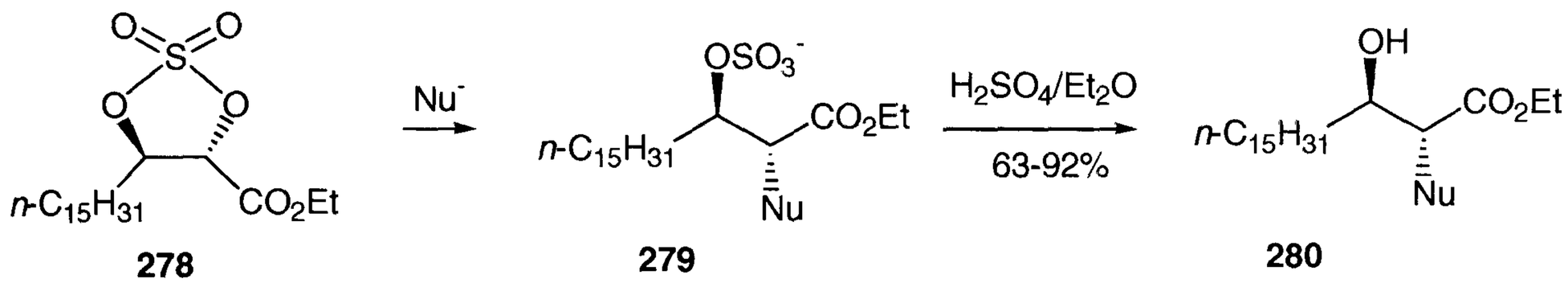

278 **279** **280**

Scheme 2.73. The cyclic sulfate **278** is very reactive towards a wide range of nucleophiles (Nu: H^-, N_3^-, $PhCO_2^-$, SCN^-, F^-). The resulting monoalkylsulfate **279** is typically hydrolysed under acidic conditions.

Not only is the stereoselectivity of the process high, but also the regioselectivity can be controlled in most cases. Cleavage of compound **278** proceeds exclusively from the side of the heterocycle, which is activated by the adjacent ester group. This tendency is in contrast to the regioselectivity observed for the cleavage of epoxides under acidic conditions, and thus these methods represent valuable tools to direct the introduction of functional groups from one specific side of the molecule (Scheme 2.69).

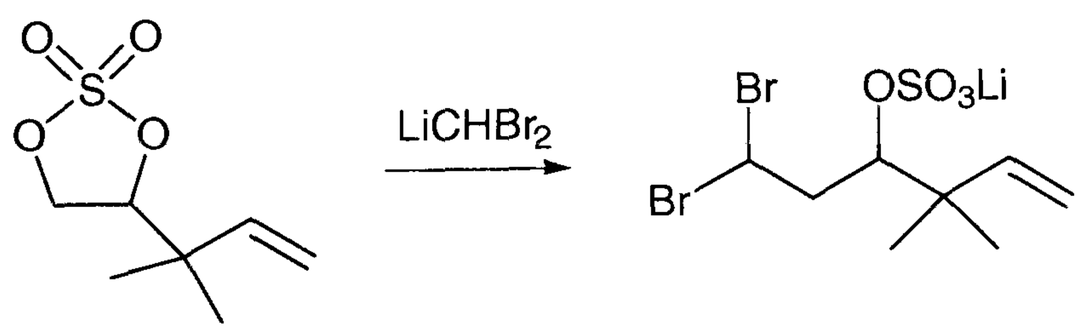

281 **282**

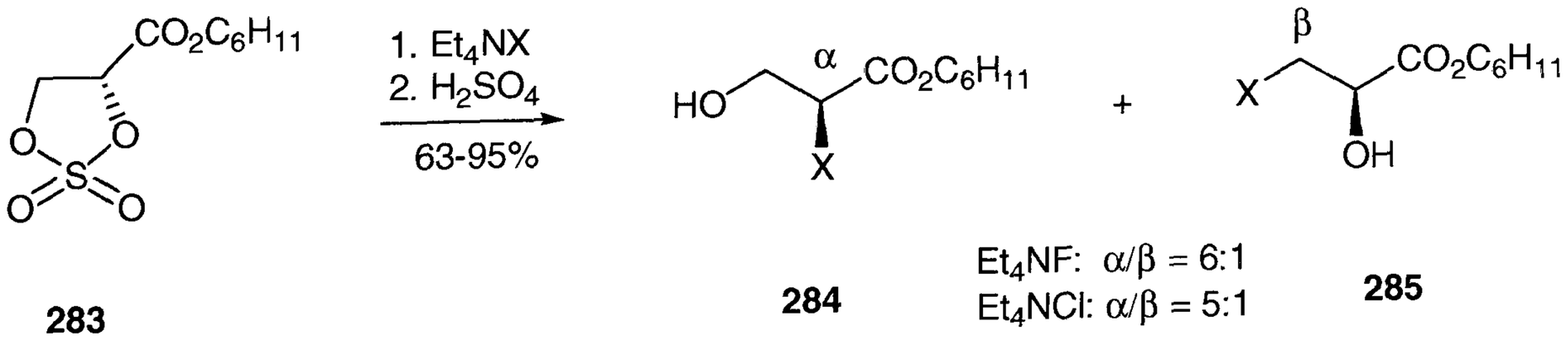

283 **284** **285**

Scheme 2.74. Regioselectivity in the nucleophilic ring opening of dioxothiolanes **281** and **283**.[22]

Steric effects will also control the regioselectivity of the nucleophilic attack. For instance, one side of the dioxathiolane **281** is blocked by a bulky substituent, and as a result, nucleophilic attack of the organolithium reagent occurs from the sterically more accessible side of the molecule. In cases where the molecule is influenced by both steric and electronic effects, product mixtures may be obtained. For instance, cyclic sulfates derived from α,β-dihydroxy esters undergo cleavage from both sides, with nucleophilic attack dominating at the α-position of the ester due to the electron-withdrawing nature of the substituent (Scheme 2.74).

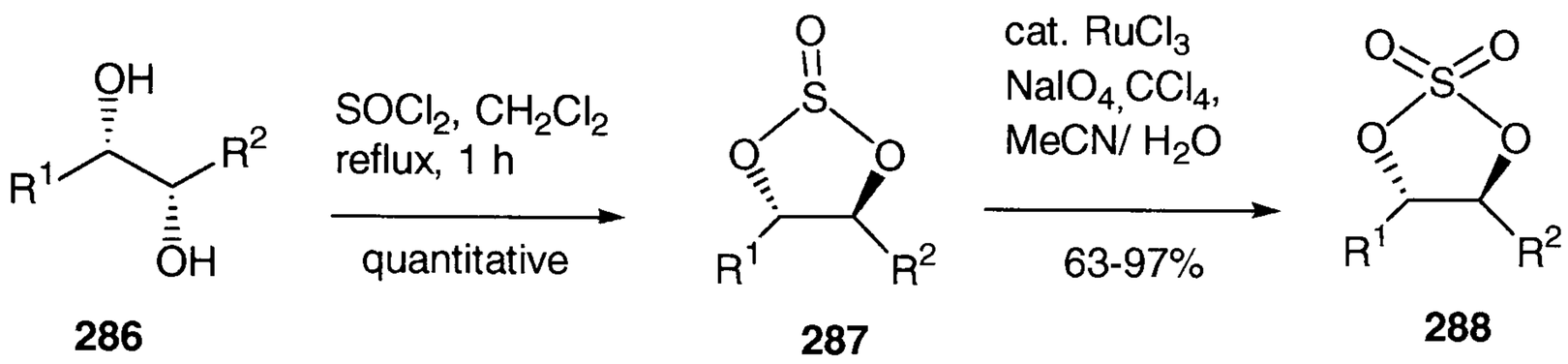

286 **287** **288**

Scheme 2.75. Dioxathiolanes **288** are most commonly generated from *vicinal* diols **286** by reaction with thionyl chloride followed by oxidation.[23]

The preparation of cyclic sulfates is especially straightforward from 1,2-diols, compounds that are readily accessible from alkenes using OsO_4, RuO_4, or $KMnO_7$ oxidations. The preparation of dioxothiolanes from 1,2-diols **286** typically involves the generation of a cyclic sulfite **287** by reaction with thionyl chloride. The intermediate sulfite **287** is oxidised after isolation or without further purification to generate the cyclic sulfate **288**. A one-pot procedure for the synthesis of cyclic sulfates from 1,2-diols employing catalytical amounts of ruthenium trichloride has been developed in the Sharpless group (Scheme 2.75).

The Sharpless asymmetric dihydroxylation facilitates the synthesis of *vicinal* diols in a stereoselective manner and has been elaborated in order to increase the usefulness of the asymmetric dihydroxylation methodology.[24]

The catalytic oxidation approach developed by Sharpless *et al.* obviously excludes compounds with functional groups that are prone to oxidation (e.g., alkenes, amines, and alcohols). In these cases, alternative synthetic methods are required and some of them are illustrated in Scheme 2.76.

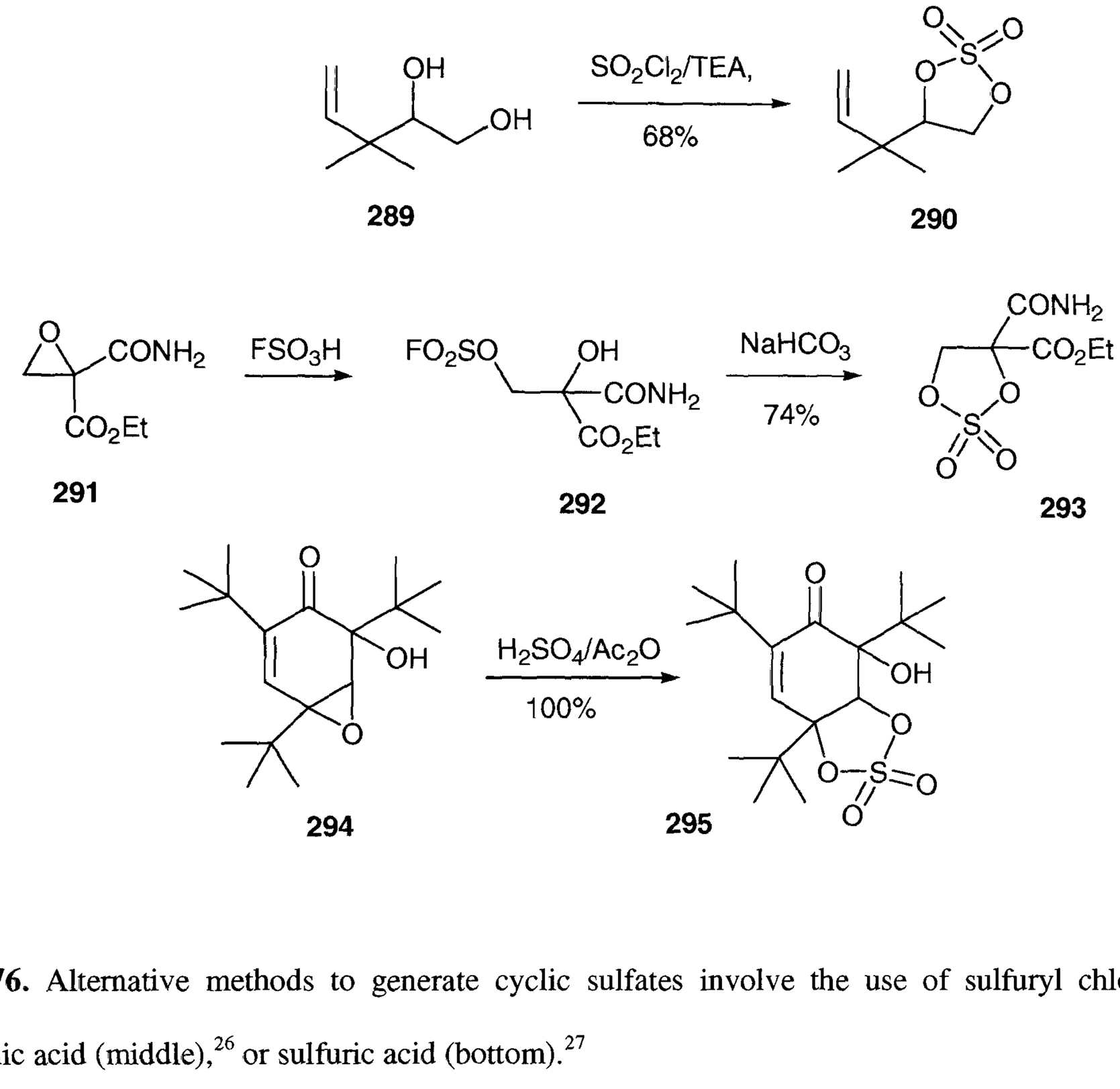

Scheme 2.76. Alternative methods to generate cyclic sulfates involve the use of sulfuryl chloride (top),[25] fluorosulfonic acid (middle),[26] or sulfuric acid (bottom).[27]

Cyclic sulfates are extraordinary reactive towards nucleophilic attack and therefore the ideal substrates for the introduction of fluorine into organic molecules. Fluorination is generally more problematic than other nucleophilic substitutions, mainly due to the high solvation energy of fluoride ion which renders it a weak nucleophile. On the other hand the inherent basicity of fluoride ion often represents a problem, which favours elimination rather than substitution. Application of 1,2-cyclic sulfate chemistry has proved immensely useful for the stereo- and regioselective introduction of fluoride ion to generate *vicinal* trifluoroalkanes. The combination of cyclic sulfate chemistry and Sharpless asymmetric epoxidation led to the

stereoselective formation of diastereoisomers.[28] Generation of the cyclic sulfate of (*R,R*)-diethyl tartrate allowed the introduction of fluoride ion into the molecule. The cyclic sulfate was obtained according to a modified literature procedure starting from diethyl tartrate **84** (Scheme 2.77).

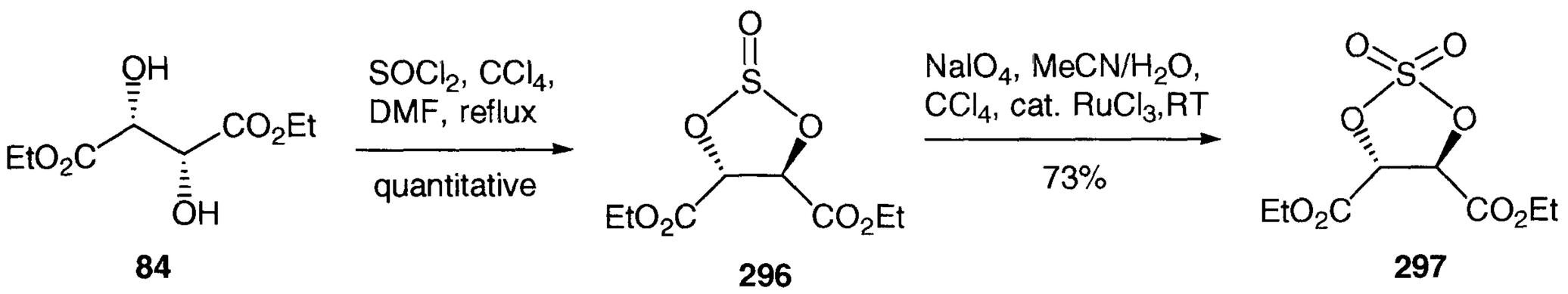

Scheme 2.77. Synthesis of the dioxothiolane derived from diethyl (*R,R*)-tartrate **84**. The use of catalytic amounts of DMF leads to complete conversion of the starting material. The oxidation of **296** can be carried out conveniently in the same reaction medium as a one-pot reaction.[29]

Initially, reaction of the diethyl tartrate with thionyl chloride was slow and did not go to completion, even with an excess of reagent at elevated temperatures. Addition of pyridine resulted in a fast conversion of the starting material, but this necessitates the isolation of the intermediate sulfite **296** before the oxidation can be carried out. As the addition of catalytic amounts of DMF has been used to catalyse the reaction of carboxylic acids with acid chlorides,[30] the use of dimethylformamide to catalyse the reaction was explored. It was found that DMF did indeed accelerate the reaction between thionyl chloride and the tartrate **84**, and the synthesis of the sulfite **296** could be carried out at ambient temperature only with catalytic amounts of DMF. The oxidation of **296** was performed in a two-phase system according to a literature procedure.[31] When a homogeneous solution of water in acetonitrile was used, the yield of the reaction dropped significantly. Presumably the sulfate **297**, which is very reactive, undergoes hydrolysis in the aqueous medium, and the resulting anion is lost during aqueous work up.

The enantiomeric structure **300** derived from diethyl (*S*,*S*)-tartrate **298** is readily accessible using the aforementioned procedure (Scheme 2.78). In analogy to **297** its enantiomer **300** undergoes cleavage on reaction with a nucleophile to yield a single stereoisomer with the opposite absolute configuration that can be obtained from **297**. The method has also been used to prepare the *meso* compound **312**, starting from diethyl (*R*,*S*) tartrate **311** (Scheme 2.83).

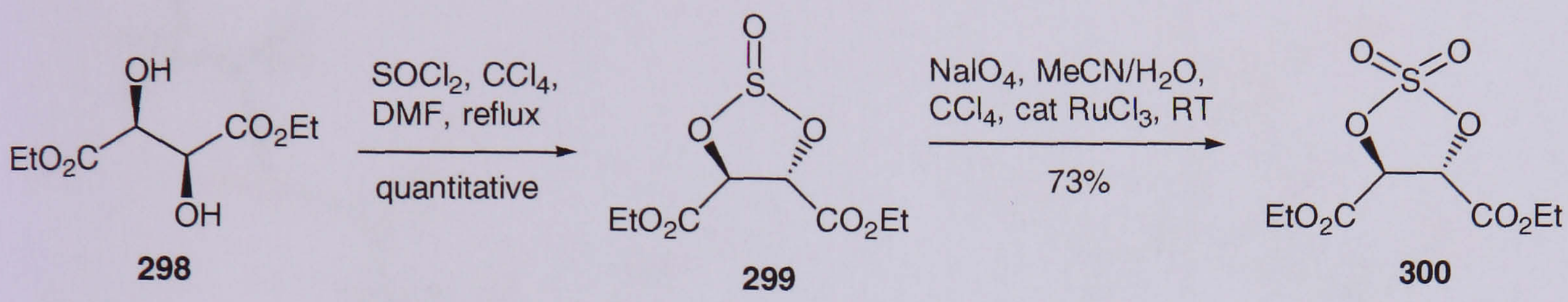

Scheme 2.78. Synthesis of the dioxothiolane **300** derived from diethyl (*S*,*S*)-tartrate **298**. The oxidation of **299** was carried out in a one-pot reaction.

The cyclic sulfate **297** was conveniently purified by recrystallisation to give the product as large colourless crystals, which proved to be stable over a period of more than three years (Figure 2.29).

Figure 2.29. Crystals of the cyclic sulfates **297** derived from diethyl (*R*,*R*)-tartrate (left), and **312** derived from diethyl (*R*,*S*)-tartrate **311** (right).

Both stereoisomers were amenable to X-ray crystallography. Compound **297** shows a solid state conformation in which the large R groups adopt axial positions, pointing away from each other. This is rather surprising as transannular ring strain is minimised when the largest substituents adopt equatorial positions (Figure 2.30).

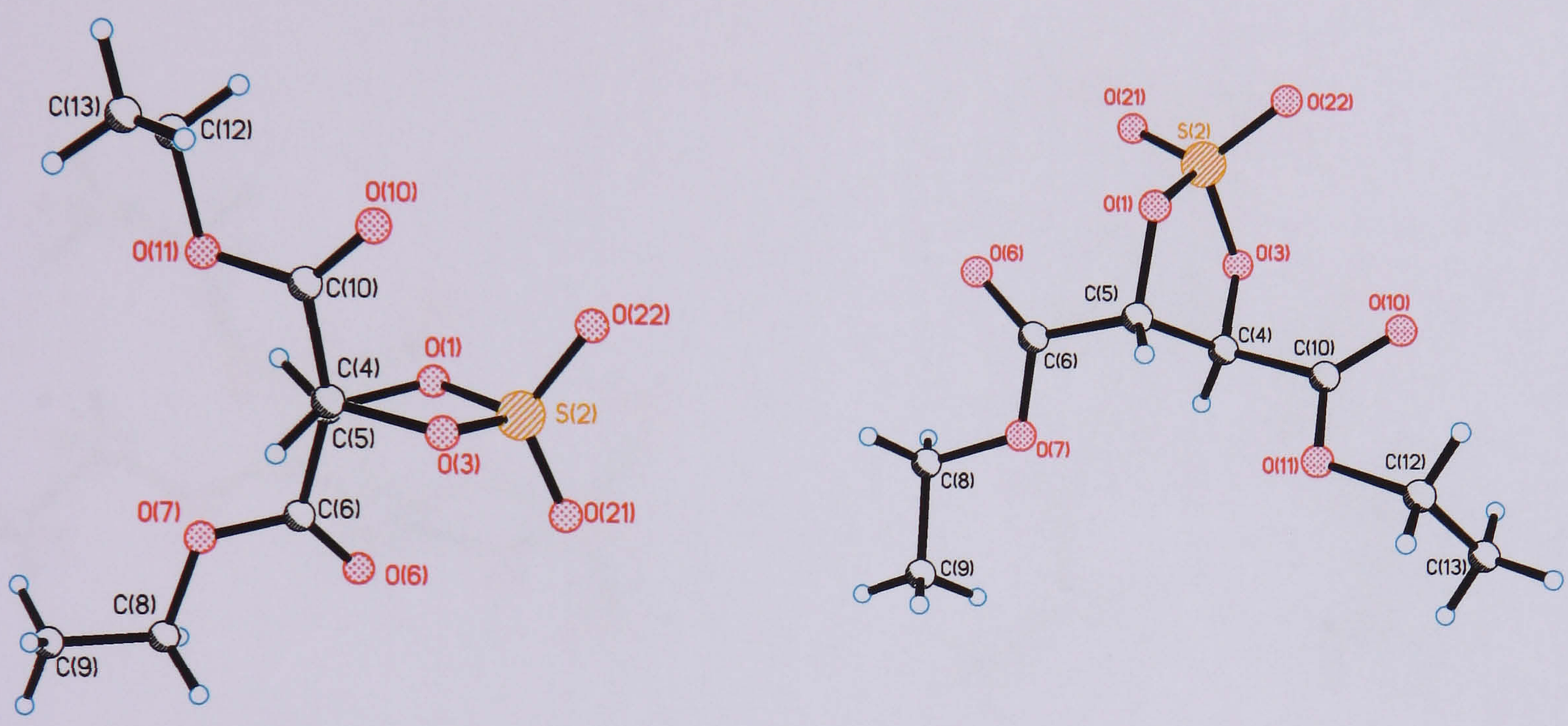

Figure 2.30. X-ray structures of the dioxathiolane **297**. The left hand structure illustrates the confomation of the 5-membered ring, whereas the right hand structure shows the conformation of the main chain. Selected bond lengths (Å), bond and torsion angles (°): O1-S2 1.579(2), S2-O3 1.51(2), O3-C4 1.441(4), C4-C5 1.543(4), C5-O1 1.444(4), S2-O22 1.416(2), S2-O21 1.422(3); O1-S2-O3 97.68(12), S2-O3-C4 112.40(19), O3-C4-C5 104.6(3), C4-C5-O1 103.4(3), C5-O1-S2 111.3(2); C5-O1-S2-O3 -16.9(2), O1-S2-O3-C4 -4.8(2), S2-O3-C4-C5 22.8(3), S2-O1-C5-C4 30.8(3), O3-C4-C5-O1 -32.2(3).

The heterocyclic ring appears to adopt a twisted envelope conformation presumably in order to reduce ring strain. The O(1)-S(2) and O(3)-S(2) bond lengths of 1.571 and 1.579 Å respectively are significantly shorter than typical sulfur-oxygen single bonds. This supports the theory of partial double bond character of the intra-annular oxygen-sulfur bond, used to explain the high reactivity of the adjacent carbon atoms towards nucleophilic substitution.The

cyclic sulfate derived from (*R*,*S*)-tartaric acid **312** shows similar behaviour in its solid state structure (Figure 2.31). The heterocycle again adopts a twisted envelope conformation in order to reduce ring strain. By contrast, the large substituents are equatorial in one case and axial in the other, due to the relative configuration of the molecule. The compound was synthesised according to the aforementioned procedure.

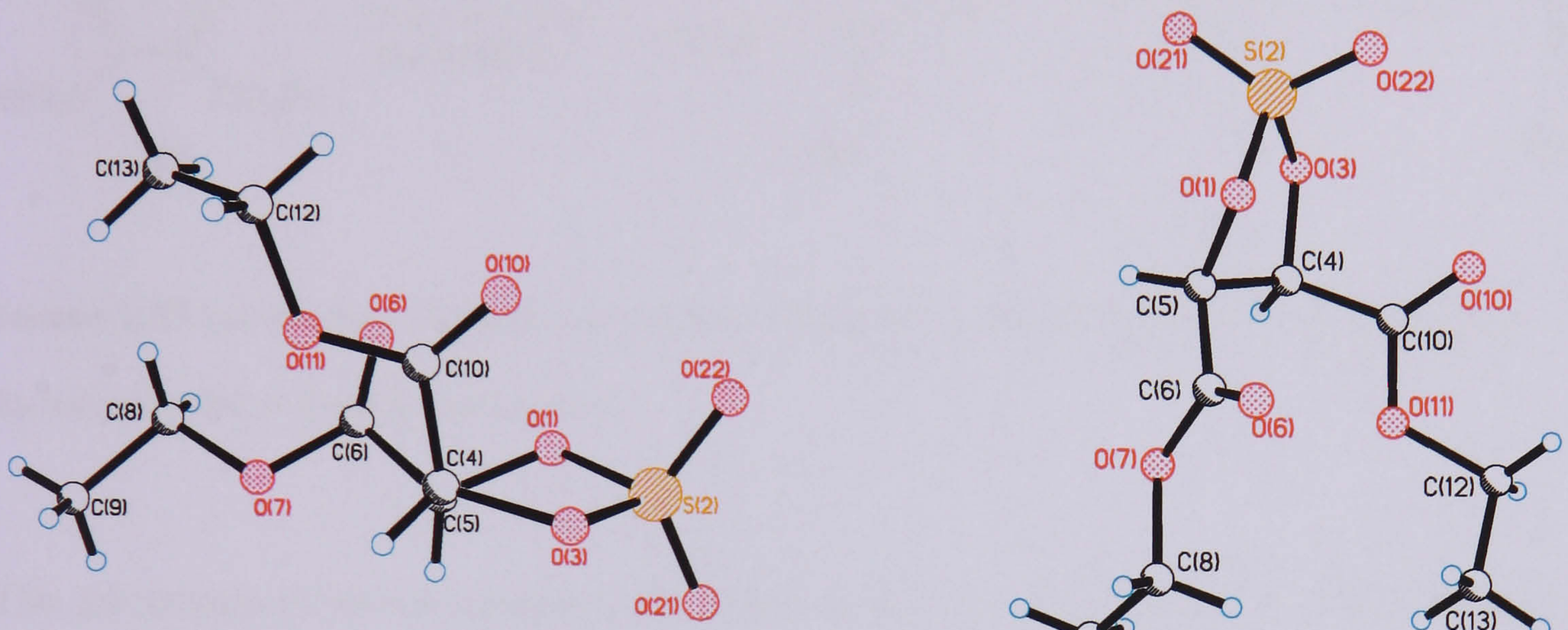

Figure 2.31. X-ray structures of the dioxathiolane **312**. The left hand structure illustrates the confomation of the 5-membered ring, whereas the right hand structure shows the conformation of the main chain. Selected bond lengths (Å), bond and torsion angles (°): O1-C5 1.452(16), O1-S2 1.597(9), S2-O22 1.385(11), S2-O21 1.429(10), S2-O3 1.619(9), O3-C4 1.474(16), C4-C5 1.598(18); C5-O1-S2 111.4(8), O1-S2-O3 97.0(5), C4-O3-S2 110.3(7), O3-C4-C5 104.2(10), O1-C5-C4 99.8(10); C5-O1-S2-O3 -25.3(12), O1-S2-O3-C4 -2.1(10), S2-O3-C4-C5 25.2(12), S2-O1-C5-C4 40.4(13), O3-C4-C5-O1 -39.3(13).

The fluorination of **297** was conveniently achieved by treatment with fluoride ion, which can be delivered in form of inorganic fluoride salts. Cesium fluoride, as expected from consideration of the crystal lattice energies, has the highest reactivity of the alkali-metal fluorides according to CsF > RbF > KF >> NaF >> LiF.[32] Alkaline-earth metal fluorides are unsuitable due to their extreme insolubility even in aqueous solutions. CsF was readily used for cleavage of the cyclic sulfate and concomitant C-F bond formation even though the

solubility of inorganic fluoride salts in organic solvents is generally quite poor. THF, acetone, and acetonitrile proved to be suitable solvents for the cleavage of the cyclic sulfate by fluoride ion. In the more polar solvents such as acetonitrile even inorganic fluoride ion can be used effectively (Scheme 2.79).

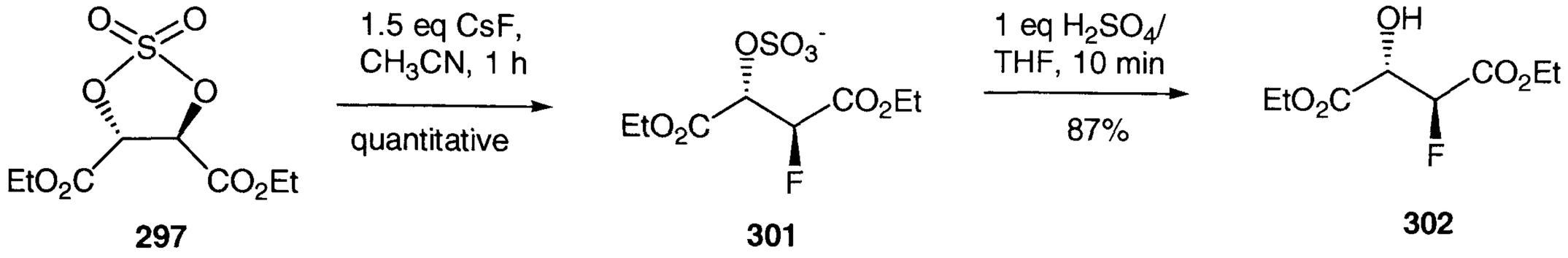

Scheme 2.79. Introduction of fluorine by reaction of the cyclic sulfate **297** with TBAF to generate the fluorohydrin **302** as a single stereoisomer.

The advantage of using inorganic fluorides is that the fluoride salt, which is used in slight exess can conveniently be removed by aqueous work up after hydrolysis of the monoalkylsulfate. Due to the inherent C_2-symmetry of **297**, nucleophilic attack from either site of the molecule leads to the same compound. Therefore the fluorohydrin **302** is obtained as a single stereoisomer after hydrolysis of the monoalkylsulfate **301**. Initially, the hydrolysis of **301** was carried out according to the literature procedure in a biphasic reaction medium.[33] Under these conditions the hydrolysis was slow and only moderate yields of the fluorohydrin **302** were obtained even after prolonged reaction times.

Optimisation attempts led to improved reaction conditions for the hydrolysis of **301**, using only traces of H_2O and a catalytic amount of sulfuric acid in a homogenous solution of THF. Instead of adding 1 mol equivalent of H_2O, the use of commercially available undried THF was sufficient to initiate the reaction. The hydrolysis could be followed by ^{19}F-NMR spectroscopy, which indicated complete hydrolysis of the monoalkylsulfate under these

conditions within minutes. The improved yield in the synthesis of fluorohydrin **302** using the homogeneous medium suggests that an excess of water is in fact interfering with hydrolysis of the alkylsulfate. Mechanistically, the aforementioned hydrolysis occurs by cleavage of the sulphur-oxygen bond under acidic conditions (Scheme 2.80).

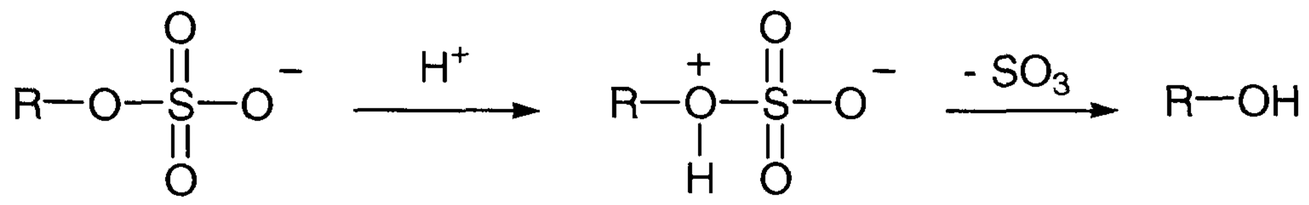

303 **304** **305**

Scheme 2.80. Proposed mechanism of the hydrolysis of the monoalkylsulfate catalysied by mineral acids.

Alkylsulfate **303** is hydrolysed to alcohol **305** while retaining the original configuration at the stereogenic centre. In that reaction, zwitterion **304** has been suggested as the reactive intermediate.[34] The absolute configuration of the product was thus assumed on the basis of an S_N2 cleavage of the cyclic sulfate, and a retention of configuration upon hydrolysis of the monoalkyl sulfate group. The stereochemical course of the reaction was confirmed by X-ray analysis of the bis(benzylamide) **306**. The compound was obtained upon heating of **302** with benzylamine in diethyl ether (Scheme 2.81).

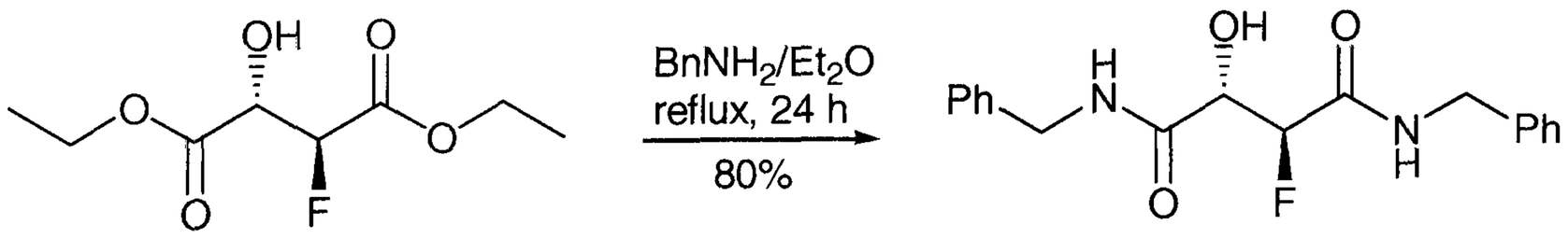

302 **306**

Scheme 2.81. Synthesis of dibenzyl (*2S,3R*)-2-fluoro-3-hydroxysuccinate **306** from diethyl ester **302**.

The fluorohydrin **302** is stable under the basic conditions generated by the amine and does not eliminate hydrogen fluoride in the process. The benzylamide **306** conveniently precipitates on cooling and can be filtered off to give the pure product. The X-ray structure of dibenzylamide **306** shows the molecule in a conformation where the C-F bond is *gauche* to the C-OH bond (Figure 2.32).

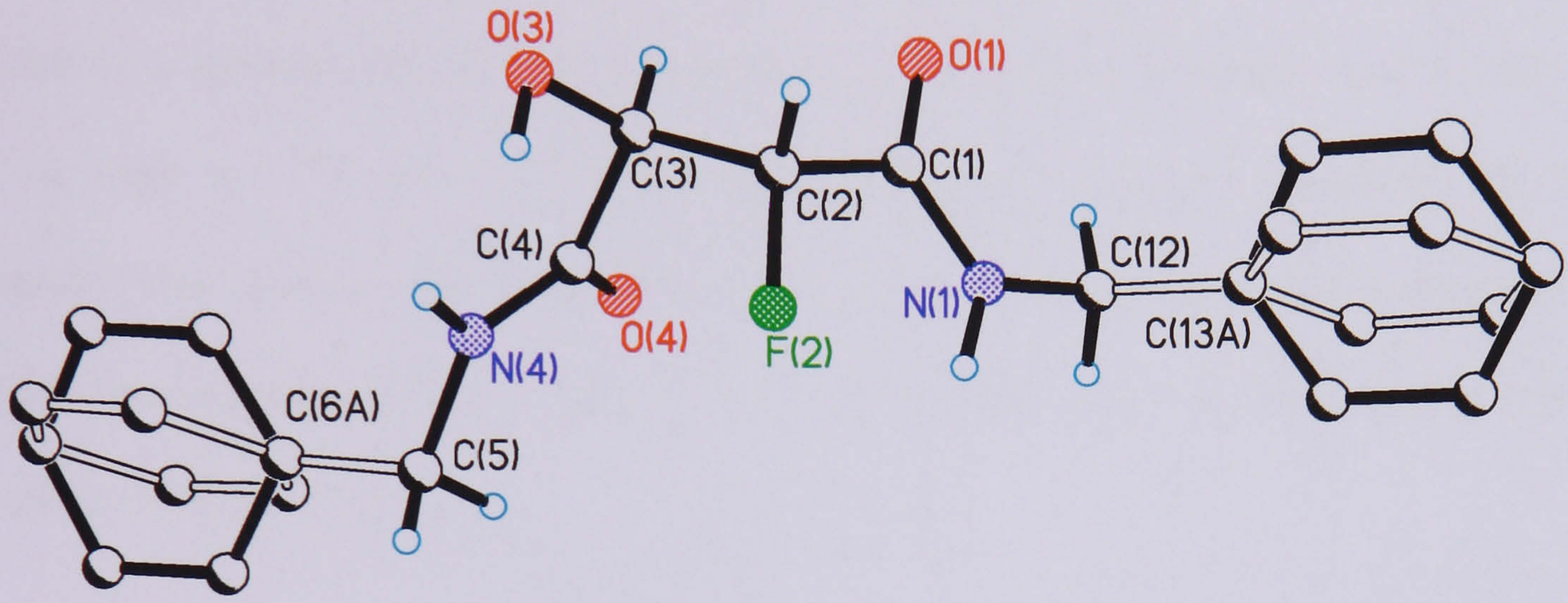

Figure 2.32. X-ray structure of *N,N*-dibenzyl 2-fluoro-3-hydroxysuccinate **306**. Selected bond lengths (Å), bond and torsion angles (°): N1-C1 1.333(6), C1-O1 1.221(7) C1-C2 1.546(7), C2-F2 1.407(7), C2-C3 1.542(6), C3-O3 1.396(6), C3-C4 1.520(7), C4-O4 1.224(7), C4-N4 1.327(8) Å; C1-C2-F2 110.6(4), F2-C2-C3 112.9(4), N1-C1-C2-F2 –1.5(6), O1-C1-C2-F2 –179.9(4), C1-C2-C3-C4 85.0(5), O3-C3-C4-O4 157.6(4), O3-C3-C4-N4 –24.2(6)°.

This conformation is consistent with the "generalised *gauche* effect", which predicts the two most electronegative substituents to align *gauche* to each other. The *gauche* conformation of the α-fluorohydroxy moiety in **306** is not surprising as the electronegativity of oxygen is second only to fluorine. In addition, the α-fluoroamide moiety adopts a planar conformation in which the C-F bond is *anti* periplanar to the carbonyl bond and *syn* planar to the N-H bond. This conformation again is consistent with predicted stereoelectronic effects as outlined earlier in the introduction.

Basic conditions force carbon-oxygen bond cleavage where the sulphate functionality acts as a leaving group (Scheme 2.82).[35] The ambident reactivity of the sulfate group has been used for the conversion of cyclic sulfates to aziridines.[36] The ambident reactivity of the sulfate group appeared to be useful for the introduction of the second fluorine atom simultaneously into the succinate moiety. This hypothesis was investigated using excess TBAF under otherwise standard reaction conditions. Substitution of the sulfate group with fluoride ion could lead to a symmetrical difluoro compound. Such molecules exhibit an AA'XX' spin system in both the ^{19}F and ^{1}H NMR spectra (Chapter 2.4), and therefore, ^{19}F NMR spectroscopy was used as a means to follow the course of the reaction. The reaction of **297** with TBAF did not afford the desired product even at prolonged reaction time and elevated temperatures (Scheme 2.82).

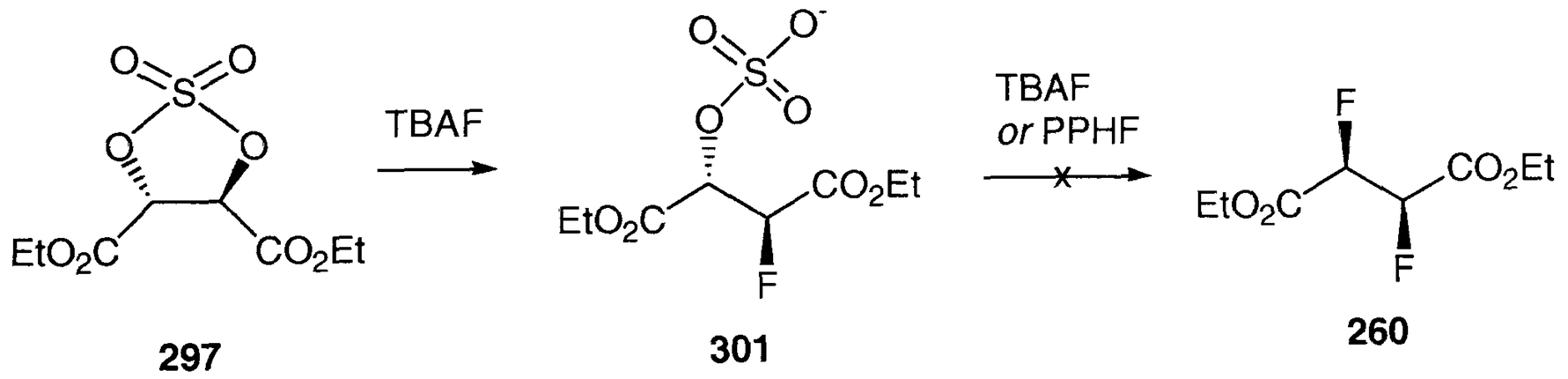

Scheme 2.82. Attempted synthesis of diethyl 2,3-difluorosuccinate by nucleophilic substitution of the sulfate group with TBAF or PPHF.

Presumably, nucleophilc displacement of the sulfate group is only favoured in intramolecular cases with good nucleophiles such as amines. An attempt was made to carry out the reaction under acidic conditions using PPHF. These conditions should force protonation of the sulfate group rendering it a better leaving group than the ionic form. However, this approach was equally unsuccessful.

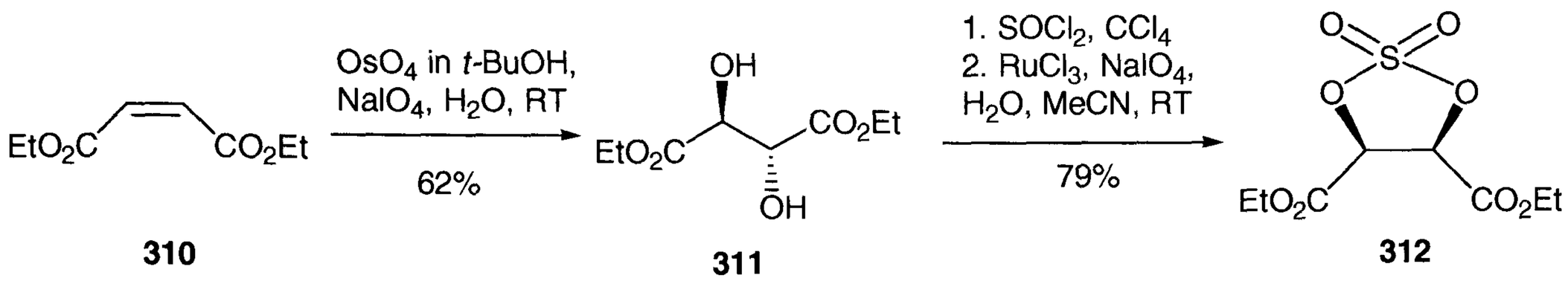

Scheme 2.83. Synthesis of diethyl (*R*,*S*)-tartrate **311** and its conversion into the cyclic sulfate **312**.

As diethyl *meso* tartrate **311** is not commercially available, the compound was synthesised from diethyl maleate **310** using the method reported by Crout *et al.*.[37] Oxidation of the electron-deficient alkene was achieved with sodium periodate in the presence of osmium tetroxide (Scheme 2.83). The oxidation of diethyl maleate **310** could be scaled up and the product purified by recrystallisation. The ruthenium species was applied in catalytic amounts only, thus reducing the danger of exposure and minimising toxic heavy metal waste. Alternatively, diethyl *meso*-tartrate was obtained by esterification of (*R*,*S*)- tartaric acid in dry ethanol in the presence of Dowex-H^+ ion exchange resin. Surprisingly, treatment of dioxathiolane **312** with fluoride ion suffered from low yield due to the formation of diethyl oxaloacetate as a by-product (Scheme 2.84).

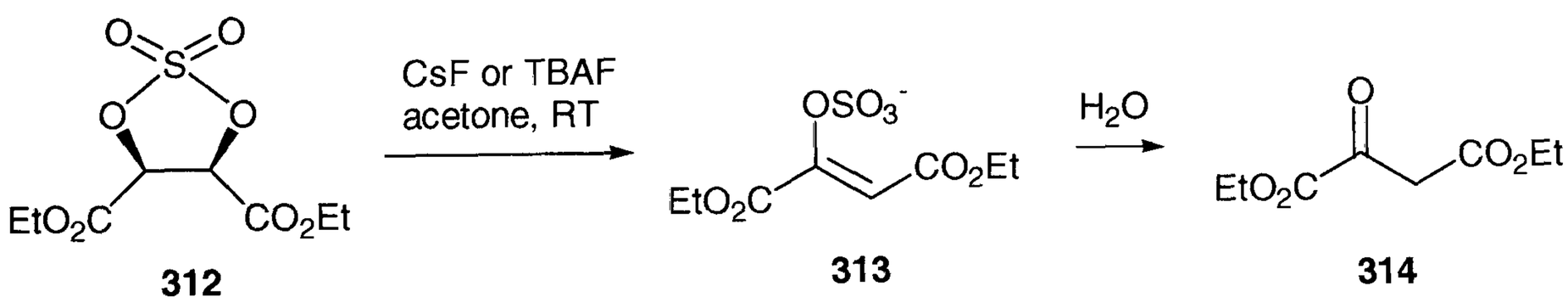

Scheme 2.84. TBAF treatment of the cyclic sulfate **312** derived from diethyl (*R*,*S*) tartrate generated diethyl oxalacetate **314** as the major product.

Oxaloacetate, which emerged as the major product from the reaction, clearly arises from deprotonation adjacent to the ester group to generate the enolate **313**. This intermediate hydrolyses under acidic conditions to give the free enolate which tautomerises to form **314**.

The different reactivity of the two diastereoisomers is quite surprising, but similar examples are frequently found in the literature.[38] For instance, fluorination of 4-*tert*-butyl cyclohexanol proceeds more readily when the nucleophilic fluoride ion can approach from an axial position. Thus, fluorination of the *cis*-isomer **316** with morpho-DAST **252** gives the *trans* isomer **318** in relatively high yield, compared to its *cis* isomer **317** (Scheme 2.85).

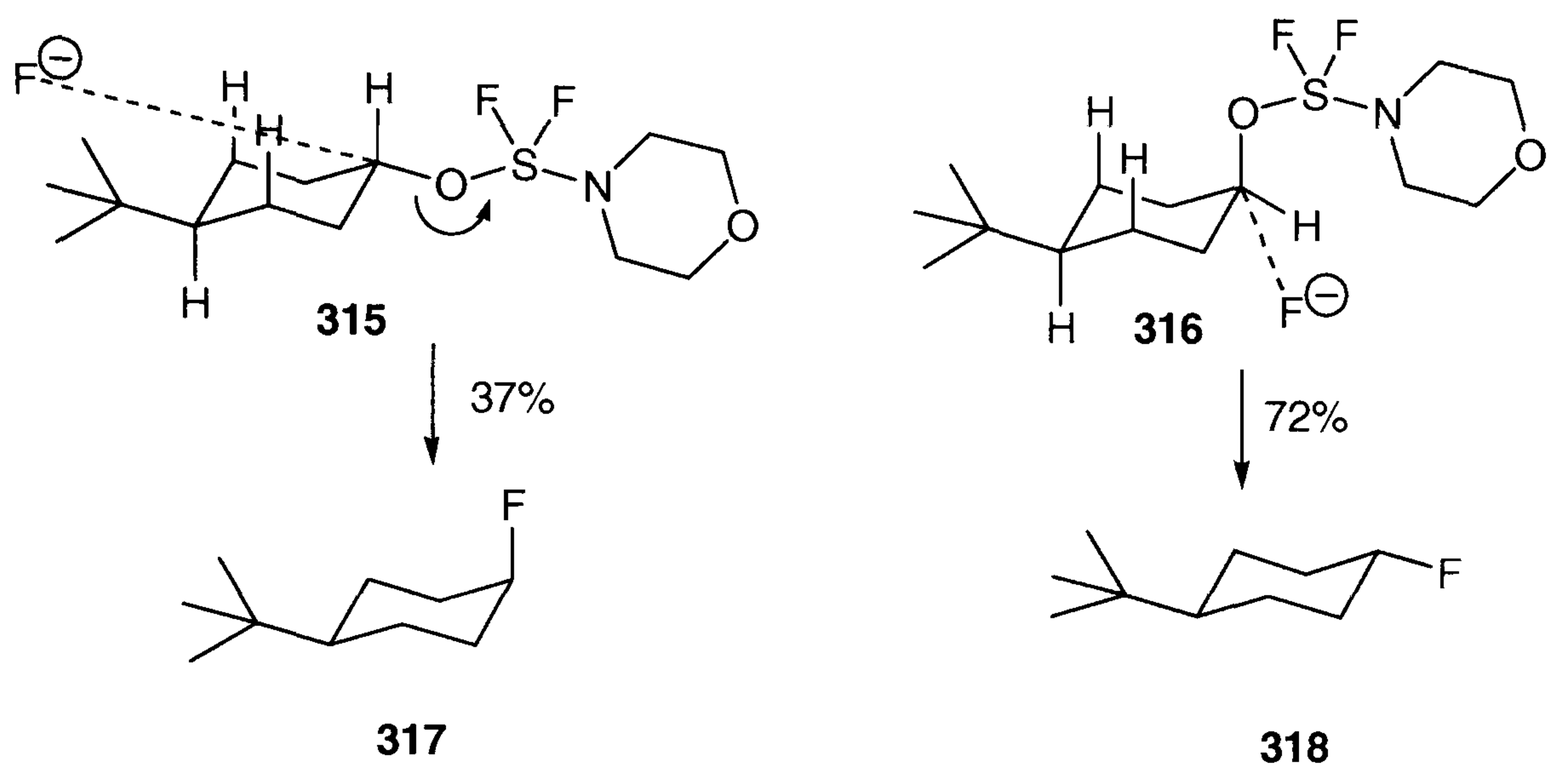

Scheme 2.85. Fluorination of the *cis* and *trans* 4-*tert*.-butylcyclohexanol **316** and **315** using morpho-DAST.

An alternative route to access *threo* 2-fluoro-3-hydroxysuccinate **319** involves the inversion of the stereogenic centre at the hydroxyl group of diethyl fluoromalate. The reaction would afford the *threo* compound **319** in a stereoselective manner, whereas the synthetic route *via* the cyclic sulfate **312** affords *threo* 2-fluoro-3-hydroxysuccinate **319** only as a racemic mixture. The enantioselective synthesis of diethyl 2-fluoromalate **319** was envisaged as the compound may exhibit biological activity for enzymes involved in the citric acid cycle.[39] Inversion of the hydroxyl carbon of (*2S,3R*)-2-fluoro-3-hydroxysuccinate **321** was attempted *via* the well-known Mitsunobu inversion methodology.[40]

Schlosser *et al.* have used the Mitsunobu reaction for the epimerisation at the hydroxyl group of aliphatic fluorohydrins.[41] Attempts were made to apply the conditions to the parent diethyl fluoromalate (Scheme 2.86).

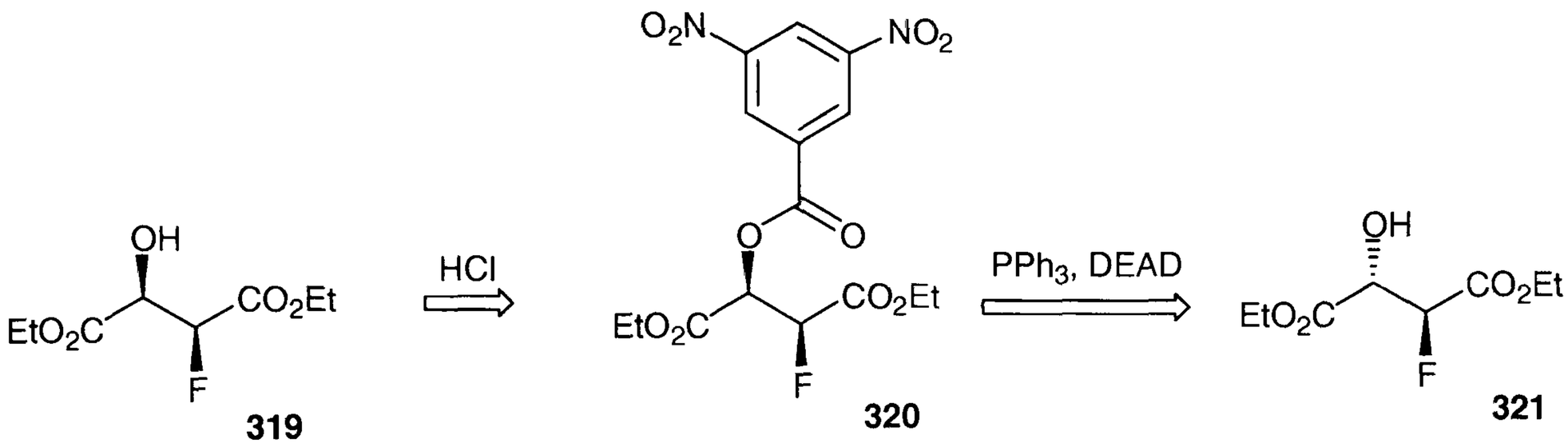

Scheme 2.86. Attempted synthesis of (*2R,3S*)-2-fluoro-3-hydroxysuccinate *via* Mitsunobu methodology.

The reaction however did not yield the expected compound **319** and resulted in undentifiable product mixtures. Subsequently, attempts were made to access the *threo* 2-fluoro-3-hydroxysuccinate **319** *via* double inversion at the adjacent stereogenic centre. The introduction of weak nucleophiles such as bromine or iodine that can act as a good leaving group is feasible due to the extraordinary reactivity of **297** towards nucleophilic attack. Consequently, cyclic sulfate **312** was converted into the bromosulfate **322** using TBAB as the bromide source (Scheme 2.87).

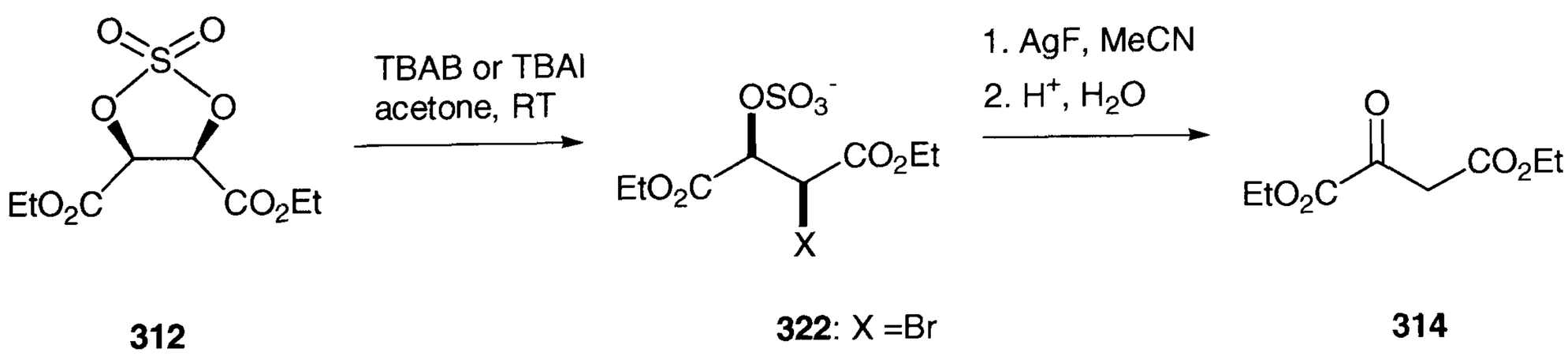

Scheme 2.87. Attempted synthesis of diethyl (*2R,3S*)-2-fluoro-3-hydroxysuccinate **319** from cyclic sulfate **322**.

The cyclic sulfate approach is unique as it affords an intermediate in which the hydroxyl group is still protected as an alkylsulfate (such as **301**, Scheme 2.79). This protection can be

utilised for a second reaction step, as it prevents from neighbouring group participation of the hydroxyl group. In the fluorination, this protection is essential, as the basic nature of fluoride ion will cause deprotonation of the adjacent hydroxyl group and concomitant intramolecular nucleophilic substitution to form an epoxide.[42] Disappointingly, the treatment of the bromosulfate **322** with AgF or TBAF did not lead to the desired fluorinated compound. Instead, diethyl oxalacetate **314** was formed as the major product in the reaction (Scheme 2.87). It can be assumed that formation of oxalacetate proceeds in a similar way as described in Scheme 2.84. Deprotonation at the β-carbon atom takes place and hydrolysis of the intermediate enolsulfate **313** results in formation of the β-ketoester **314**.

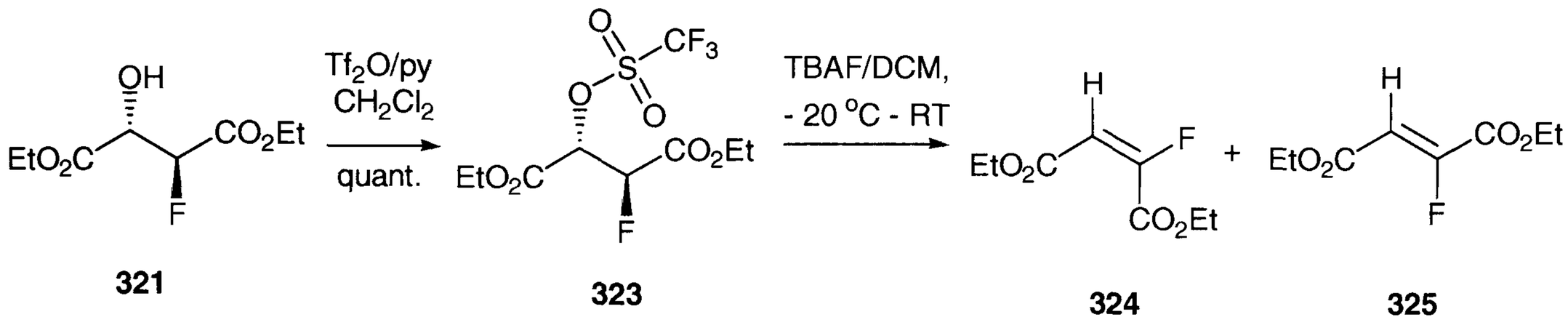

321 **323** **324** **325**

Scheme 2.88. Synthesis of **323** and attempted fluorination with *N*-tetrabutylammonium fluoride (TBAF). [43]

The conversion of the fluorohydrin into the difluorosuccinate was the next objective in the synthesis. A standard methodology for this process involves transformation of the hydroxyl group into a leaving group and subsequent treatment with nucleophilic fluorine.[44] TBAF is perhaps the most popular reagent in this class, and the reaction with a triflate generally proceeds with high S_N2 character. Therefore, the synthesis of trifluorosulfonate **323** was envisaged and achieved using standard synthetic protocols (Scheme 2.88). The reaction was straightforward and the product **323** found to be surprisingly stable towards hydrolysis and flash chromatography. However, when the triflate **323** was treated with TBAF the anticipated difluorosuccinate **260** was not formed. Instead, two new compounds were observed by ^{19}F

NMR spectroscopy, each having doublets with coupling constants of 28.6 Hz and 16.3 Hz respectively (Figure 2.35). These signals were assigned to fluorofumarate **325** and fluoromaleate **324**. Corresponding coupling patterns were observed in the ^{1}H-NMR spectrum. The identity of these products was also confirmed by GC-MS analyses as well as by comparison with published data.[45]

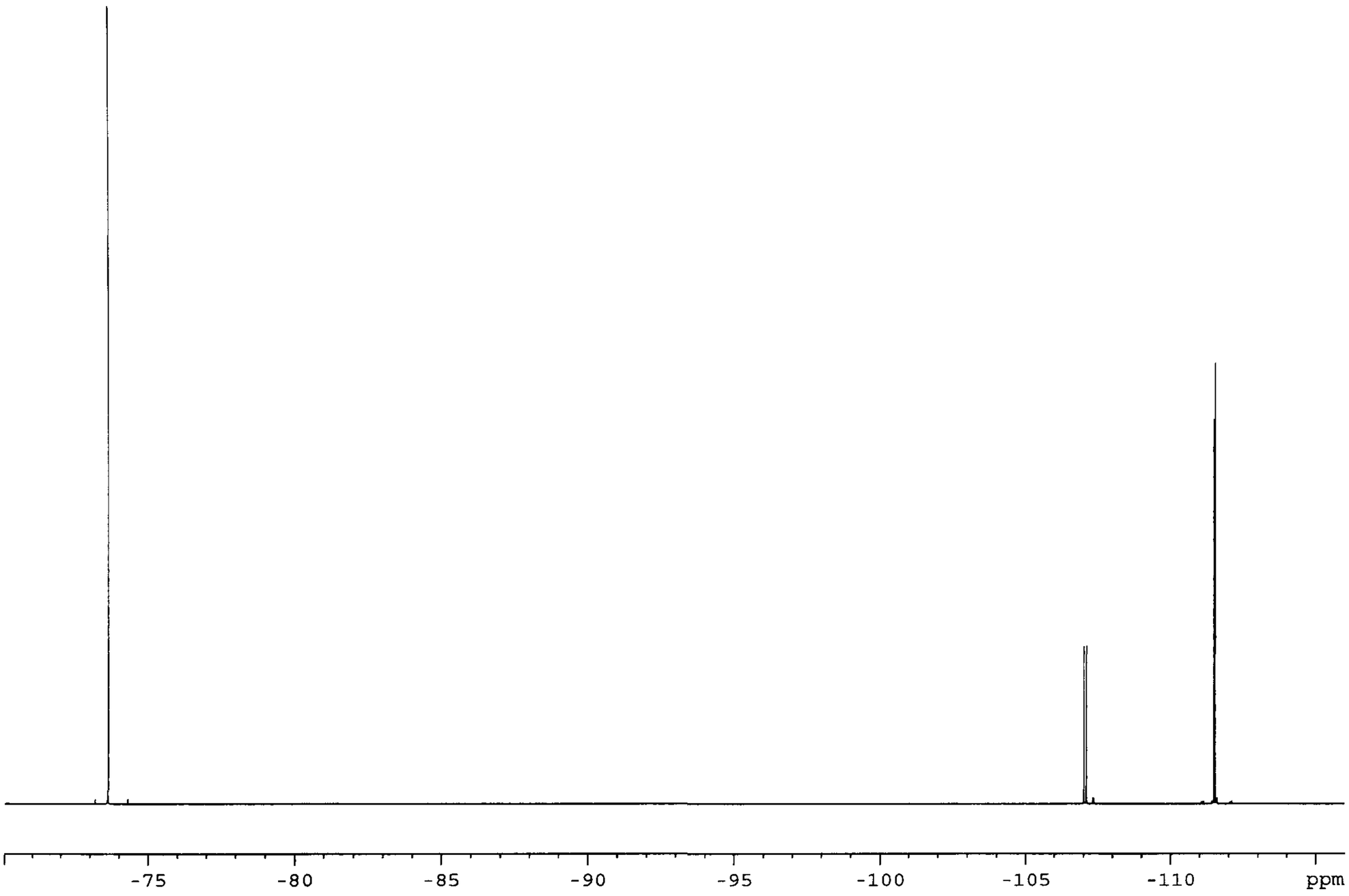

Figure 2.35. ^{19}F NMR of the crude reaction mixture obtained after fluorination of triflate **323**. The two doublets at -107 ppm and -112 ppm indicate the formation of fluorofumarate **325** and fluoromaleate **324** respectively. The singlet at -74 ppm denotes a trifluoromethyl group, which is indicative for the starting material **323**.

Integration of the ^{19}F NMR signals of the crude reaction mixture gave a ratio of 2:1 of fluoromaleate **324** to fluorofumarate **325**. Clearly, fluoride has acted as a base promoting elimination over substitution. The formation of the vinyl fluorides **324** and **325** is rather surprising, since deprotonation *geminal* to the fluorine leads to α-fluorocarbanions, which are destabilised by electronic effects (Scheme 1.2). On the other hand, the trifluorosulfonate

group is of much better leaving group ability than the fluoride ion and this appears to be the dominating factor rather than the acidity of the protons. Interestingly, not only the *anti*-elimination product fluoromaleate **324** was obtained, but also fluorofumarate **325**. This suggests that the lifetime of the carbanionic intermediate arising from deprotonation is long enough to allow for rotation around the central C-C bond. Rotational isomerism will result in formation of the two geometric isomers. The reaction most likely proceeds *via* a non-concerted E1cB mechanism (Scheme 2.89).

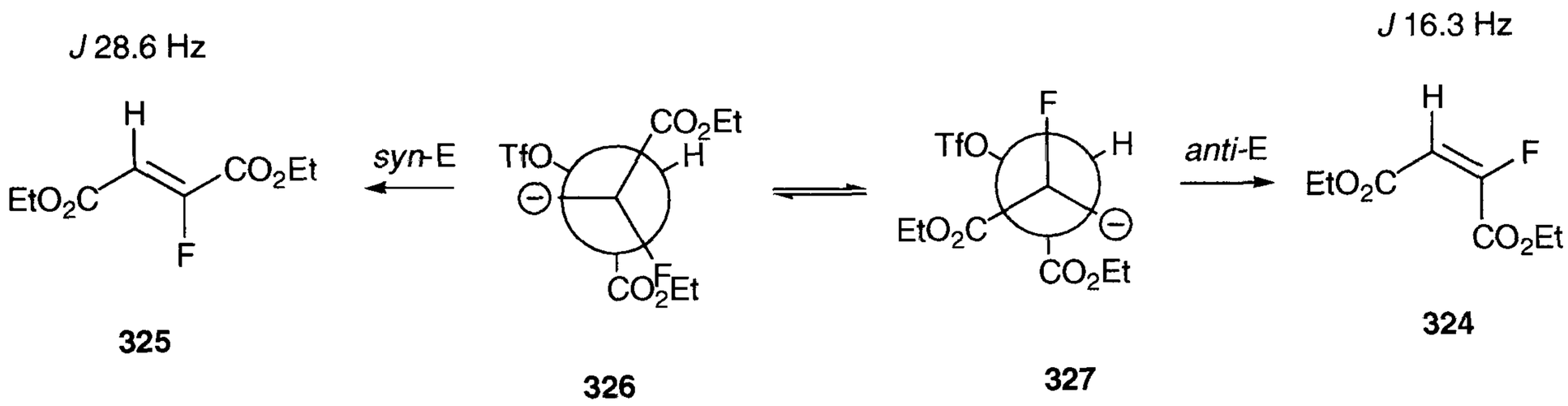

Scheme 2.89. Formation of vinyl fluorides **324** and **325** by elimination of the triflic acid from compound **323**.

The corresponding mesylate **328** was prepared in order to suppress elimination (Scheme 2.90). It was anticipated that the reduced leaving group ability of the mesyl group would provide more suitable conditions for an S_N2 reaction. Not surprisingly, elimination again dominated over substitution.

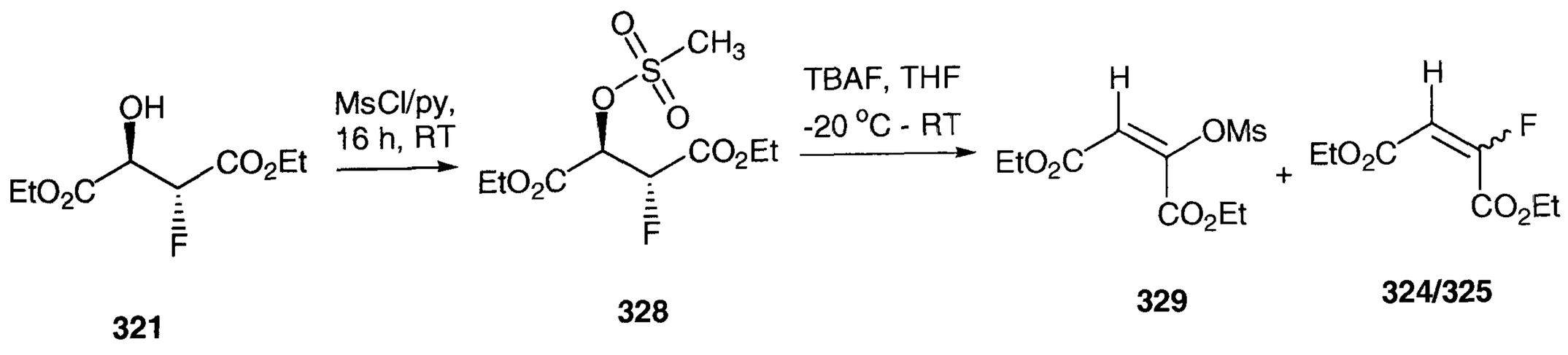

Scheme 2.90. Attemped fluorination of **328** after mesylation of the fluorohydrin **321** with mesyl chloride.

In addition to fluoromaleate **324** and fluorofumarate **325**, methanesulfonylenol **329** was identified as the main product by means of GC-MS and NMR spectroscopy. This compound formed as a result of HF loss from the mesylate **328**. Another attempt was made to prepare the *vicinal* difluoro compound **260** using tris(dimethylamino)sulfur (trimethylsilyl)difluoride (TASF). The reagent offers mild reaction conditions and good solubility in apolar organic solvents, providing a "semi-naked" fluoride ion under anhydrous conditions. The reagent has been mainly used for the fluorination of triflates,[46] but it has also been used effectively for the conversion of epoxides to fluorohydrins.[47] When TASF was reacted with triflate **323** at low temperature, diethyl fluorofumarate **325** and diethyl fluoromaleate **324** were obtained in a diasteromeric ratio of 1:3.

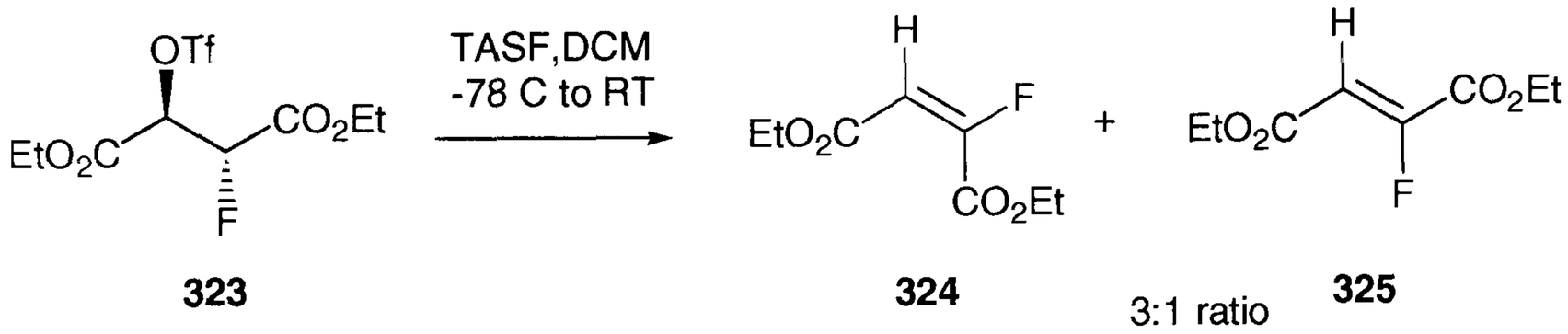

Scheme 2.91. Attempted fluorination of the triflate **323** with TASF $[(CH_3)_2N_3S^+ [(CH_3)_3SiF_2]^-$ (TASF).

Although this approach did not prove to be suitable for the generation of the desired *vicinal* difluoro compound **260** the vinyl fluorides **324** and **325** may be of interest in their own right. For instance, maleates and fumarates are known to be excellent substrates for cycloaddition reactions. Due to their electron deficient character, vinyl fluorides have been shown to be comparatively more reactive in these reactions.[48] Rearrangement reactions of vinyl fluorides, which involve the rehybridisation of fluorinated centres from sp^2 to sp^3 are generally strongly accelerated. This has recently been reported for the Claisen rearrangement of fluorinated cyclodecenones.[49]

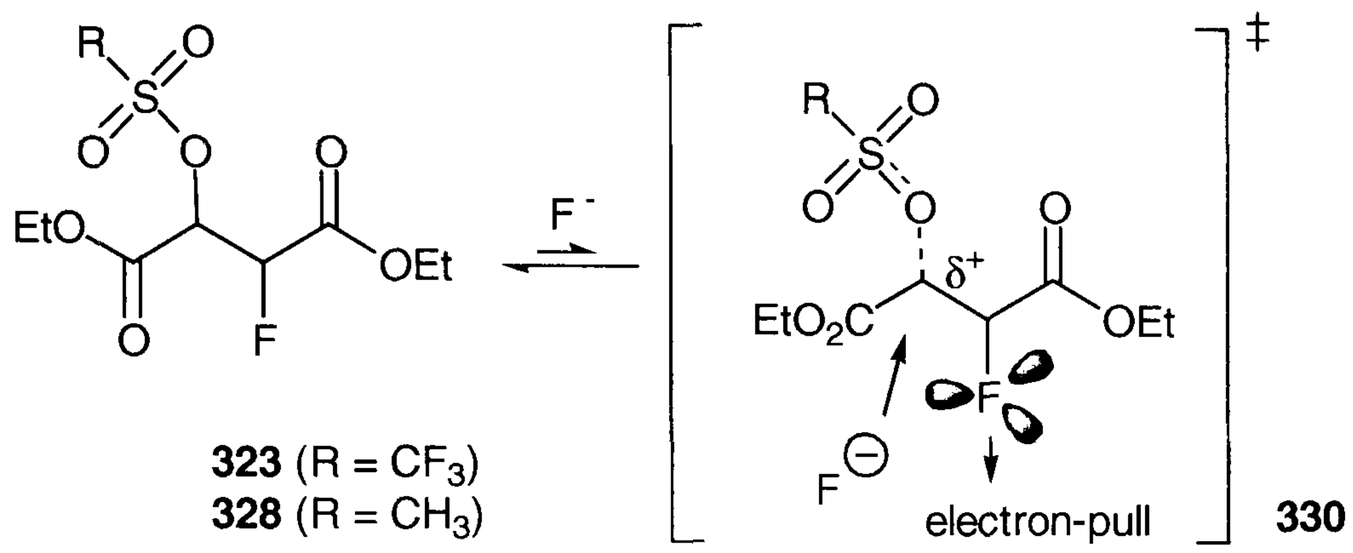

323 (R = CF_3)
328 (R = CH_3)

330

Scheme 2.92. Transition state for the nucleophilic substitution of the triflate **321** with fluoride ion.

The obvious difficulty to achieve a nucleophilic substitution at the carbon centre adjacent to the C-F bond of **321** may be rationalised in terms of electronic effects exerted by the neighbouring groups. The transition-state of the nucleophilic substitution, which is of considerable cationic character, may be difficult to establish due to the electron-deficient character of the adjacent C-F bond. The electron-deficient α-ester may reinforce this effect and also, the incoming nucleophile may experience significant electrostatic repulsion by the carbon-bonded fluorine (Scheme 2.92).

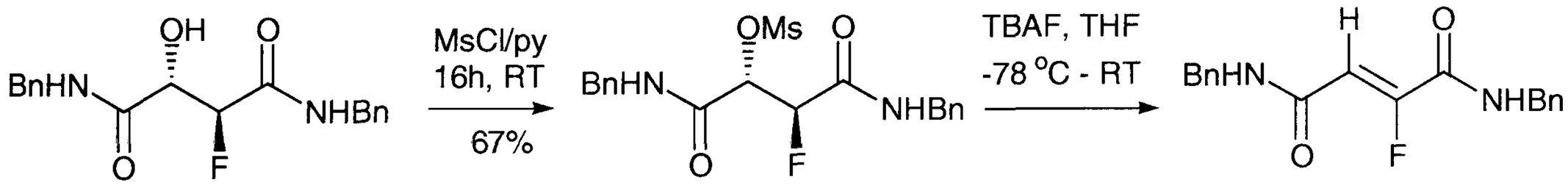

306 **332** **333**

Scheme 2.93. Attemped fluorination of the dibenzylamide **306** *via* its mesylate **332** using TBAF.

The diamide **306** was anticipated to be more amenable to fluorination due to the less electron-deficient nature of both carbonyl groups. The conversion of diamide **306** into its mesylate **332** was readily achieved with methanesulfonyl chloride. Treatment of the mesylate **332** with

TBAF however, again resulted in elimination of methanesulfonic acid to form dibenzyl fluorofumaramide **333** as the major product (Scheme 2.93).

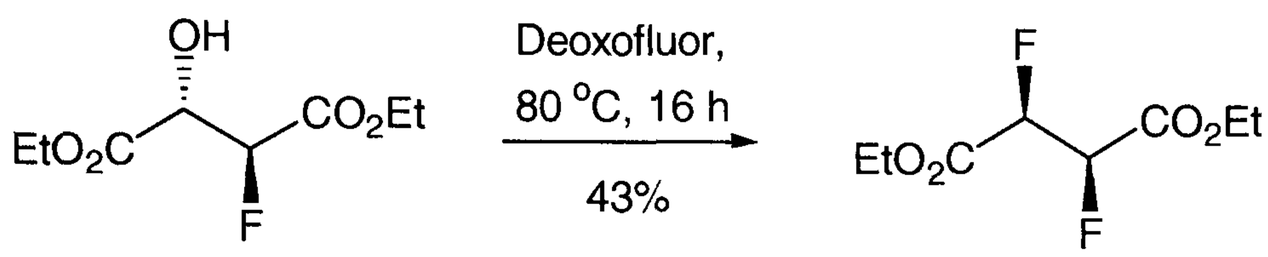

321 **260**

Scheme 2.94. Synthesis of diethyl 2,3-difluorosuccinate **260** after treatment of fluorohydrin **260** with Deoxo-fluor™ reagent at elevated temperatures.

The breakthrough in the synthesis of 2,3-difluorosuccinate was finally achieved by treating diethyl fluoromalate **321** with Deoxofluor™ (Scheme 2.94). Initially, the reaction was carried out at ambient temperature using dichloromethane as the solvent. Fast conversion of the starting material was observed by means of GC-MS, although the resulting intermediate compounds could not be identified. Deoxofluor™ **250** is structurally very similar to DAST **251** (Scheme 2.63), and it tolerates a wide range of functional groups such as ester and amide bonds, butoxycarbonyl and certain silyl protecting groups.[50] Although of quite similar reactivity to DAST, the reagent offers higher thermally stability and thus can be employed more safely at elevated temperatures and in large-scale applications.[51] For instance, the higher thermal stability of Deoxofluor™ has been used for the conversion of ketones and acylfluorides into difluoro and trifluoromethyl groups.[52, 53] The reagent appears to be particularly useful for the synthesis of *vicinal* difluoro compounds.[54] The synthesis of such compounds is difficult to achieve due to the deactivating effect of the adjacent carbon fluorine bond (Introduction).

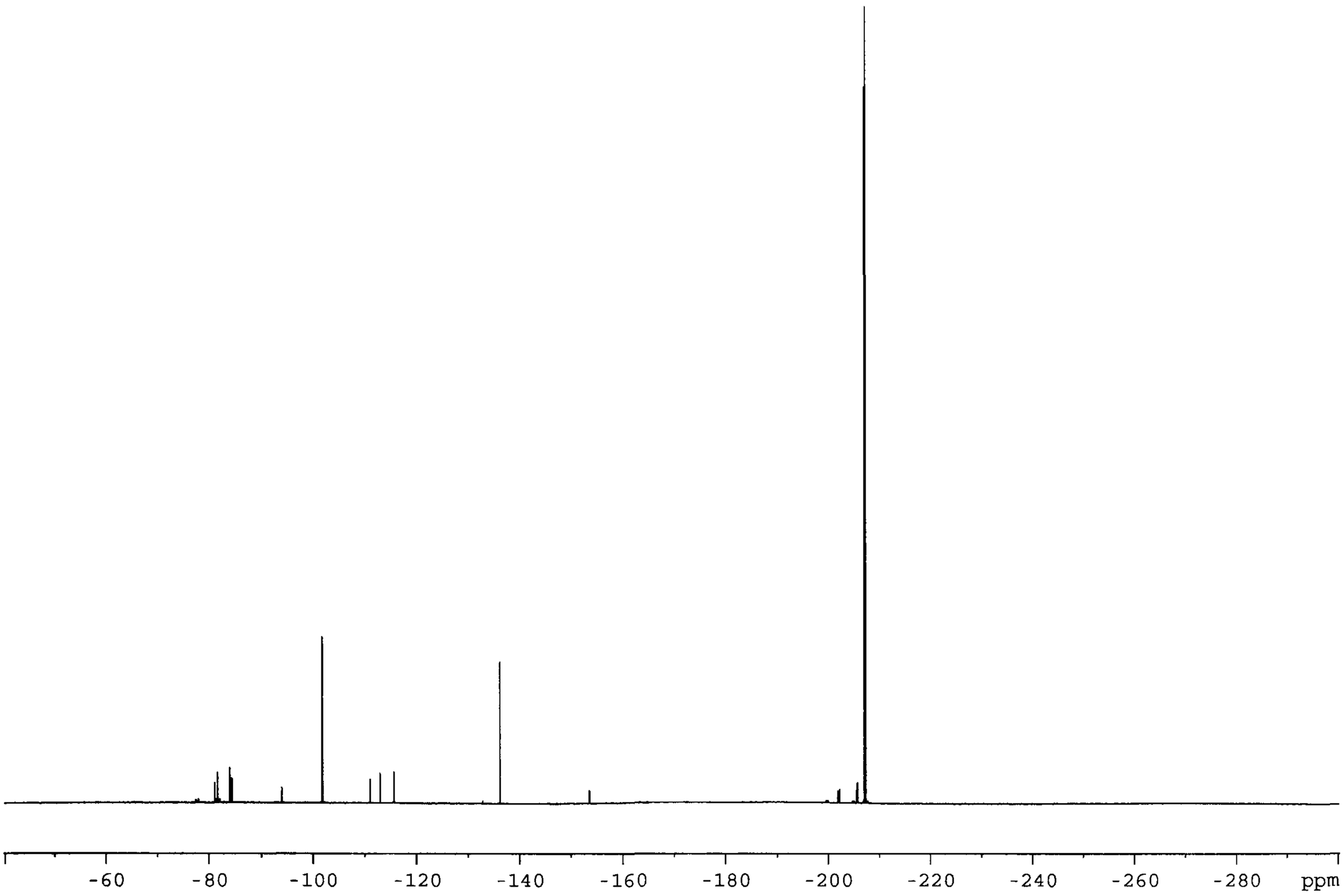

Figure 2.36. ^{19}F NMR spectrum of the crude product **260** after aqueous work up. The AA'XX' pattern at -207 indicates the presence of diethyl (*R,R*)-2,3-difluorosuccinate **260**, whereas the doublet at -106 ppm indicates the formation of diethyl fluorofumarate **325**.

The course of the reaction can conveniently be followed by ^{19}F NMR spectroscopy. Presumably, the addition of the reagent results in liberation of one molecular equivalent of hydrogen fluoride and formation of an alkoxysulfur intermediate, which gives similarly to the starting material rise to a doublet of doublet in the ^{19}F NMR spectrum. There are several different species apparent in the GC-MS and ^{19}F NMR spectrum that may arise from decomposition or dimerisation of the reagent. The spectrum considerably simplifies after acidic hydrolysis or basic wash during work up (Figure 2.36). Although the conversion of the hydroxyl group is fast, ^{19}F-NMR spectroscopy indicated formation of the AA'XX' pattern of **260** at –207 ppm only after prolonged heating using excess reagent. Consequently, the reaction was performed by heating fluorohydrin **321** in neat Deoxofluor™ which resulted in

complete conversion of the starting material after several hours. Remarkably, diethyl fluoromaleate **324** and diethyl fluorofumarate **325**, indicated by doublets at –100 ppm and -140 ppm respectively (Figure 2.36), are formed only in trace amounts. This indicates that Deoxofluor effectively suppresses elimination as a side reaction, presumably due to the slightly acidic nature of the reagent. Moreover, the absence of a similar AA'XX' signal at –202 for the *erythro* isomer **159** indicates that the reaction is entirely stereospecific. Since the *erythro* and *threo* diastereoisomers are separated in terms of their chemical shift by a surprisingly large 6 ppm, the relative configuration of the product can be unambiguously assigned to the *threo* isomer (Table 2.8).

Table 2.8. Chemical shifts of several *vicinal* difluoro compounds in dependence of relative stereochemistry.

Structure	**Chemical shift [ppm]**	
	erythro isomers	*threo* isomers
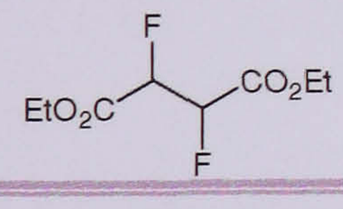	- 202.0	- 207.1
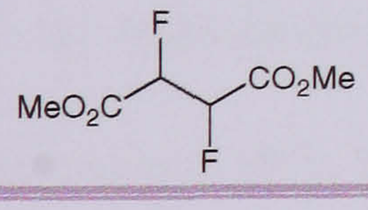	- 202.1	- 207.2
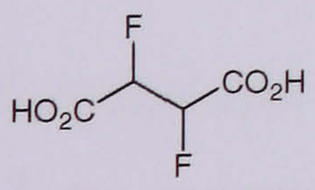	- 202.0	- 207.0
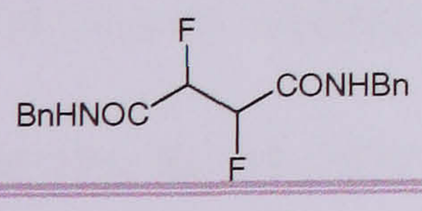	- 199.8	- 207.1
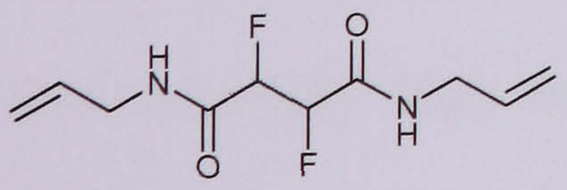	- 199.8	- 207.5
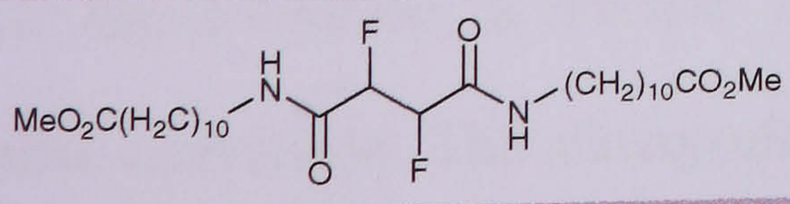	- 201.7	- 207.5

NMR and GC-MS data indicate that the conversion of the hydroxyl group of the fluorohydrin **321** results in the formation of a single stereoisomer **260**. This indicates clean inversion of configuration according to an S_N2 process, as it is typical for all trifluorosulfur alkylamine reagents.[55] Retention of configuration is generally only observed when neighbouring groups such as oxygen or nitrogen become involved in the reaction.[56]

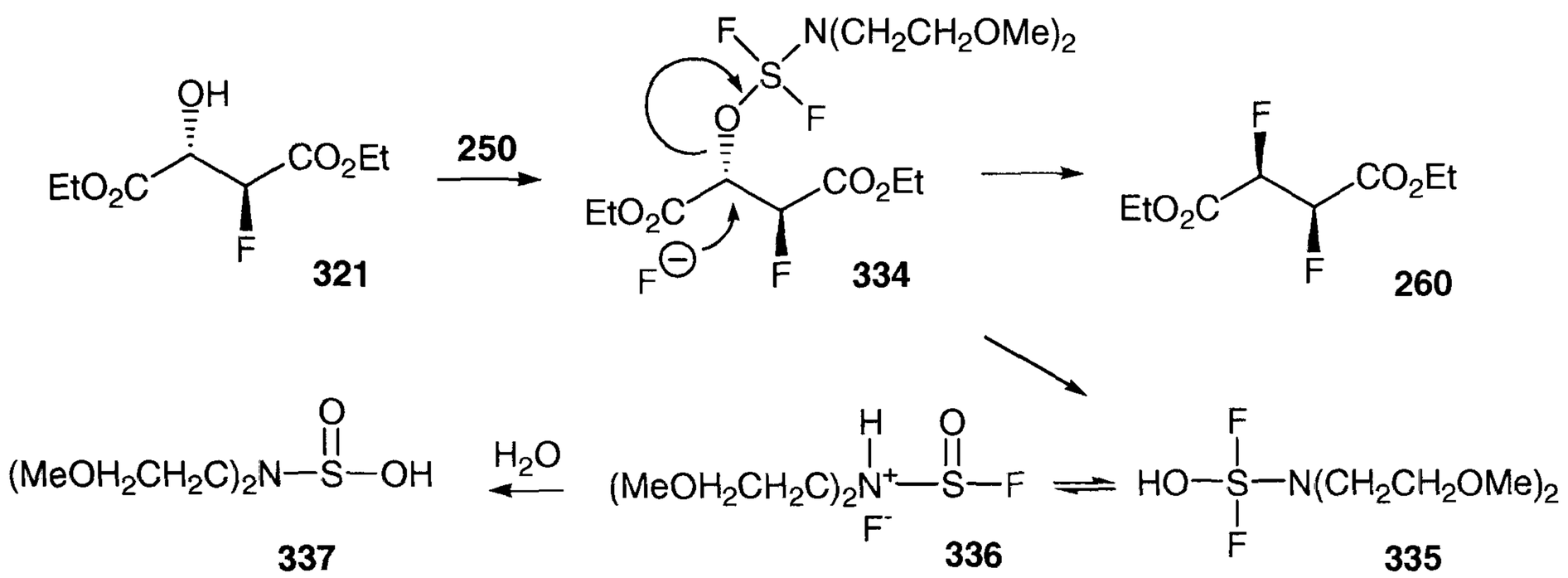

Scheme 2.95. Mechanism for the conversion of fluorohydrin **321** with Deoxo-Fluor™. The intermediate alkoxysulfur difluoride **334** undergoes nucleophilic substitution with fluoride ion resulting in clean inversion of configuration.

Formation of an intermediate alkoxysulfur difluoride **334** represents the first step in the mechanism (Scheme 2.95). This intermediate, which is stable enough to be isolated, has been confirmed by chemical and spectroscopic evidence.[57] The aminosulfurdifluoride **335** is a good nucleofug, which can undergo displacement by fluoride ion readily. In the intermediate **334**, the β-fluorine and the α-ester group clearly deactivate the nucleophilic centre against fluoride ion, and thus relatively high temperatures are necessary to facilitate this process. In the current transformation, a reaction temperature higher than 80 °C is essential to achieve complete conversion. The alkoxysulfur difluoro intermediate **334**, which is relatively easily formed by action of Deoxo-Fluor™ from fluorohydrin **321**, is stable at lower temperatures

and does not convert at appreciable reaction rate to the difluorinated product. The reaction was carried out in neat reagent, but higher boiling solvents such as toluene may also be employed successfully. Hydrogen fluoride, formed *in situ* by reaction of the alcohol **321** with the reagent is apparently complexed in the reaction mixture, as etching of the reaction vessel and condenser was not observed even at higher temperatures. The aminosulfurdifluoride **335** displaced in the process may be in equilibrium with the ammonium fluoride **336**, which is presumably basic enogh to complex liberated hydrogen fluoride. Such co-products are eventually quenched during work up with aqueous bicarbonate or dilute NaOH to form the sulfonic acid derivative **337**.

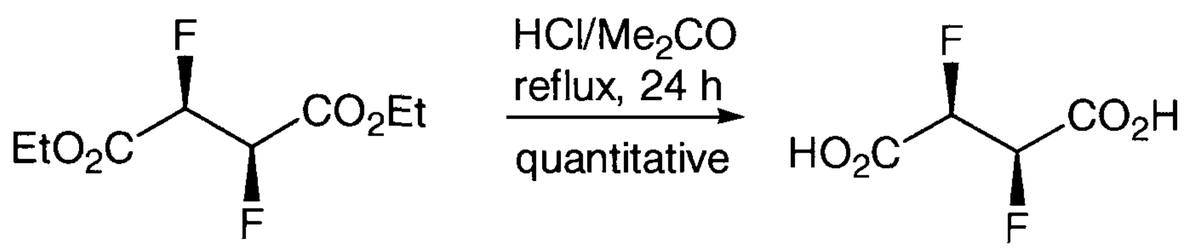

260 **338**

Scheme 2.96. Acidic hydroysis of diethyl 2,3-difluorosuccinate **260** using a mixture of aqueous HCl in acetone.

Diethyl 2,3-difluorosuccinate **260** is not stable towards basic conditions and was therefore hydrolysed with acid to yield the dicarboxylic acid **338** (Scheme 2.96). In contrast, hydrolysis of diethyl 2-fluoro-3-hydroxysuccinate was achieved under mild basic conditions using lithium hydroxide. The stability of the fluorohydrin **277** to base is remarkable but not unexpected, as diethyl 2-fluoro-3-hydroxysuccinamide **321** proved to be stable in the presence of primary amines at elevated temperatures (Scheme 2.81). Application of these conditions to diethyl 2,3-difluorosuccinate **260** resulted in rapid elimination of HF (Scheme 2.97).

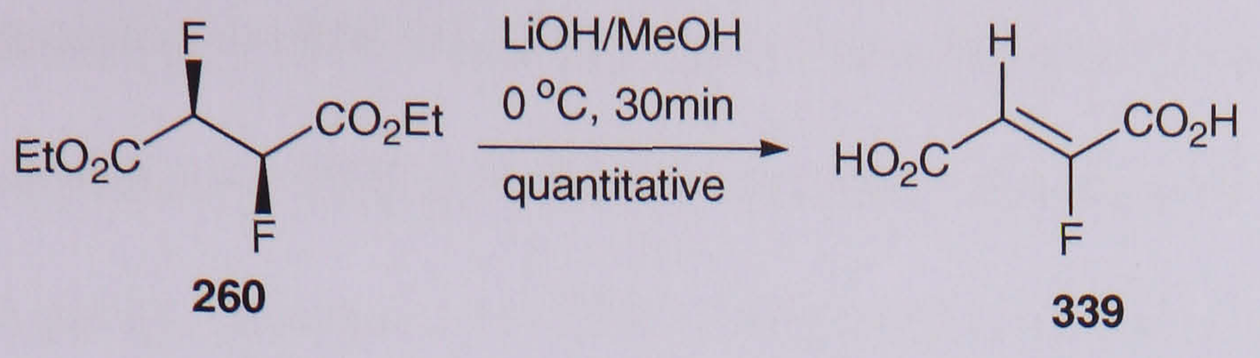

260 **339**

321 **340**

Scheme 2.97. Hydrolysis of diethyl 2-fluoro-3-hydroxusuccinate **321** proceeds under mild basic conditions.

Recrystallisation of 2-fluoro-3-hydroxysuccinic acid **340** also afforded crystals suitable for X-ray structure analysis. Interestingly, the hydroxyl group and the fluorine substituent align *gauche* with respect to each other (Figure 2.37).

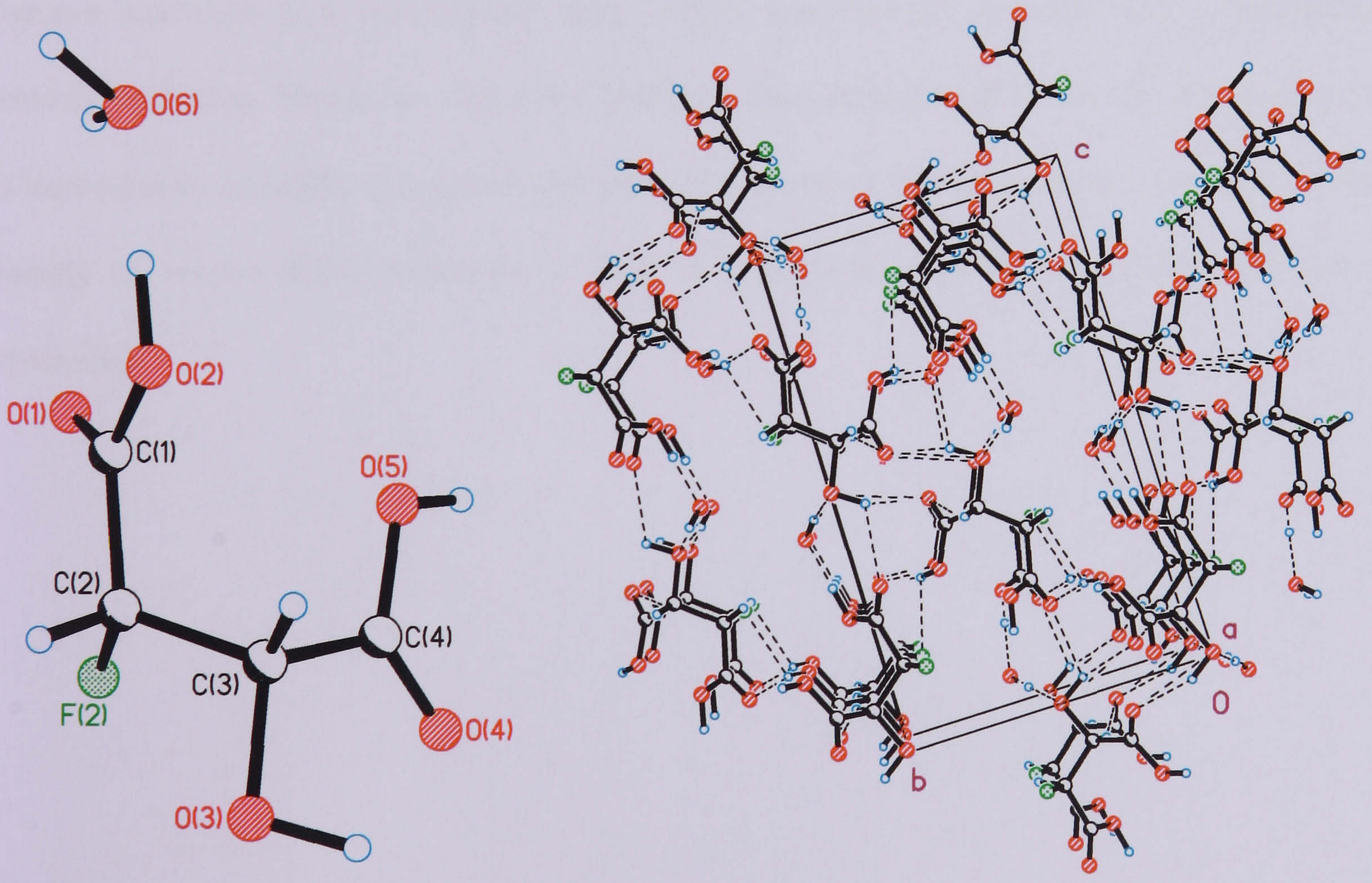

Figure 2.37. X-ray structure and crystal packing of (*2S,3R*)-2-fluoro-3-hydroxysuccinic acid **340**. Selected bond lengths (Å), bond and torsion angles (°): O1-C1 1.213(3), O2-C1 1.313(3), C1-C2 1.507(3), C2-F2 1.404(3), C2-C3 1.522(3), C3-O3 1.418(3), C3-C4 1.519(3), C4-O4 1.209(3), C4-O5 1.312(2), F2-C2-C1 108.18(17), F2-C2-C3 108.34(17), C1-C2-C3 115.08(18); O1-C1-C2-F2 10.9(3), O2-C1-C2-F2 -171.50(16), F2-C2-C3-O3 -65.6(2), F2-C2-C3-C4 55.3(2).

The solid state conformation of **340** resembles that of the difluoro compound **132** in that the two electronegative substituents align *gauche* to each other, and the C-F bond is *syn* planar to the adjacent carbonyl group (Scheme 2.13). The conformation of **340** is not unexpected and is also similar to the solid state structure of dibenzyl 2-fluoro-3-hydroxysuccinate **306** (Figure 2.33). The *gauche* arrangement of the fluorohydroxyl moiety appears to arise for fluorohydrins as well as for *vicinal* difluoro compounds. This behaviour is consistent with the generalised *gauche* effect and confirms experimentally the conformational preference predicted by *ab initio* calculations for fluoroalcohols (Introduction).

The formation of (*2S,3S*)-2,3-difluorosuccinic acid **338** offers a synthetic route which can be readily scaled and carried out with standard laboratory equipment. The synthesis allows for one-pot reactions and purification steps, which conveniently involve only crystallisation and/or distillation. Moreover, (*2R,3R*)-2,3-difluorosuccinate derived from (*2S,3S*)-tartaric acid is immediately available using this approach. The scope of this method may extend to a broad variety of *vicinal* difluoroalkanes, a class of compounds, which is generally difficult to synthesise.

References

[1] A.I. Burmakov, L. A. Motnyak, B. V. Kunshenko, L. A. Alexeeva and L. M. Yagupolskii, *J. Fluorine Chem.*, 1981, **19**, 151.

[2] J. A. Wilkinson, *Chem. Rev.*, 1992, **92**, 505.

[3] R. P. Singh, J. M. Shreeve, *Synthesis*, 2002, **17**, 2561.

[4] D. Seebach, *ChemBioChem*, 2004, **5**, 691.

[5] M. R. Kilbourn, National Academic Press, Washington DC, 1990.

[6] D. Seebach, E. Hungerbuehler: In *Modern Synthetic Methods*, Vol. 2, 1980, 131.

[7] For a review see: R. A. Johnson, K. B. Sharpless, In *Catalytic Asymmetric Synthesis*, New York, 1993, 103.

[8] E. N. Jacobsen, In *Catalytic Asymmetric Synthesis*, New York, 1993.

[9] V. A. Soloshonok, In *Enantiocontrolled Synthesis of Fluoro-organic compounds*, Wiley, Chichester, 1999.

[10] T. Hamatani, S. Matsubara, H. Matsuda, M. Schlosser, *Tetrahedron*, 1988, **44**, 2875.

[11] J. A. Wilkinson, *Chem. Rev.*, 1992, **92**, 505.

[12] M. Muehlbacher, C. D. Poulter, *J. Org. Chem.*, 1988, **53**, 1026.

[13] R. Skupin, G. Haufe, *J. Flourine Chem.*, 1998, **92**, 157.

[14] R. E. Parker, N. S. Isaacs, *Chem. Rev.*, 1959, **59**, 737.

[15] A. Ayi, M. Remli, R. Condom, R. Guedj, *J. Fluorine Chem.*, 1981, **17**, 565.

[16] O. Meth-Cohn, C. Moore, H. C. Taljaard, *J. Chem. Soc., Perkin Trans* 1, 1988, 2663.

[17] K. S. Kirshenbaum, K. B. Sharpless, *J. Org. Chem.*, 1985, **50**, 1979.

[18] D. H. G. Crout, V. S. B. Gaudet, K. O. Hallinan, *J. Chem. Soc., Perkin Trans 1*, 1993, 805.

[19] K. Mori, *Tetrahedron*, 1974, **30**, 4223.

[20] B. B. Lohray, *Synthesis,* 1992, 1035; H.-S. Byun, L. He, R. Bittman, *Tetrahedron,* 2000, **56**, 7051.

[21] E. T. Kaiser, M. Panar, F. H. Westheimer, *J. Am. Chem. Soc.*, 1963, **85**, 602.

[22] M. Nicoletti, *Novel Approach to Asymmetric Synthesis in Organic and Organo-fluorine Chemistry*, PhD thesis, 2004.

[23] Y. Gao, K. B. Sharpless, *J. Am. Chem. Soc.,* 1988, **110**, 7538.

[24] J. M. Holland, M. Lewis, A. Nelson, *J. Org. Chem.*, 2003, **68**, 747.

[25] R. W. Hoffmann, H. C. Stiasny, *Tetrahedron. Lett.*, 1995, **36**, 4595.

[26] C.S. Poorker, J. Kagan, *Tetrahedron Lett.*, 1985, **26**, 6405.

[27] A. Nishinaga, S. Wakabayashi, *Chem. Lett.*, 1978, 913.

[28] M. Nicoletti, D. O'Hagan, A. M. Z. Slawin, *J. Am. Chem. Soc.*, 2005, **127**, 482.

[29] Y. Gao, K. B. Sharpless, *J. Am. Chem. Soc.*, 1988, **110**, 7538.

[30] K. Tenza, *Synthetic Methodologies in Organofluorine Chemistry using Chiral Amines*, PhD Thesis, St Andrews University, 2004.

[31] M. Metz, T. Honda, *Liebigs Ann. Chem.*, 1993, 55.

[32] R. E. Banks, B. E. Smart, J. C. Tatlow, In *Organofluorine Chemistry: Principles and Commercial Applications,* Plenum Press, New York, 1994, 199.

[33] K. B. Sharpless, *Tetrahedron Lett.*, 1989, **30**, 655.

[34] M. Goren, *J. Org. Chem.*, 1973, **38**, 3510.

[35] K. K. Andersen, *Compr. Org. Chem.*, Vol. 3, 367.

[36] S. J. Brois, G. P. Beardsley, *Tetrahedron Lett.,* 1966, **42**, 5113; A. Galindo, L. O. F., D. Gnecco, R. G. Enriquez, R. A. Toscano, W. F. Reynolds, *Tetrahedron: Asymmetry*, **8**, 17, 2877; Y. Goa, K. B. Sharpless, *J. Am. Chem. Soc.*, 1988, **110**, 7538.

[37] Van Rheenen, D. Y. Cha, W. M. Hartley, *Org. Synth.,* 1978, **58**, 43.

[38] W. J. Middleton, K. C. Mange, *J. Fluorine Chem.*, 1989, **43**, 405.

[39] W. G. Night, j. H. J. Richards, *J. Am. Chem. Soc.*, 1969, **91**, 5847; M. A. Marletta, Y. Cheung, C. Walsh, *Biochemistry*, 1982, **21**, 2637.

[40] K. Mori, M. Ishikura, *Liebigs Ann. Chem.,* 1989, 1263; D. L. Hughes, *Org. Reactions*, 1992, **42**, 335.

[41] T. Hamatani, S. Matsubara, H. Matsuda, M. Schlosser, *Tetrahedron*, 1988, **44**, 2875.

[42] M. Schueler, *The synthesis of vicinal difluoro compounds*, First Year report, 2003

[43] D. O. Kiesewetter, J. A. Katzenellenbogen, M. R. Kilbourn, M. J. Welch, *J. Org. Chem.*, 1984, **49**, 4900.

[44] *For a review of fluorinating agents, see:* S. Rozen, R. Filler, *Tetrahedron*, 1985, **41**, 1111.

[45] M. A. Tius, J. K. Kawakami, *Tetrahedron,* **51**, 3997.

[46] Y. Tagaki, N. Kobayashi, M. S. Chang, G. Lim, T. Tsuchiya, *Carbohyd. Res.,* 1998, **307**, 217; W. A. Szarek, G. W. Hay, W. Dobroszewski, *J. Chem. Soc., Chem. Comm.,* 1985, 663; P. J. Card, W. D. Hitz, *J. Am. Chem. Soc.*, 1984, **106**, 5348.

[47] S. V. Ley, M. Parra, A. J. Redgrave, F. Sternfield, *Tetrahedron Lett.*, 1989, **30**, 3557.

[48] A. Arany, P. J. Crowley, J. Fawcett, M. B. Hursthouse, B. M. Kariuki, M. E. Light, A. C. Moralee, J. M. Percy, V. Salafia, *Org. Biomol. Chem.*, 2004, **4**, 455.

[49] G. DiMartino, M. B. Hursthouse, M. E. Light, J. M. Percy, N. S. Spencer, M. Tolley, *Org. Biomol. Chem.*, 2003, **24**, 4423.

[50] R. P. Singh, J. M. Shreeve, *Synthesis*, 2002, **17**, 2561.

[51] A. D. Becke, *J. Chem. Phys.* 1993, **98**, 1362.

[52] S. Lal, G. P. Pez, R. J. Pesaresi, F. M. Prozonic, H. Cheng, *J. Org. Chem.*, 1999, **64**, 7048.

[53] G. S. Lal, E. Lobach, A. Evans, *J. Org. Chem.*, 2000, **65**, 4830.

[54] R. P. Singh, J. M. Shreeve, *J. Fluorine Chem.*, 2002, **116**, 23.

[55] M. Hudlicky, *Org. Reactions*, 1988, **35**, 513.

[56] G. Resnati, *Tetrahedron*, 1993, **49**, 9385.

[57] P. L. Coe, L. D. Procter, J. A. Martin, W. A. Thomas, *J. Fluorine Chem.*, 1992, **58**, 87.

2.4 NMR and conformational analysis

X-ray structure analysis, although undoubtedly a powerful technique in which to explore the conformation of organic molecules, is naturally restricted to the solid state. Also, intermolecular hydrogen bonding and other crystal packing forces may affect the conformation of the individual molecules, making it difficult to establish conformational preferences unambiguously. In order to gain information about conformational equilibria in solution and in the gas phase, techniques based on nuclear magnetic resonance, rotational and infrared spectroscopy, measurement of dipole moments,[1] electron diffraction,[2] and *ab initio* calculations have been used. Among these techniques NMR analysis is certainly the most powerful tool, not only for structural elucidation, but also for conformational analysis of molecules in solution. In the course of this project, a method based on the angular dependence of NMR coupling constants was developed in order to establish conformational preferences for the *vicinal* difluoro compounds obtained (Chapter 2.1 and 2.2).

2.5.1 Coupling constants and conformational analysis

The angular dependence of the *vicinal* proton-proton coupling is a well-documented fact and led to the guidelines outlined by Karplus.[3] The Karplus equation is most conveniently illustrated in the form of a diagram showing that the $^{3}J_{HH}$ coupling constant is dependent on the dihedral angle of their coupled nuclei (Figure 2.38). Reliable values for the coupling constants can be obtained for compounds that have restricted conformational mobility or from compounds where individual rotational isomers are frozen out at low temperature.[4] For most acyclic compounds however the energy differences between the rotational isomers are too small and the freezing point of the solvents or lack of solubility can make this experiment difficult.

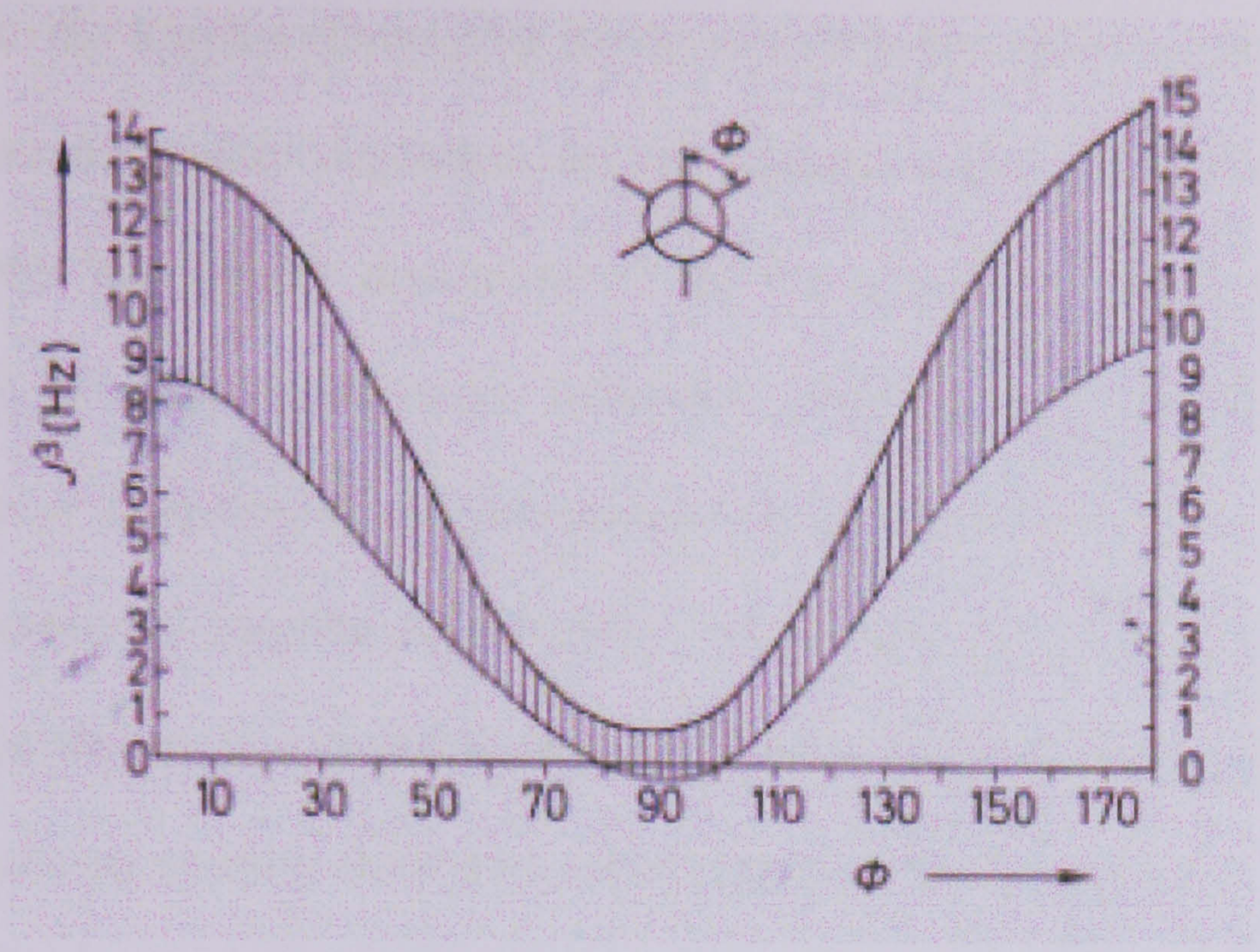

Figure 2.38. The angular dependence of *vicinal* J_{HH} couplings according to the Karplus equation.[5]

In aliphatic compounds, even at ambient temperatures fast rotation about the central C-C bond occurs. Any NMR coupling constant will therefore consist of an average value of the coupling constants for the individual rotational isomers (Scheme 2.103).[6] If the exact values for J_{trans} and J_{gauche} are known, the angular dependence of the coupling constants can be used to estimate conformational equilibria.[7] This is valid only if all other factors affecting the measured coupling are kept constant. Such factors include the chemical environment (e.g., neighbouring groups), bond angle, bond length, temperature, and the solvent. To a first approximation, these requirements are met when diastereoisomers are analysed and compared with each other. Accordingly, comparison of coupling constants obtained from the *threo* and *erythro* difluoro compounds was anticipated to yield information on the preferred conformation of these compounds in solution.

By analogy to the Karplus relationship for the *vicinal* proton-proton coupling, the $^3J_{HF}$ coupling constant is also dependent on the dihedral angle of the coupled nuclei (Scheme 2.39). This angular dependence of the $^3J_{HF}$ coupling is very large, and may conveniently be used to determine molecular conformation.[8] However, the $^3J_{HF}$ coupling is also dependent on the electronegativity of the substituents, exceeding that of the proton-proton coupling considerably.[9] As fluorine has a strong impact on the electronic distribution in a molecule, this factor has to be taken into consideration for the conformational analysis of fluorine containing organic compounds.

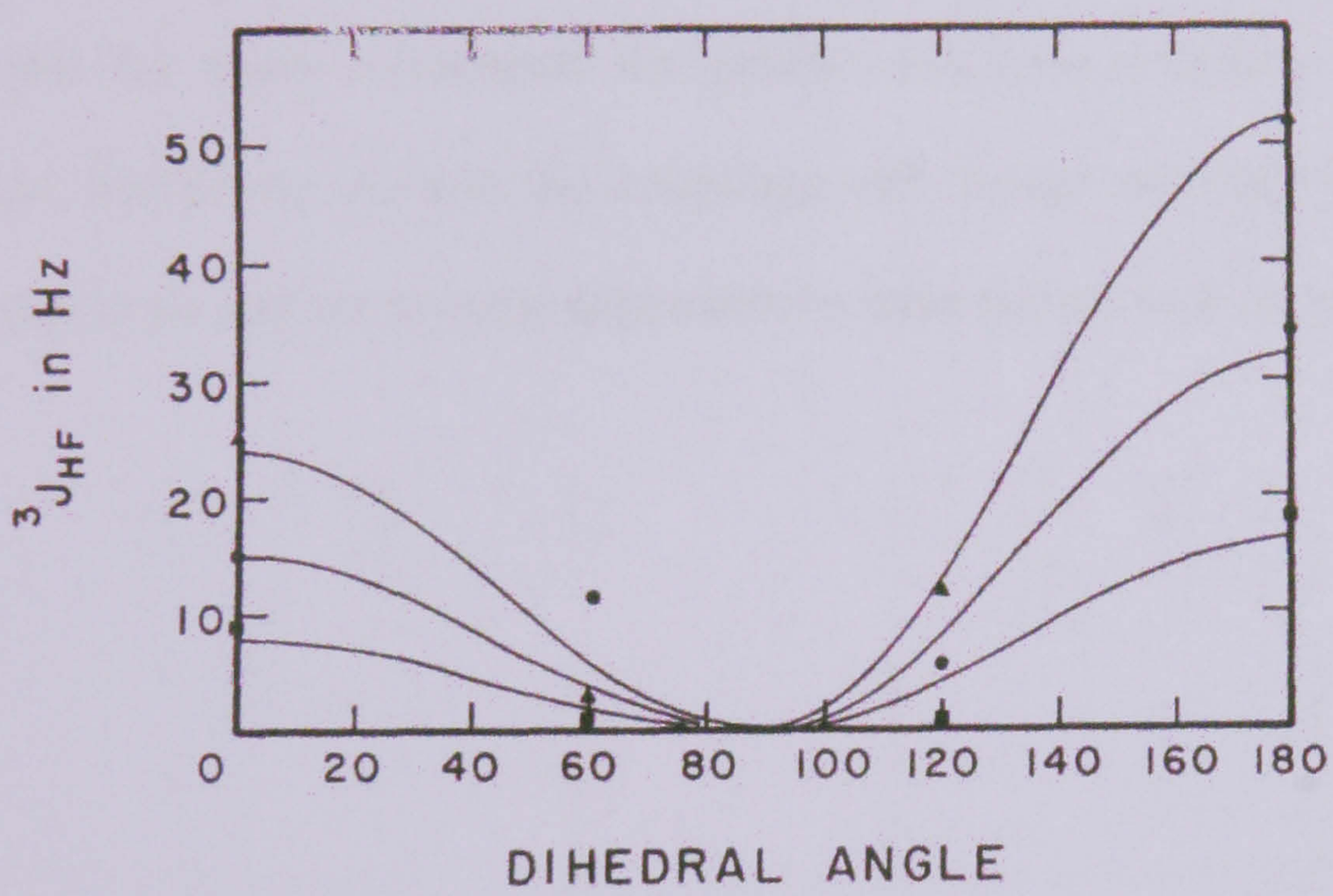

Figure 2.39. The angular dependence of the *vicinal* $^3J_{HF}$ coupling constant.[10] The three lines in the diagram represent $^3J_{HF}$ couplings obtained from compounds of different electronegativity Σ = 13.0, 11.0, 9.0 (bottom line to top).

The impact of substitution on the $^3J_{HF}$ coupling constant has been described in terms of the sum of the Huggins electronegativity Σ of the of the substituent directly attached to the coupled nuclei.[11] Figure 2.39 illustrates the angular dependence of three compounds with different Σ value. According to the Huggins electronegativities illustrated in Scheme 2.98,[12] all *vicinal* difluoro compounds synthesised fall into the middle curve of the diagram in Figure 2.39.

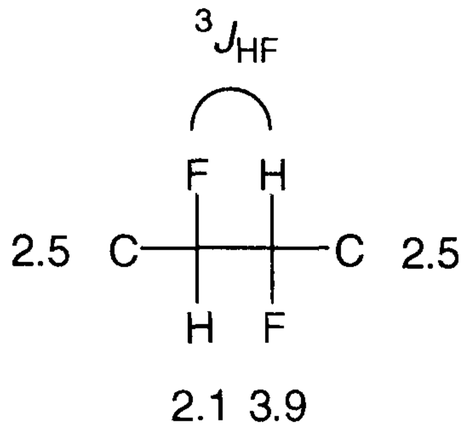

Scheme 2.98. Huggins electronegativities for the *vicinal* difluoro moiety. According to the model, all compounds derived from 2,3-difluorosuccinic acid have $\Sigma = 11.0$.

Any other nuclear coupling may in principle also be used to estimate the populations for the individual rotational isomers. However, the *geminal* $^2J_{HF}$ coupling is mainly dependent on the bond angle of the nuclei that couple and the *vicinal* $^3J_{FF}$ coupling is unique in that for many compounds the *gauche* and *trans* couplings may be of different sign. Moreover, $^3J_{FF}$ and $^2J_{HF}$ couplings will change only little with respect to the dihedral angle and are strongly dependant on other factors such as temperature.

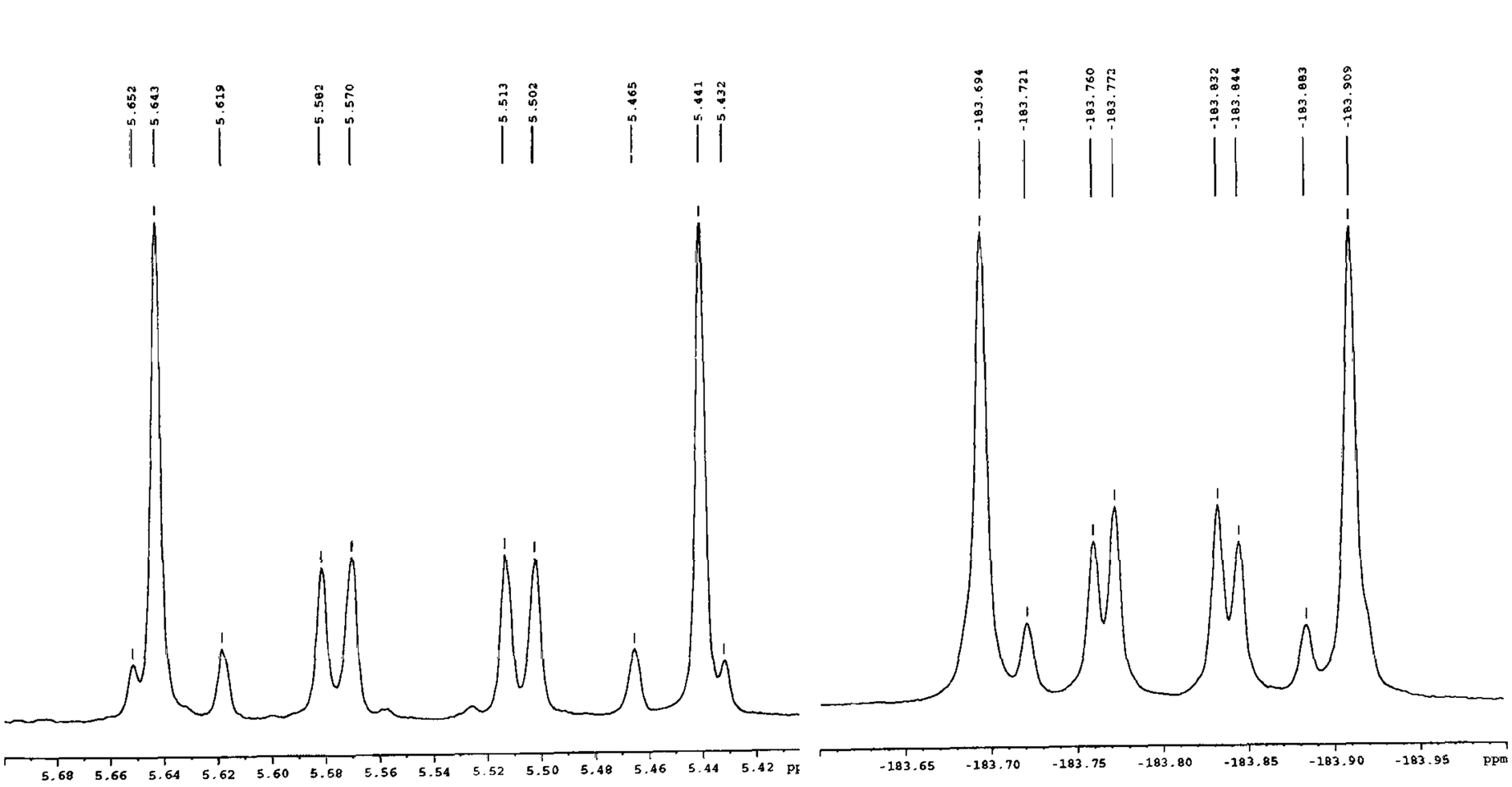

Figure 2.40. Expanded regions of the AA'XX' spin systems in the ^1H (left) and ^{19}F NMR spectrum (right) of *threo* 1,2-difluoro-1,2-biphenylethane **104**.

The conformational behaviour around the central C-C bond of 1,2-difluoro-1,2-diphenylethanes **103** and **104** was studied. The most obvious feature in the NMR spectra of both diastereoisomers is the complex coupling pattern of their ^1H and ^{19}F

NMR spectra (Figure 2.40). The signals are typical for all symmetrical *vicinal* difluoro compounds and represent a second-order spectrum from which the coupling constants cannot be extracted directly. Many types of compounds exibit AA'XX' spin systems (Scheme 2.99). These include 1,2-disubstituted ethanes **350** and their fluorinated analogues **351**, *ortho* and *para* disubstituted benzenes **354** and **355**, substituted furanes **353**, and certain heterocyclic structures such as **356** and **357**.

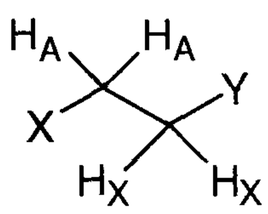

350

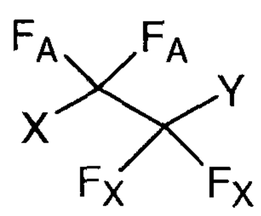

351

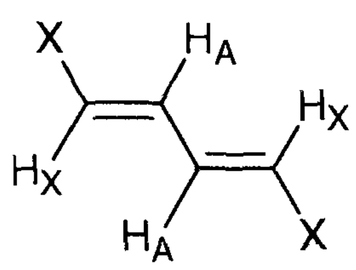

352

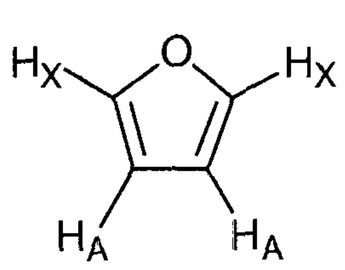

353

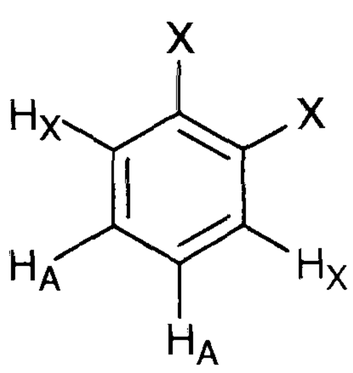

354

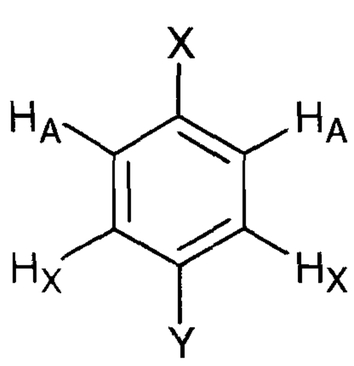

355

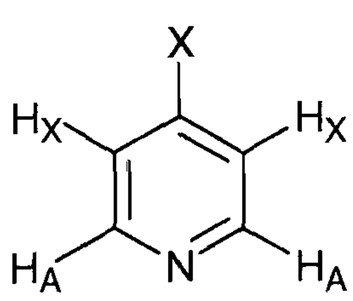

356

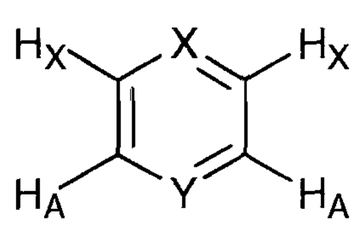

357

Scheme 2.99. Various classes of fluorinated compounds, which exhibit second-order NMR spectra.

The second-order spin pattern of 1,2-difluoro-1,2-biphenylethanes results from the coupling of the central proton and fluorine nuclei, which are chemically equivalent but magnetically non-equivalent. The chemically equivalence of the nuclei results from the similar chemical environment. The nuclei are however magnetically non-equivalent because they couple differently to each other, eg F_1 has a different coupling constant to H_1 and H_2 respectively (Scheme 2.100). There are in principle two *vicinal* HF couplings and two *geminal* HF couplings. Due to the symmetry plane of the molecules the $^3J_{HF}$ and $^2J_{HF}$ couplings are of the same value, and hence, four different coupling constants are obtained giving rise to an AA'XX' spin system

(Scheme 2.100). The NMR spectrum for the *vicinal* difluoro compounds consists of an A-part in the ^{1}H spectrum, and an X-part corresponding to the ^{19}F spectrum. The coupling patterns observed in either the A or X part are identical and the full set of coupling constants can thus be obtained from either part of the spectrum.

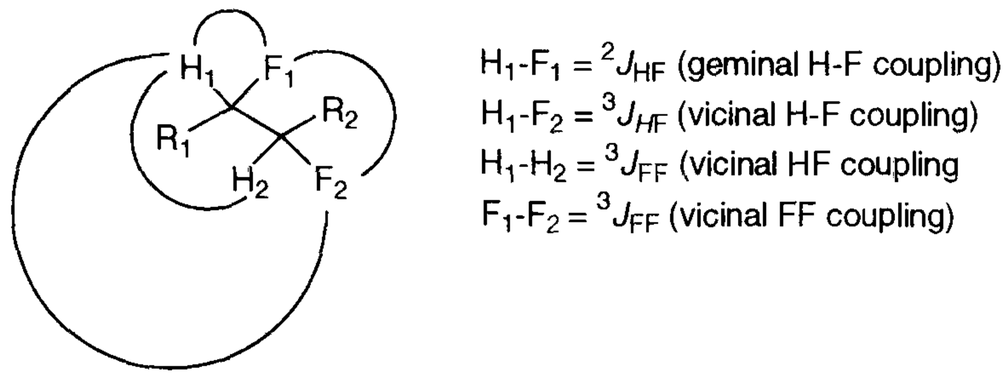

Scheme 2.100. The four individual coupling constants for the central ^{1}H and ^{19}F nuclei in 1,2-difluoro-1,2-diphenylethane **104**.

The first challenge on the way to investigate the conformational equilibria was to obtain $^{3}J_{HF}$ and $^{3}J_{HH}$ coupling constants of the *vicinal* difluoro compounds. The analysis of such spectra has been elucidated previously,[13] and software to calculate coupling constants and chemical shifts from such second order spectra are also available.[14] A precise and comprehensible method to calculate coupling constants from second-order spectra such as the AA'XX' spin systems has been given by Abrahams *et. al.*[15] Ten lines are observed in each part of the spectrum, e.g. 20 lines in all (Figure 2.40). The signals arise from the 24 transitions of the nuclear spin wave functions for the four nuclei involved. The transitions 1 & 2 and 3 & 4 coalesce and each part of the spectrum consists of only 10 lines which are completely symmetrical about the mid- points ν_A and ν_X. The intense lines of transitions 1,2 and 3,4 have each a quarter of the total intensity. Furthermore, two AB-type quartets of a quarter of the total intensity arise from transitions 5, 6, 7, 8 and 9, 10, 11, 12 respectively (Figure 2.41).

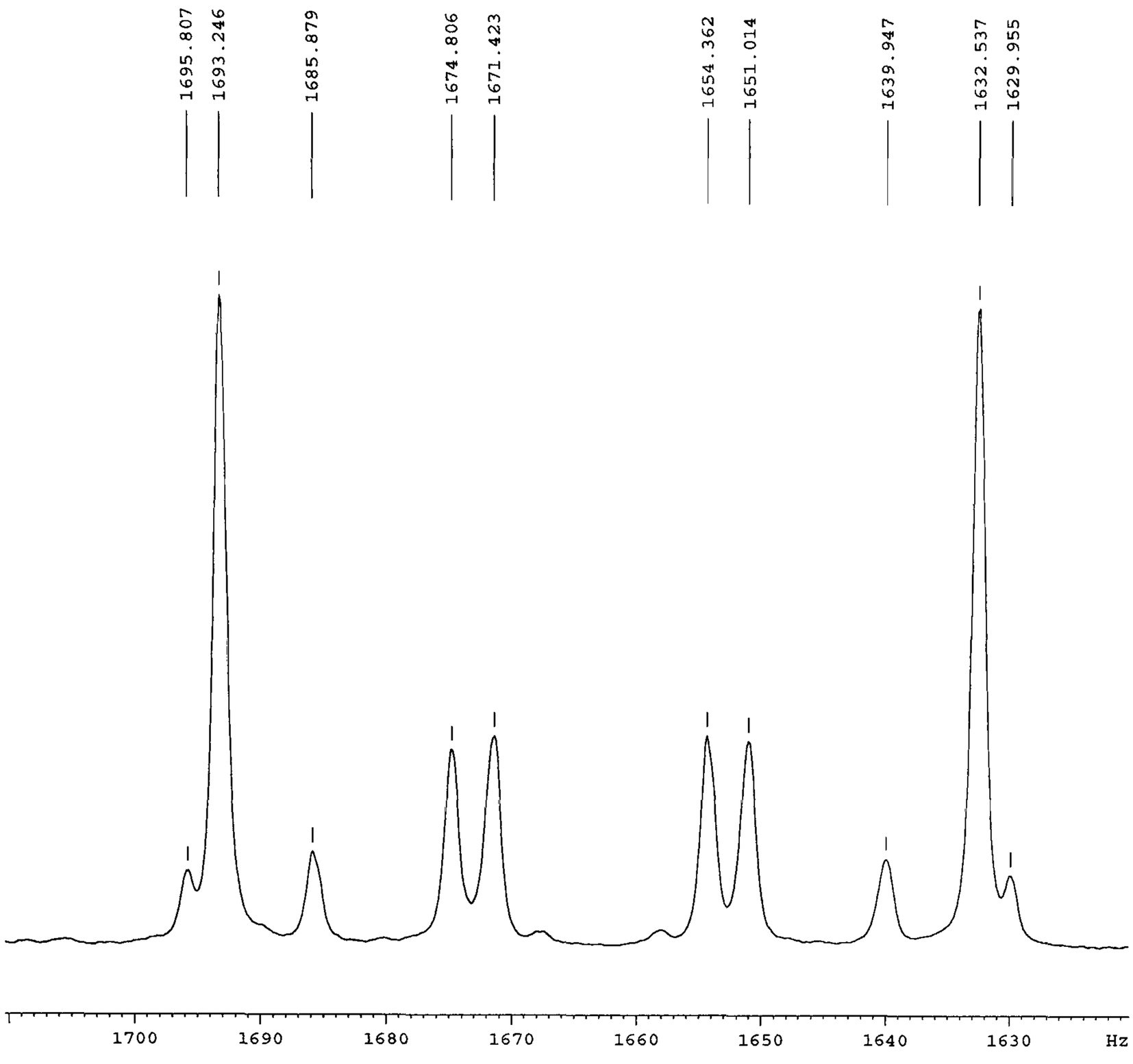

Figure 2.41. Expanded region of the AA'XX' spin system of *threo* 1,2-difluoro-1,2-diphenylethane **104** showing the ten lines necessary for calculation of the $^3J_{HF}$, $^3J_{HH}$, $^2J_{HF}$, and $^3J_{FF}$ coupling constants.

For the calculation of the four coupling constants from these spectra it is convenient to define the new quantities K, L, M, N according to Abrahams *et al.*.[16] These parameters are interconnected with the coupling constants $^3J_{HH}$, $^3J_{HF}$, $^2J_{HH}$, $^3J_{HF}$ according to simple mathematical algorithms (Scheme 2.101).

$K = J_A + J_B$

$M = J_A - J_B$

$N = J + J'$

$L = J - J'$

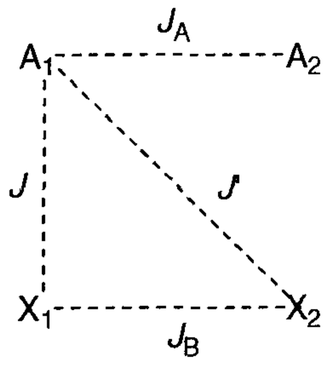

Scheme 2.101. Assignment of the resonances obtained for the AA' part of *threo* 1,2-difluorobiphenylethane **104**.

In order to calculate the parameters K, L, M, N it is necessary to identify the two intense lines and the two AB-type quartets. These lines have to be assigned according as the 12 aforementioned transitions. The assignment of transitions 1, 2, 3 and 4 is unambiguous and refers to the two intense lines at the left and the right end of the spectrum. For the assignment of the two AB-type quartets, each quartet is of the same intensity, thus the most and the least intense lines belong to one of the quartets, the four remaining lines to the other one. The assignment is illustrated for *threo* 1,2-biphenylethane **104** in Table 2.9.

Table 2.9. Chemical shifts and assignment of transition in the AA' part of compound **104**.

Transition	Frequency
5	1695.807
1,2	1693.246
9	1685.879
10	1674.806
6	1671.423
7	1654.362
11	1651.014
12	1639.947
3,4	1632.537
8	1629.955

The parameters K, L, M, and N can be calculated according to the rules given by Abrahams (Equation 2.1). It is important to note that the calculations are neutral to the sign of any of the parameters K or M. Thus, the values for K and M can be interchanged without consequence. This is not possible for the parameters L and N. Using the equations which define the parameters K, L, M, and N, the coupling constants J_A, J_B, J, and J' can be obtained immediately (Table 2.10).

Equations 2.1. The parameters K, L, M, N can be obtained from simple mathematical algorithms based on the chemical shift of the individual transitions.

$$N = \nu(1,2) - \nu(3,4)$$
$$K = \nu(5) - \nu(6) = \nu(7) - \nu(8)$$
$$M = \nu(9) - \nu(10) = \nu(11) - \nu(12)$$
$$L = \sqrt{\nu(6) - \nu(7) \times \nu(5) - \nu(8)} = \sqrt{\nu(9) - \nu(12) \times \nu(10) - \nu(11)}$$

Table 2.10. Calculated parameters N, K, M, L and the resulting coupling constants for *threo* 1,2-difluoro-1,2-diphenylethane **104** determined from the resonances listed in Table 5.1.

N	60.71	J_A ($^3J_{FF}$)	-17.7 Hz
K	24.40	J_B ($^3J_{HH}$)	6.7 Hz
M	11.07	J ($^2J_{HF}$)	47.1 Hz
L	33.52	J' ($^3J_{HF}$)	13.6 Hz

The specific assignment of the coupling constants obtained can be made by rational considerations. The large value of 47.1 Hz clearly refers to a *geminal* $^2J_{HF}$ coupling, and thus the value of 13.6 Hz is the *vicinal* $^3J_{HF}$ coupling. The small coupling constant of 6.7 Hz most appropriately refers to the $^3J_{HH}$ coupling, and the value of 17.7 Hz can be assigned for the *vicinal* $^3J_{FF}$ coupling. From the $^3J_{FF}$ coupling constants in related compounds, it can be concluded that the sign of this coupling is negative,[17] and all other coupling constants are positive in sign. The XX' part of the ^{19}F NMR spectrum can be assigned similarly to the AA' part of the ^{1}H NMR spectrum. The multiplet of 1,2-difluorobiphenylethane **103** resolves into 8 lines only as the outer lines for the transitions 5 and 8 disappear under the intense lines of 1,2 and 3,4. Increasing the concentration of the field strength (500 MHz) did not improve the resolution, and thus, the coupling constants given for *threo* 1,2-difluoro-1,2-diphenylethane are solely based on its ^{1}H NMR spectrum.

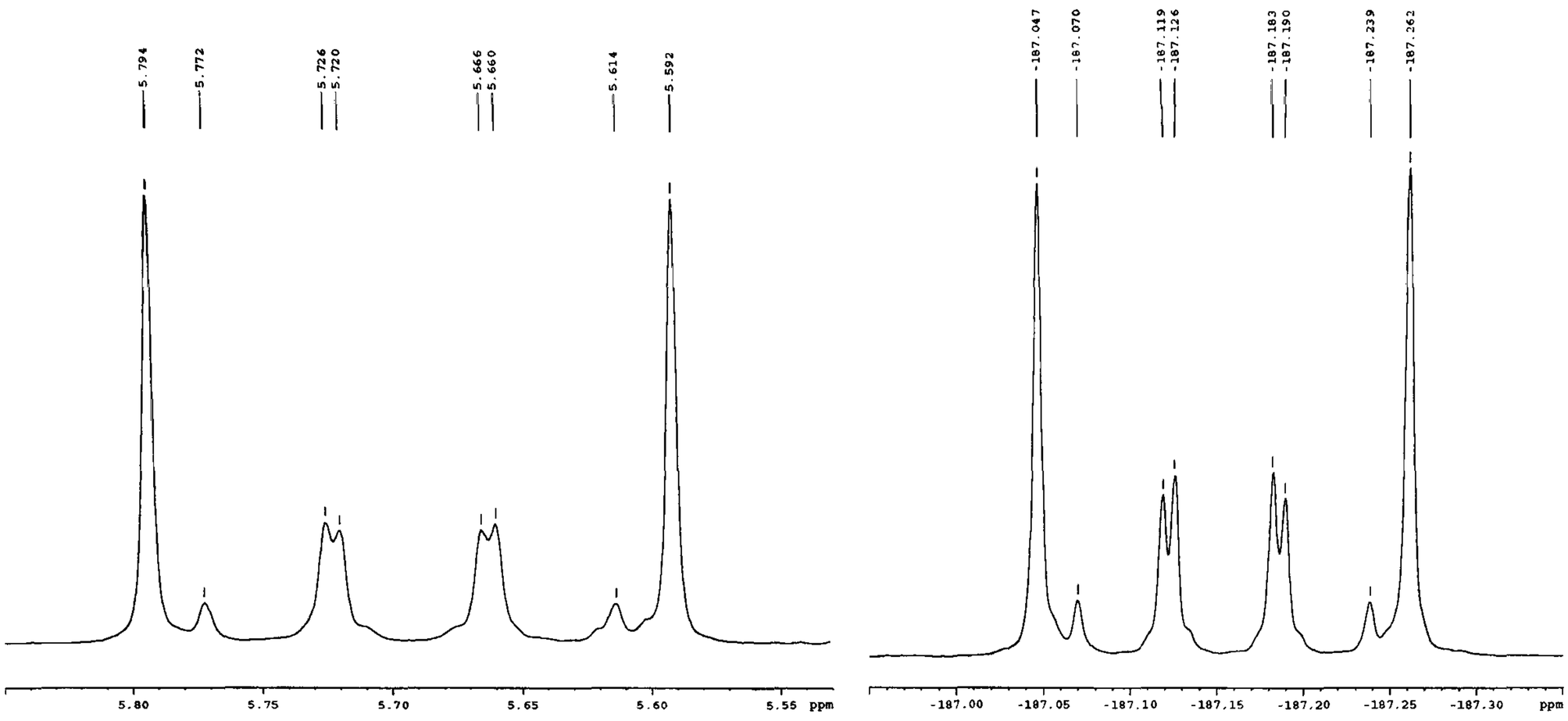

Figure 2.42. Expanded regions of the AA'XX' spin systems in the ^{1}H (left) and ^{19}F NMR spectrum (right) of *erythro* 1,2-difluoro-1,2-biphenylethane **103**.

In cases where transitions 5 and 8 are not observed in both the ^{1}H and the ^{19}F NMR spectrum, analysis of the coupling constants is compromised. This was the case for *erythro* 1,2-difluoro-1,2-biphenylethane **103** (Figure 2.42). Transitions 5 and 8 may be overlaid by the intense lines of transitions 1,2 and 3,4 or, the absence of these line may simply be a consequence of poor resolution. In order to estimate the position of all lines in the AA'XX' system, a NMR prediction program based on an EXCEL spreadsheet was developed. Incorporation of the equations 2.1 allows for the automated calculation of the coupling constants $^{2}J_{HF}$, $^{3}J_{HF}$, $^{3}J_{HH}$, and $^{3}J_{FF}$ simply by listing the measured NMR resonance's into the Excel table. This considerably simplified otherwise time-consuming manual calculations, and offered the possibility of visualising the ^{19}F and ^{1}H NMR spectrum in the form of a diagram (Figure 2.43).

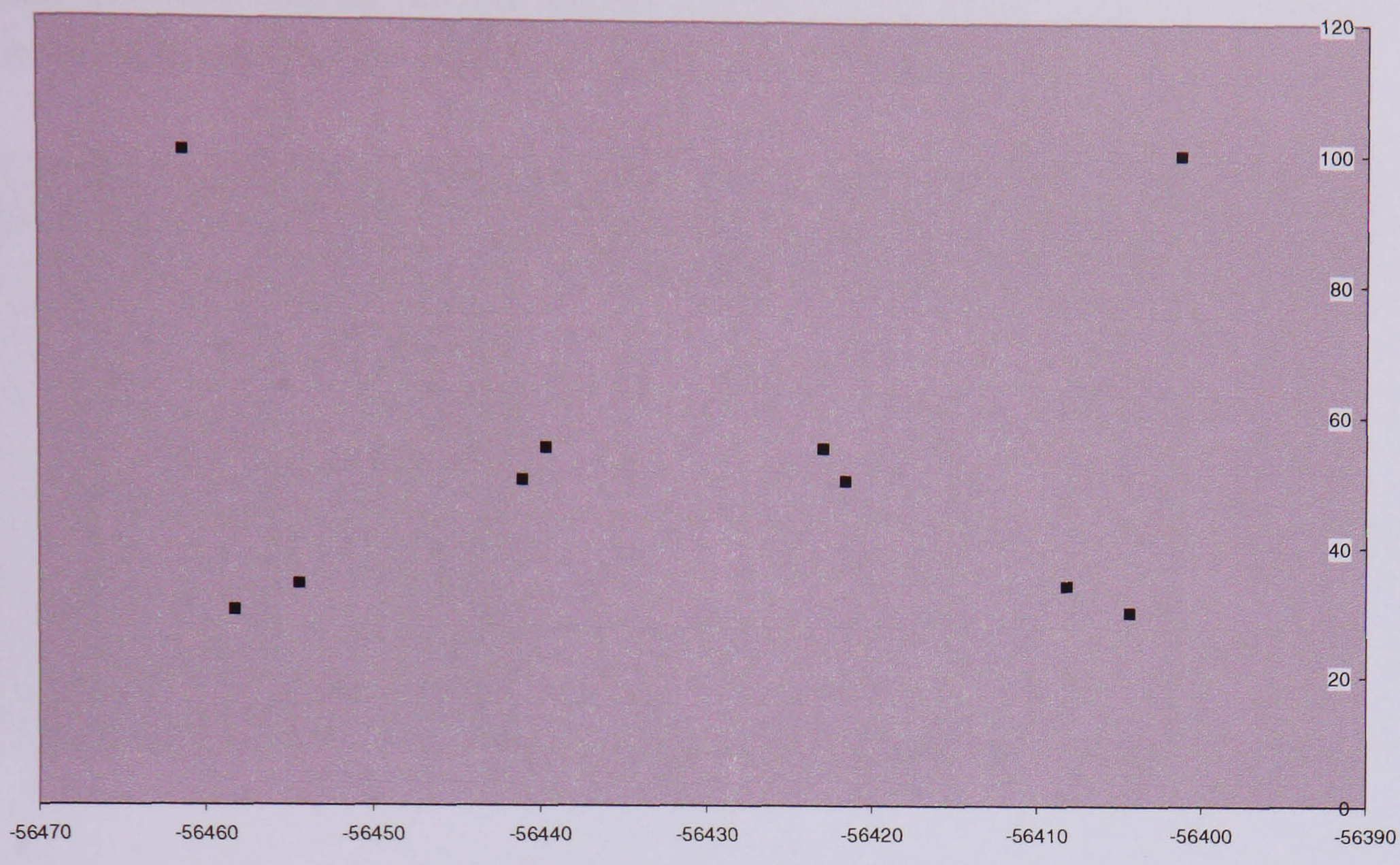

Figure 2.43. EXCEL diagram showing the calculated positions of the 10 lines for the X part of the AA'XX' system of *erythro* 1,2-difluoro-1,2-diphenylethane **103** in a virtual ^{19}F NMR spectrum.

The appearance of the NMR pattern of **103** is calculated for a set of coupling constants 45 Hz, 15 Hz, -16 Hz, and 2.6 Hz respectively (Scheme 2.43). The peak tops are illustrated by a dot which indicate the transitions 1(2), 5, 9, 10, 6, 7, 11, 12, 8, 3(4) from the left to the right. The diagram impressively illustrates that the lines of lowest intensity (5 and 8) for **103** will come into close proximity to the lines of highest intensity (1,2 and 3,4). This apparently causes these signals to coalesce, so that only 8 lines are observed in both ^{1}H and ^{19}F NMR spectra. The coupling constants for *erythro* 1,2-difluoro-1,2-diphenylethane **103** thus obtained were later confirmed and processed by LAOCOON III analysis of the spectra (Table 2.11).[18] The LAOCOON analysis was performed in Professor Abrahams laboratory for several *vicinal* difluoro compounds, which allowed for comparison of the calculated coupling constants (Chapter 6.3).

Table 2.11. NMR coupling constants obtained from the EXCEL calculation of **103** and **104** and LAOCOON III analysis of the spectra kindly supplied by Professor Abrahams of Liverpool University.

Stereoisomer	Coupling constant	$^3J_{HH}$	$^3J_{HF}$	$^3J_{FF}$	$^2J_{HF}$
threo	Calculated	6.7	13.6	-17.7	47.1
	Laocoon III	6.0	14.1	-17.3	47.2
erythro	Calculated	3.0	15.0	-16.0	45.0
	Laocoon III	2.5	15.2	-16.5	45.2

The *vicinal* $^3J_{HF}$ and the *vicinal* $^3J_{HF}$ coupling constant observed for the stereoisomers **103** and **104** were compared. The *vicinal* $^3J_{HF}$ coupling constants are approximately of the same value for both compounds. However, the observed *vicinal* $^3J_{HH}$ coupling constants are significantly different. This can be rationalised in terms of rotational isomerism. As mentioned previously, the observed coupling constants will be an average over the individual rotational isomers of the molecule. Due to the high energy of the eclipsed rotamers, only the three staggered conformations are usually considered. For *erythro* and *threo* 1,2-difluoro-1,2-biphenylethane **103** and **104** the ground state conformations are illustrated in Scheme 2.102.

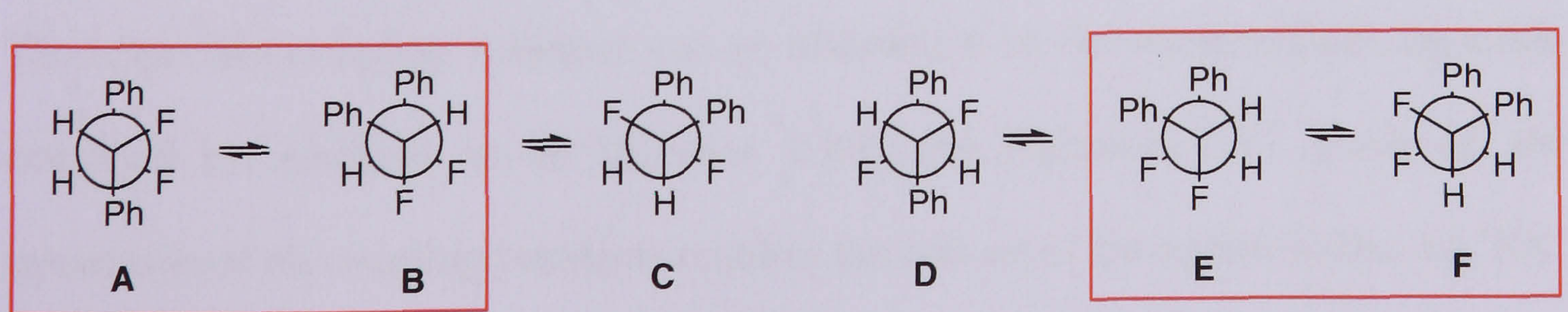

Scheme 2.102. Ground state rotational isomers of *threo* (left) and *erythro* (right) 1,2-difluoro-1,2-diphenylethane **103** and **104** and preferred solution state conformations (boxed).

The relatively high $^3J_{HH}$ coupling constant for the *threo* compound **104** suggests a significant population of the rotational isomer **B**, which has the C-H bonds *anti* to each other. Interestingly, this also is the preferred conformation for this compound in the solid state (Figure 2.8). For the *erythro* isomer, we can infer a higher population for the rotamers with the C-H bonds *gauche* on the basis of a much smaller $^3J_{HH}$ value (Scheme 2.102). Remarkably, the $^3J_{HF}$ coupling constants of the *threo* isomer **104** is of approximately the same order to that of the *erythro* isomer **103**. This may be explained by a significant contribution of rotamer **A**, which compensates the low value of $^3J_{HF}$ for rotamer **B** of the *threo* isomer. From these considerations it is apparent that the rotamers having their *vicinal* C-F bonds *gauche* to each other (boxed structures) are highly preferred over the structures, where the C-F bonds are *anti*. These findings are perhaps surprising, as rotamers **A** and **D** appear to be structures causing the least steric and electrostatic clash, but they do not dominate the rotational equilibrium of **103** and **104**. It can be concluded that factors other than steric effects determine the conformation of these molecules in solution, and the "g*auche* effect" may offer a reasonable explanation for these experimental results.

The NMR spectra of symmetrical derivatives of 2,3-difluorosuccinic acid show a similar AA'XX' spin pattern for the central fluorine and proton nuclei (Figure 2.44). The respective coupling constants can be obtained from the mathematical algorithm described by Abraham *et al.* (Scheme 2.101 and Equations 2.1). However, the calculation of all coupling constants requires the full set of ten signals in the AA'XX' system. This condition is problematic in most cases, as the lines of low intensity often merge with lines of higher intensity or entirely disappear in the signal to noise background (Figure 2.42). The intensity of the inner lines as well as their chemical

shift difference varies inherently with the coupling constants of the molecule, and therefore such effects can occur independently from the resolution of the NMR instrument.

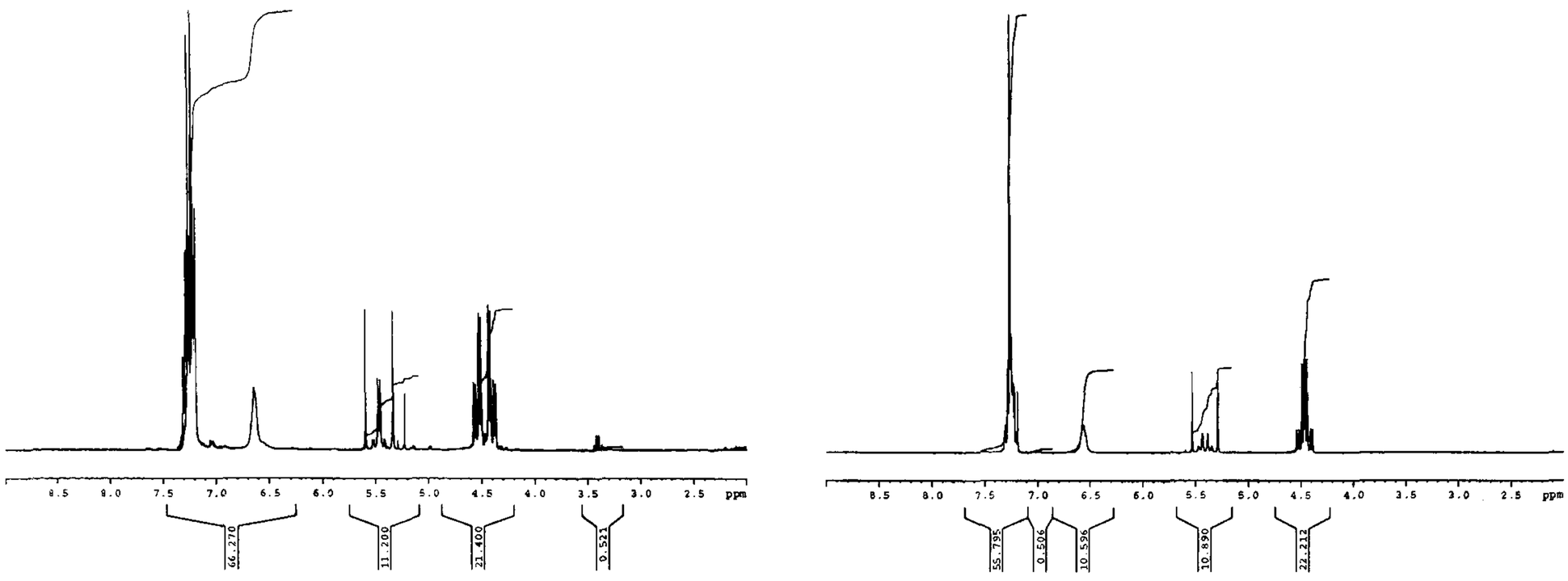

Figure 2.44. ^{1}H NMR spectra of *threo* (left) and *erythro* (right) *N,N*-dibenzyl-2,3-difluorosuccinamide **161** and **162**. The spectra show the ^{1}H AA'XX' spin pattern for the C2 and the C3 protons at 5.0-5.5 ppm.

In order to obviate these problems the software package PERCH was evaluated for calculation of the AA'XX' part of the NMR spectrum. The full version of PERCH features an option, which can be used to assess the individual lines by an integration mode. This allows the coupling constants to be obtained even in cases with eight or still fewer signals in the NMR spectrum. The idealised case of an AA'XX' pattern has 10 defined lines, which in fact comprise of twelve individual signals arising from the nuclear spin wave function of the four coupled nuclei. Thereby transitions 1 and 2 as well as 3 and 4 are equal and thus appear as a single line each.[19] NMR spectra featuring the full set of ten lines are analysed most accurately using the peak-top-fitting option (Figure 2.45). It is also possible to combine the integration analysis with the peak-top-fitting; this however does not give more accurate data in every case. The

errors of the PERCH analysis are automatically given by the program and can be used to estimate the accuracy of the coupling constants thus obtained.

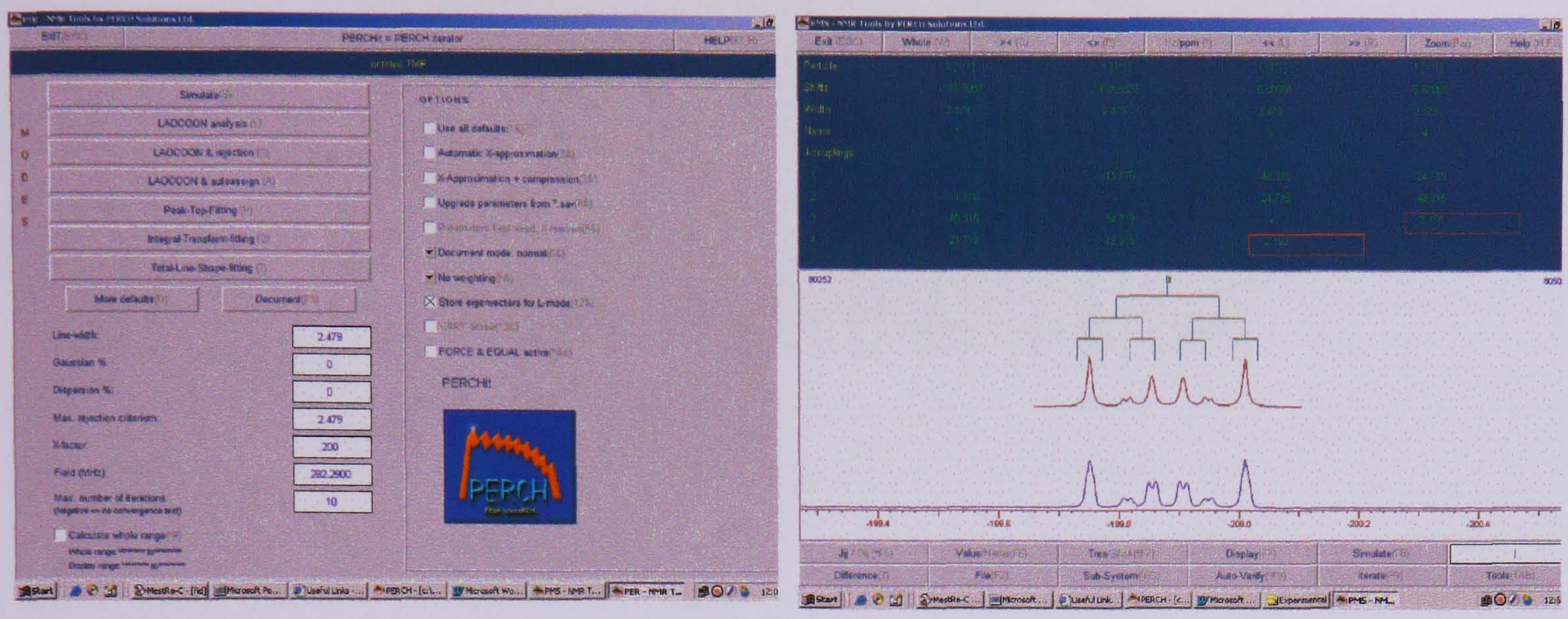

Figure 2.45. The calculation modes of PERCH (left). Reasonable values for the coupling constants have to be estimated prior to calculation for convergence of the calculation (right). The coupling constants and chemical shifts are fitted such that the parent (bottom spectrum) and the calculated resonances (above) match as closely as possible.

The coupling constants of various derivatives of 2,3-difluorosuccinic acid were determined using the PERCH program, and then compared (Figure 2.46). Interestingly, the $^{3}J_{HF}$ coupling constants are very similar to each other within each diastereoisomeric series, essentially independent of the nature of the substituents attached to the carboxylate group. The only exception to this trend is the set of 1,2-difluoro-1,2-diphenylethanes **103** and **104**, the analysis of which has been described in the previous paragraph. Clear differences in terms of the $^{3}J_{HF}$ coupling constants exist for the series of *erythro* and *threo* diastereoisomers. The *threo* compounds generally have much higher values for the *vicinal* proton-fluorine coupling constants compared to the *erythro* compounds. This is the case for all of the 2,3-difluorosuccinic acid derivatives and even extends to the more complex pseudopeptide structures.

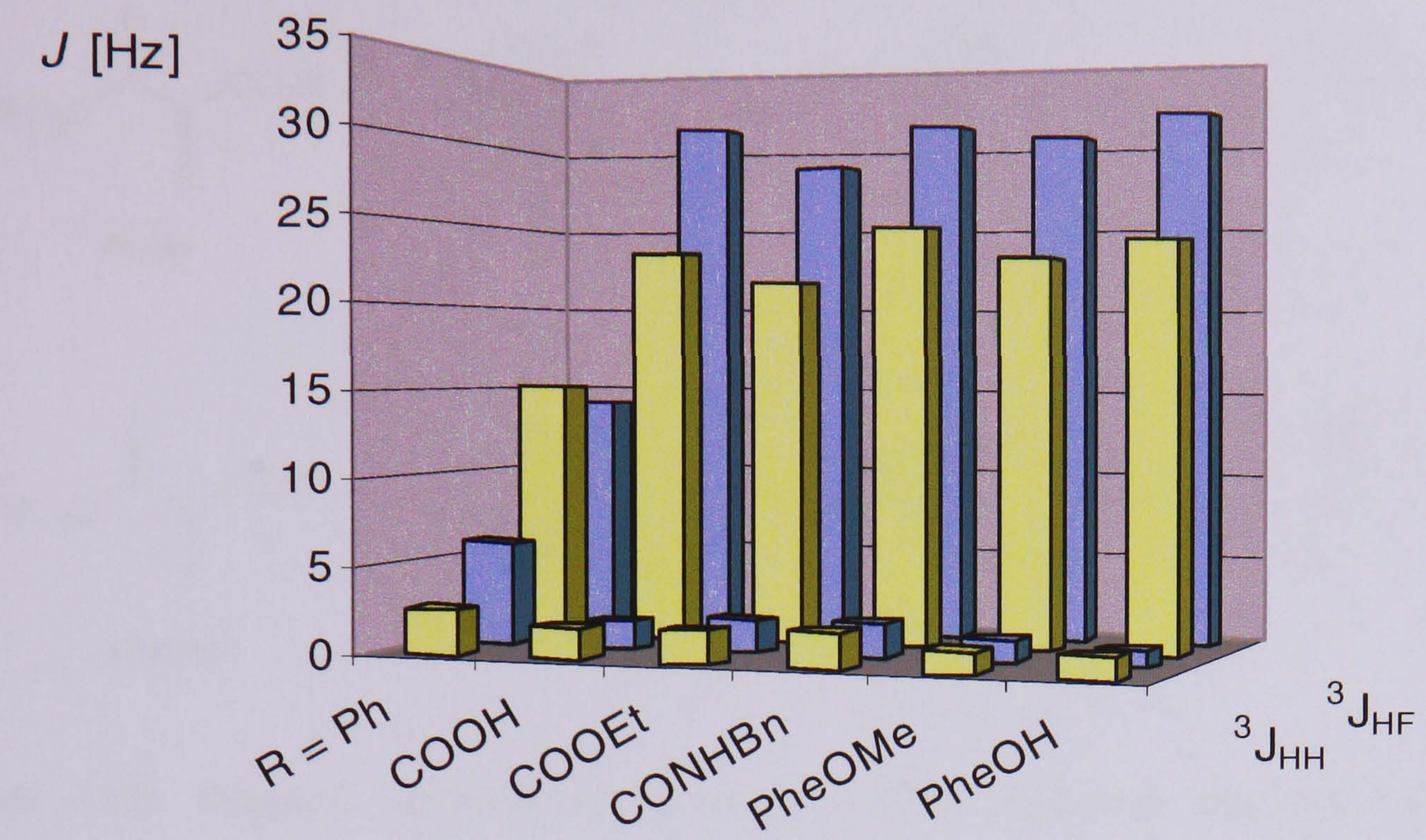

Figure 2.46. *Vicinal* H-F and H-H coupling constants of *erythro* (yellow) and *threo* (blue) diasteroisomers derived from 2,3-difluorosuccinic acid. The NMR spectra were recorded in $CDCl_3$ with the exception of 2,3-difluorosuccinic acids, which were measured in CD_3CN. All coupling constants were determined using the software PERCH.

The similarity of the $^3J_{HF}$ values within the diastereomeric series is noticeable and the difference between *threo* and *erythro* series gives reason to consider the conformational equilibria in these systems (Scheme 2.103). In order to understand the data in Figure 2.46, it is necessary to consider the staggered conformations of the diastereoisomers. Each rotational isomer has two *vicinal* H-F couplings, which can be *trans* or *gauche* in geometry. These two *vicinal* H-F couplings will then combine with the respective couplings of all other rotational isomers. Each rotational isomer may be differently populated and the combination of all three weighted by their population will give rise to the observed coupling constant J_{obs}.

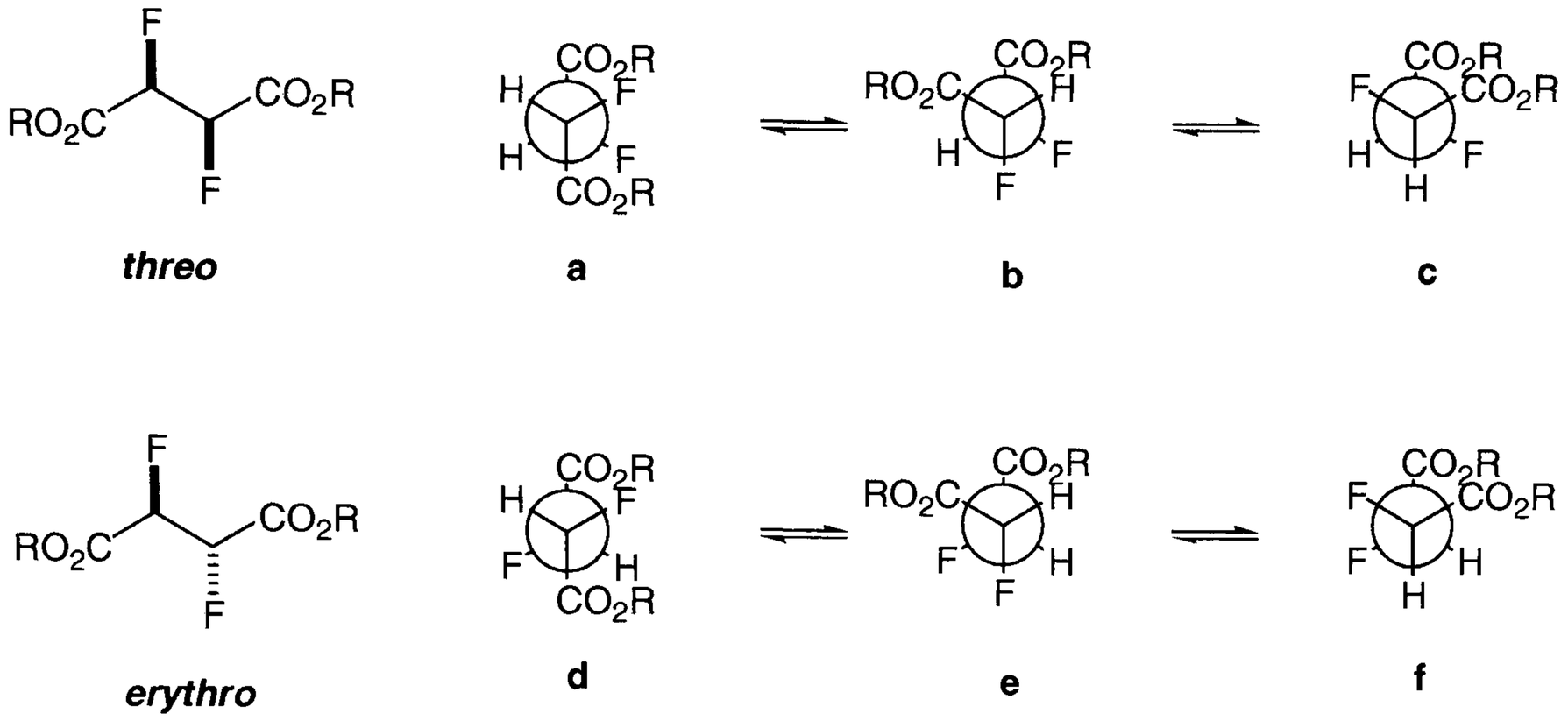

Scheme 2.103. Staggered conformations of *vicinal* difluoro compounds shown by Newman projections. The observed coupling constant for each diastereoisomer will essentially consist of a contribution from the three rotational isomers shown.

At this point it is convenient to introduce the parameter of the average coupling constant $\overline{J}$, which is the mathematical average of all of the coupling constants based on equally populated rotational isomers (Equation 2.2 and 2.3).

$$\overline{J}_{HF}(threo) = \frac{1}{3}\times\frac{J_t + J_t}{2} + \frac{1}{3}\times\frac{J_g + J_g}{2} + \frac{1}{3}\times\frac{J_g + J_g}{2} \sim 16Hz$$

$$\overline{J}_{HF}(erythro) = \frac{1}{3}\times\frac{J_g + J_g}{2} + \frac{1}{3}\times\frac{J_t + J_g}{2} + \frac{1}{3}\times\frac{J_t + J_g}{2} \sim 16Hz$$

Equations 2.2 and **2.3**. The concept of the average coupling constant. Each rotational isomer will contribute with two $^3J_{HF}$ coupling constants to the average coupling constant $\overline{J}$. The limiting coupling constants J_g = 8 Hz and J_t = 32 Hz are estimated values based on Figure 2.39.

The values of J_{trans} and J_{gauche} can be estimated from the average coupling constant according to the relationships in Figure 2.39. At sufficiently high temperatures, the populations of the individual rotational isomers will be equal for a molecule with free rotation. It is important to realise that in this case the average coupling constant $\overline{J}$ will

have the same value for the *threo* and the *erythro* diastereoisomers as the individual rotational isomers will be equally populated.

$$J_{HF}(erythro) = 0 \times \frac{J_g + J_g}{2} + 0.5 \times \frac{J_t + J_g}{2} + 0.5 \times \frac{J_t + J_g}{2} \sim 20Hz$$

$$J_{HF}(threo) = 1.0 \times \frac{J_t + J_t}{2} + 0 \times \frac{J_g + J_g}{2} + 0 \times \frac{J_g + J_g}{2} \sim 32Hz$$

Equation 2.4 and **2.5**. The observed $^3J_{HF}$ coupling constants are an average over the rotational isomers. The data from figure 2.39 suggest estimated values of 32 Hz and 20 Hz respectively for J_{trans} and J_{gauche}.

The fact that the observed $^3J_{HF}$ coupling constants are very different for the analysed *erythro* and *threo* difluoro compounds necessarily leads to the conclusion that the individual rotational isomers cannot be equally populated. From this the question follows, which of the rotational isomers are the preferred ones in the *threo* and in the *erythro* series that give rise to different $^3J_{HF}$ and $^3J_{HH}$ coupling constants. To answer this question the data in figure 2.46 have to be considered and applied to equations 2.2 and 2.3. The *threo* compounds generally have a much higher $^3J_{HF}$ coupling constant. It follows that there are more *trans* H-F relationships in the *threo* series than for the *erythro* compounds at room temperature. The high $^3J_{HF}$ coupling constant of 32 Hz for the *threo* series suggests that the rotational isomer **a** in Scheme 2.103 must be the preferred structure, whereas the two other rotamers are only of minor importance. This can be understood by considering Equation 2.4. On the other hand, the lower $^3J_{HF}$ coupling constant of 22 Hz for the *erythro* series suggests a significant contribution of rotamers **e** and **f** with a *gauche* and a *trans* H-F coupling (Scheme 2.103). As the rotational isomers **e** and **f** are enantiotopic and thus of the same energy, they will be equally populated in solution (Equation 2.5). The conformational

preferences for the rotational isomer **a** in the *threo* series and the rotamers **e** and **f** in the *erythro* series is reinforced by the low *vicinal* H-H couplings observed. These were measured at about 2 Hz, suggesting a *gauche* relationship of the proton nuclei for the *threo* as well as the *erythro* compounds (Figure 2.38). This obviously discriminates against rotamers **d** and **c** as significant structures as they have an *anti* relationship of their *vicinal* protons. In conclusion, it can be stated that there are conformational preferences within these compounds that apparently favour structures in which the C-F bonds have a *gauche* relationship. These results once again suggest the influence of the "*gauche* effect" in *vicinal* difluoro compounds in solution.

2.5.2 VT NMR experiments

The results in the previous section were confirmed by variable temperature NMR studies. Generally, solvent and temperature will affect the rotational equilibrium for compounds whose rotational barriers are small. Exploring temperature and solvent effects may therefore give an indication of the most stable rotational isomers of such equilibria and can even give the exact populations of the individual rotational isomers. The basic requirement underlying these experiments is that the inherent temperature dependence of the coupling constants is negligible compared to the variation caused by the change of proportions for the individual rotational isomers with temperature. This condition is generally met for the $^3J_{HF}$ and $^3J_{HH}$ NMR coupling constants, provided that they are considered in a relatively small temperature range.[20]

The rotational isomers of 2,3-difluorosuccinates are very different in energy terms, and thus, the observed coupling constant J_{obs} will change with temperature. The effect was investigated for the *erythro* and *threo* diethyl 2,3-difluorosuccinates **159** and **160**

in order to explore their conformational behaviour. The esters **159** and **160** were chosen as substrates for the variable temperature experiments since they gave the best defined spectra of all derivatives of 2,3-difluoroduccinic acids. The presence of ten resolved lines in the AA'XX' pattern of the NMR spectra is necessary to determine the $^3J_{HF}$ and $^3J_{HH}$ coupling constants accurately in order to draw comparison between the two diastereoisomers (Figure 2.47).

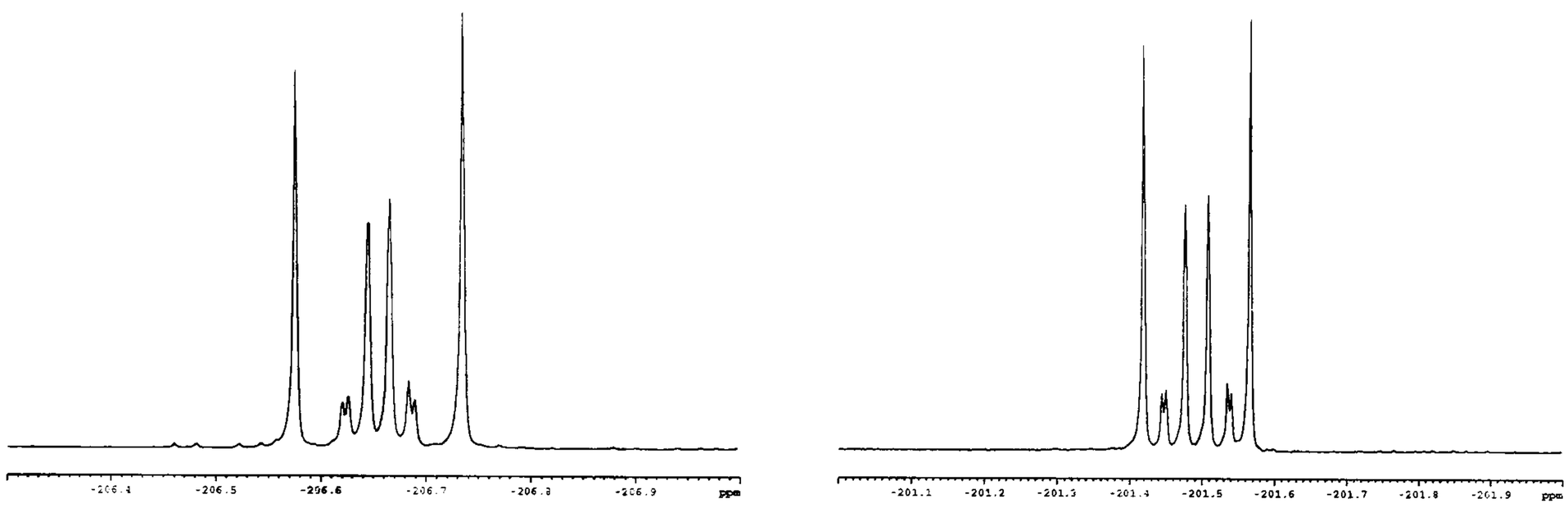

Figure 2.47. NMR spectra of *threo* (left) and *erythro* (right) 2,3-difluorosuccinates **159** and **160**.

The other advantage of using the esters of 2,3-difluorosuccinic acid is that they offer excellent solubility in all common organic solvents. Especially the more polar solvents like DMSO and DMF gave line broadening even at ambient temperature and their use is also restricted due to a relatively high melting point. Acetone and dichloromethane are solvents commonly used for low temperature NMR experiments, but their application in this case is hampered by a relatively low boiling point. The aromatic hydrocarbons like toluene and benzene offer the best compromise, and therefore d_6-toluene was chosen as the medium for these VT experiments. The physical properties of the solvent allow for NMR measurements over a wide temperature range and the apolar nature for maximum resolution.

Table 2.12. Coupling constants obtained for ethyl *erythro*-2,3-difluorosuccinate **159** after VT experiments in d_6-toluene. The coupling constants were determined using the PERCH software.

T [K]	$^3J_{HH}$	$^3J_{HF}$	$^3J_{FF}$	$^2J_{HF}$	Shift
370	2.17	21.04	-13.52	47.56	1478.6
360	2.13	21.30	-13.57	47.45	1474.7
350	2.04	21.36	-13.55	47.52	1470.9
340	2.01	21.50	-13.60	47.45	1467.9
330	1.99	21.64	-13.68	47.40	1464.1
320	1.98	21.71	-13.68	47.48	1459.8
310	1.90	21.82	-13.72	47.45	1455.1
300	1.89	21.89	-13.74	47.38	1449.8
290	1.88	21.92	-13.86	47.34	1446.8
280	1.85	22.15	-13.89	47.44	1441.2
270	1.82	22.19	-13.99	47.33	1434.5
260	1.75	22.30	-13.93	47.42	1428.1
250	1.73	22.20	-13.90	47.43	1420.8
240	1.78	22.06	-13.79	47.64	1412.8
230	1.78	22.00	-13.54	47.80	1403.4

The data for the 2,3-difluorosuccinates clearly indicate a decrease of $^3J_{HF}$ and an increase of $^3J_{HH}$ with temperature (Table 2.12). Although the differences between the individual coupling constants are relatively small, the trend clearly suggests an increasing population of rotamer **d** at higher temperatures (Scheme 2.103). This at the same time indicates a conformational preference for the rotamers **e** and **f** at ambient temperatures, which both have the C-F bonds *gauche* to each other.

Table 2.13. Coupling constants obtained for diethyl *threo* 2,3-difluorosuccinate **160** after a variable temperature profile in d_6-toluene. The coupling constants were determined using PERCH.

T [K]	$^3J_{HH}$	$^3J_{HF}$	$^3J_{FF}$	$^2J_{HF}$	Shift
370	2.62	26.47	-10.04	46.21	1504.9
360	2.42	26.7	-9.87	46.27	1504.0
350	2.33	27.00	-9.99	46.15	1502.3
340	2.31	27.29	-9.87	46.37	1500.6
330	2.21	27.75	-10.01	46.12	1498.6
320	2.23	27.89	-10.04	45.11	1496.3
310	2.15	27.92	-10.29	45.08	1493.3
300	2.03	28.51	-10.18	45.99	1482.5
290	1.85	28.90	-10.16	45.87	1477.8
280	1.83	29.12	-10.12	46.03	1473.5
270	1.80	29.57	-10.34	45.82	1468.4
260	1.79	29.44	-9.94	45.97	1462.8
250	1.64	29.73	-10.0	45.97	1456.2

A similar trend was observed for the $^3J_{HF}$ and $^3J_{HH}$ coupling constants of the *threo* isomer of 2,3-difluorosuccinate **160** (Table 2.13). The $^3J_{HF}$ value decreases at higher temperatures, whereas the $^3J_{HH}$ coupling constant increases. The variations are quite significant and again indicate a change in population for the rotational isomers with temperature. For the *threo* compound **160**, three rotational isomers have to be taken into account, which all have a different chemical configuration and thus are different in energies terms (Scheme 2.103). A large $^3J_{HF}$ coupling constant of about 31 Hz indicates a *trans* H-F coupling, whereas a small $^3J_{HH}$ coupling constant of about 1.5 Hz is typical for a *gauche* H-H relationship. The amplitude of these coupling constants suggests that at low temperature the molecule exists almost entirely as the rotamer **a**, which have two H-F *trans* relationships whereas the *vicinal* protons are gauche. Increasing the temperature leads to a higher population of the rotamers **b** and

c, as indicated by the smaller $^3J_{HF}$ coupling constants. The temperature dependence of the population for the individual rotational isomers may be described in terms of a Bolzmann distribution,[21] which can be used to describe rotational equilibria quantitatively (Equations 2.6).

$$A \rightleftharpoons B$$

$$K = \frac{n_B}{n_A} = \exp\left(-\frac{\Delta G^S}{RT}\right)$$

$$n_A + n_B = 1$$

$$M_{obeserved} = n_A M_A + n_B M_B$$

Equations 2.6. The parameters n_A and n_B refer to the populations of two molecules equilibrating in states A and B. The parameter ΔG^S is the free-energy difference for the equilibrium in any solvent S. R is the ideal gas constant and T the temperature. The single quantity *M* determined by the experimental technique is the weighted average of the values in the various rotamers.

The measurement of any values M_A and M_B for which the individual rotational isomers are different may be used to obtain relatively exact values for their respective populations. The most common method involves measurement of the NMR coupling constants, which can be used to describe the equilibrium between the rotational isomers for *erythro* 2,3-difluorosuccinate **160** quantitatively. A consideration of the individual rotational isomers in Scheme 2.103 reveals that the $^3J_{HF}$ coupling constants for rotamer **d** is different compared to the rotamers **e** and **f**, which are energetically equivalent. This allows for a straightforward comparison of ratios between these rotational isomers, and the respective populations can be obtained from the observed coupling constants.

$$J_{obs} = n_A \frac{(J_g + J_g)}{2} + n_B \frac{(J_g + J_t)}{2}$$

Equation 2.7. The observed $^3J_{HF}$ coupling constant for the *erythro* isomer **160** consists of two energetically different rotational isomers, which are described in terms of the populations n_A and n_B.

The limiting coupling constants J_g and J_t are necessary to determine the populations n_A and n_B for the individual rotational isomers of diethyl *erythro* 2,3-difluorosuccinates **159** and **160** (Equation 2.7). These parameters are difficult to obtain, but can be estimated with reasonable accuracy. The relatively high coupling constant of 21.9 Hz for J_{obs} suggests a value of 34 Hz for J_t and 12 Hz for J_g. Application of these coupling constants to Equations 2.7 immediately gives populations for the individual rotamers and their rotational barrier ΔG^S, according to equations 2.6 (Scheme 1.104).

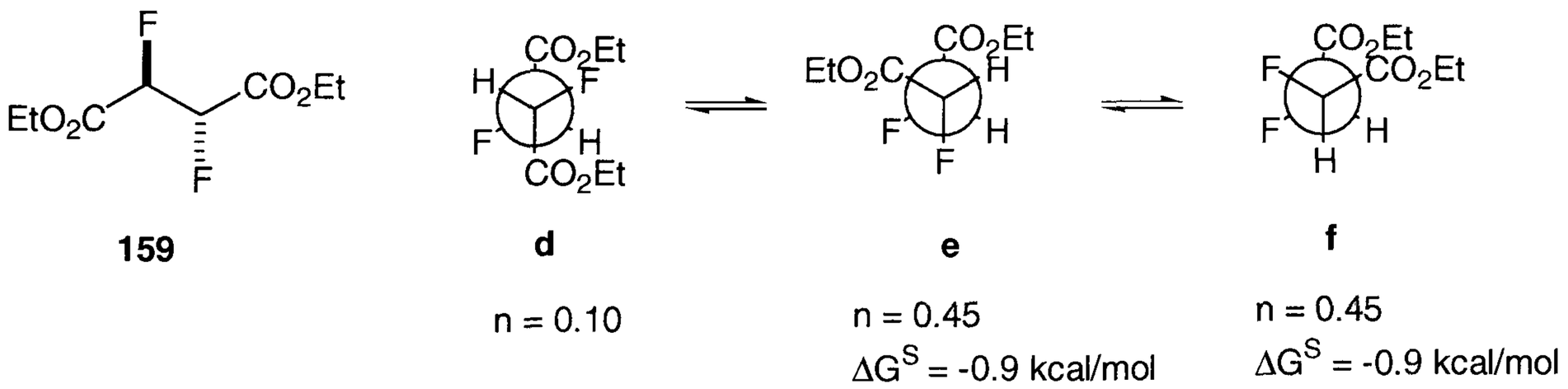

Scheme 2.104. Populations and energy barriers fro the *erythro* isomer of 2,3-difluorocuccinate **159**.

Although the result in scheme 2.104 are based on estimated values for J_g and J_t, they may be useful in describing the equilibrium between the rotational isomers in *erythro* 2,3-difluorosuccinate **159**. Clearly, the rotamers having the C-F bonds *gauche* with respect to each other (**e** and **f**) significantly outnumber those of the *trans* rotamer **d**.

The situation is somewhat more complex for the *threo* isomer **160** as it consists of the three energetically nonequivalent rotational isomers **a, b** and **c** (Scheme 2.105). The fact that two of these rotamers have similar $^3J_{HF}$ geometries (i.e., the $^3J_{HF}$ coupling of the rotamers **b** and **c** has the same value) makes it necessary to include the $^3J_{HH}$ coupling constants in the calculation. The limiting $^3J_{HH}$ coupling constants J_g and J_t are necessary to distinguish between rotamers **b** and **c**. These values can be borrowed from the values of J_{HH} which can be calculated from the measured populations of the *erythro* isomer **159** (Scheme 2.104). Application of 1.5 Hz and 5.5 Hz for J_g and J_t respectively, and the values of 12 Hz and 34 Hz for the $^3J_{HF}$ coupling constants were applied to calculate the populations of the *threo* isomer **160** (Scheme 2.105).

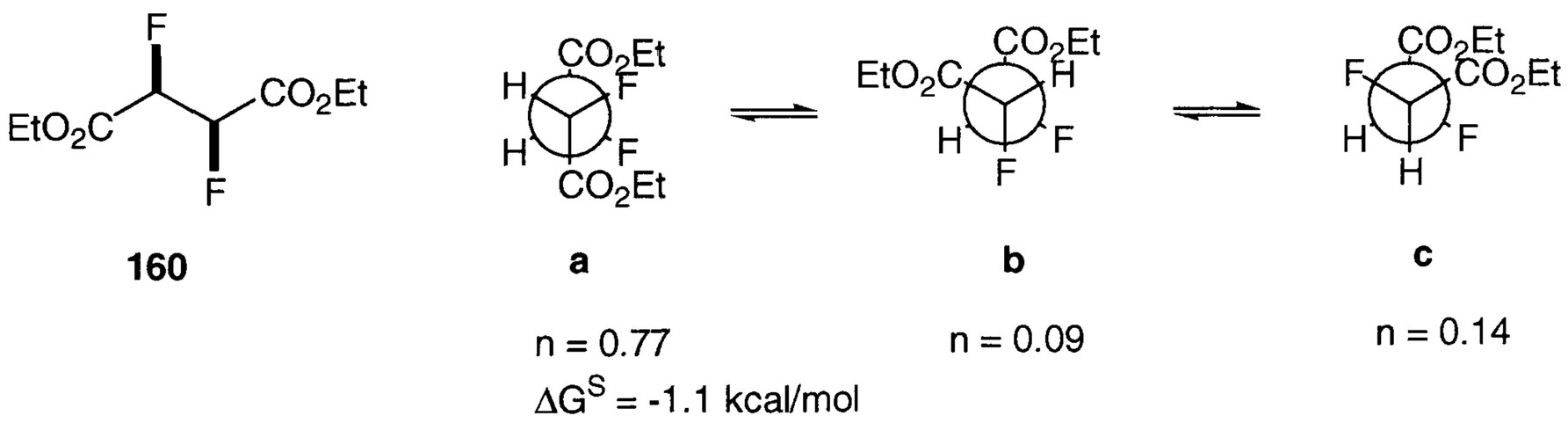

Scheme 2.105. Populations and energy barriers of the *threo* isomer of ethyl 2,3-difluorocuccinate **160**.

The calculation is based on the assumption that the limiting coupling constants J_g and J_t are similar for the stereoisomers **159** and **160**. These values rely on the Karplus relationships according to Figures 2.38 and 2.39. The energy differences for the two least favoured rotational isomer **b** and **c** of **160** are very small and possibly not very representative for the ratio of the two rotamers. In order to obtain more accurate values for the limiting coupling constants J_g and J_t the data from Tables 2.12 and 2.13 were fitted into an equation derived from the Bolzmann distribution. The value of the coupling constant J_{obs} as a function of T can give values for the parameters J_g and

J_t, and ΔG will follow from this. The plot of J_{obs} *versus* temperature generates a four-parameter curve for ΔH, ΔS, J_g, and J_t. In order to reduce the problem to a three-parameter fit, ΔS is very generally assumed to be zero.[22] The appropriate equation derived from the Bolzmann distribution can be solved by iteration starting with estimated values of the parameters using the software ORIGIN (Figure 2.48)

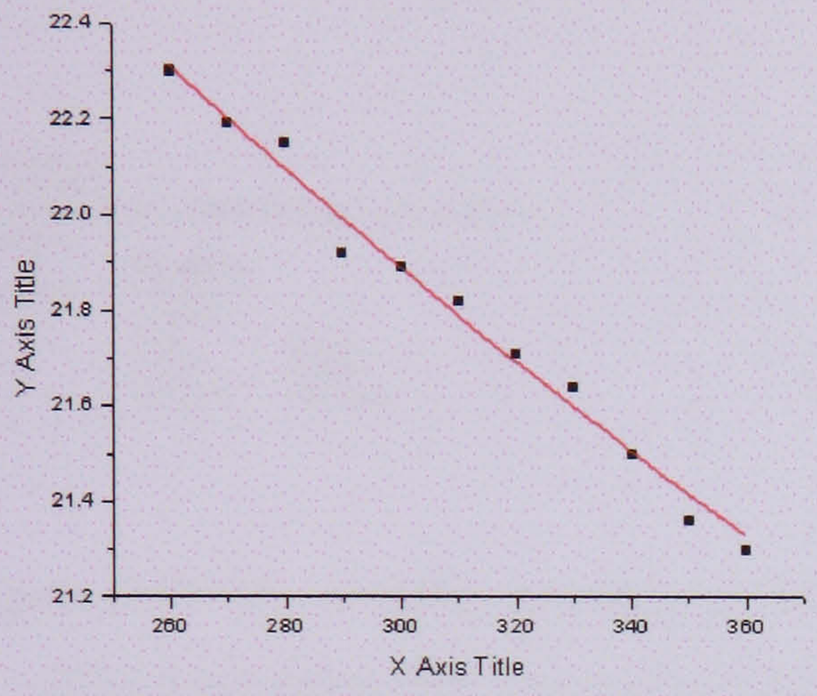

Data: Data1_B
Model: EErythroHF
Equation: (P1*exp(-P3/(8.314*T))+2*(P1+P2)/2)/(exp(-P3/(8.314*T))+2)
Weighting:
J No weighting
Chi^2/DoF = 0.00191
R^2 = 0.98628
P1 1.46348 ±4.58942
P2 46.57151 ±1.99932
P3 3910.85585 ±2220.29615

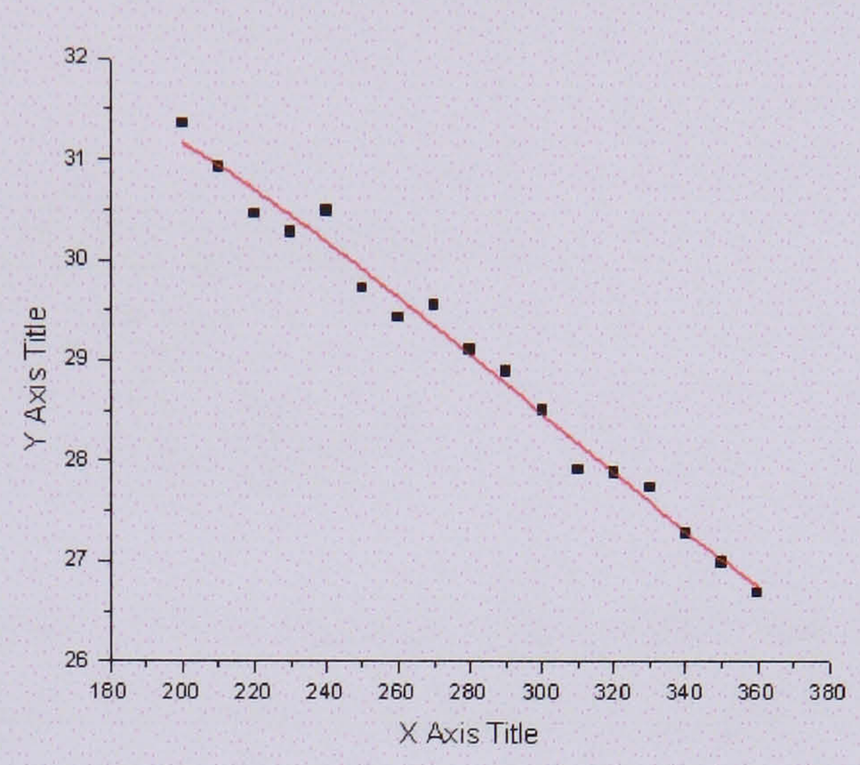

Data: Data1_B
Model: EEthreoHF
Equation: (P1*exp(-P3/(8.314*T))+P1*exp(-P4/(8.314*T))+P2)/(exp(-P3/(8.314*T))+exp(-P4/(8.314*T))+1)
Weighting:
J No weighting
Chi^2/DoF = 0.03499
R^2 = 0.98614
P1 1.60714 ±5.04135
P2 32.27868 ±0.43175
P3 6602.82181 ±6427304523.44098
P4 6602.82181 ±6427304519.48061

Figure 2.48. $^3J_{HF}$ coupling constants for *erythro* 2,3-difluorosuccinate **159** (top left) and *threo* (top right) 2,3-difluorosuccinate **160** *versus* temperature. The red lines indicate a fit of the data points to the Bolzmann distribution generated with the ORIGIN software. The parameter P1, P2 indicate the *gauche* and *trans* H-F coupling constant; P3 refers to the free-energy values in J*mol^{-1} obtained from the fit.

A modification of the published method allowed for the application of these equations to the *vicinal* $^3J_{HF}$ coupling constants for **159** and **160** (Figure 2.48). Unfortunately, the large error for the unknown parameters J_g, J_t, and in particular ΔH made these data of little value. From the distribution of the data points in Figure 2.48, it becomes quite obvious that the accuracy of the coupling constants is limited, thus leading to the large error observed. The scattering of the data points is even larger for the $^3J_{HH}$ coupling constants (Figure 2.49).

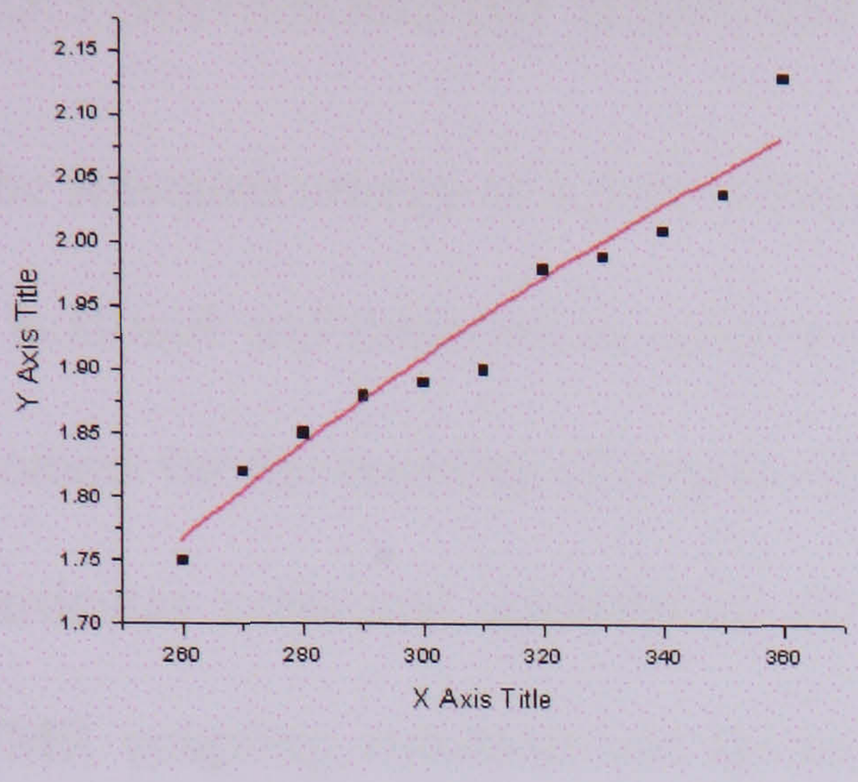

Data: Datal_B
Model: Gutkow
Equation: (2*P1+P2*exp(-P3/(8.314*T)))/(2+exp(-P3/(8.314*T)))
Weighting:

J	No weighting	
Chi^2/DoF	= 0.00071	
R^2	= 0.95257	
P1	0.7828	±2.39612
P2	8.20248	±1.6938
P3	2564.40703	±4696.74649

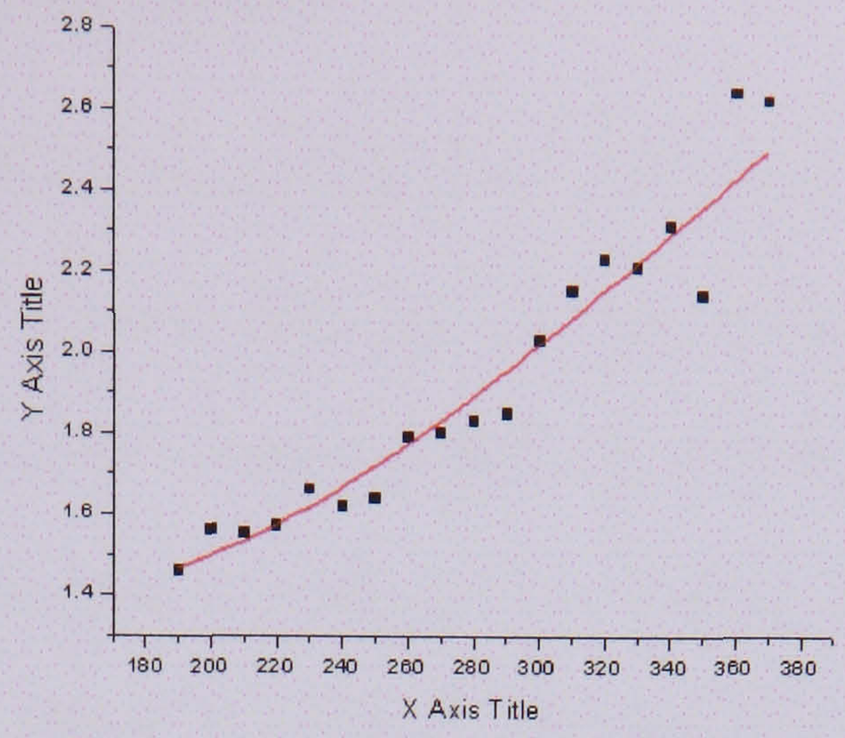

Data: Datal_B
Model: EEthreoHH
Equation: (P1*exp(-P3/(8.314*T))+P2*exp(-P4/(8.314*T))+P1)/(exp(-P3/(8.314*T))+exp(-P4/(8.314*T))+1)
Weighting:

J	No weighting	
Chi^2/DoF	= 0.0099	
R^2	= 0.93636	
P1	1.35689	±0.12483
P2	20.54332	±290.89343
P3	-6332.50397	±243748.72094
P4	1791.65788	±266594.09296

Figure 2.49. $^{3}J_{HH}$ coupling constants *versus* temperature for *erythro*- (top left) **159** and *threo* (top right) 2,3-difluorosuccinate **160**. The red lines indicate a fit of the data points to the equation derived from the Bolzmann-distributions.

From the data in table 2.12 and 2.13 it is apparent that the measurement of the $^{3}J_{HH}$ coupling constants itself is of reasonable accuracy ($\Delta < 0.5$ Hz). The error in these measurements however is apparently large enough to cause a large deviation in the parameters determined by the software. The parameter P1, P2 in figure 2.49 indicate the *gauche* and *trans* H-H coupling constants J_g and J_t, and P3 refers to the free energy ΔG values in J*mol^{-1} obtained from the fit. Although the parameters represent reasonable values, the large error in these calculations is not satisfactory. It has to be concluded that either the calculation of the coupling constants from the AA'XX' NMR system is not accurate enough, or the method itself cannot be applied due to temperature related changes of the NMR coupling constants, other than the dihedral angle. For instance, the bond angle of the coupled nuclei may change over the relatively large temperature range applied and are thereby effecting the NMR coupling constants.

2.5.3 Solvent and pH dependant NMR experiments

The solvation energy of a polar solute in a polar medium is typically in the range of 0-3 kcal/mol and therefore is quite similar to the energy difference between rotational isomers for the majority of acyclic compounds. Also, solvation effects can influence a particular rotational equilibrium considerably, and in contrast to chemical shifts, NMR coupling constants are solvent independent.[23] Therefore such effects can be used to investigate conformational equilibria of molecules. Diethyl 2,3-difluorosuccinates **159** and **160** again served as substrates for these measurements and the changes of $^{3}J_{HF}$ and $^{3}J_{HH}$ with solvent are illustrated (Table 2.14).

Table 2.14. Solvent dependant coupling constants of both stereoisomers of ethyl 2,3-difluorosuccinate, recorded at room temperature at 300 MHz. Coupling constants were calculated using PERCH.

***threo*-2,3-Difluorosuccinate**				
Solvent	$^{3}J_{HH}$	$^{3}J_{FF}$	$^{3}J_{HF}$	$^{2}J_{HF}$
CCl_4	2.1	14.9	27.6	46.0
C_6H_6	2.0	10.2	29.0	46.0
$CDCl_3$	1.5	10.1	28.4	46.2
CD_3CN	1.8	9.1	30.3	45.1
CD_3OD	1.4	9.0	30.0	45.5
DMSO	1.3	9.6	31.8	44.6
***threo*-2,3-Difluorosuccinate**				
Solvent	$^{3}J_{HH}$	$^{3}J_{FF}$	$^{3}J_{HF}$	$^{2}J_{HF}$
CCl_4	1.9	13.6	21.3	47.7
C_6H_6	1.9	14.0	21.8	47.2
$CDCl_3$	1.7	13.8	21.6	47.2
CD_3CN	2.1	13.8	22.3	46.4
CD_3OD	1.7	13.8	22.4	46.8
DMSO	1.9	14.6	23.1	45.8

A small but noticeable variation in going from nonpolar (CCl_4) towards the more polar solvents (DMSO) was observed. For the *threo* isomers the $^3J_{HF}$ values increases by about 4 Hz, whereas the $^3J_{HH}$ value decreases by about 0.8 Hz. This change may be understood in terms of rotational isomerism. The general trend is that the dipole of the solute will increase on going from an apolar solvent to a more polar one, and this will change the conformational equilibrium. Considering the rotational isomers in scheme 2.103, the dipole moments of the rotamers **b** and **c** point in opposite direction, thereby reducing their dipole moment (Scheme 2.103). This behaviour is consistent with changing populations of rotamers **c** (and **b**) in favour to a higher population of rotamer **a**, the most polar structure. These changes are consistent with a stabilisation of the more polar rotamer with increasing polarity of the solvent.

The observed changes are small, presumably because even in the nonpolar solvents rotamer **a** has a much higher population than that of the other two rotamers. The solvent induced changes for the coupling constants $^3J_{HF}$ and $^3J_{HH}$ are much smaller in the *erythro* isomer **160**. The $^3J_{HF}$ values increase by only 2 Hz in going from the least polar, to the most polar solvent. The $^3J_{HH}$ values of **160** remain essentially constant. This observation is consistent with the fact that rotamers **e** and **f** are much more populated than the rotamer **d**, and thus population shifts will remain very small. Also, the amplitude of the $^3J_{HH}$ coupling is small and deviations will lie within the experimental error of the NMR measurements. No unambiguous conclusions are therefore yet to be drawn from these experiments.

The influence of pH on the conformational equilibrium of 2,3-difluorosuccinic acids **130** and **132** was also investigated. It was assumed that the electrostatic repulsion of the negatively charged carboxylate anions in 2,3-difluorosuccinic acids **130** and **132** would influence the populations of the individual rotational isomers (Scheme 2.106). The experiments were carried out in an aqueous solution with a sodium hydrogen carbonate buffer as the medium. The pH of the solution was adjusted by addition of solid sodium bicarbonate to the buffer and measured with a thin pH-electrode directly in the NMR tube. The changes in coupling constants with respect to pH were found to be quite small and essentially take place between pH 2 and 4 (Table 2.15).

Table 2.15. Coupling constants and chemical shifts determined at different pH values for 2,3-difluorosuccinic acids **130** and **132** at room temperature. The coupling constants were determined using the PERCH software.

pH	Shift		$^3J_{HH}$		$^3J_{HF}$		$^3J_{FF}$	
	erythro	*threo*	*erythro*	*threo*	*erythro*	*threo*	*erythro*	*threo*
1,9	196.3	201.0	1.6	1.5	24.2	32.5	15.1	11.1
2,5	195.5	198.8	1.5	1.5	24.7	33.0	15.3	11.8
3.4	193.4	197.6	1.4	1.4	25.0	33.8	15.4	11.9
4.1	191.9	197.5	1.4	1.2	25.1	33.8	15.5	11.8
4.8	189.7	197.4	1.3	1.0	25.6	33.9	15.6	11.9
5.4	189.7	197.4	1.3	1.0	25.3	33.9	15.5	11.9
6.0	189.8	197.4	1.3	1.0	25.5	33.8	15.6	11.9
6.8	189.8	197.4	1.3	1.0	25.4	33.8	15.5	11.8
7.5	189.8	197.4	1.3	1.0	25.5	33.8	15.6	11.9
8.0	189.8	197.4	1.3	1.0	25.6	33.8	15.6	11.9

As expected, the changes take place at about the pH range where the carboxyl groups become deprotonated. The fluorine atoms will lower the acidity of the carboxyl groups of succinic acid (pK_a = 4.19 and 5.57) presumably into the pH 3-4 range. There is a small but clear trend with an increase in the $^3J_{HF}$ coupling constant in going to higher pH values and a decrease of the $^3J_{HH}$ coupling constant. This behaviour may be explained by a change in the population of rotamer **b** to rotamer **a** for the *threo* compound **132**. This seems reasonable, as rotamer **b** becomes less stable at higher pH due to electrostatic clash between the carboxylate groups (Scheme 2.106).

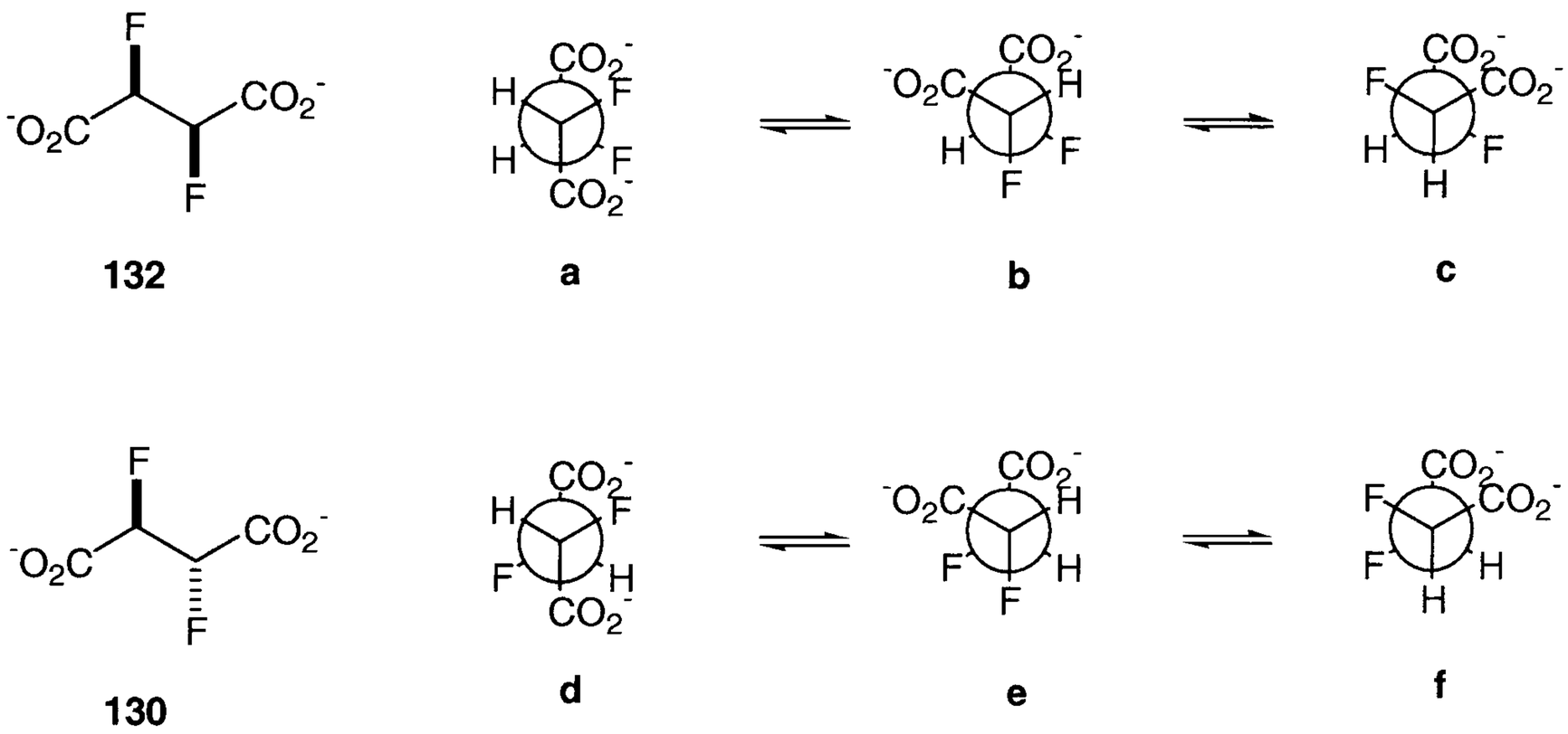

Scheme 2.106. Staggered conformations of *vicinal* difluorosuccinic acids by their Newman projections.

For the *erythro* isomer **130** however, the explanation is less obvious. The $^3J_{HF}$ coupling constant increases with higher pH and decreases for $^3J_{HH}$. This suggests a change of rotamer populations to **e** and **f** at the cost of **d**. The conclusion however is difficult to rationalise as electrostatic repulsion is expected to be higher in **e** and **f**.

Another important aspect to consider here is the substituent effect on the NMR coupling constants. Protonation or deprotonation at the carboxyl groups will change the electronic distribution of the molecule considerably and this may in turn affect the coupling constant. Therefore a concise conclusion about the stability of the individual rotational isomers was not forthcoming from the pH dependant measurements.

References

[1] A. J. de Hoog, H. R. Buys, C. Altona, E. Havinga, *Tetrahedron*, 1969, **25**, 3365.

[2] P. L. Timms, N.C. Norman, J. A .J. Pardoe, I. D. Mackie, S. L. Hinchley, S. Parsons, D. W. H. Rankin, *Dalton Trans.*, 2005, 607.

[3] M. Karplus, *J. Chem. Phys.*, 1959, **300**, 11; M. Karplus, *J. Am. Chem. Soc.*, 1963, **85**, 2870.

[4] R. A. Newmark, C. H. Sederholm, *J. Chem. Phys.* 1965, **43**, 602.

[5] M. Hesse, H. Meier, B. Zeh, In *Spektroskopische Methoden in der organischen Chemie*, 4. Auflage, Thieme Verlag, Stuttgard, 1991, 105.

[6] M. Hesse, H. Meier, B. Zeh, In *Spektroskopische Methoden in der Organischen Chemie*, 4. Auflage, 1991, New York, 105.

[7] R. J. Abrahams, K. G. R. Pachler, *J. Mol. Phys.*, 1963, **7**, 165.

[8] R. J. Abraham, L. Cavalli, K. G. R. Pachler, *Mol. Phys.*, 1966, **11**, 271.

[9] R. J. Abraham, L. Cavalli, *Mol. Phys.* 1965, **9**, 67.

[10] A. M. Ihring, S. L. Smith, *J. Am. Chem. Soc.*, 1070, **92**, 759.

[11] M. L. Huggins, *J. Am. Chem. Soc.*, 1953, **75**, 4123.

[12] R. E. Glick, A. A. Bothner-By, *J. Chem. Phys.*, 1956, **25**, 362.

[13] J. A. Pole, W. G. Schneider, H. J. Bernstein, *High Resolution Nuclear Magnetic Resonance*, McGraw-Hill, New York, 1959.

[14] R. J. Abraham, P. Loftus, *Tetrahedron*, 1977, **33**, 1227.

[15] R. J. Abrahams, E. Bretschneider, In *Internal Rotations in Molecules*, Wiley & Sons, London, 1974.

[16] R. J. Abraham, L. Cavalli, K. G. R. Pachler, *Mol. Phys.*, 1966, **11**, 271.

[17] M. Hudlicky, *J. Fluorine Chem.*, 1987, **36**, 373.

[18] The coupling constants of 1,2-difluoro-1,2-diphenylethane were calculated using LAOCOON III analysis performed by Professor Abrahams of Liverpool University.

[19] J. A. Pople, W. G. Schneider, H. J. Bernstein, *Can. J. Chem.*, 1957, **35**, 1060.

[20] R. J. Abrahams, E. Bretschneider, Medium effects on rotational and confromational equilibria, In *Internal Rotations in Molecules*, Acad. Press, 1974, 489.

[21] P. W. Atkins, In *Physikalische Chemie*, 2. Auflage, VCH, Weinheim, 1996, 675.

[22] H. S. Gutkowski, G. Belford, P. E. McMahon, *J. Chem. Physics*, 1962, 3353.

[23] R. Abrahams, E. Bretschneider, In *Internal Rotations in Molecules*, Wiley & Sons, London, 1974, 483.

2.5 Conclusion

Several *vicinal* difluoro compounds were analysed in order to investigate conformational preferences that arise from stereoelectronic effects associated with the carbon-fluorine bond. New synthetic routes were developed in order to access such compounds and the synthesis of diasteriomerically pure *erythro* and *threo* 2,3-difluorosuccinic acids was a key object towards this goal.

Erythro 2,3-difluorosuccinic acid was obtained from *trans*-stilbene after halofluorination and subsequent halogen exchange, resolution by crystallisation and oxidative degradation of the phenyl rings. The *threo* isomer of 2,3-difluorosuccinic acid were obtained as single enantiomers by multistep synthesis from either (*R,R*) or (*S,S*) diethyl tartrates. The synthetic route involves the generation of cyclic sulfates, nucleophilic fluorination with inorganic fluoride, and subsequent deoxofluorination of the intermediate fluorohydrin. The diethyl 2,3-difluorocuccinates were readily hydrolysed under acidic conditions to give the free carboxylic acids. Derivatives of 2,3-difluorosuccinic acids were obtained by standard synthetic methods such as acid catalysed esterification and amide coupling. Crystals suitable for X-ray crystallography were obtained for the *erythro* and *threo* 2,3-difluorosuccinic acid and their benzylamides. These sets of diastereoisomers were compared in terms of their molecular conformation and the comparison was extended to their nonfluorinated analogues.

For all these compounds, a strong preference was observed to align the *vicinal* C-F bonds *gauche* to each other, thereby reinforcing the concept of the *gauche* effect by experimental results. In case of the amides, the C-F bonds aligned preferentially *anti* periplanar to the amide carbonyl bond, an effect, which has been described in terms of stereoelectronic effects. These conformational preferences are pronounced and appear

to override steric and electrostatic interactions in *vicinal* difluoro amides. A similar tendency is observed for the free carboxylic acids; however in this case the C-F bonds have a strong tendency to adopt a *syn* planar conformation with respect to the carbonyl bond. The analysis was extended to the solution state and NMR experiments were carried out in order to establish conformational preferences for the *vicinal* difluoro compounds. Again, the data indicated a strong preference for the central C-F bonds to align *gauche* with respect to each other, and the conformational analysis developed in the course of these experiments will be the subject of a scientific publication in the near future.[1]

The F-C-C-F motif was incorporated into small peptide chains to assess its influence on their molecular conformation.[2] Several pseudopeptides derived from 2,3-difluorosuccinic acid were synthesised and their conformation was investigated by X-ray analysis and NMR experiments. The conformations of such fluorine-containing peptides show a remarkable dependence on the stereochemical orientation of the fluorine substituents, an effect that may serve as a tool to influence the secondary and consequently tertiary structure of peptides in a predictable way. These stereoelectronic effects associated with the C-F bond may be exploited for the synthesis of peptide mimics with improved binding properties and enhanced activity profile to have an impact in the search for new pharmacological lead structures.

---

[1] M. Schueler, R. Abrahams, D. O'Hagan, H. R. Rzepa, A. M. Z. Slawin, The vicinal difluoro motif. The synthesis and conformation of *erythro* and threo- diastereoisomers of 1,2-difluoro-1,2-diphenylethanes, 2,3-difluorosuccinic acids and their derivatives, *Beilstein J. Org. Chem.*, submitted.

[2] M. Schueler, D. O'Hagan, A. M. Z. Slawin, The *vicinal* F-C-C-F moiety as a tool for influencing peptide conformation, *J. Chem. Soc., Chem. Comm.*, 2005, **34**, 4324.

3 Experimental

3.1 General

^{1}H- and ^{13}C-NMR spectra were recorded on either a Varian Gemini 300 MHz spectrometer (^{1}H at 299.98 MHz, ^{13}C at 75.43 MHz) or on a Bruker AV-300 (^{1}H at 299.98 MHz, ^{13}C at 75.45 MHz, ^{19}F at 282.40 MHz) instrument. High-resolution mass spectra were obtained from a VG AUTOSPEC spectrometer. GC-MS analyses were performed on an Agilent 6890 gas chromatograph (equipped with a HP-5MS 5% PhMe Siloxane column, 1.5 μm thickness, 15m, 0.53 diameter) connected to an Agilent 5973N mass-selective detector. Chiral HPLC was carried out on a Chiralcel OD-H column with a Varian 9012 HPLC pump and Varian 9012 detector. Infrared spectra were recorded with a Perkin Elmer 2000 FT-IR instrument using NaCl glass plates. Optical Rotations were determined on an A-1000 polarimeter (Optical Polarimeter Ltd.) using a 2 dm cell, $[\alpha]_D$ values are given in units of 10^{-1} deg cm^2 g^{-1}. A GallenKamp GRIFFIN MPA350.BM2.5 melting point apparatus was used to determine melting points, which are uncorrected. Crystal structure determination was performed on a Bruker SMART diffractometer with graphite monochromated Mo-Kα radiation (λ = 0.7107 A) using 0.3° with steps accumulating area detector frames spanning a hemisphere of reciprocal space for both structures; the reflections were corrected for Lorentz and polarisation effects. Absorption effects were corrected on the basis of multiple equivalent reflections.

Reaction progress was monitored on thin-layer chromatography using glass plates coated with silica gel 60 (Merck F_{254}). TLC plates were examined under UV light (254 nm, 366 nm) and/or colouring with cerium-(IV)-sulfate stain. Column

chromatography was performed on Merck silica gel 60 (60-200μm, 70-230 mesh). Eluent volumes are given as a ratio of v/v. Air- and moisture sensitive reactions were carried out under a positive pressure of nitrogen in oven-dried glassware (200°C). All reagents are of synthetic grade and were used without further purification. Solvents were dried according to standard methods prior to use.[1]

3.2 Synthetic protocols

3.2.1 Preparation of *erythro* 1,2-diphenyl-1-bromo-2-fluoroethane **100**

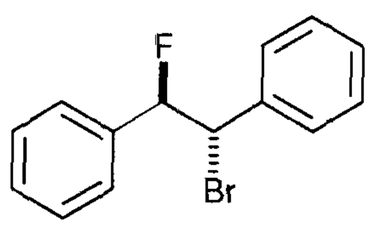

NBS (0.9g, 5mmol) was added to a mixture of *trans*-stilbene **91** (0.9 g, 5 mmol) in diethyl ether (5 cm^3) and HF/pyridine (5 cm^3) at room temperature. The suspension was stirred overnight and then water (10 cm^3) was added. The precipitate was filtered, washed with water and recrystallised in methanol to give the title compound as a white solid (1.1g, 79%), **mp** 98°C (lit.,[2] 105 °C); (**Found**: C, 60.28; H, 4.21. $C_{14}H_{12}BrF$ requires: C, 60.24; H, 4.33%); ν_{max} /cm^{-1} (nujol) 3064, 3033, 2959, 2360, 2339, 1950, 1882, 1496, 1455 and 961; δ_H ($CDCl_3$) 7.3-7.0 (10 H, m, Ar-H) and 5.8 (2H, dd, *J* 46.0 Hz, *J* 6.7 Hz, CHF) and 5.1 (2H, dd, *J* 15.0 Hz, *J* 6.7 Hz, CHBr); δ_C ($CDCl_3$) 137.4, 136.3, 129.6, 129.2, 128.9, 128.7, 127.3, 127.2 (Ar-C), 95.9 (d, *J* 181.3 Hz, CHF) and 55.0 (d, *J* 28.2 Hz, CHBr); δ_F ($CDCl_3$) –170.0 (dd, *J* 46.0 Hz, *J* 15.0 Hz); ***m/z*** (EI) 280, 278 (1, M^+), 199 (100, M-Br^-), 171 (33), 169 (32) and 109 (85). The *threo*-isomer of 1,2-diphenyl-1-bromo-2-fluoroethane was present as a minor component in a 1:10 ratio, δ_H ($CDCl_3$) 7.3-7.0 (10H, m, Ar-H), 5.8 (2H, dd, *J*

45.7 Hz, *J* 7.7 Hz, CHF) and 5.6 (2H, dd, *J* 12.9 Hz, *J* 7.7 Hz, CHBr); δ_F ($CDCl_3$) – 169.5 (dd, *J* 45.7 Hz, *J* 12.9 Hz).

3.2.2 Preparation of *E*-fluorostilbene **102**

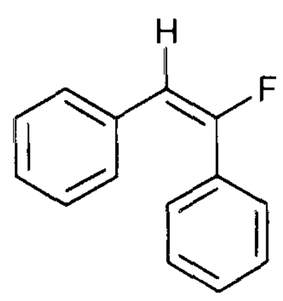

Potassium *tert*-butoxide (0.17 g, 1.5 mmol) was added to a solution of the fluorobromide **96** (0.28 g, 1.0 mmol) in pentane (10 cm^3) and the reaction mixture was heated under reflux for 5 h. The reaction mixture was then diluted with hexane (10 cm^3) and water (10 cm^3) was added. The organic layer was washed with brine (10 cm^3) and dried over $MgSO_4$. The solution was concentrated in *vacuo* to give the product (0.16 g, 82%) as a white crystalline solid, **mp** 93-97 °C (lit.[3] 94-95 °C); (**Found**: M^+, 198.0845. $C_{14}H_{11}F$ requires MH^+, 198.0840 ppm); ν_{max} /cm^{-1} (film) 3084, 3058, 3027, 1662, 1602, 1498, 1446, 1360, 1219, 1180, 1083, 1052, 1026, 918, 867, 842, 772, 731 and 694; δ_H ($CDCl_3$) 7.5-7.1 (10H, m, Ar-*H*), 6.4 (1H, d, *J* 21.8 Hz, C*H*); δ_F ($CDCl_3$) –96.5 (d, *J* 21.8 Hz, CH*F*); δ_C ($CDCl_3$) 132.0-127.5 (Ar-*C*), 109.7 (*J*, d, 31.0 Hz), 106.7 (*J*, d, 256.9 Hz); ***m/z*** (EI): 198 (100), 197 (80), 196 (61), 183 (27), 178 (15) and 170 (11).

3.2.3 Preparation of *erythro* 1,2-difluoro-1,2-diphenylethane **103**

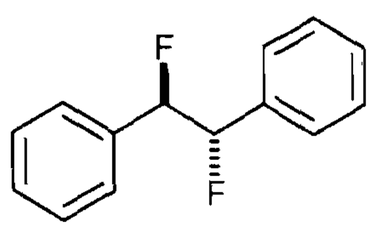

NBS (3.6 g, 20 mmol) was added to a solution of *trans*-stilbene (3.6 g, 20 mmol) in dry diethyl ether (20 cm^3) and 70% HF/pyridine (20 cm^3). The reaction mixture was stirred for 3 h and Ag(I)F (2.5 g, 20 mmol) was added. The reaction then was stirred for 12 h in the dark and was quenched into H_2O (20 cm^3). The mixture was extracted into diethyl ether (3 x 20 cm^3). The combined organic phases were washed with $NaHCO_3$ solution (10 cm^3), H_2O (10 cm^3) and brine (10 cm^3). The solvent was dried under Na_2SO_4 and the removed to give the crude product. The solid was recrystallised in methanol and then petroleum ether to give the product as white crystals (3.3 g, 76 %), **mp** 102–103 °C (lit.,[4] 100-102.5 °C); (**Found**: C, 77.04; H, 5.53. $C_{14}H_{12}F_2$ requires: C, 77.05; H, 5.54%); ν_{max} /cm^{-1} (KBr) 1618, 1508, 1498, 1457, 1243, 1208, 1001, 918, 829, 761, 699 and 598; δ_H ($CDCl_3$) 7.4-7.1 (10H, m, Ar-H), 5.8-5.5 (2H, AA'XX', *J* 45.2 Hz, *J* 15.2 Hz, *J* –16.5 Hz, *J* 2.6 Hz, 2 x CHF; δ_C ($CDCl_3$) 129.3, 128.7, 128.6, 127.2, 127.1 (Ar-C) and 94.7 (dd, *J* 181.9 Hz, *J* 28.7 Hz, 2 x CHF); δ_F ($CDCl_3$) –187.1 (AA'XX', *J* 45.2 Hz, *J* 15.2 Hz, *J* -16.5 Hz); ***m/z*** (EI) 218 (15), 109 (100) and 83 (8).

3.2.4 Preparation of *threo* 1,2-difluoro-1,2-diphenylethane **104**

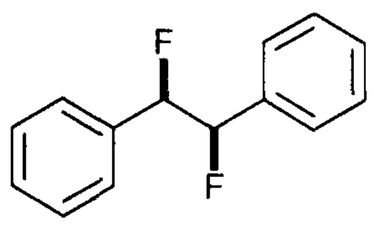

NBS (3.6g, 20 mmol) was added to a solution of *trans*-stilbene **91** (3.6 g, 20 mmol) in dry diethyl ether (20 cm^3) and 70% HF/pyridine (20 cm^3). The reaction mixture was stirred for 3 h and Ag(I)F (2.5g, 20 mmol) was added. The reaction mixture was stirred overnight in the dark and H_2O (20 cm^3) was added. The mixture was extracted into diethyl ether (3 x 20 cm^3). The combined organic phases were washed with $NaHCO_3$ solution (10 cm^3), H_2O (10 cm^3) and brine (10 cm^3). The solvent was dried under Na_2SO_4 and removed to give a crude product. The *threo*-isomer was purified from the 1:4 mixture of stereoisomers by a combination of crystallisation (methanol), flash chromatography (hexane/dichloromethane 20:1), and again crystallisation (hexane), **mp** 94°C (lit.,[5] 90-91 °C); (**Found**: C, 77.13; H, 6.05. $C_{14}H_{12}F_2$ requires: C, 77.05; H, 5.54%); ν_{max} /cm^{-1} (KBr) 3033, 2970, 1495, 1214, 1074, 1004, 849 and 699; δ_H ($CDCl_3$) 7.4-7.1 (10H, m, Ar-H) and 5.8-5.5 (2H, AA'XX', *J* 47.2 Hz, *J* 14.1 Hz, *J* –17.3 Hz, *J* 6.0 Hz, 2 x CHF); δ_C ($CDCl_3$) 129.4, 128.7, 127.2, 127.2, 127.1, (Ar-C) and 95.46 (dd, *J* 184.1 Hz, *J* 25.4 Hz); δ_F ($CDCl_3$) –187.1 (AA'XX', *J* 47.2 Hz, *J* 14.1 Hz, *J* –17.3 Hz); ***m/z*** (EI) 218 (7), 109 (100) and 83 (8).

3.2.5 Synthesis of *erythro* 2,3-difluorosuccinic acid **130**

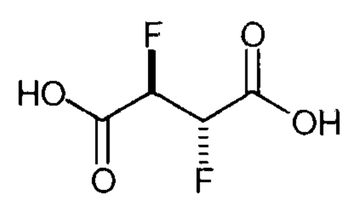

A solution of *erythro*-1,2-difluorobiphenylethane **103** (0.630 g, 3 mmol) in acetic acid (600 cm^3) was treated with ozone over a period of 16 h at ambient temperature. 30% H_2O_2 (100 cm^3) was then added, and the reaction mixture stirred for 12 h. Platinum black (0.02 g) was added and stirring continued for 2 h to remove excess of hydrogen peroxide. When gas evolution had ceased, the mixture was concentrated in vacuum and the solid filtered off under reduced pressure. The remaining solution (50 cm^3) was diluted with H_2O (25 cm^3) and extracted into diethyl ether (2 x 25 cm^3) to remove starting material and by-products. The aqueous phase was freeze dried to give the crude product (0.208 g, 45%) as an amorphous brown solid. The compound was sublimed in a Kugelrohr apparatus (100 °C/0.1 mm) to give colourless crystals, **mp** 174-175 °C; (**Found**: C, 31.46, H, 2.69. $C_4H_4O_4F_2$ requires: C, 31.18; H, 2.62 %); ν_{max} /cm^{-1} (KBr) 2946, 1719, 1450, 1271, 1240, 1122, 1096, 857 and 744; δ_H (CD_3CN) 5.5 (2H, AA'XX', *J* 46.7 Hz, *J* 23.3 Hz, *J* -14.0 Hz, *J* 1.8 Hz, C*H*F); δ_C (CD_3CN) 87.6 (*J* 191.6 Hz, *J* 22.9 Hz); δ_F (CD_3CN) –202.0 (AA'XX', *J* 46.7 Hz, *J* 23.3 Hz, *J* -14.0 Hz, *J* 1.8 Hz); ***m/z*** (ESI-) 153.22 (M-H).

3.2.6 Preparation of dimethyl *erythro* 2,3-difluorosuccinate **131**

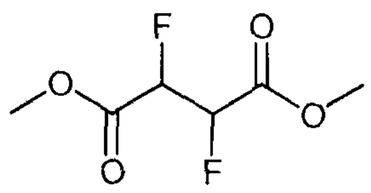

Erythro and threo 2,3-difluorosuccinic acids (0.157 g, 1.0 mmol) were heated under reflux in dry methanol (20 cm^3) in the presence of Dowex 50WX8-400 ion-exchange resin (200 mg) for 24 h. The resin was filtered and the solvent was removed under reduced pressure. The crude product was purified over silica gel (hexane/diethyl ether 10:1) to give the title compound (140 mg, 76%) as a clear colourless liquid, (**Found**: MH^+, 183.0466. $C_8H_{13}O_8S$ requires: 183.0469, 1.5 ppm); ν_{max}/cm^{-1} (film) 2962, 2856, 1772, 1745, 1443, 1360, 1304, 1227, 1129, 1092, 1031, 990, 955, 869, 830, 775, 682 and 603; δ_H ($CDCl_3$) 5.5 (2H, AA'XX', *J* 47.0 Hz, *J* 21.7 Hz, *J* -13.8 Hz, *J* 1.8 Hz, 2 x C*H*F), 4.0 (6 H, s, 2 x CH_3); δ_C ($CDCl_3$) 88.2 (dd, *J* 197.2 Hz, *J* 23.2 Hz, 2 x *C*HF), 53.5 (O*C*H_3); δ_F ($CDCl_3$) –202.1 (AA'XX', *J* 47.0 Hz, *J* 21.8 Hz, *J* -13.8 Hz, *J* 1.8 Hz); ***m/z*** (EI): 151 (20) 131 (5), 123 (10), 93 (51), 73 (40) and 59 (100).

Methyl *threo* 2,3-difluorosuccinate, δ_H ($CDCl_3$) 5.5 (2H, AA'XX', *J* 45.7 Hz, *J* 28.9 Hz, *J* -10.1 Hz, *J* 1.8 Hz, 2 x C*H*F), 4.0 (6 H, s, CH_3); δ_C ($CDCl_3$) 87.7 (dd, *J* 197.9 Hz, *J* 21.0 Hz, 2 x *C*HF) and 53.7 (O*C*H_3); δ_F ($CDCl_3$) –202.45 (AA'XX', *J* 45.7 Hz, *J* 28.9 Hz, *J* -10.1 Hz, *J* 1.8 Hz, 2 x CH*F*); ***m/z*** (EI): 151 (20) 131 (5), 123 (10), 93 (51), 73 (40) and 59 (100).

3.2.7 Synthesis of *threo* 2,3-difluorosuccinic acid **132**

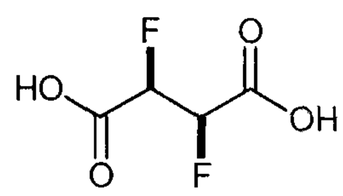

Ozone was bubbled trough a mixture of 1,2-difluoro1,2-biphenylethanes **95** (0.440 g, 2.1 mmol) in acetic acid (400 cm^3) over a period of 16 h at ambient temperature. 30% H_2O_2 (100 cm^3) was added and the reaction mixture stirred for 12 h. Platinum black (0.02 g) was added, and the stirring continued for 2 h to remove excess of hydrogen peroxide. When gas evolution had ceased, the mixture was concentrated in vacuum and the solid filtered off under reduced pressure. The remaining solution was diluted with H_2O and extracted into diethyl ether to remove unreacted starting material and by-products. The aqueous phase was freeze dried to give the crude product (0.097 g, 30%) as a brown gum. The compound was crystallised in hot acetone/benzene to give the product as light-brown crystals; **mp** 203-204 °C; (**Found**: MH^+, 153.0002. $C_4H_3O_4F_2$ requires: 152.9999, 1.9 ppm); ν_{max} /cm^{-1} (KBr) 3526, 1986, 1707, 1448, 1346, 1290, 1233, 1143, 1073, 912, 886, 830, 764, 671, 618 and 493; δ_H (CD_3CN) 5.5 (2H, AA'XX', *J* 45.3 Hz, *J* 31.2 Hz, *J* -8.8 Hz, *J* 1.6 Hz, CHF); δ_C (CD_3CN) 87.1 (dd, *J* 190.7 Hz, *J* 21.0 Hz); δ_F (CD_3CN) –202.0 (AA'XX', *J* 45.3 Hz, *J* 31.2 Hz, *J* -8.8 Hz, *J* 1.6 Hz); ***m/z*** (CI+) 155.02 ($M+H^+$).

3.2.8 Preparation of methyl *erythro* 2,3-difluoro-3-phenylpropionate **134**

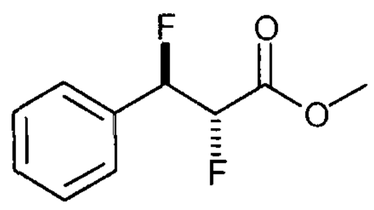

A mixture of *erythro* and *threo* 1,2-difluoro-2-phenylpropionic acid was obtained after ozonolysis from ether extraction of the crude product as described in 3.16. The combined organic extracts were dried over $MgSO_4$ and concentrated under reduced pressure. The residue was dissolved in dry methanol and heated under reflux for 12 h in the presence of Dowex 50WX8-400 ion-exchange resin (50 mg). The resin was filtered and the filtrate concentrated *en vacuo* to give a crude product, which was purified over silica gel (hexane/diethyl ether 10:1) to afford the title compound (ms321) as a colourless oil, (**Found**: $M+Na^+$, 223.0543. $C_{10}H_{10}O_2F_2Na$ requires 223.0547, -1.5 ppm); ν_{max} /cm^{-1} (KBr) 3039, 2958, 2927, 2854, 1770, 1748, 1455, 1440, 1363, 1300, 1288, 1270, 1220, 1123, 1037, 1015, 718, 699 and 558; δ_H ($CDCl_3$) 7.4-7.2 (5 H, m, Ar-*H*), 6.0-5.7 (1H, ddd, *J* 44.0 Hz, *J* 20.7 Hz, *J* 3.6 Hz, Ph-C*H*F), 5.2-4.9 (1H, ddd, *J* 49.2 Hz, *J* 12.5 Hz, *J* 3.6 Hz, CO-C*H*F) and 3.7 (3H, s, OCH_3); δ_C ($CDCl_3$) 129.9, 129.0, 127.0, 126.9 (Ar-*C*), 92.2 (dd, *J* 180.8 Hz, *J* 21.6 Hz, *C*HF), 89.9 (dd, *J* 195.2 Hz, *J* 27.9 Hz, *C*HF) and 53.1 (s, CH_3O); δ_F ($CDCl_3$) – 187.6 (ddd, *J* -15.4 Hz, CH*F*), –203.1 (ddd, *J* 15.4 Hz, CH*F*); ***m/z*** (EI): 200 (M^+, 2), 180 (35), 149 (21) and 109 (100).

3.2.9 Preparation of methyl *threo* 2,3-difluoro-3-phenylpropionate **135**

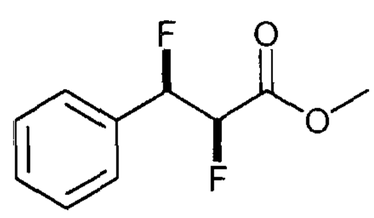

The title compound was isolated from the mixture of *erythro* and *threo* diastereoisomers after separation over silica gel (hexane/diethyl ether 10:1), **mp** 48-49 °C (**Found**: $M+Na^+$, 223.0548. $C_{10}H_{10}O_2F_2Na$ requires 223.0547, 0.1 ppm); ν_{max}/cm^{-1} (KBr) 3040, 2955, 2851, 1769, 1745, 1494, 1455, 1437, 1360, 1294, 1222, 1127, 1081, 1028, 766, 714,633 and 577; δ_H ($CDCl_3$) 7.4-7.3 (5 H, m, Ar-*H*), 6.0-5.7 (1H, ddd, *J* 44.6 Hz, *J* 23.6 Hz, *J* 2.8 Hz, Ph-C*H*F), 5.5-5.2 (1H, ddd, *J* 46.9 Hz, *J* 26.1 Hz, *J* 2.8 Hz, CO-C*H*F) and 3.8 (3 H, s, OCH_3); δ_C ($CDCl_3$) 129.8, 129.1, 129.0, 126.7, 126.6 (Ar-*C*), 92.3 (dd, *J* 182.4 Hz, *J* 19.4 Hz, *C*HF), 90.2 (dd, *J* 197.0 Hz, *J* 23.5 Hz, *C*HF) and 53.2 (s, CH_3O); δ_F ($CDCl_3$) –192.7 (ddd, *J* -10.1 Hz, CH*F*), –206.3 (ddd, *J* 10.1 Hz, CH*F*); ***m/z*** (EI): 200 (M^+, 2), 180 (30), 149 (22) and 109 (100).

3.2.10 Ethyl 2,3-difluoro-3-[3,5-dimethoxyphenyl]propionate **156**

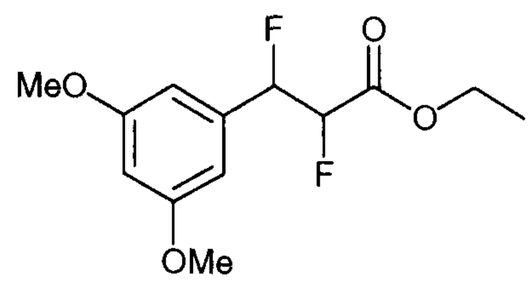

Ethyl fluoroacetate (0.1 g, 1 mmol) was added to a solution 3,5-dimethoxybenzaldehyde (0.17 g, 1 mmol) in dry THF (2 cm^3). The reaction mixture was cooled to –78 °C and a 2M solution of LDA (0.5 cm^3, 1 mmol) in hexane was added dropwise under nitrogen. The temperature was elevated to –20 °C and the reaction mixture was stirred at ambient temperature for 12 h. Aqueous ammonium chloride solution (1 cm^3) was added, the mixture diluted with H_2O (10 cm^3) and extracted into diethyl ether (3 x 10 cm^3). The combined organic extracts were washed with brine and dried over $MgSO_4$. Evaporation of the solvent gave the fluorohydrin **155** as yellowish oil, which was used without further purification for the next step. A solution of this product in dry dichloromethane (1 cm^3) was cooled to –78 °C and Deoxo-Fluor™ reagent **250** (0.2 cm^3, 1.5 mmol) was then added dropwise *via* syringe under nitrogen. The reaction was stirred at ambient temperature for 12 h, then diluted with diethyl ether (10 cm^3) and cold 10% sodium bicarbonate solution (10 cm^3) was added slowly. The phases were separated, and the organic layer washed with 1N HCl (2 x 10 cm^3), saturated sodium bicarbonate solution (10 cm^3) and brine (10 cm^3). Drying with $MgSO_4$ and removal of the solvent gave a crude product (100mg, 42%), that was purified over silica gel (hexane/Et_2O 2:1) to afford the title compound (ms513) as a yellow liquid. Ethyl *threo* 2,3-difluoro-3-[3,5-dimethoxyphenyl]-propionate**,** (**Found**: $M+Na^+$, 297.0914. $C_{13}H_{16}N_2O_2F_2Na$ requires 297.0914, -0.1 ppm); δ_H ($CDCl_3$) 6.5-6.3 (3H, m, Ar-*H*), 5.8 (1H, ddd, *J* 44.5 Hz, *J* 23.6 Hz, *J* 2.8 Hz, Ph-C*H*F), 5.0 (1H, ddd, *J* 44.5 Hz, *J* 26.4 Hz, *J* 2.8 Hz, CO-C*H*F), 4.2 (2H, q, *J*

7.1 Hz, OCH_2), 3.7 (6H, s, 2 x OCH_3), and 1.2 (6H, t, *J* Hz, 2 x CH_3); δ_C ($CDCl_3$) 161.4 (C=O), 104.9, 104.5, 101.6 (Ar-*C*), 92.4 (dd, *J* 183.3 Hz, *J* 19.6 Hz, *C*HF), 90.2 (dd, *J* 197.4 Hz, *J* 23.2 Hz, *C*HF), 62.7 (OCH_2Me), 55.8 (OCH_3) and 14.4 (CH_3); δ_F ($CDCl_3$) –193.2 (ddd, *J* 44.5 Hz, *J* 26.4 Hz, -10.1 Hz, PhCH*F*), and –205.6 (ddd, *J* 44.5 Hz, *J* 23.6 Hz, *J* –10.1, COCH*F*); ***m/z*** (ESI): 297.10 (M^+, 2).

Ethyl *erythro* 2,3-difluoro-3-[3,5-dimethoxyphenyl]propionate, (**Found**: M+Na^+, 297.0914. $C_{13}H_{16}N_2O_2F_2Na$ requires 297.0914, -0.1ppm); δ_H ($CDCl_3$) 6.5-6.3 (3H, m, Ar-*H*), 5.7 (1H, ddd, *J* 44.3 Hz, *J* 28.0 Hz, *J* 3.6 Hz, Ph-C*H*F), 5.2 (1H, ddd, *J* 49.4 Hz, *J* 20.8 Hz, *J* 3.6 Hz, CO-C*H*F), 4.2 (2H, q, *J* Hz, OCH_2), 3.7 (6H, s, 2 x OCH_3), and 1.2 (6H, t, *J* Hz, 2 x CH_3); δ_C ($CDCl_3$) 161.2 (C=O), 104.8, 104.4, 101.6 (Ar-*C*), 92.1 (dd, *J* 181.9 Hz, *J* 22.1 Hz, *C*HF), 89.8 (dd, *J* 194.9 Hz, *J* 27.4 Hz, *C*HF), 62.5 (OCH_2Me), 55.8 (OCH_3) and 14.4 (CH_3); δ_F ($CDCl_3$) –187.9 (ddd, *J* 44.3, *J* 28.0, *J* -15.1, PhCH*F*), and –202.5 (ddd, *J* 49.4, *J* 20.8, -15.9, COCH*F*); ***m/z*** (ESI): 297.04 (M+Na^+).

3.2.11 Preparation of diethyl *erythro* 2,3-difluorosuccinate **159**

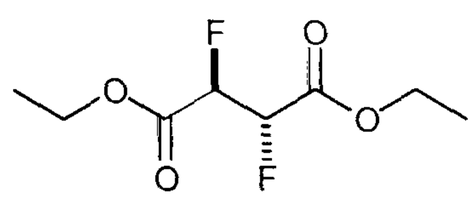

Erythro 2,3-difluorosuccinic acid **130** (0.208 g, 1.0 mmol) was heated under reflux in dry ethanol (20 cm^3) in the presence of Dowex 50WX8-400 ion-exchange resin (0.1 g) for 24 h. The resin was filtered off and excess solvent removed by evaporation. The residue was purified over silica gel (hexane/Et_2O 10:1) to give the compound (0.14 g, 91%) as a clear colourless liquid, (**Found**: MH^+, 211.079231. $C_8H_{13}O_4F_2$ requires MH, 211.078191 ppm); ν_{max} /cm^{-1} (film) 2986, 2946, 2908, 1765, 1746, 1462, 1376, 1299, 1217, 1124, 1094, 1026, 856 and 679; δ_H ($CDCl_3$) 5.30 (2H, AA'XX', *J* 48.0 Hz, *J* 21.5 Hz, *J* -14.0 Hz, *J* 1.9 Hz, 2 x C*H*F), 4.2 (4H, q, *J* 7.2 Hz, 2 x OCH_2), 1.2 (6H, t, *J* 7.2, 2 x OCH_2CH_3); δ_C ($CDCl_3$) 88.3 (dd, *J* 196.8 Hz, *J* 23.2 Hz, CHF), 63.0 (OCH_2), 14.4 OCH_2CH_3; δ_F ($CDCl_3$) –202.0 (AA'XX', *J* 48.0 Hz, *J* 21.5 Hz, *J* -14.0 Hz, *J* 1.9 Hz, 2 x CH*F*); ***m/z*** (EI): 210 (1), 183 (17), 165 (29), 137 (71), 109 (17), 90 (50), 73 (30) and 45 (25).

3.2.12 Preparation of *N,N'*-dibenzyl *erythro* 2,3-difluorosuccinamide **161**

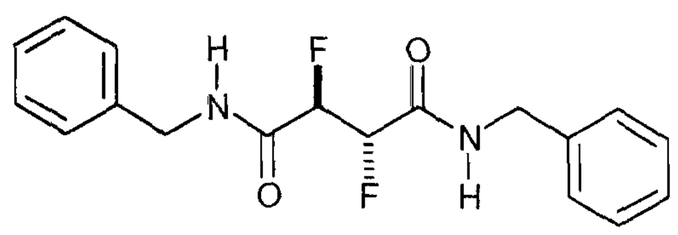

Benzylamine (0.43 g, 4.0 mmol) and HOBt (0.54 g, 4.0 mmol) were added to a solution of 2,3-difluorosuccinic acids **118** (0.31 g, 2.0 mmol) in DMF (10 cm^3) at ambient temperature. The reaction mixture was cooled to 0 °C, and a solution of EDC (0.84 g, 4.2 mmol) in $CHCl_3$ was added slowly. The reaction mixture was stirred for 24 h at ambient temperature. The mixture was then quenched with H_2O (10 cm^3) and extracted into ethyl acetate (3 x 10 cm^3). The combined organic extracts were washed with 1N HCl (2 x 10 cm^3), saturated sodium bicarbonate solution (10 cm^3), and brine (10 cm^3). The solvent was dried over $MgSO_4$ and removed under reduced pressure to give the product (0.155 g, 93%) as a mixture of stereoisomers. Separation by flash chromatography yielded the *erythro* isomer as a white solid, **mp** 159-160 °C (**Found**: C, 64.85; H, 5.32; N, 8.42. $C_{18}H_{18}F_2N_2O_2$ requires: C, 65.05; H, 5.46; 8.43 N%); ν_{max} /cm^{-1} (KBr) 3287, 3101, 3070, 3034, 2933, 2434, 1662, 1555, 1455, 1068, 1045, 1003, 747 and 695; δ_H ($CDCl_3$) 7.4-7.2 (10 H, m, Ar-H), 6.6 (2 H, m, N*H*), 5.4 (2 H, AA'XX', *J* 48.4 Hz, *J* 24.8 Hz, *J* -11.9 Hz, *J* 2.1 Hz, 2 x C*H*F) and 4.5-4.3 (4H, m, Ph-CH_2); δ_C ($CDCl_3$) 137.5, 129.2, 128.2, 128.1 (Ar-*C*) and 91.2 Hz (*J* 197.4 Hz, *J* 22.7 Hz, 2 x *C*HF); δ_F ($CDCl_3$) –199.8 (2 F, AA'XX', *J* 48.4 Hz, *J* 24.8 Hz, *J* -11.9 Hz, *J* 2.1 Hz, CH*F*); ***m/z*** (ESI-) 331.34 ($M\text{-}H^+$).

3.2.13 Preparation of *N,N'*-dibenzyl *threo*-2,3-difluorosuccinamide **162**

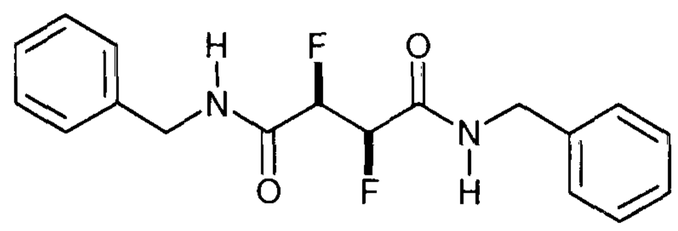

Benzylamine (0.43 g, 4.0 mmol) and HOBt (0.54 g, 4.0 mmol) were added to a solution of 2,3-difluorosuccinic acid (0.31 g, 2.0 mmol) in DMF (10 cm^3) at ambient temperature. The reaction mixture was cooled to 0 ^oC, and a solution of EDC (0.84g, 4.2 mmol) in $CHCl_3$ was added slowly. The reaction mixture was stirred for 24 h at room temperature. H_2O (10 cm^3) was added and the mixture extracted into ethyl acetate (3 x 10 cm^3). The combined organic extracts were washed with 1N HCl (2 x 10 cm^3), saturated sodium bicarbonate solution (10 cm^3), and brine (10 cm^3). The solvent was dried over $MgSO_4$ and removed under reduced pressure to give the product (0.155 g, 93%) as a mixture of stereoisomers. Separation by flash chromatography yielded the *threo* isomer as an amorphous white solid, **mp** 133-147 ^oC; (**Found**: C, 65.00; H, 5.50; N, 8.41. $C_{18}H_{18}F_2N_2O_2$ requires: C, 65.05; H, 5.46; 8.43 N%); ν_{max} /cm^{-1} (KBr) 3324, 1666, 1554, 1495, 1455, 1430, 1363, 1295, 1247, 1116, 1086, 1073, 1048, 1028, 862, 825, 737, 700, 620 and 575; δ_H ($CDCl_3$) 7.4-7.2 (10 H, m, Ar-*H*), 6.7 (2 H, m, N*H*), 5.3 (2H, AA'XX', *J* 46.0 Hz, *J* 31.3 Hz, *J* -12.6 Hz, *J* 2.0 Hz, 2 x C*H*F), 4.5-4.3 (4H, m, Ph-CH_2); δ_C ($CDCl_3$) 137.4, 129.2, 128.2, 128.1 (Ar-*C*) and 90.0 (dd, *J* 198.5 Hz, *J* 21.0 Hz, 2 x *C*HF); δ_F ($CDCl_3$) –207.1 (AA'XX', *J* 46.0 Hz, *J* 31.3 Hz, *J* -12.6 Hz, *J* 2.0 Hz, CH*F*).

3.2.14 Preparation of 11-[N-butoxycarbonyl]aminoundecanoic acid **168**

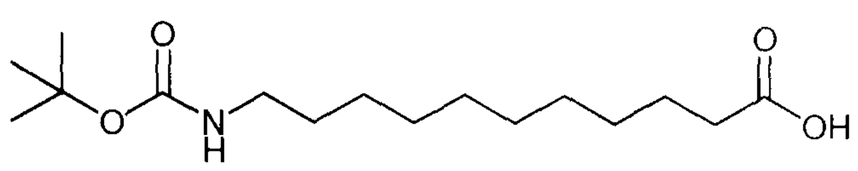

2N NaOH (15 cm^3) was added to a solution of 11-aminoundecanoic acid (2.0 g, 10 mmol) in dioxane (15 cm^3). The reaction was cooled to 0 °C and *tert*-butoxycarbonyl anhydride (2.5 cm^3, 11 mmol) was added. The mixture was stirred for 3 h and then acidified with 1N HCl under cooling in an ice-bath. A white precipitate was obtained which was purified over silica gel (hexan/diethyl ether 1:1) to obtain the product (ms534) as an amorphous white powder (1.84 g, 61%), **mp** 67-68 °C; (**Found**: C, 63.92; H, 10.53; N, 4.50. $C_{16}H_{31}NO_4$ requires: C, 63.76; H, 10.37; 4.65 N%); ν_{max} /cm^{-1} (KBr) 3370, 2986, 2920, 2853, 1687, 1522, 1470, 1281, 1239, 1173, 1010, 936, 870, 782, 722 and 594; δ_H ($CDCl_3$) 4.6 (1H, m, N*H*), 3.1 (2H, m, NCH_2), 2.3 (2H, t, *J* 7.4 Hz, CH_2CO_2Me), 1.6 (2H, m, C$H_2CH_2CO_2$Me), 1.4 (9H, s, *C*$(CH_3)_3$), 1.3 (12H, m, 7 x CH_2); δ_C ($CDCl_3$) 179.8 (CO_2Me), 156.5 ($CO_2{}^tBu$), 80.0 (C$(CH_3)_3$), 41.0 (NCH_2), 34.5 (CH_2CO_2Me), 30.4, 29.8, 29.7, 29.6, 29.6, 29.4 (6 x CH_2), 28.8 (C(*C*$H_3)_3$, 27.1 and 25.1 (2 x CH_2); ***m/z*** (ESI, -ve): 300.143 ($M\text{-}H^+$).

.

3.2.15 Synthesis of methyl 11-[N-butoxycarbonyl]aminoundecanoate **169**

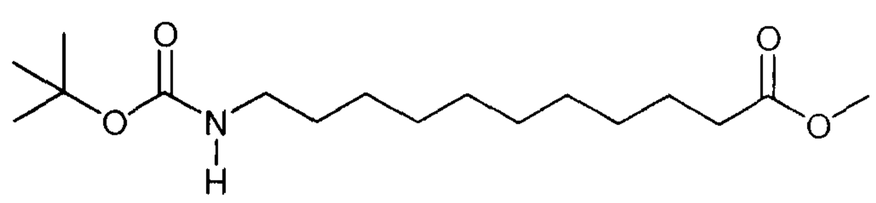

Methyl iodide (0.54 g, 3.8 mmol), followed by solid sodium hydrogen carbonate (0.32 g, 3.8 mmol) were added to a solution of the Boc-protected aminoacid (1.14 g, 3.8 mmol) in dry DMF (15 cm^3). The reaction mixture was stirred for 12 h at ambient temperature and then quenched into H_2O (30 cm^3). The suspension was extracted into diethyl ether (3 x 30 cm^3) and the combined organic extracts were washed with H_2O, brine and then dried over $MgSO_4$. The crude product (ms536) was purified over silica gel (diethyl ether/hexane 1:5) to afford the desired compound (0.46 g, 38%) as colorless gum, (**Found**: M+Na^+, 338.2305. $C_{17}H_{33}NO_4Na$ requires 338.2304, -0.7 ppm); ν_{max} /cm^{-1} (KBr) 2956, 2930, 2854, 1670, 1648, 1456, 1428, 1360, 1301, 1289, 1273, 1215, 1038, 1014, 708, 689 and 548; δ_H ($CDCl_3$) 4.9 (1H, m, N*H*), 3.6 (3H, s, OCH_3), 3.0 (2H, m, NCH_2), 2.2 (2H, t, *J* 7.1 Hz, CH_2COOMe), 1.6 (2H, m, CH_2CH_2COOMe), 1.4 (9H, s, Boc-CH_3), 1.2 (14H, m, 7 x CH_2); δ_C ($CDCl_3$) 174.4 (COOMe), 156.0 (NHCOO^{t}Bu), 78.9 ($C(CH_3)_3$), 51.6 (OCH_3), 40.8 ($NHCH_2$), 34.3 (CH_2COOMe), 29.7, 29.6, 29.5, 29.4, 29.3 (CH_2), 28.7 $(CH_3)_3$, 27.0 (CH_2) and 25.2 (CH_2); ***m/z*** (ESI, +ve): 337.992 (M+Na^+).

Removal of the Boc-group to form the ammonium chloride salt **170** was achieved by treatment of the parent compound with HCl-etherate for 12 h at ambient temperature, ***m/z*** (ESI +ve) 216 (M^+, 100).

3.2.16 Preparation of methyl *erythro* 11-[2,3-Difluoro-3-(10-methoxy-carbonyl-decylcarbamoyl)-propionylamino]-undecanoate **171**

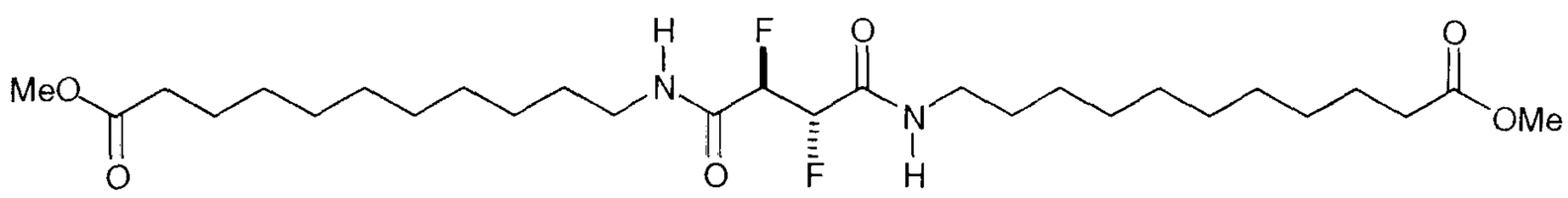

Methyl 11-aminoundecanoate hydrochloride **170** (0.25 g, 1.0 mmol), neutralised with NMM (0.5 cm^3, 1.5 mmol) prior to addition, was added to a solution of *erythro* 2,3-difluorosuccinic acid **130** (0.77 g, 0.5 mmol) in DMF (5 cm^3). HOBt (0.14 g, 1.0 mmol) was added and then a solution of EDC (0.40 g, 2.1 mmol) in $CHCl_3$ at 0 °C. The reaction mixture was stirred at room temperature for 24 h. H_2O (10 cm^3) was added and the mixture extracted into ethyl acetate (3 x 10 cm^3). The combined extracts were washed with 1 N HCl (2 x 10 cm^3), saturated $NaHCO_3$ (2 x 10 cm^3) and brine (10 cm^3). The solvent was dried over $MgSO_4$ and removed under reduced pressure to give the product (0.21g, 77%) as a colourless gel, (**Found**: M+Na^+, 571.3544. $C_{28}H_{50}N_2O_6F_2Na$ requires 571.3535, 1.6 ppm); ν_{max} /cm^{-1} (KBr) 3299, 2927, 2853, 1737, 1664, 1553, 1468, 1438, 1370, 1272, 1208, 1175 and 1115; δ_H ($CDCl_3$) 6.4 (2H, m, N*H*), 5.3 (2H, AA'XX', 2 x C*H*F), 3.6 (3H, s, OCH_3), 3.2 (4H, m, NH-CH_2), 2.2 (t, *J* 7.6 Hz, CH_2COOMe), 1.5, 1.2 (32H, m, 16 x CH_2); δ_C ($CDCl_3$) 174.7 (s, COOMe), 165.0 (m, CONH), 91.1 (dd, *J* 197.1 Hz, *J* 22.7 Hz, 2 x CHF), 51.8 (OCH_3), 39.7 ($NHCH_2$), 34.4, 29.8, 29.7, 29.6, 29.6, 29.5, 29.3, 27.1 and 25.2 (s, CH_2); δ_F ($CDCl_3$) –199.6 (AA'XX', *J* 46.4 Hz, *J* 24.5 Hz, *J* -11.9 Hz, *J* 2.1 Hz, CH*F*); ***m/z*** (ESI, +ve): 571.20 (M+Na^+).

3.2.17 Preparation of methyl *threo* 11-[2,3-Difluoro-3-(10-methoxy-carbonyl-decylcarbamoyl)-propionylamino]-undecanoate **172**

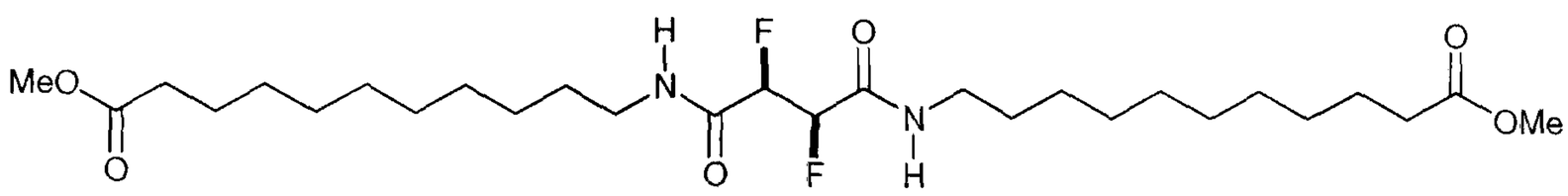

Methyl 11-aminoundecanoate hydrochloride **170** (0.18 g, 0.72 mmol) was added to a solution of *threo* 2,3-difluorosuccinic acid **132** (0.5 g, 0.3 mmol) in DMF (5 cm^3), which had been neutralised prior to addition with NMM (0.15 cm^3, 0.5 mmol). HOBt (0.9 g, 0.72 mmol) was added and a solution of EDC (0.19 g, 1.0 mmol) in $CHCl_3$ (2 cm^3) at 0 °C. The mixture was stirred at room temperature for 24 h, then H_2O (10 cm^3) was added and the mixture extracted into ethyl acetate (3 x 10 cm^3). The combined extracts were washed with 1 N HCl (2 x 10 cm^3), saturated $NaHCO_3$ (2 x 10 cm^3) and brine (10 cm^3). The solvent was dried over $MgSO_4$ and removed by evaporation to give a crude product. The material was purified over silica gel to give the product as a colourless gum (0.418g, 90%), (Found: M+Na^+, 571.3525. $C_{28}H_{50}N_2O_6F_2Na$ requires 571.3535, -1.7 ppm); ν_{max} /cm^{-1} (KBr) 3329, 2920, 2852, 1736, 1663, 1559, 1457, 1438, 1240, 1210, 1177, 1120, 1046, 881, 823, 723 and 604; δ_H ($CDCl_3$) 6.5 (2 H, m, N*H*), 5.4 (2H, AA'XX', *J* 44.8 Hz, *J* 30.9 Hz, *J* –12.1 Hz, *J* 1.9 Hz, 2 x C*H*F), 3.6 (3 H, s, OCH_3), 3.3 (4H, m, NH-CH_2), 2.2 (t, *J* 7.6 Hz, CH_2COOMe), 1.5, 1.2 (32H, m, 16 x CH_2); δ_C ($CDCl_3$) 174.7 (s, COOMe), 165.7 (m, CONH), 89.9 (dd, *J* 198.3 Hz, *J* 20.6 Hz, 2 x CHF), 51.8 (OCH_3), 39.8 ($NHCH_2$), 34.4, 29.7, 29.65, 29.55, 29.5, 29.45, 28.8, 27.0 and 25.3 (s, CH_2); δ_F ($CDCl_3$) –207.5 (AA'XX', CH*F*); ***m/z*** (ESI-) 571.112 (M+Na^+).

3.2.18 Synthesis of *erythro* 11-[2,3-Difluoro-3-(10-carboxyl-decyl-carbamoyl)-propionylamino]-undecanoic acid **173**

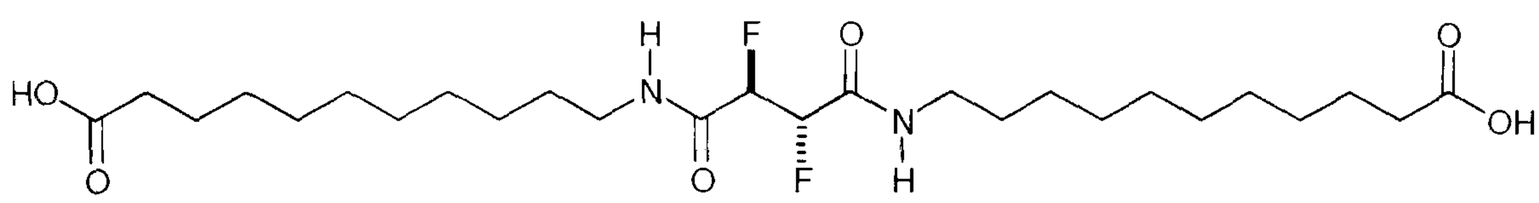

A solution of *erythro* 2,3-difluorosuccinamide **171** (0.2 g, 0.36 mmol) in acetone (5 cm^3) and 1N HCl (5 cm^3) was heated under reflux for 48 h. The solvent was removed under reduced pressure, and the remaining yellow salt was recrystallised in acetone (10 cm^3) to give the pure product as white powder (0.16 g, 83%), **mp** 138-141 ^oC; $\boldsymbol{\nu_{max}}$ /cm^{-1} (KBr) 3315, 3059, 2919, 2850, 1699, 1665, 1560, 1469, 1290, 1246, 1219, 1119, 1047, 924, 823, 722 and 606; $\boldsymbol{\delta_H}$ (DMSO) 8.3 (2H, m, N*H*), 5.4 (2H, AA'XX', *J* 46.4 Hz, *J* 24.7 Hz, *J* –11.8 Hz, *J* 1.8 Hz, 2 x C*H*F), 3.4 (3H, s, OCH_3), 3.0 (4H, m, NH-CH_2), 2.2 (t, *J* 7.6 Hz, CH_2COOMe), 1.5 and 1.2 (32H, m, 16 x CH_2); $\boldsymbol{\delta_C}$ (DMSO) 171.8 (s, COOH), 168.8 (s, COOH), 164.2 (m, CONH), 90.1 (dd, *J* 193.4 Hz, *J* 23.3 Hz, 2 x CHF), 38.7 ($NHCH_2$), 38.4 ($NHCH_2$), 33.6, 29.1, 28.9, 28.8, 28.7, 28.5, 26.9, 26.4, 26.3, 26.2, 25.8, and 24.5 (s, CH_2); $\boldsymbol{\delta_F}$ (DMSO) –199.3 (2F, AA'XX', CH*F*); ***m/z*** (ESI-) 543.22 ($M+Na^+$).

3.2.19 Preparation of *threo* 11-[2,3-Difluoro-3-(10-carboxyl-decyl-carbamoyl)-propionylamino]-undecanoic acid **174**

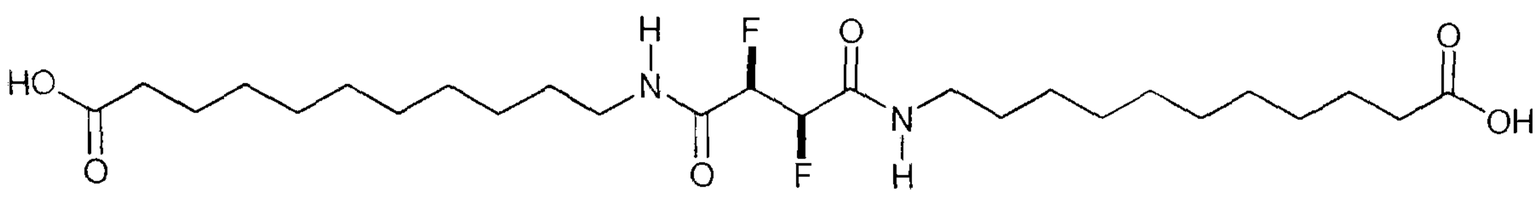

A solution of *threo* 2,3-difluorosuccinamide (0.4 g, 0.73 mmol) in acetone (5 cm^3) and 1N HCl (5 cm^3) was heated under reflux for 48 h. The solvent was removed by evaporation to give the crude product as a yellow salt. The solid was recrystallised in hot acetone (5 cm^3) to give the pure product as white powder (0.35 g, 92%), **mp** 145-146 °C (**Found**: C, 59.69; H, 9.14; N, 5.29. $C_{26}H_{46}O_6N_2F_2$ requires: C, 59.98; H, 8.90; 5.38 N%); ν_{max} /cm^{-1} (KBr) 3318, 2918, 2850, 1698, 1665, 1557, 1470, 1436, 1289, 1119, 1946, 925, 823, 722 and 604; δ_H (DMSO) 8.4 (2H, m, N*H*), 5.3 (2H, AA'XX', *J* 45.0 Hz, *J* 31.5 Hz, *J* –12.1 Hz, *J* 2.2 Hz, 2 x C*H*F), 3.1 (4H, m, NH-CH_2), 2.2 (t, *J* 7.6 Hz, CH_2COOH), 1.4 and 1.2 (32 H, m, 16 x CH_2); δ_C (DMSO) 174.9 (s, COOH), 165.3 (m, CONH), 89.6 (dd, *J* 195.9 Hz, *J* 20.5 Hz, 2 x CHF), 38.8 ($NHCH_2$), 34.0, 29.3, 29.3, 29.3, 29.1, 29.1, 28.9, 26.6 and 24.9 (s, CH_2); δ_F (DMSO) –206.6 (2 F, AA'XX', CH*F*).

3.2.20 Preparation of *N,N'*-dipropenyl 2,3-difluorosuccinamides **175**, **176**

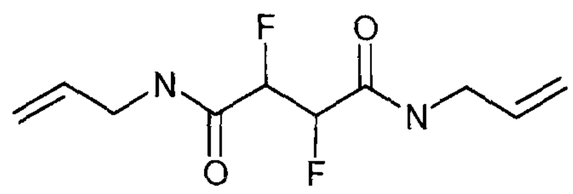

Allylamine (0.3 g, 2.0 mmol) and HOBt (0.54 g, 4.0 mmol) were added to a solution of *erythro* and *threo* 2,3-difluorosuccinic acids **118** (0.31 g, 2.0 mmol) in DMF (10 cm^3) at ambient temperature. A solution of EDC (1.15 g, 6.0 mmol) in $CHCl_3$ (2 cm^3) was added at 0 °C and the reaction mixture was stirred at ambient temperature for 24 h. H_2O (20 cm^3) was then added and the mixture extracted with ethyl acetate (3 x 10 cm^3). The combined extracts were washed with 1 N HCl (2 x 10 cm^3), saturated $NaHCO_3$ (2 x 10 cm^3), and brine (10 cm^3). The solvent was dried over $MgSO_4$ and removed by evaporation give the crude product (0.418 g, 90%). The material was purified by flash chromatography to give the *threo* isomer as the major compound, (**Found**: M+Na^+, 255.0923. $C_{10}H_{14}N_2O_2F_2Na$ requires 255.0921, 0.9 ppm); δ_H ($CDCl_3$) 6.6 (2 H, m, N*H*), 5.8 (1H, m, CH_2=C*H*), 5.4 (2 H, AA'XX', *J* 45.7 Hz, *J* 31.3 Hz, *J* 1.5 Hz, *J* -12.8 Hz, 2 x C*H*F), 5.2 (2 H, m, CH_2=CH), 3.9 (4H, m, NH-CH_2); δ_C ($CDCl_3$) 165.6 (d, *J* 12.0 Hz, C=O), 133.4 (*C*H=CH_2), 117.4 (CH=CH_2), 90.1 (dd, *J* 198.7 Hz, *J* 21.0 Hz) and 42.0 (NH-CH_2); δ_F ($CDCl_3$) –207.5 (AA'XX', *J* 45.7 Hz, *J* 31.3 Hz, *J* 1.5 Hz, *J* -12.8 Hz, CH*F*); ***m/z*** (ESI-) 255.04 (M+Na^+). The *erythro* isomer was obtained as the minor compound in the reaction, δ_H ($CDCl_3$ 6.4 (2H, m, N*H*), 5.8 (1 H, m, CH_2=C*H*), 5.3 (2 H, AA'XX', *J* 48.3 Hz, *J* 24.7 Hz, *J* – 11.8 Hz, *J* 2.2 Hz, 2 x C*H*F), 5.2 (2H, m, CH_2=CH), 3.9 (4H, m, NH-CH_2); δ_C ($CDCl_3$) 165.0 (m, C=O), 133.5 (*C*H=CH_2), 117.5 (CH=CH_2), 91.3 (dd, *J* 196.8 Hz, *J* 22.7 Hz) and 42.9 (NH-CH_2); δ_F ($CDCl_3$) –199.8 (AA'XX', *J* 48.3 Hz, *J* 24.7 Hz, *J* – 11.8 Hz, *J* 2.2 Hz, CH*F*).

3.2.21 Preparation of (*2R,3S*) MeO-(*S*)-Ala-2,3-difluorosuccinyl-(*S*)-Ala-OMe **209**

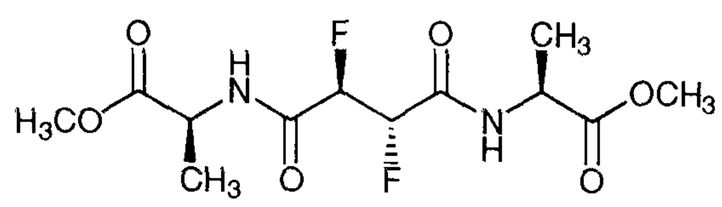

L-alanine methyl ester hydrochloride **223** (150 mg, 1.1 mmol), and HOBt (150 mg, 1.1 mmol) were addad to a solution of *erythro* 2,3-difluorosuccinic acid **130** (75 mg, 0.5 mmol) in DMF (2 cm^3). A solution of EDC (200 mg, 1.1 mmol) in $CHCl_3$ (2 cm^3) added dropwise at 0 °C, and the reaction mixture was stirred at ambient temperature for 24 h. H_2O (10 cm^3) was added and the mixture extracted into ethyl acetate (3 x 10 cm^3). The combined organic extracts were washed with 1N HCl (10 cm^3), saturated sodium bicarbonate solution (10 cm^3), and brine (10 cm^3), dried over $MgSO_4$ and the solvent removed under reduced pressure. The crude product was purified over silica gel (hexane/ethyl acetate 1:1) to give the product as colourless gum (31 mg, 22%), (**Found**: M+Na^+, 347.1027. $C_{12}H_{18}O_6N_2F_2Na$ requires 347.1031, -1.1 ppm); $[\alpha]_D$ – 50.0 (c 0.2, CH_3OH); ν_{max}/cm^{-1} 3332, 2988, 2936, 1740, 1686, 1677, 1541, 1452, 1449, 1207, 1115, 1056, 853, 780, 750, and 625; δ_H ($CDCl_3$) 7.0 (1H, m, NH), 6.8 (1H, m, NH), 5.5-5.2 (2H, m, *J* 48.0 Hz, *J* 23.0 Hz, *J* -12.0 Hz, *J* 1.3 Hz, 2 x CHF), 4.6 (2H, m, 2 x CH), 3.7 (3H, s, OCH_3), 3.7 (3H, s, OCH_3), 3.4 (3H, d, *J* 3.6 Hz, CH_3), 3.4 (3H, d, *J* 3.6 Hz, CH_3); δ_C ($CDCl_3$) 172.7 (s, CO_2Me), 172.6 (s, CO_2Me), 92.0 (dd, *J* 197.0 Hz, *J* 22.0 Hz), 89.0 (dd, *J* 197.0 Hz, *J* 22.0 Hz), 53.0 (s, CH), 52.7 (s, CH), 48.2 (t, OCH_3), 48.1 (s, OCH_3), 18.4 (d, CH_3), 18.2 (d, CH_3); δ_F ($CDCl_3$) – 201.0 (m, CHF), -199.7 (m, CHF); ***m/z*** (ESI) 347.00 (M+Na^+, 40), 325.01 (M+H^+, 100), 293.00 (M-OCH_3, 72), 265.02 (M-CO_2CH_3, 55).

3.2.22 Preparation of *(2R,3S)*-MeO-(*S*)-Phe-2,3-difluorosuccinyl-(*S*)-Phe-OMe **210**

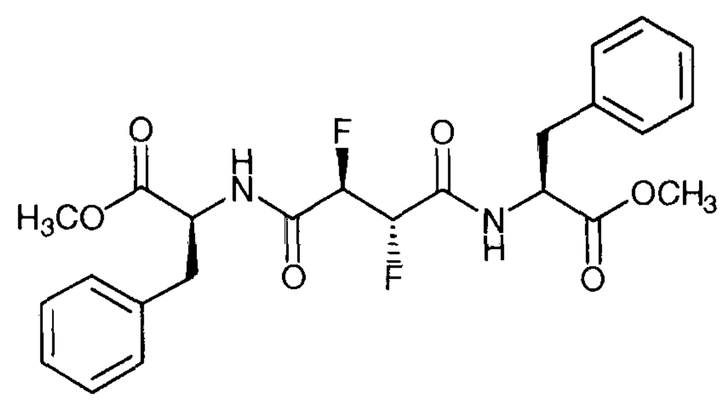

L-phenylalanine methyl ester hydrochloride **213** (115 mg, 0.52 mmol), pyridine (0.05 cm^3, 0.6 mmol) and HOBt (70 mg, 0.52 mmol) were added to a solution of *erythro* 2,3-difluorosuccinic acid **130** (40 mg, 0.26 mmol) in DMF (2 cm^3). A solution of EDC (100 mg, 0.52 mmol) in $CHCl_3$ (2 cm^3) was added dropwise at 0 °C and the reaction was stirred at room temperature for 24 h. H_2O (10 cm^3) was then added and the mixture extracted into ethyl acetate (3 x 10 cm^3). The combined organic phases were washed with 1N HCl (10 cm^3), saturated sodium bicarbonate solution (10 cm^3), and brine (10 cm^3), dried over $MgSO_4$ and the solvent removed under reduced pressure. The crude product was purified over silica gel (hexane/ethyl acetate 1:1) to give a colourless gum (70 mg, 57%), (**Found**: M+Na^+, 499.1661. $C_{24}H_{26}O_6N_2F_2Na$ requires 499.1657); $\mathbf{[\alpha]_D}$ +15.4 (c 1.0, CH_3OH); $\mathbf{\nu_{max}/cm^{-1}}$ (film) 3429, 3340, 3029, 2950, 1741, 1682, 1530, 1494, 1434, 1370, 1215, 1153, 1098, 1058, 833, 744, 702 and 636; $\mathbf{\delta_H}$ ($CDCl_3$) 7.3-7.0 (10H, m, Ar-H), 6.8 (1H, m, NH), 6.7 (1H, m, NH), 5.5-5.1 (2H, m, *J* 48.0 Hz, *J* 23 Hz, *J* -12.0 Hz, *J* 1.3 Hz, 2 x CHF), 4.9 (2H, m, 2 x CH), 3.7 (3H, s, CH_3), 3.6 (3H, s, CH_3), 3.1 (4H, m, 2 x CH_2Ph); $\mathbf{\delta_C}$ ($CDCl_3$) 171.5 (s, CO_2Me), 171.4 (s, CO_2Me), 135.8 (q, Ar-C), 135.7 (q, Ar-C), 129.8, 129.6, 129.1, 129.0, 127.7, 127.6 (t, Ar-C), 90.8 (dd, *J* 196.8 Hz, *J* 21.6 Hz), 90.6 (dd, *J* 197.4 Hz, *J* 21.6 Hz), 53.6 (s, CH), 53.2 (s, CH), 52.9 (t, OCH_3), 52.8 (s, OCH_3), 38.3 (d, CH_2Ph), 38.1 (d, CH_2Ph); $\mathbf{\delta_F}$ ($CDCl_3$) –200.4 (m, CHF), -201.1 (m, CHF); ***m/z*** (ESI) 498.99 (M+Na^+, 100), 477.00 (M+H^+, 90).

3.2.23 Preparation of MeO-(*S*)-Val-2,3-difluorosuccinyl-(*S*)-ValOMe **211**

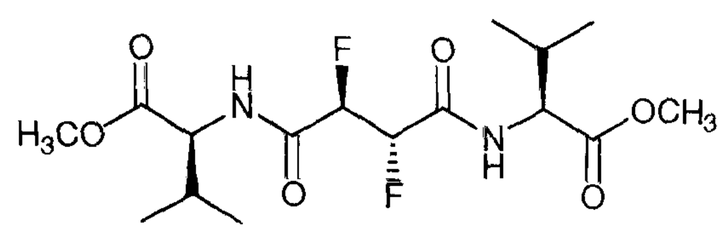

L-valine methyl ester hydrochloride (184 mg, 1.1 mmol), pyridine (0.1 cm^3, 1.2 mmol) and HOBt (150 mg, 1.1 mmol) were added to a solution of *erythro* 2,3-difluorosuccinic acid **130** (75 mg, 0.5 mmol) in DMF (2 cm^3). A solution of EDC (200 mg, 1.1 mmol) in $CHCl_3$ (2 cm^3) added dropwise at 0 °C. The reaction mixture was stirred at ambient temperature for 24 h. H_2O (10 cm^3) was added and the mixture extracted into ethyl acetate (3 x 10 cm^3). The combined organic extracts were washed with 1N HCl (10 cm^3), saturated sodium bicarbonate solution (10 cm^3), and brine (10 cm^3), dried over $MgSO_4$ and the solvent removed under reduced pressure. The crude product was purified over silica gel (hexane/ethyl acetate 1:1) to give the product as colourless gum (100 mg, 51%), (Found: $M+Na^+$, 403.1650. $C_{16}H_{26}O_6N_2F_2Na$ requires 403.1657, -1.7 ppm); $[\alpha]_D$ – 29.6 (c 1.0, CH_3OH); ν_{max}/cm^{-1} (film) 3420, 2960, 2356, 1739, 1685, 1525, 1437, 1371, 1313, 1270, 1205, 1147, 1053, 1000, 772 and 668; δ_H ($CDCl_3$) 6.8 (2H, m, 2 x NH), 5.4 (2H, m, *J* 48.0 Hz, *J* 25.0 Hz, *J* 12.0 Hz, *J* 1.3 Hz, 2 x CHF), 4.5 (2H, m, NCH), 3.7 (3H, s, OCH_3), 3.7 (3H, s, OCH_3), 2.2 (2H, m, C*H*$(CH_3)_2$), 0.9 (3H, d, *J* 6.9 Hz, CH_3), 0.9 (6H, d, *J* 6.9 Hz, 2 x CH_3), 0.9 (3H, d, *J* 6.9 Hz, CH_3); δ_C ($CDCl_3$) 172.1 (s, CO_2Me), 171.8 (s, CO_2Me), 91.1 (dd, *J* 197.9 Hz, *J* 22.1 Hz), 90.9 (dd, *J* 196.5 Hz, *J* 22.1 Hz), 57.4 (s, NCH), 57.3 (s, NCH), 52.7 (t, OCH_3), 52.6 (s, OCH_3), 31.9 (d, $CH(CH_3)_2$), 31.7 (d, $CH(CH_3)_2$), 19.2 (CH_3), 19.1 (CH_3), 18.2 (CH_3), 18.0 (CH_3); δ_F ($CDCl_3$) –200.6 (m, CHF), -199.0 (m, CHF); ***m/z*** (ESI) 403.00 ($M+Na^+$, 100), 381.04 ($M+H^+$, 40), 349.03 (M-OCH_3, 26), 321.03 (M-CO_2Me, 62).

3.2.24 Preparation of MeO-(*S*)-Leu-2,3-difluorosuccinyl-(S)-LeuOMe

212

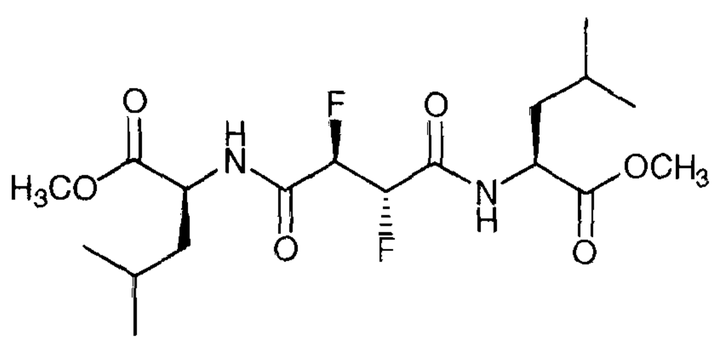

L-leucine methyl ester hydrochloride (200 mg, 1.1 mmol), pyridine (0.1 cm^3, 1.2 mmol) and HOBt (150 mg, 1.1 mmol) was added to a solution of *erythro* 2,3-difluorosuccinic acid **130** (75 mg, 0.5 mmol) in DMF (2 cm^3). A solution of EDC (200mg, 1.1mmol) in $CHCl_3$ (2 cm^3) was added dropwise at 0 °C. The reaction mixture was stirred at ambient temperature for 24 h. H_2O (10 cm^3) was added and the mixture extracted into ethyl acetate (3 x 10 cm^3). The combined organic phases were washed with 1N HCl (10 cm^3), saturated sodium bicarbonate solution (10 cm^3), and brine (10 cm^3), dried over $MgSO_4$ and the solvent removed under reduced pressure. The crude product (ms306) was purified over silica gel (hexane/ethyl acetate 1:1) to give the product as colourless gum (32mg, 16%), (**Found**: M+Na^+, 431.1967. $C_{18}H_{30}O_6N_2F_2Na$ requires 431.1970, -0.6 ppm); $[\alpha]_D$ -44.2 (c 2.0, CH_3OH); ν_{max}/cm^{-1} (film) 3340, 2952, 1740, 1682, 1526, 1436, 1368, 1275, 1200, 1147, 1053, 982, 831, 775 and 668; δ_H ($CDCl_3$) 6.8 (1H, d, *J* 7.9 Hz, NH), 6.7 (1H, d, *J* 8.4 Hz, NH), 5.5-5.2 (2H, m, *J* 47.9 Hz, *J* 48.6 Hz, *J* 25.1 Hz, *J* 23.6 Hz, *J* 11.8 Hz, *J* 1.3 Hz, 2 x CHF), 4.6 (2H, m, 2 x NCH), 3.7 (3H, s, OCH_3), 3.7 (3H, s, OCH_3), 1.6 (2H, m, CH_2), 1.6 (1H, m, C*H*(CH_3)$_2$), 0.9 (3H, d, *J* 3.6 Hz, CH_3), 0.9 (3H, d, *J* 3.6 Hz, CH_3); δ_C ($CDCl_3$) 173.2 (s, CO_2Me), 173.0 (s, CO_2Me), 91.0 (dd, *J* 196.3 Hz, *J* 21.6 Hz), 90.7 (dd, *J* 196.8 Hz, *J* 22.1 Hz), 52.9 (s, NCH), 52.8 (s, NCH), 51.0 (OCH_3), 50.9 (OCH_3), 41.8, 41.7 (CH_2), 25.2 (CH_3), 25.0 (CH_3), 23.1 ($CH(CH_3)_2$), 22.3 CH_3), 22.2 (CH_3); δ_F ($CDCl_3$) –202.1 (m, CHF), -199.6 (m, CHF); ***m/z*** (ESI) 431.04 (M+Na^+, 100), 409.08 (M+H^+, 45), 377.07 (M-OCH_3, 15).

3.2.25 Preparation of (2*S*,3*S*) MeO-(*S*)-Phe-2,3-difluorosuccinyl-(*S*)-PheOMe **214**

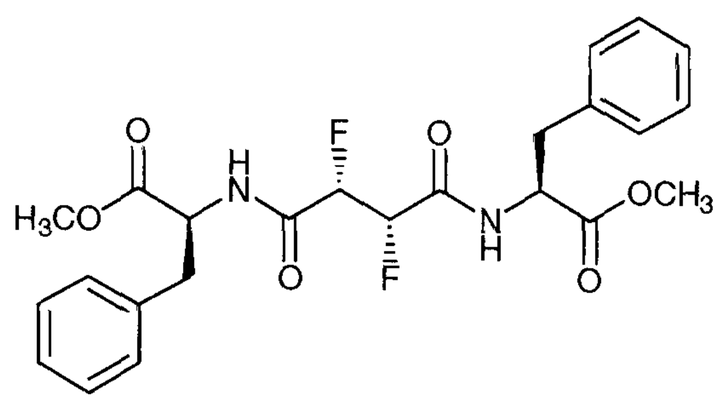

L-phenylalanine methyl ester hydrochloride **213** (0.86 g, 4.0 mmol), and HOBt (0.54 g, 4.0 mmol) were added to a solution of 2,3-difluorosuccinic acids **118** (0.3 g, 2.0 mmol) in DMF (5 cm^3). A solution of EDC (1.0 g, 5.0 mmol) in $CHCl_3$ (5 cm^3) was added dropwise at 0 °C, and the reaction mixture was stirred at ambient temperature for 24 h. H_2O (20 cm^3) was added and the mixture extracted into ethyl acetate (3 x 20 cm^3). The combined organic extracts were washed with 1N HCl (20 cm^3), saturated sodium bicarbonate solution (10 cm^3), and brine (20 cm^3), and the solvent was removed under reduced pressure. The crude product was purified over silica gel (hexane/ethyl acetate 1:1), and the stereoisomers separated by preparative TLC (diethyl ether/dichloromethane 5:1). The title compound gave a white powder, **mp** 76-79 °C, (Found: $M+Na^+$, 499.1673. $C_{24}H_{26}O_6N_2F_2Na$ requires 499.1657); $\mathbf{[\alpha]_D}$ -58.0 (c 1.0, CH_3OH); $\mathbf{\nu_{max}/cm^{-1}}$ (KBr) 3254, 3077, 3023, 1739, 1663, 1558, 1495, 1436, 1343, 1294, 1188, 1130, 1050, 1097, 1001, 743, 692 and 606; $\mathbf{\delta_H}$ ($CDCl_3$) 7.3-7.0 (10H, m, Ar-H), 6.8 (2H, d, J 8.7, NH), 5.3 (2H, AA`XX`, *J* 46.1 Hz, *J* 30.5 Hz, *J* -12.0 Hz, *J* 1.3 Hz, 2 x CHF), 4.9 (2H, m, 2 x CH), 3.7 (6H, s, OCH_3), 3.1 (4H, m, 2 x CH_2Ph); $\mathbf{\delta_C}$ ($CDCl_3$) 171.4 (s, CO_2Me), 164.5 (s, CONH), 164.6 (s, CONH), 135.4 (*ipso*-Ar-C), 129.7, 129.1, 127.7, (Ar-C), 89.8 (dd, *J* 199.6 Hz, *J* 20.5 Hz), 89.5 (dd, *J* 199.0 Hz, *J* 19.9 Hz), 53.5 (s, CH), 53.0 (s, CH), 38.3 (d, $BnCH_2$); $\mathbf{\delta_F}$ ($CDCl_3$) –207.7 (AA`XX`, *J* 44.4 Hz, *J* 32.6 Hz, *J* -12.2 Hz, *J* 2.8 Hz, CHF); ***m/z*** (ESI) 499.04 ($M+Na^+$, 100).

3.2.26 Preparation of (*2R,3R*) MeO-(*S*)-Phe-2,3-difluorosuccinyl-(*S*)-PheOMe **215**

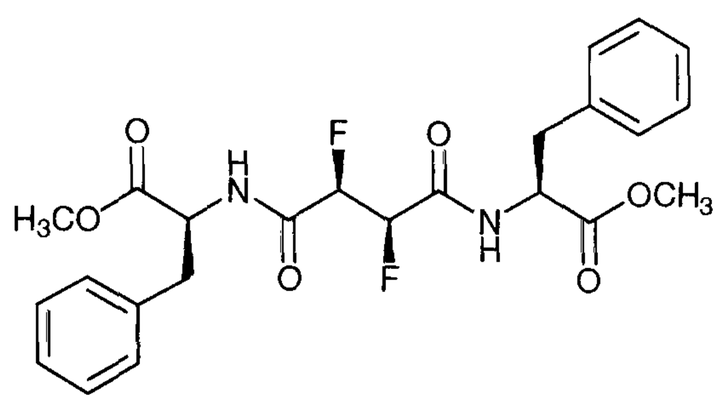

L-phenylalanine methyl ester hydrochloride **213** (0.86 g, 4.0 mmol), and HOBt (0.54 g, 4.0 mmol) were added to a solution of 2,3-difluorosuccinic acids **118** (0.3 g, 2.0 mmol) in DMF (5 cm^3). A solution of EDC (1.0 g, 5.0 mmol) in $CHCl_3$ (5 cm^3) added dropwise at 0 °C, and the reaction mixture stirred at ambient temperature for 24 h. H_2O (20 cm^3) was added and the mixture extracted into ethyl acetate (3 x 20 cm^3). The combined organic phases were washed with 1N HCl (20 cm^3), saturated sodium bicarbonate solution (10 cm^3), and brine (20 cm^3), dried over $MgSO_4$ and the solvent removed under reduced pressure. The crude product was purified over silica gel (hexane/ethyl acetate 1:1), and the stereoisomers separated by preparative thin layer chromatography (diethyl ether/dichloromethane 5:1). The first stereoisomer eluting from the TLC was obtained as a white powder after removal of the solvent, **mp** 126-128 °C, (**Found**: $M+Na^+$, 499.1657. $C_{24}H_{26}O_6N_2F_2Na$ requires 499.1657, -0.8 ppm); $\mathbf{[\alpha]_D}$ + 19.4 (c 1.0, CH_3OH); $\mathbf{\nu_{max}/cm^{-1}}$ (film) 3269, 2951, 2922, 2855, 1749, 1667, 1557, 1537, 1456, 1436, 1249, 1215, 1177, 1128, 1104, 1042, 748, and 700; $\mathbf{\delta_H}$ ($CDCl_3$) 7.2 (6H, m, Ar-H), 7.0 (4H, m, Ar-H), 6.8 (2H, d, *J* 8.7 Hz, NH), 5.3 (2H, AA`XX`, *J* 45.6 Hz, *J* 30.9 Hz, *J* -12.3 Hz, *J* 1.4 Hz, 2 x CHF), 4.8 (2H, m, 2 x CH), 3.7 (6H, s, CH_3), 3.1 (4H, m, 2 x CH_2Ph); $\mathbf{\delta_C}$ ($CDCl_3$) 171.3 (s, CO_2Me), 165.6 (s, CONH), 164.6 (s, CONH), 135.6 (q, Ar-C), 129.5, 129.2, 127.8, (t, Ar-C), 89.4 (dd, *J* 200.1 Hz, *J* 21.0 Hz), 89.2 (dd, *J* 199.6 Hz, *J* 20.5 Hz), 53.5 (s, CH), 53.0 (s, CH), 38.2 (d, $BnCH_2$); $\mathbf{\delta_F}$ ($CDCl_3$) –207.7 (AA`XX`, CHF); ***m/z*** (ESI) 499.03 ($M+Na^+$, 100).

3.2.27 Preparation of *(2S,3S)* HO-(*S*)-Phe-2,3-difluorosuccinyl-(*S*)-PheOH **217**

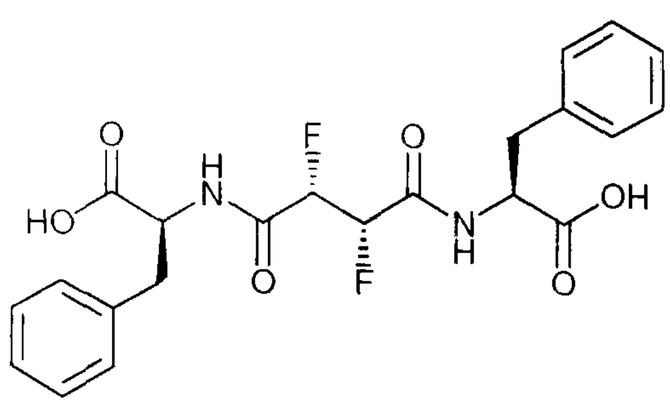

A solution of diester **214** (78 mg, 0.2 mmol) in acetone (2 cm^3) and 2N HCl (2 cm^3) was heated under reflux for 48 h. The solvent was removed with a continuos stream of air and the crystalline residue washed with H_2O (1 cm^3). Recrystallisation from acetone/CCl_4 gave the product as white crystals, **mp** 162-164 °C, (Found: M+Na^+, 471.1341. $C_{22}H_{22}O_6N_2F_2Na$ requires 471.1344, -0.6 ppm); $[\alpha]_D$ –18.2° (c 1.0, CH_3OH); ν_{max}/cm^{-1} (KBr) 3415, 3320, 3032, 1725, 1677, 1542, 1222, 1192, 1118, 1055, 816, 739, and 701; δ_H (CD_3CN) 7.3-7.1 (10H, m, Ar-H), 5.2 (2H, AA`XX`, *J* 44.9 Hz, *J* 31.8 Hz, *J* -12.0 Hz, *J* 1.0 Hz, 2 x CHF), 4.6 (2H, m, 2 x CH), 3.1 (4H, m, 2 x CH_2Ph); δ_C (CD_3CN) 170.9 (s, COOH), 165.2 (m, CONH), 136.2 (Ar-C), 129.0, 128.1, 126.5, (Ar-C), 89.1 (dd, *J* 197.4 Hz, *J* 19.9 Hz), 88.9 (dd, *J* 197.4 Hz, *J* 19.9 Hz), 52.8 (s, CH), 36.1 (d, $PhCH_2$); δ_F (CD_3CN) –208.7 (m, CHF); ***m/z*** (ESI) 471.06 (M+Na^+, 100), 463.10 (M+H^+, 90).

3.2.28 Preparation of (*2R,3S*) HO-(*S*)-Phe-2,3-difluorosuccinyl-(*S*)-PheOH **218**

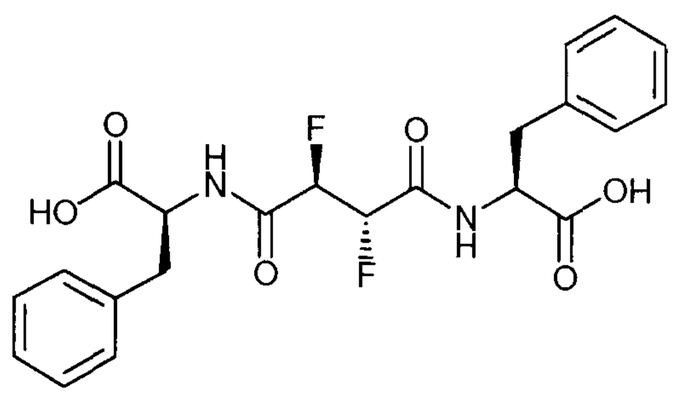

A solution of diester **210** (120 mg, 0.26 mmol) in acetone (2 cm^3) and 2N HCl (2 cm^3) was heated under reflux for 24 h. The solvent was removed with a continuos stream of air and the residue was washed with H_2O (1.0 cm^3) to give a yellow solid. Recrystallisation from hot $CHCl_3$ gave the product as a white solid, **mp** 134-138 °C (Found: C, 58.65; H, 4.93; N, 6.29. $C_{22}H_{22}O_6N_2F$ requires: C, 58.93; H, 4.94; N, 6.25%); (**Found**: M-H^+, 447.1371. $C_{22}H_{21}O_6N_2F_2$ requires 447.1368, 0.6 ppm); $[\alpha]_D$ + 65.6° (c 0.5, CH_3OH); ν_{max}/cm^{-1} (KBr) 3051, 2937, 2542, 1737, 1680, 1534, 1498, 1451, 1410, 1337, 1223, 1192, 1119, 1099, 1068, 1031, 834, 735 and 699; δ_H (CD_3CN) 7.4-7.2 (10H, m, Ar-H), 5.5-5.2 (2H, m, *J* 47.4 Hz, *J* 24.1 Hz, *J* -12.3 Hz, *J* 1.3 Hz, 2 x CHF), 4.7 (2H, m, CH), 3.3-3.0 (4H, m, CH_2Ph; δ_C (CD_3CN) 170.9 (s, COOH), 170.8 (s, COOH), 136.4 (Ar-C), 136.3 (Ar-C), 129.1, 128.9, 128.1, 128.0, 126.5, 117.0 (Ar-H), 89.9 (dd, *J* 191.3 Hz, *J* 18.2 Hz, CHF), 89.7 (dd, *J* 194.6 Hz, *J* 21.0 Hz, CHF), 52.8, 52.7 (CH), 36.2 (CH_2Ph), 36.1 (CH_2Ph); δ_F (CD_3CN) –201.8 (m, CHF), –202.3 (m, CHF); *m/z* (ESI) 447 (M-H, 100).

3.2.29 Preparation of (*2R,3R*) HO-(*S*)-Phe-2,3-difluorosuccinyl-(*S*)-PheOH **219**

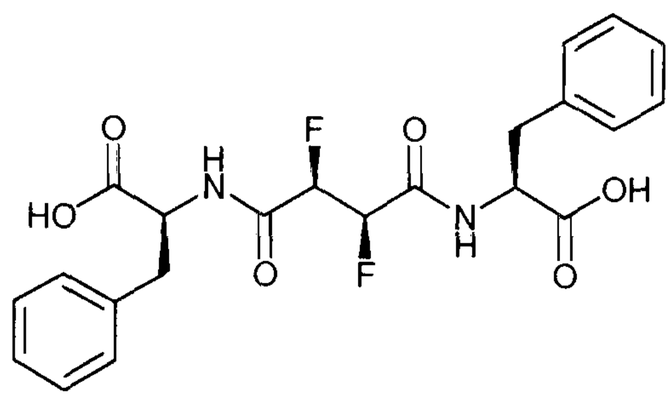

A solution of diester **215** (75 mg, 0.2 mmol) in acetone (2 cm^3) and 2N HCl (2 cm^3) was heated under reflux for 48 h. The solvent was removed with a continuous stream of air and the residue washed with H_2O (1 cm^3). Recrystallisation from hot $CHCl_3$ gave the product as brownish crystals, **mp** 118-122 °C, (Found: M+Na^+, 471.1364. $C_{22}H_{22}O_6N_2F_2Na$ requires 471.1344, 4.4 ppm); $[\alpha]_D$ +31.5° (c 1.0, CH_3OH); ν_{max}/cm^{-1} (KBr) 3400.7, 2959, 2924, 2851, 1732, 1682, 1538, 1456, 1378, 1262, 1216, 1134, 1108, 1051, and 811; δ_H (CD_3CN) 7.1 (10H, m, Ar-H), 5.3 (2H, AA`XX`, *J* 45.6 Hz, *J* 31.1 Hz, *J* -10.0 Hz, *J* 2.5 Hz, 2 x CHF), 4.6 (2H, m, 2 x CH), 3.1 (4H, m, 2 x CH_2Ph); δ_C (CD_3CN) 171.3 (s, COOH), 165.3 (dd, *J* 24.0 Hz, *J* 2.1 Hz, CONH), 165.2 (dd, *J* 20.0 Hz, *J* 10.0 Hz, CONH), 136.8 (Ar-C), 129.4, 128.5, 127.0, (Ar-C), 89.5 (dd, *J* 196.8 Hz, *J* 19.6 Hz), 89.2 (dd, *J* 196.8 Hz, *J* 19.6 Hz), 53.3 (s, CH), 53.2 (s, CH), 36.6 (d, $PhCH_2$); δ_F (CD_3CN) –208.8 (m, CHF); ***m/z*** (ESI) 471.04 (M+Na^+, 24), 242 (M-Phe-CO_2, 100).

3.2.30 Preparation of MeO-(*S*)-Phe-succinyl-(*S*)-PheOMe **221**

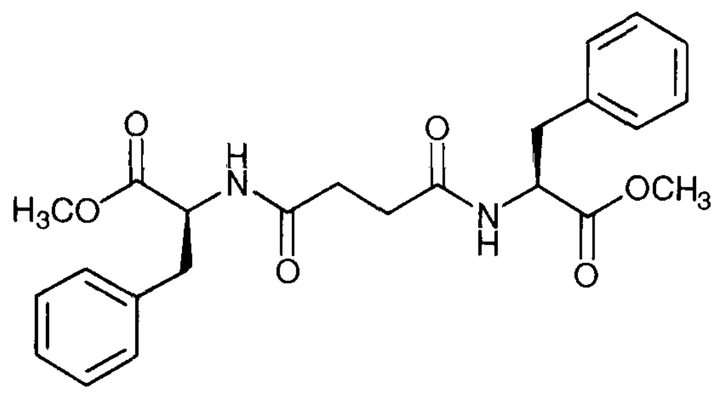

L-Phenylalanine hydrochloride **213** (6.9 g, 32 mmol) and HOBt (4.3 g, 32 mmol) was addad to a solution of succinic acid **87** (1.87 g, 16 mmol) in DMF (32 cm^3). The mixture was stirred until homogeneous and then a solution of EDC (6.1g, 32mmol) in $CHCl_3$ was added dropwise at 0 °C. The reaction mixture was stirred at ambient temperature for 16 h. The reaction was quenched with H_2O (100 cm^3) and the mixture extracted into ethyl acetate (3 x 50 cm^3). The combined organic extracts were washed with 1N HCl (50 cm^3), saturated sodium bicarbonate solution (50 cm^3), and brine (50 cm^3), dried over $MgSO_4$ and removed under reduced pressure to give the crude product as yellow oil (3.5 g, 50%). Purification over silica gel (hexanes/diethyl ether/ethyl acetate 1:5:1) afforded the title compound as white solid, **mp** 177-179 °C (Found: M+Na^+, 463.1831. $C_{24}H_{28}O_6N_2Na$ requires 463.1845, -3.1); $[\alpha]_D$ + 2.7 (c 1.0, CH_3OH); ν_{max}/cm^{-1} (KBr) 3313, 3064, 3030, 2952, 1739, 1644, 1538, 1436, 1353, 1279, 1212, 1177, 1031, 748, 701, 562, 531 and 497; δ_H ($CDCl_3$) 7.4-7.1 (10H, m, Ar-H), 6.5 (1H, m, NH), 4.9 (2H, m, 2 x CH), 3.7 (3H, s, CH_3), 3.2-3.0 (4H, m, 2 x CH_2Ph), 2.5 (4H, s, 2 x CH_2); δ_C ($CDCl_3$) 172.1 (s, CO_2Me), 171.7 (s, CONH), 135.9 (Ar-C), 129.2, 128.6, 127.1 (Ar-C), 53.4 (CH), 52.3 (OCH_3), 37.8 (CH_2Ph), 31.4 (CH_2); ***m/z*** (ESI) 463.08 (M+Na^+).

3.2.31 Preparation of HO-(S)-Phe-succinyl-(S)-PheOH **222**

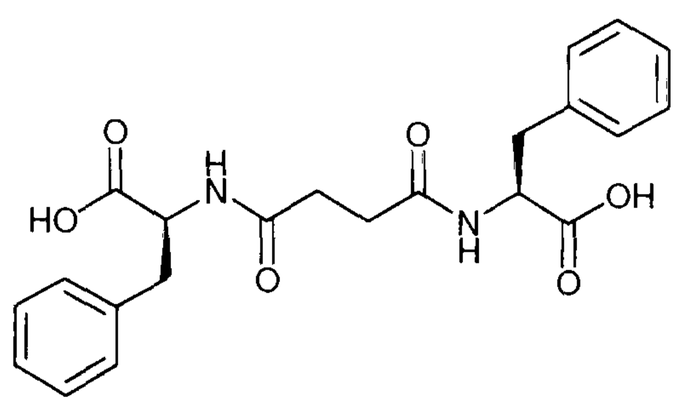

A solution of the diester **221** (600 mg, 1.4 mmol) in acetone (5 cm^3) and 1N HCl (5 cm^3) was heated under reflux for 24 h. The solvent was removed with a continuous stream of air and the residue washed with H_2O (1 cm^3). Recrystallisation in acetonitrile gave the product as white crystals, **mp** 188-190 °C (**Found**: $M+Na^+$, 435.1533. $C_{22}H_{24}O_6N_2Na$ requires 435.1532, 0.1 ppm); $[\alpha]_D$ +22.5 (c 1.0, CH_3OH); ν_{max}/cm^{-1} (KBr) 3349, 3069, 3029, 2943, 2602, 2549, 1725, 1656, 1613, 1533, 1496, 1455, 1352, 1218, 1192, 1117, 738, 701, 539 and 491; δ_H (CD_3OD) 7.3-7.2 (10H, m, Ar-H), 4.6 (2H, m, 2 x CH), 3.2-2.9 (4H, m, $PhCH_2$), 2.4 (4H, s, 2 x CH_2); δ_C (CD_3OD) 174.7 (s, CO_2H), 174.4 (s, CONH), 138.4 (Ar-C), 130.3, 129.4, 127.8 (Ar-C), 55.1 (CH), 38.4 (CH_2Ph), 32.0 (CH_2); ***m/z*** (ESI) 435.08 ($M+Na^+$, 100).

3.2.32 Preparation of (2R,3S) MeO-(S)-Ala-(S)-Phe-2,3-difluorosuccinyl-(S)-Phe-(S)-AlaOMe **224**

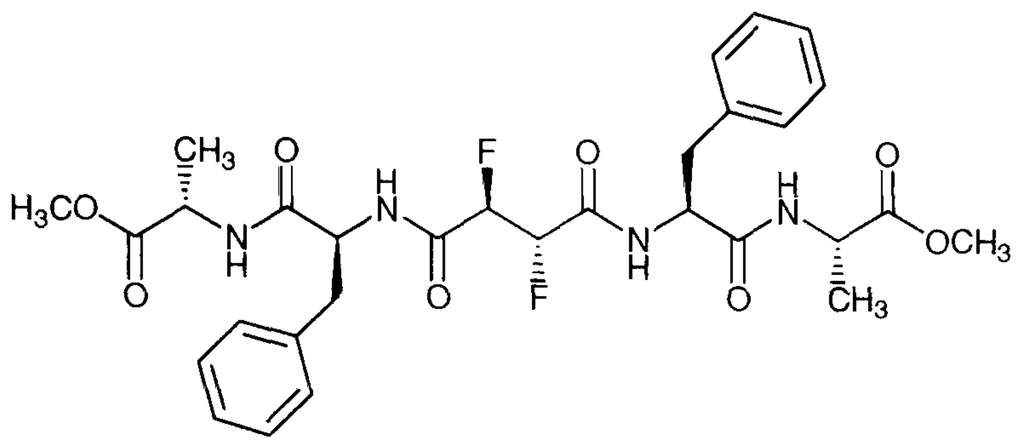

L-alanine methyl ester hydrochloride **223** (140 mg, 1.0 mmol) and HOBt (135.0 mg, 1.0 mmol) was added to a solution of diacid **218** (20 mg, 0.45 mmol) in DMF (2 cm^3). The mixture was stirred for 10 min and then a solution of EDC (192 mg, 1.0 mmol) in $CHCl_3$ (2 cm^3) was added at 0 °C. The reaction was stirred at ambient temperature for 12 h. H_2O (10 cm^3) was added and the mixture extracted into ethyl acetate (3 x 10 cm^3). The combined organic extracts were washed with 1N HCl (10 cm^3), saturated sodium bicarbonate solution (10 cm^3), and brine (10 cm^3), dried over $MgSO_4$ and the solvent removed under reduced pressure. The crude product was purified by preparative TLC (diethyl ether) to give the product as white solid, **mp** 158-159 °C (**Found**: M+Na^+, 619.2573 $C_{30}H_{37}O_8N_4F_2$ requires 619.2579, -1.0 ppm); $\mathbf{[\alpha]_D}$ – 43.8 (c 0.5, CH_3OH); $\mathbf{\nu_{max}/cm^{-1}}$ 3299, 3279, 1735, 1658, 1550, 1524, 1451, 1436, 1379, 1337, 1300, 1202, 1145, 1094, 1057, 746, 701, 637 and 502; $\mathbf{\delta_H}$ ($CDCl_3$) 7.4 (1H, d, *J* 7.4 Hz, NH), 7.3 (1H, m, NH), 7.3-7.1 (10H, m, Ar-H), 6.4 (1H, dd, *J* 8.4 Hz, *J* 3.3 Hz, NH), 6.3 (1H, d, *J* 7.2 Hz, NH), 5.5-5.2 (1H, ddd, *J* 47.1 Hz, *J* 28.2 Hz, *J* -12.0 Hz, *J* 1.3 Hz, CHF), 5.3-5.0 (1H, ddd, *J* 49.4 Hz, *J* 20.0 Hz, *J* 12.0 Hz, *J* 1.3 Hz, CHF), 4.7 (1H, m, CHMe), 4.6-4.4 (3H, m, 2 x CHBn, CHMe), 3.7 (3H, s, OCH_3), 3.6 (3H, s, OCH_3), 3.2 (2H, m, CH_2Ph), 3.2 (2H, m, CH_2Ph), 1.3 (3H, d, *J* 7.2 Hz, $CHCH_3$), 1.3 (3H, d, *J* 7.2 Hz, $CHCH_3$); $\mathbf{\delta_C}$ ($CDCl_3$) 173.00 (COPhe), 172.8

(COPhe), 169.5 (CO_2Me), 169.0 (CO_2Me), 164.6 (m, 2 x COCHF), 136.1, 136.0, 129.3, 129.3, 128.9, 128.6, 127.3, 127.1 (Ar-C), 90.8 (dd, *J* 198.3 Hz, *J* 21.8 Hz), 90.2 (dd, *J* 198.3 Hz, *J* 21.8 Hz), 54.9 (AlaCH), 53.4 (AlaCH), 53.4 (AlaCH), 52.6 (CHPhe), 52.4 (CHPhe), 48.4 (OCH_3), 48.2 (OCH_3), 38.1 (CH_2Ph), 36.9 (CH_2Ph), 18.1 ($AlaCH_3$), 17.6 ($AlaCH_3$); δ_F ($CDCl_3$) –198.2 (m, CHF), -202.1 (m, CHF); ***m/z*** (ESI) 619.26 ($M+H^+$, 95), 587.23 (M^+-OMe, 54), 559.24 (M^+-CO_2CH_3, 26), 516.20 (M^+-AlaOMe, 62), 488.20, (M^+-COAlaOMe, 100).

3.2.33 Preparation of Boc-(S)-Phe-(S)-AlaOMe **230**

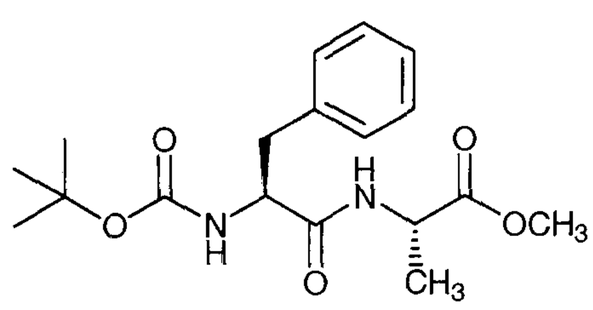

NMM (2.0 cm^3) was added to a solution of Boc-PheOH (4.85 g, 18.28 mmol) in dry THF (40 cm^3), followed by ethyl chloroformate (1.74 cm^3, 20 mmol) at –10 °C. The solution was stirred for 15 min, and then a suspension of L-alanine methyl ester hydrochloride (2.8 g, 20 mmol) in THF (80 cm^3), previously neutralised with NMM (2 cm^3), was added. The reaction was stirred at ambient temperature for 12 h and then diluted with ethyl acetate (50 cm^3). The organic phase was washed with 1N HCl (3 x 20 cm^3), $NaHCO_3$ (3 x 20 cm^3) and brine, dried over $MgSO_4$ and the solvent removed by evaporation to give the product as a white solid (5.91g, 91%), **mp** 104-105 °C (lit.[6], 108-109 °C); (**Found**: C, 61.76; H, 7.74; N, 7.98. $C_{18}H_{26}N_2O_5$ requires: C, 61.70; H, 7.48; 7.99 N%); $[\alpha]_D$ – 3.9° (c 1.0, CH_2Cl_2); ν_{max} /cm^{-1} (KBr) 3334, 3064, 3029, 2987, 2951, 1754, 1695, 1654, 1542, 1446, 1388, 1368, 1171, 1051, 1026, 990, 861, 757, 717, 702, 670 and 574; δ_H ($CDCl_3$) 7.3-7.1 (5H, m, Ar-*H*), 6.5 (1H, d, Ala-

NH), 5.0 (1H, d, Phe-NH), 4.5 (1H, m, Ala-CH), 4.3 (1H, m, Phe-CH), 3.6 (3H, s, OCH_3), 3.0 (1H, d, *J* 6.1 Hz, Ph-CH_2), 1.4 (9H, s, $C(CH_3)_3$), 1.3 (3H, d, *J* 7.2 Hz, Ala-CH_3); δ_C ($CDCl_3$) 173.3 (d, COOMe), 171.2 (CONH), 136.9, 129.8, 129.0, 127.3 (Ar-C), 56.0 (Phe-CH), 52.8 (OCH_3), 48.5 (Ala-CH), 38.8 (Phe-CH_2), 28.6 ($C(CH_3)_3$) and 18.8 (Ala-CH_3); ***m/z*** (ESI+ve) 373.169 ($M+Na^+$).

3.2.34 Preparation of Boc-(*S*)-Phe-(*S*)-Ala-(*S*)-ValOMe **232**

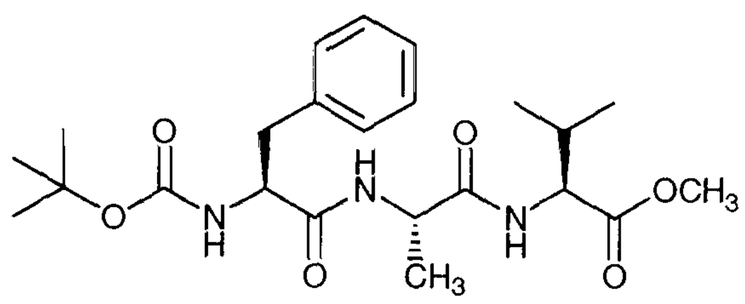

An aqueous solution of NaOH (10 mmol, 10 cm^3) was added to a solution of Boc-Phe-AlaOMe (3.5 g, 10 mmol) in MeOH (30 cm^3) at 0 °C. The mixture was stirred for 2 h at 0 °C. The mixture was concentrated in *vacuo* to obtain the sodium salt, which was recrystallised in acetone prior to use. The aminoester (1.75 g, 10.4 mmol) and HOBt (1.35 g, 10 mmol) were added to a suspension of the sodium salt in DMF (20 cm^3). A solution of EDC (2.0 g, 10.4 mmol) in $CHCl_3$ (20 cm^3) was then added dropwise at 0 °C. The reaction mixture was stirred at ambient temperature for 12 h and then quenched with H_2O (40 cm^3). The mixture was extracted into ethyl acetate (2 x 50 cm^3) and the combined organic phases were washed with 1N HCl (3 x 20 cm^3), $NaHCO_3$ (3 x 20 cm^3), dried over $MgSO_4$ and the solvent removed under reduced pressure to give the crude product as a white solid (2.0 g, 44%), **mp** 82-85 °C; (**Found**: $M+Na^+$, 472.2425 $C_{23}H_{35}O_6N_3$ requires 472.2424, 0.3 ppm); $[\alpha]_D$ – 19.8° (c 1.0, CH_2Cl_2); ν_{max} /cm^{-1} (KBr) 3305, 3032, 2976, 1746, 1649, 1528, 1455, 1392, 1367, 1252, 1168, 1079, 1022, 859, 747 and 700; δ_H ($CDCl_3$) 7.3-7.1 (5H, m, Ar-*H*), 6.9 (1H, d, NH), 6.7 (1H, d, NH), 5.1 (1H, d, NH), 4.5 (1H, m, Phe-CH), 4.4 (1H, m,

Val-CH), 4.3 (1H, m, Ala-CH), 3.7 (3H, s, OCH_3), 3.0 (1H, m, Ph-CH_2), 2.1 (1H, m, $CH(CH_3)_2$), 1.4 (9H, s, $C(CH_3)_3$), 1.3 (3H, d, J 22.0 Hz, Ala-CH_3), 0.9 (6H, m, Val-CH_3); δ_C ($CDCl_3$) 172.6, 172.3, 171.7 (CONH), 136.8, 129.7, 129.0, 127.4 (Ar-C), 57.7 (Val-CH), 55.9 (OCH_3), 52.6 (Ala-CH), 49.3 (Phe-CH), 38.7 (Ph-CH_2), 31.5 ($CH(CH_3)_2$), 28.6 ($C(CH_3)_3$, 19.4, 18.8, 18.2 (3 x CH_3); ***m/z*** (ESI+ve) 472.223 ($M+Na^+$), 450.210 ($M+H^+$).

3.2.35 Preparation of Boc-(*S*)-Val-(*S*)-LeuOMe **240**

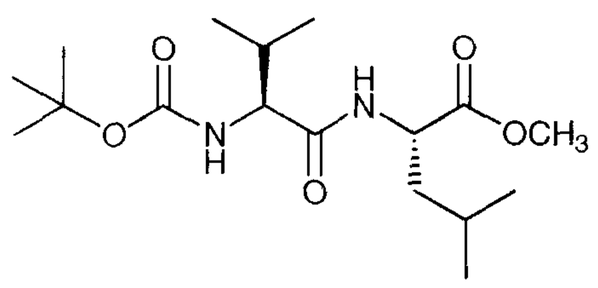

NMM (0.5 cm^3) was added to a solution of Boc-ValOH (1.085 g, 5.0 mmol) in dry THF (20 cm^3). Ethyl chloroformate (0.48 cm^3, 5.5 mmol) was then added dropwise at –10 °C and the solution stirred for 15 min. A suspension of L-leucine methyl ester hydrochloride (1.0 g, 5.5 mmol) in THF (20 cm^3), previously neutralised with NNM (0.5 cm^3) was added and the reaction stirred at ambient temperature for 12 h. The reaction mixture was diluted with ethyl acetate (50 cm^3), washed with 1N HCl (3 x 20 cm^3), $NaHCO_3$ (3 x 20 cm^3), dried over $MgSO_4$ and the solvet removed under reduced pressure to give the product as a white solid (1.09g, 63%), **mp** 119-121 °C (lit.,[7] 121-124 °C); (Found: $M+Na^+$, 367.2206 $C_{17}H_{32}N_2O_5Na$ requires: 367.2209, -0,8 ppm); $[\alpha]_D$ – 26.6° (c 1.0, CH_2Cl_2); ν_{max} /cm^{-1} (KBr) 3352, 3279, 3082, 2961, 1760, 1687, 1652, 1553, 1521, 1438, 1392, 1367, 1298, 1253, 1162, 1093, 1043, 1016, 985, 880, 794, 736 and 625; δ_H ($CDCl_3$) 6.4 (2H, d, N*H*), 5.1 (1H, d, BocNH), 4.6 (1H, m, LeuCH), 3.9 (1H, m, ValCH), 3.7 (3H, s, OMe), 2.1 (1H, m, $CH(CH_3)_2$), 1.7 (2H, m, $CH_2CH(CH_3)_2$), 1.6 (1H, m, $CH_2CH(CH_3)_2$), 1.5 (9H, s, $C(CH_3)_3$), 0.9 (12H, m, 2 x

$CH(CH_3)_2$); δ_C ($CDCl_3$) 173.6, 171.9, 156.0 (CONH), 60.3 (Val-CH), 52.7 (OCH_3), 51.0 (Leu-CH), 41.8 (Leu-CH_2), 31.2, 28.7 ($C(CH_3)_3$, 25.1, 23.2, 22.2, 19.6; ***m/z*** (ESI+ve) 367.059 ($M+Na^+$).

3.2.36 Preparation of diethyl (*R,R*)-2,3-bismethanesulfonyloxysuccinate **258**

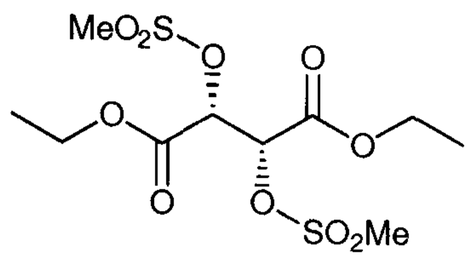

Methanesulfonyl chloride (0.4 cm^3, 5 mmol) was added to a solution of L-(+)-diethyl-tartrate **257** (5 mmol) and DMAP (80 mg, 0.5 mmol) in dry dichloromethane (10 cm^3) dropwise at 0 °C. The reaction mixture was stirred at ambient temperature for 72 h and then quenched into ice water (10 cm^3). The mixture was extracted into ethyl acetate (2 x 20 cm^3). The combined organic extracts were washed with saturated $NaHCO_3$ solution (15 cm^3), 1N HCl (15 cm^3) and brine (10 cm^3), dried over $MgSO_4$ and the solvent was removed under reduced pressure. Purification over silica gel (ethyl acetate/hexane 1:3) afforded the product as colourless oil (50 mg, 7 %), **mp** 91-93 °C (lit.,[8] 88-90 °C); δ_H ($CDCl_3$) 5.6 (2H, s, 2 x CH), 4.3 (4H, q, *J* 7.2 Hz, OCH_2), 3.2 (6H, s, CH_3), and 1.3 (6H, t, *J* 7.2 Hz, 2 x CH_3); δ_C ($CDCl_3$) 165.2 (C=O), 76.8 (2 x CH), 63.9 OCH_2CH_3, 40.0 (OSO_2CH_3), and 14.3 OCH_2CH_3; ***m/z*** (EI) 289 (M^+, 10%), 243 (7), 217(5), 193 (33), 175 (35), 149 (52), 97 (100) and 79 (100).

The main product was *diethyl 2-Methanesulfonyloxy-but-2-enedioate*, which eluted in the first fraction of the column, δ_H ($CDCl_3$) 6.75 (1H, s, CH), 4.3 (4H, q, *J* 7.2 Hz, OCH_2), 3.2 (6H, s, CH_3) and 1.3 (6H, t, *J* 7.2 Hz, 2 x CH_3); m/z (EI) 221 (30), 193 (100), 165(40), 125 (31), 115 (82), 97 (81) and 69 (100).

3.2.37 Preparation of diethyl *(R,R)-2,3*-difluorosuccinate **260**

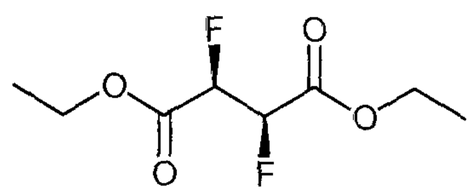

Deoxofluor™ **250** (2.0 cm^3) was added to a solution of diethyl (*2R,3S*)-2-fluoro-3-hydroxysuccinate **277** (440 mg, 2.1 mmol) in dry dichloromethane (4.0 cm^3) under nitrogen at –78 °C. The mixture left stirring until ambient temperature, and then heated at 80 °C for 12 h. The reaction mixture was cooled to room temperature, diluted with diethyl ether (10 cm^3) and cold 10% aqueous bicarbonate solution (10 cm^3). The mixture was stirred vigorously until gas evolution had ceased (10-30 min). The phases were separated and the organic layer washed with 2N hydrochloric acid (10 cm^3), saturated sodium bicarbonate solution (10 cm^3), and brine (10 cm^3). The solvent was dried with $MgSO_4$ and then removed under reduced pressure to afford the product as a yellow oil (190mg, 43%). The compound was purified over silica gel (hexane/CH_2Cl_2 10:1) to give the title compound as a clear colourless liquid, (**Found**: MH^+, 211.07866. $C_8H_{13}O_4F_2$ requires MH, 211.078191 (ppm)); $\mathbf{[\alpha]^{20}_D}$ -12.2 (c 1.0, CH_2Cl_2); $\mathbf{\nu_{max}}$ /cm^{-1} (film) 2988, 2944, 2913, 1771, 1746, 1470, 1397, 1374, 1285, 1213, 1080, 1019, 858, 702 and 599; $\mathbf{\delta_H}$ ($CDCl_3$) 5.35 (2H, AA'XX', *J* 45.9 Hz, *J* 28.8 Hz, *J* -9.8 Hz, *J* 1.9 Hz, 2 x C*H*F), 4.34 (4H, q, *J* 7.2 Hz, 2 x OCH_2) and 1.34 (6H, t, *J* 7.2, 2 x OCH$_2$CH_3); $\mathbf{\delta_C}$ ($CDCl_3$) 87.7 (*J* 197.4 Hz, *J* 21.3 Hz, 2 x CH*F*), 63.1 (OCH_2) and 14.4 OCH$_2$CH_3; $\mathbf{\delta_F}$ ($CDCl_3$) –207.1 (AA'XX', *J* 45.9 Hz, *J* 28.8 Hz, *J* -9.8 Hz, *J* 1.9 Hz, 2 x CH*F*); ***m/z*** (EI): 210 (1), 183 (14), 165 (31), 137 (100), 117 (8), 109 (11), 90 (78), 73 (43), 45 (30) and 29 (95).

3.2.38 Preparation of diethyl (*2R,3R*)-3-acetoxy-2-bromosuccinate **274**

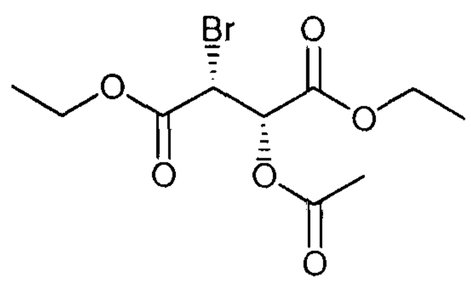

A solution of HBr (30 %) in glacial acetic acid (34 cm^3) was added to stirred and ice-cooled L-(+)-diethyl tartrate **257** (11.6 g, 56.0 mmol). The mixture was stirred for 4 h in the dark at ambient temperature. Ice water (20 cm^3) was added and the solution was extracted with diethyl ether (2 x 20 cm^3). The combined organic extracts were washed with saturated brine (20 cm^3), dried over $MgSO_4$ and evaporated under reduced pressure to give diethyl (*2R,3R*)-3-acetoxy-2-bromosuccinate as a pale yellow oil (10.5 g, 61 %), **bp** 159-170 °C (1.0 Torr), lit.,[9] 145-150°C (0.5 Torr); $\mathbf{[\alpha]^{20}_D}$ **-6.60** (c 2.5, CH_2Cl_2); $\mathbf{\nu_{max}/cm^{-1}}$ (film) 2986, 1756, 1468, 1447, 1373, 1269, 1025, 936; δ_H ($CDCl_3$) 5.6 (1H, d, *J* 5.4 Hz, CHBr), 4.8 (1H, d, *J* 5.4 Hz, CHOR, 4.3 (4H, q, *J* 7.2 Hz, OCH_2), 2.2 (3H, s, CH_3COO) and 1.3 (3H, t, *J* 7.2 Hz, 2 x CH_3; δ_C ($CDCl_3$) 73.1 *C*HOR); 63.4 O*C*H_2CH_3, 62.7 (O*C*H_2CH_3), 44.3 CHBr, 20.8 *C*H_3CO), 14.4 CH_3 and 14.3 CH_3; ***m/z*** (CI-CH_4) 194 (MH^+), 151 (100), 149 (46), 133 (48), 95 (48), 93 (79), 81 (66), 79 (54), 67 (48), 55 (62) and 43 (72).

3.2.39 Preparation of diethyl (*2R,3R*)-2-bromo-3-hydroxysuccinate **275**

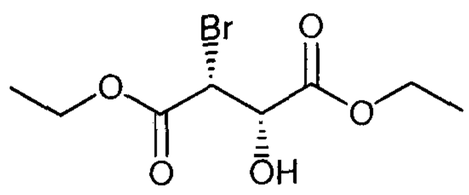

HBr (30 %) in glacial acetic acid (3 cm^3) was added to a solution of diethyl (*R,R*)-2-bromo-3-acetoxy-succinate **274** (10.5 g) in dry ethanol (9 cm^3). The solution was

heated under reflux for 4 h and the solvent then removed under reduced pressure. The residue was purified by distillation to give diethyl (*2R,3R*)-2-bromo-3-hydroxysuccinate as a colourless oil (6.9 g, 76 %), **bp** 144 °C (1.0 Torr), $\mathbf{[\alpha]^{20}_D}$ –27.4 ° (c 1.0, CH_2Cl_2); lit.,[10] $[\alpha]^{20}_D$ -29.9° (c 4.51, $CHCl_3$), $\mathbf{\nu_{max}/cm^{-1}}$ (film) 3482, 2984, 1738, 1631, 1468, 1446, 1371, 1025 and 860; $\mathbf{\delta_H}$ ($CDCl_3$) 4.8 (1H, d, *J* 3.9 Hz, CHF); 4.77 (1H, dd, *J* 7.7 Hz, *J* 3.9 Hz, C*H*OH); 4.5-4.3 (4H, m, OCH_2) and 1.4 (t, *J* 7.2 Hz, 6H, CH_3); $\mathbf{\delta_C}$ ($CDCl_3$) 170.7 (C=O), 167.0 (C=O), 72.9 (CHOH); 63.3 (OCH_2), 63.0 (OCH_2), 48.2 (CHBr), 14.44 (OCH_2CH_3) and 14.33 (OCH_2CH_3); ***m/z*** (EI) 197 (100) 195 (100), 169 (57), 167 (57), 71 (86) and 43 (24).

3.2.40 Preparation of diethyl (*2S,3R*)-epoxysuccinate **276**

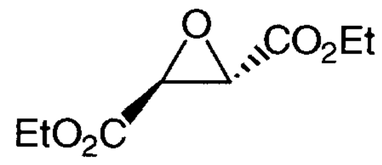

A solution of diethyl (*2R,3R*)-2-bromo-3-hydroxysuccinate **275** (2.63 g, 9.8 mmol) in dry ethanol (2.3 cm^3) was added dropwise to a solution of sodium ethoxide, prepared from sodium (0.28 g, 12 mmol) and dry ethanol (6.6 cm^3) at 0 °C. The reaction was stirred at ambient temperature for 1 h, then neutralised with acetic acid and concentrated under reduced pressure. The residue was taken up in ice-water (10 cm^3) and the solution was extracted into diethyl ether (3 x 30 cm^3). The combined ether extracts were washed with saturated brine (10 cm^3), dried over $MgSO_4$ and the solvent removed under reduced pressure to give the product as a pale yellow oil (1.4 g). Purification over silica gel (hexane/ethyl acetate 9:1) afforded the product as a colourless oil (1.0 g, 56 %), **bp** 135 °C (0.5 Torr), $\mathbf{[\alpha]^{20}_D}$ –76.1 (c 0.89, diethyl ether), (lit.[11], $[\alpha]^{20}_D$ -105.5 (c 1.41, diethyl ether); $\mathbf{\nu_{max}/cm^{-1}}$ 3510, 2985, 1736, 1657, 1468,

1448, 1394, 1372, 1031, 964; δ_H ($CDCl_3$) 4.28 (4H, q, *J* 7.2 Hz, 2 x OCH_2); 3.67 (2H, s, 2 x CH) and 1.32 (6H, t, *J* 7.2 Hz, CH_3); δ_C ($CDCl_3$) 167.2 (C=O); 62.7 OCH_2; 52.4 CH and 14.4 OCH_2CH_3; ***m/z*** (CI-CH_4) 194 (MH^+), 151 (100), 149 (46), 133 (48), 95 (48), 93 (79), 81 (66), 79 (54), 67 (48), 55 (62) and 43 (72).

3.2.41 Preparation of diethyl (*2S,3R*)-2-fluoro-3-hydroxysuccinate **277**

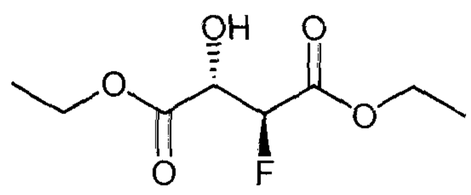

A solution of TBAF in dry THF (20 cm^3) was added to a solution of the cyclic sulfate **297** (9.8 g, 36.5 mmol) in dry THF (40 cm^3) at 0 °C. The reaction mixture was stirred for 2 h at ambient temperature. H_2O (0.2 cm^3) and H_2SO_4 (1.0 cm^3) were added at 0 °C and the reaction mixture stirred vigorously for 2 h. The reaction mixture was concentrated to one third of its volume, then quenched with water (20 cm^3), and the mixture extracted into ethyl acetate (3 x 50 cm^3). The combined organic extracts were washed with saturated $NaHCO_3$ solution (20 cm^3), 1N HCl (20 cm^3), and brine (20 cm^3), dried over $MgSO_4$ and the solvent removed under reduced pressure to give the crude product as a colourless oil (6.85g, 87%), **bp** 133 °C (1 Torr), lit.,[12] 144-146 °C (16 Torr), (**Found**: MH^+, 209.0834. $C_8H_{14}O_5F$ requires MH, 209.0825); $[\alpha]^{20}_D$ -10.8 (c 1.0, CH_2Cl_2); ν_{max}/cm^{-1} (film) 3489, 2987, 1752, 1461, 1377, 1028, 950; δ_H ($CDCl_3$) 5.24 (1H, dd, *J* 47.0 Hz, *J* 2.3 Hz, CHF); 4.70 (1H, dd, *J* 23.5 Hz, *J* 2.0 Hz, C*H*OH); 4.30 (4H, 2 x q, *J* 7.2 Hz, 2 x CH_2CH_3); 3.36 (1H, d, OH, D_2O exchangeable) and 1.33 (3H, t, *J* 7.2 Hz, OCH_2CH_3) and 1.32 (3H, t, *J* 7.2 Hz, OCH_2CH_3); δ_C ($CDCl_3$) 167.0 (C=O); 166.4 (C=O); 90.15 (d, *J* 193.0 Hz, CHF); 71.8 (d, *J* 21.6 Hz, CHOH); 63.3 CH_2; 62.4 CH_2; 14.45 CH_3 and 14.40 CH_3; δ_F (282 MHz, $CDCl_3$) -202.2 (dd, *J* 47.1 Hz, *J* 23.6 Hz, CHF); ***m/z*** (CI-CH_4) 194 (MH^+), 151 (100),

133 (48), 95 (48), 93 (79), 81 (66), 79 (54), 55 (62) and 43 (72). *Diethyl (2R,3S)-2-fluoro-3-hydroxysuccinate* $[\alpha]^{20}_{D}$ +10.8 (c 1.0, CH_2Cl_2); (**Found**: MH^+, 231.0645. $C_8H_{13}O_5FNa$ requires MH, 231.0645).

3.2.42 Preparation of (*R,R*)-2,3-cyclic sulfate of tartaric acid **297**

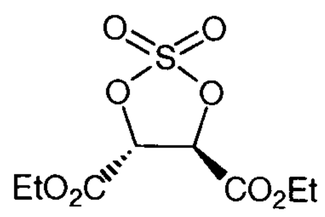

Thionyl chloride (4.4 cm^3, 60 mmol) was added to a solution of L-(+)-diethyl tartrate **257** (10.3 g, 50 mmol) in CCl_4 (50 cm^3) at 0 °C. DMF (0.2 cm^3) was added and the solution stirred vigorously at ambient temperature for 12 h. The reaction mixture was then heated under reflux for additional 2 hr to remove excess of the reagent. H_2O (75 cm^3), MeCN (50 ml), $NaIO_4$ (16 g, 75 mmol) and $RuCl_3$ (8 mg, 0.03 mmol) were added subsequently, and the suspension was stirred at ambient temperature for 2 h. The solid was then filtered off and the phases of the filtrate were separated. The water phase was extracted with diethyl ether (3 x 50 cm^3) and the combined organic phases were washed with saturated sodium hydrogen carbonate (30 cm^3), 1N HCl (30 cm^3), and brine (30 cm^3) and dried over $MgSO_4$. The solvent was removed under reduced pressure to afford pale yellow oil, which formed a white powder on standing. Recrystallisation in diethyl ether/hexane gave chunky colourless crystals (9.8 g, 73%) of the title compound **mp** 76-77 °C (lit.,[13] 75-76 °C); (**Found**: C, 36.24; H, 4.43; S, 11.96. $C_8H_{13}O_8S$ requires: C, 35.82; H, 4.51; S, 11.95%); **Found**: MH^+, 269.0337. $C_8H_{13}O_8S$ requires MH, 269.0331); $[\alpha]_D$ –67.2 (c 0.51, $CHCl_3$); ν_{max}/cm^{-1} (KBr) 2945, 1761, 1560, 1458, 1377 and1058; δ_H ($CDCl_3$) 5.6 (2H, s, CH); 4.5 (4H, q, *J* 7.2

Hz, 2 x OCH_2) and 1.49 (6H, t, *J* 7.2 Hz, 2 x CH_3); δ_C ($CDCl_3$) 164.7 (2 x C=O); 77.5 (CH); 64.3 (CH_2CH_3) and 14.3 (CH_2CH_3); ***m/z*** (EI) 151 (100), 149 (46), 133 (48), 93 (79), 81 (66), 55 (62) and 43 (72).

3.2.43 Preparation of diethyl (*2S,3R*)-2-fluoro-3-trifluoromethane-sulfonyloxysuccinate **323**

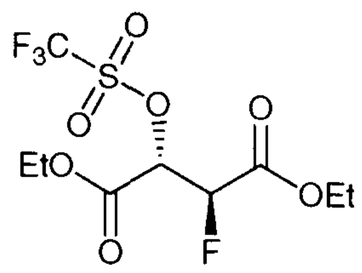

Trifluoromethanesulfonic anhydride (0.095 cm^3, 0.58 mmol) was added to a solution of diethyl 2-fluoro-3-hydroxysuccinate **277** (100 mg, 0.48 mmol) and pyridine (0.058 ml, 0.75 mmol) in dry dichloromethane (2 cm^3) at -15 °C. The reaction mixture was stirred for 30 min and then diluted with pentane (2 cm^3). The suspension was filtered through a small plug of silica and the solvent removed under reduced pressure to give the product as colorless oil (153 mg, 94%), (**Found**: M+Na^+, 363.0130. $C_9H_{12}O_7F_4SNa$ requires: 363.0138 (-2.1 ppm)); ν_{max}**/cm**$^{-1}$ (film) 2989, 1777, 1470, 1426, 1376, 1307, 1099, 1026; δ_H ($CDCl_3$) 5.67 (1H, dd, *J* 18.1 Hz, *J* 1.4 Hz, $CHOSO_2CF_3$); 5.55 (1H, dd, *J* 46.5 Hz, *J* 7.2 Hz); 4.5-4.4 (4H, m, *J* 7.2 Hz, 2 x OCH_2), 1.33 (3H, t, *J* 7.2 Hz, OCH_2CH_3) and 1.31 (3H, t, *J* 7.2 Hz, OCH_2CH_3); δ_C ($CDCl_3$) 164.2 (d, *J* 23.8 Hz, C=O), 162.9 (d, *J* 8.8 Hz, C=O); 118.7 (q, *J* 319.6 Hz, CF_3); 86.9 (d, *J* 199.0 Hz, CHF); 81.4 (d, *J* 22.1 Hz, $CHOSO_2CF_3$); 64.1 (CH_2CH_3); 63.4 (CH_2CH_3); 14.3 (CH_2CH_3) and 14.2 (CH_2CH_3); δ_F ($CDCl_3$) -74 (3F, s, CF_3); -199.3 (1F, dd, *J* 46.5 Hz, *J* 18.1 Hz); ***m/z*** 295 (10), 267 (22), 135 (48), 107 (100) and 69 (53).

3.2.44 Preparation of diethyl fluoromaleate **324**

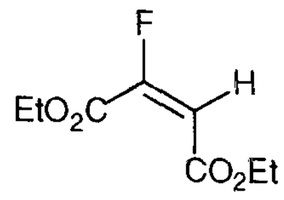

A 1M solution of TBAF (2.7 mmol, 2.7 cm^3) in THF was added to a solution of the triflate **323** in dry acetone (6 cm^3) slowly at 0 °C. The reaction mixture was stirred at ambient temperature for 1h. Ice water (10 cm^3) was added and the solution extracted into diethyl ether (3 x 10 cm^3). The combined organic extracts were washed with brine (10 cm^3) and the solution was dried over $MgSO_4$. The solvent was removed under reduced pressure and the remaining oil purified over silica gel to give the product (240 mg, 71 %) as a colourless oil, (**Found**: M+Na^+, 213.0539. $C_8H_{11}O_4FNa$ requires: 213.0539, 0.9 ppm); ν_{max}/cm^{-1} 2986, 2937, 1733, 1667, 1432, 1371, 1272, 1206, 1136, 1079, 1028, 931, and 857; δ_H (300 MHz, $CDCl_3$) 6.1 (1H, d, *J* 28.8 Hz, CH), 4.3 (4H, q, *J* 7.1 Hz, OCH_2), 4.2 (4H, q, *J* 7.1 Hz, OCH_2), 1.4 (6H, t, 7.1 Hz, CH_3), and 1.3 (6H, t, 7.1 Hz, 2 x CH_3); δ_C ($CDCl_3$) 163.9-153.6 (m, 2 x C=O), 109.2 (d, *J* 21.6 Hz, CF), 108.2 (d, *J* 3.2 Hz, CH), 63.0, 62.1 (2 x OCH_2), 14.4, 14.3 (2 x CH_3); δ_F ($CDCl_3$) –111.5 (d, *J* 21.6 Hz, CF); **m/z** (EI) 161 (21), 145 (100) and 117 (76). D*iethyl fluorofumarate* **325** was formed as a minor by-product in the reaction: δ_H($CDCl_3$) 6.3 (1H, d, *J* 30.0 Hz, CH), 4.4-4.2 (4H, m, 2 x OCH_2) and 1.4-1.3 (6H, m, 2 x CH_3); δ_F ($CDCl_3$) -107.1 (d, *J* 30.0 Hz, CF); ***m/z*** (EI) 161 (11), 145 (20) and 117 (100).

3.2.45 Preparation of diethyl (*2S,3R*)-2-fluoro-3-methanesulfonyloxy-succinate **328**

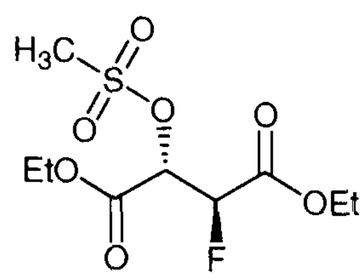

Methanesulfonyl chloride (0.070 cm^3, 0.89 mmol) was added to a solution of diethyl (*2R,3S*)-2-fluoro-3-hydroxysuccinate **277** (155 mg, 0.74 mmol) and *N,N*-dimethylaminopyidine (109 mg, 0.89 mmol) in dry dichloromethane (2 cm^3) at –15 ºC. The reaction mixture was stirred at ambient temperature for 5 h, then diluted with diethyl ether (5 cm^3) and quenched with ice-water (5 cm^3). The phases were separated and the organic layer was washed with 1N HCl (5 cm^3), H_2O (5 cm^3), and brine (5 cm^3), and dried over $MgSO_4$. The solvent was removed under reduced pressure to give the product (186 mg, 88%) as a colourless oil, (**Found**: M+Na^+, 309.0426. $C_9H_{15}O_7FSNa$ requires: 309.0420, ppm); ν_{max}/cm^{-1} (film) 2989, 2941, 1769, 1741, 1371, 1305, 1261, 1222, 1176, 1097, 1030, 971, 923, 857, 791 and 756; δ_H ($CDCl_3$) 5.5 (1H, dd, *J* 20.2 Hz, *J* 2.1 Hz, C*H*OSO_2CH_3); 5.4 (1H, dd, *J* 46.6 Hz, *J* 2.1 Hz, CHF); 4.3 (4H, q, *J* 7.2 Hz, 2 x OCH_2CH_3), 3.2 (3H, s, CH_3SO_3) and 1.3 (6H, dt, *J* 7.2 Hz, 2 x CH_2CH_3); δ_C ($CDCl_3$) 164.9, 164.6 (2 x C=O), 87.9 (t, *J* 196.3 Hz, CHF), 77.3 (t, *J* 22.1 Hz, $CHOSO_2Me$), 63.5 (d, CH_2), 63.1 (d, CH_2), 39.8 (s, SO_3Me), 14.4 (OCH_2CH_3) and 14.3 (OCH_2CH_3); δ_F ($CDCl_3$) -199.2 (dd, *J* 46.6 Hz, *J* 20.2 Hz); ***m/z*** 241 (M-45, 2), 221 (M-73, 15), 193 (75), 135 (80), 107 (100), 97 (50), 79 (78) and 69 (91).

3.2.46 Preparation of diethyl (*2S,3R*)-2-Fluoro-3-(toluene-4-sulfonyloxy)-succinate **329**

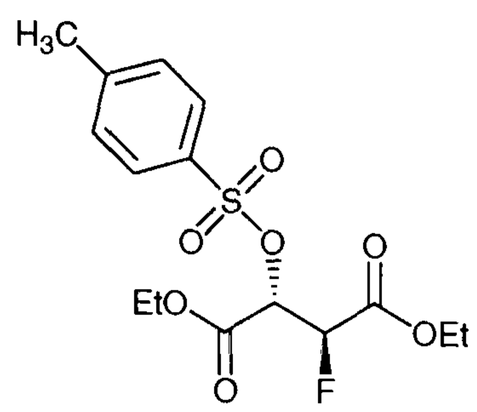

A solution of *p*-toluenesulfonyl chloride (238 mg, 0.125 mmol) in CH_2Cl_2 (2 cm^3) was added to a solution of diethyl 2-fluoro-3-hydroxysuccinate (130 mg, 0.62 mmol) and DMAP (115 mg, 0.94 mmol) in dry dichloromethane (3 cm^3) at 0 °C. The reaction mixture was stirred for 16 h and then quenched with ice-water (10 cm^3). The phases were separated and the organic layer washed with 1N HCl (10 cm^3), H_2O (10 cm^3) and brine (10 cm^3). After drying over $MgSO_4$, the solvent was removed under reduced pressure. The crude product was purified by preparative TLC (petroleum/ethyl acetate 3:1) to give the title compound as a colourless oil (204 mg, 91 %), (**Found** MH^+, 363.092039. $C_8H_{13}O_8S$ requires MH, 363.0914); δ_H ($CDCl_3$) 7.83 (2H, d, *J* 8.45 Hz, Ar-H), 7.35 (2H, d, *J* 7.94 Hz, Ar-H), 5.45 (1H, dd, *J* 21.2 Hz, *J* 2.0 Hz, $CHSO_3Ar$); 5.26 (1H, dd, *J* 47.1 Hz, *J* 2.3 Hz, CHF); 4.27 (2H, q, *J* 7.2 Hz, OCH_2), 4.21 (2H, m, *J* 7.2 Hz, OCH_2), 2.44 (3H, s, Ph-CH_3), 1.28 (3H, t, *J* 7.2 Hz, OCH_2CH_3) and 1.23 (3H, t, *J* 7.2 Hz, CH_2CH_3); δ_C ($CDCl_3$) 165.2 (d, *J* 23.8 Hz, C=O), 164.4 (d, *J* 8.3 Hz, C=O), 145.9 (Ar-C), 133.2 (Ar-C), 130.14 (Ar-H), 128.7 (Ar-H), 87.8 (d, *J* 197.4 Hz, CHF), 76.7 (d, *J* 22.7 Hz, $CHOSO_2Ar$), 63.2 (OCH_2), 62.9 (OCH_2CH_3), 22.1 (CH_3-Ar), 14.35 (OCH_2CH_3) and 14.24 (CH_2CH_3); δ_F ($CDCl_3$) –200.5 (dd, *J* 46.7 Hz, *J* 21.3 Hz).

3.2.47 Preparation of *(2R,3S)*-2-fluoromalic acid **240**

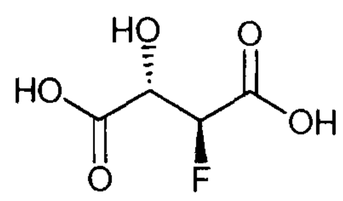

1N NaOH (1 cm^3) was added to a solution of diethyl (*2R,3S*)-2-fluoromalate **277** in ethanol (2 cm^3) dropwise at ambient temperature. The reaction mixture was neutralised after 30 min with of 4N HCl (5 cm^3). The concentrated under reduced pressure and the residue acidified to pH 1 by addition of concentrated HCl. The mixture was extracted into ethyl acetate (6 x 10 cm^3), and the combined organic extracts were washed with brine and concentrated under reduced pressure. The solid residue was recrystallised in acetone to afford the product as a white crystalline powder (60 mg, 88 % yield), **mp** 149-152 °C; (Found: M-H, 151.0040. $C_4H_4O_5F$ requires M-H, 151.0760); $\boldsymbol{[\alpha]_D}$ + 4.6 (c 7.0, H_2O); $\boldsymbol{\nu_{max}/cm^{-1}}$ (KBr) 3507, 2924, 2854, 1759, 1726, 1632, 1462, 1377 and 1111; $\boldsymbol{\delta_H}$ (D_2O) 5.40 (1H, dd, *J* 46.85 Hz, *J* 2.30 Hz, CHF) and 4.85 (1H, dd, *J* 22.8 Hz, *J* 2.0 Hz, C*H*OH); $\boldsymbol{\delta_C}$ (D_2O) 172.8 (q, *J* 9.9 Hz, C=O), 170.0 (q, *J* 24.3 Hz, C=O); 90.5 (t, *J* 186.9 Hz, CHF); 71.2 (t, *J* 22.1 Hz, CHOH); $\boldsymbol{\delta_F}$ (D_2O) -198.9 (dd, *J* 47.0 Hz, *J* 23.0 Hz); ***m/z*** (ESI) 151 (MH^+, 100).

3.2.48 Preparation of diethyl 2-methanesulfonyloxy-but-2-enedioate **259**

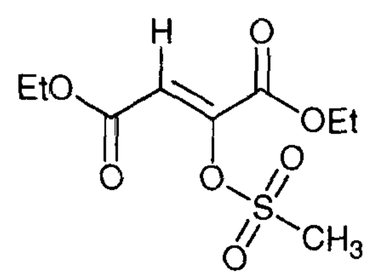

A 1M solution of TBAF in tetrahydrofuran (0.38 cm^3) was added to a solution of diethyl 2-fluoro-3-methanesulfonyloxysuccinate **328** (90 mg, 0.32 mmol) in dry tetrahydrofuran (1 cm^3) dropwise at –78 °C. After stirring for 1 h, a 1:1 mixture of methanol and H_2O (2 cm^3) was slowly added to the reaction mixture. The mixture was diluted with diethyl ether (2 cm^3) and the phases were separated. The combined organic extracts were washed with H_2O (2 cm^3) and brine (2 cm^3), dried over $MgSO_4$ and the solvent was removed under reduced pressure. The residue was purified by preparative TLC (hexane/diethyl ether 1:1) to give the compound as a colourless oil (40 mg, 47%), (**Found** MH^+, 267.05249. $C_8H_{13}O_8S$ requires MH, 267.05385); δ_H ($CDCl_3$) 6.75 (1H, s, CH); 4.33 (2H, q, *J* 7.2 Hz, OCH_2); 4.27 (2H, q, *J* 7.2 Hz, OCH_2), 3.40 (3H, s, CH_3-SO_3), 1.35 (3H, t, *J* 7.2 Hz, OCH_2CH_3) and 1.32 (3H, t, *J* 7.2 Hz, OCH_2CH_3); δ_C ($CDCl_3$) 162.7 (C=O), 161.6 (C=O), 144.2 C(2), 120.4 C(3), 63.5 (OCH_2), 62.1 (OCH_2CH_3), 40.8 (CH_3SO_3), 14.38 (OCH_2CH_3) and 14.36 (OCH_2CH_3).

3.2.49 Preparation of *N,N*-dibenzyl *(2S,3R)*-2-fluoro-3-hydroxyl-succinamide **306**

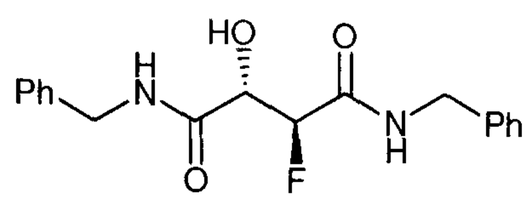

Benzylamine (3.3 cm^3, 30 mmol) was added to a solution of diethyl 2-fluoro-3-hydroxysuccinate **277** (1.55 g, 7.5 mmol) in dry diethyl ether (20 cm^3) under cooling in an ice bath. The reaction mixture was heated under reflux for 16 h and the suspension was then cooled to ensure complete precipitation of the product. The solid was filtered, washed with diethyl ether (2 x 10 cm^3) and dried *en vacuo*. The remaining solid (ms88) was recrystallised in hot chloroform to afford the product as a white powder (1.875 g, 80%), **mp** 155 ^oC, (**Found**: C, 65.55; H, 5.81; N, 8.52 $C_{18}H_{19}O_5N_2F_2$ requires: C, 65.44; H, 5.80; N 8.48%); $[\alpha]_D$ + 24.2 (c 0.5, CH_3OH); ν_{max}/cm^{-1} (KBr) 3375, 3300, 2932, 2104, 2037, 1650, 1555, 1493, 1453, 1432, 1343, 1261, 1238, 1127, 1046, 1026, 746, 724, 696; δ_H (CD_3OD) 7.25-7.10 (10H, m, Ar-H), 5.2 (1H, dd, *J* 47.9 Hz, *J* 2.3 Hz, CHF); 4.5 (1H, dd, *J* 22.3 Hz, *J* 2.0 Hz, C*H*OH); 4.4-4.25 (4H, m, Ph-CH_2); δ_C (CD_3OD) 172.3 (q, *J* 10.5 Hz, C=O), 169.5 (q, *J* 20.5 Hz, C=O), 140.1, 140.0, 129.9, 129.8, 128.9, 128.8, 128.5, 128.5 (Ar-C), 93.9 (t, *J* 191.8 Hz, CHF), 74.1 (t, *J* 22.1 Hz, CHOH), 44.1, 43.9 (d, Ph-CH_2); δ_F (CD_3OD) – 199.9 (dd, *J* 47.8 Hz, *J* 2.3 Hz); ***m/z*** (EI) 197 (100) 195 (100), 169 (57), 167 (57), 151 (33), 149 (33), 117 (31), 99 (19), 89 (43), 71 (86) and 43 (24).

3.2.50 Preparation of diethyl *meso* 2,3-Dihydroxysuccinate **311**

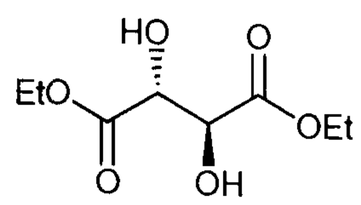

A stock solution of OsO_4 (4 mg) in *tert*-butanol (4 cm^3) was added to a solution of *N*-methyl morpholine *N*-oxide (6.8 g, 50 mmol) in a 2:1 mixture of H_2O and acetone (30 cm^3). Diethyl maleate **310** (8.6 g, 50 mmol) was added dropwise under cooling in an ice-bath and the reaction mixture stirred at ambient temperature for 12 h. A slurry of $NaHSO_3$ (0.5 g) and magnesium silicate (4 g) in H_2O (25 cm^3) was added. After stirring for 30 min, the solids were filtered off and the filtrate neutralised with concentrated sulfuric acid. Acetone was removed under reduced pressure and the remaining aqueous solution acidified to pH 2. The residue was extracted into ethyl acetate (3 x 20 cm^3) and the combined organic extracts were washed with H_2O (2 x 15 cm^3) and brine, dried over $MgSO_4$ and the solvent removed by evaporation. The remaining solid was recrystallised in hot diethyl ether to afford the product (6.36 g, 62 %) as white needles, **mp** 51-52 °C, (**Found**: C, 45.84; H, 6.99. $C_8H_{14}O_6$ requires: C, 46.6; H, 6.84%); ν_{max}/cm^{-1} (KBr) 3419, 2987, 1747, 1639, 1447, 1371, 1216, 1126, 1029, 949, 866, 792 and 627; δ_H ($CDCl_3$) 4.58 (2H, s), 4.25 (4H, q, *J* 7.2 Hz, OCH_2), 3.33 (1H, s, OH) and 1.28 (t, *J* 7.2 Hz, 6H, CH_3); δ_C ($CDCl_3$) 71.4 (C=O), 73.3 (C-OH), 62.7 (OCH_2) and 14.5 (CH_3); ***m/z*** (EI) 207 (2) 133 (47), 104 (100) and 76 (82).

3.2.51 Preparation of dibenzyl (*2S,3R*)-2-fluoro-3-methanesulfonyloxy-succinicamide **332**

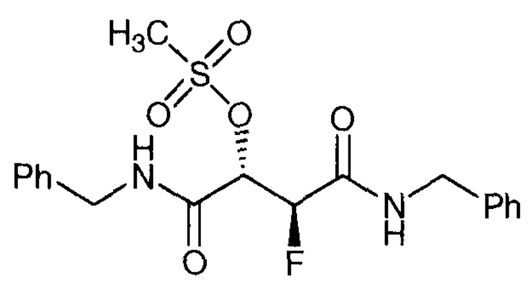

Methanesulfonyl chloride (0.025 cm^3, 0.3 mmol) was added to a solution of dibenzyl *(2S,3R)*-2-fluoro-3-hydroxysuccinamide **306** (63 mg, 0.2 mmol) in pyridine (1 cm^3). The reaction mixture was stirred for 12 h at ambient temperature, and then diluted with ethyl acetate (5 cm^3). The solution was washed with saturated bicarbonate solution (2 cm^3), 1N HCl (2 cm^3), and brine (2 cm^3). After drying over $MgSO_4$, the solvent was removed under reduced pressure. The residue was purified by preparative TLC (hexane/ethyl acetate 1:1) to afford the product (84 mg, 67 %) as a colorless oil, δ_H ($CDCl_3$) 7.3-7.1 (10H, m, Ar-H), 6.6, 6.8 (2H, m, 2 x NH), 5.6 (1H, dd, *J* 16.4 Hz, *J* 1.8 Hz, CHOMs); 5.4 (1H, dd, *J* 46.8 Hz, *J* 1.8 Hz, CHF); 4.5-4.3 (4H, m, $PhCH_2$) and 3.0 (3H, s, SO_2CH_3); δ_C (CD_3OD) 137.52, 137.36, 129.27, 129.17, 128.33, 128.26, 128.1, 127.99 (Ar-C), 90.9 (d, *J* 196.8 Hz, CHF), 79.15 (d, *J* 21.6 Hz, CHOMs), 44.0, 43.6 ($PhCH_2$) and 39.1 (SO_2CH_3); δ_F ($CDCl_3$) –196.5 (ddd, *J* 47.2 Hz, *J* 20.1 Hz, *J* 3.44 Hz).

References

[1] Perrin, D. D., Armarego, W. L. F., *Purification of Laboratory Chemicals*, Pergamon, New York, 1999.

[2] M. Brand, S. Rozen, *J. Fluorine Chem.*, 1982, **20**, 419.

[3] D. H. R. Barton, *J. Chem. Soc., Perkin Trans. 1*, 1974, 739.

[4] S. A. Lermontov, A. Sergei, S. I. Zavorin, I. V. Bakhtin, A. N. Pushin, N. S. Zefirov, P. J. Stang, *J. Fluorine Chem.*, 1998, **87**, 75.

[5] D. H. R. Barton, *J. Chem. Soc., Perkin Trans. 1*, 1974, 739.

[6] D. Seebach, A. Thaler, D. Blaser, S. Y. Koo, *Helv. Chim. Acta*, 1991, **74**, 1102.

[7] T. Abiko, H. Shishido, H. Sekino, *Chem. Pharm. Bull.*, 1986, **34**, 2133.

[8] B. Bretschneider, *Monatsh. Chem.*, 1949, **80**, 256.

[9] M. C. Pirrung, H. Han, D. S. Nunn, *J. Org. Chem.*, 1994, **59**, 2423.

[10] S. Seito, T. Ishikawa, A. Kuroda, K. Koga, T. Moriwake, *Tetrahedron*, 1992, **48**, 4067.

[11] K. Mori, H. Iwasawa, *Tetrahedron*, 1980, **36**, 87.

[12] M. Hudlicky, *Coll. Czech. Chem. Comm.*, 1961, **26**, 1414.

[13] Y. Gao, K. Sharpless, K. Barry, *J. Am. Chem. Soc.*, 1988, **110**, 7538.

3.3 Crystallographic data for Chapter 2

3.3.1 *Erythro* 1,2-difluoro-1,2-diphenylethane **103**

Identification code	msdh8	
Empirical formula	C14 H12 F2	
Formula weight	218.24	
Temperature	373(2) K	
Wavelength	0.71073 Å	
Crystal system	Monoclinic	
Space group	P2(1)/n	
Unit cell dimensions	a = 7.916(5) Å	α= 90°.
	b = 5.936(3) Å	β= 104.145(12)°.
	c = 12.041(7) Å	γ = 90°.
Volume	548.6(5) Å^3	
Z	2	
Density (calculated)	1.321 Mg/m^3	
Absorption coefficient	0.099 mm^{-1}	
F(000)	228	
Crystal size	0.2000 x 0.1000 x 0.0800 mm^3	
Theta range for data collection	2.80 to 27.48°.	
Index ranges	-9<=h<=8, -6<=k<=7, -13<=l<=14	
Reflections collected	3755	
Independent reflections	1098 [R(int) = 0.0728]	
Completeness to theta = 27.48°	87.3 %	
Absorption correction	MULTISCAN	
Max. and min. transmission	1.0000 and 0.3438	
Refinement method	Full-matrix least-squares on F^2	
Data / restraints / parameters	1098 / 0 / 74	
Goodness-of-fit on F^2	1.119	
Final R indices [I>2sigma(I)]	R1 = 0.1131, wR2 = 0.2989	
R indices (all data)	R1 = 0.1995, wR2 = 0.3734	
Extinction coefficient	0.06(4)	
Largest diff. peak and hole	0.261 and -0.276 e.Å^{-3}	

3.3.2 *Threo* 1,2-difluoro-1,2-diphenylethane **104**

Identification code	msdh14	
Empirical formula	C14 H12 F2	
Formula weight	218.24	
Temperature	125(2) K	
Wavelength	0.71073 Å	
Crystal system	Monoclinic	
Space group	P2(1)/n	
Unit cell dimensions	a = 10.8973(16) Å	α= 90°.
	b = 7.3270(11) Å	β= 90.629(2)°.
	c = 13.940(2) Å	γ = 90°.
Volume	1112.9(3) $Å^3$	
Z	4	
Density (calculated)	1.302 Mg/m^3	
Absorption coefficient	0.098 mm^{-1}	
F(000)	456	
Crystal size	.19 x .1 x .1 mm^3	
Theta range for data collection	2.36 to 25.39°.	
Index ranges	-13<=h<=8, -8<=k<=8, -16<=l<=16	
Reflections collected	5541	
Independent reflections	1996 [R(int) = 0.0095]	
Completeness to theta = 25.39°	97.8 %	
Absorption correction	MULTISCAN	
Max. and min. transmission	1.00000 and .940988	
Refinement method	Full-matrix least-squares on F^2	
Data / restraints / parameters	1996 / 0 / 146	
Goodness-of-fit on F^2	1.057	
Final R indices [I>2sigma(I)]	R1 = 0.0316, wR2 = 0.0785	
R indices (all data)	R1 = 0.0335, wR2 = 0.0799	
Extinction coefficient	0.020(3)	
Largest diff. peak and hole	0.222 and -0.164 $e.Å^{-3}$	

Bond lengths [Å] and angles [°] for msdh14.

3.3.3 *Erythro* 2,3-difluorosuccinic acid **130**

Identification code	msdh11	
Empirical formula	C4 H4 F2 O4	
Formula weight	154.07	
Temperature	125(2) K	
Wavelength	0.71073 Å	
Crystal system	Orthorhombic	
Space group	P2(1)2(1)2(1)	
Unit cell dimensions	a = 6.6240(19) Å	α= 90°.
	b = 8.868(3) Å	β= 90°.
	c = 9.582(3) Å	γ = 90°.
Volume	562.8(3) $Å^3$	
Z	4	
Density (calculated)	1.818 Mg/m^3	
Absorption coefficient	0.200 mm^{-1}	
F(000)	312	
Crystal size	.1 x .1 x .01 mm^3	
Theta range for data collection	3.74 to 25.43°.	
Index ranges	-7<=h<=7, -8<=k<=10, -11<=l<=11	
Reflections collected	3454	
Independent reflections	987 [R(int) = 0.0300]	
Completeness to theta = 25.43°	97.6 %	
Absorption correction	MULTISCAN	
Max. and min. transmission	1.00000 and 0.589892	
Refinement method	Full-matrix least-squares on F^2	
Data / restraints / parameters	987 / 2 / 100	
Goodness-of-fit on F^2	0.990	
Final R indices [I>2sigma(I)]	R1 = 0.0274, wR2 = 0.0615	
R indices (all data)	R1 = 0.0306, wR2 = 0.0622	
Absolute structure parameter	2.3(10)	
Extinction coefficient	0.005(4)	
Largest diff. peak and hole	0.133 and -0.143 e.$Å^{-3}$	

3.3.4 *Threo* 2,3-difluorosuccinic acid **132**

Identification code	msdh27	
Empirical formula	C4 H8 F2 O6	
Formula weight	190.10	
Temperature	93(2) K	
Wavelength	0.71073 Å	
Crystal system	Monoclinic	
Space group	C2/c	
Unit cell dimensions	a = 18.025(6) Å	α= 90°.
	b = 4.7156(15) Å	β= 115.758(11)°.
	c = 9.731(3) Å	γ = 90°.
Volume	744.9(4) $Å^3$	
Z	4	
Density (calculated)	1.695 Mg/m^3	
Absorption coefficient	0.187 mm^{-1}	
F(000)	392	
Crystal size	0.100 x 0.100 x 0.020 mm^3	
Theta range for data collection	4.65 to 25.34°.	
Index ranges	-19<=h<=21, -5<=k<=5, -9<=l<=11	
Reflections collected	1826	
Independent reflections	615 [R(int) = 0.0486]	
Completeness to theta = 25.34°	90.2 %	
Absorption correction	Multiscan	
Max. and min. transmission	1.0000 and 0.0402	
Refinement method	Full-matrix least-squares on F^2	
Data / restraints / parameters	615 / 3 / 68	
Goodness-of-fit on F^2	1.086	
Final R indices [I>2sigma(I)]	R1 = 0.0410, wR2 = 0.1100	
R indices (all data)	R1 = 0.0420, wR2 = 0.1113	
Largest diff. peak and hole	0.240 and -0.213 $e.Å^{-3}$	

3.3.5 Methyl *threo* 2,3-difluoro-3-phenylpropionate **135**

Identification code	msdh23	
Empirical formula	C10 H10 F2 O2	
Formula weight	200.18	
Temperature	293(2) K	
Wavelength	0.71073 Å	
Crystal system	Monoclinic	
Space group	P2(1)/c	
Unit cell dimensions	a = 16.096(5) Å	α= 90°.
	b = 10.072(3) Å	β= 111.552(15)°.
	c = 12.286(4) Å	γ = 90°.
Volume	1852.5(10) $Å^3$	
Z	8	
Density (calculated)	1.435 Mg/m^3	
Absorption coefficient	0.125 mm^{-1}	
F(000)	832	
Crystal size	0.20 x 0.20 x 0.04 mm^3	
Theta range for data collection	3.30 to 25.34°.	
Index ranges	-18<=h<=12, -10<=k<=12, -14<=l<=14	
Reflections collected	9681	
Independent reflections	3183 [R(int) = 0.2710]	
Completeness to theta = 25.34°	94.1 %	
Absorption correction	Multiscan	
Max. and min. transmission	1.0000 and 0.0032	
Refinement method	Full-matrix least-squares on F^2	
Data / restraints / parameters	3183 / 0 / 256	
Goodness-of-fit on F^2	1.047	
Final R indices [I>2sigma(I)]	R1 = 0.0965, wR2 = 0.2308	
R indices (all data)	R1 = 0.1419, wR2 = 0.2764	
Largest diff. peak and hole	0.364 and -0.382 e.$Å^{-3}$	

3.3.6 *N,N*-dibenzyl *erythro* 2,3-difluorosuccinamide **161**

Identification code	msdh13	
Empirical formula	C18 H18 F2 N2 O2	
Formula weight	332.34	
Temperature	93(2) K	
Wavelength	0.71073 Å	
Crystal system	Monoclinic	
Space group	P2(1)/c	
Unit cell dimensions	a = 4.8021(16) Å	α= 90°.
	b = 17.147(7) Å	β= 91.428(10)°.
	c = 9.776(4) Å	γ = 90°.
Volume	804.7(5) $Å^3$	
Z	2	
Density (calculated)	1.372 Mg/m^3	
Absorption coefficient	0.106 mm^{-1}	
F(000)	348	
Crystal size	0.2000 x 0.0300 x 0.0300 mm^3	
Theta range for data collection	2.38 to 25.35°.	
Index ranges	-4<=h<=5, -18<=k<=20, -7<=l<=11	
Reflections collected	5032	
Independent reflections	1373 [R(int) = 0.0954]	
Completeness to theta = 25.35°	93.1 %	
Absorption correction	Multiscan	
Max. and min. transmission	1.0000 and 0.4223	
Refinement method	Full-matrix least-squares on F^2	
Data / restraints / parameters	1373 / 1 / 123	
Goodness-of-fit on F^2	0.985	
Final R indices [I>2sigma(I)]	R1 = 0.0733, wR2 = 0.1705	
R indices (all data)	R1 = 0.1372, wR2 = 0.2021	
Extinction coefficient	0.014(9)	
Largest diff. peak and hole	0.310 and -0.278 $e.Å^{-3}$	

3.3.7 *N,N*-dibenzyl *erythro* 2,3-difluorosuccinamide **161**

Identification code	msdh16	
Empirical formula	C18 H18 F2 N2 O2	
Formula weight	332.34	
Temperature	93(2) K	
Wavelength	0.71073 Å	
Crystal system	Triclinic	
Space group	P-1	
Unit cell dimensions	a = 5.1156(7) Å	α= 91.807(10)°.
	b = 8.6935(13) Å	β= 90.945(10)°.
	c = 35.584(6) Å	γ = 91.986(10)°.
Volume	1580.5(4) $Å^3$	
Z	4	
Density (calculated)	1.397 Mg/m^3	
Absorption coefficient	0.108 mm^{-1}	
F(000)	696	
Crystal size	0.100 x 0.100 x 0.040 mm^3	
Theta range for data collection	3.33 to 25.35°.	
Index ranges	-6<=h<=6, -8<=k<=10, -32<=l<=41	
Reflections collected	10732	
Independent reflections	4988 [R(int) = 0.0703]	
Completeness to theta = 25.35°	86.3 %	
Absorption correction	MULTISCAN	
Max. and min. transmission	1.0000 and 0.6866	
Refinement method	Full-matrix least-squares on F^2	
Data / restraints / parameters	4988 / 0 / 426	
Goodness-of-fit on F^2	2.639	
Final R indices [I>2sigma(I)]	R1 = 0.2046, wR2 = 0.5570	
R indices (all data)	R1 = 0.2133, wR2 = 0.5610	
Extinction coefficient	0.19(5)	
Largest diff. peak and hole	1.030 and -0.716 e.$Å^{-3}$	

3.3.8 *N,N*-dibenzylsuccindiamide **164**

Identification code	msdh18	
Empirical formula	C18 H20 N2 O2	
Formula weight	296.36	
Temperature	93(2) K	
Wavelength	0.71073 Å	
Crystal system	Triclinic	
Space group	P-1	
Unit cell dimensions	a = 5.586(3) Å	α= 85.52(3)°.
	b = 7.921(4) Å	β= 83.01(2)°.
	c = 17.265(9) Å	γ = 89.81(3)°.
Volume	755.9(7) $Å^3$	
Z	2	
Density (calculated)	1.302 Mg/m^3	
Absorption coefficient	0.086 mm^{-1}	
F(000)	316	
Crystal size	0.2000 x 0.1000 x 0.0300 mm^3	
Theta range for data collection	2.38 to 25.34°.	
Index ranges	-6<=h<=6, -9<=k<=8, -20<=l<=13	
Reflections collected	3846	
Independent reflections	2285 [R(int) = 0.0654]	
Completeness to theta = 25.34°	82.2 %	
Absorption correction	Multiscan	
Max. and min. transmission	1.0000 and 0.2797	
Refinement method	Full-matrix least-squares on F^2	
Data / restraints / parameters	2285 / 2 / 208	
Goodness-of-fit on F^2	0.684	
Final R indices [I>2sigma(I)]	R1 = 0.0474, wR2 = 0.0977	
R indices (all data)	R1 = 0.0928, wR2 = 0.1126	
Extinction coefficient	0.015(2)	
Largest diff. peak and hole	0.201 and -0.227 $e.Å^{-3}$	

3.3.9 (*2R,3S*) HO-(*S*)-Phe-2,3-difluorosuccinyl-(*S*)-PheOH **218**

Identification code	msdh17	
Empirical formula	C22 H22 F2 N2 O6	
Formula weight	448.42	
Temperature	93(2) K	
Wavelength	0.71073 Å	
Crystal system	Monoclinic	
Space group	P2(1)	
Unit cell dimensions	a = 11.121(2) Å	α= 90°.
	b = 6.1323(10) Å	β= 90.179(6)°.
	c = 30.671(6) Å	γ = 90°.
Volume	2091.8(7) $Å^3$	
Z	4	
Density (calculated)	1.424 Mg/m^3	
Absorption coefficient	0.115 mm^{-1}	
F(000)	936	
Crystal size	0.2000 x 0.2000 x 0.2000 mm^3	
Theta range for data collection	1.95 to 25.34°.	
Index ranges	-11<=h<=13, -7<=k<=6, -36<=l<=28	
Reflections collected	13463	
Independent reflections	6970 [R(int) = 0.0887]	
Completeness to theta = 25.34°	98.9 %	
Absorption correction	MULTISCAN	
Max. and min. transmission	1.0000 and 0.3854	
Refinement method	Full-matrix least-squares on F^2	
Data / restraints / parameters	6970 / 9 / 611	
Goodness-of-fit on F^2	1.008	
Final R indices [I>2sigma(I)]	R1 = 0.0825, wR2 = 0.1525	
R indices (all data)	R1 = 0.1584, wR2 = 0.1924	
Absolute structure parameter	-1.6(14)	
Extinction coefficient	0.0104(14)	
Largest diff. peak and hole	0.338 and -0.326 e.$Å^{-3}$	

3.3.10 (*2R,3R*) HO-(*S*)-Phe-2,3-difluorosuccinyl-(*S*)-PheOH **219**

Identification code	msdh22	
Empirical formula	C22.25 H22 Cl F2 N2 O6	
Formula weight	486.87	
Temperature	173(2) K	
Wavelength	1.54178 Å	
Crystal system	Orthorhombic	
Space group	P2(1)2(1)2(1)	
Unit cell dimensions	a = 4.9826(19) Å	α= 90°.
	b = 22.066(10) Å	β= 90°.
	c = 24.319(9) Å	γ = 90°.
Volume	2673.7(18) $Å^3$	
Z	4	
Density (calculated)	1.210 Mg/m^3	
Absorption coefficient	1.709 mm^{-1}	
F(000)	1010	
Crystal size	0.3000 x 0.0200 x 0.0100 mm^3	
Theta range for data collection	7.56 to 67.99°.	
Index ranges	-5<=h<=5, -26<=k<=26, -28<=l<=29	
Reflections collected	35848	
Independent reflections	4760 [R(int) = 0.1355]	
Completeness to theta = 67.99°	98.0 %	
Absorption correction	Multiscan	
Max. and min. transmission	1.0000 and 0.2037	
Refinement method	Full-matrix least-squares on F^2	
Data / restraints / parameters	4760 / 8 / 347	
Goodness-of-fit on F^2	1.347	
Final R indices [I>2sigma(I)]	R1 = 0.1260, wR2 = 0.3296	
R indices (all data)	R1 = 0.1414, wR2 = 0.3451	
Absolute structure parameter	0.23(13)	
Extinction coefficient	0.0059(17)	
Largest diff. peak and hole	0.795 and -0.445 e.$Å^{-3}$	

3.3.11 HO-(*S*)-Phe-succinyl-(*S*)-PheOH **222**

Identification code	msdh19	
Empirical formula	C22 H24 N2 O6	
Formula weight	412.43	
Temperature	93(2) K	
Wavelength	0.71073 Å	
Crystal system	Monoclinic	
Space group	C2	
Unit cell dimensions	a = 20.677(13) Å	α= 90°.
	b = 7.603(5) Å	β= 101.443(19)°.
	c = 14.021(9) Å	γ = 90°.
Volume	2160(2) $Å^3$	
Z	4	
Density (calculated)	1.268 Mg/m^3	
Absorption coefficient	0.093 mm^{-1}	
F(000)	872	
Crystal size	0.2000 x 0.2000 x 0.1000 mm^3	
Theta range for data collection	2.72 to 25.35°.	
Index ranges	-24<=h<=24, -9<=k<=6, -16<=l<=16	
Reflections collected	6405	
Independent reflections	2799 [R(int) = 0.0393]	
Completeness to theta = 25.35°	94.4 %	
Absorption correction	MULTISCAN	
Max. and min. transmission	1.0000 and 0.3483	
Refinement method	Full-matrix least-squares on F^2	
Data / restraints / parameters	2799 / 5 / 289	
Goodness-of-fit on F^2	0.955	
Final R indices [I>2sigma(I)]	R1 = 0.0517, wR2 = 0.1340	
R indices (all data)	R1 = 0.0613, wR2 = 0.1447	
Absolute structure parameter	-0.5(17)	
Extinction coefficient	0.0028(11)	
Largest diff. peak and hole	0.220 and -0.211 e.$Å^{-3}$	

3.3.12 (*R*,*R*)-Cyclic sulfate of tartaric acid **297**

Identification code	msdh6/MS8	
Empirical formula	C8 H12 O8 S	
Formula weight	268.24	
Temperature	100(2) K	
Wavelength	0.71073 Å	
Crystal system	Orthorhombic	
Space group	P2(1)2(1)2(1)	
Unit cell dimensions	a = 8.727(2) Å	α= 90°.
	b = 9.106(3) Å	β= 90°.
	c = 14.519(4) Å	γ = 90°.
Volume	1153.7(5) $Å^3$	
Z	4	
Density (calculated)	1.544 Mg/m^3	
Absorption coefficient	0.309 mm^{-1}	
F(000)	560	
Crystal size	0.1300 x 0.1500 x 0.2000 mm^3	
Theta range for data collection	2.72 to 25.68°.	
Index ranges	-8<=h<=10, -8<=k<=10, -14<=l<=16	
Reflections collected	6013	
Independent reflections	2009 [R(int) = 0.0284]	
Completeness to theta = 25.68°	93.9 %	
Absorption correction	MULTISCAN	
Max. and min. transmission	1.0000 and 0.7741	
Refinement method	Full-matrix least-squares on F^2	
Data / restraints / parameters	2009 / 0 / 155	
Goodness-of-fit on F^2	1.154	
Final R indices [I>2sigma(I)]	R1 = 0.0457, wR2 = 0.1081	
R indices (all data)	R1 = 0.0517, wR2 = 0.1140	
Absolute structure parameter	0.00(12)	
Extinction coefficient	0.018(3)	
Largest diff. peak and hole	0.266 and -0.356 e.$Å^{-3}$	

3.3.13 (*R,R*)-Cyclic sulfate of tartaric acid **312**

Identification code	msdh7	
Empirical formula	C8 H12 O8 S	
Formula weight	268.24	
Temperature	293(2) K	
Wavelength	0.71073 Å	
Crystal system	Monoclinic	
Space group	Cc	
Unit cell dimensions	a = 8.9187(18) Å	α= 90°.
	b = 21.055(4) Å	β= 109.15(3)°.
	c = 6.5604(13) Å	γ = 90°.
Volume	1163.8(4) $Å^3$	
Z	4	
Density (calculated)	1.531 Mg/m^3	
Absorption coefficient	0.306 mm^{-1}	
F(000)	560	
Crystal size	0.1000 x 0.0500 x 0.0500 mm^3	
Theta range for data collection	1.93 to 26.36°.	
Index ranges	-11<=h<=10, -24<=k<=24, -6<=l<=8	
Reflections collected	3799	
Independent reflections	1679 [R(int) = 0.1173]	
Completeness to theta = 26.36°	87.7 %	
Absorption correction	MULTISCAN	
Max. and min. transmission	1.00000 and 0.0774	
Refinement method	Full-matrix least-squares on F^2	
Data / restraints / parameters	1679 / 2 / 155	
Goodness-of-fit on F^2	0.993	
Final R indices [I>2sigma(I)]	R1 = 0.1104, wR2 = 0.2479	
R indices (all data)	R1 = 0.1752, wR2 = 0.3084	
Absolute structure parameter	0.1(3)	
Extinction coefficient	0.031(10)	
Largest diff. peak and hole	0.615 and -0.381 e.$Å^{-3}$	

3.3.14 *N,N*-dibenzyl (2S,3R)-2-fluoro-3-hydroxylsuccindiamide **306**

Identification code	msdh5	
Empirical formula	C18 H19 F N2 O2	
Formula weight	314.35	
Temperature	293(2) K	
Wavelength	0.71073 Å	
Crystal system	Monoclinic	
Space group	P2(1)	
Unit cell dimensions	a = 4.848(2) Å	α= 86.226(7)°.
	b = 5.027(2) Å	β= 84.550(7)°.
	c = 17.196(7) Å	γ = 75.400(7)°.
Volume	403.3(3) $Å^3$	
Z	1	
Density (calculated)	1.294 Mg/m^3	
Absorption coefficient	0.093 mm^{-1}	
F(000)	166	
Crystal size	.14 x .1 x .1 mm^3	
Theta range for data collection	2.38 to 26.50°.	
Index ranges	-6<=h<=4, -6<=k<=6, -21<=l<=19	
Reflections collected	2618	
Independent reflections	2219 [R(int) = 0.1073]	
Completeness to theta = 26.50°	96.5 %	
Absorption correction	Multiscan	
Max. and min. transmission	1.000000 and 0.801830	
Refinement method	Full-matrix least-squares on F^2	
Data / restraints / parameters	2219 / 3 / 133	
Goodness-of-fit on F^2	1.069	
Final R indices [I>2sigma(I)]	R1 = 0.0952, wR2 = 0.2585	
R indices (all data)	R1 = 0.0991, wR2 = 0.2645	
Absolute structure parameter	3(2)	
Largest diff. peak and hole	0.698 and -0.590 e.$Å^{-3}$	

3.3.15 (*2S,3R*)-2-Fluoro-3-hydroxysuccinic acid **340**

Identification code	msdh26	
Empirical formula	C4 H7 F O6	
Formula weight	170.10	
Temperature	173(2) K	
Wavelength	1.54178 Å	
Crystal system	Orthorhombic	
Space group	P2(1)2(1)2(1)	
Unit cell dimensions	a = 4.9895(7) Å	α= 90°.
	b = 9.0272(12) Å	β= 90°.
	c = 14.936(2) Å	γ = 90°.
Volume	672.75(16) $Å^3$	
Z	4	
Density (calculated)	1.679 Mg/m^3	
Absorption coefficient	1.597 mm^{-1}	
F(000)	352	
Crystal size	0.100 x 0.100 x 0.010 mm^3	
Theta range for data collection	5.92 to 67.79°.	
Index ranges	-5<=h<=5, -10<=k<=10, -17<=l<=17	
Reflections collected	8635	
Independent reflections	1150 [R(int) = 0.0786]	
Completeness to theta = 67.79°	95.1 %	
Absorption correction	Multiscan	
Max. and min. transmission	1.0000 and 0.0288	
Refinement method	Full-matrix least-squares on F^2	
Data / restraints / parameters	1150 / 5 / 121	
Goodness-of-fit on F^2	1.077	
Final R indices [I>2sigma(I)]	R1 = 0.0361, wR2 = 0.0898	
R indices (all data)	R1 = 0.0374, wR2 = 0.0910	
Absolute structure parameter	-0.4(3)	
Largest diff. peak and hole	0.177 and -0.210 e.$Å^{-3}$	

3.4 Laocoon III analysis for *vicinal* difluoro compounds

3.4.1 *Erythro* 1,2-difluoro-1,2-diphenylethane **103**

```
NN= 4  FREQUENCY RANGE     0.000   600.000
   MINIMUM INTENSITY0.01000

INPUT PARAMETERS:

1        W(1)=  424.000
1        W(2)=  424.000
2        W(3)= 6424.000
2        W(4)= 6424.000
        A(1,2)=   2.680
        A(1,3)=  47.250
        A(1,4)=  26.000
        A(2,3)=  26.000
        A(2,4)=  47.250
        A(3,4)=  11.960


   PARAMETER SETS
1
   W(1)
   W(2)
2
   A(1,2)
3
   A(1,3)
   A(2,4)
4
   A(1,4)
   A(2,3)
5
   A(3,4)
 ITERATION  0  R.M.S.ERROR =  46.737
 ITERATION  1  R.M.S.ERROR =   0.294
 ITERATION  2  R.M.S.ERROR =   0.294

 BEST VALUES CASE   1


1        W(1)=  377.620
1        W(2)=  377.620
2        W(3)= 6424.000
```

2 W(4)= 6424.000
A(1,2)= 2.548
A(1,3)= 45.251
A(1,4)= 15.210
A(2,3)= 15.210
A(2,4)= 45.251
A(3,4)= 16.457

PROBABLE ERRORS OF PARAMETER SETS

1 0.075
2 0.166
3 0.174
4 0.174
5 0.183

ORDERED LINES CASE 1

LINE	EXP.FREQ.	CALC.FREQ.	INTEN.	ERROR
51	347.460	347.390	2.000	0.070
55	347.460	347.390	2.000	0.070
37	349.980	350.343	0.465	-0.363
24	354.180	354.114	0.580	0.066
42	367.790	368.022	1.420	-0.232
21	369.770	369.349	1.535	0.421
45	385.610	385.891	1.535	-0.281
26	387.590	387.217	1.420	0.373
34	401.440	401.126	0.580	0.314
19	404.320	404.896	0.465	-0.576
5	407.920	407.850	2.000	0.070
1	407.920	407.851	2.000	0.069

3.4.2 *Threo* 1,2-difluoro-1,2-diphenylethane **104**

NN= 4 FREQUENCY RANGE 0.000 600.000
MINIMUM INTENSITY0.01000

INPUT PARAMETERS:

1 W(1)= 424.000
1 W(2)= 424.000

```
2       W(3)= 6424.000
2       W(4)= 6424.000
      A(1,2)=   2.680
      A(1,3)=  47.250
      A(1,4)=  26.000
      A(2,3)=  26.000
      A(2,4)=  47.250
      A(3,4)=  11.960

   PARAMETER SETS
1
   W(1)
   W(2)
2
   A(1,2)
3
   A(1,3)
   A(2,4)
4
   A(1,4)
   A(2,3)
5
   A(3,4)

ITERATION  0  R.M.S.ERROR =  456.685
ITERATION  1  R.M.S.ERROR =   0.088
ITERATION  2  R.M.S.ERROR =   0.080
ITERATION  3  R.M.S.ERROR =   0.080


BEST VALUES CASE   1

1       W(1)=  880.652
1       W(2)=  880.652
2       W(3)= 6424.000
2       W(4)= 6424.000
      A(1,2)=   5.971
      A(1,3)=  47.166
      A(1,4)=  14.103
      A(2,3)=  14.103
      A(2,4)=  47.166
      A(3,4)=  17.301

PROBABLE ERRORS OF PARAMETER SETS
```

1 0.024
2 0.161
3 0.057
4 0.057
5 0.149

ORDERED LINES CASE 1

LINE	EXP.FREQ.	CALC.FREQ.	INTEN.	ERROR
51	850.100	850.017	2.000	0.083
55	850.100	850.017	2.000	0.083
24	857.530	857.512	0.676	0.018
42	868.730	868.842	1.324	-0.112
21	872.000	872.072	1.576	-0.072
45	889.160	889.232	1.576	-0.072
26	892.350	892.462	1.324	-0.112
34	903.810	903.792	0.676	0.018
5	911.370	911.286	2.000	0.084
1	911.370	911.287	2.000	0.083

3.4.3 *Erythro* 2,3-difluorosuccinic acid **130**

NN= 4 FREQUENCY RANGE 0.000 600.000
MINIMUM INTENSITY0.01000

INPUT PARAMETERS:

1 W(1)= 424.000
1 W(2)= 424.000
2 W(3)= 6424.000
2 W(4)= 6424.000
A(1,2)= 2.680
A(1,3)= 47.250
A(1,4)= 26.000
A(2,3)= 26.000
A(2,4)= 47.250
A(3,4)= 11.960

PARAMETER SETS
1
W(1)
W(2)

2
A(1,2)
3
A(1,3)
A(2,4)
4
A(1,4)
A(2,3)
5
A(3,4)

ITERATION 0 R.M.S.ERROR = 375.060
ITERATION 1 R.M.S.ERROR = 0.080
ITERATION 2 R.M.S.ERROR = 0.078
ITERATION 3 R.M.S.ERROR = 0.078

BEST VALUES CASE 1

1 W(1)= 48.944
1 W(2)= 48.944
2 W(3)= 6424.000
2 W(4)= 6424.000
A(1,2)= 1.756
A(1,3)= 46.678
A(1,4)= 23.314
A(2,3)= 23.314
A(2,4)= 46.678
A(3,4)= 14.005

PROBABLE ERRORS OF PARAMETER SETS

1 0.020
2 0.044
3 0.047
4 0.047
5 0.049

ORDERED LINES CASE 1

LINE	EXP.FREQ.	CALC.FREQ.	INTEN.	ERROR
51	13.910	13.948	2.000	-0.038

55	13.910	13.949	2.000	-0.039
37	26.910	26.972	0.441	-0.062
24	29.600	29.630	0.536	-0.030
42	42.070	41.879	1.464	0.191
21	42.710	42.733	1.559	-0.023
45	55.190	55.155	1.559	0.035
26	56.150	56.010	1.464	0.140
34	68.210	68.258	0.536	-0.048
19	70.870	70.916	0.441	-0.046
5	83.900	83.940	2.000	-0.040
1	83.900	83.941	2.000	-0.041

3.4.4 *Threo* 2,3-difluorosuccinic acid **132**

NN= 4 FREQUENCY RANGE 0.000 600.000
MINIMUM INTENSITY0.01000

INPUT PARAMETERS:

1 W(1)= 424.000
1 W(2)= 424.000
2 W(3)= 6424.000
2 W(4)= 6424.000
A(1,2)= 2.680
A(1,3)= 47.250
A(1,4)= 26.000
A(2,3)= 26.000
A(2,4)= 47.250
A(3,4)= 11.960

PARAMETER SETS
1
W(1)
W(2)
2
A(1,2)
3
A(1,3)
A(2,4)
4
A(1,4)
A(2,3)
5

A(3,4)
ITERATION 0 R.M.S.ERROR = 185.706
ITERATION 1 R.M.S.ERROR = 0.048
ITERATION 2 R.M.S.ERROR = 0.047
ITERATION 3 R.M.S.ERROR = 0.047

BEST VALUES CASE 1

1 W(1)= 609.671
1 W(2)= 609.671
2 W(3)= 6424.000
2 W(4)= 6424.000
A(1,2)= 1.587
A(1,3)= 45.331
A(1,4)= 31.209
A(2,3)= 31.209
A(2,4)= 45.331
A(3,4)= 8.809

PROBABLE ERRORS OF PARAMETER SETS

1 0.012
2 0.026
3 0.029
4 0.029
5 0.029

ORDERED LINES CASE 1

LINE	EXP.FREQ.	CALC.FREQ.	INTEN.	ERROR
51	571.430	571.400	2.000	0.030
55	571.430	571.400	2.000	0.030
37	595.710	595.705	0.407	0.005
24	598.090	598.129	0.545	-0.039
42	605.420	605.351	1.455	0.069
21	606.000	606.100	1.593	-0.100
45	613.250	613.241	1.593	0.009
26	613.970	613.991	1.455	-0.021
34	621.140	621.213	0.545	-0.073
19	623.670	623.637	0.407	0.033
5	647.970	647.941	2.000	0.029
1	647.970	647.942	2.000	0.028

3.4.5 Dimethyl *erythro* 2,3-difluorosuccinate **126**

```
                NN= 4  FREQUENCY RANGE     0.000   600.000
 MINIMUM INTENSITY0.01000

 INPUT PARAMETERS:

 1        W(1)=  424.000
 1        W(2)=  424.000
 2        W(3)= 6424.000
 2        W(4)= 6424.000
          A(1,2)=   2.680
          A(1,3)=  47.250
          A(1,4)=  26.000
          A(2,3)=  26.000
          A(2,4)=  47.250
          A(3,4)=  11.960

    PARAMETER SETS
 1
    W(1)
    W(2)
 2
    A(1,2)
 3
    A(1,3)
    A(2,4)
 4
    A(1,4)
    A(2,3)
 5
    A(3,4)
 ITERATION  0  R.M.S.ERROR =  361.011
 ITERATION  1  R.M.S.ERROR =   0.095
 ITERATION  2  R.M.S.ERROR =   0.095

 BEST VALUES CASE   1

 1        W(1)=   62.997
 1        W(2)=   62.997
 2        W(3)= 6424.000
 2        W(4)= 6424.000
          A(1,2)=   1.793
          A(1,3)=  47.009
          A(1,4)=  21.702
          A(2,3)=  21.702
```

A(2,4)= 47.009
A(3,4)= 13.751

PROBABLE ERRORS OF PARAMETER SETS

1 0.024
2 0.053
3 0.056
4 0.056
5 0.059

ORDERED LINES CASE 1

LINE	EXP.FREQ.	CALC.FREQ.	INTEN.	ERROR
51	28.690	28.641	2.000	0.049
55	28.690	28.642	2.000	0.048
37	40.390	40.375	0.476	0.015
24	43.020	43.023	0.573	-0.003
42	55.050	54.981	1.427	0.069
21	55.730	55.919	1.524	-0.189
45	70.160	70.075	1.524	0.085
26	70.840	71.013	1.427	-0.173
34	82.870	82.970	0.573	-0.100
19	85.720	85.619	0.476	0.101
1	97.400	97.353	2.000	0.047
5	97.400	97.353	2.000	0.047

3.4.6 Dimethyl *threo* 2,3-difluorosuccinate **127 + 128**

NN= 4 FREQUENCY RANGE 0.000 600.000
MINIMUM INTENSITY0.01000

INPUT PARAMETERS:

1 W(1)= 424.000
1 W(2)= 424.000
2 W(3)= 6424.000
2 W(4)= 6424.000
A(1,2)= 2.680
A(1,3)= 47.250
A(1,4)= 26.000
A(2,3)= 26.000

```
          A(2,4)=  47.250
          A(3,4)=  11.960

     PARAMETER SETS
1
     W(1)
     W(2)
2
     A(1,2)
3
     A(1,3)
     A(2,4)
4
     A(1,4)
     A(2,3)
5
     A(3,4)

               ITERATION  0  R.M.S.ERROR =  52.874
 ITERATION  1  R.M.S.ERROR =   0.330
 ITERATION  2  R.M.S.ERROR =   0.330

BEST VALUES CASE   1

1        W(1)= 476.828
1        W(2)= 476.828
2        W(3)= 6424.000
2        W(4)= 6424.000
          A(1,2)=   1.766
          A(1,3)=  45.666
          A(1,4)=  28.863
          A(2,3)=  28.863
          A(2,4)=  45.666
          A(3,4)=  10.140

PROBABLE ERRORS OF PARAMETER SETS

 1    0.084
 2    0.183
 3    0.199
 4    0.199
 5    0.206

ORDERED LINES CASE   1

LINE   EXP.FREQ.  CALC.FREQ.  INTEN.     ERROR
```

51	439.740	439.563	2.000	0.177
55	439.740	439.564	2.000	0.176
37	460.620	460.578	0.422	0.042
24	463.440	463.254	0.554	0.186
42	471.740	471.628	1.446	0.112
21	471.740	472.485	1.578	-0.745
45	481.360	481.172	1.578	0.188
26	481.360	482.029	1.446	-0.669
34	490.290	490.402	0.554	-0.112
19	493.370	493.079	0.422	0.291
1	514.270	514.092	2.000	0.178
5	514.270	514.093	2.000	0.177

3.4.7 Dibenzyl *erythro* 2,3-difluorosuccinamide **161**

NN= 4 FREQUENCY RANGE 0.000 600.000
MINIMUM INTENSITY0.01000

INPUT PARAMETERS:

1 W(1)= 424.000
1 W(2)= 424.000
2 W(3)= 6424.000
2 W(4)= 6424.000
A(1,2)= 2.680
A(1,3)= 47.250
A(1,4)= 26.000
A(2,3)= 26.000
A(2,4)= 47.250
A(3,4)= 11.960

PARAMETER SETS
1
W(1)
W(2)
2
A(1,2)
3
A(1,3)
A(2,4)
4

A(1,4)
A(2,3)
5
A(3,4)

ITERATION 0 R.M.S.ERROR = 1.238
ITERATION 1 R.M.S.ERROR = 0.566
ITERATION 2 R.M.S.ERROR = 0.565

BEST VALUES CASE 1

1 W(1)= 424.682
1 W(2)= 424.682
2 W(3)= 6424.000
2 W(4)= 6424.000
A(1,2)= 2.139
A(1,3)= 48.414
A(1,4)= 24.836
A(2,3)= 24.836
A(2,4)= 48.414
A(3,4)= 11.938

PROBABLE ERRORS OF PARAMETER SETS

1 0.144
2 0.322
3 0.330
4 0.330
5 0.352

ORDERED LINES CASE 1

LINE	EXP.FREQ.	CALC.FREQ.	INTEN.	ERROR
51	388.070	388.057	2.000	0.013
55	388.070	388.058	2.000	0.012
37	404.270	403.913	0.487	0.357
24	406.670	407.016	0.616	-0.346
42	415.950	416.815	1.384	-0.865
21	418.910	417.990	1.513	0.920
45	430.330	431.375	1.513	-1.045
26	433.360	432.550	1.384	0.810
34	442.750	442.348	0.616	0.402
19	445.170	445.451	0.487	-0.281
1	461.320	461.308	2.000	0.012
5	461.320	461.308	2.000	0.012

3.4.8 Dibenzyl *threo* 2,3-difluorosuccinamide **162**

NN= 4 FREQUENCY RANGE 0.000 600.000
MINIMUM INTENSITY0.01000

INPUT PARAMETERS:

1 W(1)= 424.000
1 W(2)= 424.000
2 W(3)= 6424.000
2 W(4)= 6424.000
A(1,2)= 2.680
A(1,3)= 47.250
A(1,4)= 26.000
A(2,3)= 26.000
A(2,4)= 47.250
A(3,4)= 11.960

PARAMETER SETS
1
W(1)
W(2)
2
A(1,2)
3
A(1,3)
A(2,4)
4
A(1,4)
A(2,3)
5
A(3,4)

ITERATION 0 R.M.S.ERROR = 62.403
ITERATION 1 R.M.S.ERROR = 0.838
ITERATION 2 R.M.S.ERROR = 0.824
ITERATION 3 R.M.S.ERROR = 0.824

BEST VALUES CASE 1

1 W(1)= 486.350
1 W(2)= 486.350
2 W(3)= 6424.000
2 W(4)= 6424.000

A(1,2)= 2.005
A(1,3)= 46.029
A(1,4)= 31.340
A(2,3)= 31.340
A(2,4)= 46.029
A(3,4)= 12.552

PROBABLE ERRORS OF PARAMETER SETS

1 0.210
2 0.433
3 0.540
4 0.540
5 0.513

ORDERED LINES CASE 1

LINE	EXP.FREQ.	CALC.FREQ.	INTEN.	ERROR
51	447.680	447.665	2.000	0.015
55	447.680	447.667	2.000	0.013
37	468.880	468.732	0.296	0.148
24	471.990	472.035	0.417	-0.045
42	481.270	482.582	1.583	-1.312
21	484.690	483.288	1.704	1.402
45	487.790	489.412	1.704	-1.622
26	491.260	490.118	1.583	1.142
34	501.270	500.666	0.417	0.604
19	503.590	503.968	0.296	-0.378
1	525.050	525.035	2.000	0.015
5	525.050	525.035	2.000	0.015